ABSTRACT

Synthetic Studies Toward the Total Syntheses of
Scholarisine A and Phomoidride D

Aaron A. Bedermann, Ph.D.

Advisor: John L. Wood, Ph.D.

Isolated in 2008 from a leaf extract of an *Alstonia scholaris* variant, scholarisine A contains a unique pentacyclic architecture that makes it a challenging target for total synthesis. Our approach toward the molecule's polycyclic core consists of a nucleophilic olefin addition into an activated isonitrile with subsequent addition of an adjacent ester into the resultant carbocation to produce a polycyclic imine. The feasibility of this proposed cascade cycloaddition was explored in a model system that presented an analogous array of functionality within a similar, but not identical, carbon framework. Although we were delighted to find that the model substrate was capable of undergoing the desired cyclization process, it occurred in low yield and only when using an acyl group as an activating agent, the product of which is not suited as an intermediate en route to scholarisine A. Our efforts to access an advanced isonitrile-containing intermediate was met with only limited success and concerns regarding overall efficiency led us to eventually abandon the scholarisine A effort.

Phomoidrides A and B were isolated in 1996 from an unidentified fungus, believed to be a steril *Phoma* variant. Phomoidrides C and D were later isolated from the same fungus and were shown to be epimeric at the C7 stereocenter. The synthetic challenges inherent to the phomoidrides have inspired many creative synthetic approaches that have culminated in four completed total syntheses of members of the phomoidride family. Our unique approach consist of a phenolic oxidation Diels-Alder sequence and eventual radical cascade cyclization to produce a functionalized isotwistane intermediate that undergoes a Grob-type fragmentation to produce the bicyclo[4.3.1]decadiene core of the phomoidrides. Attempts to install the maleic anhydride and complete the synthesis from a diester precursor failed. Subsequent model studies determined the maleic anhydride can be accessed from a β-keto ester functionality. In our current third-generation approach toward phomoidride D, we have achieved fragmentation to produce the phomoidride core and attempts to install the maleic anhydride and complete the total synthesis are currently underway.

Synthetic Studies Toward the Total Syntheses of Scholarisine A and Phomoidride D

by

Aaron A. Bedermann, B.S.

A Dissertation

Approved by the Department of Chemistry and Biochemistry

_____

Patrick J. Farmer, Ph.D., Chairperson

Submitted to the Graduate Faculty of
Baylor University in Partial Fulfillment of the
Requirements for the Degree
of

Doctor of Philosophy

Approved by the Dissertation Committee

_____

John L. Wood, Ph.D., Chairperson

_____

Charles M. Garner, Ph.D.

_____

Kevin G. Pinney, Ph.D.

_____

Caleb D. Martin, Ph.D.

_____

William Hockaday, Ph.D.

Accepted by the Graduate School

May 2015

_____

J. Larry Lyon, Ph.D., Dean

Page bearing signatures is kept on file in the Graduate School.

TABLE OF CONTENTS

LIST OF FIGURES

CHAPTER ONE

CHAPTER THREE

CHAPTER FOUR

APPENDIX A

APPENDIX B

APPENDIX C

APPENDIX D

LIST OF SCHEMES

CHAPTER ONE

CHAPTER TWO

CHAPTER THREE

CHAPTER FOUR

CHAPTER FIVE

LIST OF TABLES

CHAPTER TWO

CHAPTER FOUR

CHAPTER FIVE

APPENDIX D

LIST OF ABBREVIATIONS

Ac	acetyl
ACHN	1,1'-azobis(cylohexanecarbonitrile)
AIBN	2,2′-Azobis(2-methylpropionitrile)
Ar	aromatic
BtCN	cyanobenzotriazole
BTPP	*tert*-butylimino(pyrrolidino)phosphorane
Bu	*n*-butyl
Bz	benzoyl
CAM	ceric ammonium molybdate
Cat.	catalyst
COSY	correlation spectroscopy
CSA	camphorsulfonic acid
DCM	dichloromethane
DEAD	diethyl azodicarboxylate
DEPT	distortionless enhancement by polarisation transfer
DIBAL	diisobutylaluminum hydride
DMAP	4-(dimethylamino)pyridine
DMF	*N,N*-dimethylformamide
DMP	Dess-Martin Periodinane
DMS	dimethylsulfide
DMSO	dimethyl sulfoxide
DPPA	diphenylphosphorylazide
EDCI	1-ethyl-3-(3-dimethylaminopropyl)carbodiimide
ESI	electrospray ionization
Et	ethyl
EtOAc	ethyl acetate
FTIR	fourier transform infrared spectroscopy
HMBC	heteronuclear multiple-bond correlation
HMPA	hexamethylphosphoramide
Hex	hexanes
HRMS	high resolution mass spectrometry
HSQC	heteronuclear single quantum correlation
hν	irradiation by light
IBX	2-iodosybenzoic acid
*i*Pr	*iso*-propyl
KHMDS	potassium bis(trimethylsilyl)amide
LDA	lithium diisopropylamine

LiHMDS	lithium bis(trimethylsilyl)amide
*m*CPBA	3-chloroperbenzoic acid
Me	methyl
MeCN	acetonitrile
MS	molecular sieves
Ms	methanesulfonyl
NBS	*N*-bromosuccinimide
NCS	*N*-chlorosuccinimide
NIS	*N*-iodosuccinimide
NMM	*N*-methylmorpholine
NMO	*N*-methylmorpholine oxide
NMR	nuclear magnetic resonance
Ns	2-nitrophenylsulphonyl
Nu	nucleophile
Ph	phenyl
Pin	pinacolato
Piv	pivaloyl
PMB	4-methoxybenzyl
PPTS	pyridinium *p*-toluenesulfonate
Red-Al	reductive aluminum
rt	room temperature
TBAF	tetrabutylammonium fluoride
TBDPS	*tert*-butyldiphenylsilyl chloride
TBS	*tert*-butyldimethylsilyl
*t*Bu	*tert*-butyl
TEMPO	2,2,6,6-tetramethyl-1-piperidinyloxy
Tf	trifluoromethylsulfonyl
TFA	trifluoroacetic acid
TFAA	trifluoromethylacetic anhydride
THF	tetrahydrofuran
TLC	thin-layer chromatography
TMG	trimethylguanidine
TMS	trimethylsilyl
TPAP	tetrapropylammonium perruthenate
Ts	4-toluenesulfonyl
TTMP	tris(2,4,6-trimethoxyphenyl)phosphine
uv	ultraviolet

ACKNOWLEDGMENTS

First and foremost I would like to thank my advisor Professor John L. Wood for taking me into his group. I am amazed at how much I have learned both chemically and professionally under your guidance. You have been a phenomenal mentor and I cannot thank you enough for the doors you have helped open and opportunities you have given me.

To my family and my parents above all, without your love and support I would not have been able to achieve what I have. This has not been an easy road but you both have seen me through it to the end, and for this I am eternally grateful. I know I don't say this very often, but I love you all very much.

To the Wood group, you have all been great assets and friends for the better part of a decade. Jenn and Genessa, thank you both for looking after an optimistic young graduate student and helping me through the difficulties of total synthesis. Your knowledge and advice helped set a foundation so that I could become the chemist I am today and I thank you for that. Ke thank you for being a great role model and hoodmate. I am very glad I was able to learn from you both in my early stages and also at the end of my graduate studies. Enquist, your chemical knowledge is both daunting and inspiring. I cannot thank you enough for all the help you have given me over the years, especially during my literature seminar. Sam, thank you for all the treats you supplied us with over the years and I have never met a better proofreader. Dave, Matt, Chris, and Graham, thank you all for the help, advice, and laughs. Naoto, thank you for giving me the

phomoidride project, without your help on the model system we wouldn't be where we are today. Yutaka, thank you for allowing me to sleep in your living room these last few months and for being a good friend. Joyce, good luck finishing phomoidrides, I have all the faith in you and know you can do it. Jonas, thank you for working mechanisms with us, bringing us Swiss chocolate, visiting us in Waco, and your overall friendship; you always knew how to make lab fun and I look forward to visiting you in Switzerland. Monica, thank you for being a great labmate, hoodmate, and friend. You are a phenomenal chemist and you will do great things. Heemal, thank you for all the chemistry discussions/debates they have been great challenges and learning experiences for both of us. Thank you too for allowing me to crash in your living room and use your shower. You truly are a great friend. Last but certainly not least, Travis, thank you for being one of my best friends. Graduate school would not have been bearable without the game nights, fantasy football or baseball, softball, or just hanging out at the steakout. It truly has been a pleasure getting to know you all!

Eric, thank you for being such a great friend from our first summer of research to our defenses (that occurred within 30 minutes of each other). Whether it was studying in the chemistry library or visiting on my way to get ice every morning, I greatly enjoyed our discussions about chemistry and life in general. You are just as good a chemist as you are a friend and you will do great things. Curtis, thank you for spending Sundays getting lost in the mountains of both Colorado and Wyoming with me. Brett, Sandy (and Juna), Sandra, and Tim, thank you all for including me in your lives. Some of my fondest memories of graduate school were spending a Friday night drinking wine, eating late night pasta, and playing with Juna at Brett and Sandy's apartment. Tim, Sandra, and

Newton thank you so much for watching the Packers and Badgers with me, it was always a great time.

To my climbing friends, it was a blast spending what little free time I had tromping around Colorado with each an every one of you. Tim and Brandon, thank you both for introducing me to mountaineering. Although the days were grueling they were some of the best I've ever had. Nick, thank you for always being willing to go to lunch with me and being a great drinking buddy. A great day climbing is rarely due to what you accomplish but always attributed to the company you are with and you all made sure every day (or trip) was worth remembering.

Finally, I'd like to thank Eric Ferreira and Brian McNaughton for all their help and for pushing me to become a better chemist each and every day. Eric your class was one of the best I have ever taken and I still find myself referring to your notes. Brian, thank you for including me in your group activities and offering great advice throughout the years. It was always fun having a beer with your group on a Friday evening.

CHAPTER ONE

Introduction To Scholarisine A and Related Natural Products

1.1 Isolation, Characterization, and Biosynthesis

1.1.1 The Scholarisines

In 2008, Luo and coworkers isolated scholarisine A (**1.10,** Figure 1.10) from the leaves of an *Alstonia scholaris* variant that is native to the Yunnan province of the People's Republic of China.[1] *A. scolaris*, more commonly known as milk wood or devil's tree, is native to Asia, Africa, and Australia. After the initial isolation of **1.10**, Luo and coworkers isolated scholarisines B-G from a bark extract of *A. scholaris*.[2] Both the leaves and bark of *A. scholaris* have been used as traditional medicines for centuries due to their anti-inflammatory, anti-asthmatic, anti-tussive, and anti-bacterial properties. While the biological activity of **1.10** (as opposed to the whole extract of *A. scholaris*) has yet to be determined, scholarisine B (**1.11**), E (**1.14**), and G (**1.15**) exhibit moderate activity toward COX-1, COX-2, and 5-LOX inflammatory enzymes. Scholarisine G (**1.15**) in particular exhibited selectivity toward COX-2 (91.1% inhibition at 100 μM), over COX-1 (38.5 %, 100 μM) and 5-LOX (57.3%, 100 μM).[3]

The structure and connectivity of **1.10** was elucidated through extensive spectroscopic studies. The molecular formula was determined to be $C_{19}H_{18}N_2O_2$ based upon high resolution electrospray ionization mass spectrometry (HRESIMS) (307.1440 *m/z*, $[M+H]^+$). A UV spectrum of **1.10** indicated the presence of an indolenine motif (220, 268 nm), while the presence of a lactone and aromatic ring was determined by

FTIR spectroscopy (1766 cm^{-1} and 1641, 1575 cm^{-1}, respectively). The basic structural makeup, including the presence of a substituted indole ring, was determined by ^{1}H, ^{13}C, and DEPT NMR studies. While HMBC, HSQC, and COSY NMR experiments were utilized to determine the structural connectivity. NOE correlations, obtained via ROESY, between H19-H21 and H-18-H15 aided in the structural determination of the core, while the correlations between H3, H15, and H16 helped determine the relative stereochemistry.[1] The absolute stereochemistry of **1.10** was recently confirmed by Smith and coworkers via the enantioselective total synthesis of (+)-**1.10**.[4]

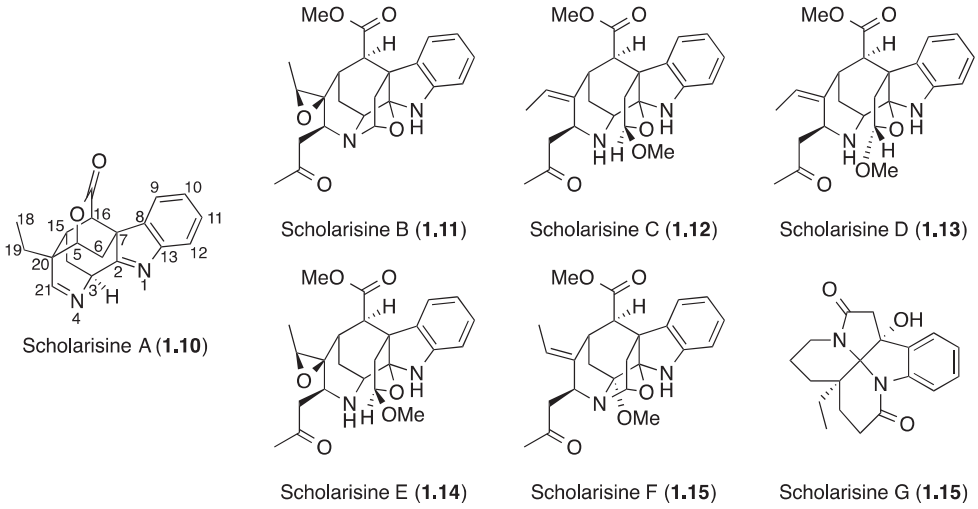

Figure 1.10 The scholarisine family

1.1.2 Biosynthetic Origins

Scholarisines A-F are members of the akuammiline family of natural products which all possess similar C7-C16 connectivity, representative examples of the family are illustrated in Figure 1.11.[5] The family's namesake akuammiline (**1.16**) was isolated in 1932,[6] and is considered to be a biogenic precursor to several members the family.

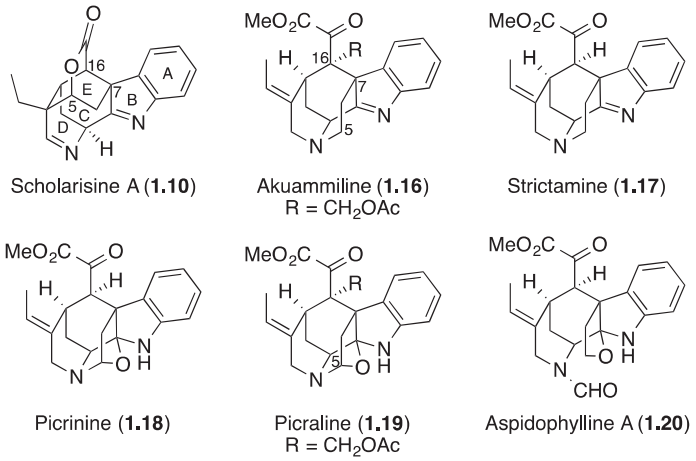

Figure 1.11 Representative examples of the akuammiline family

The akuammiline alkaloids are believed to arise from the same biogenic precursor, geissoschizine (**1.26**, Scheme 1.10), through formation of a C16-C7 bond. The biosynthetic origins of **1.10** have been traced back through strictosidine to geraniol (**1.21**) and tryptophan (**1.23**).[7c] The monoterpene secoirodoid pathway converts **1.21** to secologanin (**1.22**), while tryptophan decarboxylate (TDC) converts **1.23** to tryptamine (**1.24**). Strictosidine synthase then catalyzes a Pictet-Spengler type reaction to convert secologanin (**1.22**) and tryptamine (**1.24**) into strictosidine (**1.25**).[7] Strictosidine (**1.25**) is thought to be converted to geissoschizine (**1.26**) via a sequence involving loss of glucose, aldehyde condensation, and reduction.[8] Oxidative coupling at C7 of geissoschizine can then lead to the formation of the C7-C16 bond, characteristic of the akuammaline alkaloids, delivering rhazimal (**1.27**).[9]

Rhazimal (**1.27**) can be further manipulated to give many other members of the akuammiline family. For example, akuammiline (**1.16**) is believed to derive from **1.27** by the reduction of the aldehyde followed by acylation of the resultant alcohol (Scheme 1.11).[10] Subsequent oxidation of **1.16** at C5, followed by nucleophilic addition of the

resultant hemiaminal hydroxyl to the pendant imine at C2 would deliver oxabicycle contained in picraline (**1.19**).[11]

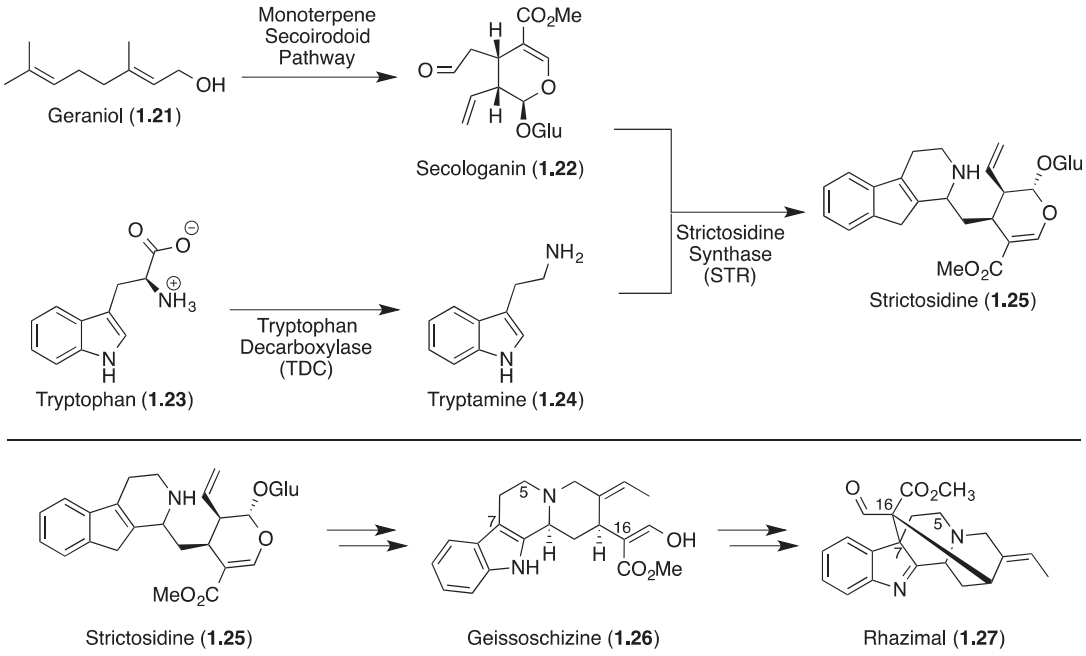

Scheme 1.10 Biosynthesis of Rhazimal

A parallel biosynthetic pathway from rhazimal (**1.27**) can be envisioned as giving rise to several other members of the akuammiline family. In this sequence a deformylation event producing strictamine (**1.17**)[12] precedes C5 oxidation and oxabicyle formation to yield picrinine (**1.18**), which in turn can serve as a biogenetic precursor to aspidophylline A (**1.20**) via C5 reduction and *N*-formylation.[13,14] Picrinine (**1.18**) is proposed to be a direct precursor to scholarisine A (**1.10**) through the opening of the oxabicycle to **1.18a** followed by olefin migration to generate enamine **1.18b**. Addition of the derived enamine to the pendant aldehyde, forming alcohol **1.18c**. Lactonization and loss of methanol could then furnish scholarisine A (**1.10**).[1,15] Alternatively one could

imagine ring closure of aldehyde **1.18b** by direct addition of the adjacent olefin followed by 1,3-hydride shift to produce alcohol **1.18c**.[16]

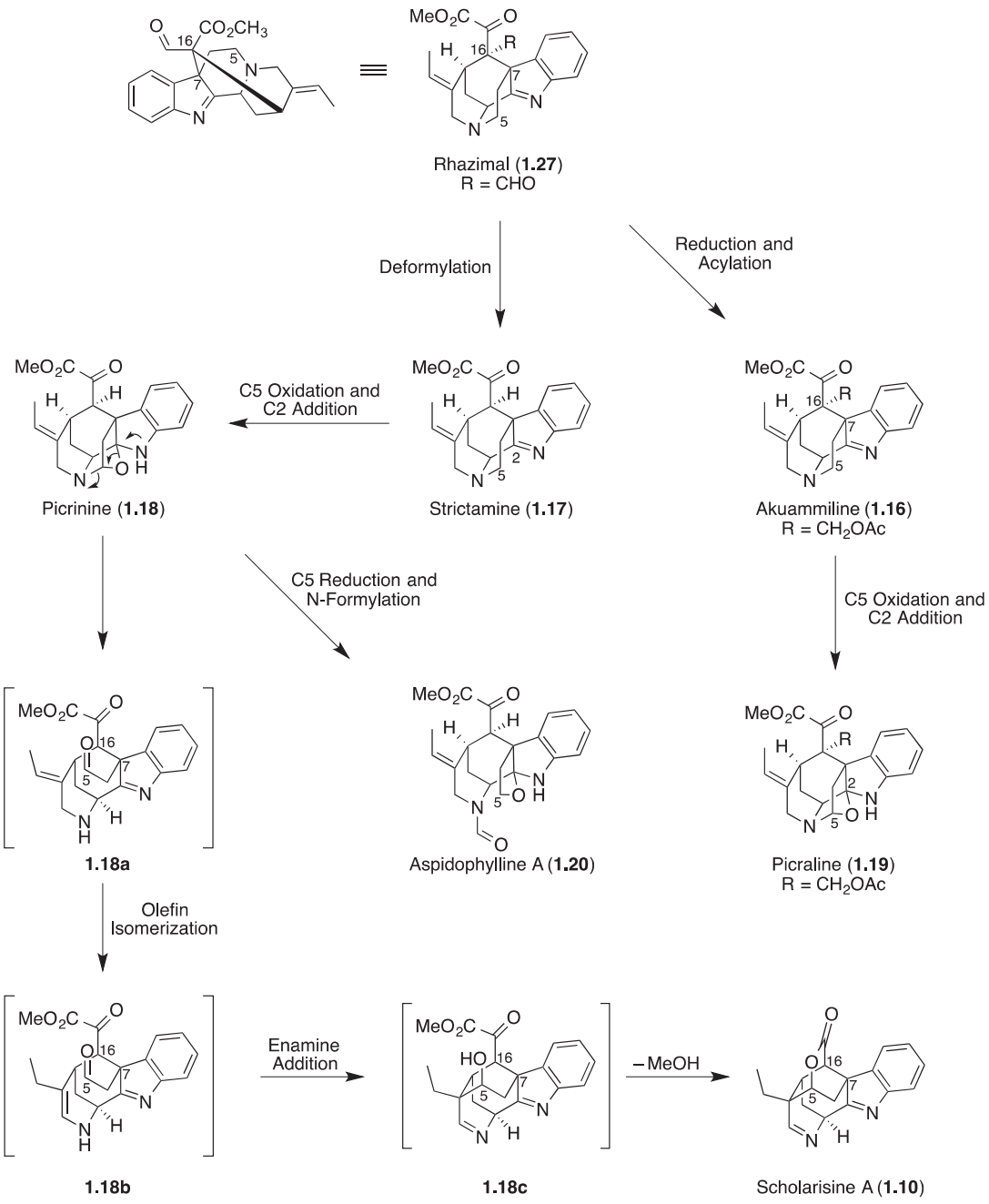

Scheme 1.11 Biosynthesis of scholarisine A and related alkaloids[1,16]

1.2 Completed Syntheses and Synthetic Attempts Toward Scholarisine A

1.2.1 Smith and Coworkers Enantioselective Synthesis

In 2012, Smith and coworkers reported the first total synthesis of **1.10**.[4,6a] As illustrated retrosynthetically in Scheme 1.12, the Smith approach employed a late stage cyclization and oxidation to furnish **1.10** from alcohol **1.28**. The lactone of **1.28** was obtained via oxidation, lactonization, and deprotection of diol **1.29** which, in turn, was derived from the reduction and homologation of lactone **1.30**. Indole **1.30** was produced by employing Fischer's protocol on the oxidation product of alcohol **1.31**, which was derive from epoxide **1.32** by reductive cyclization of the nitrile and epoxide moieties. The latter compound was prepared by alkylation and epoxidation of known lactone **1.33**.

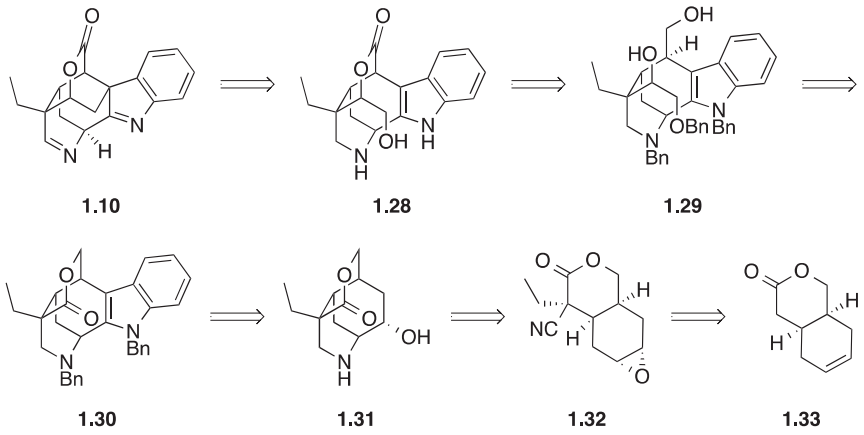

Scheme 1.12 Smith's retrosynthetic analysis

In the forward sense (Scheme 1.13) Smith's synthesis commenced with the reduction of commercially available anhydride **1.34** with lithium aluminum hydride ($LiAlH_4$) to produce diol **1.35** in 90% yield. Diol **1.35** was resolved by selective acylation under enzymatic conditions to deliver the desired isomer (+)-**1.36** (95% ee) accompanied by the corresponding diacetate **1.37** (3.4:1, respectively). The mixture was

moved forward through a tosylation/substitution sequence to give nitrile **1.38**. Subsequent basic hydrolysis and acidification delivered lactone (−)-**1.33** in 70% yield from diol **1.36**. Under the basic conditions, the diacetate was saponified to the diol, which was then chromatographically separated from the desired lactone **1.33**. Deprotonation of lactone **1.33** with lithium diisopropylamide (LDA) and functionalization with cyanobenzotriazole (BtCN) gave the nitrile, which was stereoselectively alkylated on the convex face to generate (−)-**1.39**. Epoxidation of **1.39** (*m*CPBA) produced epoxides (−)-**1.32** (desired) and (−)-**1.40** as a 3:1 mixture of diastereomers. Fortunately, the major diastereomer could be isolated by crystallization from toluene in a 58% yield.

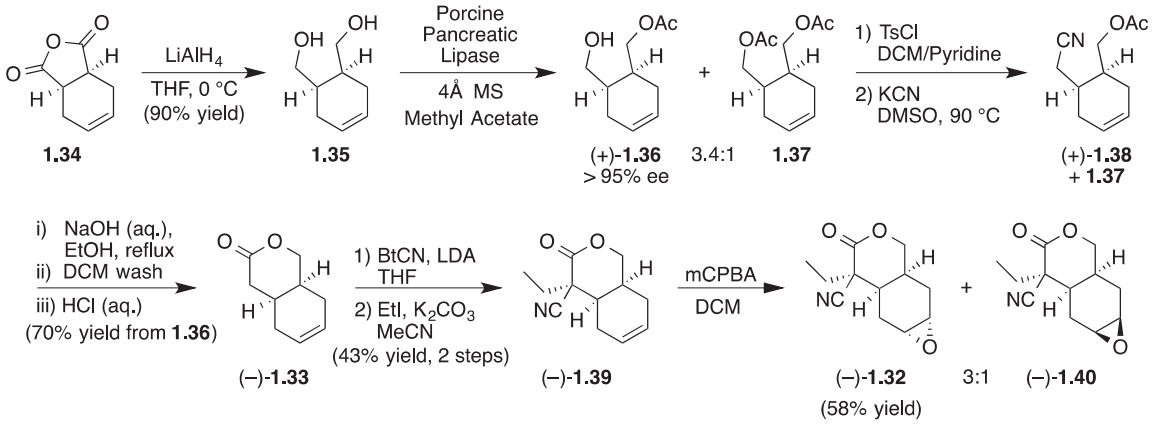

Scheme 1.13 Epoxide formation

Nitrile (−)-**1.32** was subjected to rhodium mediated reduction upon which the resultant amine cyclized onto the epoxide to deliver alcohol (−)-**1.31**. Amine protection with benzoyl chloride and alcohol oxidation with Dess-Martin Periodinane (DMP) furnished ketone (+)-**1.41** in a 71% yield over 2 steps. Condensation of (+)-**1.41** with 1-benzyl-1-phenylhydrazine initiated a Fischer indole synthesis which produced benzyl

protected indole (−)-**1.42** which, without purification was subjected to $LiAlH_4$ reduction of the lactone and benzoyl moieties followed by selective protection of the sterically least hindered of the two derived alcohols (70% yield over three steps). Oxidation of alcohol (−)-**1.43** using Ley's conditions delivered aldehyde (+)-**1.44** in good yield.

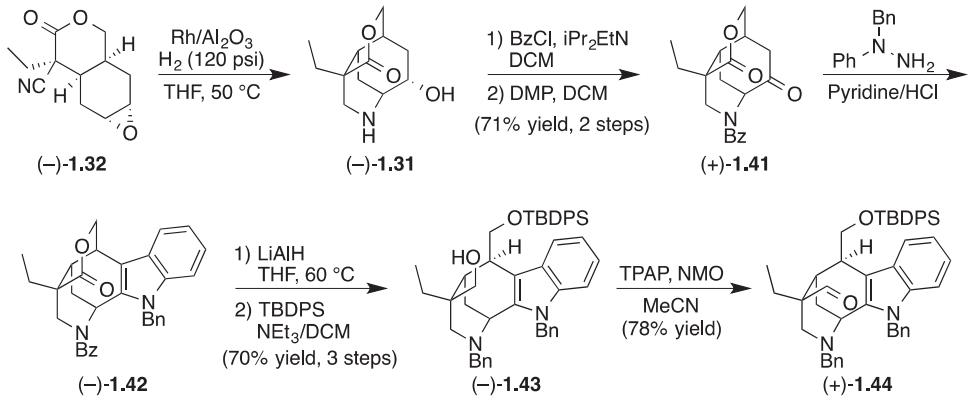

Scheme 1.14 Formation of the tetracycle

To complete the synthesis, aldehyde (+)-**1.44** was alkylated with benzyloxymethyl lithium, followed by the removal of the silyl protecting group with a potassium hydroxide (KOH) wash to form diol (+)-**1.29** in 63% yield as a single diastereomer. Oxidation of the primary alcohol with 2-iodoxybenzene (IBX) and further oxidation of the resultant lactol under Ley's conditions generated lactone (−)-**1.45** in a 57% yield over two steps. A two step global benzyl deprotection ($AlCl_3$) and hydrogenation with Pearlman's catalyst furnished alcohol (−)-**1.45**. Protection of the secondary amine as the corresponding trifluoracetamide and tosylation of the primary alcohol set the stage for a *t*-butylimino(pyrrolidino)phosphorous mediated cyclization that produces the bridging lactone (+)-**1.46** in a 53% yield over five steps. Hydrolysis of the trifluoroacetamide and oxidation of the resultant secondary amine to the cyclic imine furnished synthetic (+)-**1.10** in 25 overall steps from commercially available materials.

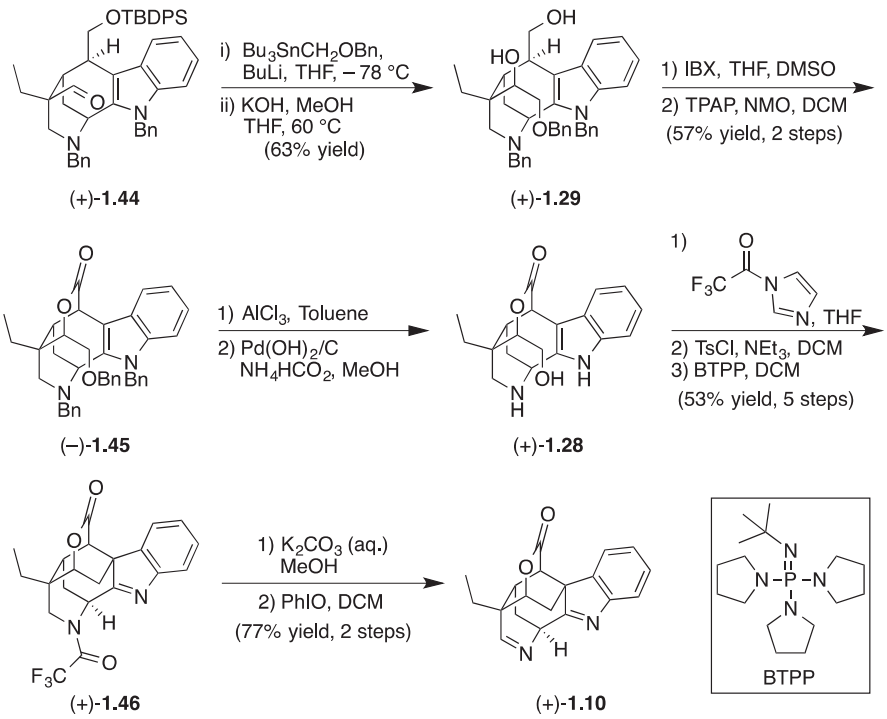

Scheme 1.15 Completion of Smith's synthesis

1.2.2 Snyder and Coworkers Synthesis

Snyder and coworkers completed the second total synthesis of (+)-**1.10** in 2013, utilizing a novel alpha-arylation strategy that introduces the indolenine ring at a late stage.[17] As illustrated retrosynthetically in Scheme 1.16, Snyder and coworkers introduced the indolenine motif of (+)-**1.10** by intramolecular arylation of lactone **1.47**, which in turn was generated by condesation of ketone **1.48** with *o*-iodoanaline. The lactam present in **1.48** arose from ester **1.49** via epimerization and lactamization. The requisite tricycle (**1.49)** was produced by 6-*exo*-*trig* radical cyclization of enoate **1.50** which, in turn, arose from a Diels-Alder reaction utilizing an appropriately functionalized pyrone.

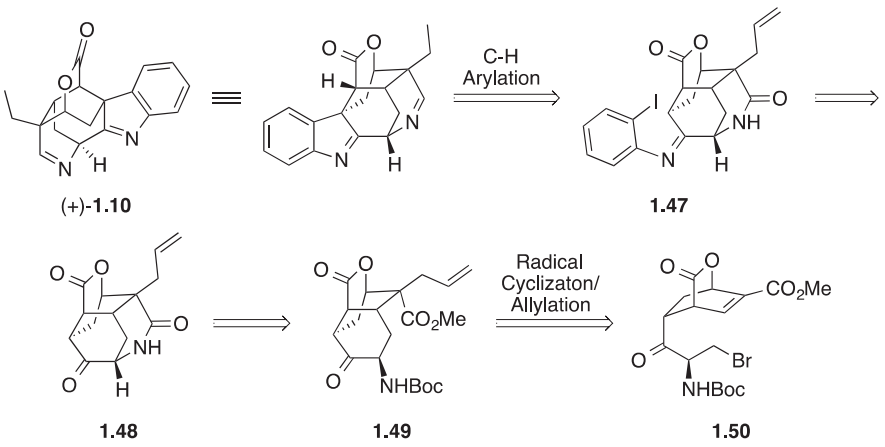

Scheme 1.16 Snyder's retrosynthetic analysis

In the forward sense, Snyder's synthesis was initiated by conversion of *N*-Boc-*D*-serine to corresponding Weinreb amide (**1.52**). Oxazolidine formation in the presence of boron trifluoride diethyl etherate (BF_3•OEt_2) and subsequent vinyl Grignard addition gave enone **1.53** in excellent yield over two steps. Subsequent Diels-Alder cycloaddition with pyrone **1.54** furnished an 83% yield of diastereomeric *endo*-cycloadducts that proved separable and favored the desired isomer (**1.55)**. Deprotection of oxazole **1.55** with trifluoroacetic acid (TFA) and following bromination under Appel's conditions delivered bromide **1.50**, in a 71% yield over two steps.

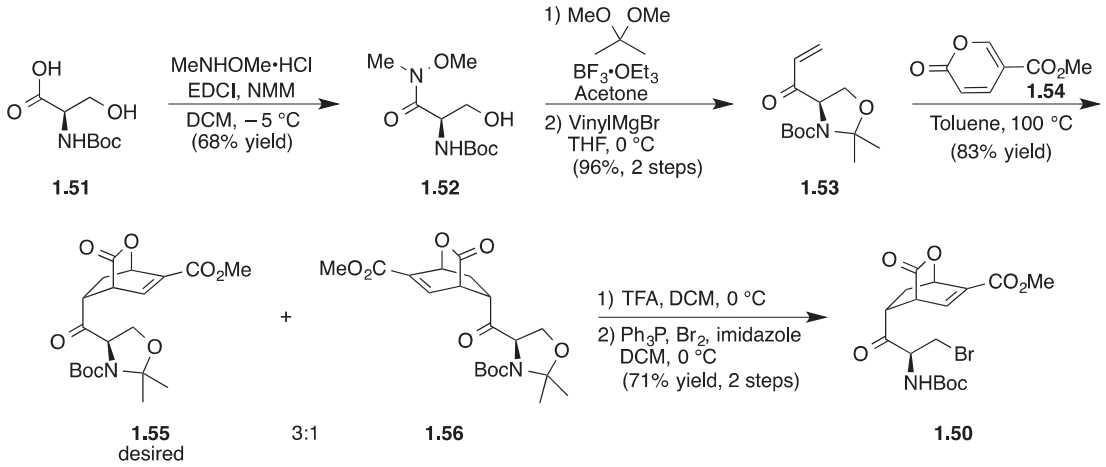

Scheme 1.17 Formation of ester **1.50**

With bromide **1.50** in hand, Snyder and coworkers attempted their desired 6-*exo*-*trig* cyclization in the presence of allyltributylstannane as a radical trap and triethylborane (Et_3B)/O_2 as an initiator (Scheme 1.18). In the event, the reaction occurred to deliver a moderate yield of a single diastereomer (**1.49**) possessing the requisite stereochemistry at C20 for conversion to the natural product. Initial attempts to epimerize amide **1.49** for subsequent lactamization failed and resulted only in the formation of pyrazine dimers. Thus, as illustrated a two-step oxidation-reduction sequence was developed that employs trimethylguanidine (TMG) and TEMPO under an atmosphere of air to furnish an enamine (**1.57**, 68% yield) which, in turn, is reduced to the desired amine upon exposure to sodium cyanoborohydride ($NaBH_3CN$). Heating of the reaction mixture to 80 °C following the reduction event promotes lactamization to deliver alcohol **1.58** in an excellent yield over two steps. Oxidation of **1.58** with IBX to produce ketone **1.48** and concomitant imine formation with 2-iodoaniline resulted in C-H arylation precursor **1.47**.

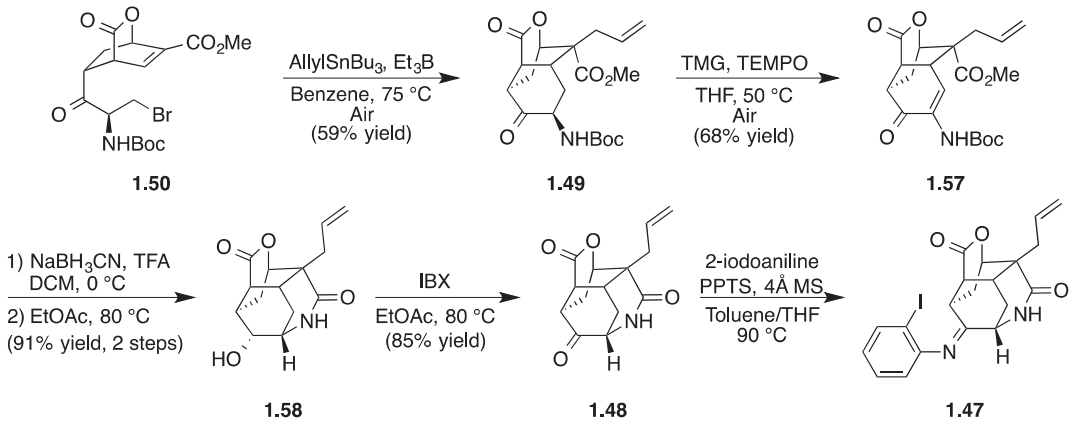

Scheme 1.18 Formation of the scholarisine A core

With aryl iodide **1.47** in hand, the key C-H arylation could be attempted. In the presence of tributyltinhydride (Bu_3SnH) and 1,1'-azobis(cylohexanecarbonitrile)

(ACHN) as a radical initiator, the desired indolenine **1.59** was formed in a 25% yield as a 3:1 mixture of regioisomers. The regioisomeric ratio may be derived from the initial condensation to form imine **1.47,** as the mixture was moved forward crude. Ozonolysis of alkene **1.59**, utilizing a reductive workup, delivered alcohol **1.61** in a 68% yield. Treatment of **1.61** with Lawesson's reagent produced thioimidate **1.62** and subsequent reaction with Raney nickel furnished imine **1.63** in a moderate yield over two steps. The synthesis was completed with the oxidation to the indolenine utilizing iodosobenzene (PhIO), delivering (+)-**1.10** in 15 steps from commercially available **1.51**.

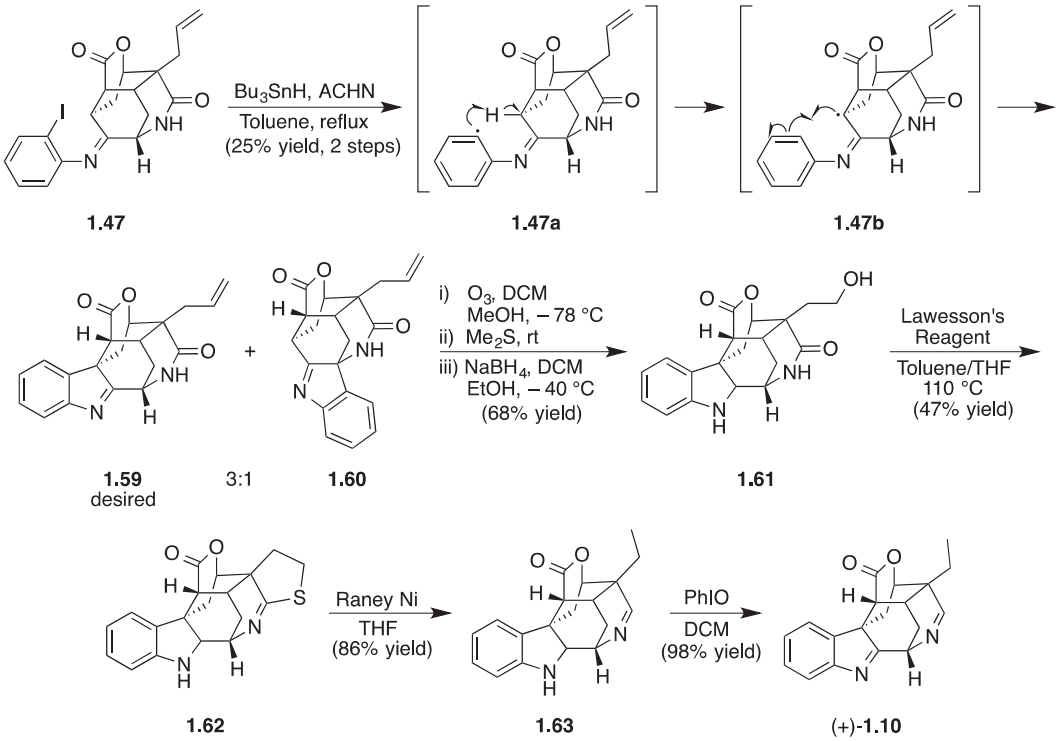

Scheme 1.19 Completion of Snyder's synthesis

1.2.3 Higuchi and Coworkers Model Study

In 2013, Higuchi and coworkers published a model study toward the core of **1.10** wherein an oxidative enolate coupling is employed to create the partial core structure of **1.10**.[18] In a retrosynthetic sense, model substrate **1.64** derives from oxidative coupling of bicyclo[7.3.1]decane **1.65** which, in turn, arises from lactonization of acid **1.66**. Assembly of the requisite eight-membered ring was achieved by a ring-closing metathesis/hydrogenation sequence originating from diene **1.67**. Alcohol **1.67** was generated through an alkyllithium addition to aldehyde **1.68**.

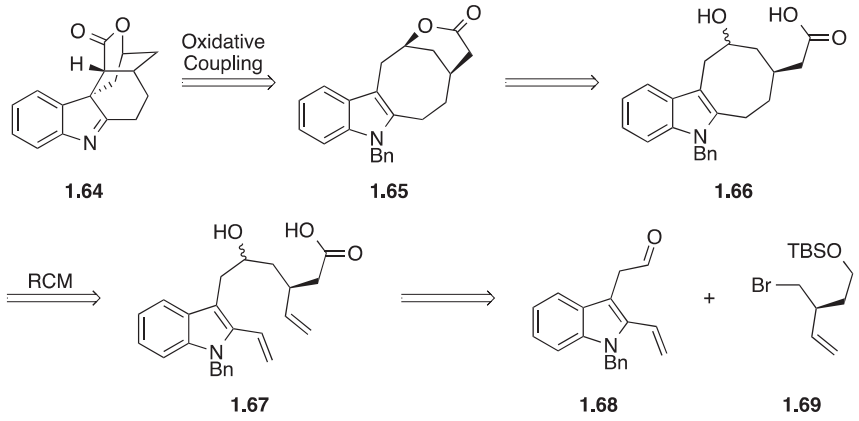

Scheme 1.20 Higuchi's model studies

In the forward sense Higuchi's model study was initiated with the lithiation of alkyl bromide **1.69**, which is produced in six steps from commercially available *cis*-2-butene-1,4-diol **1.70**. The derived alkyllithium was then combined with aldehyde **1.68** (produced from commercially available alcohol **1.72**), to deliver the corresponding secondary alcohol which was then acylated with acetic anhydride to give diene **1.74** in a 56% yield as a 1:1 mixture of diastereomers. Ring closing metathesis of **1.74** followed by hydrogenation of the disubstituted alkene (PtO_2), and silyl deprotection produced

alcohol **1.75** in a 60% yield, over 3 steps. Oxidation to the carboxylic acid, silver mediated acetate hydrolysis, and benzyl deprotection under dissolving metal reduction conditions furnished indole **1.77**. At this point the *cis* and *trans* diastereomers were separated and *cis*-**1.77** was lactonized, by formation of the mixed anhydride with Ac_2O, to deliver lactone **1.65**. To complete the model study lactone **1.65** was treated with lithium bis(trimethylsilyl)amide (LiHMDS) using NIS as an oxidant to deliver the desired indolenine **1.64**, which contains the ABCE ring system of **1.10**.

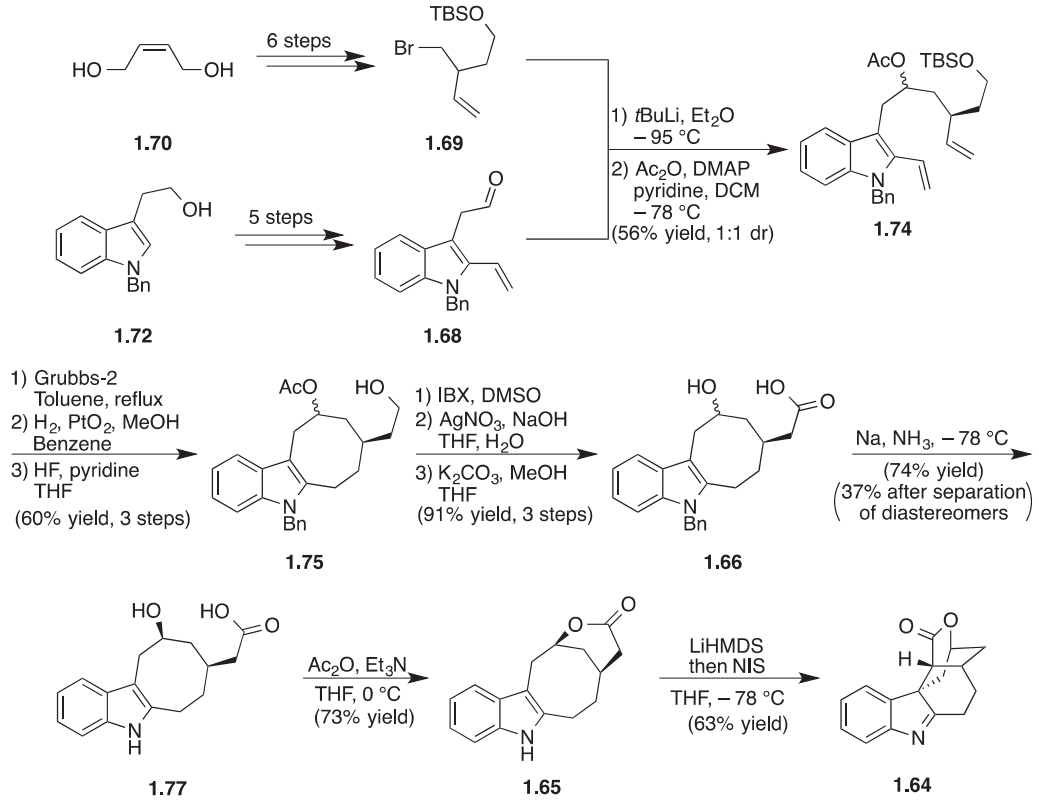

Scheme 1.21 Completion of Higuchi's model study

1.3 Conclusion

Due to their interesting and complex structures, the akuammiline alkaloids have garnered considerable attention from the synthetic community. Scholarisine A (**1.10**) is

no exception and since its isolation in 2008, has been the focus of two total synthesis efforts (Smith and Snyder) as well as several model system studies. The first total synthesis, by Smith and coworkers, not only confirmed the structure and absolute stereochemistry of **1.10** but also featured an interesting one-pot reductive cyclization process that provides access to complex core architecture of scholarisine. In contrast, Snyder and coworkers developed a novel C-H arylation strategy to form the indolenine motif. The dramatic differences taken in these two approaches serve to illustrate how the complex core architectures found in many natural products can serve as inspirational challenges to synthetic chemists and lead to the development of both new chemical methods and strategies that can serve to improve our ability to access important molecules. Importantly these completed syntheses represent only two of many approaches one can envision employing to access scholarisine A and other interesting members of this large and growing family of alkaloids. Our efforts in this latter regard will be detailed in the subsequent chapters of this thesis.

1.4 References

[1] Cai, X.-H.; Tan, Q.-G.; Liu, Y.-P., Feng, T.; Du, Z.-Z.; Li, W.-Q.; Luo, X.-D. *Org. Lett.* **2008**, *10*, 577.

[2] Feng, T.; Cai, X.-H.; Zhao, P.-H.; Du, Z.-Z.; Li, W.-Q.; Luo, X.-D. *Planta Med.* **2009**, *75*, 1537.

[3] (a) Shang, J.-H.; Cai, X.-H.; Zhao, Y.-L.; Feng, T.; Luo, X.-D. *J. Ethnopharmacol*. **2010**, *129*, 293. (b) Shang, J.-H.; Cai, X.-H.; Feng, T.; Zhao, Y.-L.; Wang, J.-K.; Zhang, L.-Y.; Yan, M.; Luo, X.-D. *J. Ethnopharmacol.* **2010**, *129*, 174.

[4] Adams, G. L.; Carroll, P. J.; Smith, A. B., III. *J. Am. Chem. Soc.* **2012**, *134*, 4037.

[5] Wenkert, E.; Wickberg, B. *J. Am. Chem. Soc.* **1965**, *87*, 1580.

[6] For a brief review of akuammilline alkaloids. (a) Adams, G. L.; Carroll, P. J.; Smith, A. B., III. *J. Am Chem. Soc.* **2013**, *135*, 519. (b) Llopart, C. C.; Joule, J. A. *Arkivoc* **2004**, (*x*), 20.

[7] (a) Stöckigt, J.; Zenk, M. H. *FEBS Lett.* **1977**, *79*, 233. (b) Mahroug, S.; Burlat, V. *Phytochem. Rev.* **2007**, *6*, 363. (c) Courdavault, V.; Burlat, V.; St-Pierre, B.; Giglioli-Guivarc'h, N. *Plant Cell Rep.* **2009**, *28*, 83. (d) Guirimand, G.; Guihur, A.; Ginis, O.; Poutrain, P.; Héricourt, F.; Oudin, A.; Lanoue, A.; St-Pierre, B.; Burlat, V.; Courdavault, V. *FEBS Journal* **2011**, *278*, 749.

[8] (a) Rapoport, H.; Onak, T. P.; Hughes, N. A.; Reinecke, M. G. *J. Am. Chem. Soc.* **1958**, *80*, 1601. (b) Cardoso, C. L.; Silva, D. H. S.; Tomazela, D. M.; Verli, H.; young, M. C. M.; Furlan, M.; Eberlin, M. N.; da Silva Bolani, V. *J. Nat. Prod.* **2003**, *66*, 1017.

[9] a) Ahmad, Y.; Fatima, K.; Le Quesne, P. W.; Atta-Ur-Rahman *Phytochemistry* **1983**, *22*, 1017.

[10] Henry, T. A. *J. Chem. Soc.* **1932**, 2759.

[11] Britten, A. Z.; Smith, G. F. *J. Chem. Soc.* **1963**, 3850.

[12] (a) Schnoes, H. K.; Biemann, K.; Mokry, H. K.; Kompis, I.; Chatterjee, A.; Ganguli, G. *J. Org. Chem.* **1966**, *31*, 1641. (b) Ahmad, Y.; Fatima, K.; Rahman, A.-U.; Occolowitz, J. L.; Solheim, B. A.; Clardy, J.; Garnick, R. L.; Le Quesne, P. W. *J. Am. Chem. Soc.* **1977**, *99*, 1943.

[13] (a) Chatterjee, A.; Mukherjee, B.; Ray, A. B.; Das, B. *Tet. Lett.* **1965**, *6*, 3633. (b) Ghosh, R.; Roychowdhury, P.; Chattopadhyay, D. Iitaka, Y. *Acta Crys., Sect. C: Cryst. Struct. Commun.* **1988**, *44*, 2151. (c) Smith, J. M.; Moreno, J.; Boal, B. W.; Garg, N. K. *J. Am. Chem. Soc.* **2014**, *136*, 4504.

[14] (a) Subramanium, G.; Hiraku, O.; Hayashi, M.; Koyano, T.; Komiyama, K.; Kam, T.-S. *J. Nat. Prod.* **2007**, *70*, 1783. (b) Zu, L.; Boal, B. W.; Garg, N. K. **2011**, *133*, 8877.

[15] Cai, X.-H., Du, Z.-Z.; Luo, X.-D. *Org. Lett.* **2007**, *9*, 1817.

[16] For an excellent review of the biosynthesis and total synthesis of several akuammiline alkaloids see: Smith, J. M.; Moreno, J.; Boal, B. W.; Garg, N. K. *Angew. Chem. Int. Ed.* **2014**, *53*, 2.

[17] Smith, M. W.; Snyder, S. A. *J. Am. Chem. Soc.* **2013**, *135*, 12964.

[18] Watanabe, T.; Kato N, Umezawa, N.; Higuchi, T. *Chem. Eur. J.*, **2013**, *19*, 4255.

CHAPTER TWO

Studies Toward the Total Synthesis of Scholarisine A

2.1 A Retrosynthetic Analysis

2.1.1 A Novel Disconnect

The complex core architecture of scholarisine A (**2.10**) has made it an inspiring target for both total synthesis and methods development. Smith and coworkers utilized a reductive cyclization strategy and Fischer indole synthesis to generate the core structure of **2.10**.[1] In contrast, Snyder and coworkers developed an approach to the tetracyclic core of **2.10** that employed a Diels-Alder, radical cyclization, and lactamization sequence. To complete the synthesis, Snyder developed a novel C-H arylation strategy to install the indolenine motif (Scheme 2.10).[2]

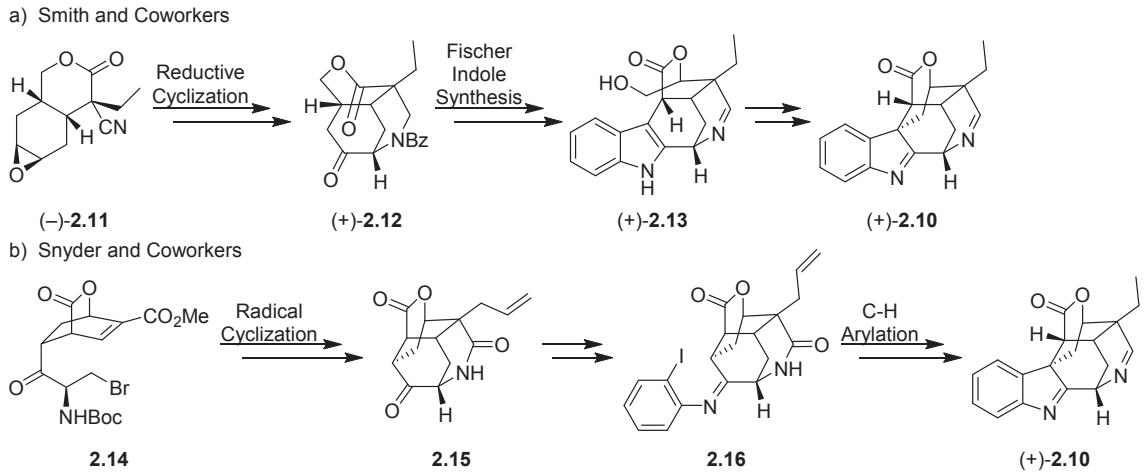

Scheme 2.10 Comparison of completed syntheses

Prior to the published reports from the Smith and Snyder groups we too had been inspired by scholarisine A in terms of the challenges it presents for total synthesis and began thinking about possible approaches. Having completed syntheses of the isonitrile containing natural products welwitindolinone A and kalihinol C we became intrigued with the possibility of using this functional group as an intermediate to nitrogen heterocycles. Moreover, Baran's recently reported syntheses of (+)-ambiguine (**2.19**) and cortistatin (Scheme 2.11) wherein activation of isonitrile-containing intermediates with chloronium ion or copper initiates intramolecular attack by a pendent nucleophile (olefin or hydroxyl, respectively) to furnish cyclized synthetic intermediates (see **2.17** to **2.19** and **2.20** to **2.22**, Scheme 2.11) served to further pique our interest in the potential of isonitrile chemistry. [3,4]

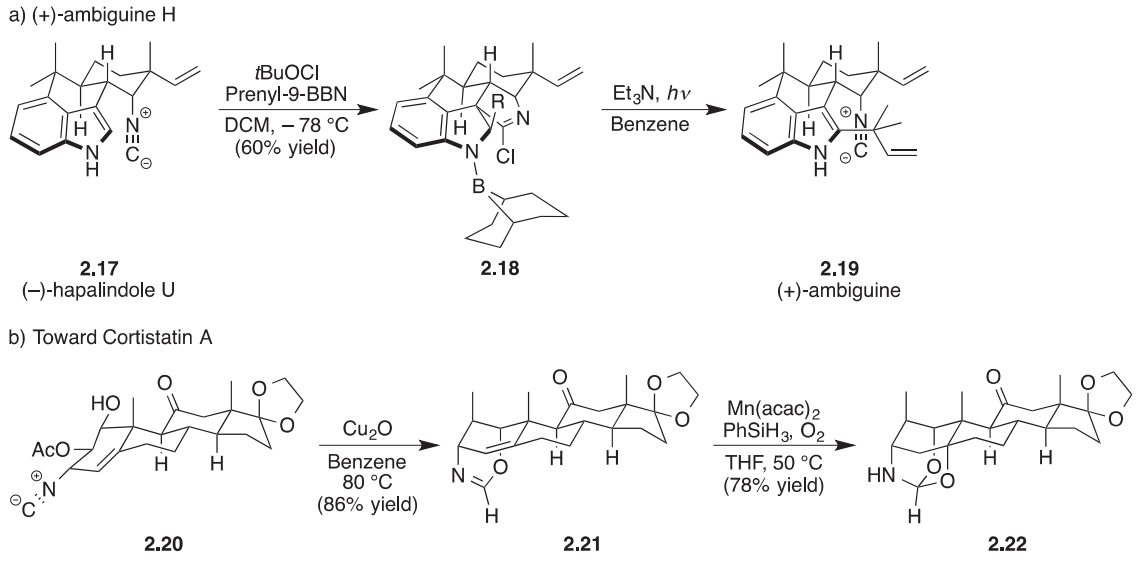

Scheme 2.11 Baran's isonitrile activation methods

The combination of literature precedent and experience within the Wood Group led us to envision an approach to scholarisine A which, in a retrosynthetic sense (Scheme

2.12.), involves disconnection adjacent to the cyclic imine of **2.10** to furnish an intermediate isonitrile (**2.23)**. In the forward sense, activation of the isonitrile and olefin addition would furnish a secondary carbocation that could be trapped intramolecularly with a pendant ester to deliver the lactone and E-ring of **2.10** in one synthetic step. Isonitrile **2.23** was further envisioned to derive from a substituted indole such as **2.24**.

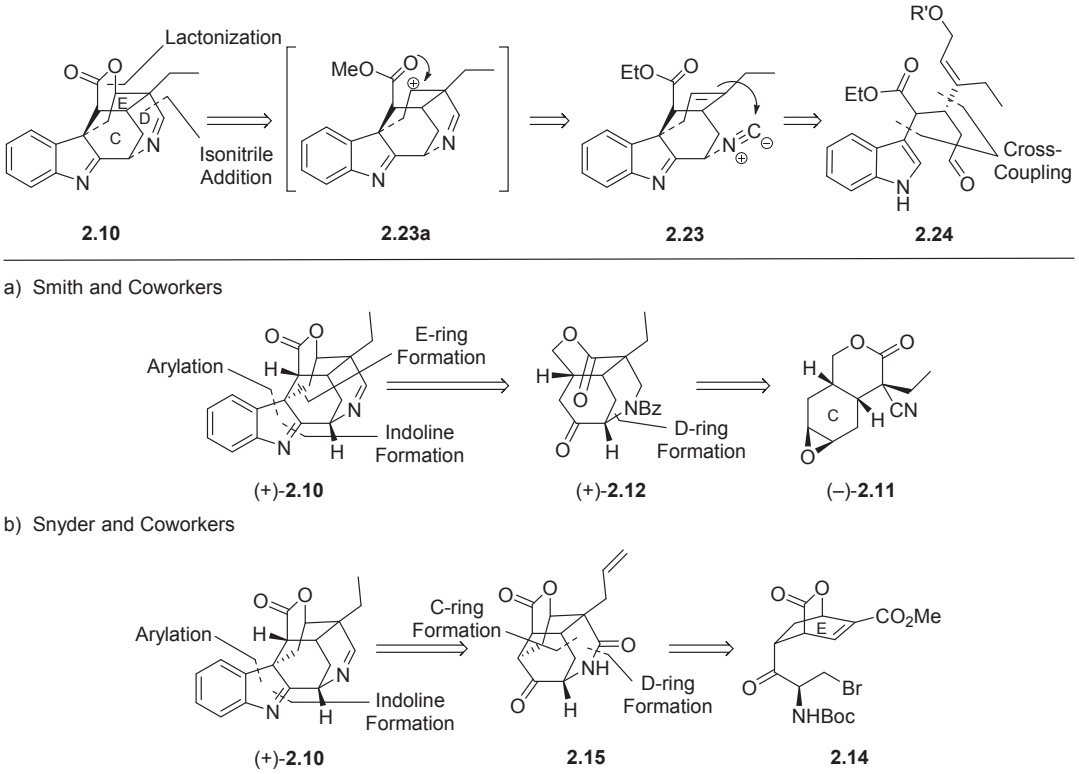

Scheme 2.12 Comparison of approaches

Our overall retrosynthetic plan would allow the access of **2.10**, in a method that is orthogonal to previously completed syntheses. The previous syntheses by Snyder and Smith both utilized a similar overall synthetic strategy. In each synthesis the core structure (C, D, and E rings) of **2.10** was constructed before the installation of the indole/indoline ring system. Such a strategy offers an element of convergency, but we

believed it neglected the indole motifs potential as a functional handle. Our strategy, consisting of the sequential formation of the D and E-rings would allow the incorporation of the indole early and subsequently allow us to harness its innate reactivity to construct the polycyclic architecture of **2.10**.

2.1.2 Retrosynthetic Analysis

Having become intrigued by the reaction cascade illustrated in Scheme 2.12, we began considering approaches toward the requisite substrate **2.23** (Scheme 2.13). To this end, isonitrile **2.23** was envisioned to derive from amine **2.25**, through a formylation/dehydration sequence. The requisite indolenine (**2.25**) would arise from **2.26** via intramolecular allylation of an intermediate Pd-π-allyl complex. Indole **2.26** was seen as accessible from an intramolecular Mannich reaction of aldehyde **2.24** which, in turn, would be produced via conjugate addition of a vinyl nucleophile to α,β-unsaturated ester **2.27**.

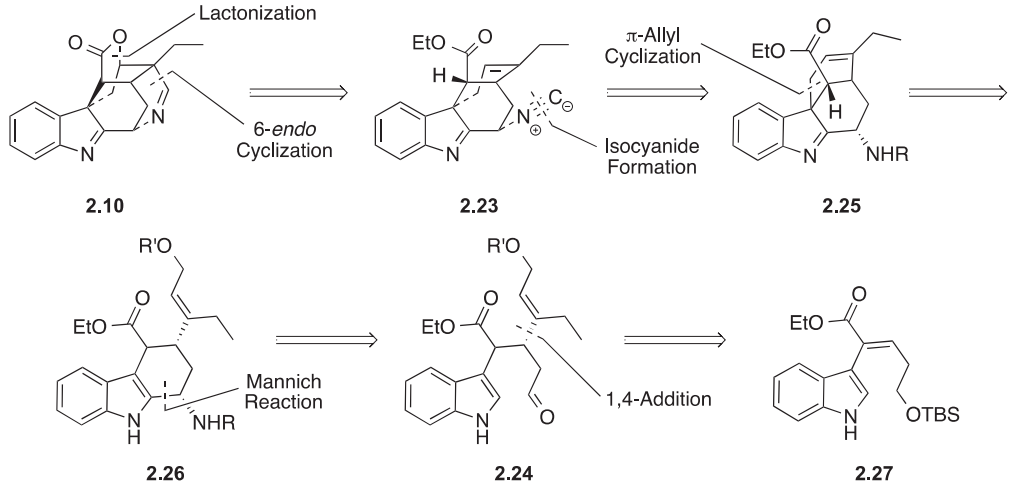

Scheme 2.13 Our retrosynthetic analysis of **2.10**

After developing a retrosynthetic plan, one often steps back and assesses feasibility. In this latter regard there are clearly some issues one would need to consider in the approach illustrated in Scheme 2.13. For example, there is very little precedence in the literature for the Mannich reaction we hope to use in preparing **2.26** and ones ability to effectively control the stereochemical outcome in the preparation of **2.24** is difficult to predict. Although these concerns seem discouraging, in fact they are relatively minor and addressing them would likely serve as opportunities to explore new chemistry. However, with regard to the overall synthesis, efforts to develop the early stages of this route would be wasted if the key transformation from **2.23** to **2.10** proves unworkable.[5] Thus, rather than focus on the early steps our early investigations were devoted to assessing the feasibility of the key transformation, the conversion of **2.23** to **2.10**.

As eluded to above, we were well aware of the fact that nucleophilic additions into activated isonitriles are precedented in literature reports and some specific examples include: a) activation by electrophilic halogen sources, such has hypochlorites or elemental bromine, followed by *in situ* addition of alcohols to generate imidates or thio imidates (Scheme 2.14a and bi) and;[6] b) activation by acyl electrophiles followed by intramolecular electrophilic aromatic substitution to produce dihydroisquinolines (Scheme 2.14bii).[7]

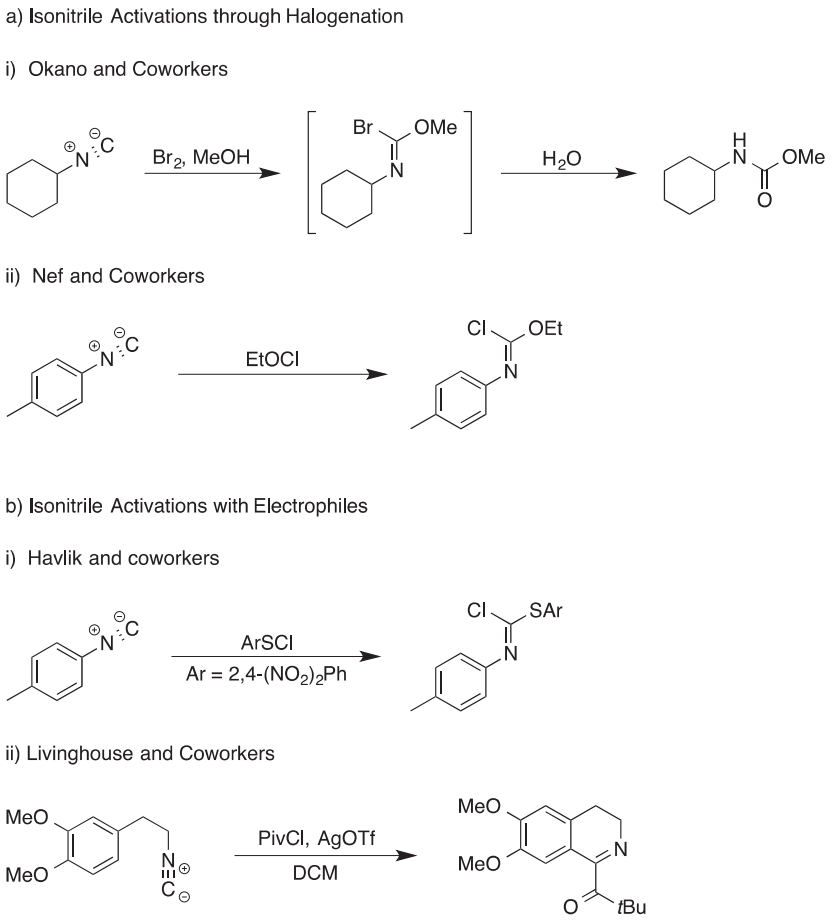

Scheme 2.14 Isonitrile activations

Activation of isonitriles with metals is also known (Scheme 2.15). For example, Saegusa and coworkers have demonstrated that copper catalysts can promote the addition of amines, alcohols, thiols, and silanes into isocyanides. They also reported the use of isonitriles, activated by a copper catalyst, as substrates in cycloaddition reactions with electron deficient alkenes to form pyrrolines (Scheme 2.15b).[8] To our knowledge, these are the earliest reports describing the metal activation of isonitriles.[10b]

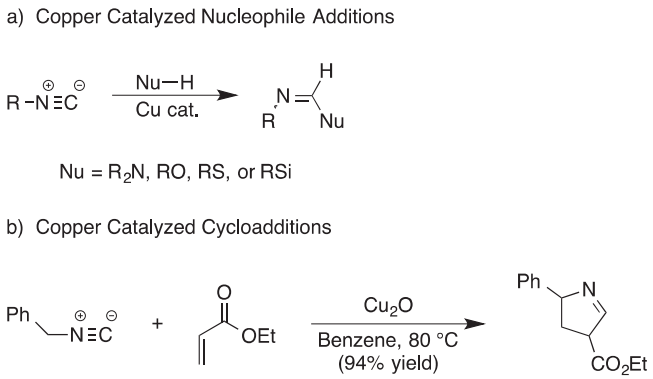

Scheme 2.15 Isonitrile activation by copper

The use of activated isonitriles as electrophiles in reactions with alkenes has been further studied by Livinghouse and coworkers, using their *in situ* generated acyl nitrilium chemistry (Scheme 2.16).[9] In contrast to Saegusa's cycloaddition chemistry, which employs electron deficient alkenes, Livinghouse has studied electron rich and neutral alkenes and demonstrated that aromatics,[10c] silyl enol ethers,[10a] and allyl silanes[10b] make excellent nucleophiles for the formation of cyclic imines from nitrilium species (Scheme 2.16a-c). Livinghouse also demonstrated the utility of this chemistry in extended systems to form fused ring system. As illustrated in Scheme 2.16c, appropriately functionalized disubstituted alkenes will react with acyl nitrilium ions to furnish intermediate carbocations that can be trapped intramolecularly via Friedel-Crafts reaction. In addition to the intramolecular trapping of the intermediate carbocation, Livinghouse and coworkers have employed external nucleophiles. As shown in Scheme 2.16d, the cyclization of an unactivated olefin with an acyl nitirlium was followed by successful intermolecular trapping of the carbocation with water, albeit in a 33% yield.

The precedent established by Livinghouse and coworkers for olefin addition across the π-system of an isonitrile provides excellent precedent for our proposed cascade

cycloaddition to form **2.10**. However, their use of an acyl activating group was viewed as undesirable given the potential difficulty of amide hydrolysis following cyclization. Therefore, we sought an alternative mode of activation that would lead to a more malleable intermediate. Precedent for this exists (e.g., **2.20** to **2.21** in Scheme 2.11), but has not been studied using unactivated alkenes as nucleophiles. Given that were now proposing a late stage cascade cyclization that was based on tangential precedent and thus of questionable feasibility for our synthesis, we decided to develop a model substrate to test the reactivity.

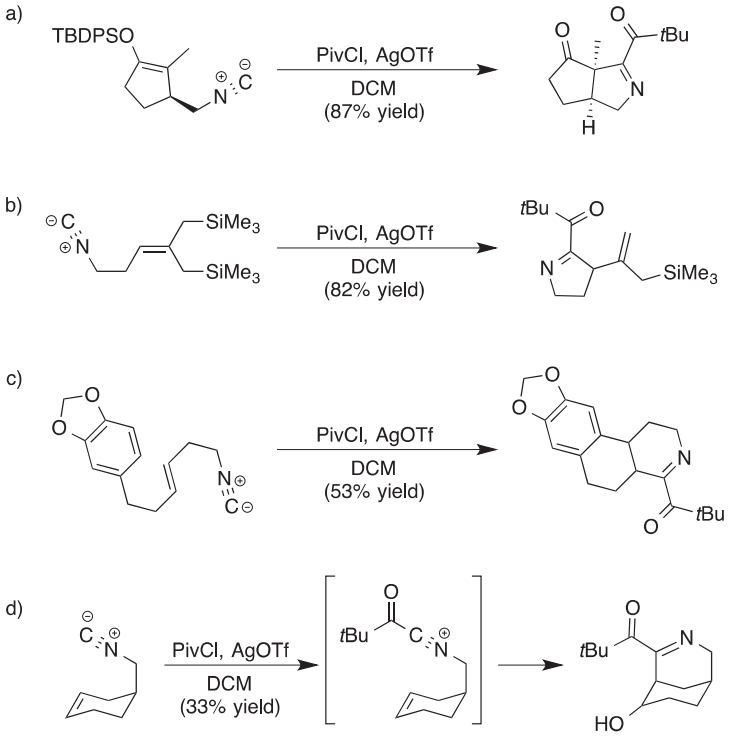

Scheme 2.16 Livinghouse's isonitrile activation methods

2.2 Developing a Model System

2.2.1 Retrosynthetic Analysis

With a lack of literature precedent for our desired late stage isonitrile cascade cyclization to form **2.10**, we decided to test the reactivity on a model substrate that could be accessed quickly. A proper model substrate would need to contain an ester, olefin, and isonitrile poised to undergo an analogous cascade process. To this end, we decided upon norbornene **2.28** (Scheme 2.17) as a suitable substrate since it not only contains the necessary functional groups but also was envisioned to be readily accessible. In the cyclization events, activation of the isocyanate moiety with concomitant 6-*endo-dig* cyclization would form a 6-membered cyclic imine in both model (**2.28a**) and desired (**2.23a**) substrates. Also, in both cases an ester would be used to trap the resultant secondary carbocation. However, these substrates differ in that **2.10** contains a bicyclo[2.2.2]octane motif, while the model **2.29** contains a bicyclo[2.2.1]heptane.

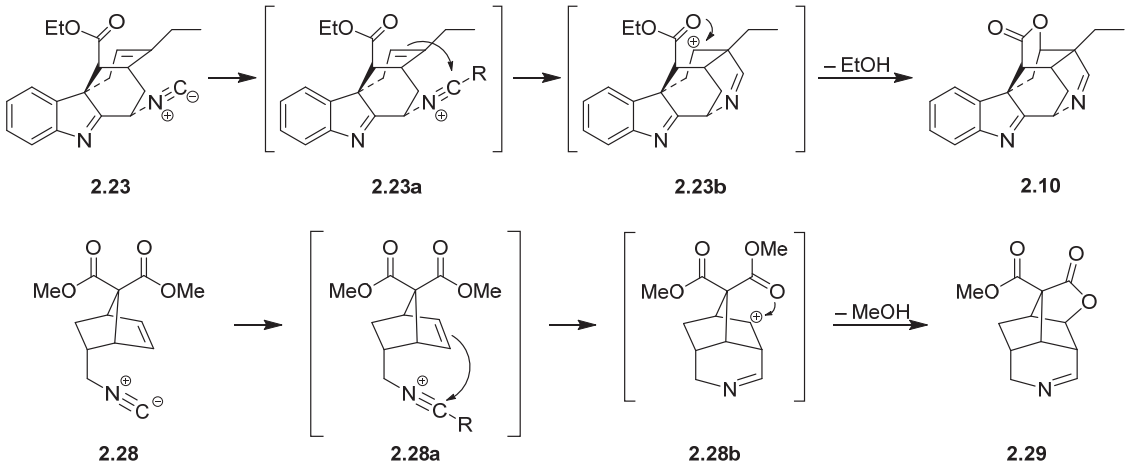

Scheme 2.17 Model system comparison

A retrosynthetic analysis for model substrate **2.29** is shown in Scheme 2.18. The envisioned cascade cyclization would develop through activation of the isonitrile **2.28**. The isonitrile itself would originate from aldehyde **2.30** through a reductive amination/formylation/dehydration sequence. Aldehyde **2.30** was seen as arising from a Diels-Alder reaction with acrolein and diene **2.31**. The diene could be obtained from known cyclopentene **2.32** through a bromination/elimination sequence.

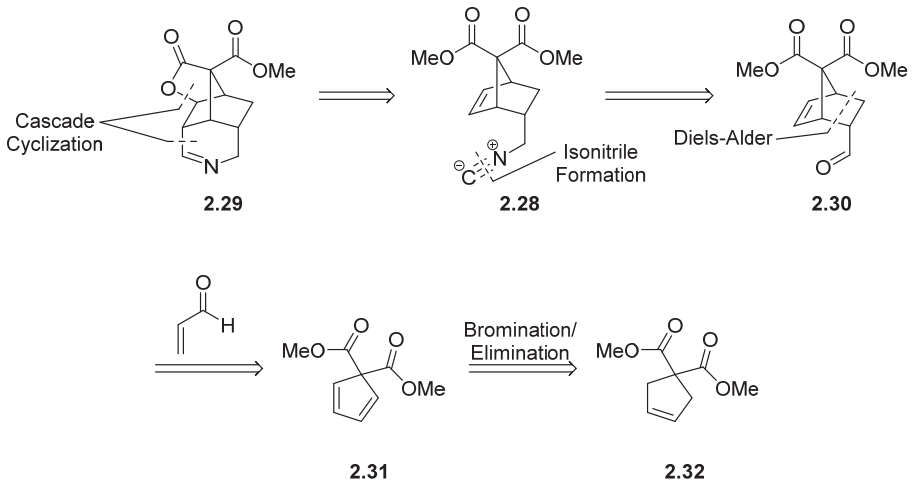

Scheme 2.18 Model retrosynthetic analysis

2.2.2 Cascade Cyclization Model Studies

We began our approach to isonitrile **2.28** by reacting commercially available *cis*-1,4-dichloro-2-butene **2.33** with dimethyl malonate in the presence of lithium hydride (LiH) and DMPU at 45 °C. Under these conditions the known cyclopentene (**2.32**) was produced in a 73% yield following chromatographic purification (Scheme 2.19).[10] Exposure of **2.32** to Br_2 produced a 95% yield of dibromide **2.34**, that when treated with potassium bis(trimethylsilyl)amide (KHMDS) furnished cyclopentadiene **2.31**. Heating the crude diene **2.31** with acrolein formed the desired norbornene **2.30** as a single

diastereomer, which was subsequently assigned as the illustrated *endo* product.[11] The aldehyde was subjected to sodium borohydride ($NaBH_4$) to produce alcohol **2.35**. At this point the *endo* stereochemistry was confirmed by exposure of alcohol **2.35** to bromoetherfication conditions, which produced cyclic ether **2.36**.

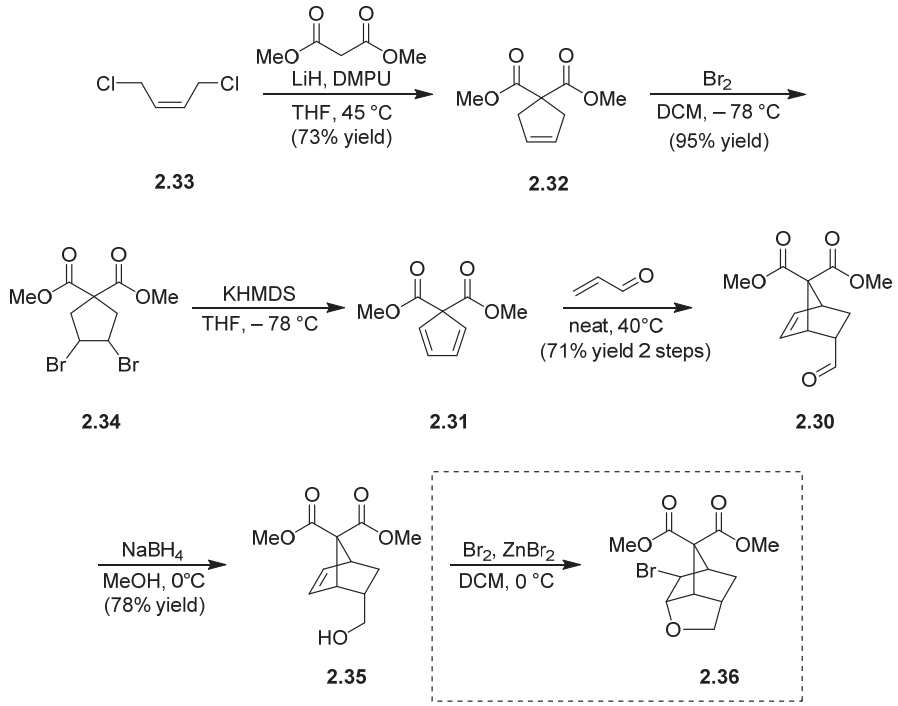

Scheme 2.19 Norbornene formation

Having determined that alcohol **2.35** possessed our desired stereochemistry, we sought to convert it to the necessary isonitrile (Scheme 2.20). This was done through a two step amination sequence beginning with a Mitsunobu reaction of alcohol **2.35** and diphenylphosphoryl azide (DPPA), which was then subjected to a Staudinger reduction to deliver amine **2.37** in an 82% yield over 2 steps.[12] To complete the synthesis, amine **2.37** was reacted with formic acetic anhydride to deliver the formamide.[13] Dehydration of the

formamide with phosphorous oxychloride ($POCl_3$) in the presence of Et_3N gave desired isocyanide **2.28** in good yield over two steps.[14]

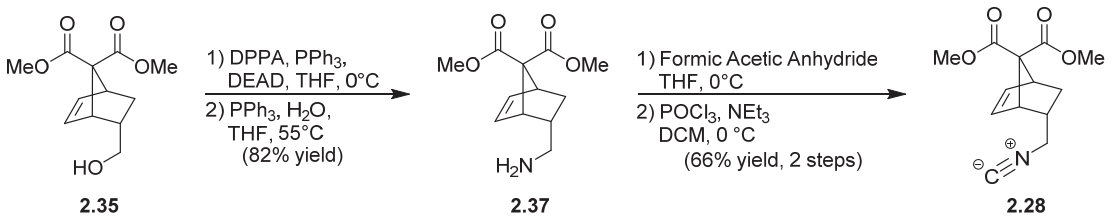

Scheme 2.20 Isonitrile formation

With isonitrile **2.28** in hand, we could attempt the desired cascade cyclization sequence. In preliminary studies we simply employed the conditions developed by Livinghouse and, as illustrated in Scheme 2.21a, the first experiment was done in the absence of silver(I) triflate (AgOTf) so as to explore the ability of pivaloyl chloride (PivCl) to activate the isonitrile.[11d] Upon an aqueous workup, ketone **2.38** was obtained indicating that isonitrile **2.28** was indeed being activated by the acyl chloride (Scheme 2.21a). With these promising results, isonitrile **2.28** was again subjected to the Livinghouse conditions; however, this time AgOTf was added after a 24-hour period. To our delight, tricycle **2.39** was obtained in a 34% yield and the structure was confirmed by X-ray crystallography. Although the pendent acyl moiety does not exist in the natural product and expanding our investigations to include traceless or cleavable isonitrile activation was required, we could pursue these studies knowing that the substrate is capable of undergoing the cascade cyclization.

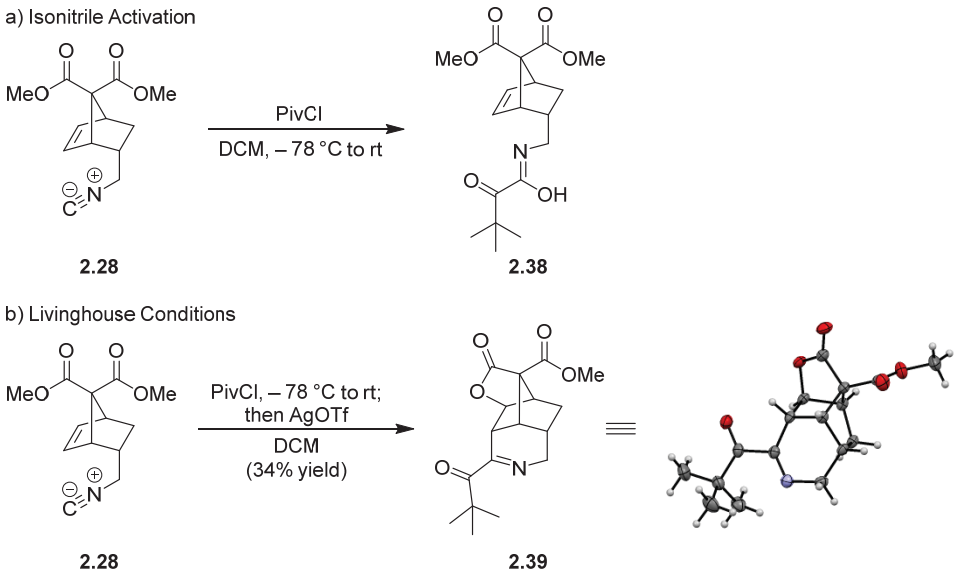

Scheme 2.21 Cascade cyclization

In considering possibilities for incorporating a traceless or removable activating group it is worthwhile to consider the possible mechanistic course of the cascade cyclization. In this regard we believe that **2.28** arises via a mechanism consistent with that proposed by Livinghouse and coworkers (Scheme 2.22).[11] Thus, nucleophilic addition of isocyanide **2.28** to pivaloyl chloride creates an intermediate acyl nitrilium (e.g. **2.41**) which undergoes nucleophilic attack by a tight ion-paired chloride to furnish imine **2.40**. The addition of silver triflate sequesters the chloride, forcing the reformation of the free acyl nitrilium ion (**2.41**), which then undergoes addition by the adjacent olefin in a 6-*endo*-*dig* fashion to generate carbocation **2.42**. Trapping of the intermediate carbocation by the ester oxygen would furnish an oxocarbenium ion that upon aqueous workup produces a transient ortho acid that loses methanol to produce lactone **2.39**.

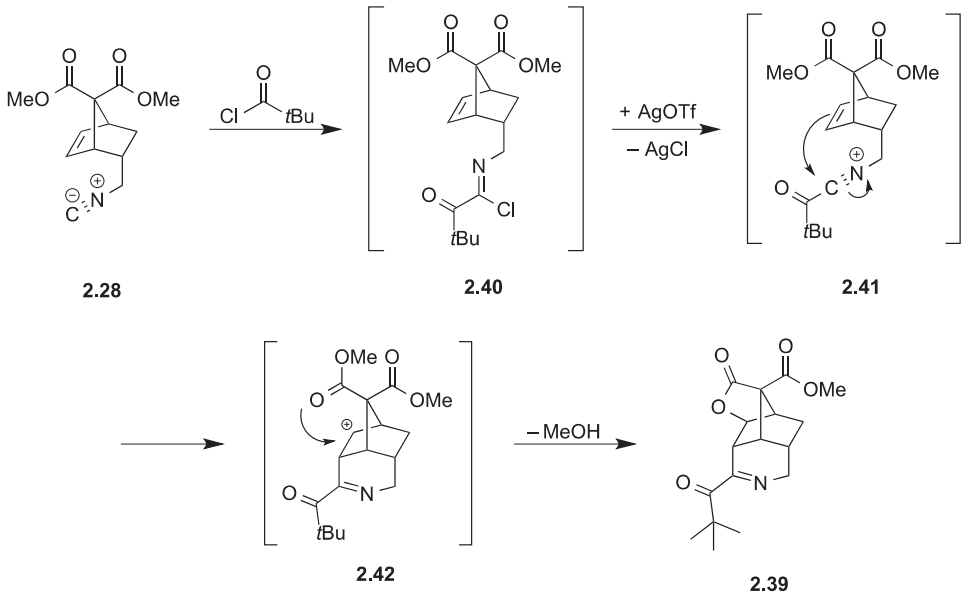

Scheme 2.22 Proposed mechanism for the cascade cyclization

Having established that the model substrate is capable of undergoing the desired 6-*endo*-*dig* cyclization, we attempted various modes of isonitrile activation. As illustrated in Table 2.10, our studies included the use of reagents that have been shown previously to activate isonitriles toward nucleophilic additions (Table 2.10, entries 1-4). To our great frustration, the Livinghouse conditions employed in our initial investigations were the only activating agents that delivered our desired cycloaddition product! Halogenating agents, such as *tert*-butyl hypochlorite, *N*-chlorosuccinimide, and iodine returned only the unreacted isonitrile **2.28**. Using transition metals known to activate isonitriles (Cu_2O and $GaCl_3$) and exposure to Lewis or Brønsted acids such as TMSCl, $Zn(OTf)_2$ or trifluoroacetic acid (TFAA) and methanesulfonic acid (MsOH) all failed to furnish any cyclized product. Attempts to activate the isonitrile with π-acidic metals known to activate alkynes, like $Pd(OAc)_2$, AgOTf, or Au(I) salts returned only isonitrile **2.28**.[15]

Table 2.10 Isonitrile activation attempts

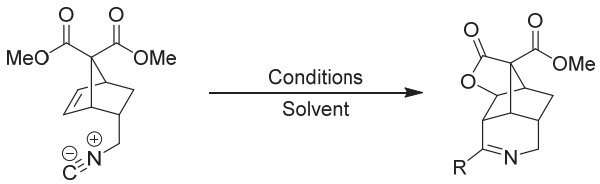

2.28

Entry	Conditions	R	Solvent	Yield
1	PivCl, AgOTf	Piv	DCM	30%
2	tBuOCl, NCS, I_2	Cl or I	DCM, Benzene	0%
3	TMSCl	TMS	DCM	0%
4	Cu_2O	H	Benzene	0%
5	TFAA, MsOH	H	DCM	0%
6	AgOTf, Au(I)	H	DCM	0%
7	$GaCl_3$, $Zn(OTf)_2$	H	Toluene, THF	0%
8	$Pd(OAc)_2$	H	THF	0%
9	AIBN, $HSnBu_3$	$SnBu_3$	Benzene	0%

In an effort to circumvent the requisite acyl activation, we began to pursue an alternative activation method, where activation of the olefin of **2.28** with bromine in hopes of nucleophilic opening of the bromonium intermediate with the isonitrile also proved to be futile. Livinghouse and coworkers had also investigated acyl electrophiles that would have been more amenable to hydrolysis. In these studies the Livinghouse group attempted to replace pivaloyl chloride with methyl chloroformate; however, under these conditions no nucleophilic addition of the isocyanide was ever seen, even when using the chloroformate as the solvent.[9] In light of this information, and combined with our discouraging attempts at alternative activation conditions, we began to rethink our desired end game strategy toward **2.10**.

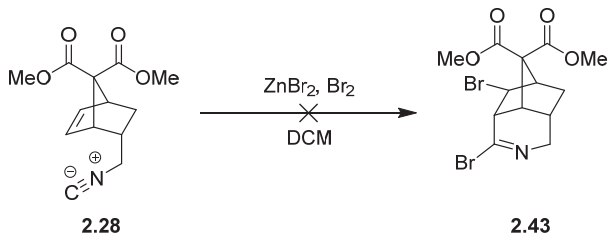

Scheme 2.23 Alternate cyclization attempts

In considering the studies done thus far as well as possible alternatives we were left unconvinced that the cascade reaction would not work and began to wonder if the model system had not adequately represented the desired cyclization precursor **2.23** (*vide supra,* Scheme 2.17). In the natural product **2.10** a bicyclo[2.2.2]octane would form upon lactonization, while in the model system a bicyclo[2.2.1]heptane ring is formed. In considering this difference we became concerned that perhaps the excess ring strain required to make the lactone in the model system was preventing the reaction from being driven forward. With this in mind, and a desire to further investigate the desired cascade cyclization in the real system, we decide to continue efforts toward the synthesis of scholarisine A (**2.10**).

2.3 Synthetic Studies Toward Scholarisine A

2.3.1 1,4-Addition Route

In accord with the synthetic plan outlined above (Scheme 2.13) our synthetic efforts toward the total synthesis of **2.10** began with investigations into the initial conjugate addition of enoate **2.27**. In contrast to the known syntheses of **2.10**, our plan called for incorporation of the indole from the beginning. Thus, for our initial step we

envisioned preparing enoate **2.27** via a Stille coupling between known stannane **2.44** and vinyl iodide **2.45**.

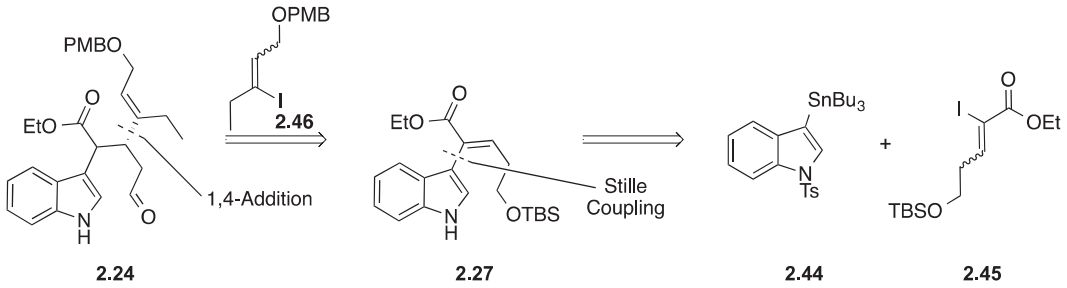

Scheme 2.24 1,4-Addition route

Indole stannane **2.44** was derived from indole (**2.47**) via a known procedure that involves the reaction with iodine and tosyl chloride in the presence of potassium hydroxide (KOH) to initially furnish iodide **2.48** (Scheme 2.25).[16] Exposure of **2.48** to magnesium-iodide exchange conditions and subsequently treating with tributyltin chloride (Bu_3SnCl) produces stannane **2.44** in a 66% yield.[17]

With **2.44** in hand, we now turned our attention to the formation of the vinyl iodide. Following a known protocol, 1,3-propanediol was monoprotected with TBSCl and oxidized to aldehyde **2.50** under Swern conditions.[18] Premixing phosphonate **2.51**, iodine, and sodium hydride led to an intermediate α-iodophosphonate, which, upon reaction with aldehyde **2.50**, gave the Horner-Wadsworth-Emmons product **2.45** as a mixture of olefin isomers.[19] Conjugate addition precursor **2.27** was produced through a Stille coupling of stannane **2.44** with iodide **2.45** in the presence of $Pd_2(dba)_3$ and triphenylarsine ($AsPh_3$), isolating the *E* olefin isomer in a 78% yield.[20]

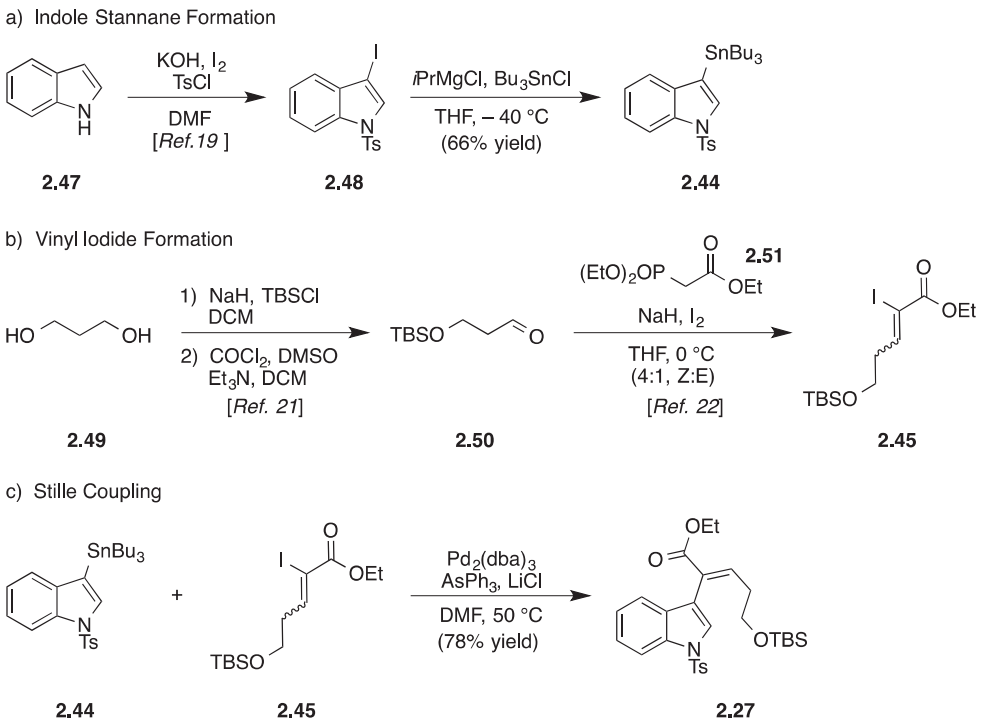

Scheme 2.25 Enoate **2.27** formation

In order to attempt the 1,4-addition on enoate **2.27**, we had to first access vinyl iodide **2.46** (Scheme 2.26). To this end, reduction of commercially available propargyl alcohol (**2.52**) with Red-Al in the presence of iodine produced vinyl iodide **2.53**, which when exposed to the illustrated trichloroacetimidate underwent smooth conversion to the corresponding *para*-methoxybenzyl ether (**2.46**) in a good yield over two steps.[21] Unfortunately, metal halogen exchange of **2.46** to the vinyl cuprate (various conditions) and subsequent exposure to enoate **2.27** did not lead to the desired coupling product **2.54**. Although it was unclear why **2.27** failed to undergo conjugate addition we decided to move forward with a slight variation wherein cross coupling would deliver the desired product (Scheme 2.26c).

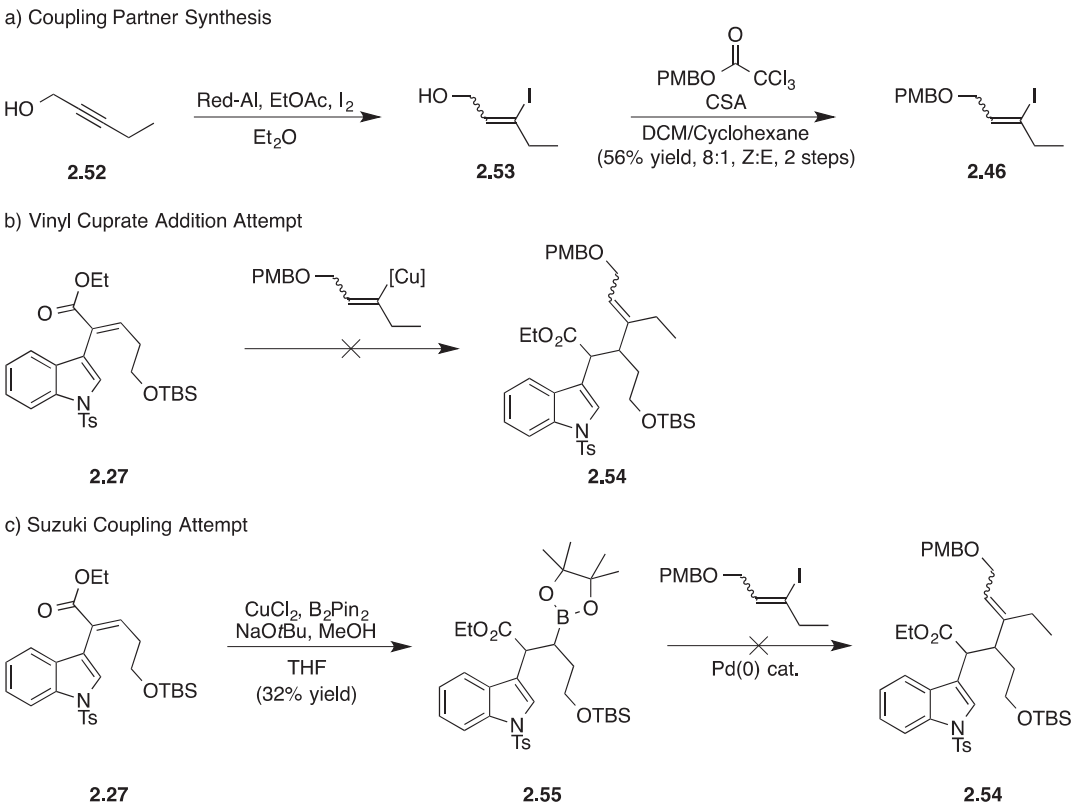

Scheme 2.26 1,4-Addition attempts

In the event, it was found that a copper(I) catalyzed β-boration was effective in delivering the requisite boronic ester (**2.55**), albeit in low yield (32% yield). Unfortunately, attempts to effect the B-alkyl Suzuki reaction under various cross coupling conditions failed to deliver any of the desired coupling product.[22] This was perhaps not too surprising, as sp^3-sp^2 cross-coupling reactions are known to be challenging due to beta-hydride elimination and, in the realm of organoboron nucleophiles for transmetallation, our substrate, which manifests as a B-Pin boronic ester, is among the least reactive. Subsequent, attempts to address this latter issue by converting boronic ester **2.55** to the corresponding (and more reactive) potassium trifluoroborate (KBF_4) also met with failure.[23] At this point, it was necessary to find an alternate pathway to access ester **2.24** (Scheme 2.27).

2.3.2 Ireland-Claisen Rearrangement Route

A possible alternative way of accessing ester **2.24** presented itself, as it contains and γ,δ-unsaturated ester motif, we believed the use of an Ireland-Claisen rearrangement could produce the desired ester (Scheme 2.27). Therefore, ester **2.24** would arrive by enolization of ester **2.57** to form a 1,5-diene (i.e., **2.56**) that would be poised to undergo the desired [3,3]-sigmatropic rearrangement to form a carboxylic acid, which upon esterification would deliver **2.24**.

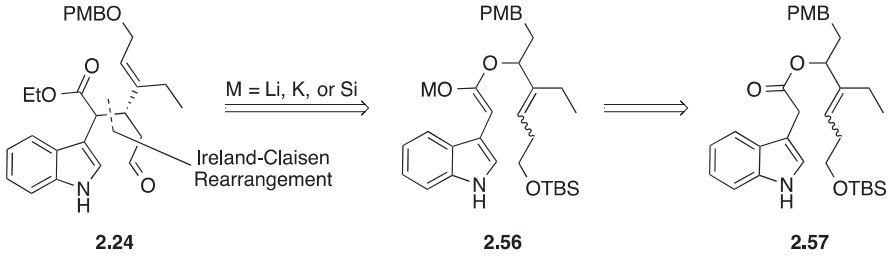

Scheme 2.27 Ireland-Claisen route

Initial efforts to prepare **2.57** are illustrated in Scheme 2.28 and began with commercially available homopropargyl alcohol **2.58** which, upon hydroalumination and subsequent trapping with iodine gave homoallylic alcohol **2.59** as 1:1 mixture of olefin isomers.[24] Silyl protection of **2.59** followed by lithium-halogen exchange with *tert*-butyl lithium produced an intermediate vinyllithium that was reacted with known aldehyde **2.61** to generate alcohol **2.62** as a 1:1 mixture of olefin isomers.[25,26] Unfortunately, initial esterification of **2.63** with alcohol **2.62** proved to be more difficult than anticipated, since only trace product could be isolated. It was clear further optimization would be required to obtain enough material to attempt the Ireland-Claisen rearrangement. Although we had invested a considerable amount of effort in the Scholarisine project, we began to question our ability to efficiently access a suitable isonitrile intermediate for cascade

cyclization, a transformation that was itself proving somewhat dubious; thus, we chose to abandon the Scholarisine project.

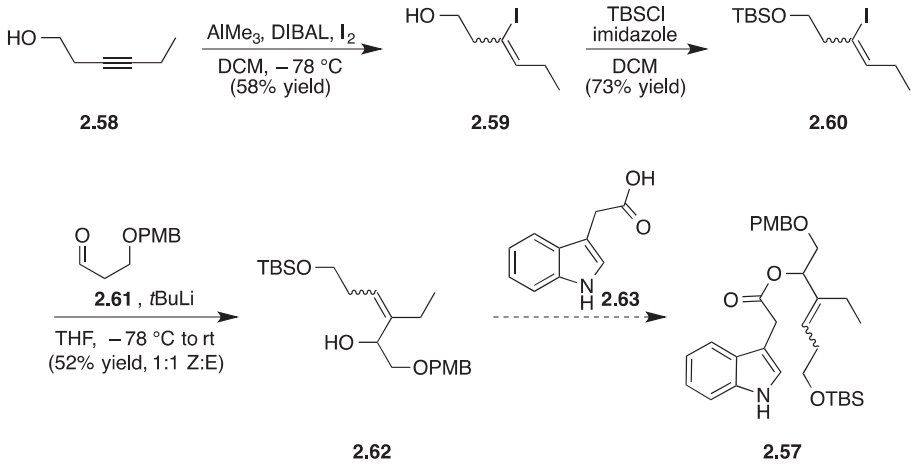

Scheme 2.28 Ireland-Claisen attempts

2.4 Conclusion

In our approach toward the synthesis of scholarisine A (**2.10**), we sought to develop a novel disconnection to set us apart from others who have or are currently working toward the total synthesis. We were inspired by the work of Phil Baran and coworkers who utilized isocyanides as electrophiles for cyclization reactions to form cyclic imines. With regard to scholarisine we envisioned a pendent olefin acting as a nucleophile in the attack of an activated isonitrile. In a cascade event, the derived carbonium ion was seen as undergoing attack by an adjacent ester to deliver the polycyclic imine **2.10**. The feasibility of this proposed cascade cycloaddition was explored in a model system that presented an analogous array of functionality within a similar but not identical carbon framework. Although we were delighted to find that the model substrate was capable of undergoing the desired cyclization process, it occurred in low yield and only when using an acyl group as an activating agent. Unfortunately the

acylated intermediate that is produced under these conditions is not suited as an intermediate en route to **2.10**. Attempts to find a traceless or cleavable activating agent failed.

While the model system did establish that the desired bond connectivity could be produced by this approach, it did not fully mimic the system presented by **2.10** and thus the lack of desired reactivity was put aside in hopes of preparing a fully functionalized substrate. With this in mind we initiated studies to prepare an intermediate that could be advanced to the natural product. However, despite promising early results using an Ireland-Claisen rearrangement, our efforts to access an advanced isonitrile-containing intermediate met with only limited success and concerns regarding overall efficiency led us to eventually abandon the scholarisine A effort.

2.5 Experimentals

General

Unless stated otherwise, all reactions were performed using flame or oven-dried glassware and under an atmosphere of nitrogen. DCM, THF, diethyl ether, benzene, and toluene were dried using a solvent purification system manufactured by SG Water U.S.A., LLC. Acetonitrile, ethyl acetate, pentanes, hexanes, DMF, DMSO, and DCE were supplied by either Fisher Scientific or Sigma-Aldrich and were used as received. Triethylamine, diisopropylamine, and methanol were stirred over calcium hydride and distilled before use. All other commercially available reagents were used as received.

Unless stated otherwise, reactions were monitored by thin-layer chromatography using Silicycle SiliaPlate® TLC glass backed extra hard layer, 60 Å (F-254 indicator,

250 μm thickness). All purifications were performed using Silicyle SiliaFlash® P60 silica (40-63 μm, 230-400 mesh) as a stationary phase. High-resolution mass spectroscopy was performed by the central instrument facility at Colorado State University or on a Thermo Orbitrap ESI mass spectrometer at Baylor University. Single-crystal X-ray crystallography was performed by Brian Newell at Colorado State University or Prof. Caleb Martin at Baylor University. ^{1}H and ^{13}C-NMR spectra were taken on Varian VNMRS 500, Varian Inova 400, Bruker Ascend 400, and Bruker Ascend 600 cryoprobe spectrometers. Infrared spectra were taken on a Nicolet Avatar 320 FTIR or Bruker Alpha Platinum ATR. Chemical Shifts (δ) are reported in parts per million (ppm) and coupling constants (*J*) are reported in hertz (Hz). The reported chemical shifts are relative to the residual solvent peaks of the indicated deuterated solvents.

Preparation of Cyclopentene **2.32**[12]

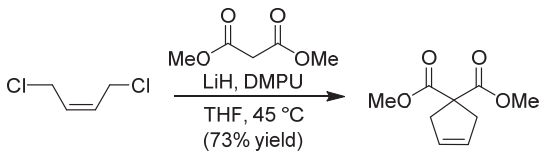

2.33 **2.32**

To a round bottom flask equipped with a magnetic stir bar was added dimethyl malonate (2.30 g, 19.9 mmol), *N,N′*-dimethylpropylene urea (DMPU) (4.40 mL, 36.4 mmol), and THF (30.0 mL). The solution was cooled in an ice/water bath 15 minutes before lithium hydride (0.395 g, 49.7 mmol) was added in one portion. After 1.5 hours of stirring at 0 °C a solution of *cis*-1,4-dichloro-2-butene (2.73 g, 21.9 mmol) in THF (10.0 mL) was added and the reaction was heated to 45 °C. TLC was used to follow the reaction progress and the TLC plates were developed using a 25% EtOAc/Hexanes solution and visualized with $KMnO_4$. After 72 hours the reaction was quenched with the

addition of sat. aq. NH_4Cl (20.0 mL) and H_2O (10.0 mL). The organic was then washed with H_2O (3 x 20.0 mL) and brine (30.0 mL) before drying over $MgSO_4$. Concentration and purification via silica gel flash column chromatography (5% gradient, 0% → 20% EtOAc/Hex) afforded cyclopentene **2.32** (2.92 g, 73% yield) as a white solid.

R_f = 0.38 (25% EtOAc/Hex); m.p. 61-63 °C; ^{1}H-NMR (400 MHz; $CDCl_3$): δ 5.60 (s (br), 2H), 3.73 (s, 6H), 3.01 (s (br), 4H); ^{13}C-NMR (100 MHz; $CDCl_3$) δ 172.8, 127.9, 58.9, 53.0, 41.1; FTIR (neat): 2959, 1720 cm^{-1}; HRMS (ESI) *m/z* Calc'd.for $C_9H_{12}O_4$ $[M+H]^+$: 185.0814, found: 185.0807.

Preparation of Dibromide **2.34**

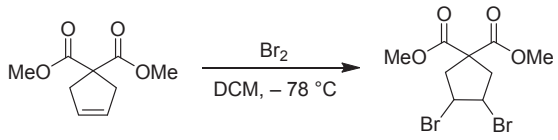

2.32 **2.34**

To a round bottom flask equipped with a magnetic stir bar was added cyclopentene **2.32** (2.63 g, 14.3 mmol) and DCM (143 mL). The solution was cooled in a dry ice/acetone bath and bromine (0.800 mL, 15.0 mmol) was added dropwise over 5 minutes. The reaction was stirred at this temperature for 2 hours before slowly warming to room temperature over an addition 2 hours. TLC was used to follow the reaction progress and the TLC plates were developed using a 25% EtOAc/Hexanes solution and visualized with $KMnO_4$. After reaching room temperature the reaction was diluted with DCM and transferred to a separatory funnel. The solution was washed with sat. aq. $Na_2S_2O_4$ (30.0 mL), H_2O (3 x 40.0 mL), and brine (40.0 mL) before drying over $MgSO_4$. Concentration and purification via silica gel flash column chromatography (10% EtOAc/Hex) afforded dibromide **2.34** (4.70 g, 95% yield) as a white solid.

R_f = 0.43 (25% EtOAc/Hex); m.p. 48-49 °C; ^{1}H-NMR (400 MHz; $CDCl_3$): δ 4.47-4.44 (m, 2H), 3.77 (d, *J* = 1.9 Hz, 6H), 3.48-3.38 (m, 2H), 2.73-2.67 (m, 2H); ^{13}C-NMR (100 MHz; $CDCl_3$) δ 171.2, 58.6, 56.0, 53.6, 42.1; FTIR (neat): 2855, 1732 cm^{-1}; HRMS (ESI) *m*/*z* Calc'd.for $C_9H_{12}Br_2O_4$ $[M+H]^+$: 342.9181, found: 342.9166.

Preparation of Aldehyde **2.30**

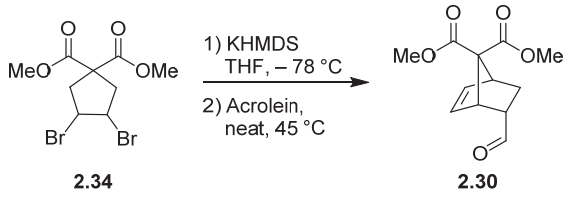

2.34 **2.30**

Diene Formation. To a round bottom flask equipped with a magnetic stir bar was added the dibromide **2.34** (3.00 g, 8.77 mmol) and THF (88.0 mL). The solution was cooled in a dry ice/acetone bath and potassium bis(trimethylsilyl)amide (KHMDS) (38.6 mL, 0.5 M in toluene, 19.3 mmol) was added. The reaction was allowed to slowly warm to room temperature with the bath. TLC was used to follow the reaction progress and the TLC plates were developed using a 50% EtOAc/Hexanes solution and visualized with *p*-anisaldehyde stain. After 3 hours the reaction was diluted in EtOAc and washed with sat. aq. NH_4Cl (3 x 20.0 mL), H_2O (2 x 20.0 mL), and brine (25.0 mL) before drying over $MgSO_4$. Concentration delivered the crude diene, which was moved onto the next reaction.

Diels-Alder. To a round bottom flask equipped with a magnetic stir bar and water cooled condensor was added the crude diene and acrolein (14.7 mL, 220 mmol). The flask was sealed and heated to 45 °C. The reaction progress was followed by ^{1}HNMR. After 85 hours the reaction was worked up by concentration and purification via silica gel

flash column chromatography (10% gradient, 0% → 30% EtOAc/Hex) afforded aldehyde **2.30** (1.50 g, 71% yield from **2.34**) as a yellow oil.

R_f = 0.44 (50% EtOAc/Hex); ^{1}H-NMR (400 MHz; $CDCl_3$): δ 9.51 (d, *J* = 1.3 Hz, 1H), 6.21-6.12 (m, 1H), 6.03-5.99 (m, 1H), 3.79-3.77 (m, 1H), 3.73 (s, 3H), 3.64 (s, 3H), 3.47-3.44 (m, 1H), 3.20-3.11 (m, 1H), 2.07 (ddd, *J* = 12.8, 9.1, 3.8 Hz, 1H), 1.60 (dd, *J* = 12.7, 4.2 Hz, 1H); ^{13}C-NMR (100 MHz; $CDCl_3$) δ 201.8, 168.7, 168.3, 136.6, 131.1, 76.7, 53.0, 52.9, 50.4, 48.4, 47.5, 26.0; FTIR (neat): 2955, 1719 cm^{-1}; HRMS (ESI) *m*/*z* Calc'd.for $C_{12}H_{14}O_5$ $[M+Na]^+$: 261.0733, found: 261.0735.

Preparation of Alcohol **2.35**

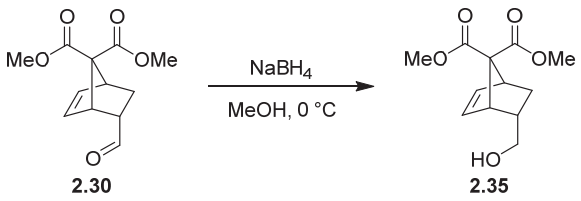

2.30 **2.35**

To a cone shaped flask equipped with a magnetic stir bar was added aldehyde **2.30** (0.81 g, 3.4 mmol) and MeOH (17 mL). The reaction was cooled in an ice/water bath and sodium borohydride ($NaBH_4$) (0.15 g, 4.1 mmol) was added in one portion. TLC was used to follow the reaction progress and the TLC plates were developed using a 75% EtOAc/Hexanes solution and visualized with $KMnO_4$. After 1 hour the reaction was quenched with the addition of 1M HCl (5.0 mL) and removal of MeOH. The solution was extracted with EtOAc (20 mL) and the organic was washed with sat. aq. $NaHCO_3$ (2 x 10 mL), H_2O (10 mL), and brine (10 mL) before drying over $MgSO_4$. Concentration and purification via silica gel flash column chromatography (50% EtOAc/Hex) afforded alcohol **2.35** (0.64 g, 78% yield) as a white solid.

R_f = 0.32 (50% EtOAc/Hex); m.p. 67-69 °C; ^{1}H-NMR (400 MHz; $CDCl_3$): δ 6.14-6.11 (m, 1H), 6.03-6.00 (m, 1H), 3.71 (s, 3H), 3.63 (s, 3H), 3.50-3.48 (m, 1H), 3.40-3.23 (m, 3H), 2.46-2.36 (m, 1H), 2.09 (ddd, *J* = 12.7, 9.1, 3.9 Hz, 1H), 1.51 (s, 1H), 0.64 (dd, *J* = 12.3, 4.6 Hz, 1H); ^{13}C-NMR (100 MHz; $CDCl_3$) δ 169.5, 168.8, 135.3, 131.7, 77.0, 65.1, 52.8, 52.7, 48.6, 47.0, 39.3, 27.5; FTIR (neat): 3175, 2934, 1721 cm^{-1}; HRMS (ESI) *m*/*z* Calc'd.for $C_{12}H_{16}O_5$ $[M+H]^+$: 241.1076, found: 241.1062.

Preparation of Amine **2.37**

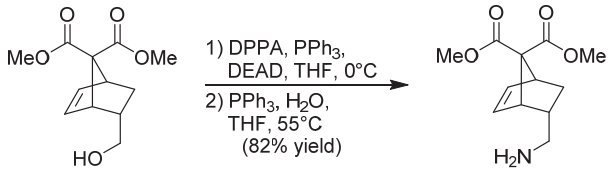

2.35 **2.37**

Azide Formation. To a round bottom flask equipped with a magnetic stir bar was added alcohol **2.35** (0.16 g, 1.9 mmol), PPh_3 (1.0 g, 3.9 mmol), and THF (19 mL). The solution was cooled in an ice/water bath before the addition of diphenyl phosphoryl azide (DPPA) (0.88 mL, 3.9 mmol) and diethyl azodicarboxylate (DEAD) (2.0 mL, 40%, 3.9 mmol). The reaction was allowed to slowly warm to room temperature with the bath. TLC was used to follow the reaction progress and the TLC plates were developed using a 75% EtOAc/Hexanes solution and visualized with $KMnO_4$. After 19 hours the reaction was diluted with EtOAc and washed with H_2O (2 x 15 mL) and brine (15 mL) before drying over $MgSO_4$. Concentration and purification via silica gel flash column chromatography (2% gradient, 0% → 10% EtOAc/Hex) afforded the slightly impure azide (0.76 g) as a colorless oil.

Staudinger Reduction. To a round bottom flask equipped with a magnetic stir bar was added the azide (0.76 g, 2.9 mmol) and THF (29 mL). PPh_3 (1.1 g, 4.3 mmol) and H_2O (0.26 mL, 14 mmol) were then added and the reaction heated to 55 °C. TLC was used to follow the reaction progress and the TLC plates were developed using a 75% EtOAc/Hexanes solution and visualized with $KMnO_4$. After 24 hours the reaction was worked up by concentration and purification via silica gel flash column chromatography (2% gradient, 0% → 10% EtOAc/Hex) afforded amine **2.37** (0.18 g, 82% yield from alcohol **2.35**) as a yellow oil.

Azide. R_f = 0.61 (50% EtOAc/Hex); ^{1}H-NMR (600 MHz; $CDCl_3$): δ 6.18 (dd, *J* = 6.0, 3.0 Hz, 1H), 6.00 (dd, *J* = 6.0, 3.0 Hz, 1H), 3.72 (s, 3H), 3.64 (s, 3H), 3.48-3.47 (m, 1H), 3.35-3.34 (m, 1H), 3.08-2.93 (m, 1H), 2.49-2.44 (m, 1H), 2.14 (ddd, *J* = 12.6, 9.0, 3.8 Hz, 1H), 0.68 (dd, *J* = 12.5, 4.5 Hz, 1H); ^{13}C-NMR (150 MHz, $CDCl_3$) δ 169.2, 168.5, 136.0, 131.3, 77.04, 54.2, 52.9, 52.8, 49.1, 47.1, 36.7, 28.6; FTIR (neat): 2953, 2092, 1731 cm^{-1}; HRMS (ESI) *m*/*z* Calc'd.for $C_{12}H_{15}N_3O_4$ $[M+Na]^+$: 288.0955, found: 288.0957.

Amine. ^{1}H-NMR (400 MHz; $CDCl_3$): δ 6.12 (dd, *J* = 6.0, 2.9 Hz, 1H), 5.98 (dd, *J* = 6.0, 2.9 Hz, 1H), 3.70 (s, 3H), 3.62 (s, 3H), 3.45-3.43 (m, 1H), 3.32-3.30 (m, 1H), 2.46-2.38 (m, 2H), 2.23-2.18 (m, 1H), 2.12 (ddd, *J* = 12.5, 8.9, 3.8 Hz, 1H), 1.29 (s, 2H), 0.65 (dd, *J* = 11.9, 4.3 Hz, 1H); ^{13}C-NMR (100 MHz; $CDCl_3$) δ 169.6, 168.8, 135.3, 131.5, 77.03, 52.7, 52.6, 49.0, 47.1, 45.4, 40.3, 28.9; FTIR (neat): 2952, 1730, 1658 cm^{-1}; HRMS (ESI) *m*/*z* Calc'd.for $C_{12}H_{17}NO_4$ $[M+H]^+$: 240.1236, found: 240.2134.

Preparation of Isonitrile **2.28**

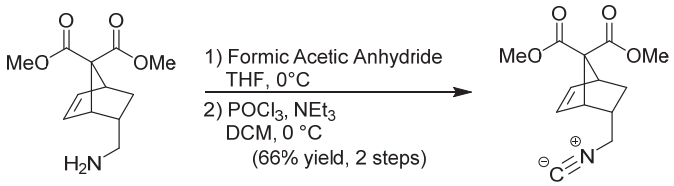

2.37 **2.28**

Formamide Formation. To a round bottom flask equipped with a magnetic stir bar was added amine **2.37** (0.27 g, 1.1 mmol) and THF (13 mL). The solution was cooled in and ice/water bath and formic acetic anhydride (0.12 mL, 1.6 mmol) was added dropwise. TLC was used to follow the reaction progress and the TLC plates were developed using a 75% EtOAc/Hexanes solution and visualized with $KMnO_4$. After 2 hours, concentration and purification via silica gel flash column chromatography (10% gradient, 40% → 100% EtOAc/Hex) afforded the amide (0.27 g) as a colorless oil.

Isonitrile Formation. To a round bottom flask equipped with a magnetic stir bar was added the amide (0.10 mL, 0.37 mmol) and DCM (3.7 mL). The solution was cooled in an ice/salt/water bath and Et_3N (0.17 mL, 1.9 mmol) was added. After thorough cooling $POCl_3$ (0.77 mL, 3.7 mL) was added drowise. TLC was used to follow the reaction progress and the TLC plates were developed using a 50% EtOAc/Hexanes solution and visualized with $KMnO_4$. After 45 minutes the reaction was quenched with the addition of H_2O (4.0 mL). The aqueous layer was extracted with DCM (3 x 8.0 mL) and the combined organics were dried over Na_2SO_4. Concentration and purification via silica gel flash column chromatography (50% EtOAc/Hex) afforded the isonitrile **2.28** (0.067 g, 66% yield from amine **2.37**) as a white solid.

R_f = 0.40 (50% EtOAc/Hex); m.p. 73-75 °C; ^{1}H-NMR (400 MHz; $CDCl_3$): δ 6.26 -6.23 (m, 1H), 6.06-6.04 (m, 1H), 3.76 (s, 3H), 3.66 (s, 3H), 3.58-3.54 (m, 1H), 3.42-3.37 (m, 1H), 3.17-3.05 (m, 2H), 2.67-2.64 (m, 1H), 2.19 (ddd, *J* = 12.0, 8.0, 4.0 Hz, 1H), 0.70 (d, *J* = 16.0, 4.0 Hz, 1H); ^{13}C-NMR (100 MHz; $CDCl_3$) δ 168.8, 168.2, 156.6, 136.8, 130.7, 77.1, 53.0, 52.8, 49.0, 47.4, 44.1 (t, *J* = 6.0 Hz), 36.7, 28.4; FTIR (neat): 2935, 2143, 1738, 1717 cm^{-1}; HRMS (ESI) *m/z* Calc'd.for $C_{12}H_{17}NO_4$ $[M+H]^+$: 250.1079, found: 250.1077.

Preparation of Ether **2.36**

2.35 **2.36**

To a vial equipped with a magnetic stir bar was added alcohol **2.35** (0.050 g, 0.21 mmol), zinc bromide (0.047 g, 0.21 mmol), and DCM (0.70 mL). The solution was cooled in an ice/water bath and bromine (0.011 mL, 0.21 mmol) was added dropwise. TLC was used to follow the reaction progress and the TLC plates were developed using a 75% EtOAc/Hexanes solution and visualized with $KMnO_4$. After 1 hour the reaction was diluted with DCM (6.0 mL) and washed sat. aq. $Na_2S_2O_3$ (2 x 2.0 ml), H_2O (6.0 mL), and brine (6.0 mL) before drying over Na_2SO_4. Concentration and purification via silica gel flash column chromatography (10% gradient, 0% → 60% EtOAc/Hex) afforded ether **2.36**.

^{1}H-NMR (400 MHz; $CDCl_3$): δ 4.90-4.88 (m, 1H), 3.89-3.85 (m, 1H), 3.79-3.70 (m, 7H), 3.68-3.63 (m, 1H), 3.25-3.19 (m, 1H), 2.99 (s (br), 1H), 2.59-2.51 (m, 1H), 2.46-2.41 (m, 1H), 1.24-1.19 (m, 1H); ^{13}C-NMR (100 MHz; $CDCl_3$) δ 169.0, 168.9, 88.9,

74.8, 69.5, 55.7, 53.1, 53.0, 51.3, 48.5, 37.1, 35.6; HRMS (ESI) *m/z* Calc'd.for $C_{12}H_{15}BrO_5$ $[M+NH_4]^+$: 336.0441, found: 336.0436.

Preparation of Ketone **2.38**

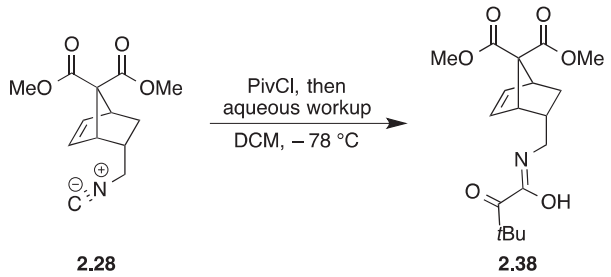

2.28 **2.38**

To a vial equipped with a magnetic stir bar was added isonitrile **2.28** (0.015 g, 0.060 mmol) and DCM (0.60 mL). The solution was cooled in a dry ice/acetone bath and pivaloyl chloride (0.0078 g, 0.063 mmol) was added. TLC was used to follow the reaction progress and the TLC plates were developed using a 25% EtOAc/Hexanes solution and visualized with $KMnO_4$. After 8 hours at this temperature the reaction was removed from the cooling bath and warmed to room temperature overnight. The reaction was quenched with the addition of sat. aq. $NaHCO_3$ (0.6 mL) and diluted with DCM. The organic layer was washed with H_2O and brine. Concentration and purification via silica gel flash column chromatography (10% gradient, 0% → 100% EtOAc/Hex) afforded ketone **2.38**.

R_f = 0.23 (50% EtOAc/Hex); ^{1}H-NMR (400 MHz; $CDCl_3$): δ 6.89 (s (br), 1H), 6.22-6.18 (m, 1H), 6.07-6.02 (m, 1H), 3.71 (s, 3H), 3.63 (s, 3H), 3.38-3.32 (m, 2H), 3.05-3.01 (m, 2H), 3.43-3.35 (m, 1H), 2.13 (ddd, *J* = 12.7, 9.1, 3.8 Hz, 1H), 1.32 (s, 9H), 0.72 (dd, *J* = 12.4, 4.5 Hz, 1H); ^{13}C-NMR (100 MHz; $CDCl_3$) δ 203.6, 169.2, 168.6, 159.7, 135.9, 131.5, 77.1, 52.9, 52.8, 49.1, 47.2, 43.1, 41.8, 36.7, 28.8, 26.4; FTIR (neat): 3369,

2955, 1733, 1672, 1519 cm^{-1}; HRMS (ESI) *m/z* Calc'd.for $C_{19}H_{19}NO_9S$ $[M+H]^+$: 352.1760, found: 352.1761.

Preparation of Imine **2.39**

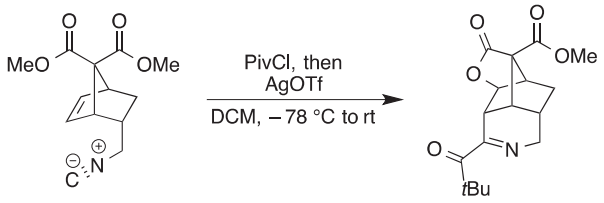

2.28 **2.39**

To a vial equipped with a magnetic stir bar was added isonitrile **2.28** (0.025 g, 0.10 mmol) and DCM (1.0 mL). The solution was cooled in a dry ice/acetone bath and pivaloyl chloride (0.013 g, 0.11 mmol) was added. The reaction was allowed to warm to room temperature, with the bath, over 3 hours and the vial was sealed. After a total of 19 hours AgOTf (0.028 g, 0.11 mmol) was added, in one portion, and the vial was recapped and stirred at room temperature. TLC was used to follow the reaction progress and the TLC plates were developed using a 50% EtOAc/Hexanes solution and visualized with $KMnO_4$. After a total of 48 hours the reaction was quenched with the addition of sat. aq. NH_4Cl (1.0 mL) and diluted with DCM. The organic layer was washed with H_2O and brine before drying over $MgSO_4$. Concentration and purification via silica gel flash column chromatography (5% gradient, 0% → 40% EtOAc/Hex) afforded imine **2.39** (0.011 g, 34% yield) as a white solid.

R_f = 0.43 (50% EtOAc/Hex); m.p. 152-154 °C; ^{1}H-NMR (400 MHz; $CDCl_3$): δ 4.55 9d, *J* = 2.6 Hz, 1H), 4.14 (d, *J* = 24.0 Hz, 1H), 3.85-3.74 (m, 4H), 3.17-3.15 (m, 1H), 2.87-2.86 (m, 1H), 2.67-2.65 (m, 1H), 2.55 (s (br), 1H), 2.04 (ddd, *J* = 16.7, 11.3, 5.4 Hz, 1H), 1.31 (d, *J* = 1.7 Hz, 9H), 1.03 (dd, *J* = 14.2, 6.3 Hz, 1H); ^{13}C-NMR (150

MHz, $CDCl_3$) δ 171.2, 167.2, 162.8, 81.7, 67.6, 54.3, 53.1, 51.2, 44.0, 39.2, 32.1, 27.3, 24.0; FTIR (neat): 2954, 1781, 1738, 1678 cm^{-1}; HRMS (ESI) *m/z* Calc'd.for $C_{17}H_{21}NO_5$ $[M+H]^+$: 320.1498, found: 320.1503.

Preparation of Stannane **2.44**

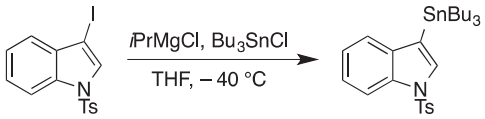

2.48 **2.44**

To a round bottom flask equipped with a magnetic stir bar was added iodide **2.48** (0.79 g, 2.0 mmol) and THF (12.0 mL). The reaction was cooled in a dry ice/MeCN bath and *i*PrMgCl (1.3 mL, 1.7M, 2.2 mmol) was added dropwise. After 1 hour, tributyltin chloride (Bu_3SnCl) (0.81 mL, 1.5 mmol) was added dropwise and the reaction was allowed to slowly warm to room temperature with the bath. TLC was used to follow the reaction progress and the TLC plates were developed using a 25% EtOAc/Hexanes solution and visualized with $KMnO_4$. After 3 hours the reaction was quenched with the addition of sat. aq. NH_4Cl (4.0 mL). The organic was washed with H_2O (15 mL) and brine (15 mL) before drying over $MgSO_4$. Concentration and purification via silica gel flash column chromatography (96%:2%:2% Hex:EtOAc:Et_3N) afforded stannane **2.44** (0.074 g, 66% yield) as a colorless oil. [CAS: 156021-25-9]

Preparation of α,β-Unsaturated Ester **2.27**

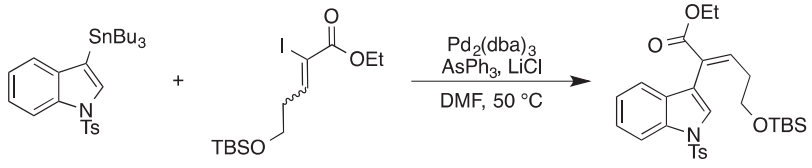

2.44 **2.45** **2.27**

To a round bottom flask equipped with a magnetic stir bar was added stannane **2.44** (0.28 g, 0.50 mmol), $Pd_2(dba)_3$ (0.012 g, 0.013 mmol), and $AsPh_3$ (0.015 g, 0.050 mmol). A solution of vinyl iodide **2.45** (0.19 g, 0.50 mmol) in DMF (2.0 mL) was added and the entire solution was degassed (freeze-pump-thaw). The reaction was then heated to 60 °C. TLC was used to follow the reaction progress and the TLC plates were developed using a 25% EtOAc/Hexanes solution and visualized with $KMnO_4$. After 43 hours the reaction was worked up by the addition of H_2O (60 mL) and diluting with Et_2O. The organic layer was washed with H_2O (2 x 60 mL) and brine (60 mL) before drying over Na_2SO_4. Concentration and purification via silica gel flash column chromatography (0% → 8% Et_2O/Toluene) afforded α,β-unsaturated ester **2.27** (0.21 g, 78% yield) as a yellow oil.

R_f = 0.54 (25% EtOAc/Hex); ^{1}H-NMR (400 MHz; $CDCl_3$): δ 7.96 (m, 1H), 7.78-7.71 (m, 2H), 7.50 (s, 1H), 7.32-7.13 (m, 6H), 4.16 (q, *J* = 7.1 Hz, 2H), 3.65 (t, *J* = 6.3 Hz, 2H), 2.35-2.22 (m, 6H), 1.18 (t, *J* = 7.1 Hz, 3H), 0.85 (s, 9H), 0.00 (s, 6H); ^{13}C-NMR (100 MHz; $CDCl_3$) δ 166.6, 144.9, 135.4, 134.9, 130.7, 132.0, 127.0, 126.3, 125.1, 124.7, 123.4, 120.8, 116.9, 113.8, 110.2, 61.9, 61.0, 33.7, 26.1, 21.7, 18.5, 14.3, -5.2; FTIR (neat): 2928, 1713, 1597 cm^{-1}; HRMS (ESI) *m/z* Calc'd.for $C_{28}H_{37}NO_5SSi$ $[M+Na]^+$: 550.2054, found: 550.2055.

Preparation of Allylic Alcohol **2.53**

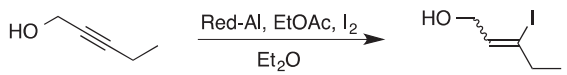

2.52 **2.53**

To a round bottom flask equipped with a magnetic stir bar was added Red-Al (2.1 mL, 7.1 mmol) and Et_2O (9.7 mL). The solution was cooled in an ice/water bath and a

solution of alcohol **2.52** (0.30 g, 3.6 mmol) in Et_2O (3.0 mL) was added. The reaction was removed from the cooling bath and warmed to room temperature. After 8 hours the reaction was again cooled to 0 °C and EtOAc (0.35 mL, 3.6 mmol) was added. The reaction was immediately placed into a dry ice/acetone bath and iodine (1.4 g, 5.4 mmol) was added. The reaction was then removed from the cooling bath and stirred at room temperature overnight. TLC was used to follow the reaction progress and the TLC plates were developed using a 10% EtOAc/Hexanes solution and visualized with $KMnO_4$. The reaction was worked up by washing the organic layer with sat. aq. $Na_2S_2O_3$, H_2O, and brine before drying over Na_2SO_4. Concentration and purification via silica gel flash column chromatography (25% EtOAc/Hex) afforded allylic alcohol **2.53** (0.45 g, 60% yield) as an orange oil. [CAS: 161630-78-5 (Z); 161530-76-3 (E)]

Preparation of Vinyl Iodide **2.46**

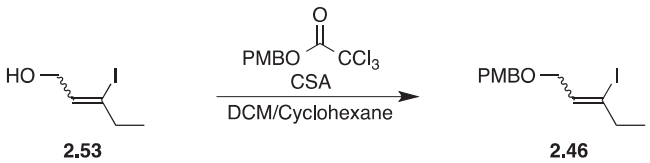

To a round bottom flask equipped with a magnetic stir bar was added allylic alcohol **2.53** (0.20 g, 0.94 mmol), DCM (4.4 mL), cyclohexane (1.1 mL), PMB acetimidate (0.30 mL, 1.4 mmol), and CSA (0.022 g, 0.094 mmol). TLC was used to follow the reaction progress and the TLC plates were developed using a 25% EtOAc/Hexanes solution and visualized with $KMnO_4$. After 21 hours the reaction was worked up by washing with sat. aq. $NaHCO_3$ before drying over Na_2SO_4. Concentration and purification via silica gel flash column chromatography (0% → 12% EtOAc/Hex) afforded vinyl iodide **2.46** (0.29 g, 94% yield, 8:1 E:Z) as an orange oil.

R_f = (50% EtOAc/Hex); ^{1}H-NMR (400 MHz; $CDCl_3$): δ 7.32-7.24 (m, 2H), 7.11-7.06 (m, 0.25H), 6.92-6.85 (m, 2H), 6.83-6.81 (m, 0.25H), 5.82-5.79 (m, 1H), 4.52 (s, 0.25H), 4.46(s, 2H), 4.16 (dt, *J* = 5.7, 1.3 Hz, 0.25H), 4.07 (dt, *J* = 5.6, 1.2 Hz, 2H), 3.81 (s, 3H), 3.78 (s, 0.38H), 2.58 -2.51 (m, 2H), 2.28-2.22 (m, 0.25H), 1.16 (t, *J* = 7.5 Hz, 0.38H), 1.09 (t, *J* = 7.3 Hz, 3H); ^{13}C-NMR (100 MHz; $CDCl_3$) δ 159.34, 157.96, 133.77, 130.77, 130.21, 129.81, 129.79, 129.58, 113.91, 113.89, 112.18, 74.43, 72.31, 71.08, 57.45, 55.36, 55.32, 40.20, 39.15, 14.77, 13.96, 12.59; FTIR (neat): 2967, 1611, 1510 cm^{-1}; HRMS (ESI) *m*/*z* Calc'd.for $C_{13}H_{17}IO_2$ $[M+Na]^+$: 355.0165, found: 355.0165.

Preparation of Boronic Ester **2.55**

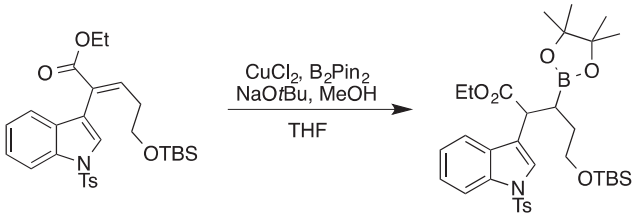

2.27 **2.55**

To a round bottom flask equipped with a magnetic stir bar was added CuCl (0.0060 g, 0.061 mmol), NaO*t*Bu (0.016 g, 0.17 mmol), and THF (0.5 mL). After 30 minutes a solution of bis(pinacolato)diboron (B_2Pin_2) (0.27 g, 1.0 mmol) in THF (0.7 mL) was added. After 10 additional minutes a solution of α,β-unsaturated ester **2.27** (0.50 g, 0.95 mmol) in THF (0.7 mL) was added, followed immediately by MeOH (0.080 mL, 1.9 mmol). TLC was used to follow the reaction progress and the TLC plates were developed using a 5% Et_2O/Toluene solution and visualized with $KMnO_4$. After 16 hours the reaction was worked up by vacuum filtration through celite. Concentration and purification via silica gel flash column chromatography (0% → 6% Et_2O/Toluene)

afforded boronic ester **2.55** (0.20 g, 32% yield) as an inconsequential mixture of diastereomers.

R_f = 0.43 (25% EtOAc/Hex); ^{1}H-NMR (400 MHz; $CDCl_3$): δ 7.99 (d, *J* = 8.2 Hz, 1H), 7.85-7.57 (m, 3H), 7.35-7.18 (m, 5H), 4.20-3.90 (m, 3H), 3.72-3.48 (m, 2H), 2.37-2.35 (m, 3H), 2.05-1.73 (m, 2H), 1.56-1.48 (m, 1H), 1.31 (d, *J* = 16.4 Hz, 9H), 0.95-0.87 (m, 12H), 0.11-0.01 (m, 6H); ^{13}C-NMR (100 MHz; $CDCl_3$) δ 173.87, 173.41, 144.81, 144.78, 135.55, 135.41, 135.28, 134.79, 130.35, 130.19, 129.88, 129.85, 128.50, 128.47, 128.33, 128.26, 126.87, 125.53, 124.99, 124.75, 124.69, 124.67, 123.19, 123.04, 120.53, 120.45, 120.42, 120.33, 113.76, 113.44, 83.45, 83.43, 83.31, 77.48, 77.16, 76.84, 62.75, 62.54, 60.95, 60.86, 44.51, 43.96, 33.15, 32.17, 26.09, 26.06, 25.03, 24.81, 24.56, 24.44, 21.60, 18.46, 18.41, 14.22, 14.14, -5.13, -5.17, -5.22, -5.03; FTIR (neat): 2928, 1730, 1598 cm^{-1}; HRMS (ESI) *m/z* Calc'd.for $C_{34}H_{50}BNO_7SSi$ $[M+Na]^+$: 678.3063, found: 678.3065.

Preparation of Homoallylic Alcohol **2.59**

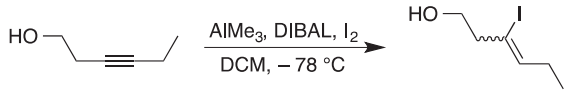

2.58 **2.59**

To a round bottom flask equipped with a magnetic stir bar was added 3-hexyn-1-ol **2.58** (0.56 mL, 5.1 mmol) and DCM (20 mL). $AlMe_3$ (3.1 mL, 2.0M in heptanes, 6.1 mmol) was added dropwise at room temperature. After 30 minutes diisobutylaluminum hydride (5.3 mL, 1.0M in hexanes, 5.3 mmol) was added. After an additional 48 hours the reaction was cooled in a dry ice/acetone bath and I_2 (3.1 g, 12 mmol) was added in one portion. The reaction was immediately placed into and ice/water bath and stirred 30 minutes. TLC was used to follow the reaction progress and the TLC plates were

developed using a 25% EtOAc/Hexanes solution and visualized with $KMnO_4$. The reaction was quenched with the dropwise addition of sat. aq. $Na_2S_2O_3$ (3.0 ml) and sat. aq. NH_4Cl (3.0 mL). The solution was then washed with Rochelle's salt, H_2O, and brine before drying over $MgSO_4$. Concentration and purification via silica gel flash column chromatography (0% → 35% EtOAc/Hex) afforded homoallylic alcohol **2.59** (0.67 g, 58% yield) as a 1.1:1 mixture of olefin isomers.

R_f = 0.28 (25% EtOAc/Hex); ^{1}H-NMR (600 MHz; $CDCl_3$): δ 6.16 (t, *J* = 7.6 Hz, 1H), 5.58 (t, *J* = 6.7 Hz, 0.9H), 3.71 (q, *J* = 6.1 Hz, 1.8H), 3.65 (q, *J* = 6.1 Hz, 2.0H, 2.47 (q, *J* = 7.3 Hz, 1.8H), 2.45-2.39 (m, 3.8H), 2.32 (q, *J* = 6.7 Hz, 2.0H), 1.40 (t, *J* = 5.7 Hz, 1.0H), 1.34 (t, *J* = 5.6 Hz, 0.90H), 1.10-1.04 (m, 5.7H); ^{13}C-NMR (150 MHz; $CDCl_3$) δ 136.2, 129.8, 114.1, 108.1, 61.6, 61.5, 39.9, 39.2, 34.1, 32.6, 15.1, 14.6; FTIR (neat): 3311, 2967, 1629 cm^{-1}; HRMS (ESI) *m*/*z* Calc'd.for $C_6H_{11}IO$ $[M+Na]^+$: 248.9747, found: 248.9748.

Preparation of Vinyl Iodide **2.60**

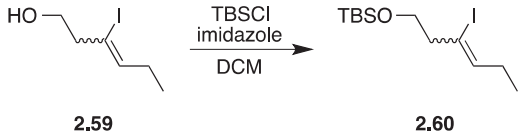

2.59 **2.60**

To a vial equipped with a magnetic stir bar was added homoallylic alcohol **2.59** (0.58 g. 2.6 mmol), imidazole (0.44 g, 6.5 mmol), *tert*-butyldimethylsilyl chloride (0.46 g, 3.1 mmol), and DMF (1.4 mL). TLC was used to follow the reaction progress and the TLC plates were developed using a 50% EtOAc/Hexanes solution and visualized with $KMnO_4$. After 19 hours, the reaction was diluted with EtOAc and washed with sat. aq. NH_4Cl. Concentration and purification via silica gel flash column chromatography (0%

→ 12% EtOAc/Hex) afforded vinyl iodide **2.60** (0.76 g, 73% yield) as a 1.4:1 mixture of olefin isomers.

R_f = 0.67 (25% EtOAc/Hex); ^{1}H-NMR (400 MHz; $CDCl_3$): δ 6.14 (tt, *J* = 7.6, 0.9 Hz 0.7H), 5.56 (tt, *J* = 6.7, 1.3 Hz, 1H), 3.65 (t, *J* 6.7 Hz, 2H), 3.60 (t, *J* = 6.7 Hz, 1.4H), 2.54-2.47 (m, 2H), 2.44-2.38 (m, 1.4H), 2.38-2.31 (m, 2H), 2.28-2.23 (m, 1.4H), 1.09-1.02 (m, 5.1H), 0.90-0.88 (m, 15.4H), 0.06-0.05 (m, 10.3H); ^{13}C-NMR (100 MHz, $CDCl_3$) δ 136.9, 130.5, 113.0, 107.1, 62.1, 61.8, 40.1, 39.2, 34.4, 32.6, 26.1, 26.1, 18.5, 15.1, 14.6, -5.08, -5.13; FTIR (neat): 2928 cm^{-1}; HRMS (ESI) *m*/*z* Calc'd.for $C_{12}H_{25}IOSi$ $[M+H]^+$: 341.0792, found: 341.0792.

Preparation of Alcohol **2.62**

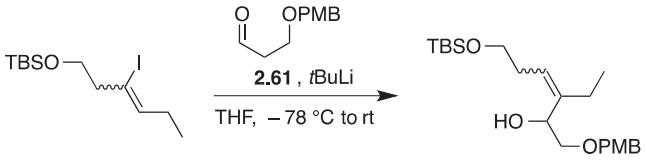

2.60 **2.62**

To a round bottom flask equipped with a magnetic stir bar was added vinyl iodide **2.60** (0.50 g, 1.5 mmol) and THF (5.0 mL). The solution was cooled in a dry ice/acetone bath and *t*BuLi (1.8 mL, 1.7M in hexanes, 3.1 mmol) was added dropwise. After 40 minutes a solution of aldehyde **2.61** (0.29 g, 1.6 mmol) in THF (2.5 mL) was added. TLC was used to follow the reaction progress and the TLC plates were developed using a 25% EtOAc/Hexanes solution and visualized with $KMnO_4$. After 45 minutes the reaction was removed from the cooling bath and allowed to stir at room temperature for an additional 40 minutes. The reaction was quenched with the addition of sat. aq. NH_4Cl and the organic layer was dried over Na_2SO_4. Concentration and purification via silica

gel flash column chromatography (0% → 3% EtOAc/Hex) afforded alcohol **2.62** (0.30 g, 52% yield) as a 1:1 mixture of olefin isomers.

R_f = 0.43 (25% EtOAc/Hex); ^{1}H-NMR (400 MHz; $CDCl_3$): δ 7.30-7.23 (m, 4H), 6.92-6.85 (m, 4H), 5.48 (t, *J* = 7.2 Hz, 1H), 5.27 (t, *J* = 8.0 Hz, 1H), 4.72-4.69 (m, 1H), 4.54-4.47 (m, 4H), 4.29-4.25 (m, 1H), 3.81-3.79 (m, 6H), 3.64-3.59 (m, 4H), 3.54-3.40 (m, 4H), 3.34 (t, *J* = 8.0 Hz, 1H), 2.40-2.26 (m, 4H), 2.21-2.08 (m, 2H), 2.06-1.94 (m, 2H), 1.04-0.98 (m, 6H), 0.90 (m, 18H), 0.06-0.04 (m, 12H); ^{13}C-NMR (100 MHz, $CDCl_3$) δ 159.42, 159.37, 141.70, 141.46, 130.26, 130.14, 129.52, 129.49, 123.37, 123.11, 113.96, 113.93, 74.11, 74.03, 73.07, 73.00, 69.98, 63.07, 62.93, 55.36, 31.36, 31.16, 26.09, 25.09, 21.26, 18.53, 18.48, 14.30, 13.32, -5.15, -5.20; FTIR (neat): 3446, 2954, 2856, 1612, 1512 cm^{-1}; HRMS (ESI) *m/z* Calc'd.for $C_{22}H_{38}O_4Si$ $[M+NH_4]^+$: 417.2437, found: 417.2437.

2.5 References

[1] Adams, G. L.; Carroll, P. J.; Smith, A. B. III. *J. Am. Chem. Soc.* **2012**, *134*, 4037.

[2] Smith, M. W.; Snyder, S. A. *J. Am. Chem. Soc.* **2013**, *135*, 12964.

[3] Baran, P. S.; Maimone, T. J.; Richer, J. M. *Nature* **2007**, *446*, 404.

[4] Shi, J.; Manolikakes, G.; Yeh, C.-H.; Guerrero, C. A.; Shenvi, R. A.; Shigehisa, H.; Baran, P. S. *J. Am. Chem. Soc.* **2011**, *133*, 8014.

[5] For reviews on asymmetric 1,4-additions see: (a) Hayahsi, T.; Yamasaki, K. *Chem. Rev.* **2003**, *103*, 2829. (b) Almasi, D.; Alonso, D. A.; Nájera, C. *Tetrahedron: Asymmetry* **2007**, *18*, 299. (c) Christoffers, J.; Koripelly, G.; Rosiak, A.; Rössle, M. *Synthesis* **2007**, *9*, 1279. (d) Alexakis, A.; Bäckvall, J. E.; Krause, N. Pàmies, O.; Diéguez, M. *Chem. Rev.* **2008**, *108*, 2796. e) Harutyunyan, S. R.; den Hartog, T.; Geurts, K.; Minnaard, A. J.; Ferigna, B. L. *Chem. Rev.* **2008**, *108*, 2824.

[6] (a) Havlik, A. J.; Wald, M. M. *J. Am. Chem. Soc.* **1955**, *77*, 5171. (b) Yamada, H.; Wada, Y.; Tanimoto, S.; Okano, M. *Bull. Chem. Soc. Jpn.* **1982**, *55*, 2480.

[7] Wesling, M.; Livinghouse, T. *Tet. Lett.*, **1985**, *26*, 5389.

[8] (a) Saegusa, T.; Ito, Y.; Kobayashi, S.; Hirota, K. *J. Am. Chem. Soc.* **1967**, *89*, 2240. (b) Saeugusa, T.; Ito, Y.; Kinoshita, H.; Tomita, S. *J. Org. Chem.* **1971**, *36*, 3316. (c) For a Review on Isonitriles in the synthesis of hetercycles see: Lygin, A. V.; de Meijere, A. *Angew. Chem. Int. Ed.* **2010**, *49*, 2.

[9] (a) Westling, M.; Livinghouse, T. *J. Am. Chem. Soc.* **1987**, *109*, 590. (b) Kercher, T.; Livinghouse, T. *J. Org. Chem.* **1997**, *62*, 805. (c) Westling, M.; Smith, R.; Livinghouse, T. *J. Org. Chem.* **1986**, *51*, 1159. (d) Luedtke, G.; Westling, M.; Livinghouse, T. *Tetrahedron* **1992**, *48*, 2209. d) Livinghouse, T. *Tetrahedron* **1999**, *55*, 9947.

[10] Deprés, J.-P.; Greene, A. E. *Organic Syntheses* **2004**, 228.

[11] Dmitrienko, G. I.; Savard, M. E.; Friesen, R. W.; Thandi, M. S. *Tet. Lett.* **1985**, *26*, 1691.

[12] Yoshimura, Y.; Kusanagi, T.; Kibayashi, C.; Yamazaki, N.; Aoyagi, S. *Heterocycles* **2008**, *75*, 1329.

[13] Krimen, L. I. *Organic Syntheses* **1988**, *6*, 8.

[14] Nayak, M.; Batra, S. *Tet. Lett.* **2010**, *51*, 510.

[15] (a) Trost, B. M.; Haffner, C. D.; Jebaratnam, D. J.; Krische, M. J.; Thomas, A. P. *J. Am. Chem. Soc.* **2008**, *130*, 16176. (b) Patil, N. T; Yamamoto, Y. *Chem. Rev.* **2008**, *108*, 3395. (c) Davies, P.; Fürstner, A. *Angew. Chem. Int. Ed.* **2007**, *46*, 3410. d) Arcadi, A. *Chem. Rev.* **2008**, *108*, 3266.

[16] Mitsudo, K.; Thansandote, P.; Wilhelm, T.; Mariampillai, B.; Lautens, M. *Org. Lett.* **2006**, *8*, 3939.

[17] Rottländer, M.; Baymond, L.; Cahiez, G.; Knochel, P. *J. Org. Chem.* **1999**, *64*, 1080.

[18] Yu, M.; Zhang, G.; Zhang, L. *Org. Lett.* **2007**, 2147.

[19] Shibahara, S.; Fujino, M.; Tashiro, Y.; Okamoto, N.; Esumi, T; Takahashi, K.; Ishihara, J.; Hatakeyama, S. *Synthesis* **2009**, *17*, 2935.

[20] Ciattini, P. G.; Morera, E.; Ortar, G. *Tet. Lett.* **35**, *35*, 2405.

[21] (a) Yasui, Y.; Takeda, H.; Takemoto, Y. *Chem. Pharm. Bull.* **2008**, *56*, 1567. (b) Lautens, M.; Paquin, J.-F. *Org. Lett.* **2003**, *5*, 3391.

[22] (a) Endo K.; Ohkubo, T.; Hirokami, M.; Shibata, T. *J. Am. Chem. Soc.* **2010**, *132*, 11033. (b) Ohmura, T.; Agwano, T.; Suginome, M. *J. Am. Chem. Soc.* **2010**, *132*, 13191. (c) Chemler, S. R.; Trauner, D.; Danishefsky, S. J. *Angew. Chem. Int. Ed.* **2001**, *40*, 4544.

[23] Lee, J. C.; McDonald, R.; Hall, D. G. *Nature Chem.* **2011**, *3*, 894.

[24] Ma, S.; Liu, F.; Negishi, E. *Tet. Lett.* **1997**, *38*, 3829.

[25] Corey, E. J.; Venkateswarlu, A. *J. Am. Chem. Soc.* **1972**, *94*, 6190.

[26] González, D. F.; Brand, J. P.; Waser, J. *Chem. Eur. J.* **2010**, *16*, 9457.

CHAPTER THREE

Studies Toward the Total Synthesis of the Phomoidrides

3.1 Isolation, Biological Activity, and Biosynthesis

3.1.1 Isolation[1]

Phomoidrides A (CP-225,917) and B (CP-263,114) (**3.10** and **3.11**, respectively) were isolated by a group at Pfizer in 1996[2] from an unidentified fungus, believed to be a steril *Phoma* variant, found on the twigs of a juniper tree in Dripping Springs, Texas. The structures assigned to **3.10** and **3.11** were based on intensive spectroscopic experiments that included FTIR, UV, FAB-MS (FAB = fast atom bombardment), and both 1-D and 2-D NMR spectroscopy. Mass spectrometry helped deliver the molecular formulas ($C_{31}H_{38}O_{10}$ and $C_{31}H_{36}O_9$, for **3.10** and **3.11,** respectively) and molecular weights (570 and 552). UV spectroscopy indicated the presence of an α,β-unsaturated carbonyl (250 nm) and FTIR spectroscopy indicated the presence of a carboxylic acid (3500-3200 cm^{-1}), an anhydride (1830, 1760 cm^{-1}), and long chain methylene motifs (720 cm^{-1}). The specific rotations were found to be $[\alpha]^{25}_D$ = + 23° and − 11° (for **3.10** and **3.11,** respectively). The basic structural makeup was determined by ^1H, ^{13}C, and DEPT, while their structural connectivities were elucidated using COSY and HMBC NMR studies. The relative configuration of H7 in **3.11** was determined by H7-H10 ROESY correlations. The *trans* configuration of H17 and H9 was obtained by NOE and bond distance modeling. It was also determined, based on interconversion experiments, that the stereochemistry at C7 was the same in both **3.10** and **3.11**. The absolute

stereochemistry as illustrated by Scheme 3.10 was confirmed by total synthesis, which will be discussed later.

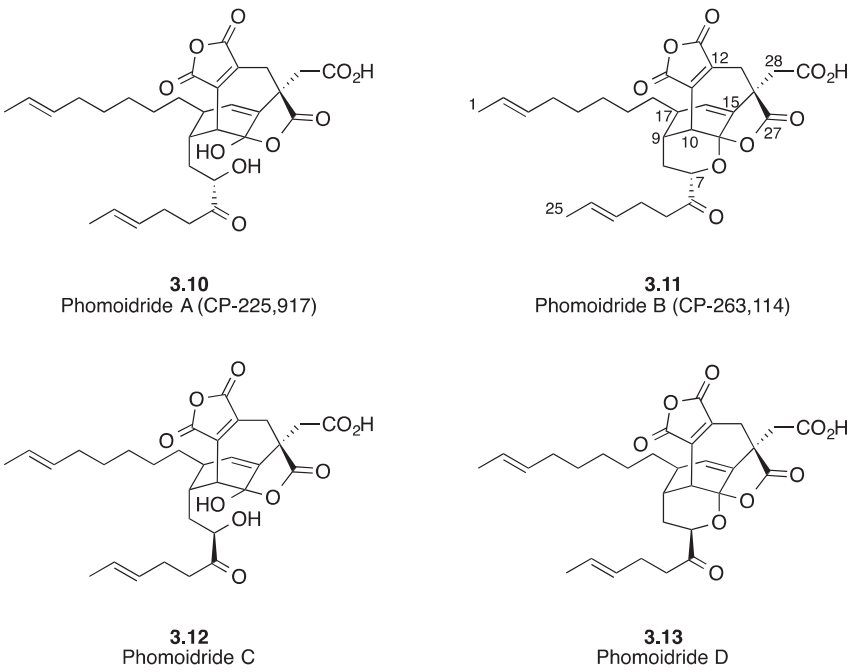

Figure 3.10 The phomoidride family

Phomoidride D (**3.13**) that is epimeric at C7, was later isolated in 1999 by Danishefsky and coworkers (from the **3.10** and **3.11** producing fungus) during their synthetic studies toward **3.10** and **3.11**.[3] They were able to fully characterize and assign absolute stereochemistry of **3.13** through comparison of their synthetic and isolated samples. They were also able to make a synthetic sample of the 7*R*-epimer of **3.10**, which was later isolated from the same organism and named phomoidride C (**3.12**).[4]

A key feature present in the phomoidrides is a bicyclo[4.3.1]decadiene core containing an "anti-bredt" olefin. Originally, Bredt's rule stated that tortional strain on the π-system of a bridgehead double bond made such a system too reactive to exist.[5] The rule was later revised to include only the ring systems studied by Bredt, of the camphene-

and pinene-like structures, while bridgehead olefins in larger ring systems (i.e bicyclo[4.3.1]decene) are considerably less strained. Even though compounds containing a bridgehead olefin in larger rings are isolable they are generally referred to as anti-Bredt.[6] Natural products containing bridgehead olefins are well represented in the literature and have offered synthetic chemist excellent challenges for total synthesis (e.g., phomactins, and taxanes).[7]

A second interesting feature is the maleic anhydride substituent, which is fused to a nine-membered ring. This combination of functional groups allows one to classify the phomoidrides as members of the nonadride family.[8] The term "nonadride" was given to the family upon isolation of its earliest members, which include glaucanic acid (**3.14**), glauconic acid (**3.15**) and byssochlamic acid (**3.16**).[9] The proposed biogenesis of the phomoidrides is based on analogy to the biosynthetic origins of **3.14**.

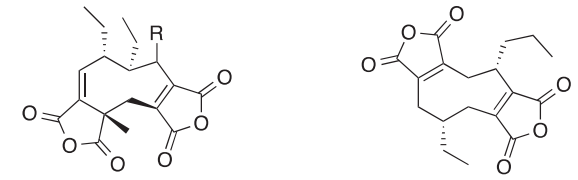

3.14 Glaucanic Acid R = H
3.15 Glauconic Acid R = OH

3.16
Byssochlamic Acid

Figure 3.11 Early nonadride examples

3.1.2 Phomoidride Biogenesis

Upon isolation of **3.10** and **3.11**, Kaneko and coworkers proposed that the biogenesis of the phomoidrides was analogous to that of **3.14** (Scheme 3.10).[2, 10] Sulikowski and coworkers later expounded upon this by drawing relation to polyketide and fatty acid biosynthesis.[11] They proposed that a condensation between oxaloactic acid (**3.18**) and an enzyme bound dodecadiene **3.20** would deliver maleic anhydride **3.21**. A

dimerization of **3.21** via successive conjugate addition is proposed to deliver enolate **3.23** that could further react in an intramolecular aldol fashion. Loss of CO_2 and oxidation at C6 and C7 furnishes phomoidride A (**3.10**) which, upon dehydration, would produce phomoidride B (**3.11**).

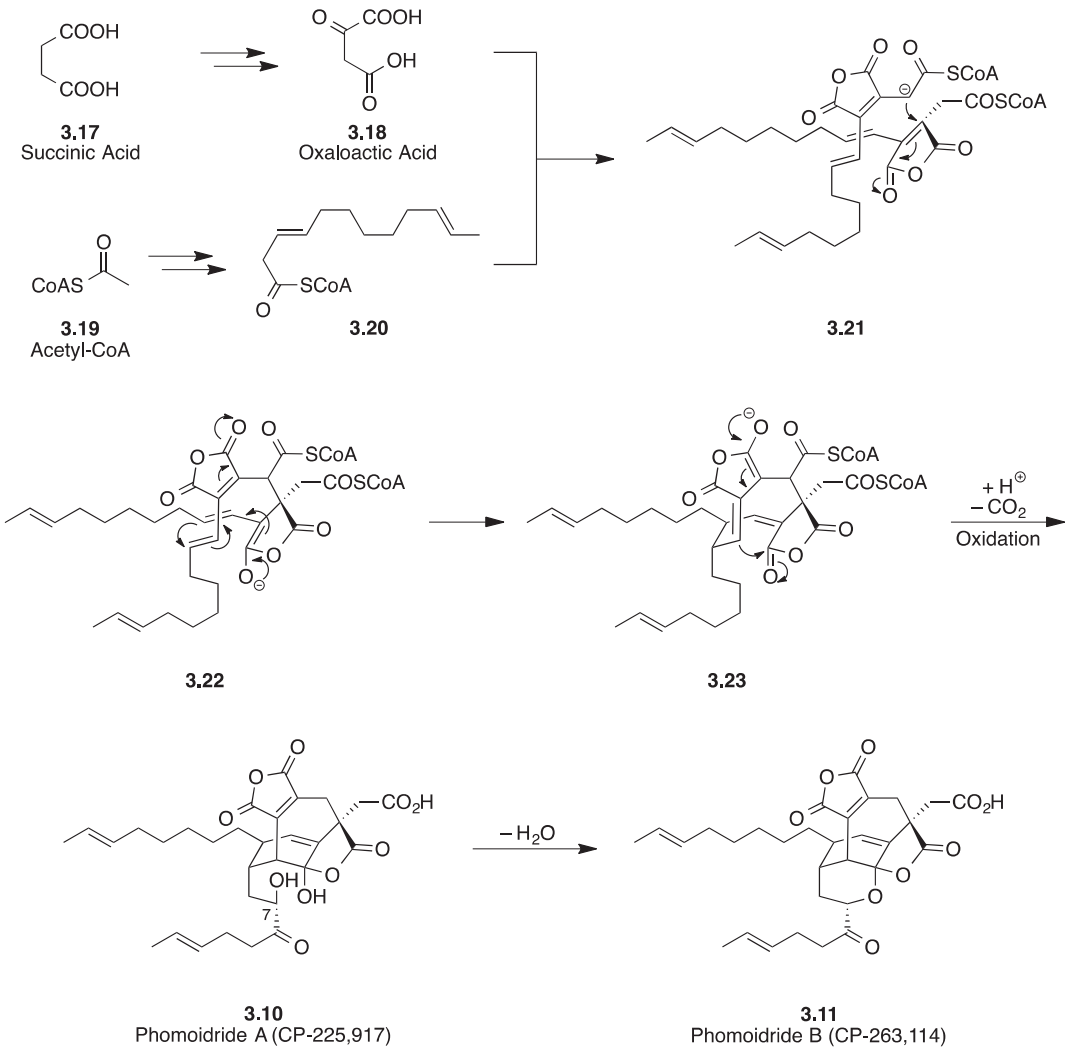

Scheme 3.10 Biosynthesis of phomoidrides A and B[1]

To support this biosynthetic proposal, Sulikowski and coworkers prepared two unsaturated maleic anhydrides. One (**3.24**) contained an *N*-acyl cysteamide (SNAC) ester and the other (**3.25**) a hydrogen. Feeding studies using the phomoidride isolating

organism (ATCC 74256) were performed on both **3.24** and **3.25**, and only the thioester **3.24** produced [*d*]-**3.11** with deuterium incorporated.[12]

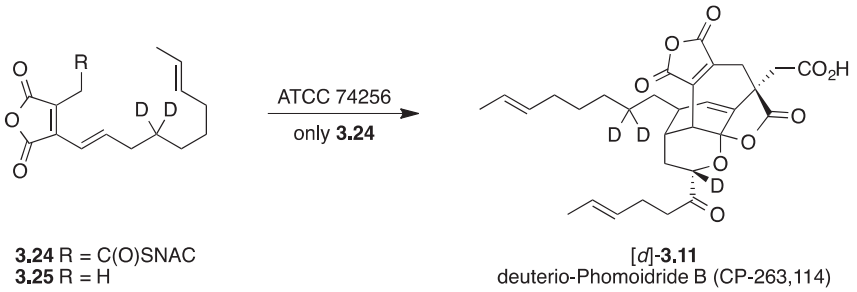

Scheme 3.11 Sulikowski's deuterium labeling studies

3.1.3 Biological Activity

Upon isolation, Phomoidrides A (**3.10**) and B (**3.11**) were shown to exhibit moderate biological activities toward the inhibition of the squalene synthase (SQS) protein (IC_{50} = 43 μM and 160 μM, respectively). SQS promotes the formation of squalene from farnesyl pyrophosphate, which is also known as the first committed step of cholesterol biosynthesis. Both molecules have also shown the ability to inhibit RAS-farnesyl transferase in rats, with IC_{50} values of 6 μM and 20 μM, respectively. Although both **3.10** and **3.11** have shown good activity toward inhibition of SQS and RAS-farnesyl transferase, phomoidride C's (**3.12**) and D's (**3.13**) bioactivities remain untested.

3.1.4 Interconversion and Epimerization

Experiments performed during the course of the isolation work and subsequent synthetic studies toward **3.10** and **3.11**, established conditions whereby these natural products could be interconverted. Specifically, Kaneko and coworkers showed that **3.10** undergoes dehydration to furnish **3.11** upon treatment with methanesulfonic acid

(MsOH),[2] while Nicolaou and coworkers observed the conversion of **3.11** to **3.10** upon exposure of the former to aqueous lithium hydroxide (LiOH).[13]

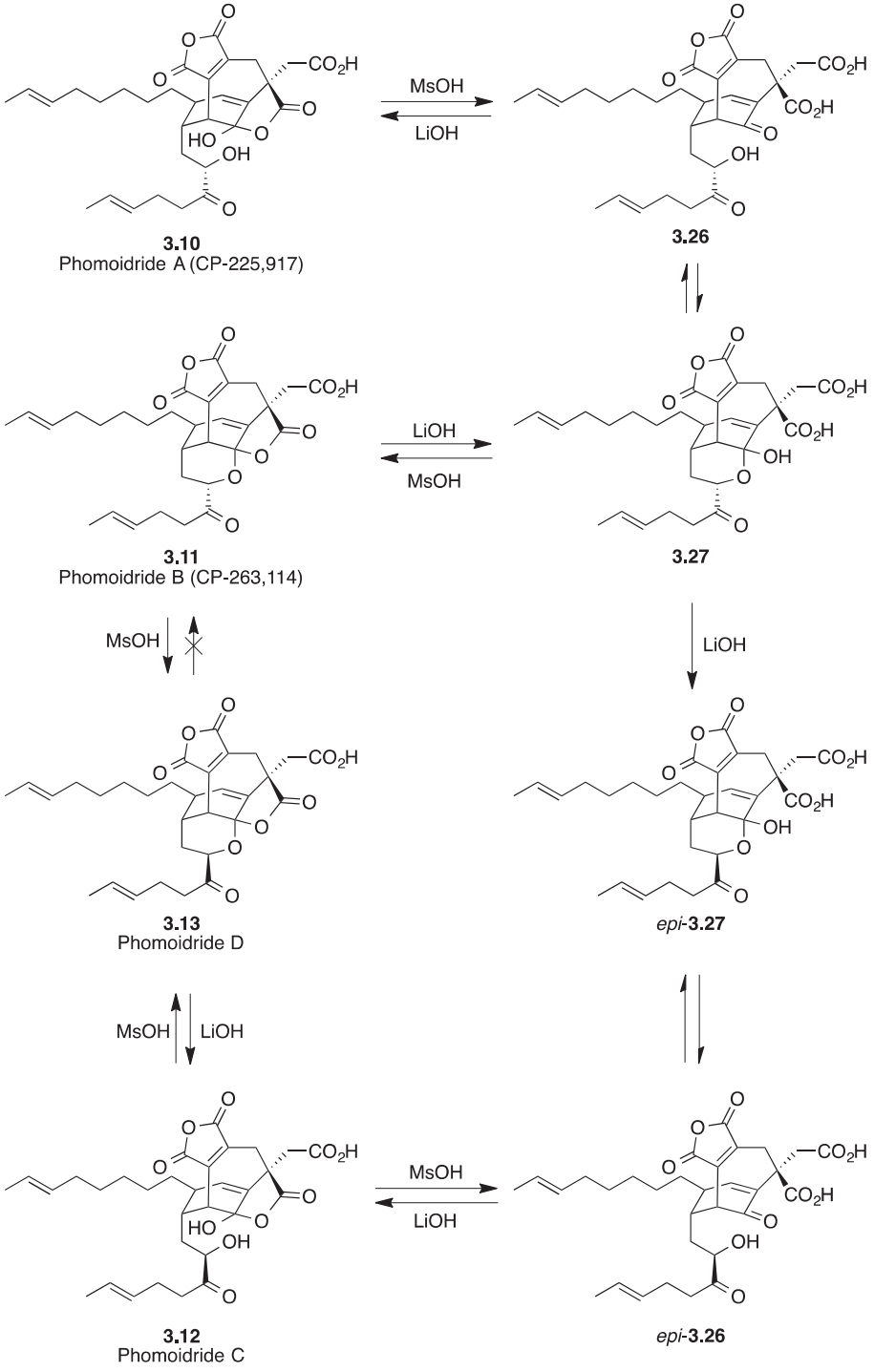

Scheme 3.12 Phomoidride interconversion and epimerization

Sulikowski and coworkers performed studies to elucidate the mechanism of the interconversion (Scheme 3.12). They found that treating **3.10** with MsOH opened the lactone to give ketone **3.26**,[2,3] which exists in equilibrium with hemi-acetal **3.27**, and **3.11** is formed upon lactonization. The reverse of this transformation also holds true. **3.11** can react with LiOH to form hemi-acetal **3.27** through the addition to the lactone carbonyl, then hemi-acetal **3.27,** that is in equilibrium with ketone **3.26,** delivers **3.10** in the presence of LiOH.

During their synthetic efforts toward the phomoidrides, Danishefsky and coworkers observed the epimerization of **3.11** to **3.13** in the presence of MsOH.[3] This was proposed to occur due to the relief of steric strain imposed upon the molecule when the C7 side chain changes from *endo* (7*S*-epimer, **3.11**) to *exo* (7*R*-epimer, **3.13**), relative to the bicyclic ring system. While it remains unclear why the 7*R*-epimer (**3.12**) of the open form is preferred over the 7*S*-epimer (**3.10**), Sulikowski and coworkers proposed that hemi-acetal **3.27**, in the presence of LiOH, epimerizes to give *epi*-**3.27**, which exists in equilibrium with *epi*-**3.26**.[2] Similar to the aforementioned pathway, *epi*-**3.26** can then form **3.12** in the presence of LiOH. Finally, Danishefsky also demonstrated that the interconversion between **3.12** and **3.13** occurs in the same manner as was observed for interconversions between **3.10** and **3.11**.

3.2 Completed Total Syntheses of the Phomoidrides

3.2.1 Synthetic Challenges

The phomoidrides' structural features make them an intriguing and challenging target for organic synthesis. As illustrated for **3.11** (Figure 3.12) challenging synthetic features include: a hydrolytically labile maleic anhydride, a stereogenic all carbon

quaternary center, a labile bridged spiroacetal (*vide supra*), two side chains containing olefins (which present an oxidation liability), and an epimerizable stereocenter; structural features which are all present on a bicyclo[4.3.1]decadiene carbocyclic core that contains a bridgehead olefin. As one might expect, this combination of intriguing structural features has attracted the attention of many synthetic chemists and led them to design creative and novel synthetic strategies for the synthesis of the phomoidrides. As a result, numerous interesting and remarkably diverse approaches have been developed, particularly for accessing the carbocyclic core.[14] Despite all these synthetic efforts, only four total syntheses have been reported to date.

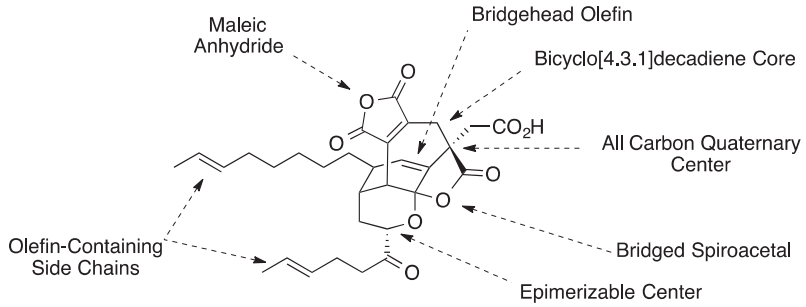

3.11
Phomoidride B (CP-263,114)

Figure 3.12 Synthetic challenges presented by the phomoidrides

3.2.2 K. C. Nicolaou and Coworkers

The first reported total synthesis of a member of the phomoidride family was completed in the laboratory of K. C. Nicolaou. Their synthetic strategy targeted phomidride A (**3.10**) and provided access to **3.11** via the acid-catalyzed dehydration eluded to previously (Scheme 3.13). As illustrated retrosynthetically, Phomoidride A

(**3.10**) was formed from the bicyclo[4.3.1]decene **3.28**, which was obtained from a key intra-molecular Diels-Alder (IMDA) cycloaddition of diene **3.29**.[15]

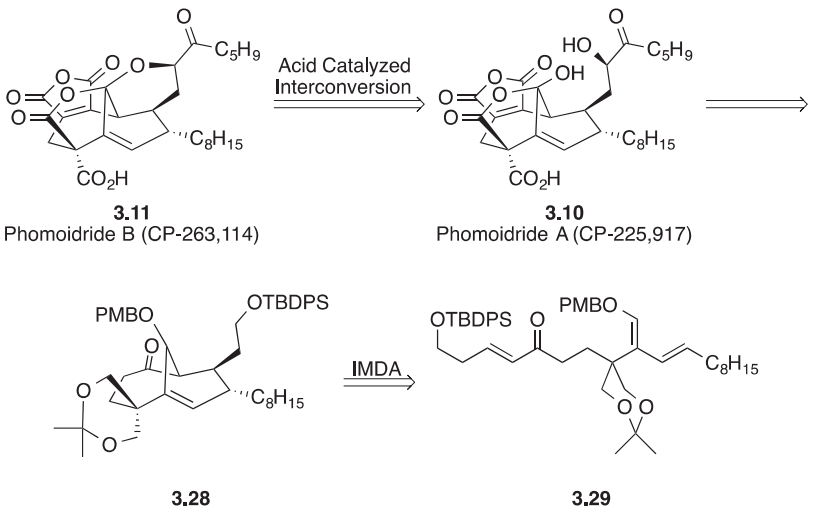

3.11
Phomoidride B (CP-263,114)

3.10
Phomoidride A (CP-225,917)

3.28

3.29

Scheme 3.13 Nicolaou's retrosynthetic analysis

In a forward sense, Nicolaou and coworkers began their synthesis with the sequential alkylation of dimethyl malonate with alkyl iodide **3.31** and allyl bromide in the presence of sodium hydride (NaH) (Scheme 3.14). Reduction of the esters and protection of the diol as the acetonide produced alkene **3.32**. Ozonolysis of the terminal alkene **3.32** then allowed them to extend their system through an enamine assisted aldol condensation of **3.33**, which effectively installed what would become the C17 side chain.

The key Diels-Alder cycloaddition, which delivers the bicyclic core of the phomoidrides, was effected using dimethyl aluminum chloride in DCM, to give **3.28** in 90% yield. Silyl deprotection and oxidation of the resultant aldehyde provided an electrophilic coupling partner for the installation of the C7 side chain, which was incorporated using the nucleophilic addition of alkyllithium **3.37** to give alcohol **3.36**.

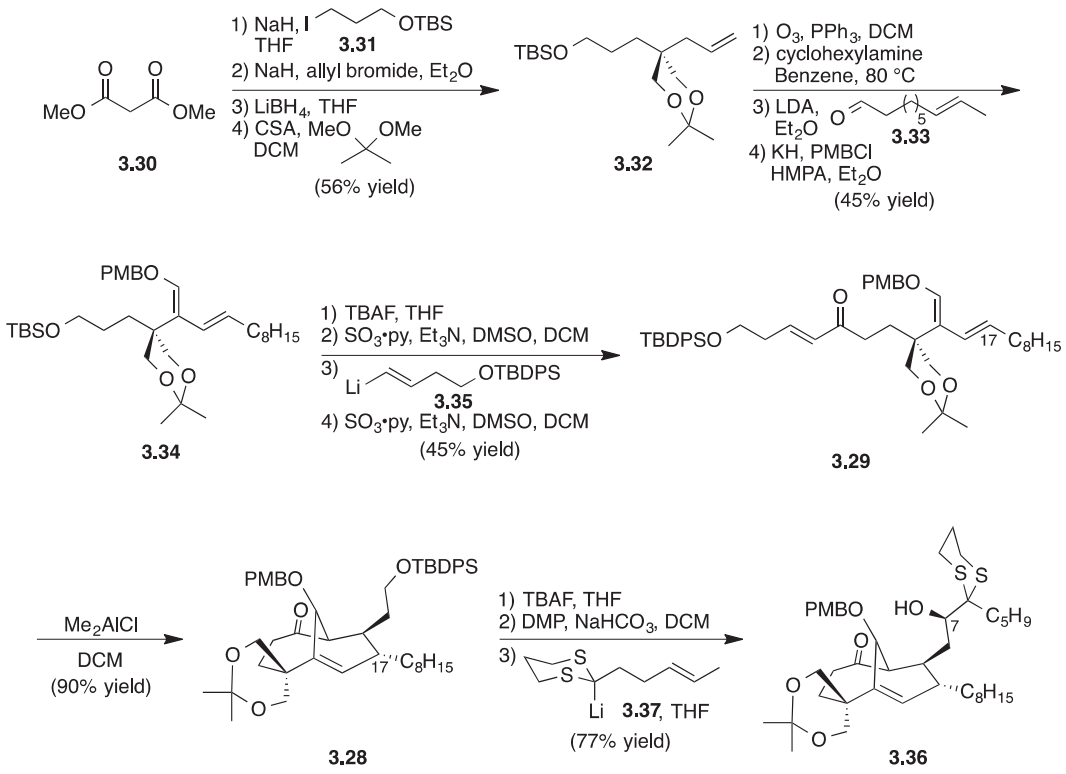

Scheme 3.14 Nicolaou's access to the phomoidride core

Upon successful formation of the bicyclo[4.3.1]decene core and installation of the two olefin-containing side chains, Nicolaou and coworkers directed their attention toward introducing the maleic anhydride (Scheme 3.15). The sequence began with ketone **3.36,** which upon undergoing palladium catalyzed carbonylation and subsequent ester reduction, provided allylic alcohol **3.39**. Epoxidation of the olefin and *syn* addition of a cyano group then furnished diol **3.40**, which then underwent a three-step sequence consisting of epoxide formation, β-elimination, cyclization and air oxidation to deliver maleic anhydride **3.41**. Further protecting group manipulations delivered alcohol **3.42**, a substrate positioned for the formation of the γ-lactone and introduction of the spiroacetal.

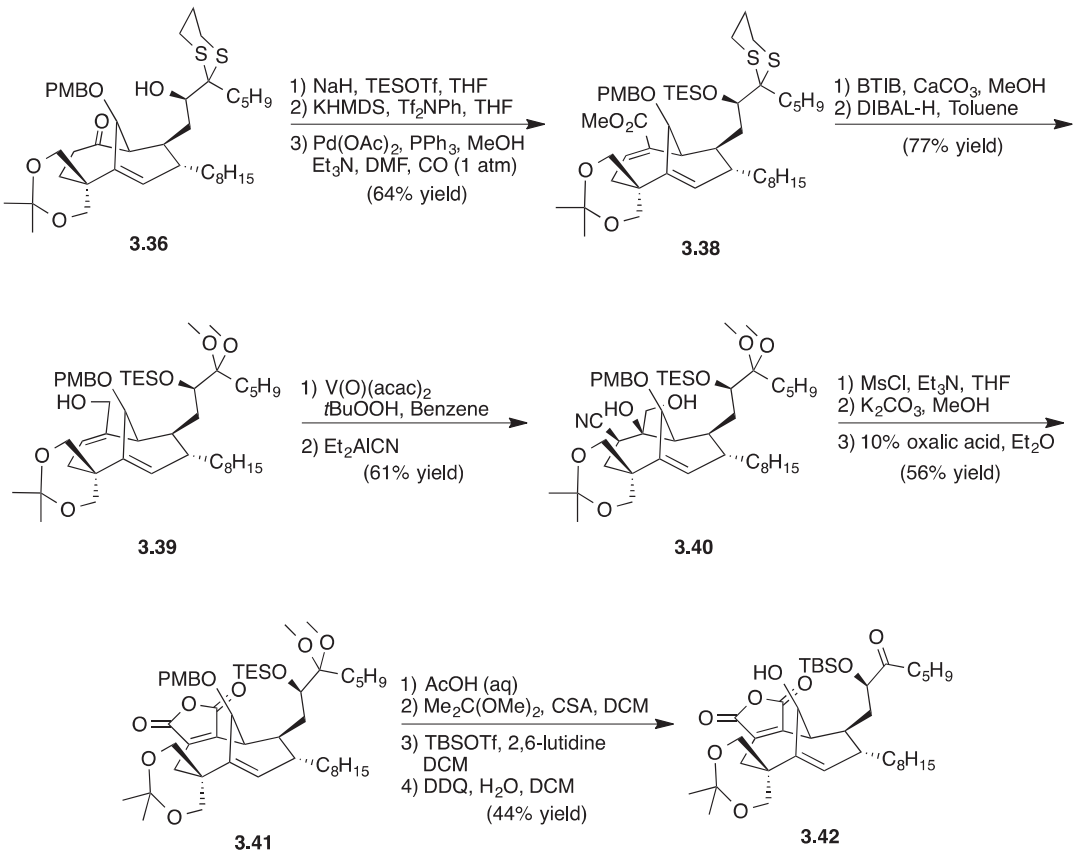

Scheme 3.15 Nicolaou's formation of the maleic anhydride

To complete the synthesis, alcohol **3.42** was oxidized and deprotected to furnish cyclized hemi-acetal **3.43** (Scheme 3.16). Further oxidations and protecting group manipulations delivered silyl acetal **3.44**, which was subjected to an Arndt-Eistert homologation sequence to deliver an intermediate acid which, upon condensation with indoline, TBS-deprotection, and oxidation of the resultant lactol to the gamma-lactone, delivered amide **3.46**. A two-step conversion of the amide to the acid delivered phomoidride A (**3.10**) in 46 steps from dimethyl malonate. The use of Kaneko's conditions for the conversion of **3.10** to **3.11** resulted in the first total synthesis of phomoidride B.[2]

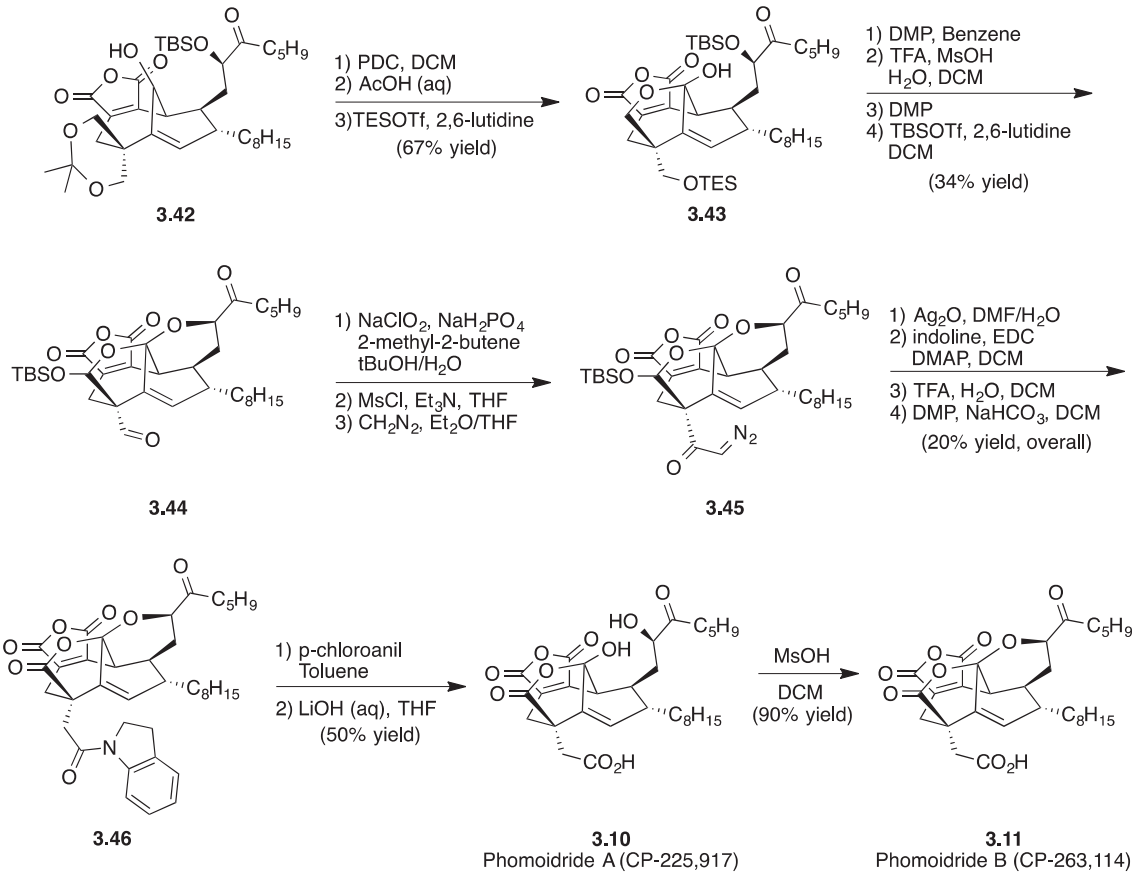

Scheme 3.16 Nicolaou's completion of **3.10** and **3.11**

Nicolaou and coworkers also sought to perform the first asymmetric synthesis toward **3.10** and **3.11** (Scheme 3.17). Using (+)-glycidol (**3.47**) as their point of departure, they were able to prepare Diels-Alder precursor **3.50** in six synthetic steps. The Diels-Alder reaction was accomplished using an aluminum catalyst **3.52**, which upon silyl deprotection and oxidation intercepted an intermediate (**3.51**) employed in their racemic synthesis. Following their previously developed synthetic route, they were able to form enantioenriched amide (+)-**3.46**, which was compared to an analogous indoline amide formed from natural (−)-**3.11**. They found their synthetic material had the opposite optical rotation compared the indoline derived from natural material. They concluded that the absolute configuration was that illustrated in Figure 3.10, and that it

could be obtained via total synthesis utilizing their previously demonstrated route, but originating from (*S*)-glycidol instead.

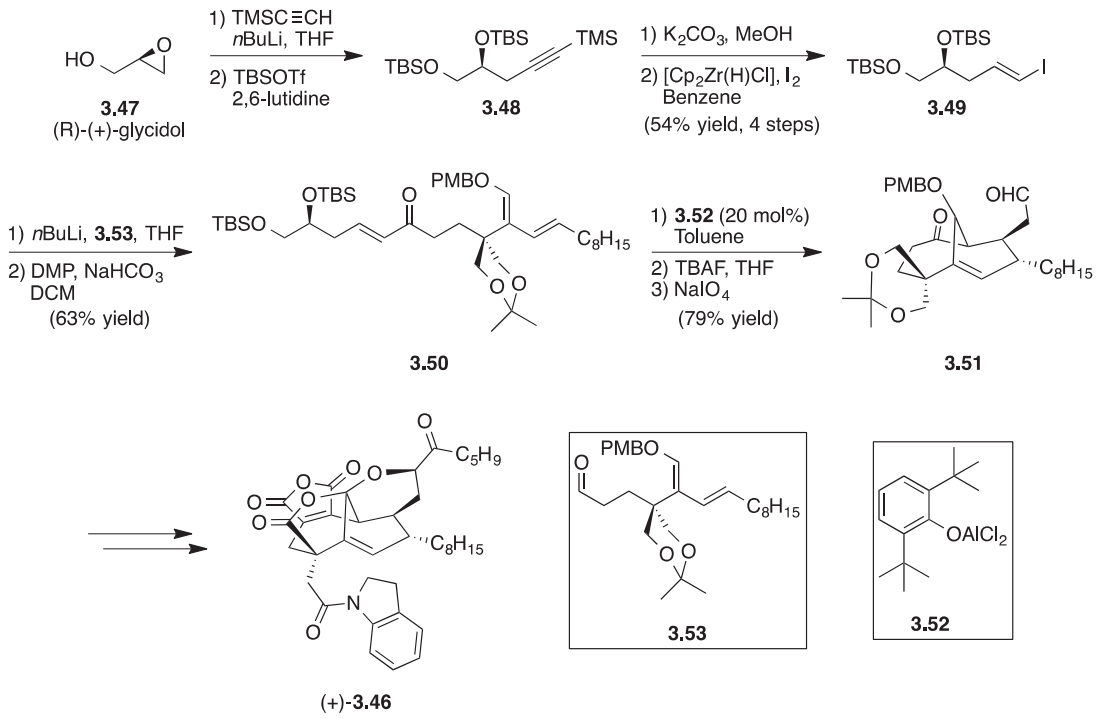

Scheme 3.17 Nicolaou's asymmetric synthesis

In summary, Nicolaou and coworkers completed the first total synthesis of phomoidrides A and B, in 46 and 47 synthetic steps, respectively, by utilizing an intramolecular Diels-Alder cycloaddition to form the bicyclo[4.3.1]decene core and installing the maleic anhydride from ketone **3.36**. Acid catalyzed conditions discovered by Kaneko and coworkers were employed to convert phomoidride A to B in one synthetic step. Adaptation of the racemic synthesis employing (+)-glycidol as the point of departure allowed the eventual assignment of absolute stereochemistry.

3.2.3 Fukuyama and Coworkers

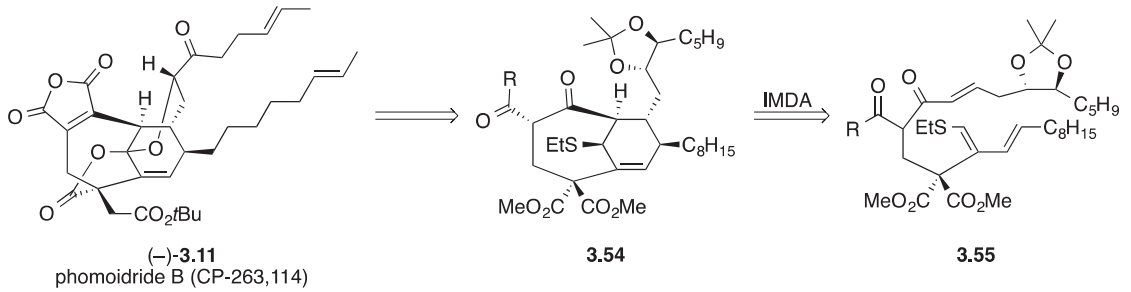

Scheme 3.18 Fukuyama's retrosynthetic analysis

In 2000, Fukuyama and coworkers' published a synthesis of (−)-**3.11** that also employs an intramolecular Diels-Alder cycloaddition strategy to establish the bicyclo[4.3.1]decadiene core of phomoidride B (Scheme 3.18). In contrast to the Nicolaou approach, Fukuyama's synthesis directly furnished **3.11** instead of utilizing the acid catalyzed conversion from **3.10**.[16]

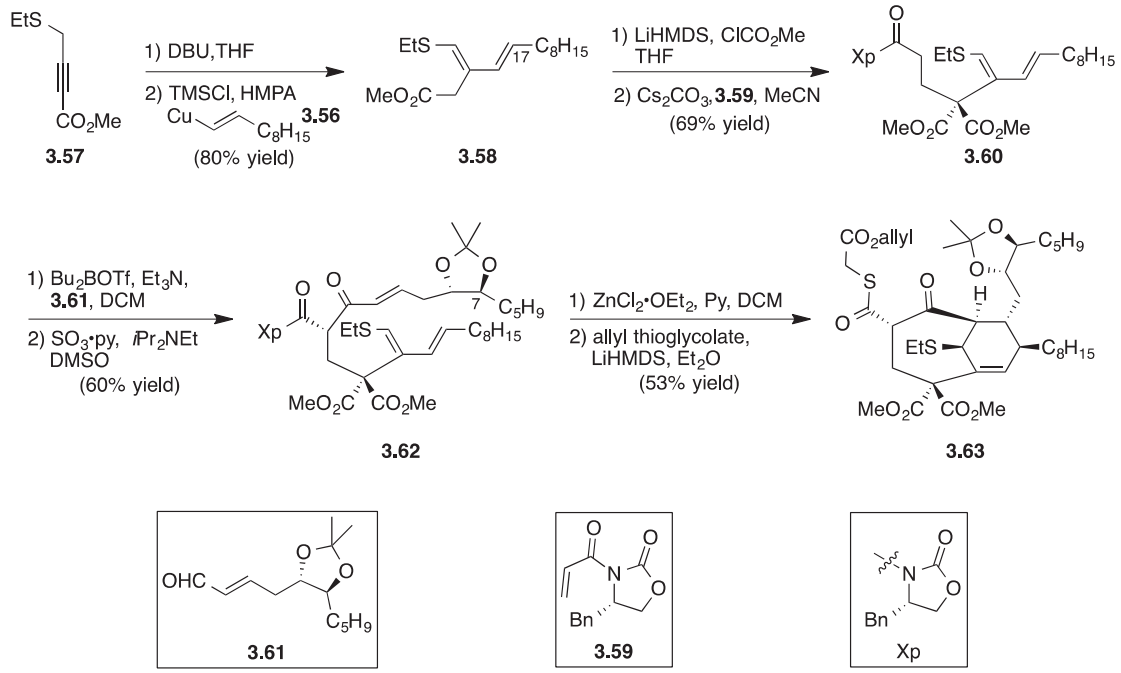

Scheme 3.19 Fukuyama's intramolecular Diels-Alder (IMDA)

As illustrated in Scheme 3.19, Fukuyama and coworkers began by converting alkyne **3.57** to the corresponding allene which was subjected to 1,4-addition of a vinyl cuprate to install the C17 side chain. Installation of the Evans chiral auxiliary set the stage for a diastereoselective aldol addition to introduce the C7 side chain and form diene **3.62.** Intramolecular Diels-Alder cycloaddition of the derived diene occurred smoothly to give intermediate **3.63** and establish the bicyclo[4.3.1]decene core.

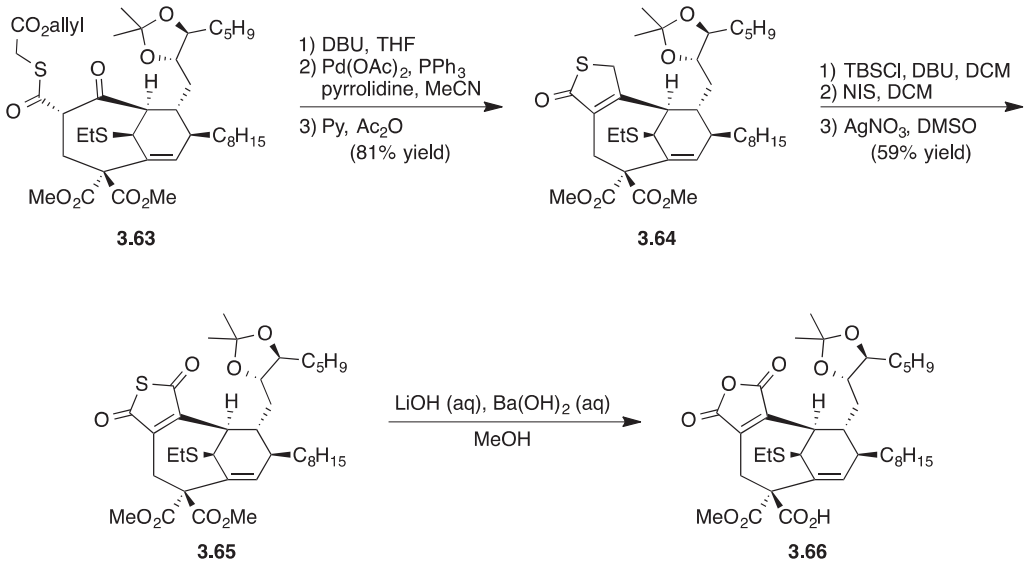

Scheme 3.20 Fukuyama's maleic anhydride synthesis

With the core structure assembled, Fukuyama and coworkers turned their attention to the formation of the maleic anhydride. To this end, an intramolecular aldol condensation and decarboxylation furnished thiobutenolide **3.64**, which was further oxidized to give thiomaleic anhydride **3.65**. Under the condition of lithium hydroxide and barium hydroxide, both the hydrolysis of the thiomaleic anhydride to the maleic anhydride and hydrolysis of the less hindered methyl ester were accomplished, delivering acid **3.66.**

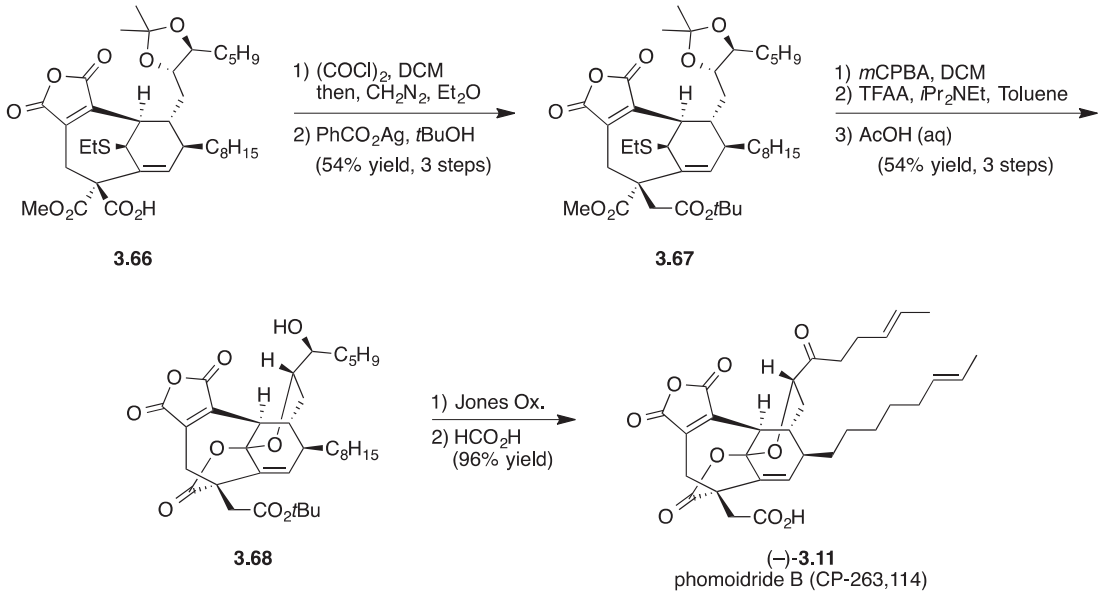

Scheme 3.21 Completion of Fukuyama's synthesis

In a manner analogous to Nicolaou, Fukuyama and coworkers completed their synthesis by employing an Arndt-Eistert homologation sequence to deliver *tert*-butyl ester **3.67**. Oxidation of the thioether to the ketone and subsequent acetonide deprotection delivered spiroacetal **3.68**. A Jones oxidation and hydrolysis of the *tert*-butyl ester completed the total synthesis of (−)-**3.11** in 27 linear steps from commercially available starting materials.

Although they achieved the total synthesis of phomoidride B, they later reported an alternative route for maleic anhydride formation.[17] Utilizing the same chemistry as previously reported to form diene **3.60**, they then performed diastereoselective aldol reaction on a similar aldehyde subunit lacking the C7 side chain. Subsequent intramolecular Diels-Alder provided the desired bicyclo[4.3.1] core of thioester **3.71**. At this point the synthetic strategy deviates from their previous report, instead of an

aldol/thiomaleic anhydride sequence, they opted to install a vinyl triflate precursor (Scheme 3.22).

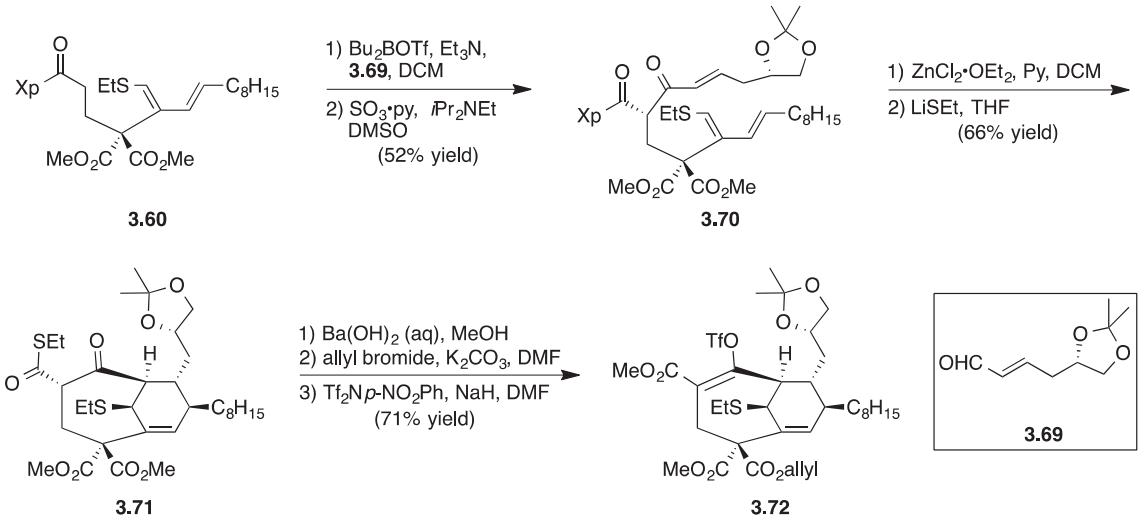

Scheme 3.22 Fukuyama's second-generation strategy

To complete their second-generation synthesis of **3.11** (Scheme 3.23), Fukuyama and coworkers selectively removed the allyl ester in **3.73** and performed an Arndt-Eistert sequence to deliver *tert*-butyl ester **3.74**. Subsequent oxidation and Pummerer rearrangement of the thioether furnished ketone **3.75**, which, upon palladium-catalyzed carbonylation and acetonide removal furnished intermediate **3.76**. The final steps of this second-generation synthesis involved installation of the side-chain attached at C7 via alcohol oxidation to the acid, conversion to the corresponding thioester and palladium catalyzed coupling between the thioester and an alkyl zinc reagent. The derived ketone was subjected to ester hydrolysis which furnsished phomoidride B.

In summary, Fukuyama and coworkers were able to prepare phomoidride B (**3.11**) utilizing a strategy similar to that reported by Nicolaou. Both groups exploited an intramolecular Diels-Alder cycloaddition to construct the bicyclic core of the

phomoidrides. Additionally, they both introduced the olefin-containing side chains early in the synthesis, followed by the installation of the maleic anhydride moiety and spiroacetal in a linear fashion. Although the routes were very similar overall, Fukuyama's asymmetric total synthesis was 20 synthetic steps shorter than that of Nicolaou, partially due to their quick access to the maleic anhydride and relatively few protecting group manipulations.

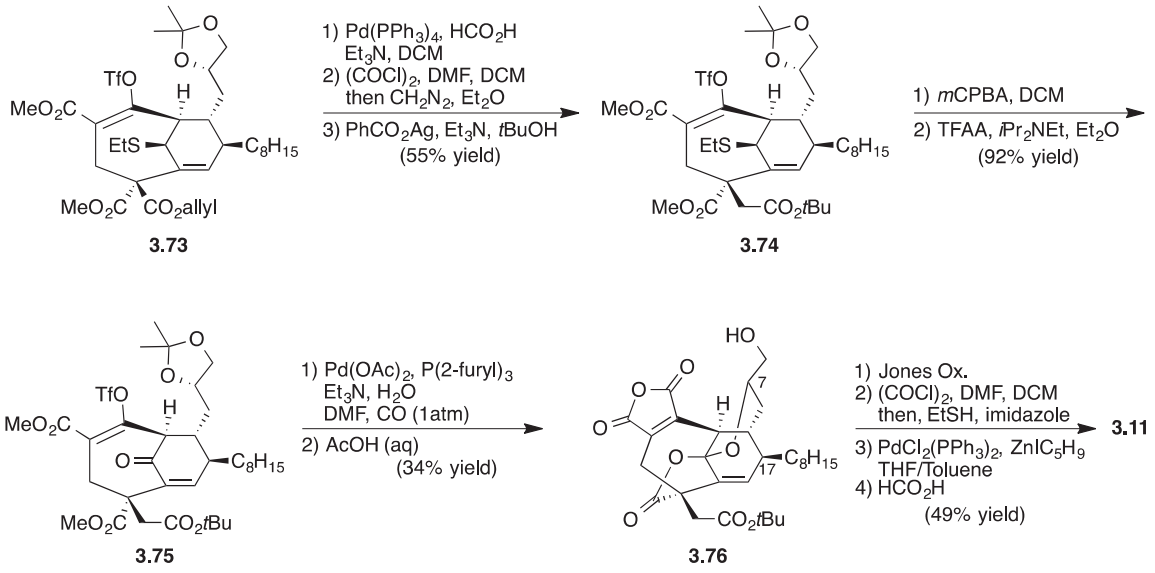

Scheme 3.23 Fukuyama's second-generation synthesis

3.2.4 Shair and Coworkers

Shair and coworkers' approach toward (+)-**3.11** was quite different to previous known syntheses. While Fukuyama made the natural enantiomer, both Nicalaou and Shair formed the unnatural isomer. In contrast to the previous syntheses, which utilized an intramolecular Diels-Alder cycloaddition, Shair and coworkers envsioned an anion accelerated oxy-cope rearrangement as giving rise to the bicyclo[4.3.1]decene core of the phomoidrides (Scheme 3.24).

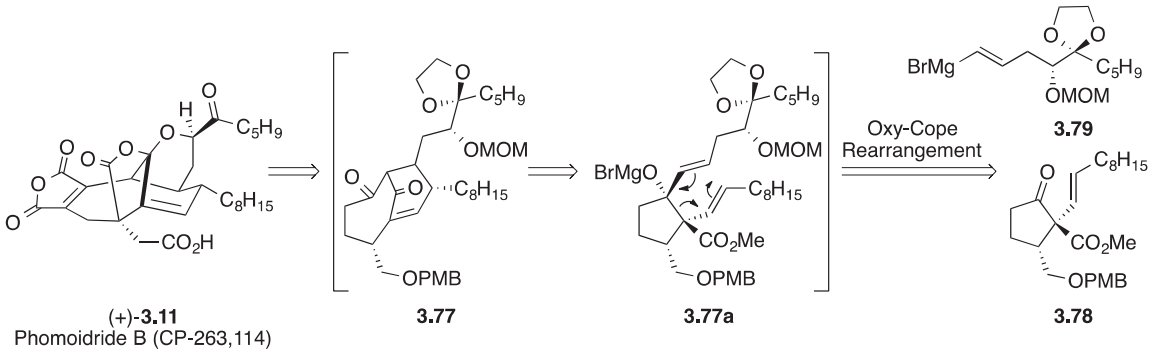

Scheme 3.24 Shair's retrosynthetic analysis

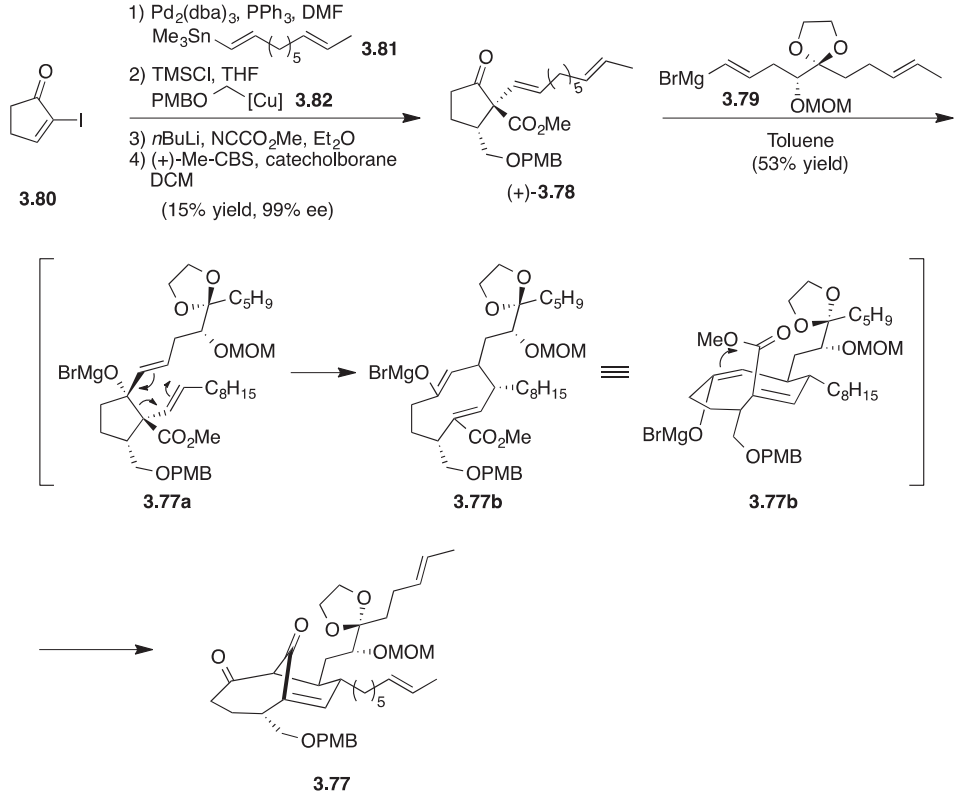

Scheme 3.25 Shair's approach toward the core

Beginning with cyclopentenone **3.80**, Shair and coworkers were able to form densely functionalized derivative (+)-**3.78** in a 99% ee via Stille coupling, conjugate addition, acylation, and kinetic resolution (Scheme 3.25). The reaction of

cyclopentanone (+)-**3.78** with vinyl Grignard **3.79** induced the desired oxy-cope rearrangement, resulting in the formation of bicycle **3.77**.[18]

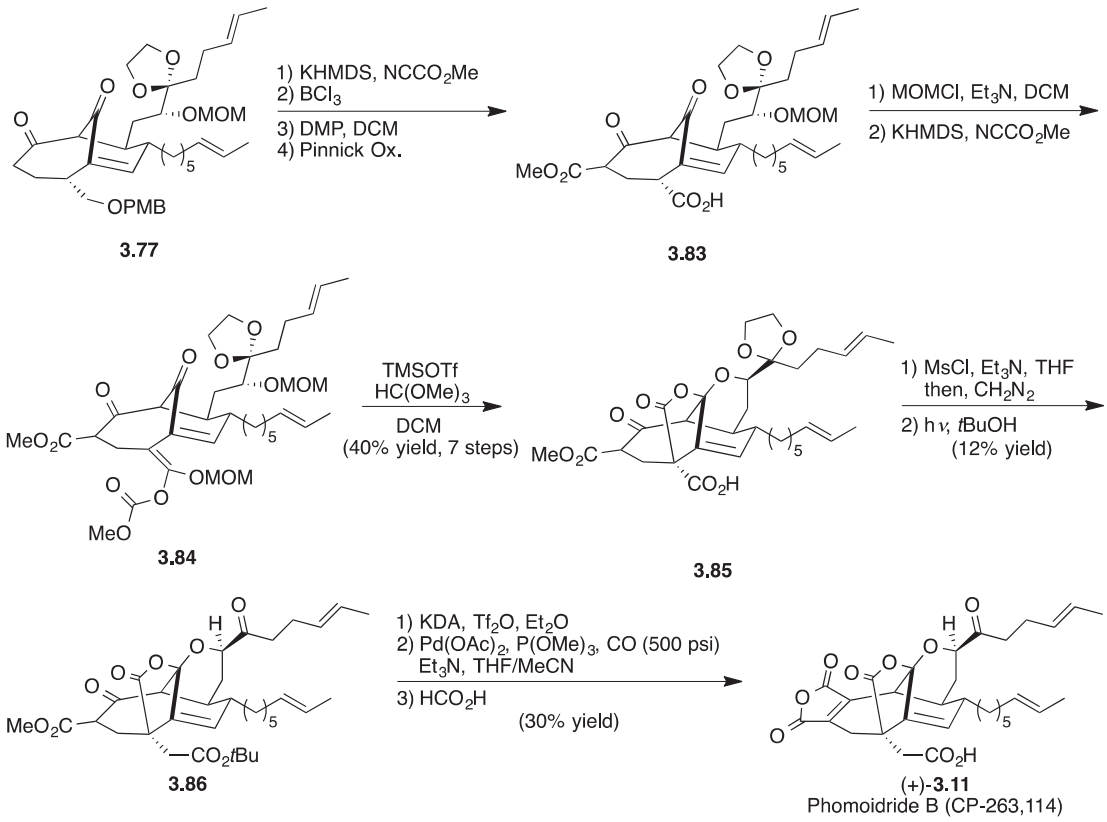

Scheme 3.26 Shair's completion of (+)-**3.11**

Acylation and oxidation of **3.77** using Mander's reagent provided acid **3.83**, which was further functionalized to afford ketene acetal **3.84**. The ketene acetal was subjected to a Fries-type rearrangement followed by subsequent cyclization to form the spiroacetal and γ-lactone of **3.85**. Lastly, an Arndt-Eistert type homologation, a carbonylative maleic anhydride formation of the vinyl triflate generated from the β-ketoester **3.86**, and hydrolysis of the ester completed the total synthesis of (+)-**3.11** in a total of 22 linear steps.

In summary, Shair and coworkers' synthesis of **3.11** is the most efficient to date, consisting of only 22 linear steps from commercially available starting materials. The efficiency of their approach derives from the convergent manner in which they access the anionic oxy-Cope substrate and the elegant Fries-type rearrangement cascade that furnishes the spiroacetal and γ-lactone simultaneously.

3.2.5 Danishefsky and Coworkers

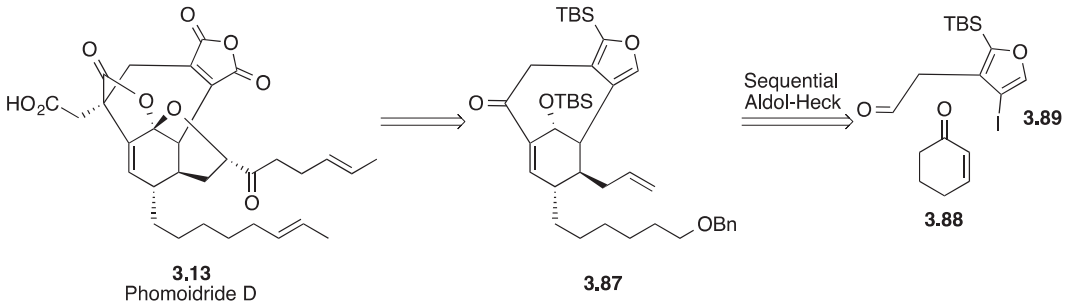

Scheme 3.27 Danishefsky's retrosynthetic analysis

Danishefsky and coworkers were the last to report a completed total synthesis of a member of the phomoidride family. In this effort it was envisioned that the bicyclo[4.3.1]decene core of the phomoidrides would arise from a sequential aldol-Heck cyclization between furan **3.89** and cyclohexenone **3.88**. In addition, this approach featured a silylated furan as a masked precursor to the maleic anhydride that could be carried through several synthetic operations..

In the forward sense, Danishefsky and coworkers began with furan **3.90**, which in five steps was converted to cyanide **3.91** (Scheme 3.28). Reduction of the cyano group to the aldehyde, followed by an aldol reaction with **3.88** and Heck cyclization, delivered bicyclo[4.3.1]decene **3.92**. Alcohol protection (TBS) followed by allylic oxidation,

enone formation and halogenation furnished vinyl iodide **3.93**. Installation of a precursor to the C17 side chain via palladium mediated cross coupling, followed by allylation, and reduction provided diol **3.94**.

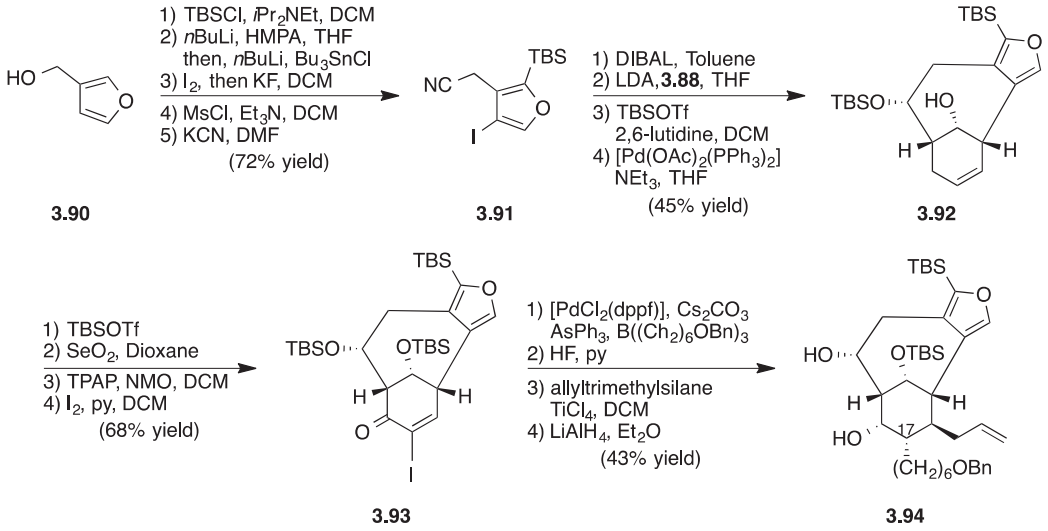

Scheme 3.28 Danishefsky's formation of the phomoidride core

As illustrated in Scheme 3.29, the bicyclic core was completed from **3.94** by installing the bridgehead olefin via an elimination sequence that delivered enone **3.87**.[19] The formation of the γ-lactone and spiroacetal commenced with an olefination and [2+2] ketene cycloaddition to deliver spirocyclobutane **3.95**. Thioether formation, Baeyer-Villager reaction, and dihydroxylation of the primary olefin produced hemiacetal **3.96**, which upon methanolysis and Swern oxidation delivered lactone **3.97**.[20]

In the final stages of the synthesis, the C7 side chain was installed by addition of alkyl magnesium bromide **3.98** to aldehyde **3.97** followed by oxidation. Deprotection of the benzyl ether, oxidation to the aldehyde, and olefination formed the C17 side chain and produced furan **3.99** (Scheme 3.30). Conversion of the furan to the maleic anhydride was effected in two-steps via exposure of **3.99** to singlet oxygen followed by TPAP.

Subsequent hydrolysis of the methyl ester produced phomoidride C, which was converted to phomoidride D (**3.13**) in the presence of acid. At this point, neither **3.12** nor **3.13** had been isolated previously and thus it was unknown if it was a natural product; hence, Danishefsky performed a seven-step sequence to epimerize the C7 stereocenter and obtained phomoidride A (**3.10**).[21]

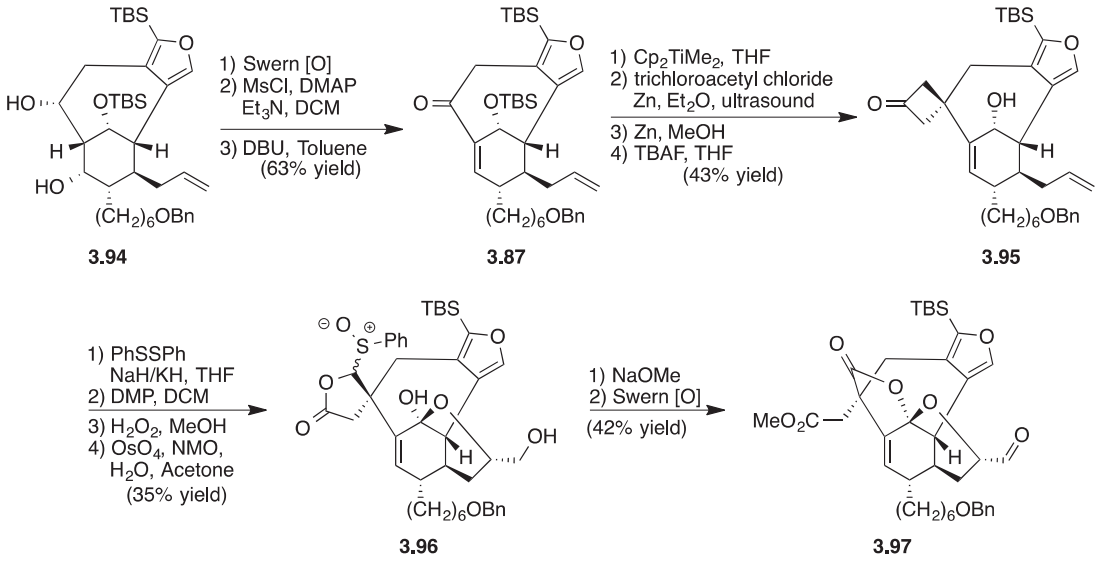

Scheme 3.29 Spiroacetal and γ-lactone formation

In summary, Danishefsky completed the first total synthesis of phomoidrides C (**3.12**) and D (**3.13**) in 39 and 40 synthetic steps, respectively, from commercially available starting materials. They utilized a sequential aldol-Heck cyclization process to form a [4.3.1]bicycle which upon dehydrative installation of the bridgehead double bond produced the phomoidride core. Incorporation of the 5-membered lactone and spiro-acetal preceded a late stage transformation of the furan motif to the maleic anhydride and completion of the total synthesis.

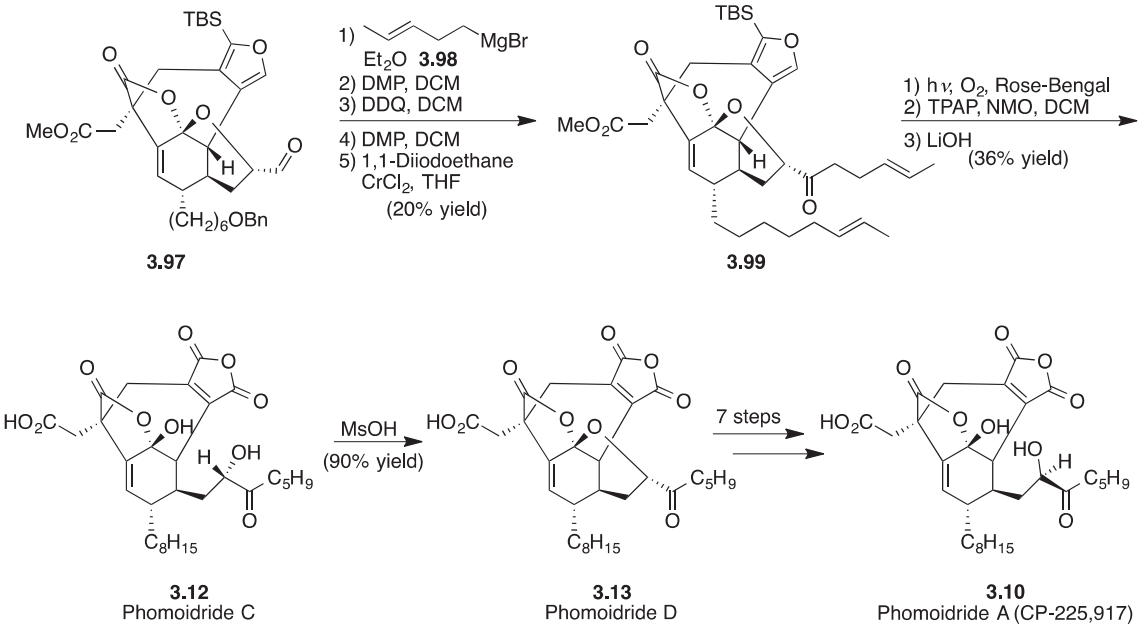

Scheme 3.30 Completion of phomoidride D

3.2.6 Comparison of the Completed Total Syntheses

Each prior synthetic strategy contains a unique approach to one of the key features contained in the phomoidrides (Figure 3.13). Nicolaou, Fukuyama, and Shair all installed the side chains prior to the construction of the bicyclic core. Additionally, all of the syntheses incorporated the spiroacetal and maleic anhydride substituents after the formation of the bicyclic core, although Danishefsky utilized a furan functionality that served as a latent precursor to the maleic anhydride. Although each synthesis differed in term of the tactics employed for introducing functionality, the overall strategies were fairly similar and key transformations were involved during assembly of the bicyclo[4.3.1]decadiene core.

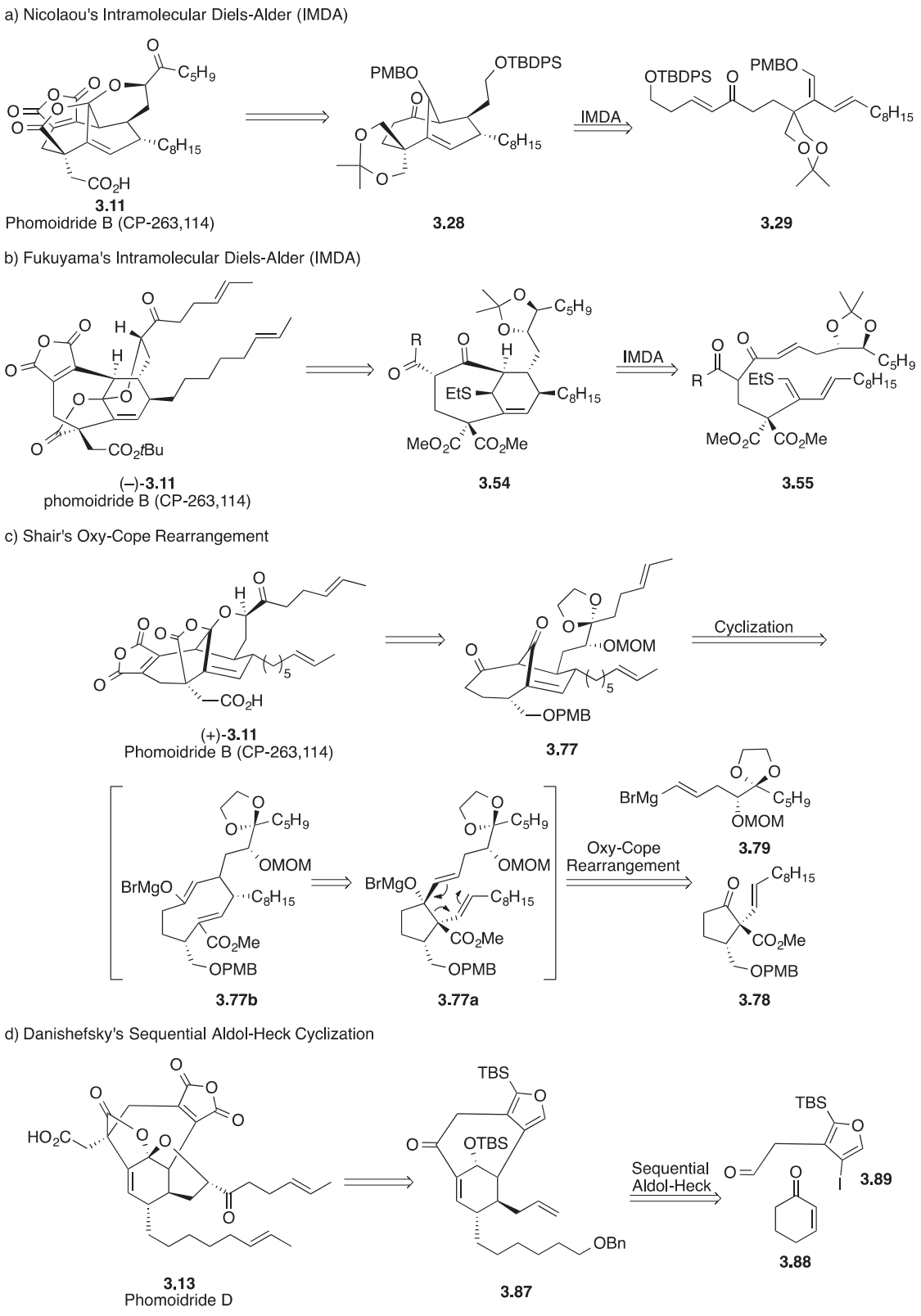

Scheme 3.31 Comparison of synthetic approaches

A comparison of the different approaches employed to access the core is illustrated in Scheme 3.31. In addition this Scheme illustrates the phomoidride structures as rendered in the original publications. Interestingly, as one often finds, different retrosynthetic disconnections become apparent when viewing the molecules from a different perspective and this, in turn, leads to the diversity of synthetic approaches reported for the same target.

3.3 The Wood Group's Previous Synthetic Efforts Toward the Phomoidrides

3.3.1 Evolution of a Fragmentation Strategy Toward the Bicyclo[4.3.1]decadiene Core

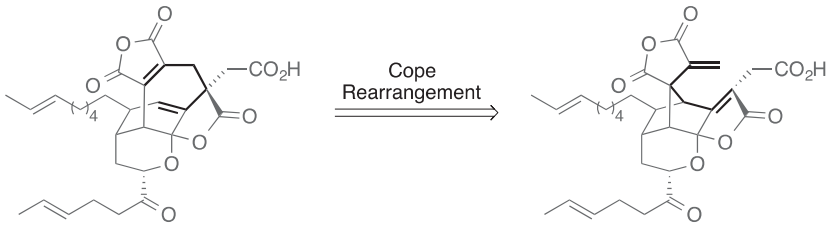

3.11
Phomoidride B

3.100

Scheme 3.32 Proposed oxy-Cope disconnection

Studies toward the phomoidrides within the Wood group began over a decade ago and, as with the syntheses illustrated above, the initial focus of this effort was the formation of the bicyclo[4.3.1]deca-1,6-diene core. At the time, considerable work in the Wood Group was occuring in the area of [3,3]-sigmatropic rearrangement chemistry and the rendering of phomoidride B (**3.11**) illustrated in Scheme 3.32, wherein the retron, (i.e., 1,5-diene) for this type of reaction is clearly evident, was most intriguing. Thus, in the very early days of the phomoidride project it was proposed that a Cope rearrangement synthon (**3.100**) would serve as a late stage intermediate. It is worth noting that this Cope

synthon contains a functionalized norbornane core with pendant butenolide, side-chain, and spirocyclic maleic anhydride units oriented with a defined relative stereochemsitry. As such this intermediate itself represented a major synthetic challenge.

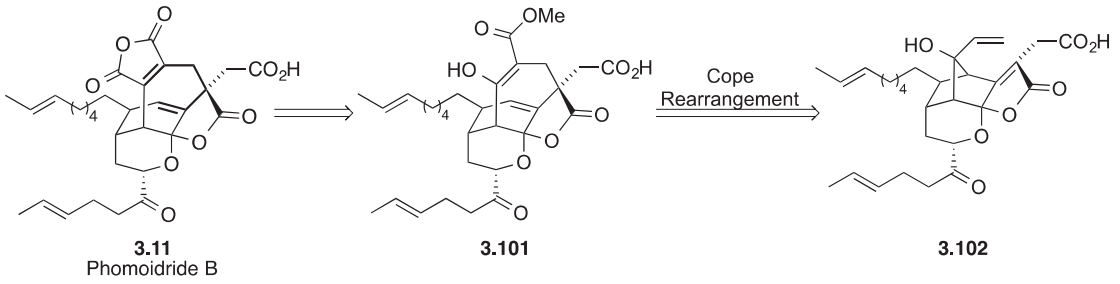

3.11
Phomoidride B

3.101

3.102

Scheme 3.33 Initial Cope disconnect

As illustrated retrosynthetically in Scheme 3.33, a plan calling for late-stage maleic anhydride installation of an advanced decadiene intermediate (**3.101**) allows one to envision a simpler Cope substrate (**3.102**, Scheme 3.33).

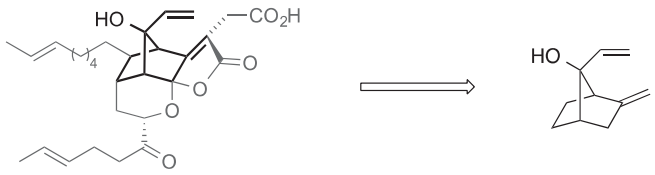

3.102 **3.103**

Scheme 3.34 Model simplification

To determine if a Cope rearrangement could occur on such a system, we constructed a simplified model substrate (i.e., **3.103** in Scheme 3.34). To this end, known diketone **3.104** was protected as its TBS-enol ether and then alkylated by addition of vinyl Grignard. Acylation of the resultant tertiary alcohol followed by hydrolysis of the enol ether furnished ketone **3.105**, which, upon olefination and saponification furnished the model Cope substrate (**3.103**). Although **3.103** was found to undergo Cope

rearrangement to deliver bicyclo[4.3.1]decene **3.106** upon addition of KHMDS in refluxing benzene, these were considered to be rather forcing conditions for what was expected to be an anion accelerated reaction;[22] thus prior to committing to this rearrangement approach a second, more densely functionalized, model Cope substrate was prepared (i.e., **3.111**). As illustrated in Scheme 3.35b this substrate was prepared in a manner similar to **3.103**; however, in contrast to **3.103**, it was found that **3.111** would not undergo Cope rearrangement, even under the more forcing conditions of toluene at reflux.

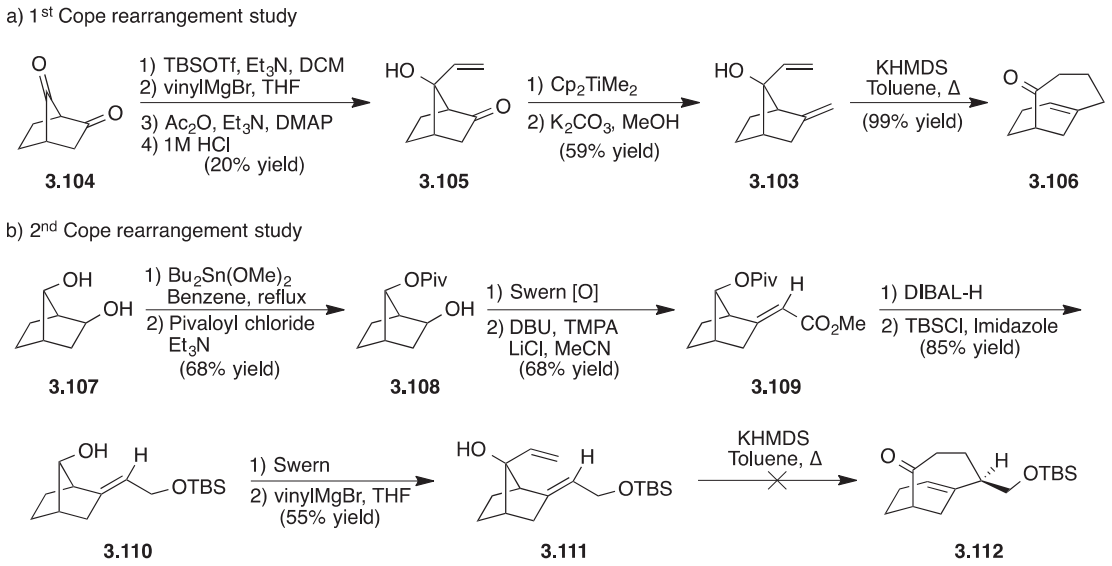

Scheme 3.35 Initial Cope rearrangement studies

Interestingly, we were not the only group attempting to employ a Cope rearrangement to access the phomoidride bicyclic core; Clive (U. Alberta) and Leighton (Columbia) also developed model substrates to test an analogous rearrangement. In Clive's model studies, they induced rearrangement of **3.113** to the corresponding bicycle **3.114** by heating in dichlorobenzene at reflux.[23] Similarly, Leighton and coworkers

utilized butenolide **3.117**, generated *in situ* through a carbonylation of **3.116**, in a thermal rearrangement to form **3.118**.

Importantly, both groups found it necessary to have the butenolide functionality embedded in the ring system in order for the Cope rearrangement to be productive. It was speculated that ring strain imparted by this subunit facilitated the rearrangement. Due to the harsh reaction conditions and level of strain required for the reaction to occur, we decided that implementing a Cope rearrangement on a heavily functionalized late stage intermediate was to risky and thus began to consider alternative approaches that would deliver **3.11**.

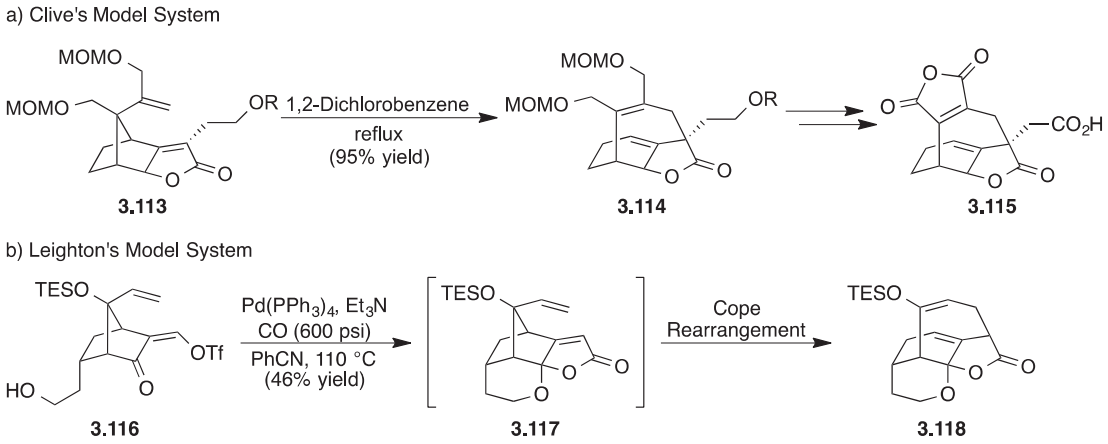

Scheme 3.36 Other model studies toward the Cope rearrangement

Although the Cope rearrangement itself is most often a concerted process; one can view the reaction as consisting of disinct bond-forming and bond-breaking events. Thus, in considering alternatives to the Cope reaction a logical alternative was one wherein the bond forming and bond breaking steps of this rearrangement are performed at different stages of the synthesis. When considered in this fashion the latter stage, our synthetic strategy changes from late stage rearrangement to late stage fragmentation. When

considering the potential viability of advancing either vinylogous acid intermediates **3.101** or **3.119**, the Cope-inspired fragmentation approach leads one to two possible precursors, norbornane derivative **3.120** or isotwistane **3.121**, respectively (Scheme 3.37).

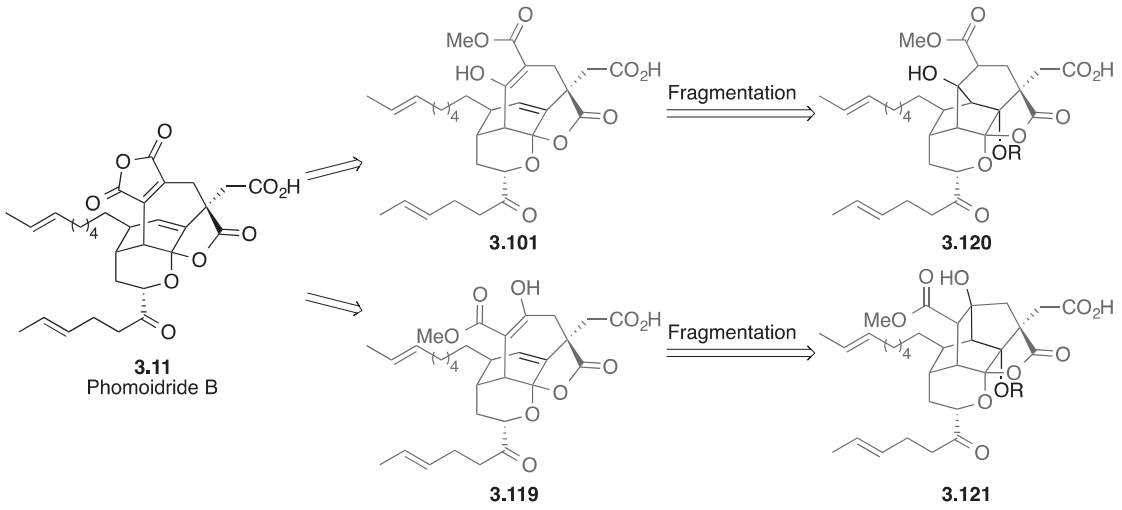

Scheme 3.37 Fragmentation retrosynthetic analysis

To determine the potential feasibility of each fragmentation route, we again turned to a model system study. As illustrated in Scheme 3.38 alkylation of norbornane **3.122** with lithiated 1-bromo-3-butene furnished an intermediate tertiary alcohol, which following acylation and enol ether hydrolysis, was subjected to SmI_2 initiated radical cycloaddition to deliver alcohol **3.123**. Mesylation of the alcohol and subsequent fragmentation upon exposure to methanolysis conditions produced bicyclo[4.3.1]decene **3.124** in excellent yield.[22] Similarly, isotwistane **3.126** was prepared through an alkylation and acylation of an intermediate silyl enol ether followed by a radical cyclization process utilizing tributyltin hydride and AIBN. Functionalization of alcohol **3.126** with MsCl and methanolysis-induced fragmentation delivered bicycle **3.127** in good yield. We were delighted that bicycles **3.124** and **3.127** could be obtained via fragmentation under such mild conditions; a stark contrast to the harsh conditions

required by the Cope rearrangement. Given that the fragmentation approach appeared much more suited to implementation at a late stage of a synthesis wherein the substrates are complex and potentially labile, we began focusing on further developing this approach. Preliminary investigations into methods for preparing fully functionalized fragmentation substrates similar to **3.123** proved untenable and efforts eventually switched to the isotwistane type intermediates.

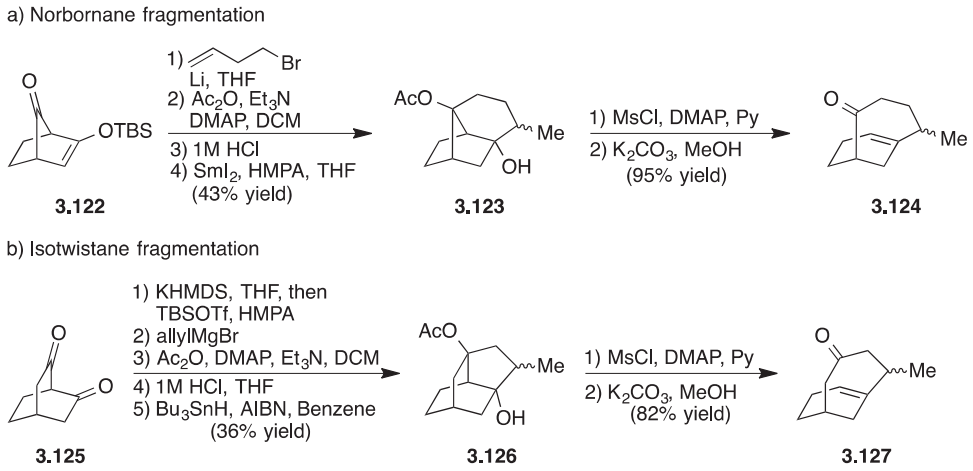

Scheme 3.38 Fragmentation model studies

3.3.2 Completing the Retrosynthetic Analysis

Taken together, the strategic shift (rearrangement to fragmentation) and greater synthetic access of isotwistane systems led to our developing the approach outlined retrosynthetically in Scheme 3.39. As illustrated we envisioned **3.11** as arising from β-keto ester **3.119** wherin the [4.3.1]bicyclic core results from the fragmentation reaction of isotwistane **3.121** (Scheme 3.39). The success with radical ring closing reactions in our model system studies led us to further proposed that **3.121** would derive from a 5-*endo-trig* cyclization of bicyclo[2.2.2]octene **3.128** which, in turn, was seen as accessible by means of a Diels-Alder reaction of a diene such as **3.129**.

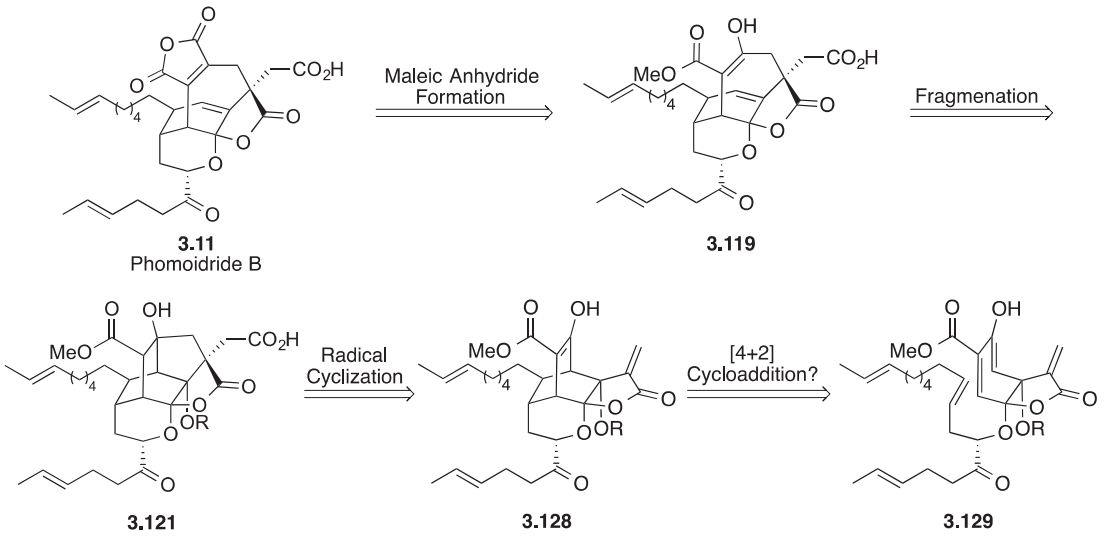

Scheme 3.39 Revised retrosynthetic analysis

In exploring the literature for dienes akin to **3.129**, we were intrigued by a report by Liao and coworkers who prepared a similar diene in the course of a sequential phenolic oxidation/Diels-Alder reaction (Scheme 3.40a).[24] In fact, Liao obtained a bicyclo[2.2.2]octane product (**3.133**) that contained a cyclic acetal quite similar to that found in our proposed intermediate (**3.128**). Further investigation into methods for accessing catechol substrates for incorporation into the Liao-type aryl-oxidation/Diels-Alder cascade revealed a known protocol to prepare catechol **3.137** that required only four synthetic steps from commercially available diketone **3.134**.[25]

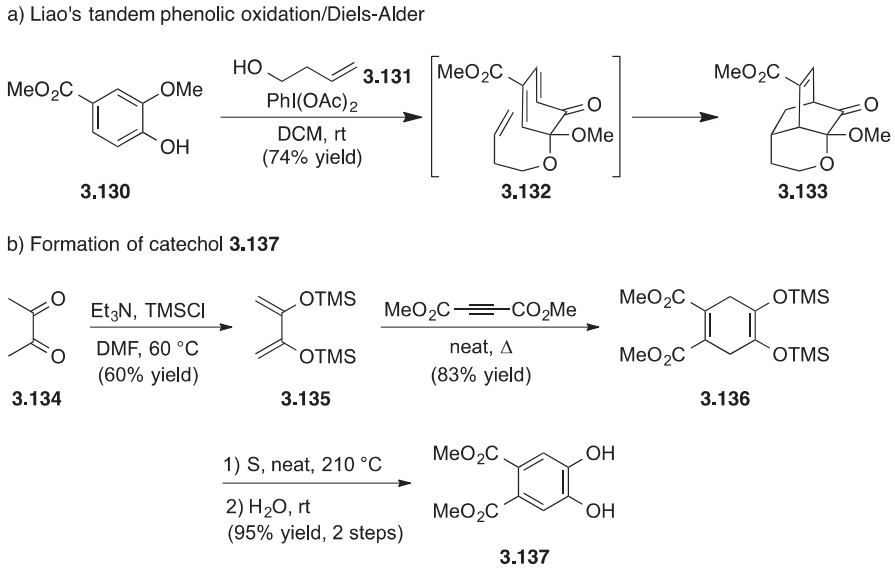

Scheme 3.40 Accessing bicyclo[2.2.2]octenes

Having identified good literature precedents for both an interesting cascade sequence and known starting materials that when combined could lead to a bicycle similar to **3.128** we again revised our strategy to phomoidride B (**3.11**) as illustrated retrosynthetically in Scheme 3.41.[26] The evolved approach now consists of a late-age maleic anhydride formation of maleate **3.138**, and continues with a Grob-type fragmentation of diester **3.139** to form the bicyclic decadiene core. The carboxylic acid of **3.139** is envisioned to arise from **3.140** through acetal opening and oxidation. The isotwistane architecture and quaternary center would be installed by a radical cyclization process that involves the maleate, *exo*-methylene, and alkyl bromide functionalities of **3.141**.

The bicyclo[2.2.2]octene is seen as deriving via the previously described phenolic oxidation/Diels-Alder sequence originating from phenol **3.144**. Importantly, all of the relative stereochemical elements needed for the synthesis are set in the course of this Diels-Alder reaction. Finally, phenol **3.144** would be obtained from a coupling reaction

between known catechol **3.137** and bromoketone **3.145**. Unlike the previous syntheses, we planned to introduce the two side chains as a single unit and differentiate them during the Diels-Alder reaction.

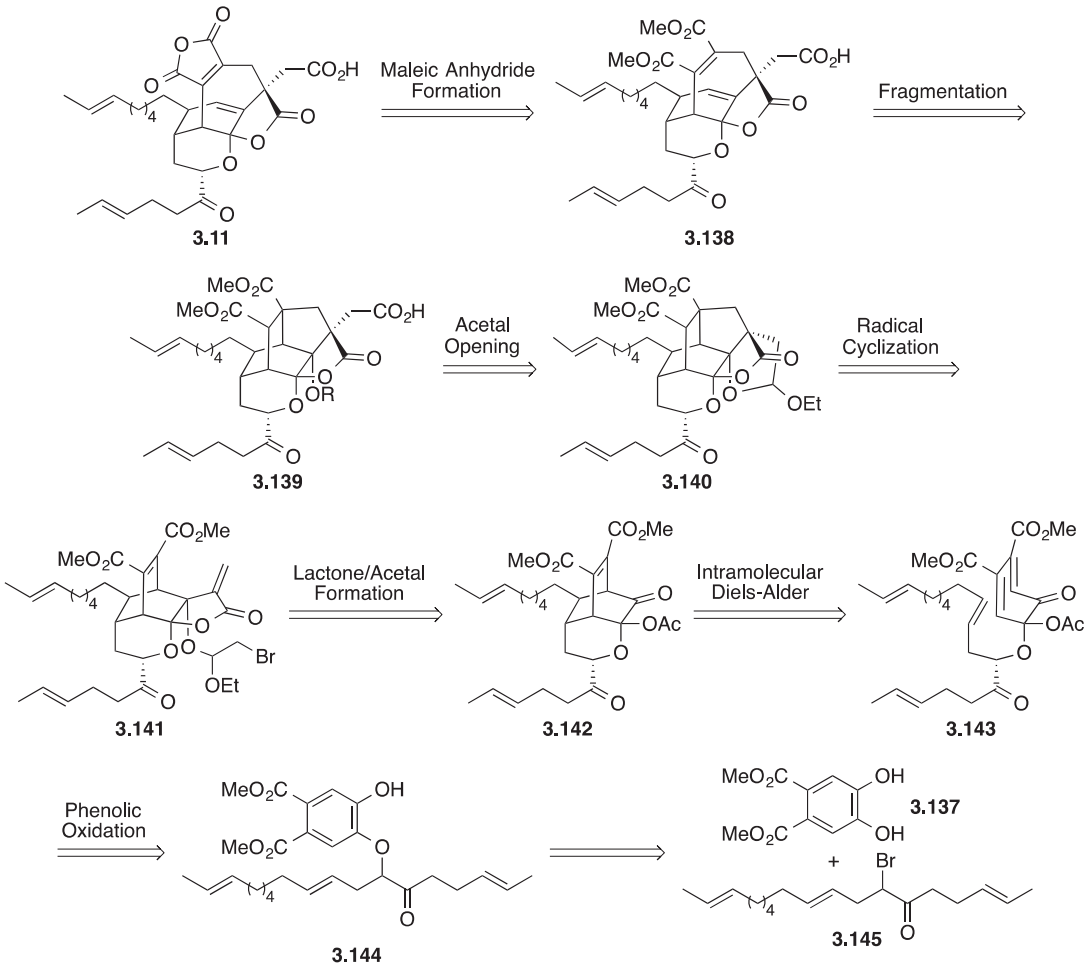

Scheme 3.41 Evolved first-generation retrosynthetic analysis

3.3.3 First-Generation Synthetic Route Toward Phomoidride B

Our synthetic investigations toward phomoidride B (**3.11**) began with the formation of α-bromoketone **3.145**. This was performed in a six-step process originating from 1,5-dibromopentane **3.146**. Displacement of the bromides with sodium acetylide and subsequent methylation formed diyne **3.147** in 35% yield over two steps. Reduction

of the internal alkyne to the *trans* alkene was affected under dissolving metal conditions in the presence of sodium amide; vinyl iodide **3.148** was produced upon hydroalumination of the enyne followed by an iodine quench. Addition of the vinyl cuprate, generated from vinyl iodide **3.148**, to the known enone **3.149** and subsequent trapping of the enolate with TMSCl furnished silyl enol ether **3.150**. Trapping the enolate as the silyl enol ether allowed the regioselective formation of bromoketone **3.145** upon reacting silyl enol ether **3.150** with NBS.

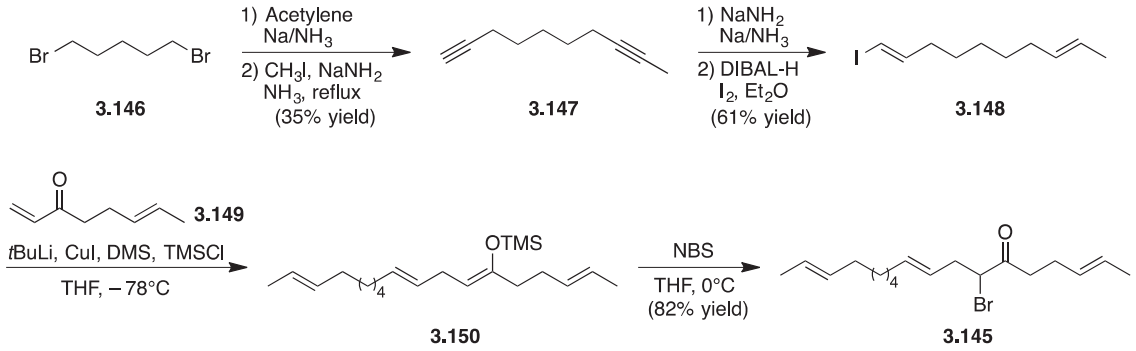

Scheme 3.42 Side chain synthesis

With the side chain fragment in hand, the known catechol **3.137**[25] was prepared for coupling by mono-protecting with allylbromide. Exposure of the derived allyl ether to bromoketone **3.145** in the presence of cesium carbonate delivered ketone **3.151** (Scheme 3.43). At this point, the ketone was protected as the ethylene glycol acetal and the phenol deprotected using $Pd(PPh_3)_4$ to afford **3.152**. In the absence of the protecting group, the ketone was found to cyclize to the hemi-acetal upon allyl deprotection and the subsequent phenolic oxidation could not proceed. Subjecting phenol **3.152** to phenolic oxidation conditions generated an intermediate diene, which underwent an intramolecular Diels-Alder reaction to give bicycle **3.153** as a mixture of separable C7 epimers. The

diastereomeric ratio favored β-**3.153**, which would be the isomer en route to phomoidride D (**3.13**); therefore, we decided to target **3.13** during our initial investigations.

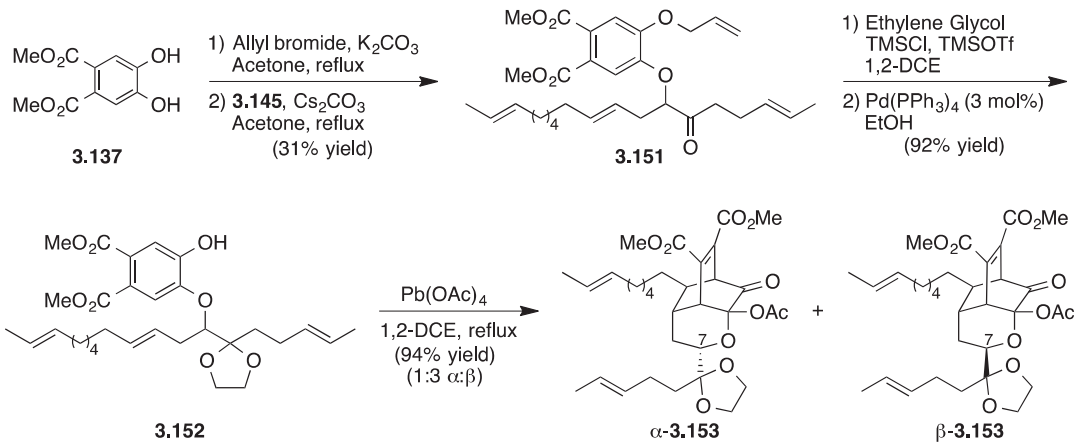

Scheme 3.43 Phenolic oxidation/Diels-Alder synthetic sequence

Having successfully completed the aryl-oxidation/Diels-Alder cascade we next investigated the radical cascade cyclization. To this end, β-**3.153** was deacylated and the resultant hemi-acetal was protected as the TMS ether. The resultant ketone (**3.154**) was treated with the lithium enolate of methyl propionate **3.155** to produce aldol adduct **3.156** in excellent yield. A Cope elimination was followed by fluoride promoted lactonization to deliver γ-lactone **3.157**. Functionalization of the tertiary alcohol with bromoacetal **3.158** produced cyclization precursor **3.159**.

With ethyl acetal **3.159** in hand, the desired 5-*exo*-*trig*/5-*exo*-*trig* cyclization was attempted using tributyltin hydride and AIBN as a radical initiator. Although we were pleased to obtain our desired cyclization product **3.160**, it was accompanied by a significant amount of the 6-*endo*-*trig*/4-*exo*-*trig* isomer **3.161**. Although the yield of **3.160** was synthetically useful, we decide to explore alternative conditions in hopes of improving efficiency; optimizations studies revealed that changing conditions from

Bu_3SnH and AIBN to samarium diiodide improved the yield of the desired product (**3.160**) to 97% and completely suppressed the formation of the unwanted isomer (**3.161**).

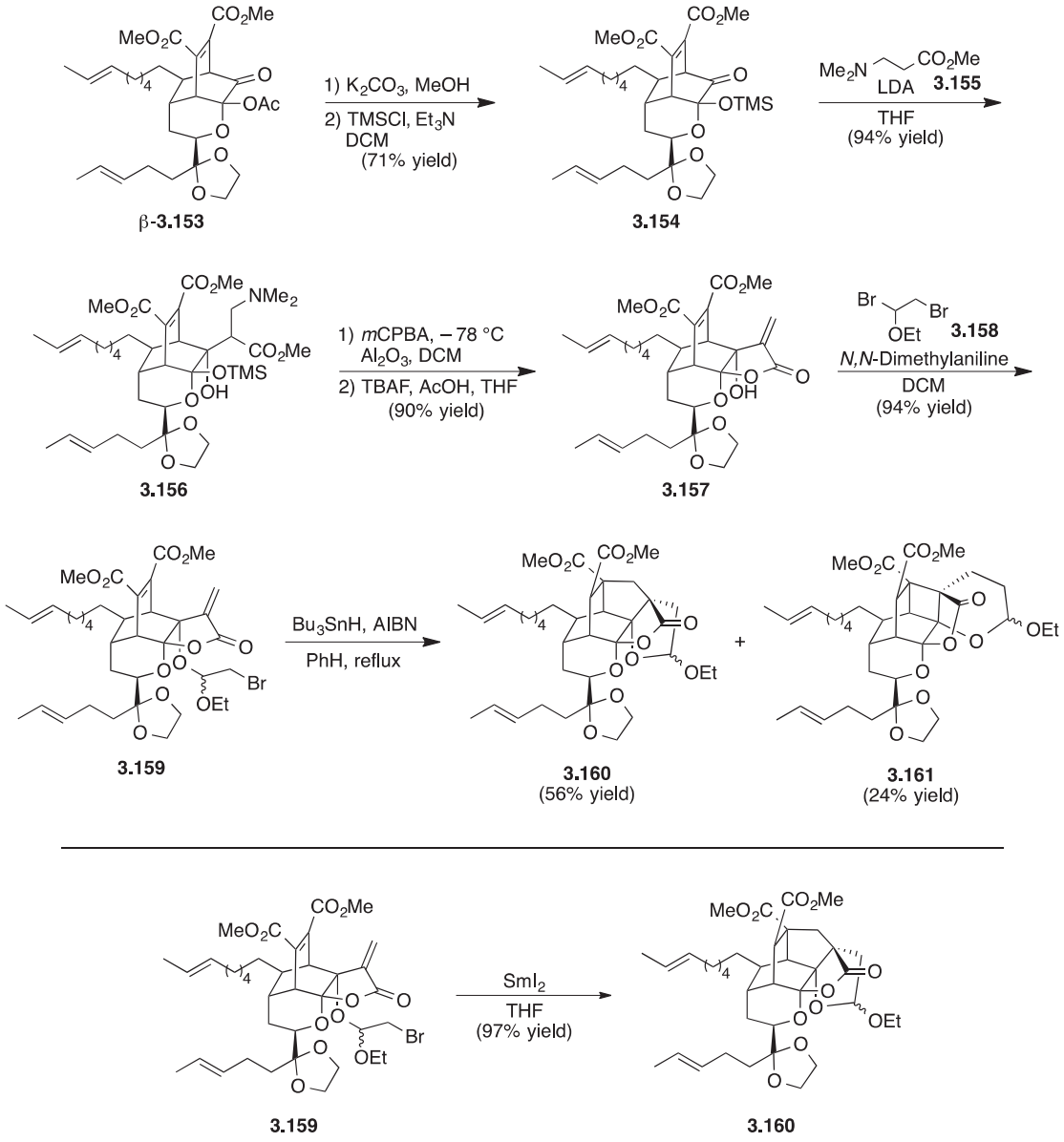

Scheme 3.44 Radical cascade cyclization

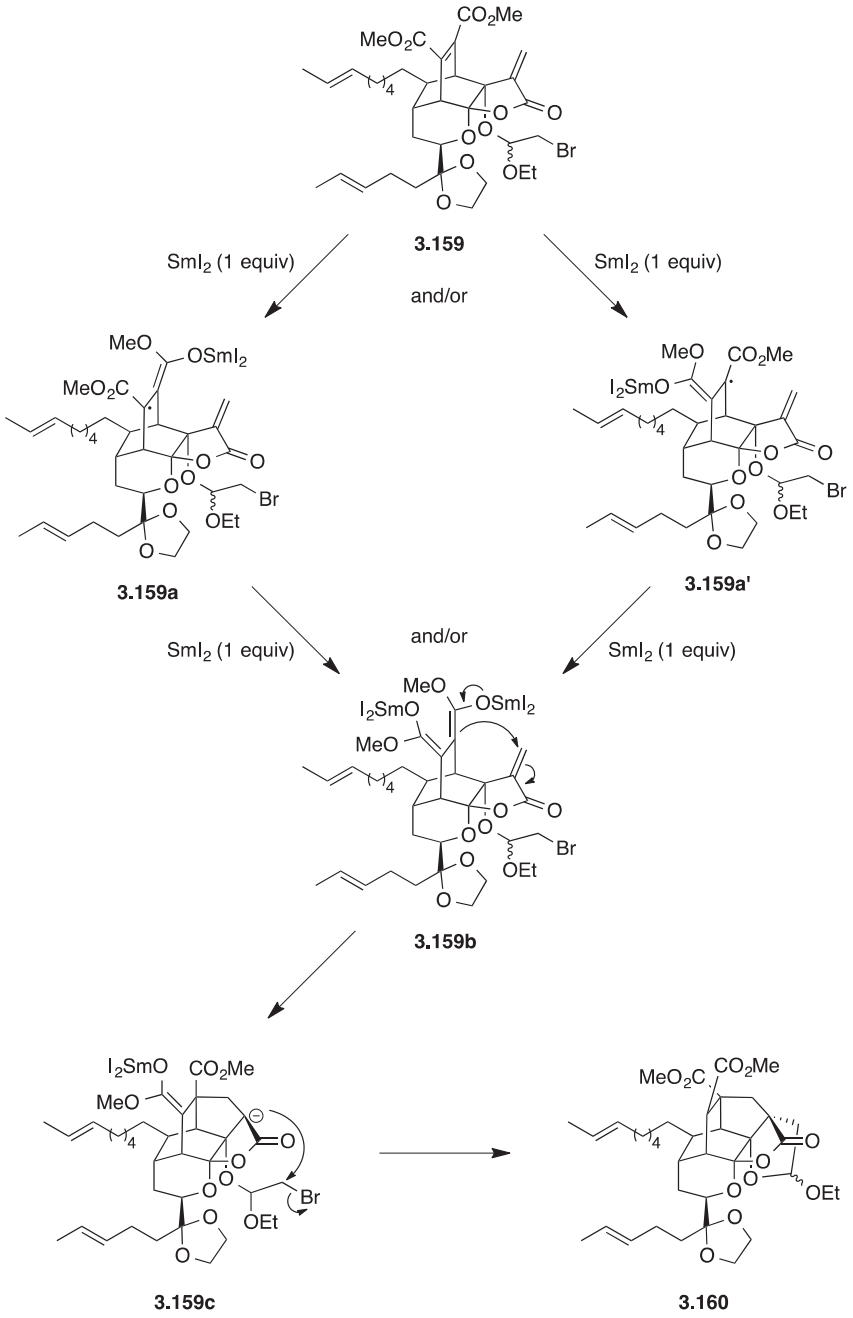

Scheme 3.45 Proposed mechanism for SmI_2 promoted cyclization

The surprising differences in reactivity between the similar sets of reaction conditions used for the radical cyclization led us to speculate that a different mechanism was operating (Scheme 3.45). Specifically, we speculated that the dimethyl maleate motif was undergoing reduction through two single-electron transfers (SET) from two

separate equivalents of SmI_2. This would effectively produce dienolate **3.159b**, which could undergo a conjugate addition with the enone to deliver enolate **3.159c**. The enolate could then further react to give ethyl ester **3.160** upon the displacement of the bromide.[25]

To further support this mechanistic proposal, two test reactions were conducted. First, alcohol **3.157** was subjected to the reaction conditions and was found to produce isotwistane **3.162** in 84% yield. The second reaction consisted of exposing bromide **3.159** to the same reaction conditions at –78 °C and quenching after 30 minutes. This produced the 5-*endo-trig* cyclization product **3.163** in a 37% yield. Taken together these results suggest that the Sm-mediated cyclization reaction occurs through a top-down process that can be classified as a 5-*endo-trig*/5-*exo-tet* cyclization.

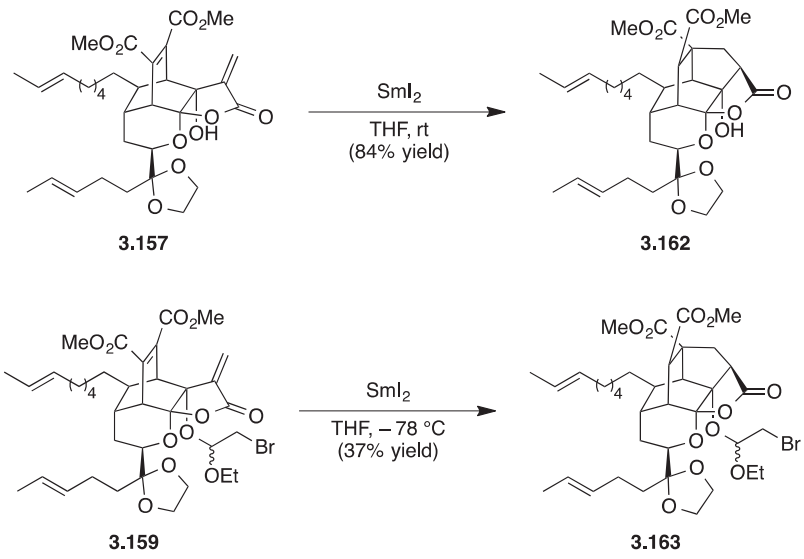

Scheme 3.46 Mechanistic investigation of the cascade cyclization

Having developed a viable route to isotwistane **3.160** we moved on to preparing the fragmentation precursor **3.165** (Scheme 3.47). To this end, ethyl acetal **3.160** was subjected to transacetalization to form the thioacetal and the resultant tertiary alcohol was

functionalized as the targeted xanthate (**3.165)**. Unfortunately, treating **3.165** with SmI_2, failed to induce fragmentation to **3.167**.[27]

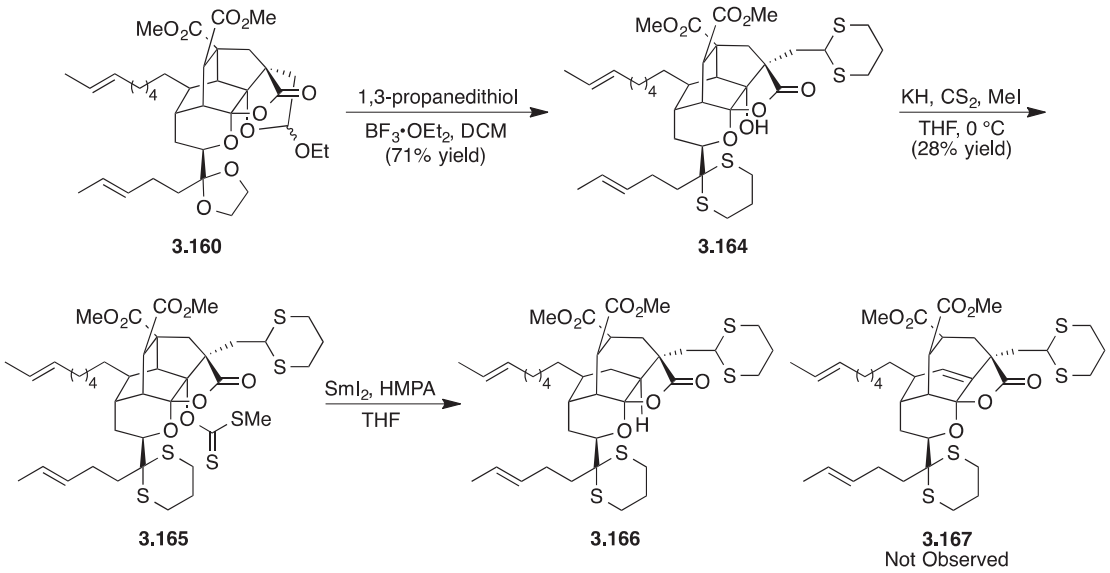

Scheme 3.47 First Grob fragmentation attempt

In considering potential reasons for the failed fragmentation, we speculated that the adjacent carbonyl functionality might be problematic due to the stability it would provide as a possible α-elimination pathway; hence, we decided to reduce lactone **3.164** to its corresponding acetal (Scheme 3.48). Thus, reduction of **3.164** to an intermediate hemi-acetal followed by conversion to the corresponding mixed acetal and xanthate formation furnished modified fragmentation substrate **3.168**. Treatment of xanthate **3.168** with SmI_2 and HMPA in THF resulted in desired Grob fragmentation to the desired bicyclo[4.3.1]decene core of the phomoidrides (**3.169**).

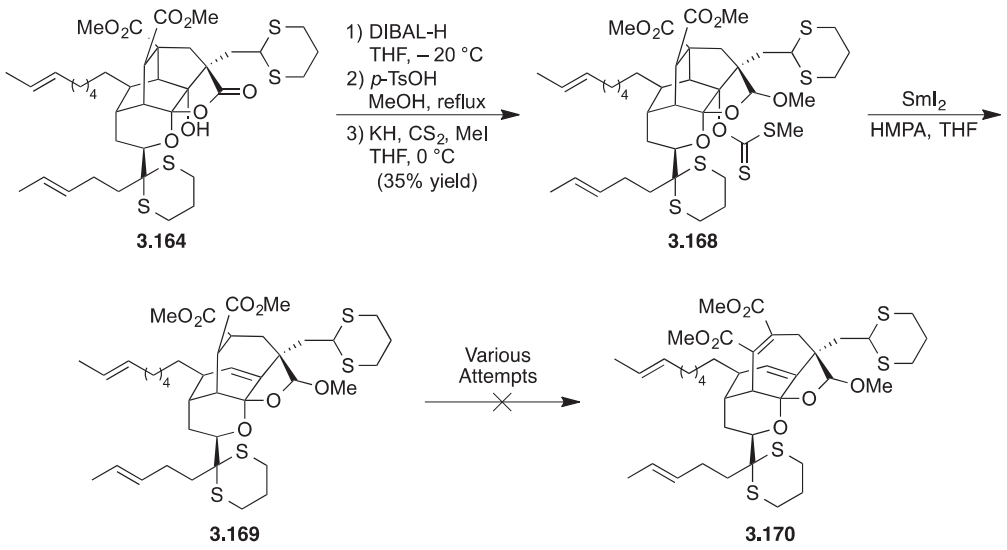

Scheme 3.48 Successful fragmentation to deliver the phomoidride core

At this point, in order to complete the synthesis of phomoidride D, **3.169** was required to undergo the formation of the maleic anhydride, removal of the thioacetal and thioketal, followed by oxidiation to form the lactone and the carboxylic acid. Unfortunately, all attempts to effect an unsaturation to produce the dimethyl maleate were futile.[28] Unable to transform the diester into the requisite maleic anhydride we were forced to develop a new end-game strategy. Of numerous possibilities, we decided to explore methods developed in previous syntheses of the phomoidrides and proposed to introduce the maleic anhydride via a carbonyl insertion akin to that developed by Shair and Fukuyama in their syntheses of **3.11** (Scheme 3.49).[17,18b]

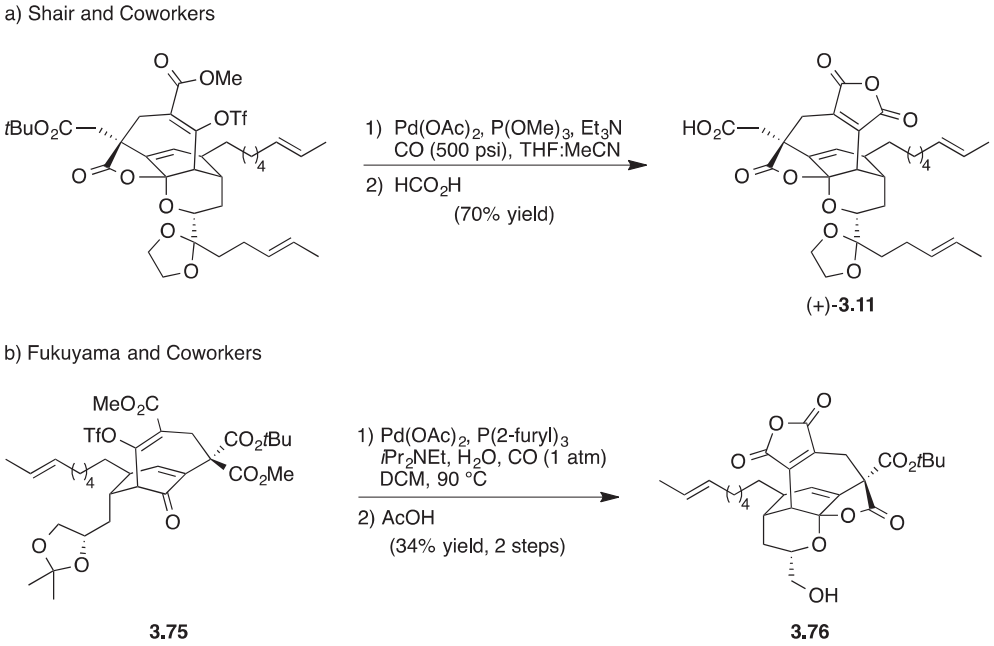

Scheme 3.49 Carbonylative maleic anhydride formation

3.3.4 Second-Generation Studies Toward the Synthesis of Phomoidride D

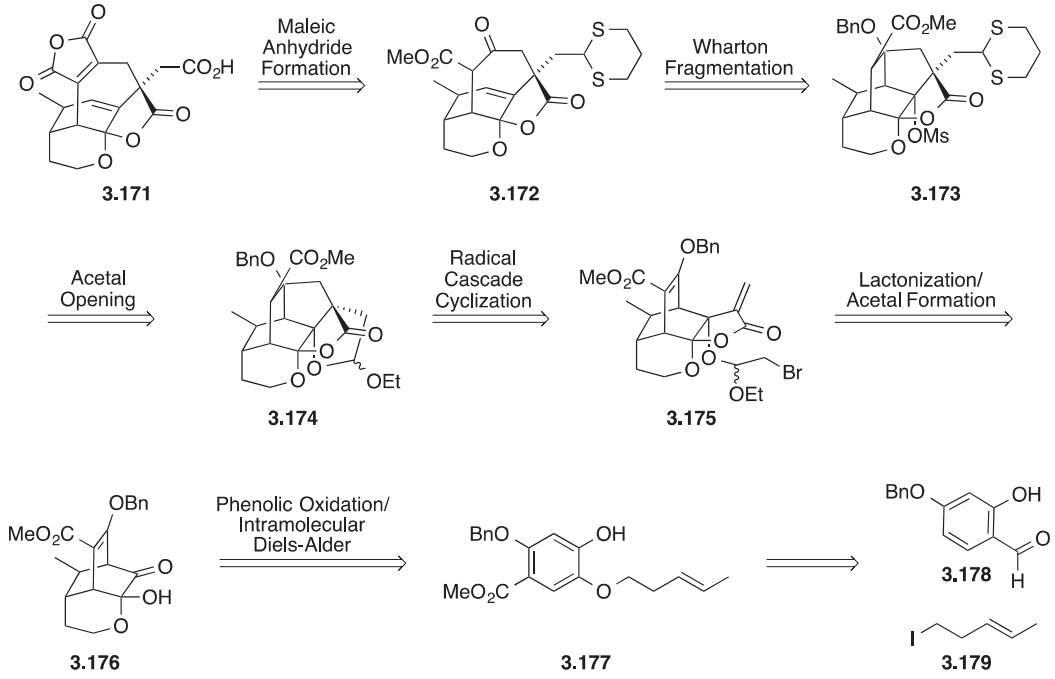

Scheme 3.50 Second-generation approach toward phomoidride D

Our second-generation approach toward phomoidride D (**3.13**) is illustrated retrosynthetically in Scheme 3.50.[29] Given that the changes reflected in the second-generation approach were to be made at a late stage in the sequence we opted to perform these exploratory studies on a simplified model system. As illustrated, the target for these investigations was maleic anhydride **3.171**, which was envisioned as arising from **3.172** through vinyl triflate formation and palladium catalyzed carbonylation. The requisite β-keto ester would derive from a Wharton fragmentation of isotwistane **3.173** which, in turn, was seen as the product of a phenolic oxidation/Diels-Alder and cascade radical cyclization strategy similar to that employed in the first-generation synthesis. Thus, the point of departure was defined as a coupling reaction of phenol **3.178** and iodide **3.179** which would furnish the first cascade substrate **3.177**.

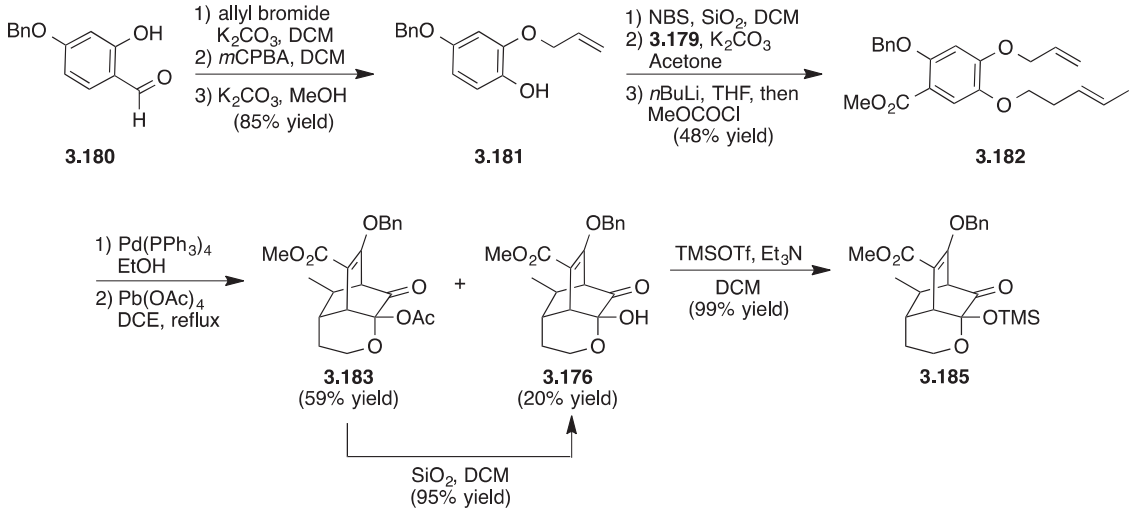

Scheme 3.51 Phenolic oxidation/Diels-Alder sequence

In a forward sense, benzaldehyde **3.180** was protected with allyl bromide and carried through a Dakin oxidation that furnished phenol **3.181** (Scheme 3.51). Alkylation

with the model side chain **3.179** and acylation with methyl chloroformate then produced protected phenol **3.182**. Allyl deprotection and treatment with $Pb(OAc)_4$ formed a mixture of acylated and deacylated Diels-Alder adducts **3.183** and **3.176**. Upon stirring with silica gel in DCM, **3.183** was converted to **3.176** in excellent yield. Alcohol protection with TMSOTf then gave ketone **3.185**.

Having completed the first cascade sequence we began setting the stage for the second by carrying **3.185** into an aldol reaction with the lithium enolate of propionate **3.155**. Subsequent Cope elimination of the aldol product generated methyl ester **3.186** which, upon fluoride promoted lactonization and functionalization of the tertiary alcohol with bromoacetal **3.158** gave the cyclization precursor **3.175**. Finally, a bottom up 5-*exo-trig*/*5-exo-trig* cyclization gave isotwistane **3.174** along with its 6-*endo-trig* isomer **3.189**.

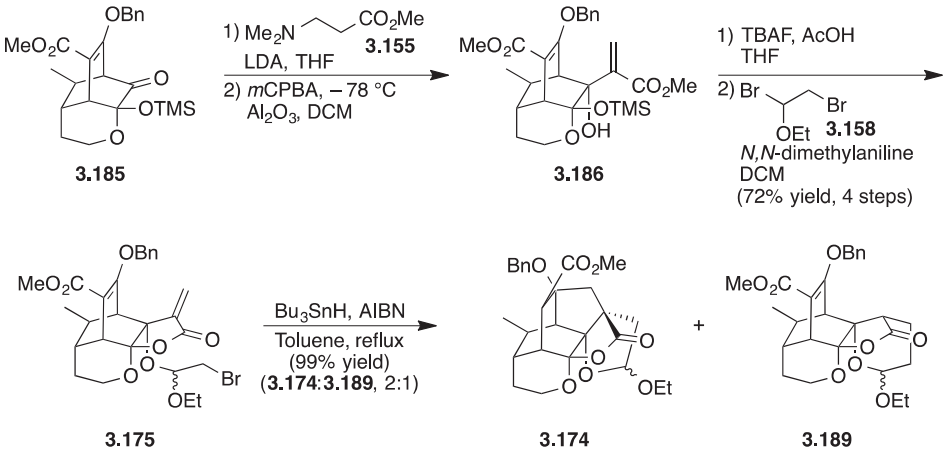

Scheme 3.52 Radical cascade cyclization

Having completed the second cascade sequence, acetal **3.174** was advanced toward the fragmentation substrate by transacetalization with 1,3-propanedithiol and conversion of the resultant tertiary alcohol to the corresponding mesylate (Scheme 3.53). Benzyl deprotection of **3.173** was performed employing BBr_3 and furnished the

corresponding alcohol, however the expected concomitant fragmentation was not observed. Spectroscopic studies eventually indicated that epimerization at C11 had accompanied the benzyl deprotection to give alcohol **3.190** in 94% yield. This puzzling result indicated that our system might not be suitable for fragmentation. As a small amount (4% yield) of the unepimerized C11-*epi*-**3.190** was obtained; we decided to investigate this reaction further by subjecting this product to potassium hydride in THF and again no desired fragmentation product **3.172** was obtained (Scheme 3.53). Instead, a retro-aldol process occurred that upon cyclization delivered our observed C11 epimer **3.190**.

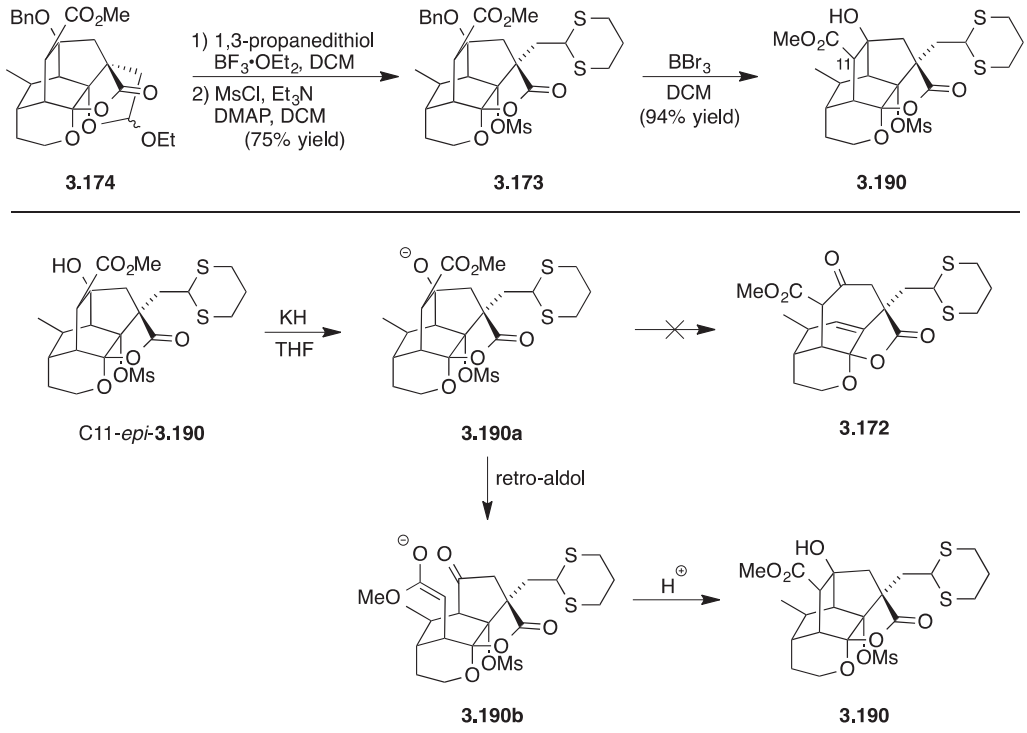

Scheme 3.53 Initial fragmentation attempt

To confirm that the non-productive retro-aldol pathway was derailing the desired fragmentation event we reduced **3.190** to the corresponding alcohol, thereby removing the driving force behind the undesired reactivity. As illustrated in Scheme 3.54, treating

the derived diol (**3.191**) with aqueous potassium hydroxide resulted in a 67% yield of **3.192**, the product of concomitant Wharton fragmentation and acetal opening. The latter is consistent with the interconversion studies performed by Nicolaou and coworkers using LiOH (section 3.1.4).[13]

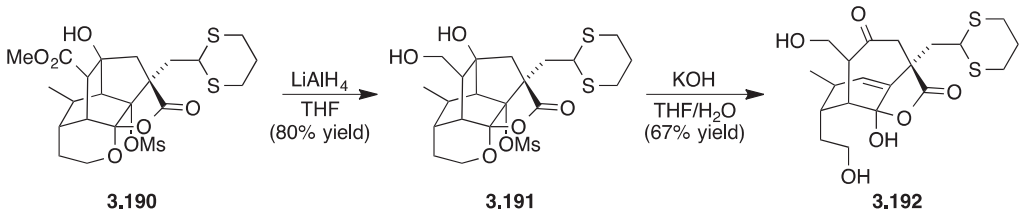

Scheme 3.54 Wharton fragmentation

Although we were able to successfully perform the key fragmentation reaction on the second-generation substrate, the additional redox manipulations required to avoid the deleterious retro-aldol reaction greatly diminished efficiency. In order to avoid unnecessary redox manipulations, we decided to install the ester functionality at a later stage in the synthesis. Hence, we decided to redesign our synthetic strategy toward phomoidride D (**3.13**) to include a late stage esterification and maleic anhydride formation (Chapter Four).

3.4 Conclusion

Since the initial isolation of the phomoidrides in 1996, they have drawn the attention of many synthetic chemists and inspired the development of many creative synthetic approaches. Despite considerable interest, only four syntheses have been completed to date. Each synthesis contained a unique approach toward one or many of the key structural features.

Utilizing a tandem phenolic oxidation/Diels-Alder sequence and radical cascade cyclization, we were able to quickly assemble a fully functionalized isotwistane precursor containing the side chains, spiroacetal, and quaternary center found in the phomoidrides. We were pleased to find that fragmentation of this precursor proceeds to furnish the desired bicyclic core. Unfortunately, the last key functionality necessary to complete the synthesis, the maleic anhydride, proved an insurmountable obstacle and led to our developing a second-generation approach designed to take advantage of existing methods for maleic anhydride incorporation. Unfortunately, the second-generation approach failed as the result of an unanticipated retro-aldol process that derailed the planned fragmentation reaction. Since overcoming this latter obstacle required additional redox manipulations it was decide to again redesign the end-game strategy.

3.5 References

[1] For an excellent review of the phomoidrides from isolation to synthesis, see: Spiegel, D. A.; Njardarson, J. T.; McDonald, I. M.; Wood, J. L. *Chem. Rev.* **2003**, *103*, 2691.

[2] Dabrah, T. T.; Kaneko, T.; Massefski, Jr. W.; Whipple, E. B. *J. Am. Chem. Soc.* **1997**, *119*, 1594.

[3] Meng, D.; Tan, Q.; Danishefsky, S. J. *Angew. Chem. Int. Ed.* **1999**, *38*, 3197.

[4] Spencer, P.; Agnelli, F.; Sulikowski, G. A. *Org. Lett.* **2001**, *3*, 1443.

[5] Bredt, J.; Thouet, H.; Schnitz, J. *J. Liebigs Ann. Chem.* **1924**, *437*, 1.

[6] (a) Buchanan, G. L. *Chem. Soc. Rev.* **1974**, *3*, 41. (b) Warner, P. M. *Chem. Rev.* **1989**, *89*, 1067.

[7] (a) Goldring, W. P. D.; Pattenden, G. *Acc. Chem. Res.* **2006**, *39*, 354. (b) Baloglu, E.; Kingston, D. G. I. *J. Nat. Prod.* **1999**, *62*, 1448.

[8] For a review on nonadride natural products, see: Chen, X.; Zheng, Y.; Shen, Y. *Chem. Rev.* **2007**, *107*, 1777.

[9] (a) Baldwin, J. E.; Barton, D. H. B.; Bloomer, J. L.; Jackman, L. M.; Rodriguez-Hahn, L.; Sutherland, J. K. *Experientia* **1962**, *18*, 345. (b) Barton, D. H. R.; Godinho, L. D. S.; Sutherland, J. K. *J. Chem. Soc.* **1965**, 1772. (c) Barton, D. H. R.; Jackman, L. M.; Rodriguez-Hahn, L.; Sutherland, J. K. *J. Chem. Soc.* **1965**, 1779. (d) Barton, D. H. R.; Sutherland, J. K. *J. Chem. Soc.* **1965**, 1769. (e) Baldwin, J. E.; Barton, D. H. R.; Sutherland, J. K. *J. Chem. Soc.* **1965**, 1787.

[10] (a) Ref. 9a-c. (b) Bloomer, J. L.; Moppett, C. E.; Sutherland, J. K. *J. Chem. Soc. C* **1968**, 588. (c) Huff, R. K.; Sutherland, J. K.; Moppett, C. E. *J. Chem Soc. Perkin Trans. 1* **1972**, 2584.

[11] Spencer, P.; Agnelli, F.; Williams, H. J.; Keller, N. P.; Sulikowski, G. A. *J. Am. Chem. Soc.* **2000**, *122*, 420.

[12] Sulikowski, G.; Agnelli, F.; Spencer, P.; Koomen, J. M.; Russell, D. H. *Org. Lett.* **2002**, *4*, 1447.

[13] Nicolaou, K. C.; Baran, P. S.; Zhong, Y. L.; Fond, K. C.; He, Y.; Yoon, W. H.; Choi, H. S. *Angew. Chem. Int. Ed.* **1999**, *38*, 1676.

[14] (a) See ref. 1 and references contained within. (b) Ashenhurst, J. A.; Isakovic, L.; Gleason, J. L. *Tetrahedron* **2010**, *66*, 368. (c) Malihi, F.; Clive, D. L. J.; Chang, C.-C.; Minaruzzaman *J. Org. Chem.* **2013**, *78*, 996. (d) Clive, D. L. J.; Cheng, H.; Gangopadhyay, P.; Huang, X.; Prabhudas, B. *Tetrahedron* **2004** *60*, 4205. (e) Clive, D. L. J.; Sgarbi, P. W. M.; He, X.; Sun, S.; Zhang, J.; Ou, L. *Can. J. Chem.* **2003**, *81*, 811 (f) Banwell, M. G.; Coster, M. J.; Edwards, A. J. Vögtle, M. *Aust. J. Chem.* **2003**, *56*, 577. (g) Armstrong, A.; Davies, N. G. M.; Martin, N. G.; Rutherford, A. P. *Tetrahedron* **2003**, *44*, 3915. (h) Yoshimitsu, T.; Sasaki, S.; Arano, Y.; Nagaoka, H. *J. Org. Chem.* **2004**, *69*, 9262.

[15] (a) Nicolaou, K. C.; Baran, P. S.; Zhong, Y.-L.; Choi, H-S.; Yoon, W. H.; He, Y.; Fong, K. C. *Angew. Chem. Int. Ed.* **1999**, *38*, 1669. (b) Nicolaou, K. C.; Baran, P. S.; Zhong, Y.-L.; Fong, K. C.; He, Y.; Yoon, W. H.; Choi, H.-S. *Angew. Chem. Int. Ed.* **1999**, *38*, 1676. (c) Nicolaou, K. C.; Postema, M. H. D.; Miller, N. D.; Yang, G. *Angew. Chem. Int. Ed.* **1997**, *36*, 2821. (d) Nicolaou, K. C.; He, Y.; Fong, K. C.; Yoon, W. H.; Choi, H. s.; Zhong, Y. L.; Baran, P. S. *Org. Lett.* **1999**, *1*, 63. (e) Nicolaou, K. C.; Baran, P. S.; Jautelat, R.; He, Y.; Fong, K. C.; Choic, H. S.; Yoon, W. H.; Zhong, Y. L. *Angew. Chem. Int. Ed.* **1999**, *38*, 549. (f) Nicolaou, K. C.; Jung, J.; Yoon, W. H.; Fong, K. C.; Choi, H. S.; He, Y.; Zong, Y. L.; Baran, P. S. *J. Am. Chem. Soc.* **2002**, *124*, 2183. (g) Nicolaou, K. C.; Baran, P. S.; Zhong, Y. L; Fong, K. C.; Choi, H. S. *J. Am. Chem. Soc.* **2002**, *124*, 2190. (h) Nicolaou, K. C.; Jung, J. K.; Yoon, W. H.; He, Y.; Zhong, Y. L.; Baran. P.S. *Angew. Chem. Int. Ed.* **2000**, *124*, 1829. (i) Nicolaou, K. C.; Zhong, Y. L.; Baran, P. S.; Zhong, Y. L.; Fong, K. C.; Choi, H. S.; Yoon, W. H. *J. Am. Chem. Soc.* **2002**, *124*, 2202. (j) Nicolaou, K. C.; Baran, P. S. *Angew. Chem. Int. Ed.* **2002**, *41*, 2678.

[16] (a) Waizumi, N.; Itoh, T.; Fukuyama, T. *Tetrahedron Lett.* **1998**, *39*, 6015. (b) Waizumi, N.; Itoh, T.; Fukuyama, T. *J. Am. Chem. Soc.* **2000**, *122*, 7825.

[17] Hayashi, Y.; Itoh, T.; Fukuyama, T. *Org. Lett.* **2003**, *5*, 2235.

[18] (a) Chen, C.; Layton, M. E.; Shair, M. D. *J. Am. Chem. Soc.* **1998**, *120*, 10784. (b) Chen, C.; Layton, M. E.; Sheehan, S. M.; Shair, M. D. *J. Am. Chem.Soc.* **2000**, *122*, 7424. (c) Sheehan, S. M.; Lalic, G.; Chen, J. S.; Shair, M. D. *Angew. Chem. Int. Ed.* **2000**, *39*, 2714.

[19] (a) Kwon, O.; Su, D.-S.; Meng, D.; Deng, W.; D'Amico, C. D.; Danishefsky, S. J. *Angew. Chem. Int. Ed.* **1998**, *37*, 1877. (d) Kwon, , O. Y.; Su, d. S.; Meng, D. F.; Deng, W.; Danishefsky, S. J. *Angew. Chem. Int. Ed.* **1998**, *37*, 1880. (c) Meng, D.; Danishefsky, S. J. *Angew. Chem. Int. Ed.* **1999**, *38*, 1485.

[20] Meng, D.; Tan, Q.; Danishefsky, S. J. *Angew. Chem. Int. Ed.* **1999**, *38*, 3197.

[21] Tan, Q.; Danishefsky, S. J. *Angew. Chem. Int. Ed.* **2000**, *39*, 4509.

[22] Njardarson, J. T.; Wood, J. L. *Org. Lett.* **2001**, *3*, 2431.

[23] Clive, D. L. J.; Ou, L. *Tetrahedron Lett.* **2002**, *43*, 4559.

[24] Chu, C.-S.; Lee, T.-H.; Rao, P. D.; Song, L.-D.; Liao, C. C. *J. Org. Chem.* **1999**, *64*, 4111.

[25] (a) Njardarson, J. T.; McDonald, I. M.; Speigel, D. A.; Inoue, M.; Wood, J. L. *Org. Lett.* **2001**, *3*, 2435. (b) Spiegel, D. A.; Njardarson, J. T.; Wood, J. L. *Tetrahedron* **2002**, *58*, 6545.

[26] Murphy, G. K.; Shirahata, T.; Hama, N.; Bedermann, A.; Dong, P.; McMahon, T. C; Twenter, B. M.; Spiegel, D. A.; McDonald, I. M.; Taniguchi, N.; Inoue, M.; Wood, J. L. *J. Org. Chem.* **2013**, *78*, 477.

[27] McDonald, I. M. *Progress Toward the Total Synthesis of the Phomoidrides*, Ph. D. Thesis, Yale University, New Haven, CT, 2005.

[28] Twenter, B. *Synthetic Approaches Toward the Phomoidrides*, Ph. D. Thesis, Yale University, New Haven, CT, 2008.

[29] Murphy, G. K.; Hama, N.; Bedermann, A.; Dong, P.; Schneider, C. M.; McMahon, T. C.; Tao, R. N.; Twenter, B. M.; Spiegel, d. A.; Wood, J. L. *Org. Lett.* **2012**, *14*, 4544.

CHAPTER FOUR

Model Studies Toward the Synthesis of Phomoidride D: A 3rd Generation Approach

4.1 A Retrosynthetic Approach

4.1.1 Phomoidride D Model Substrate Retrosynthetic Analysis

To continue our ongoing synthetic studies toward Phomoidride D, we needed to reconsider our approach. Our first-generation strategy was very successful initially, but stalled when attempting to introduce the maleic anhydride. To circumvent this, a second-generation plan was developed wherein a late stage carbonylation would deliver the maleic anhydride. Unfortunately, this route failed due to early incorporation of a requisite β-hydroxy ester which, due to an unanticipated retro-aldol reaction, thwarted the key Wharton fragmentation. Subsequent studies revealed that the Wharton fragmentation could be performed successfully following ester reduction; however, the additional redox manipulations diminished the efficiency of the route and led us to propose the current, third-generation, synthetic strategy toward phomoidride D. As with our second-generation approach, our initial efforts were performed using a model substrate which we hoped would help us to define not only the appropriate starting aromatic substrate but also develop the late-stage sequence leading to the maleic anhydride (Figure 4.10). A retrosynthetic analysis for the third generation approach is shown in Scheme 4.10.

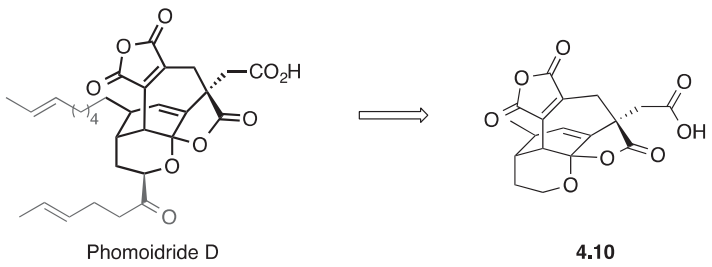

Figure 4.10 Model of the phomoidride core

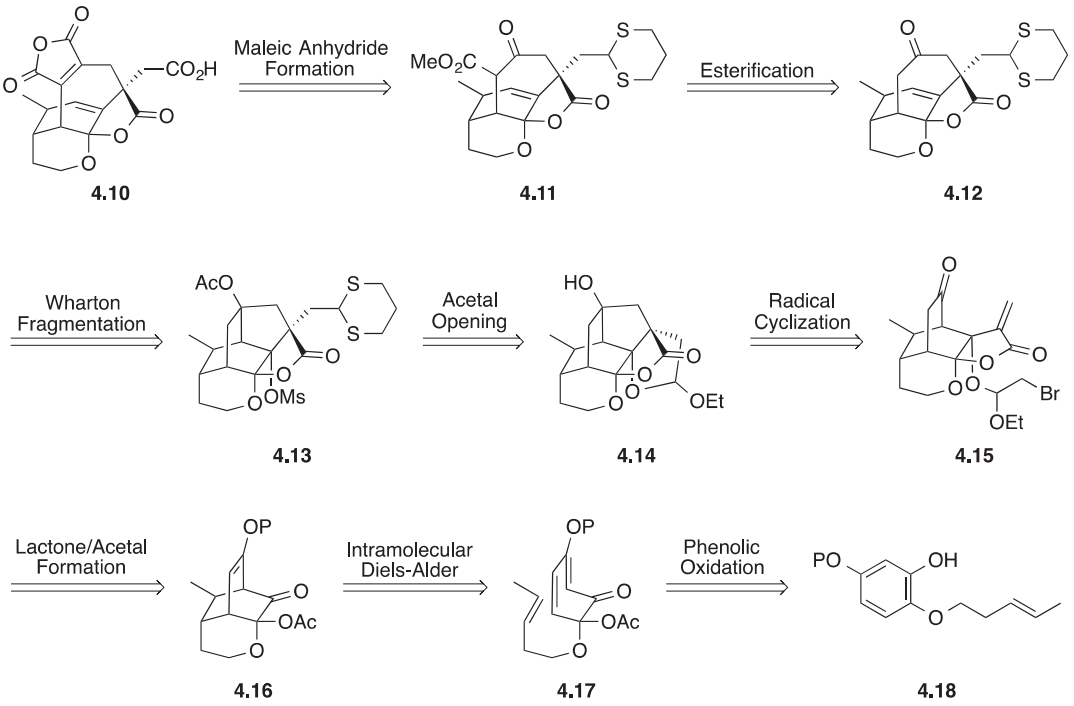

Scheme 4.10 A retrosynthetic analysis for our third-generation model study

As illustrated, the initial disconnection envisions late-stage introduction of the maleic anhydride via carbonylation of an intermediate derived from β-keto ester **4.11** (Scheme 4.10). To avoid the unproductive retro-aldol reaction observed in the second-generation approach, the current plan calls for preparation of beta-keto ester **4.11** using ketone **4.12** as substrate. The latter, in turn, is envisioned to derive from Wharton fragmentation of acetate **4.13**. The core isotwistane unit found in **4.13** and **4.14** will arise

via a radical cascade closely paralleling that employed in the early generation approaches and thus the current strategy calls for the intermediacy of ethyl acetal **4.15**. The lactone and ethyl acetal of **4.15** are seen as being introduced into the [2.2.2]bicycle **4.16** using reagents and conditions that are akin to those which had proved fruitful in our early generation approaches. Also, similar to our previous studies is the envisioned aryl oxidation/intramolecular Diels-Alder cycloaddition cascade (proceding through the intermediacy of cyclohexadiene **4.17**) that is illustrated as the initial key reaction sequence.

4.2 Model Studies Toward the Synthesis of Phomoidride D

4.2.1 The Phenolic Oxidation/Diels-Alder Sequence

In the previous two generations toward phomoidride D, our group utilized a phenolic oxidation/Diels-Alder sequence to form the [2.2.2]bicycle of **4.16**. The distinguishing feature in the substrates employed for this reaction in the first- and second-generation approaches is the number of ester moieties (two vs. one, respectively). Interestingly, exploiting this reaction in the third-generation approach toward **4.16** requires a similar change; however in this instance the number of ester substituents is reduced from one to none. As illustrated in Table 4.10, the requisite catechol substrate now possesses a single additional alcohol substituent.

In contrast to generations one and two, wherein the aryl-oxidation proceeded smoothly with all substrates we employed, our efforts to advance diol **4.18a** through a similar reaction failed to produce any of the desired product (Table 4.10). By simply comparing the nature of **4.18a** to the substrates employed in generations one and two, we

believed that the lack of an electron withdrawing substituents on the intermediate diene was causing of the loss of reactivity. In an effort to address this electronic difference we prepared a variety of substrates possessing a range of what could be considered electron withdrawing protecting groups. As indicated in Table 4.10, the presence of an acetate or trifluoroacetate did nothing to promote cycloaddition; however,, to our delight, substrates possessing sulfonyl-protecting groups, such as methanesulfonyl (**4.18d**) or 2-nitrobenzenesulfonyl (**4.18e**), underwent the desired aryl oxidation/Diels-Alder reaction to furnish bicycles (**4.16d** and **4.16e**, respectively). Given that the nosyl protected phenol (**4.18e**) gave us the best results we chose to move forward with this as our first major intermediate.[1]

Table 4.10 Optimization of the phenolic oxidation/Diels-Alder reaction

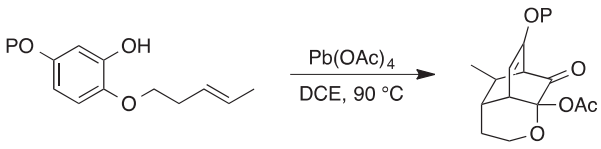

4.18 a-e **4.16 a-e**

P	Yield
H (**4.18a**)	0%
Ac (**4.18b**)	0%
$COCF_3$ (**4.18c**)	0%
Ms (**4.18d**)	42%
Ns (**4.18e**)	62%

As illustrated in Scheme 4.11 synthesis of the nosylated intermediate (**4.16e)** on-scale began with nosylation and allylation of the commercially available 2,4-dihydroxybenzaldehyde **4.19**. As one might anticipate, this is not a particularly regioselective transformation and nearly equimolar amounts of **4.20** and **4.21** are initially

produced. However, we discovered that filtering and washing the worked-up reaction mixture with methanol allows for the isolation of a 5:1 mixture of regioisomers, favoring the desired benzaldehyde **4.20**. Subsequent Dakin oxidation of **4.20** (*m*CPBA) delivers phenol **4.22**. At this point, the regioisomers were separated and the desired regioisomer was functionalized with allyl iodide **4.23** to produce **4.24** in 44% yield.[2] The aryl oxidation/Diels-Alder substrate was completed by removal of the allyl protecting group in **4.24** using $Pd(PPh_3)_4$ and potassium carbonate (K_2CO_3) in methanol.[3]

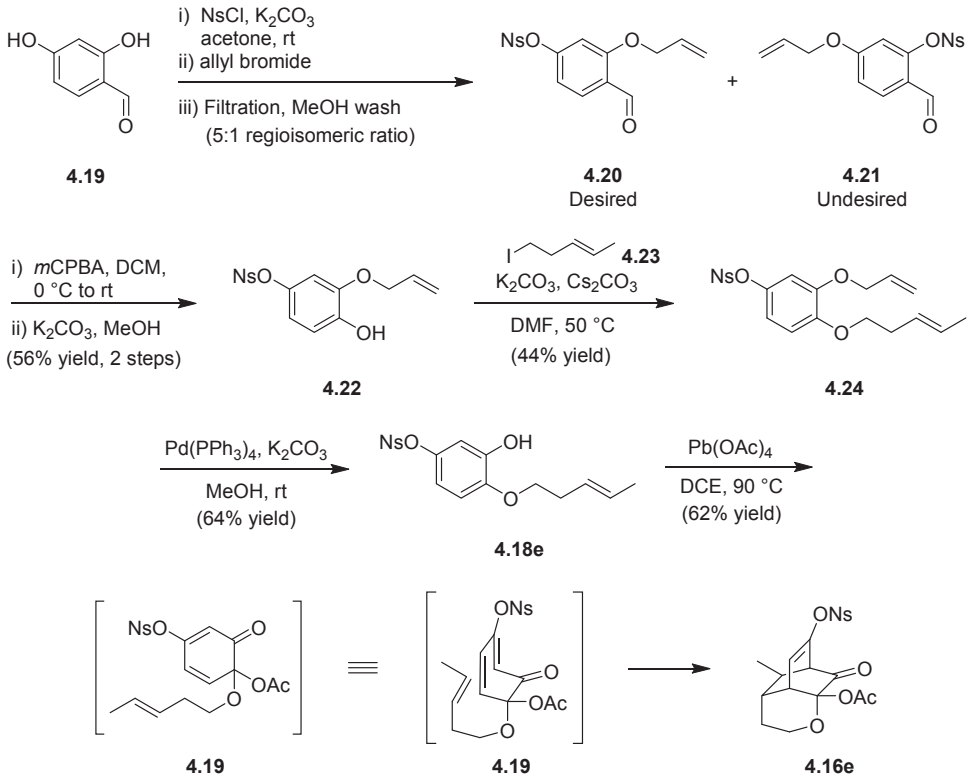

Scheme 4.11 Phenolic oxidation/Diels-Alder sequence

As with material prepared in our initial small scale studies, the resultant phenol **4.18e** was treated with lead tetraacetate ($Pb(OAc)_4$) in 1,2-dichloroethane (DCE) at reflux to induce formation of diene **4.19** via Wessely oxidation. Although this intermediate is

observable (in some instance isolable) under the 90 °C reaction conditions employed here the intermeidate undergoes further reaction via a [4+2] cycloaddition to give [2.2.2]bicycle **4.16e**.[4] The resultant Diels-Alder adduct (**4.16e**) was isolated in a 62% yield, along with a small amount (<5%) of the deacylated product.

4.2.2 Formation of the Isotwistane Core

Having successfully implemented the first cascade sequence and accessed **4.16e**, we turned next toward setting the stage for the second, a radical-mediated cascade. The two carbon atoms that would serve as the linchpin in this cascade, along with the lactone carbonyl, would be introduced using an aldol reaction that was analogous to that employed in the earlier generation approaches. As is evident from the chemistry illustrated in Scheme 4.12, we chose to employ *tert*-butyl 3-(dimethylamino)propionate (**4.25**) as the nucleophilic component in the aldol reaction. This choice to use a *t*-butyl ester was dictated by our interest in developing an acid promoted procedure that would allow us to advance the aldol product through acetate hydrolysis and lactonization in a single pot. After a thorough study of the reaction conditions, it was determined that the best yields of alcohol **4.27** are observed when magnesium bromide is used as a Lewis-acid to activate ketone **4.16e** and the lithium enolate derived from **4.25** is used as the nucleophile.[5] The nosyl protecting group was removed from the aldol product using thiophenol (PhSH) and cesium carbonate (Cs_2CO_3)[6] and the resulting keto-alcohol was subjected to oxidation (*m*CPBA) and Cope elimination to generate α,β-unsaturated ester **4.27** in 30% yield over three steps.[7] In accord with our plan, exposure of **4.27** to hydrochloric acid resulted in acetate hydrolysis and lactonization to furnish the desired lactone **4.28** in excellent yield.

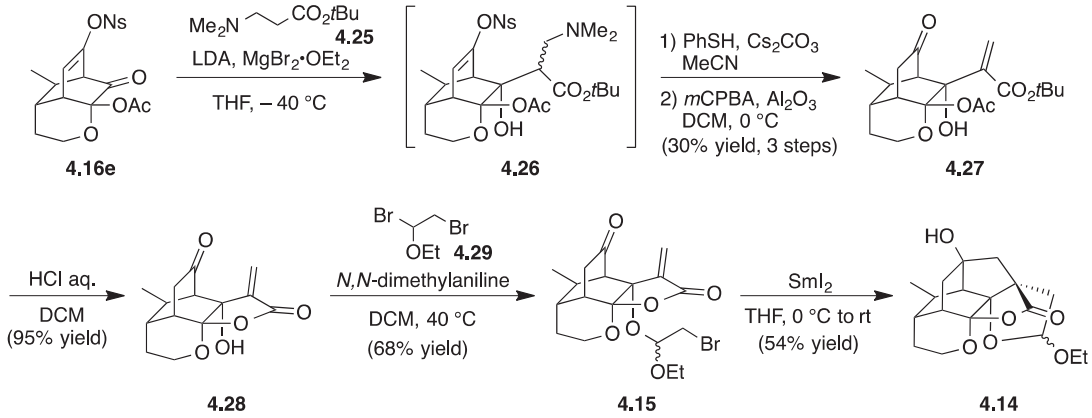

Scheme 4.12 Isotwistane formation

With lactone **4.28** in hand, the final two carbons needed to complete construction of the radical cyclization substrate were introduced via coupling of **4.28** to bromoacetal **4.29** using *N,N*-dimethylaniline as a base in DCM at reflux, conditions developed by Stork for delivering **4.29** to hindered tertiary alcohols.[8] The desired radical cyclization substrate (**4.15**) was produced as an inconsequential mixture (1:1) of diastereomeric acetals (**4.15**) in 68% yield. In previous studies several methods had been employed in our group to initiate similar radical cascade reactions. Of these, the use of SmI_2 has often proven to be the most efficient. Thus, we were delighted to find that exposure of **4.15** to SmI_2 in THF at 0 °C resulted in smooth conversion to isotwistane **4.14** (54% yield). Although no detailed mechanistic studies have been done we speculate (Scheme 4.13), based on previous studies, that this cascade event is initiated by formation of a ketyl radical (**4.15a)** which upon 5-*endo* ring closure produces an intermediate radical that undergoes further reduction to a lactone enolate (**4.15b)** capable of terminating the cascade by intramolecular alpha alkylation.[9] It is important to note that in addition to allowing for the efficient construction of the requisite isotwistane core, the radical

cascade reaction stereoselectively produces the all-carbon quaternary center, a synthetically challenging structural element.

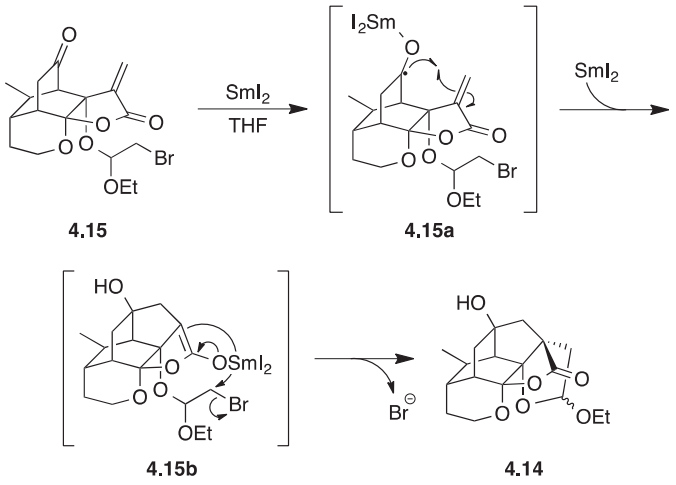

Scheme 4.13 Possible mechanism for the radical cascade cyclization

4.2.3 Formation of the Bicyclo[4.3.1] Core

Having accessed isotwistane **4.14**, the bicylodecadiene core structure found in the phomoidrides was now potentially accessible via Wharton fragmentation. As in the second-generation approach we envisioned the fragmentation proceeding by deacylation and loss of the mesylate nucleofuge. Installation of these functionalities was accomplished in a three-step sequence that began with acylation of the resident tertiary alcohol followed by transacetalization to the corresponding thioacetal, a transformation which was readily accomplished upon exposure of the acylated **4.14** to 1,3-propanedithiol in the presence of BF_3•OEt_2. The resultant crude tertiary alcohol was reacted with methanesulfonyl chloride (MsCl), delivering fragmentation precursor **4.13** in 86% yield over the three steps. Inducing fragmentation to the desired bicyclo[4.3.1] core was accomplished by the addition of aqueous potassium hydroxide (KOH) in THF. Initial analysis of the crude reaction mixture by ^{1}H NMR spectroscopy clearly indicated that the

fragmentation had occurred due to the characteristic vinyl resonance; however, loss of the distinct diastereotopic resonances associated with the protons residing on the closed acetal, coupled with the polar nature of the product, suggested that the fragmentation reaction had been accompanied by acetal opening to furnish diol **4.30**. In subsequent studies we determined that subjecting the crude reaction mixture to 4-toluenesulfonyl chloride (TsCl) and DMAP in pyridine, transforms the diol into the desired ketone **4.12** which can be isolated in 11% yield over two steps. To our delight, switching the latter conditions to NsCl and Et_3N in DCM improved the yield of ketone **4.12** to 72% yield from mesylate **4.13**.

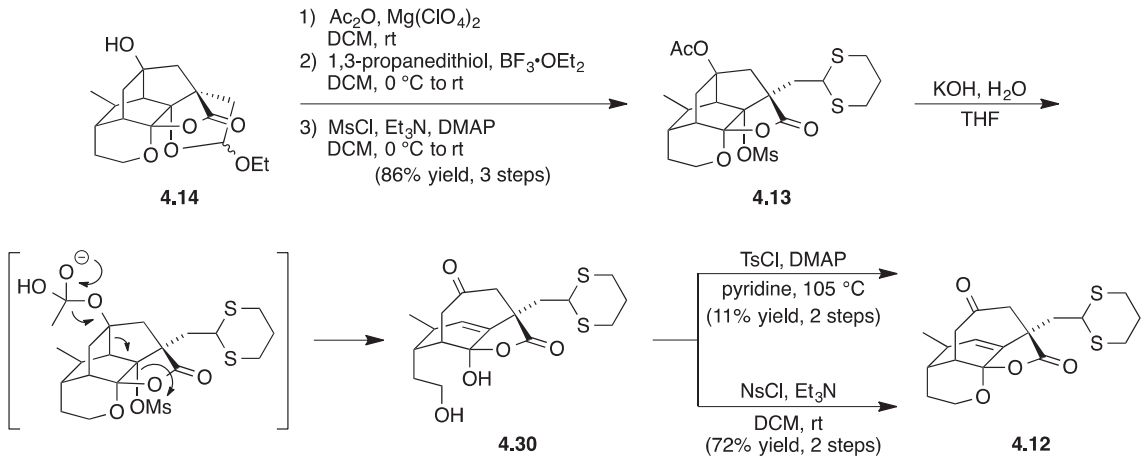

Scheme 4.14 Wharton fragmentation

At this point our model study had clearly demonstrated feasibility in the two-cascade sequences leading up to the proposed Wharton fragmentation of isotwistane **4.13**. Moreover, the latter fragmentation, in contrast to the retro-aldol plagued second-generation approach, proved effective in delivering the phomoidride core and put us in position to begin addressing potential concerns associated with maleic anhydride installation.

4.2.4 β-Keto Ester Formation

As outlined in Chapter 3, our first generation approach had been successful in delivering a diester intermediate that was only one oxidation level removed from the natural product. Our inability to complete the synthesis by oxidation of the diester to the maleic anhydride led to our developing the second-generation approach, which ultimately failed due to an unanticipated retro-aldol reaction. Although, contrary to synthetic dogma, which often calls for maximizing convergency, the results obtained from our first and second-generation attempts indicated that our fragmentation based strategy would only be successful if the carbonyl carbons of the maleic anhydride were introduced one at a time (i.e., in the least convergent manner).

Thus, as illustrated in the retrosynthetic analysis for our current approach (*vide supra*, Scheme 4.10) our plan is to first install a beta-keto ester and then, in a fashion similar to that of Shair and Fukuyama in their syntheses of phomoidride B (**4.35**), introduce the final carbon via a cabonylation reaction. Although there is a strategic similarity to the work of Shair and Fukuyama with regard to maleic anhydride construction, it is noteworthy that these groups employed the regioisomeric beta-keto ester as a substrate (Scheme 4.15). Thus, this past precedent provided some hope but by no means assured success. In any event, as outlined is Scheme 4.16, our plan next called for conversion of ketone **4.12** to the corresponding beta-keto ester, a transformation that is often best performed under conditions developed by Mander and coworkers.[10]

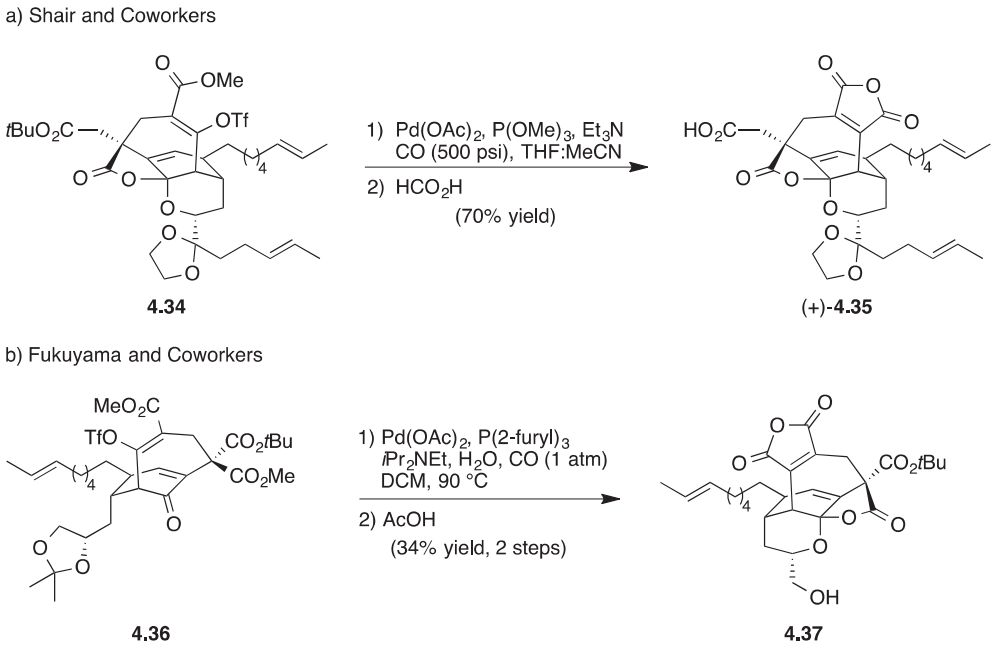

Scheme 4.15 Shair and Fukuyama's maleic anhydride formation

As illustrated in Scheme 4.16, Mander's conditions for converting a ketone to the corresponding beta-keto ester involve initial formation of a lithium enolate followed by acylation using methyl cyanoformate (a.k.a., Mander's Reagent). A complicating factor with **4.12** is the fact that the ketone is flanked by four protons, any of which could potentially be removed by a strong base. This presents a potential regioisomeric issue, which we hoped would be controlled to some extent by the quaternary center adjacent to one of the methylenes. If the quaternary center directed enolization away from the neopentyl methylene the outcome would be the desired enolate regioisomer **4.11** and **4.31** (Scheme 4.16). To our chagrin, initial studies utilizing kinetic enolization conditions (super-stoichiometric LDA) akin to those employed by Mander, furnished an acylated product which, after ^{1}H and ^{13}C NMR studies was determined to be the undesired regioisomer **4.32**.

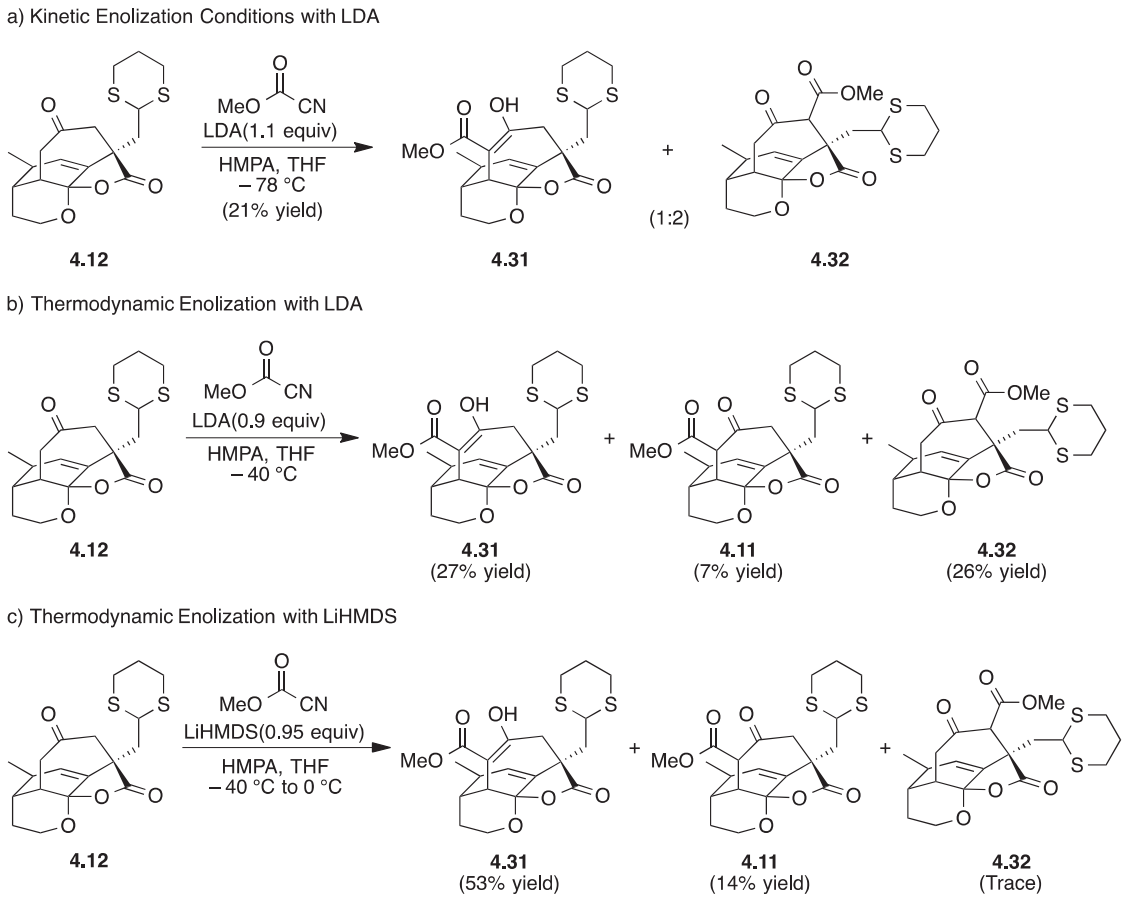

Scheme 4.16 β-Keto ester formation

Due to the poor yields and undesired regioselectivity observed in our initial studies, we decided to more closely examine the reaction conditions. It is known that one can sometimes influence the course of enolate formation by performing the deprotonation under thermodynamic conditions instead of the more common kinetic. It is, *a priori*, difficult to predict if a "kinetic enolate" (generated with a superstoichiometric amount of base) will be regioisomerically different from a "thermodynamic enolate" (generated with a substoichiometric amount of base, hence under equilibrating conditions); thus, we set out to explore these various conditions on our substrate (**4.12**). In the event, we decreased the equivalents of LDA from 1.1 to 0.9 and warmed the reaction to – 40 °C.

To our delight, we found that we could indeed influence the regioisomeric ratio and under these conditions the regioisomeric outcome favored the desired β-keto ester **4.11** (and **4.31**) (Scheme 4.16b). In addition to delivering the desired ester **4.11** (and **4.31**) these conditions also resulted in a significant increase in the yield (21% to 53%). Further optimization studies revealed that the use of a sub-stoichiometric amount of a bulkier base (LiHMDS), followed by warming the reaction to 0 °C prior to the addition of Mander's reagent, results in the formation **4.11** (and **4.31**) in 67% yield (Scheme 4.16c). Interestingly the desired beta-keto ester is produced as a mixture of isolable tautomers that favors enol (**4.31**) over the corresponding keto (**4.11**) form. The indicated yields for this transformation reflect the combined weight of the tautomers.

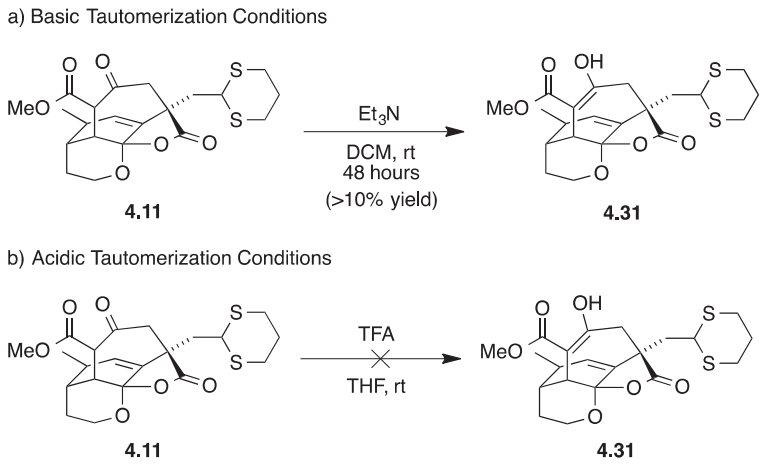

Scheme 4.17 Tautomerization experiments

Typically one finds that keto-enol tautomerization of β-keto esters is rapid and the mixtures are inseparable. Given the unusual observation in this system we decided to test the keto-enol tautomerization under both basic and acidic conditions (Scheme 4.17). Subjecting the keto form (**4.11**) to Et_3N in DCM did produce a minimal amount of enol

tautomer, but only after 48 hours, while acidic conditions resulted in no tautomerization at all.

Initial studies to form vinyl triflate **4.33** were performed on keto-tautomer **4.11** (Scheme 4.18). As might have been anticipated from our studies with Et_3N (*vide supra*) treatment of **4.11** with Hünig's base and triflic anhydride failed to produce any vinyl triflate.[11] Thus, we decided to use a stronger base (KHMDS) in conjunction with *N*-phenyl triflimide (Tf_2NPh). In the event, deprotonation employing a substoichiometric amount of KHMDS in the presence of Tf_2NPh, produced desired vinyl triflate **4.33** in 53% yield.[12] It is worth noting that we employed a slight substoichiometric amount of base simply to avoid any complications that may have arisen due to excess base.

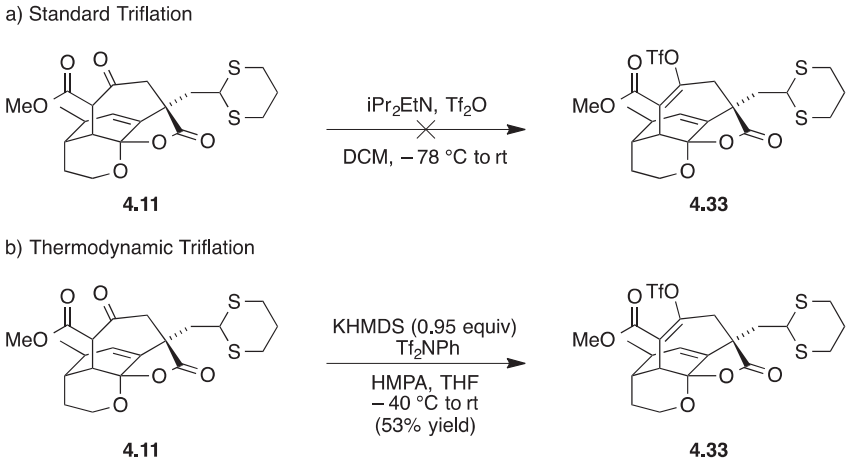

Scheme 4.18 Triflation attempts

Similarly, the enol form was converted to vinyl triflate **4.33** using KHMDS with Tf_2NPh as the triflating agent to provide vinyl triflate **4.33** in corresponding 68% yield (Scheme 4.19).

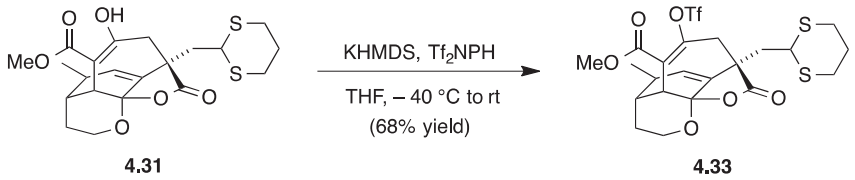

Scheme 4.19 Enol triflation

4.2.5 Maleic Anhydride Formation and Completion of the Model Study

Having prepared vinyl triflate **4.33** from either keto or enol-tautomer, we turned next to completion of the maleic anhydride. Two slightly different sets of conditions for this reaction had already been developed on similar systems and are reported in the syntheses of phomoidride B (**4.35**) by the groups of Shair and Fukuyama (Scheme 4.15).[13]

In our initial studies to advance the vinyl triflate we explored Shair's conditions and in accord with their protocol exposed **4.33** to a mixture of palladium(II) acetate ($Pd(OAc)_2$), trimethyl phosphite ($P(OMe)_3$), and Et_3N, in an atmosphere of CO. Unfortunately, only decomposition of the starting enol triflate was observed (Scheme 4.20a). Turning next to the conditions developed by Fukuyama, vinyl triflate **4.33** was exposed to a DMF solution of $Pd(OAc)_2$, tri(2-furyl)phosphine ($P(2\text{-furyl})_3$), Hünig's base, and water, all under an atmosphere of CO. After heating to 90 °C we were delighted to find that these conditions produced the required maleic anhydride **4.38** in 58% yield, the structure of which was confirmed by single crystal X-ray analysis (Scheme 4.20b).

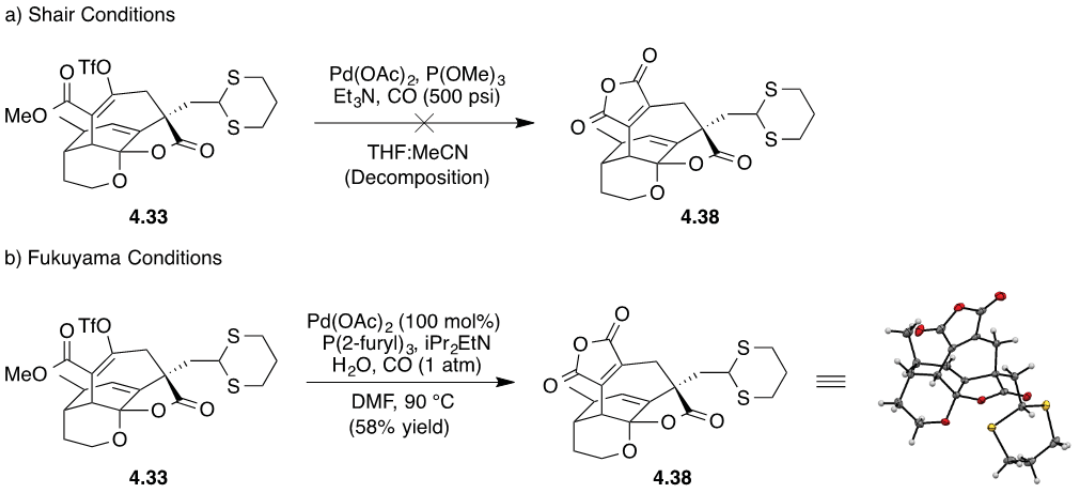

Scheme 4.20 Maleic anhydride formation

With maleic anhydride **4.38** in hand, all that was left to finish the model system synthesis was removal of the thioacetal and oxidation of the derived aldehyde to the acid. Initial attempts using iodination conditions, such as [bis(trifluoroacetoxy)iodo]benzene (BTIB) or iodine, did not give aldehyde **4.39**.[14] Similar conditions were attempted on vinyl triflate **4.33**, but this too did not deliver the desired aldehyde.

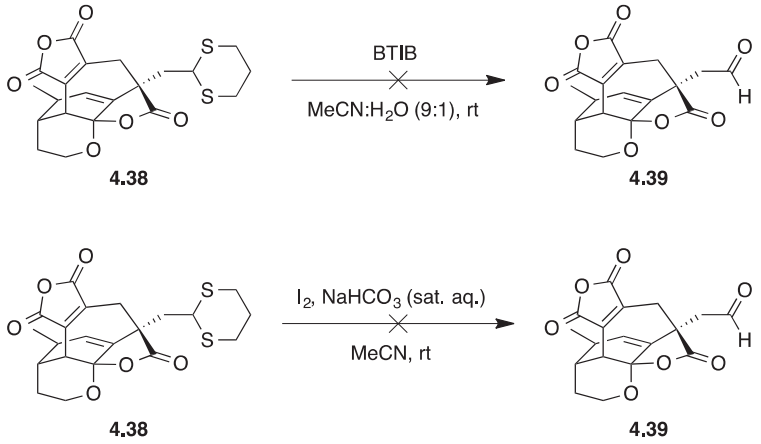

Scheme 4.21 Initial thioacetal deprotections

Given the difficulties encountered with the milder deprotection reagents we decided to attempt conditions which had been developed by Nicolaou for the removal thioketals.[15] Under these conditions, which involved exposing thioacetal **4.38** to *N*-bromosuccinimide (NBS) and silver(I) perchlorate in aqueous acetone, we were excited to see removal of the thioacetal protecting group. However, we were unable to separate the aldehyde intermediate **4.39** from succinimide and thus carried the crude mixture through the subsequent Pinnick oxidation, which furnished the final product in an unoptimized 23% yield. Importantly, this final step completed the model study and validated our third generation strategy.

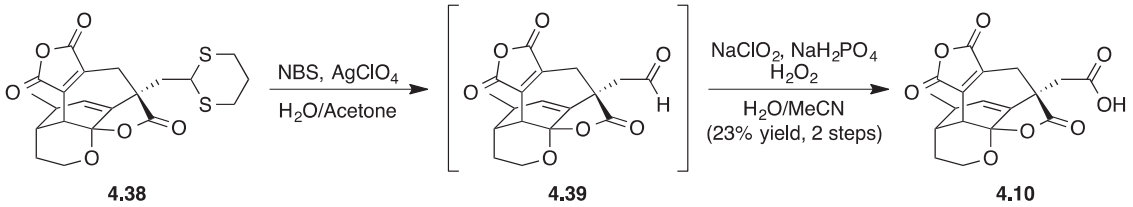

Scheme 4.22 Completion of the model study

4.3 Conclusion

In a first-generation approach toward phomoidride D, we began developing a strategy that centers around two cascade sequences as key steps in delivering the phomoidride carbocyclic core. In the first of these sequences a tandem phenolic oxidation/Diels-Alder reaction is employed to produce a [2.2.2]bicycle, which is readily transformed into a bromo acetal that is poised for conversion to a key isotwistane. The latter transformation is performed via the second cascade sequence which is mediated by SmI_2 and delivers not only the isotwistane but also sets the quaternary stereogenic center that is imbedded in the phomoidride core. Functional group manipulation sets the stage

for a Grob fragmentation which provides access to the bicyclo[4.3.1]decadiene core found in the phomoidrides (Chapter 3, section 3.47). Unfortunately, the first generation approach met its demise when conversion of a late stage diester to the corresponding maleic anhydride proved impossible. To circumvent this issue, a model study was launched to investigate an alternative (second-generation) approach wherein carbonylation of an advanced beta-keto ester would give rise to the maleic anhydride. Unfortunately, due to a deleterious retro-aldol reaction, this approach also met with an untimely demise, failing prior to the Wharton fragmentation. In our third-generation approach, which has been the focus of this chapter, we combine the strategic elements of the first two generations with a better understanding of the late stage reactivity into an approach that calls for generating the maleic anhydride unit from an isolated ketone. As described above, this approach was explored in a model study that has allowed us to define suitable substrates for the initial aryl-oxidation/Diels-Alder cascade sequence. In addition, the model study established that a simple ketone can be combined with an *exo*-methylene lactone and bromoacetal in a cascade cyclization that delivers the requisite isotwistane intermediate. Importantly, these studies also revealed that the desired Wharton fragmentation can be induced under mild conditions to furnish a ring opened acetal that can be reclosed and thus positioned for subsequent incorporation of the maleic anhydride. With regard to the latter, these models studies helped to establish feasibility with regard to the requisite regioselective acylation under Mander's conditions and established that an enol triflate derived from the resultant beta-keto ester is a viable carbonylation substrate using conditions developed by Fukuyama. Finally this model study aided in establishing the feasibility of thioacetal removal and oxidation in the

presence of the phomoidride core functionality. Efforts can now be focused on translating the model system chemistry onto substrates containing the full complement of carbons and functional groups found in natural phomoidride D.

4.4 Experimentals

General

Unless stated otherwise, all reactions were performed using flame or oven-dried glassware and under an atmosphere of nitrogen. DCM, THF, diethyl ether, benzene, and toluene were dried using a solvent purification system manufactured by SG Water U.S.A., LLC. Acetonitrile, ethyl acetate, pentanes, hexanes, DMF, DMSO, and DCE were supplied by either Fisher Scientific or Sigma-Aldrich and were used as received. Triethylamine, diisopropylamine, and methanol were stirred over calcium hydride and distilled before use. All other commercially available reagents were used as received.

Unless stated otherwise, reactions were monitored by thin-layer chromatography using Silicycle SiliaPlate® TLC glass backed extra hard layer, 60 Å (F-254 indicator, 250 μm thickness). All purifications were performed using Silicyle SiliaFlash® P60 silica (40-63 μm, 230-400 mesh) as a stationary phase. High-resolution mass spectroscopy was performed by the central instrument facility at Colorado State University or on a Thermo Orbitrap ESI mass spectrometer at Baylor University. Single-crystal X-ray crystallography was performed by Brian Newell at Colorado State University or Prof. Caleb Martin at Baylor University. ^{1}H and ^{13}C NMR spectra were taken on Varian VNMRS 500, Varian Inova 400, Bruker Ascend 400, and Bruker Ascend 600 cryoprobe spectrometers. Infrared spectra were taken on a Nicolet Avatar 320 FTIR

or Bruker Alpha Platinum ATR. Chemical Shifts (δ) are reported in parts per million (ppm) and coupling constants (*J*) are reported in hertz (Hz). The reported chemical shifts are relative to the residual solvent peaks of the indicated deuterated solvents.

Preparation of Phenol **4.22**

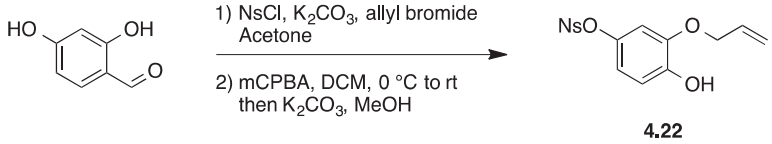

4.22

Benzaldehyde Functionalization. To a round bottom flask equipped with a magnetic stir bar was added 2,4-dihydroxybenzaldehyde (40.0 g, 290 mmol), 2-nitrobenzenesulfonyl chloride (NsCl) (64.2 g, 290 mmol), potassium carbonate (K_2CO_3) (96.2 g, 608 mmol), and Acetone (965 mL). The flask was capped with a rubber septum containing a 16 gauge needle open to air and stirred vigorously at room temperature. After 25 hours allyl bromide (36.5 mL, 434 mmol) was added rapidly via syringe and TLC was used to monitor the reaction progress. The TLC plates were developed using a 25% EtOAc/Hex solution and visualized by $KMnO_4$. The reaction was worked up after a total of 47 hours by light concentration and transferring to a separatory funnel containing EtOAc (600 mL). The organic layer was washed with 1M HCl (750 mL) and brine (250 mL) before drying over $MgSO_4$. Concentration delivered a mixture of regioisomers as a tan solid that was washed with MeOH (~ 500 mL) and filtered by vacuum filtration through a fritted funnel until the filtrate appeared colorless. The resultant white solid contained the functionalized benzaldehyde as a 5:1 (desired:undesired) mixture of regioisomers (56.9 g) which was moved onto the next step without further purification.

Dakin Oxidation. To a round bottom flask equipped with a magnetic stir bar was added the benzaldehyde (56.9 g, 157 mmol) and dichloromethane (DCM) (500 mL). The solution was cooled in an ice/water bath and *m*CPBA (35.1 g, 77%, 157 mmol) was added. The flask was capped with a rubber septum fitted with a 16 gauge needle open to air and the reaction was allowed to slowly warm to room temperature within the bath. After 19 hours K_2CO_3 (32.5 g, 235 mmol) and MeOH (660 mL) were added all at once. After 67 hours the reaction was concentrated and dissolved again in H_2O:EtOAc (1:2). The layers were separated and the aqueous extracted with EtOAc (2x) and the combined organics were washed with brine and dried over $MgSO_4$. Concentration and purification via silica gel flash column chromatography (10% gradient elution from 0% → 50% EtOAc/Hex) afforded phenol **4.22** (53.1 g, 56% yield) as a brown solid.

R_f = 0.49 (50% EtOAc/Hex); m.p. 81-83 °C; ^{1}H-NMR (600 MHz; $CDCl_3$): δ 7.95-7.91 (m, 1H), 7.84-7.80 (m, 2H), 7.67 (ddd, *J* = 7.9, 5.9, 2.9 Hz, 1H), 6.81 (dd, *J* = 5.7 Hz, 2H), 6.65 (dd, *J* = 8.7 hz, 2.6 Hz, 1H), 5.99 (ddt, *J* = 17.2, 10.5, 5.6 Hz, 1H), 5.60 9s, 1H), 5.41-5.29 (m, 2H), 4.55 (d, *J* = 12.0 Hz, 2H); ^{13}C-NMR (150 MHz; $CDCl_3$): δ 145.8, 145.3, 141.8, 135.4, 132.5, 132.0, 132.0, 128.4, 124.9, 119.3, 115.0, 114.6, 107.3, 70.3; FTIR (thin film/NaCl): 3498, 3098, 2923, 1545, 1504 cm^{-1}; HRMS (ESI) *m*/*z* Calc'd for $C_{15}H_{13}NO_7S$ $[M+Na]^+$: 374.0305, found: 374.0305.

Preparation of Allyl Ether **4.24**

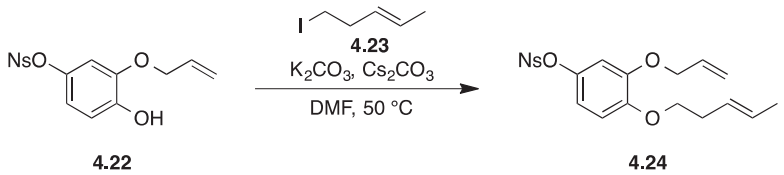

4.22 **4.24**

To a round bottom flask equipped with a magnetic stir bar was added phenol **4.22** (46.7 g, 133 mmol), alkyl iodide **4.23**, potassium carbonate (91.9 g, 665 mmol), cesium carbonate (2.17 g, 6.65 mmol), and dimethylformamide (DMF) (200 mL). The flask was capped with a polyethylene stopper and stirred at 50 °C. TLC was used to monitor the reaction progress. The TLC plates were developed using a 25% EtOAc/Hex solution and visualized by $KMnO_4$. The reaction was removed from heat after 23 hours and allowed to cool to room temperature. The reaction was slowly transferred to a separatory funnel containing 1M HCl (700 mL) and the aqueous was extracted with EtOAc (3 x 700 mL). The combined organics were then washed with 1M HCl, brine and dried over Na_2SO_4. Concentration and purification via silica gel flash column chromatography (10% gradient elution from 0% → 60% EtOAc/Hex) afforded allyl ether **4.24** (24.7 g, 44% yield) as a brown viscous oil.

R_f = 0.24 (25% EtOAc/Hex); ^{1}H-NMR (600 MHz; $CDCl_3$): δ 7.89 (d, *J* = 7.9 Hz, 1H), 7.83-7.79 (m, 2H), 7.65 (ddd, *J* = 7.9, 6.4, 2.4 Hz, 1H), 6.78-6.69 (m, 3H), 5.96 (ddt, *J* = 17.2, 10.5, 5.2 Hz, 1H), 5.61-5.53 (m, 1H), 5.50-5.45 (m, 1H), 5.36 (dd, *J* = 17.4 Hz, 1.8 Hz, 1H), 5.24 (dd, *J* = 10.2, 1.2 Hz, 1H), 4.48 (d, *J* = 5.4 Hz, 2H), 3.95 (t, *J* = 7.0 Hz, 2H), 2.50 (m, 2H), 1.66 (d, *J* = 6.0 Hz, 3H); ^{13}C-NMR (150 MHz; $CDCl_3$): δ 148.9, 148.8, 148.3, 142.3, 135.4, 132.7, 132.5, 132.0, 128.3, 128.1, 126.4, 124.8, 118.1, 114.4, 113.4, 108.8, 70.1, 69.2, 32.6, 18.2; FTIR (thin film/NaCl): 2918, 1544, 1504 cm^{-1}; HRMS (ESI) *m/z* Calc'd for $C_{20}H_{21}NO_7S$ $[M+Na]^+$: 442.0931, found: 442.0934.

Preparation of (E)-3-hydroxy-4-(pent-3-en-1-yloxy)phenyl 2-nitrobenzenesulfonate **4.18e**

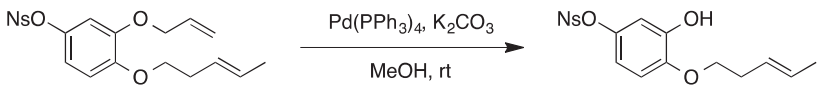

4.24 **4.18e**

To a round bottom flask equipped with a magnetic stir bar was added the allyl-protected phenol **4.24** (24.9 g, 59.3 mmol), potassium carbonate (10.7 g, 77.1 mmol), tetrakis(triphenylphosphine)palladium(0) ($Pd(PPh_3)_4$) (2.1 g, 1.8 mmol), and methanol (200 mL). The flask was purged with an over-pressure of nitrogen and then allowed to stir at room temperature overnight. TLC was used to monitor the reaction progress. The TLC plates were developed using a 25% EtOAc/Hex solution and visualized by $KMnO_4$. The reaction was worked up by filtration through a plug of silica, using ethyl acetate to flush out the organics. Concentration and purification via silica gel flash column chromatography (10% gradient elution from 0% → 70% EtOAc/Hex) afforded phenol **4.18e** (14.5 g, 64% yield) as a brown solid.

R_f = 0.16 (EtOAc/Hex); m.p. 84-85 °C; ^{1}H-NMR (400 MHz; $CDCl_3$): δ 7.93 (d, *J* = 8.0 Hz, 1H), 7.83-7.78 (m, 2H), 7.66 (ddd, *J* = 7.9, 6.4, 2.8 Hz, 1H), 7.76-7.67 (m, 3H), 5.74 (s, 1H), 5.61-5.54 (m, 1H), 5.49-5.41 (m, 1H), 4.01 (t, *J* = 6.7Hz, 2H), 2.46 (q, *J* = 6.5 Hz, 2H), 1.68 (d, *J* = 6.3 Hz, 3H); ^{13}C-NMR (100 MHz; $CDCl_3$): δ 146.6, 145.3, 143.0, 135.42, 132.4, 132.0, 128.7, 128.4, 126.2, 124.9, 113.6, 112.0, 109.1, 69.2, 32.5, 18.1; FTIR (thin film/NaCl): 3507, 3099, 3027, 2941, 1605, 1546, 1504 cm^{-1}; HRMS (ESI) *m*/*z* Calc'd for $C_{17}H_{17}NO_7S$ $[M+H]^+$: 380.0805, found: 380.0801.

Preparation of α-Acetoxy Ketone **4.16e** *and α-Hydroxy Ketone* **4.16e-OH**

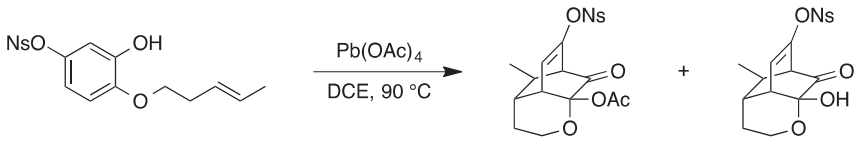

4.18e **4.16e** **4.16e-OH**

To a sealed tube equipped with a magnetic stir bar was added phenol **4.18e** (2.0 g, 5.3 mmol), lead(IV) acetate (2.8 g, 6.3 mmol), and 1,2-dichloroethane (DCE) (53 mL).

The reaction vessel was sealed and heated at 90 °C for 14 hours. Upon cooling the reaction progress was analyzed by TLC. The TLC plates were developed using 50% EtOAc/Hex solution and visualized by $KMnO_4$. The reaction was then concentrated and purified immediately by silica gel flash column chromatography (10% gradient from 20% → 100% EtOAc/Hex) affording the product as a 20:1 mixture favoring **4.16e** (1.4 g, 62% yield) as and orange foam.

α-Acetoxy Ketone **4.16e**. R_f = 0.22 (50% EtOAc/Hex); ^{1}H-NMR (400 MHz; Benzene-D_6): δ 7.67 (dd, *J* = 7.4, 2.0 Hz, 1H), 6.85 (dd, *J* = 7.8, 1.5 Hz, 1H), 6.67-6.57 (m, 2H), 5.82 (dd, *J* = 7.6, 2.8 Hz, 1H), 3.64-3.58 (m, 2H), 3.26 (td, *J* = 12.0, 4.0 Hz, 1H), 3.14 (t, *J* = 2.8 Hz, 1H), 1.51 (s, 3H), 1.39-1.29 (m, 2H), 1.09 (p, *J* = 3.6 Hz, 1H), 0.735 (q, *J* = 2.8 Hz, 1H), 0.75-0.69 (m, 1H), 0.66 (d, *J* = 7.2 Hz); ^{13}C-NMR (100 MHz, Benzene-D_6) δ 198.91, 195.14, 168.13, 146.40, 135.15, 132.02, 131.63, 128.44, 124.72, 116.48, 93.62, 62.19, 57.80, 40.63, 37.21, 35.61, 28.34, 21.44, 20.00; FTIR (thin film/NaCl): 3099, 2963, 1754, 1653, 1592, 1547 cm^{-1}; HRMS (ESI) *m/z* Calc'd.for $C_{19}H_{19}NO_9S$ $[M+H]^+$: 438.0859, found: 438.0850.

α-Hydroxy Ketone **4.16e-OH.** R_f = 0.27 (75% EtOAc/Hex); m.p. 60-62 °C; ^{1}H-NMR (400 MHz; $CDCl_3$): δ 8.01 (dt, *J* = 7.8, 1.0 Hz, 1H), 7.88-7.82 (m, 2H), 7.75-7.69 (m, 1H), 6.04 (dd, *J* = 7.6, 2.8 Hz, 1H), 3.86 (ddt, *J* = 11.2, 5.6, 1.2 Hz, 1H) 3.53 (td, *J* = 12.5, 2.7 Hz, 1H), 3.18 (t, *J* = 2.7 Hz, 1H), 2.68 (dd, *J* = 7.6, 3.6 Hz, 1H), 2.11-2.05 (m, 2H), 1.94-1.85 (m, 1H), 1.82 (p, *J* = 3.2 Hz, 1H), 1.63-1.58 (m, 1H), 1.13 (d, *J* = 7.0 Hz, 3H); ^{13}C-NMR (100 MHz, $CDCl_3$) δ 206.51, 194.81 (instrument artifact), 144.61, 135.89, 133.28, 132.36, 127.74, 125.12, 119.64, 90.18, 61.50, 57.74, 42.80, 39.32, 37.17, 34.92,

28.80, 20.20; FTIR (neat): 3382, 3099, 2961, 1742, 1651, 1592, 1543 cm^{-1}; HRMS (ESI) *m/z* Calc'd.for $C_{19}H_{19}NO_9S$ $[M+H]^+$: 396.0753, found: 396.0755.

Preparation of tert-Butyl Enoate **4.27**

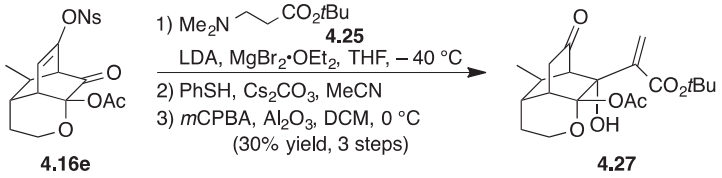

Lithium tert-Butyl 3-(dimethylamino)propionate formation. To a flame dried round bottomed flask equipped with a magnetic stir bar was added freshly distilled diisopropylamine (1.5 mL, 10.5 mmol) and THF (12 mL). The solution was then cooled in a dry ice/acetone bath and *n*-butyllithium (6.6 mL, 1.6 M in hexanes, 10.5 mmol) was added dropwise. After 20 minutes the reaction was placed into and ice water bath. After 20 more minutes the reaction was recooled to – 78 °C and a solution of methyl 3-(dimethylamino)propionate (1.8 g, 10.5 mmol) in THF (3.0 mL) was added. The reaction was allowed to stir at this temperature for 20 minutes.

To a flame dried round bottomed flask equipped with a magnetic stir bar was added ketone **4.16e** (1.4 g, 3.3 mmol), $MgBr_2$•OEt_2 (1.7 g, 6.6 mmol), and THF (33 mL). The solution was then cooled in an acetonitrile/dry ice bath. The lithium enolate was added via cannula over 25 minutes as the solution slowly turns red. The reaction progress was followed by TLC and the TLC plates were developed using 50% EtOAc/Hex solution and visualized by $KMnO_4$. After an additional 25 minutes of stirring at – 40 °C the reaction was quenched by adding saturated ammonium chloride (5.0 mL). The solution was the allowed to warm to room temperature when it was diluted with water and extracted three times with EtOAc. The combined organics were

washed with brine and dried over $MgSO_4$. Concentration afforded a brown oil which was moved forward crude.

Deprotection of the Nosyl Enol Ether. To a round bottomed flask equipped with a magnetic stir bar was added the crude enol ether, thiophenol (0.51 mL, 4.9 mmol), cesium carbonate (1.6 g, 4.9 mmol), and MeCN (17 mL). The reaction progress was followed by TLC and the TLC plates were developed using 50% EtOAc/Hex solution and visualized by $KMnO_4$. The solution was allowed to stir 1 hour when it was quenched with the addition of saturated ammonium chloride (10 mL). The solution was then extracted three times with EtOAc and the combined organics were washed with brine and dried over Mg_2SO_4. Concentration afforded the ketone as a brown oil that was carried forward to the next reaction crude.

Enoate Formation. To a round bottomed flask equipped with a magnetic stir bar was added the crude aminopropionate and DCM (25 mL). The solution was then cooled in an ice water bath and *m*CPBA (2.4 g, 77%, 10.5 mmol) was added. The cooling bath was removed and the reaction was allowed to warm for 20 minutes before basic Al_2O_3 (5.4 g) was added. The reaction progress was followed by TLC and the TLC plates were developed using 50% EtOAc/Hex solution and visualized by $KMnO_4$. The reaction was stirred 6 hours before it was filtered to remove the solid, using DCM to rinse. The filtrate was then washed twice with saturated sodium bicarbonate and once with brine. The combined organics were then dried over Na_2SO_4 and concentrated. The crude was purified via silica gel flash column chromatography (5% gradient from 0% → 35% EtOAc/Hex) affording **4.27** as a white solid in 30% yield over 3 steps.

R_f = 0.58 (50% EtOAc/Hex); m.p. 133-135 °C; ^{1}H-NMR (400 MHz; $CDCl_3$): δ 6.03 (d, *J* = 1.6 Hz, 1H), 5.76 (d, *J* = 1.2 Hz, 1H), 5.38 (d, *J* = 1.2 Hz, 1H), 4.45-4.39 (m, 1H), 4.36-4.30 (m, 1H), 3.36 (d, *J* = 3.5 Hz, 1H), 2.67-2.67 (m, 1H), 2.60 (m, 1H), 2.26 (dd, *J* = 19.6, 1.6 Hz, 1H), 2.14-2.06 (m, 2H), 1.95 (s, 3H), 1.84-1.76 (m, 1H), 1.74-1.69 (m, 1H), 1.50 (s, 9H), 0.94 (d, *J* = 7.6 Hz, 3H); ^{13}C-NMR (100 MHz; $CDCl_3$) δ 212.24, 194.96 (instrument artifact), 168.62, 167.43, 144.11, 123.66, 103.70, 82.21, 77.87, 64.07, 61.48, 38.29, 35.47, 34.29, 32.10, 30.91, 28.22, 22.38, 20.94; FTIR (thin film/NaCl): 3524, 2975, 2931, 1729, 1626 cm^{-1}; HRMS (ESI) *m*/*z* Calc'd.for $C_{20}H_{28}NO_7$ $[M+Na]^+$: 403.1733, found: 403.1735.

Preparation of γ-Lactone **4.28**

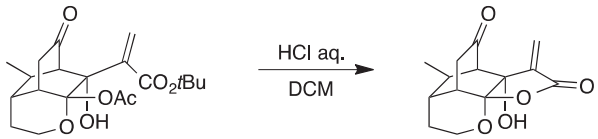

4.27 **4.28**

To a cone-shaped flask equipped with a magnetic stir bar was added the *tert*-butyl enoate **4.27** (0.38 g, 1.0 mmol) and DCM (5.2 mL). Concentrated HCl (0.05 mL, 12 M, 0.60 mmol) was added dropwise and the reaction was allowed to stir. The reaction progress was followed by TLC, and the TLC plates were developed using 50% EtOAc/Hex solution and visualized by $KMnO_4$. After 1.5 hours the reaction was filtered to remove the γ-lactone **4.28** as a white solid. The filtrate was then washed once with water and the aqueous was extracted three times with DCM. The combined organic layers were washed with brine and dried over $MgSO_4$. Concentration afforded the γ-lactone **4.28** which was combined (0.25 g, 95%) and moved forward without further purification.

R_f = 0.31 (50% EtOAc/Hex); ^{1}H-NMR (400 MHz; DMSO-d_6): δ 6.61 (s, 1H), 6.31 (s, 1H), 5.96 (s, 1H), 4.56 (td, *J* = 12.2, 3.7 Hz, 1H), 3.98 (dd, *J* = 11.5, 6.5 Hz, 1H), 2.56 (d, *J* = 2.7 Hz, 1H), 2.36 (ddd, *J* = 7.1, 4.6, 2.7 Hz, 1H), 2.18 (dd, *J* = 20.0, 3.5 Hz, 1H), 2.08 (q, *J* = 3.0 Hz, 1H), 1.91-1.81 (m, 3H), 1.60 (dt, *J* = 13.2, 3.2 Hz, 1H), 0.91 (d, *J* = 7.0, 3H); ^{13}C-NMR (100 MHz; DMSO-d_6) δ 209.45, 166.16, 140.49, 128.88, 105.35, 74.60, 63.08, 61.93, 39.97, 38.18, 37.61, 29.13, 27.89, 20.60; FTIR (neat): 3443, 3109, 2977, 2921, 2908, 2863, 1777, 1728, 1661 cm^{-1}; HRMS (ESI) *m*/*z* Calc'd.for $C_{14}H_{16}O_5$ $[M+H]^+$: 265.1076, found: 265.1078.

Preparation of α-Bromo Ethyl Acetal **4.15**

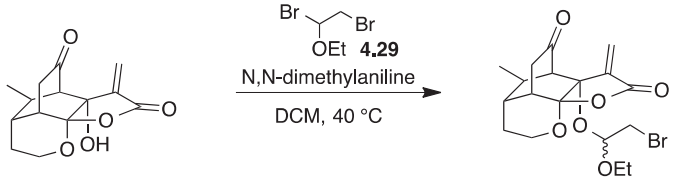

4.28 **4.15**

To a flame dried round bottomed flask, equipped with a magnetic stir bar and fitted with a water cooled condenser, was added γ-lactone **4.28** (2.5 g, 9.4 mmol), the bromoacetal (5.6 g, 2.4 mmol), dimethylaniline (3.0 mL, 2.4 mmol) and DCM (94 mL). The reaction was heated to 40 °C and after an hour at this temperature more bromoacetal (5.6 g, 2.4 mmol) and dimethylaniline (3.0 mL, 2.4 mmol) were added. This was repeated every hour for 5 more additions. After the final addition the reaction was allowed to stir 14.5 more hours at 40 °C, where the reaction progress was followed by TLC. TLC plates were developed using 50% EtOAc/Hex solution and visualized by $KMnO_4$. Upon cooling the reaction was filtered, using DCM to rinse the solid, and the filtrate was washed with water. The aqueous was extracted three times with DCM and dried over $MgSO_4$. Concentration and silica gel flash chromatography (10% gradient

from 0% → 70% EtOAc/Hex) afforded the α-bromo ethyl acetal **4.15** (2.7 g) in a 68% yield.

R_f = 0.47 (50% EtOAc/Hex); ^{1}H-NMR (400 MHz; $CDCl_3$): δ 6.68 (s, 0.6H), 6.61 (s, 0.4H), 6.00 (s, 0.6H), 5.84 (s, 0.4H), 4.85 (t, *J* = 4.3 Hz, 0.6H), 4.71 (dd, *J* = 5.9, 4.3 Hz, 0.4H), 4.61 (td, *J* = 12.4, 4.4 Hz, 0.4 H), 4.52 (td, *J* = 12.0, 4.4 Hz, 0.6H), 4.16-4.10 (m, 1H), 3.52-3.36 (m, 4H), 2.87 (d, *J* = 2.3 Hz, 0.6H), 2.75 (d, *J* = 2.7 Hz, 0.4H), 2.60-2.48 (m, 1H), 2.25-1.96 (m, 4H), 1.81 (br. s, 1H), 1.71-1.62 (m, 1H), 1.19 (t, *J* = 7.2 Hz, 1.8H), 1.12 (t, *J* = 7.2 Hz, 1.2H), 1.01 (dd, *J* = 7.2, 1.8 Hz, 3H); ^{13}C-NMR (100 MHz; $CDCl_3$) δ 208.63, 208.49, 194.91 (instrument artifact), 165.77, 135.74, 1353.30, 132.46, 130.29, 106.06, 105.65, 97.20, 97.16, 80.07, 63.73, 61.89, 61.69, 61.42, 61.30, 40.70, 40.31, 38.72, 38.61, 38.51, 38.25, 31.86, 31.75, 29.58, 29.55, 28.65, 28.19, 20.88, 15.12, 14.93; FTIR (neat): 2966, 2914, 1765, 1727, 1657 cm^{-1}; HRMS (ESI) *m*/*z* Calc'd.for $C_{18}H_{23}BrO_6$ $[M+Na]^+$: 437.0576, found: 437.0576.

Preparation of Ethyl Acetal **4.14**

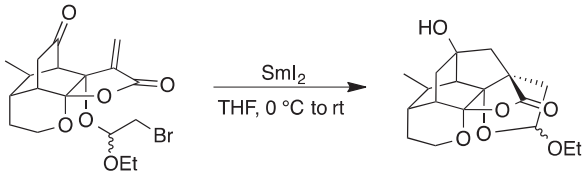

4.15 **4.14**

In the following reaction special precautions were taken to avoid light. All reaction vessels were wrapped in aluminum foil and the reaction was carried out in a darkened hood. The THF used in the following procedure was degassed over 4 Å molecular sieves via FPT.

Purification of 1,2-diiodoethane. 1,2-diiodoethane was taken up in Et_2O and placed into a separatory funnel. The organic was washed with a 50/50 mixture of saturated sodium thiosulfate and brine. The aqueous was extracted twice with Et_2O and the combined organics were dried over Na_2SO_4. Concentration afforded a white solid that was further dried under high vacuum.

Preparation of SmI_2. To a flame dried round bottomed flask, equipped with a magnetic stir bar and water cooled condenser, was added samarium powder (0.75 g, 5.0 mmol) in THF (19 mL). A separate solution of 1,2-diiodoethane (0.79 g, 2.8 mmol) in THF (9.0 mL) was added to the samarium solution. After 20 minutes of stirring the reaction mixture had turned deep blue in color and the reaction was heated to 55 °C for 14 hours.

Preparation of Ethyl Acetal **4.14**. To a solution of SmI_2 (0.10M in THF) cooled in an ice water bath was added the α-bromo ethyl acetal **4.15** (0.39 g, 0.93 mmol) in THF (8.5 mL). After 30 minutes the brown solution was allowed to warm to room temperature. The reaction progress was followed by TLC. TLC plates were developed using 50% EtOAc/Hex solution and visualized by $KMnO_4$. After 1.5 more hours the reaction solution was filtered and the organic was washed with saturated aqueous sodium thiosulfate and 1M HCl. The acidic layer was extracted twice with EtOAc. The combined organics were washed with brine and dried over $MgSO_4$. Concentration followed by purification via silica gel flash chromatography (10% gradient from 20% → 70% EtOAc/Hex) delivered the ethyl acetal **4.14** (0.17 g) in a 54% yield.

Ethyl Acetal Diastereomer A: R_f = 0.32 (50% EtOAc/Hex); ^{1}H-NMR (400 MHz; $CDCl_3$): δ 5.46 (dd, *J* = 5.9, 2.0 Hz, 1H), 4.20 (td, *J* = 12.5, 3.1 Hz, 1H), 3.99 (dd, *J* = 11.7, 5.9 Hz, 1H), 3.77 (dq, *J* = 9.8, 7.0 Hz, 1H), 3.53 (dq, *J* = 9.8, 7.0 Hz, 1H), 2.71 (dd, *J* = 14.1, 5.9 Hz, 1H), 2.32-2.29 (m, 2H), 2.21-2.03 (m, 3H), 1.99-1.90 (m, 3H), 1.82-1.68 (m, 3H), 1.48 (dt, *J* = 13.3, 2.7 Hz, 1H), 1.28 (d, *J* = 7.4 Hz, 3H), 1.21 (t, *J* = 7.0 Hz, 3H); ^{13}C-NMR (100 MHz,) δ 177.70, 109.50, 106.94, 95.91, 77.85, 63.97, 63.03, 56.94, 53.83, 52.04, 44.23, 39.39, 38.38, 37.82, 30.71, 27.74, 20.99, 15.34; FTIR (neat): 3469, 2929, 1759 cm^{-1}; HRMS (ESI) *m*/*z* Calc'd.for $C_{18}H_{24}O_6$ $[M+H]^+$: 337.1651, found: 337.1648.

Ethyl Acetal Diastereomer B: R_f = 0.20 (50% EtOAc/Hex); ^{1}H-NMR (400 MHz; $CDCl_3$): δ 5.30 (d, *J* = 4.3 Hz, 1H), 4.21 (td, *J* = 12.5, 3.1 Hz, 1H), 3.94 (dd, *J* = 11.9, 6.1 Hz, 1H), 3.83 (dq, *J* = 9.0, 7.2 Hz, 1H), 3.35 (dq, *J* = 9.3, 6.8 Hz, 1H), 2.63 (d, *J* = 12.9 Hz, 1H), 2.18 (d, *J* = 12.9 Hz, 1H), 2.10-1.89 (m, 8H), 1.81 (p, *J* = 3.6 Hz, 1H), 1.68 (dt, *J* = 14.7, 2.2 Hz, 1H), 1.45 (dt, *J* = 13.4, 2.9 Hz, 1H), 1.26 (d, *J* = 7.8 Hz, 3H), 1.13 (t, *J* = 7.0 Hz, 3H); ^{13}C-NMR (100 MHz; $CDCl_3$) δ 194.23 (instrument artifact), 177.30, 107.67, 107.16, 95.35, 79.32, 62.53, 62.35, 56.24, 54.19, 50.87, 43.74, 39.63, 38.65, 38.44, 30.81, 27.8, 20.92, 14.68; FTIR (neat): 34.36, 2913, 1789 cm^{-1}; HRMS (ESI) *m*/*z* Calc'd.for $C_{18}H_{24}O_6$ $[M+Na]^+$: 359.1471, found: 359.1466.

Preparation of isotwistane **4.13**

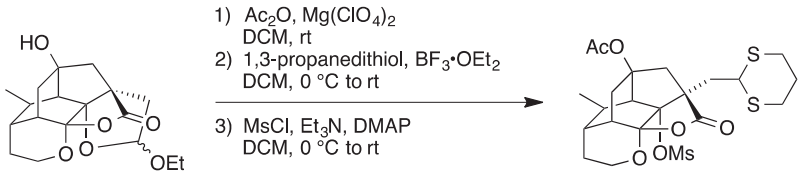

4.14 **4.13**

Acetate protection. To a cone shaped flask equipped with a magnetic stir bar was added ethyl acetal **4.14** (0.90 g, 2.7 mmol), acetic anhydride (0.82 mL, 8.0 mmol), $Mg(ClO_4)_2$ (0.09 g, 0.27 mmol), and DCM (11 mL). The reaction vessel was capped and the solution was allowed to stir 23 hours. The reaction progress was followed by TLC. TLC plates were developed using 50% EtOAc/Hex solution and visualized by $KMnO_4$. The reaction was worked up by washing with brine and drying over Na_2SO_4. Upon concentration the crude was azeotroped twice with EtOH and twice with toluene. The crude solid was moved on to the next reaction without further purification.

Preparation of the thioacetal. To a cone shaped flask equipped with a magnetic stir bar was added the protected tertiary alcohol, 1,3-propanedithiol (1.36 mL, 13.5 mmol), and DCM (27.0 mL). The solution was cooled in an ice water bath and BF_3•OEt_2 (1.70 mL, 13.5 mmol) was added. The reaction was allowed to stir at 0 °C for 45 minutes after which it was allowed to warm to room temperature. The reaction progress was followed by TLC. The TLC plates were developed using 50% EtOAc/Hex solution and visualized by UV light. After a total of 2.5 hours the reaction was recooled to 0 °C and acetone (5.00 mL) was added slowly. The solution was then washed with water and brine and dried over $MgSO_4$. Concentration yielded the solid thiophenol which was moved forward to the next reaction without further purification.

Mesylate functionalization. To a round bottomed flask equipped with a magnetic stir bar was added the thiophenol, 4-(dimethylamino)pyridine (DMAP) (0.99 g. 8.1 mmol), triethylamine (1.1 mL, 8.1 mmol), and DCM (27 mL). The solution was cooled in an ice water bath and methanesulfonyl chloride (0.63 mL, 8.1 mmol) was added. The

reaction progress was followed by TLC. The TLC plates were developed using 50% EtOAc/Hex solution and visualized by $KMnO_4$. After 3 hours of stirring at this temperature the reaction was quenched with the addition of 1M HCl (10 mL). The solution was then washed with brine and dried over $MgSO_4$. Concentration and silica gel flash chromatography (10% gradient, 20% → 60% EtOAc/Hex) delivered the isotwistane **4.13** (1.2 g, 86% yield) as a white solid.

R_f = 0.36 (50% EtOAc/Hex); ^{1}H-NMR (400 MHz; $CDCl_3$): δ 4.76 (dd, *J* = 8.2, 3.9 Hz, 1H), 4.33, (td, *J* = 12.1, 3.9 Hz, 1H), 4.01 (dd, *J* = 12.3, 5.7 Hz, 1H), 3.24 (s, 4H), 3.02-2.88 (m, 3H), 2.82-2.74 (m, 2H), 2.54-2.44 (m, 3H), 2.33 (dd, *J* = 15.7, 3.9 Hz, 1H), 2.23 (dd, *J* = 14.7, 3.7 Hz, 1H), 2.10-2.02 (m, 1H), 2.00 (s, 3H), 1.97-1.88 (m, 1H), 1.85-1.72 (m, 4H), 1.56 (d, *J* = 13.3 Hz, 1H), 1.21 (d, *J* = 7.4, 3H); ^{13}C-NMR (100 MHz; $CDCl_3$) δ 194.95 (instrument artifact), 174.61, 169.54, 105.50, 97.14, 79.82, 62.81, 52.32, 50.02, 47.53, 42.27, 40.89, 39.97, 38.40, 37.67, 36.55, 31.40, 30.75, 30.01, 27.03, 25.49, 21.73, 20.80; FTIR (neat): 2911, 1765, 1737 cm^{-1}; HRMS (ESI) *m*/*z* Calc'd.for $C_{22}H_{30}O_8S_3$ $[M+H]^+$: 519.1182, found: 519.1177.

Preparation of ketone **4.12**

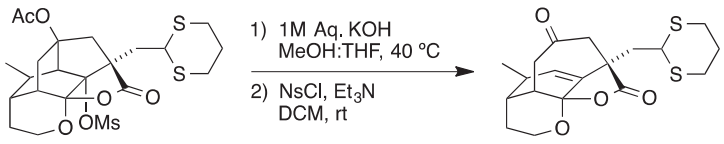

4.13 **4.12**

Wharton Fragmentation. To a flask equipped with a magnetic stir bar was added isotwistane **4.13** (1.2 g, 2.3 mmol), 1M KOH in H_2O (12 mL, 12 mmol), and MeOH:THF (1:1, 23 mL). The reaction vessel was sealed and heated to 40 °C. The reaction progress

was followed by TLC and the plates were developed using 50% EtOAc/Hex solution and visualized by $KMnO_4$. After 2.5 hours the reaction was cooled in an ice water bath and concentrated HCl was added dropwise via Pasteur pipette until the solution reached a pH of 1. The solution was then diluted with Ethyl Acetate and washed with brine (3x). The organic was then dried over Na_2SO_4. Concentration delivered a white solid (0.90 g, 98% yield), which was moved forward crude.

Acetal Formation with TsCl. To a flask equipped with a magnetic stir bar was added the crude diol (0.090 g, 0.23 mmol), pyridine (5.0 mL), and *p*-toluenesulfonyl chloride (0.086 gm, 0.45 mmol). The reaction was cooled in an ice water bath before the addition of DMAP (0.0028 g, 0.023 mmol) and the reaction was heated to 105 °C. After 6 hours the reaction was cooled to room temperature and quenched with the addition of 1M HCl. The solution was then transferred to a separatory funnel and the aqueous was extracted with EtOAc. The combined organics were then washed with brine and concentrated. Purification by silica gel flash column chromatography (30% → 50% EtOAc/Hex) delivered ketone **4.12** (0.10 g, 12% yield) as a white solid.

Acetal Formation with NsCl. To a flask equipped with a stir bar was added the crude diol (1.2 g, 3.0 mmol), 2-nitrobenzenesulfonyl chloride (NsCl) (1.3 g, 5.7 mmol), and DCM (30 mL). To the stirred heterogeneous solution was added triethylamine (Et_3N) (1.3 mL, 9.0 mmol) and the solution became homogeneous. The reaction progress was followed by TLC using 50% EtOAc/Hex solution to develop and $KMnO_4$ to visualize. After 2 hours the reaction was diluted with DCM and washed with brine (2x). The organic was dried of $MgSO_4$ and concentrated. Silica gel flash column

chromatography (1% gradient, 0% → 6% EtOAc/DCM) delivered ketone **4.12** (0.80 g, 73% yield) as a white solid.

R_f = 0.43 (50% EtOAc/Hex); m.p. 163–165 °C; ^{1}H-NMR (400 MHz; $CDCl_3$): δ 5.75 (d, *J* = 1.6 Hz, 1H), 4.06 (dd, *J* = 9.2, 7.6 Hz, 1H), 4.00-3.94 (m, 1H), 3.88-3.81 (m, 1H), 2.97-2.87 (m, 3H), 2.75-2.62 (m, 4H), 2.60-2.53 (m, 2H), 2.43 (q, *J* = 8.0 Hz, 1H), 2.24 (dd, *J* = 14.6, 7.2 Hz, 1H), 2.18 (ddd, *J* = 13.3, 4.0, 1.0 Hz, 1H), 2.07-1.91 (m, 4H), 1.69 (dq, *J* = 13.2, 3.9 Hz, 1H), 1.18 (d, *J* = 7.9 Hz, 3H); ^{13}C-NMR (100 MHz; $CDCl_3$) δ 205.00, 175.85, 138.37, 133.33, 105.64, 61.31, 60.48, 49.29, 45.66, 42.17, 41.27, 39.93, 36.96, 36.22, 33.37, 27.94, 27.45, 25.41, 22.63; FTIR (neat): 2921, 1785, 1698 cm^{-1}; HRMS (ESI) *m*/*z* Calc'd.for $C_{19}H_{19}NO_9S$ $[M+H]^+$: 381.1195, found: 381.1193.

Preparation of β-Keto Ester **4.32**

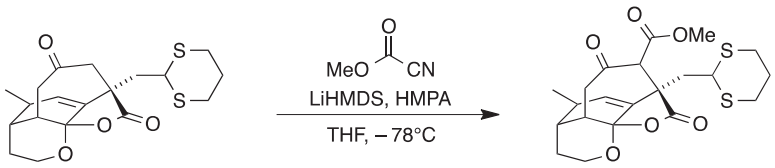

4.12 **4.32**

Mander's Reaction. To a flask equipped with a stir bar was added diisopropylamine (*i*$PrNH_2$) (8 μL, 0.06 mmol), and THF (0.2 mL). The stirred solution was cooled to – 20 °C via a dry ice/acetonitrile bath and *n*-butyllithium (*n*BuLi) (0.04 mL, 0.06 mmol, 1.53 M solution in hexanes) was added dropwise. After stirring at this temperature for 50 minutes, the enolate solution was cannulated rapidly into a flask containing a solution of ketone **4.12** (0.02 g, 0.05 mmol) in THF (0.3 mL) cooled in a dry ice/acetone bath. After 30 minutes, hexamethylphophoramide (HMPA) (9 μL, 0.05 mmol) and methyl cyanoformate (5 μL, 0.06 mmol) were added dropwise to the enolate

solution. The reaction progress was followed by TLC, using a 50% EtOAc/Hexane solution to develop and $KMnO_4$ to visualize. After 1 hour and 40 minutes the reaction was quenched with the addition of H_2O (0.2 mL). The solution was then diluted with DCM, washed with NH_4Cl (sat. aq.) and brine, and dried over Na_2SO_4. Silica gel flash column chromatography (10% gradient, 0% → 70% EtOAc/Hex) delivered β-keto ester **4.32** (5 mg, 21% yield) as a clear oil. Crude ^{1}H NMR indicated a 2:1 ratio of undesired (**4.32**):desired (**4.31**).

R_f = 0.33 (50% EtOAc/Hex); ^{1}H-NMR (400 MHz; $CDCl_3$): δ 6.06 (d, *J* = 3.0, 1H), 4.04 (t, *J* = 8.0 Hz, 1H), 3.99-3.83 (m, 1H), 3.82-3.71 (m, 1H), 3.74 (s, 3H), 3.51 (s, 1H), 3.08-2.91 (m, 3H), 2.84-2.55 (m, 7H), 2.15-2.00 (m, 4H), 1.87 (m, 1H), 1.35 (d, *J* = 7.8, 3H); ^{13}C-NMR (100 MHz, $CDCl_3$) δ 200.8, 174.5, 166.9, 135.1, 133.27, 106.1, 68.1, 60.8, 52.8, 52.3, 43.0, 41.0, 40.4, 39.3, 37.2, 33.8, 32.7, 29.9 (H grease), 27.7, 27.2, 25.4, 23.1; HRMS (ESI) *m/z* Calc'd.for $C_{21}H_{26}O_6S_2$ $[M+Na]^+$: 461.1063, found: 461.1067.

Preparation of Enol **4.31** *and β-keto Ester* **4.11**

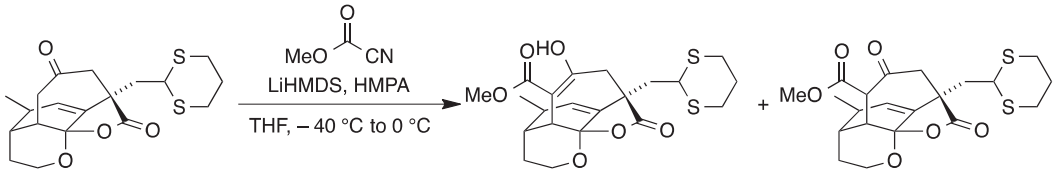

4.12 **4.31** **4.11**

To a vial equipped with a magnetic stir bar was added ketone **4.12** (20 mg, 0.05 mmol) and THF (0.5 mL). The solution was cooled in a dry ice/acetonitrile bath and lithium bis(trimethylsilyl)amide (LiHMDS) (1.0 M solution in Toluene, 0.05 mL, 0.05 mmol) was added dropwise. After 35 minutes at this temperature the reaction vessel was placed into an ice/salt water bath. After 30 minutes the reaction vessel was recooled to –

40 °C and after 10 more minutes hexamethylphosphoramide (HMPA) (0.1 mL, 0.6 mmol) was added. After stirring 20 minutes at – 40 °C, methyl cyanoformate (4 μL, 0.05 mmol) was added. The reaction progress was followed by TLC and the plates were developed using 50% EtOAc/Hex solution and visualized by $KMnO_4$. After 25 minutes the reaction was quenched with the addition of sat. aq. NH_4Cl (0.2 mL) and was warmed to room temperature. The solution was then diluted with DCM and washed sat. aq. NH_4Cl and brine. The organic was then dried of Na_2SO_4 and concentrated. Silica gel flash column chromatography (10% gradient, 0% → 50% EtOAc/Hex) delivered β-keto ester **4.11** (3 mg, 14% yield) and its enol tautomer **4.31** (12 mg, 53% yield) as colorless oils.

Enol Tautomer: R_f = 0.52 (50% EtOAc/Hex); ^{1}H-NMR (400 MHz; $CDCl_3$): δ 13.82 (s, 1H), 5.71 (s, 1H), 4.06 (t, *J* = 8.4 Hz, 1H), 3.97 (dd, *J* = 11.7, 5.4 Hz, 1H), 3.89-3.79 (m, 4H), 3.27 (d, *J* = 2.2 Hz, 1H), 3.01-2.81 (m, 4H), 2.80-2.58 (m, 3H), 2.33 (q, *J* = 8.0 Hz, 1H), 2.29-2.26 (m, 1H), 2.21 (dd, *J* = 14.5, 7.6 Hz, 1H), 2.08-1.92 (m, 3H), 1.61-1.54 (m, 1H), 1.25 (H grease), 0.97 (d, *J* = 7.7 Hz, 3H); ^{13}C-NMR (100 MHz; $CDCl_3$) δ 175.54, 174.62, 171.68, 136.10, 132.17, 103.49, 100.42, 61.52, 55.16, 52.71, 49.29, 44.62, 41.55, 38.33, 36.18, 36.04, 33.64, 29.84 (H grease), 28.13, 27.62, 25.51, 22.85; FTIR (neat) 2928, 1780, 1733, 1635, 1575 cm^{-1}; HRMS (ESI) *m/z* Calc'd.for $C_{21}H_{26}O_6S_2$ $[M+H]^+$: 439.1249, found: 438.1248.

Ketone Tautomer: R_f = 0.30 (50% EtOAc/Hex); ^{1}H-NMR (400 MHz; $CDCl_3$): δ 5.82 (d, *J* = 2.1 Hz, 1H), 4.08-3.93 (m, 2H), 3.92-3.75 (m, 1H), 3.72 (s, 3H), 3.19 (s, 1H), 2.97-2.85 (m, 4H), 2.75-2.57 (m, 4H), 2.55-2.47 (m, 1H), 2.24 (dd, *J* = 14.6, 7.0 Hz, 1H),

2.10-1.88 (m, 4H), 1.80-1.71 (m, 1H), 1.22 (d, J = 7.9 Hz, 3H); ^{13}C-NMR (100 MHz; $CDCl_3$) δ 200.58, 195.00 (instrument artifact), 174.65, 169.02, 138.83, 132.56, 104.49, 61.68, 60.90, 60.74, 52.95, 49.67, 44.27, 40.74, 40.04, 36.76, 36.06, 32.83, 27.67, 27.17, 25.36, 23.01; FTIR (neat) 2931, 1786, 1743, 1704 cm^{-1}; HRMS (ESI) *m*/*z* Calc'd.for $C_{21}H_{26}O_6S_2$ $[M+H]^+$: 439.1249, found: 439.1251.

Methyl Carbonate: R_f = 0.43 (50% EtOAc/Hex); ^{1}H-NMR (400 MHz; $CDCl_3$): δ 5.76 (s, 1H), 5.26 (ddd, J = 5.7, 2.1, 1.0 Hz, 1H), 4.09-4.02 (m, 1H), 3.99-3.92 (m, 1H), 3.83 (td, J = 12.1, 3.4 Hz, 1H), 3.76 (s, 3H), 2.87 (dddd, J = 25.5, 23.2, 11.5, 7.0 Hz, 3H), 2.76-2.61 (m, 4H), 2.48 (d, J = 16.4 Hz, 1H), 2.38 (q, J = 8.0 Hz, 1H), 2.23 (dd, J = 14.5, 7.6 Hz, 1H), 2.13-2.11 (m, 1H), 2.05-1.89 (m, 3H), 1.64-1.58 (m, 1H), (d, J = 8.0 Hz, 3H); ^{13}C-NMR (100 MHz; $CDCl_3$) δ 195.00 (instrument artifact), 175.80, 154.20, 145.93, 134.82, 133.28, 118.27, 104.05, 61.43, 55.28, 50.50, 49.37, 44.38, 41.69, 38.18, 36.81, 36.24, 33.32, 28.18, 27.68, 25.50, 22.06: FTIR (neat) 2928, 2360, 1779, 1754 cm^{-1}; HRMS (ESI) *m*/*z* Calc'd.for $C_{21}H_{26}O_6S_2$ $[M+H]^+$: 439.1249, found: 439.1249.

Preparation of Vinyl Triflate **4.33**

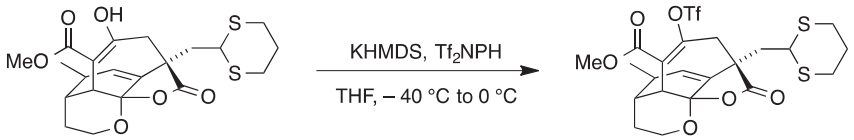

4.31 **4.33**

From Enol **4.31**. To a flask equipped with a magnetic stir bar was added enol **4.31** (0.05 g, 0.1 mmol) and THF (0.9 mL). The solution was cooled in a dry ice/acetonitrile bath and a solution of potassium bis(trimethylsilyl)amide (0.5 M in toluene, 0.4 mL, 0.2 mmol) was added dropwise. After 1 hour at this temperature a

solution of *N*-phenyl-bis(trifluoromethanesulfonimide) (0.07 g, 0.2 mmol) in THF (0.3 mL) was added. TLC was used to monitor the reaction progress. The TLC plates were developed using 50% EtOAc/Hex solution and visualized with *p*-anisaldehyde stain. After 25 minutes the cooling bath was removed and the solution allowed to warm to room temperature for additional hour. The reaction was quenched with the addition of a saturated solution of NH_4Cl (0.3 mL, aqueous) and diluted with EtOAc. The organic was washed with water and brine, and then dried over Na_2SO_4. Concentration and purification via silica gel flash column chromatography (10% gradient elution from 0% → 60% EtOAc/Hex) afforded vinyl triflate **4.33** (0.05 g, 65% yield) as a yellow residue.

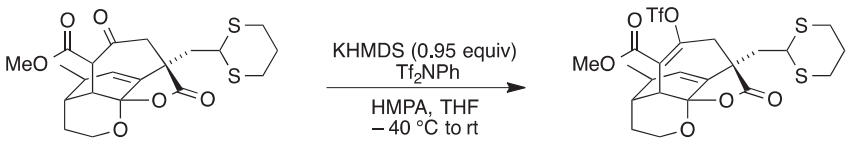

4.11 **4.33**

From Ketone **4.11**. To a flask equipped with a magnetic stir bar was added ketone **4.11** (0.13 g, 0.30 mmol) and THF (3.0 mL). The solution was cooled in a dry ice/acetonitrile bath and hexamethylphosphoramide (HMPA) (0.57 mL, 3.3 mmol) was added. After 5 minutes a solution of potassium bis(trimethylsilyl)amide (0.5 M in toluene, 0.56 mL, 0.28 mmol) was added dropwise. After 25 minutes the reaction was removed from the cooling bath and allowed to warm to room temperature where the solution became homogenous and dark red in color. After 55 minutes a solution of *N*-phenyl-bis(trifluoromethanesulfonimide) (0.11 g, 0.31 mmmol) in THF (1.0 mL) was added rapidly. TLC was used to monitor the reaction progress. The TLC plates were developed using 50% EtOAc/Hex solution and visualized with $KMnO_4$ stain. After 40

minutes the reaction was quenched with a saturated solution of NH_4Cl (1.0 mL, aqueous). The solution was diluted with EtOAc and washed with NH_4Cl (saturated, aqueous), brine, and dried over Na_2SO_4. Concentration and purification via silica gel flash column chromatography (10% gradient elution from 0% → 50% EtOAc/Hex) afforded vinyl triflate **4.33** (0.09 g, 53% yield) as a yellow residue.

R_f = 0.54 (50% EtOAc/Hex); ^{1}H-NMR (400 MHz; $CDCl_3$): δ 5.85 (d, *J* = 4.0 Hz, 1H), 4.05-3.96 (m, 2H), 3.85-3.78 (m, 4H), 3.09 (s, 1H), 2.96-2.83 (m, 3H), 2.80 (d, *J* = 4.0 Hz, 1H), 2.73-2.62 (m, 3H), 2.43 (qd, *J* = 7.8, 1.8 Hz, 1H), 2.38-2.33 (m, 1H), 2.27 (dd, *J* = 14.5, 7.5 Hz, 1H), 2.07-1.91 (m, 3H), 1.68-1.61 (m, 1H), 1.20 (d, *J* = 7.8 Hz, 3H); ^{13}C-NMR (100 MHz; $CDCl_3$) δ 174.6, 165.8, 145.2, 134.3, 134.0, 129.3, 102.7, 61.4, 53.2, 50.6, 50.0, 47.7, 41.1, 37.4, 36.5, 36.1, 33.1, 27.9, 27.4, 25.3, 21.7; FTIR (neat): 2955, 1782, 1736 cm^{-1}; HRMS (ESI) *m/z* Calc'd.for $C_{22}H_{25}F_3O_8S_3$ $[M+H]^+$: 571.0742, found: 571.0741.

Preparation of Malaic Anhydride **4.38**

4.33 **4.38**

To a flask equipped with a magnetic stir bar was added palladium(II) acetate (0.036 g, 0.164 mmol), tri(2-furyl)phosphine (0.190 g, 0.820 mmol), a solution of vinyl triflate **4.33** (0.093 g, 0.164 mmol) in DMF (3.2 mL), diisopropylethylamine (0.210 mL, 1.23 mmol), and H_2O (0.220 mL, 12.30 mmol) (in that order). The reaction vessel was purged with carbon monoxide (CO) for 15 minutes by submerging the tip of an 18-gauge syringe needle into the solution and stirring vigorously. The gas inlet was replaced with a

balloon containing CO and the reaction was heated in a 90 °C oil bath. After 2.5 hours the reaction was removed from the heating bath and allowed to cool to room temperature. After 30 minutes of cooling the reaction was quenched with 1 M HCl (3.20 mL). The aqueous was extracted with EtOAc (3x) and the organics washed with brine and dried over Na_2SO_4. Concentration and purification via silica gel flash column chromatography (10% gradient elution from 0% → 60% EtOAc/Hex) afforded maleic anhydride **4.38** (0.045 g, 63% yield) as a yellow solid.

R_f = 0.48 (50% EtOAc/Hex); ^{1}H-NMR (400 MHz; $CDCl_3$): δ 5.78 (s, 1H), 4.09-4.02 (m, 2H), 3.89 (td, *J* = 12.3, 3.1 Hz, 1H), 3.31 (s, 1H), 3.10 (d, *J* = 20.0 Hz, 1H), 3.02-2.86 (m, 3H), 2.75-2.64 (m, 2H), 2.58 (dd, *J* = 19.2, 2.3 Hz, 1H), 2.54-2.43 (m, 2H), 2.35 (dd, *J* = 14.5, 7.4 Hz, 1H), 2.17-2.08 (m, 1H), 2.07-1.94 (m, 2H), 1.72 (d, *J* = 12.0 Hz, 1H), 0.92 (d, *J* = 7.7 Hz, 3H); ^{13}C-NMR (100 MHz, $CDCl_3$) δ 174.9, 164.8, 164.5, 142.4, 140.5, 135.9, 133.7, 102.8, 61.6, 51.6, 45.4, 44.3, 41.3, 38.4, 36.9, 35.9, 32.7, 27.9, 27.4, 25.4, 22.6; FTIR (neat): 2925, 1761 cm^{-1}; HRMS (ESI) *m*/*z* Calc'd.for $C_{21}H_{22}O_6S_2$ $[M+H]^+$: 435.0936, found: 435.0933.

Preparation of Carboxylic Acid **4.10**

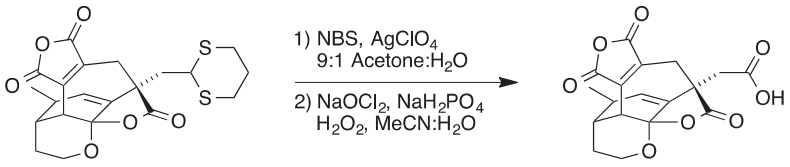

4.38 **4.10**

Thioacetal deprotection. To a flask equipped with a magnetic stir bar was added maleic anhydride (0.04 g, 0.09 mmol) **4.38** and taken up in acetone:H_2O (9:1, 0.4 mL). A solution of NBS (0.03 g, 0.2 mmol) and $AgClO_4$ (0.04g, 0.2 mmol) in acetone:H_2O (9:1,

0.6 mL) was added at room temperature. TLC was used to monitor the reaction progress. The TLC plates were developed using a 50% EtOAc/Hex solution and visualized with $KMnO_4$. After 30 minutes the reaction was worked up by diluting with EtOAc and transferred to a separatory funnel, where the solution was washed with H_2O. The aqueous layer was extracted with EtOAc (2x) and the combined organics washed with brine and then dried over Na_2SO_4. Concentration and purification via silica gel flash column chromatography (10% gradient elution from 0% → 60% EtOAc/Hex) afforded the aldehyde as an oil.

Pinnick Oxidation. To a flask equipped with a magnetic stir bar was added the aldehyde (0.02 g, 0.05 mmol) and MeCN (0.5 mL). This was allowed to dissolve before the addition of H_2O (0.5 mL) and cooling in an ice/water bath. H_2O_2 (30%, 0.005 mL, 0.05 mmol) was then added followed by a solution of $NaClO_2$ (0.01 g, 0.1 mmol) and NaH_2PO_4 (0.003 g, 0.03 mmol) in H_2O (0.5 mL). TLC was used to monitor the reaction progress. The TLC plates were developed using 75% EtOAc/Hex and visualized with $KMnO_4$. After 1 hour in the cooling bath the reaction was quenched with the addition of a saturated solution $Na_2S_2O_3$ (1 mL, aqueous). The solution was diluted with EtOAc and transferred to a separatory funnel, where the organic layer was washed with H_2O, and 1M HCl. The aqueous was extracted with EtOAc (2x) and combined organics dried over Na_2SO_4. Concentration and purification via silica gel flash column chromatography (25% gradient elution from 25% → 100% EtOAc/Hex:5% AcOH) afforded carboxylic acid **4.10** (0.008 g, 23% yield).

R_f = 0.13 (50% EtOAc/Hex:5% AcOH); ^{1}H-NMR (400 MHz; CD_3CN): δ 5.88 (s, 1H), 4.01-3.96 (m, 1H), 3.82 (td, *J* = 11.9, 3.3 Hz, 1H), 3.25 (s, 1H), 3.07 (q, *J* = 16.0 Hz,

2H), 2.90-2.72 (m, 2H), 2.48-2.40 (m, 2H), 2.08-1.99 (m, 1H), 1.77-1.71 (m, 1H), 0.91 (d, J = 8.0 Hz, 3H); ^{13}C-NMR (100 MHz; CD_3CN) δ 190.3, 190.2, 176.4, 165.9, 142.6, 141.9, 136.9, 134.1, 104.1, 62.3, 49.7, 45.2, 43.1, 39.4, 36.5, 36.3, 33.0, 22.4; FTIR (neat): 3366, 2922, 1765, 1702 cm^{-1}; HRMS (ESI) m/z Calc'd.for $C_{18}H_{16}O_8$ $[M+NH_4]^+$: 378.1189, found: 378.1182.

4.5 References

[1] Dong, P. *Synthetic Approaches Towards Cephalezomine A and Phomoidride D*, PhD Thesis, Colorado State University, Ft. Collins, CO, 2010.

[2] Hrubiec, R. T.; Smith, M. B. *J. Org. Chem.* **1984**, *49*, 431.

[3] (a) Guibe, F. *Tetrahedron* **1998**, *54*, 2967. (b) Vutukuri, D. R.; Bharathi, P.; Yu, Z.; Rajasekaran, K.; Trans, M.; Thayumanavan, S. *J. Org. Chem.* **2003**, *68*, 1146.

[4] (a) Yates, P.; Auski, H.; *Can. J. Chem.* **1979**, *57*, 2853. (b) Yates, P.; Macas, T. S. *Can. J. Chem.* **1988**, *66*, 1. (c) Chu, C. S.; Lee, T. H.; Liao, C. C. *Synlett* **1994**, 635. (d) Lai, C. H.; Shen, Y. L.; Liao, C. C. *Synlett* **1997**, 1351. (e) Chu, C. S.; Lee, T. H.; Rao, P. D.; Song L. D.; Liao, C. C. *J. Org. Chem.* **1999**, *64*, 4111. (f) Liao, C. C.; Chu, C. S.; Lee, T. H.; Rao, P. D.; Ko, S.; Song, L. D.; Shiao, H. C. *J. Org. Chem.* **1999**, *64*, 4102. (g) Rao, P. D.; Chen, C. H.; Liao, C. C. *Chem. Comm.* **1998**, 155. (h) Drutu, I.; Njardarson, J. T.; Wood, J. L. *Org. Lett.* **2002**, *4*, 493.

[5] (a) Varala, R.; Sreelatha, N.; Srinivas, R. A *Synlett* **2006**, 1549. (b) Yu, L. C.; Helquist, P. *Tetrahedron Lett.* **1978**, *37*, 3423. (c) Yu, L. C.; Helquist, P. *J. Org. Chem.* **1981**, *46*, 4536. (d) Yu, L. C.; Helquist, P. *Synthetic Commun.* **1981**, *11*, 591.

[6] Aihara, Y.; Yoshida, A.; Furuta, T.; Wakimoto, T.; Akizawa, T.; Konishi, M.; Kan, T. *Bioorg. Med. Chem. Lett.* **2009**, *19*, 4171.

[7] (a) DePuy, C. H.; King, R. W. *Chem. Rev.* **1960**, *60*, 431. (b) Garcia Martinez, A.; Teso Vilar, E.; Garcia Fraile, A.; de la Moya Cerero, S.; Lora Maroto, B. *Tetrahedron: Asymmetry* **2002**, *13*, 17.

[8] (a) Stork, G.; Kahn, M. *J. Am. Chem. Soc.* **1985**, *107*, 500. (b) Stork, G.; Mook, R. *J. Am. Chem. Soc.* **1983**, *105*, 3720. (c) Stork, G.; Mook, R.; Biller, S. A.; Rychnovsky, S. D. *J. Am. Chem. Soc.* **1983**, *105*, 3741. (d) Stork, G.; Sher, P. M. *J. Am. Chem. Soc.* **1986**, *108*, 303.

[9] (a) Molander, G. A.; Harris, C. R. *Chem. Rev.* **1996**, *96*, 307. (b) Ananthanarayan, T. P.; Gallagher, T.; Magnus, P. *J. Chem. Soc. Chem. Commun.* **1982**, 709. (c) Fang, J. M.; Chen, M. Y.; Shiue, J. S.; Lu, L.; Hsu, J. L. *Tetrahedron Lett.* **2000**, *41*, 4633. (d) Cabrera, A.; Alper, H. *Tet. Lett.* **1992**, *33*, 5007. (e) Fukuzawa, S.; Tsuchimoto, T. *Synlett* **1993**, 803. (f) Inanaga, J.; Handa, Y.; Tabuchi, T.; Otsubo, K.; Yamaguchi, M.; Hanamoto, T. A. *Tetrahedron Lett.* **1991**, *32*, 6557. (g) Inanaga, J.; Sakai, S.; Handa, Y.; Yamaguchi, M.; Yokoyama, Y. *Chem. Lett.* **1991**, 2117. (h) Shinohara, I.; Okue, M.; Yamada, Y.; Nagaoka, H. *Tetrahedron Lett.* **2003**, *44*, 4649.

[10] (a) Mander, L. N.; Sethi, S. P. *Tetrahedron Lett.* **1983**, *24*, 5425. (b) Hale, K. J.; Grabski, M.; Flasz, J. T. *Org. Lett.* **2013**, *15*, 370.

[11] Logan, A. W. J.; Parker, J. S.; Hallside, M. S.; Burton, J.W. *Org. Lett.* **2012**, *14*, 2940.

[12] Yang, D.; Xu, M. *Org. Lett.* **2001**, *3*, 1785.

[13] (a) Chen, C.; Layton, M. E.; Sheehan, S. M.; Shair, M. D. *J. Am. Chem. Soc.* **2000**, *122*, 7424. (b) Hayashi, Y.; Itoh, T.; Fukuyama, T. *Org. Lett.* **2003**, *5*, 2235.

[14] (a) Stork, G.; Zhao, K. *Tetrahedron Lett.* **1989**, *30*, 287. (b) Gbur, R. K.; Little. R. D. *J. Org. Chem.* **2012**, *77*, 2134.

[15] Nicolaou, K. C.; Ajito, K.; Patron, A. P.; Khatuya, H.; Richter, P. K.; Bertinato, P. *J. Am. Chem. Soc.* **1996**, *118*, 3059.

CHAPTER FIVE

Studies Toward the Total Synthesis of Phomoidride D

5.1 Introduction and Retrosynthetic Analysis

5.1.1 Introduction

For more than a decade, our group has been attempting to develop a novel total synthesis of phomoidride D (**5.10**). Initial synthetic studies culminated in an efficient and creative first-generation strategy consisting of a tandem phenolic oxidation/Diels-Alder sequence, cascade cyclization, and fragmentation reaction to establish the bicyclo[4.3.1] core of the phomoidrides (Scheme 5.10).[1] Although this first-generation synthesis was successful in delivering an advanced intermediate that contained all of the requisit carbon atoms, it failed when efforts to install the maleic anhydride motif in a very late stage intermediate (**5.14**) proved futile.[8] Therefore, a second-generation strategy was developed which called for installation of the troublesome maleic anhydride using a β-keto ester as substrate.[2] However, the β-hydroxy ester (**5.16**), which was envisioned to deliver the β-ketoester **5.17** via fragmentation was found to undergo retro-aldol reaction as the only bond breaking event. (Scheme 5.10b). Having encountered yet another insurmountable obstical we developed a third-generation approach toward phomoidride D (**5.10**), the results of these investigations are described below.

As with our efforts in the second-generation approach we chose to perform our initial studies on a model substrate. As discussed in Chapter Four, the third-generation

approach was successful in delivering a fully functionalized phomoidride core structure and thus gave us confidence that this approach would prove viable in delivering **5.10**.

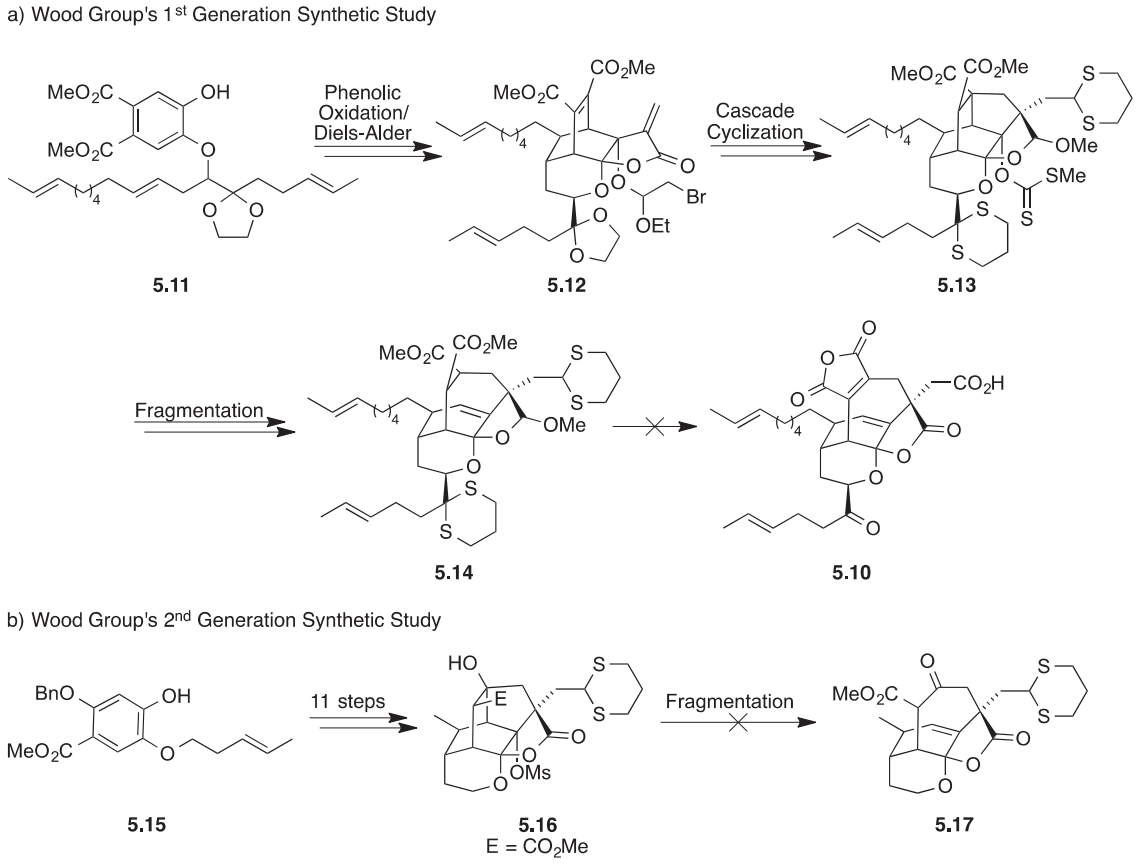

Scheme 5.10 Prior work toward phomoidride D

The synthesis of the model system was completed in 21 total steps from commercially available starting materials. Although we were thrilled to complete the synthesis of the phomoidride core (Scheme 5.11, grey), adapting this approach to the synthesis of phomoidride D would require incorporation of the olefin-containing side chains. The relatively linear nature of our approach dictated that the side chains be incorporated at an early stage of the synthesis (see Scheme 5.11 wherein the black highlights track the side chains througout the synthesis). As one familiar with the model

system synthesis would note (see Chapter Four), once the olefin-containing side chain, or "side chains" are incorporated, the total synthesis merely requires optimization of previously developed reactions. Although the side-chain incorporation appears rather benign, complications due to structural subtleties are comonplace in densly functionalized bridging ring sytems like those found in **5.10**.

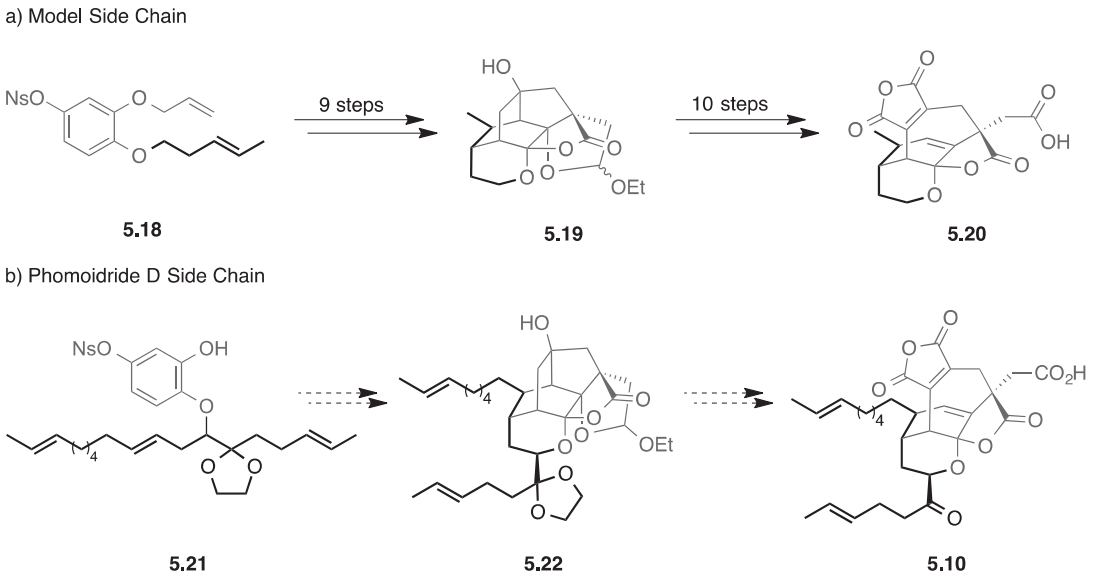

Scheme 5.11 Comparison of the model substrate and phomidride D (**5.10**)

5.1.2 Retrosynthetic Analysis

Based on our model studies, the initial retrosynthetic analysis calls for incorporation of the maleic anhydride from β-keto ester **5.23**. The ester substituent of **5.23** would be installed through acyclation of ketone **5.24**. The bicyclo[4.3.1]decene core of ketone **5.24** would be produced from a Wharton fragmentation of mesylate **5.25**, which would in turn come from an alcohol functionalization and transacetalization of ethyl acetal **5.22**.

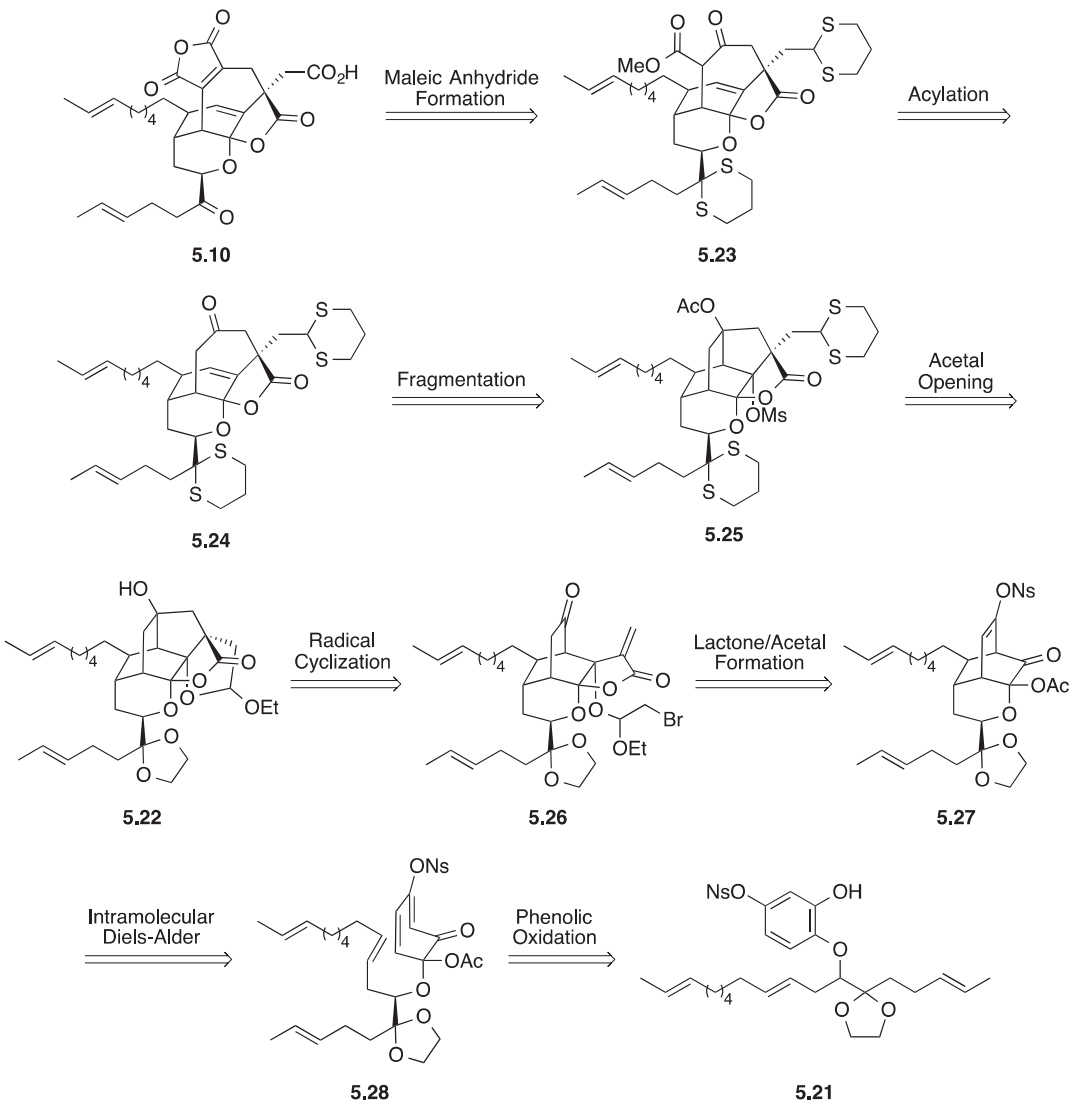

Scheme 5.12 Third-generation approach toward phomoidride D (**5.10**)

The isotwistane architecture of ethyl acetal **5.22** can be derived from alkyl bromide **5.26** through a tandem radical cyclization that utilizes the ketone, *exo*-methylene, and alkyl bromide functionalities. Lactone **5.26** is envisioned to be prepared from an aldol addition and lactonization process originating with ketone **5.27**. The [2.2.2]bicycle of **5.27**, would be constructed via an intramolecular Diels-Alder cycloaddition of triene **5.28**, which would come from a phenolic oxidation of a phenol

(**5.21**) containing the side-chains. With our synthetic strategy adapted to include the phomoidride olefinic side chains, we can now turn our attention toward the formation of phenol **5.21.**

5.2 Progress Toward the Total Synthesis of Phomoidride D

5.2.1 Phenolic Oxidation Precursor Synthesis

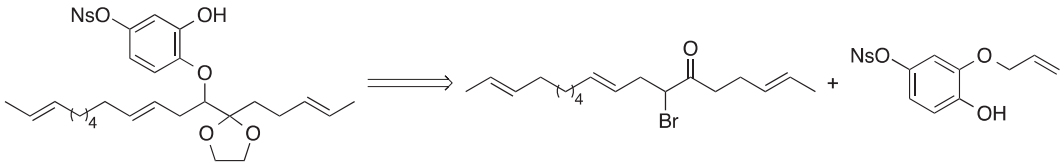

5.21 **5.29** **5.30**

Scheme 5.13

Our synthesis of phomoidride D (**5.10**) commenced with the formation of α-bromoketone **5.29** (see Scheme 5.13), an intermediate which had been previously prepared in our first-generation synthesis via the route illustrated in Scheme 5.14.

Commercially available and inexpensive 1,5-dibromopentane **5.31**, was subjected to bromide displacement with two equivalents of sodium acetylide, subsequent mono-methylation of the resultant diyne produced deca-diyne **5.32** in 35% yield over two steps.[3,4] Treating alkyne **5.32** with sodium amide in liquid ammonia effectively protected the terminal alkyne as its sodium salt, while allowing for the selective Birch reduction of the internal alkyne to the *trans* alkene.[5] A second reduction of the terminal alkyne with diisobutylaluminum hydride (DIBAL-H) and trapping the vinyl aluminum compound with iodine delivered vinyl iodide **5.33** in 61% yield over two steps.

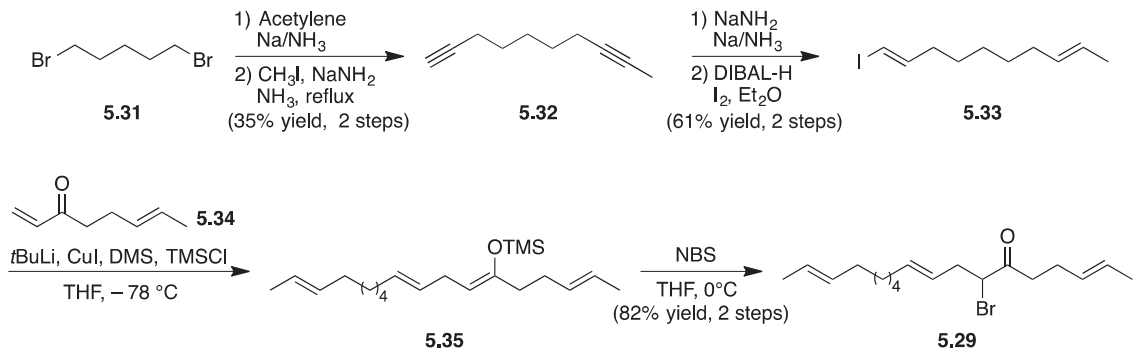

Scheme 5.14 Side chain synthesis

A conjugate addition of the vinyl cuprate, generated from vinyl iodide **5.33**, onto enone **5.34** and subsequent trapping of the resultant enolate with chlorotrimethylsilane (TMSCl) formed TMS enol ether **5.35**.[6] Reacting **5.35** with *N*-bromosuccinimide (NBS) produced α-bromoketone **5.29** in 82% yield over two steps, as a single regioisomer.[7] The key to the regioselectivity was the selective formation and trapping of the enolate during the 1,4-addition.[8]

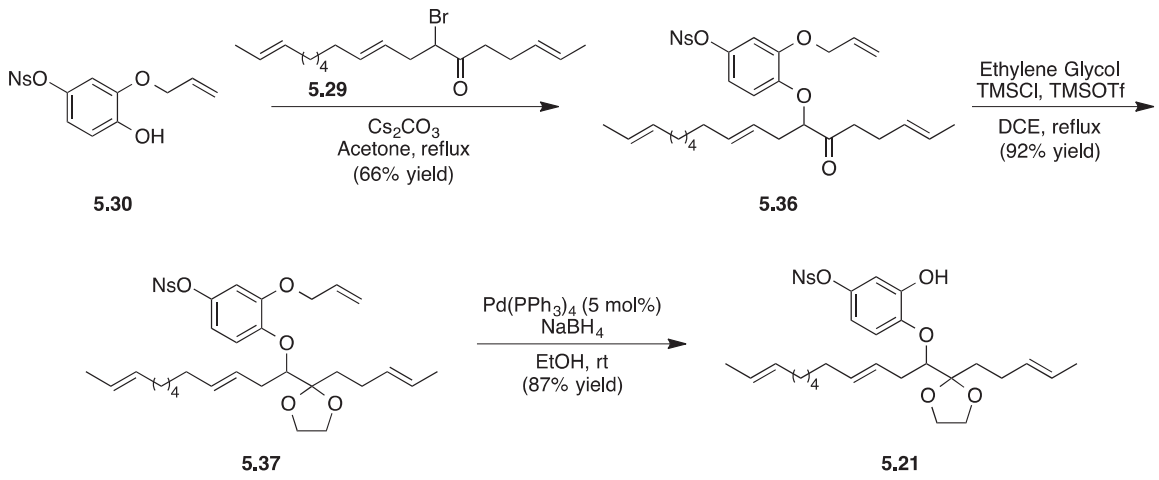

Scheme 5.15 Phenolic Oxidation/Diels-Alder precursor synthesis

At this stage the synthesis merged with our model studies and the previously employed phenol **5.30** was coupled with α-bromoketone **5.29**. The coupling performed by exposing the mixture of substrates to cesium carbonate (Cs_2CO_3) in refluxing acetone and delivered ketone **5.36** in good yield.[8] At this point it was necessary to protect the ketone to avoid the hemi-acetal formation previously observed upon deallylation.[1] The protection proceeded smoothly in the presence of TMSCl, ethylene glycol and catalytic amount of trimethylsilyl trifluoromethanesulfonate (TMSOTf) to furnish acetal **5.37** in excellent yield.[9] The synthesis of phenol **5.21** was completed with the removal of the allyl protecting group using $Pd(PPh_3)_4$ and $NaBH_4$ in ethanol.[2,10]

5.2.2 Phenolic Oxidation/Diels-Alder Reaction and Lactone Formation

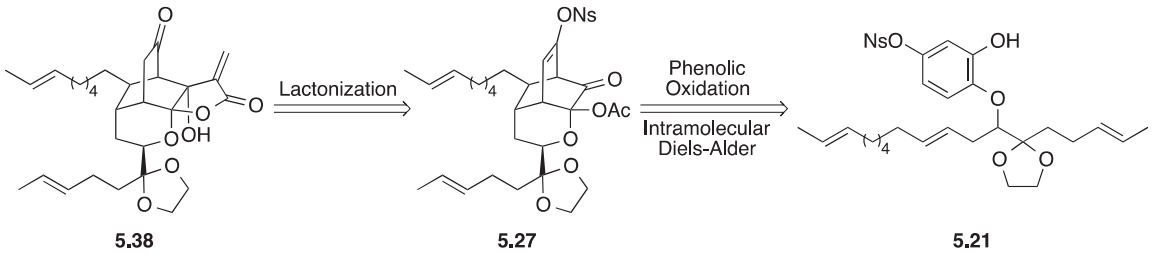

5.38 **5.27** **5.21**

Scheme 5.16

With **5.21** in hand we next investigated the phenolic oxidation/Diels-Alder sequence by exposing the phenol to $Pb(OAc)_4$ in refluxing DCE. To our delight, the desired [2.2.2]bicycle **5.27** was obtained as a 1:3 ratio of inseparable α:β epimers.[1c,8] Not

[1]See chapter 3; ref 1; it was found in our previous synthetic attempts that removal of the allyl protecting group in the presence of the ketone would result in a hemi-acetal formation. This hemi-acetal would not react during the phenolic oxidation.

[2]The deallylation could also be performed using the same procedure as in Chapter 4, Scheme 4.11. The use of $Pd(PPh_3)_4$, K_2CO_3, in MeOH gave phenol **5.21** in a lower (69%-79% yield).

only was this sequence an extremely efficient method for the introduction of molecular complexity, it also allowed us to set stereochemistry at C17 selectively based on the *trans* configuration of the dienophile (Scheme 5.17). The C7 stereocenter was also formed during the intramolecular [4+2] cycloaddition and its relative stereochemistry was assigned to favor the β-epimer as the major diastereomer. The stereochemical assignment at C7 is based upon analogy to our first-generation studies and an X-ray crystal structure obtained of a late stage intermediate (*vida infra*, Scheme 5.25, **5.24**).

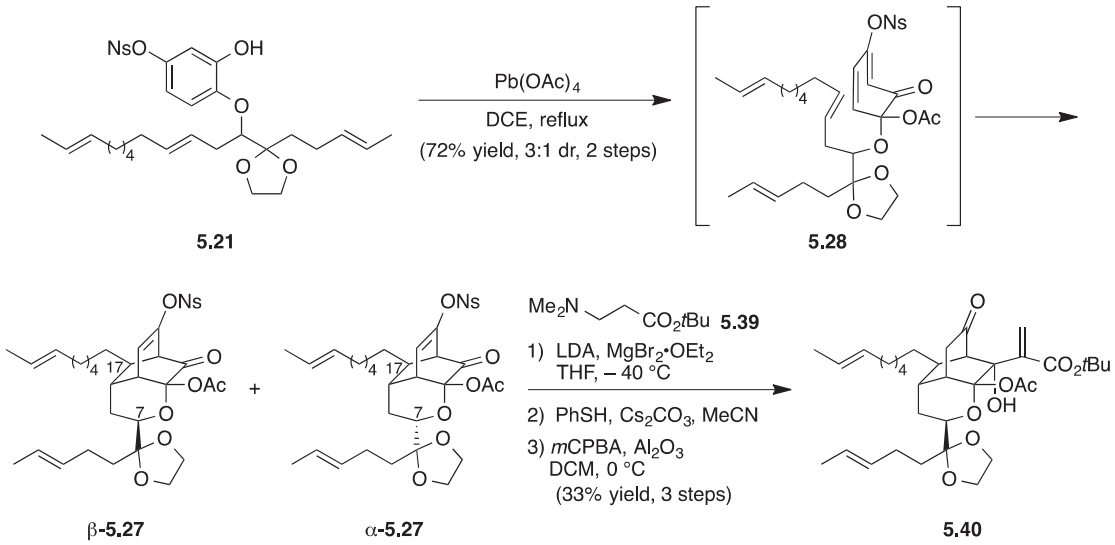

Scheme 5.17 Phenolic oxidation/Diels-Alder sequence

Subjecting a mixture of acetates, β-**5.27** and α-**5.27,** to the previously developed aldol conditions utilizing the lithium enolate of *tert*-butyl propionate **5.39** in the presence of $MgBr_2 \bullet OEt_2$, gave the desired aldol adduct, which was moved on to the next step as a crude mixture.[11] Removal of the nosyl protecting group with thiophenol (PhSH) and Cs_2CO_3, followed by Cope elimination afforded *tert*-butyl ester **5.40** in 33% yield over three steps.[12,13]

The derived *tert*-butyl ester (**5.40**) was then subjected to our previously developed acid mediated lactonization conditions. Unfortunately, this formed a complex mixture of compounds, none of which appeared to be the desired lactone (**5.38**). Spectral data also showed that the ethylene glycol was hydrolyzed under these conditions.

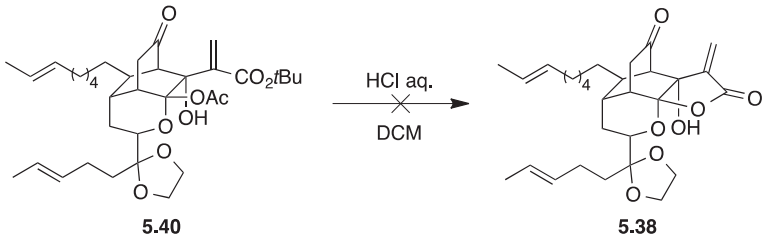

5.40 **5.38**

Scheme 5.18 Initial lactonization attempt

In order to surmount this problem, lactonization conditions were explored. As shown in Table 5.10, basic methanolysis conditions only provided decomposition of our starting material into a complex mixture of products.[14] We reasoned that this could be a result of a detrimental retro-aldol pathway as this type of retro-aldol process is known to occur on hydroxyl-bicycle[2.2.2]octanones.[15] When the reaction was performed under the conditions developed by Mandolini and coworkers (Table 5.10, entry 4), which employs an in situ derived lanthanum methoxide dimer, lactone **5.38** was obtained in 13% yield. Attempts to further optimize this reaction failed; hence, we attempted the use of acyl transfer conditions. However, KCN in ethanol or the bulky phosphine TTMP in methanol did not yield any desired product (Table 5.10, entries 5 and 6, respectively).[16]

Table 5.10 Lactonization attempts

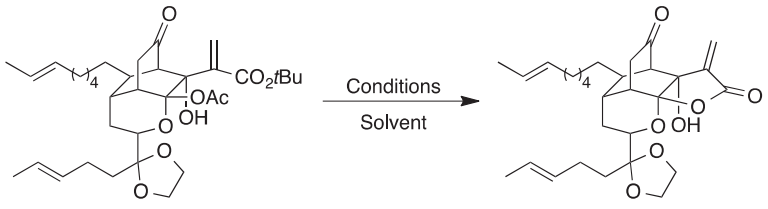

5.40 **3.38**

Entry	Conditions	Solvent	Yield
1	K_2CO_3	MeOH	Decomposition
2	KOMe	MeOH	Decomposition
3	NH_3	MeOH	S.M.
4	$La(OTf)_3$, KOMe	MeOH	13%
5	KCN	EtOH	S.M.
6	TTMPP*	MeOH	S.M.

S.M. = Starting Material
*TTMP = tris(2,4,6-trimethoxyphenyl)phosphine

These latter difficulties led to our revising the approach to lactone **5.38**. To this end, we recalled our first-generation lactonization strategy (Scheme 5.19) where the alcohol was protected as a TMS ether and underwent lactonization in the presence of tetrabutylammonium fluoride (TBAF). Exploiting this strategy in the current approach simply requires a protecting group swap after the phenolic oxidation/Diels-alder sequence.[8]

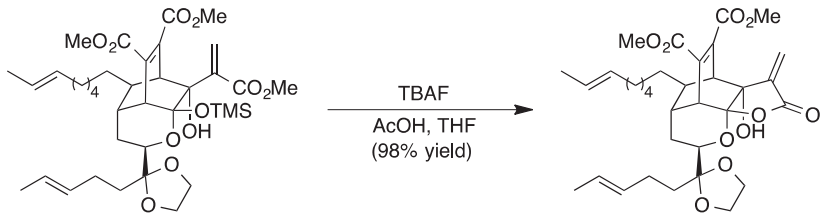

5.41 **5.42**

Scheme 5.19 First-generation lactonization strategy

In order to install the trimethylsilyl group, the acetate protecting group first needed to be removed; to our delight, we found that removal of the acetate following the Diels-Alder cycloaddition appeared to be quite facile (Scheme 5.20). Upon reacting phenol **5.21** with $Pb(OAc)_4$, the crude Diels-Alder adduct was stirred with silica gel for 24 hours, allowing an effective removal of the acetate to deliever alcohol **5.43** as a 1:3 ratio of α:β epimers at C7 in 60% overall yield. As the diastereomers were still inseparable, the mixture was carried on to the silyl protection and thus exposed to TMSCl and Et_3N which furnished silyl ether **5.44** in good yield.[8]

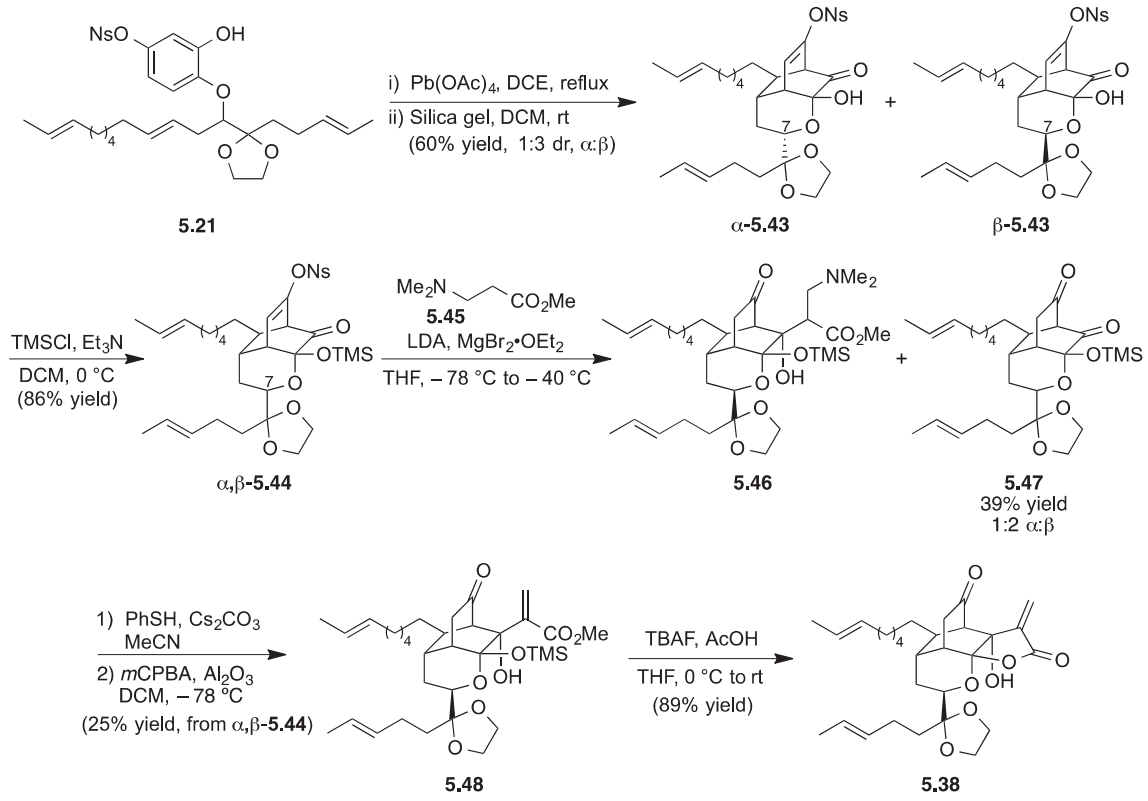

Scheme 5.20 Successful lactonization sequence

As we were hoping to mimic the lactonization conditions from our previous approach, we switched from the *t*-butyl propionate to use the lithium enolate of methyl

propionate **5.45** as our aldol nucleophile. Addition of the enolate to our diastereometic mixture delivered our desired aldol adduct **5.46** along with a 39% yield of diketone **5.47**. The desired alcohol **5.46** was obtained as a mixture of several inseperable compounds, therefore the crude mixture moved forward without further purification. Removal of the nosyl group with thiophenol followed by a cope elimination deliverd the desired α,β-unsaturated methyl ester **5.48** in 25% yield over three steps.[13b-d]

We were surprised to find that the aldol reaction delivered only one of the C7 epimers. Based on our previous results, we expected the aldol reaction to be diastereoselective (with regard to the newly formed stereocenter), but we also hoped that both epimers would react and could be moved forward through the synthesis. Our assignment of the relative stereochemistry came upon the analysis of the byproducts. In the reaction, we obtained a 39% yield of diketone **5.47** with a diastereomeric ratio of 1:2 (α:β), which was enriched in the minor-epimer (α-**5.47**) relative to the original diastereomeric mixture (1:3, α-**5.43**:β-**43**). Based on diketone **5.47**'s diastereomeric ratio, we determined that only a quarter of the α,β-**5.44** mixture underwent the aldol reaction to give alcohol **5.46**. This observation was supported by the 25% yield of methyl ester **5.48** that we obtained. Therefore, we proposed that only β-**5.44** reacts in the aldol reaction to form α,β-unsaturated ester **5.48**.

In order to enhance the reaction yield and find conditions that would allow both α-**5.44** and β-**5.44** to react, we explored various combinations of bases (LDA, MgDA, LiHMDS, and KHMDS), Lewis acids ($MgBr_2 \bullet OEt_2$, LiCl), and solvents (THF, Et_2O, and Toluene), but none gave results better than those shown in Scheme 5.20. The addition of

HMPA only led to decomposition, while absence of Lewis acid gave no reaction; hence, we decided to move forward with our current conditions.

Although our yield in the aldol reaction suffered slightly from switching to a TMS protecting group, the lactonization proceeded in excellent yield. Reacting ester **5.48** with TBAF in the presence of acetic acid (AcOH) afforded lactone **5.38** in 89% yield.[8] With a scalable route for the formation of lactone **5.38**, we could then attempt the cascade cyclization sequence.

5.2.3 Radical Cascade Cyclization

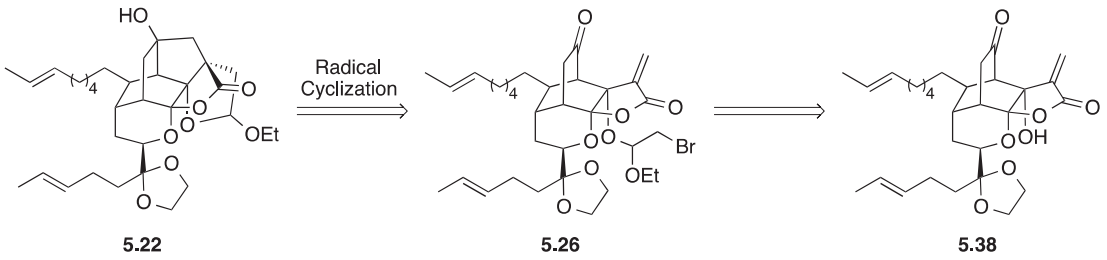

Scheme 5.21

Hoping to prepare isotwistane **5.22** using the same conditions developed for the model system (Chapter Four) we initiated a synthetic sequence by functionalizing tertiary alcohol **5.38** with bromoacetal **5.49,** under the conditions developed by Stork and coworkers, to deliver alkyl bromide **5.26**.[8,17]

Alkyl bromide **5.26** was treated with freshly prepared samarium diiodide to induce the formation of a keto-radical and sequential cyclizations to deliver isotwistane **5.22** in 60% yield as an inconsequential mixture of diastereomers. A plausible mechanism for this transformation is shown in Scheme 5.23. The single electron reduction of the ketone by SmI_2 could form a keto radical **5.26a**, which could further

cyclize in a 5-*endo-trig* manner to deliver the stabilized α-carboxy radical. This could undergo further reduction by SmI_2 to produce a lactone enolate that upon intramolecular alkylation could deliver the observed isotwistane **5.22**.[18]

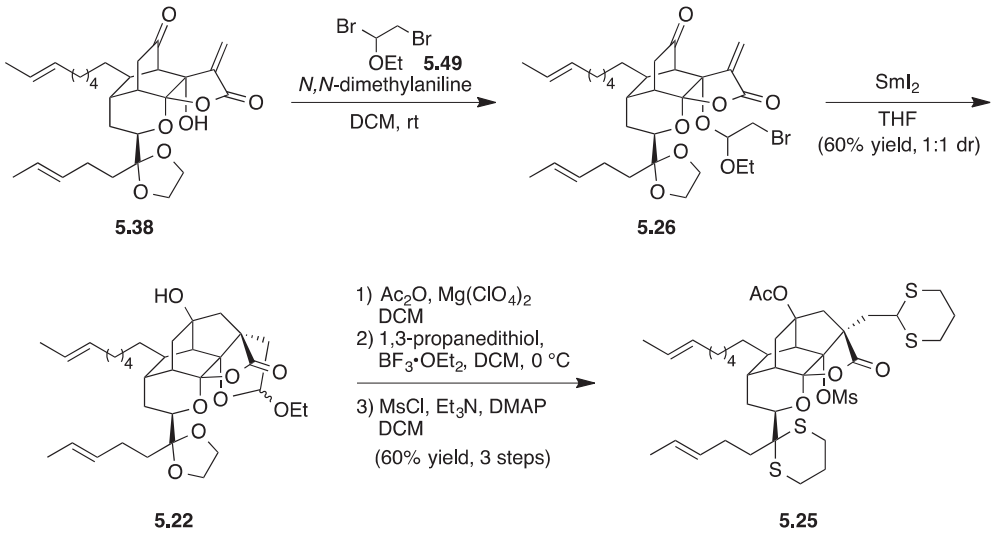

Scheme 5.22 Isotwistane formation

The tertiary alcohol **5.22** obtained from the radical cascade cyclization (Scheme 5.22) was protected as an acetate using acetic anhydride and magnesium perchlorate ($Mg(ClO_4)_2$). The ethyl acetal was exchanged to the corresponding thioacetal upon exposure to 1,3-propanedithiol and $BF_3•OEt_2$ to give a tertiary alcohol, which upon treatment with methanesulfonyl chloride, produced fragmentation precursor **5.25** in 60% yield over three steps.

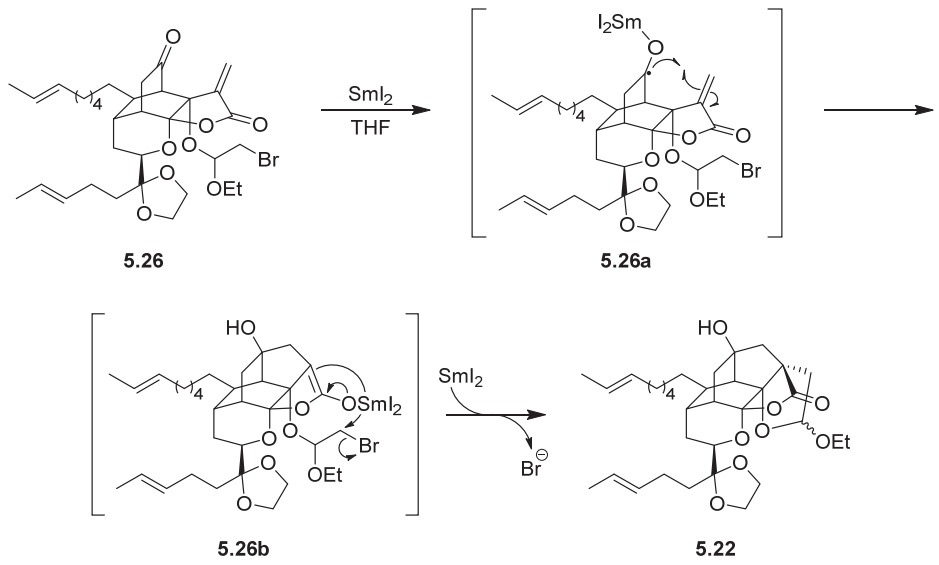

Scheme 5.23 Mechanistic proposal for the radical cycloaddition

5.2.4 Fragmentation and β-Keto Ester Formation

At this point, we have successfully arrived at the targeted fragmentation substrate (isotwistane **5.25**) and so far had encountered relatively few complications resulting from the presence of the side-chain moieties. To our delight, success continued through the Wharton fragmentation (Scheme 5.25) which was initiated via hydrolysis of acetate **5.25** and led to the ring-opened fragmentation product **5.50**, a result that closely paralleled the behavior of our model substrate.[1a,2]

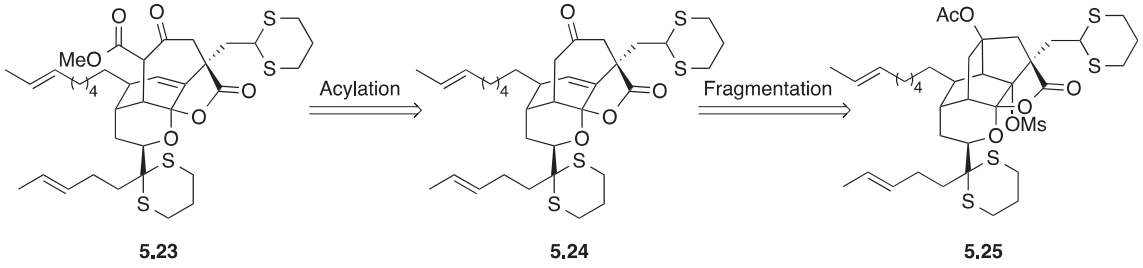

Scheme 5.24

As in our model studies, we were able to convert hemi-acetal **5.50** to acetal **5.24** (67% yield) in the presence of nosyl chloride and Et_3N. We were also able to confirm the relative stereochemistry of ketone **5.24** as the C7-β-epimer using X-ray crystallography. The stereochemical assignment of **5.24** indicates that reclosure of the acetal under the nosyl chloride conditions occurs with retention of stereochemistry, based upon our initial stereochemical assessment of α-**5.43** and β-**5.43** after the Diels-Alder reaction (Schemes 5.17 and 5.20).

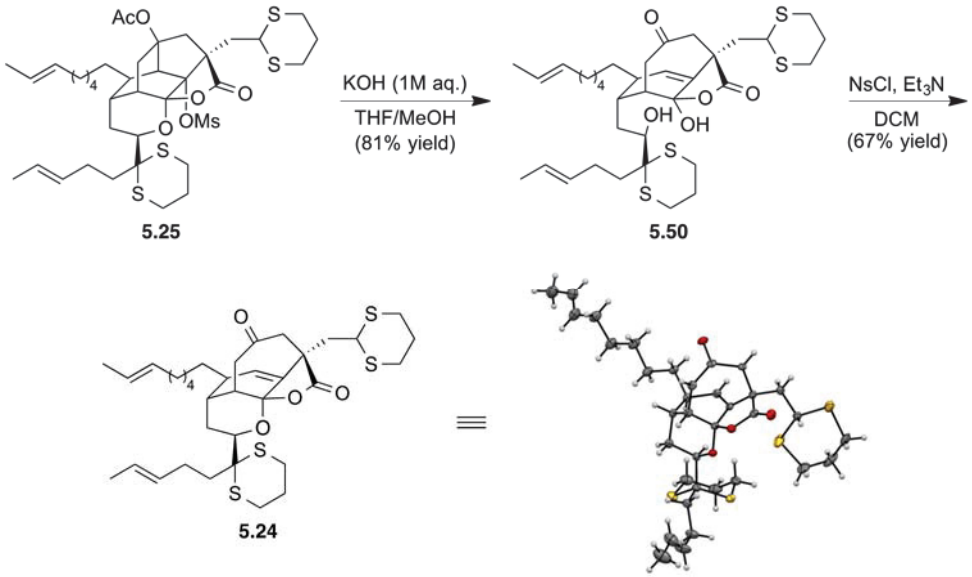

Scheme 5.25 Wharton fragmentation

With ketone **5.24** in hand, we then attempted the acylation to form β-keto ester **5.23**. Previously in our model system studies, we discovered that the ketone **5.51** had a different kinetic and thermodynamic enolate preference (Scheme 5.26). If we used more than one equivalent of base (kinetic conditions), the undesired regioisomer **5.52** was formed, while sub-stoichiometric amount of base (thermodynamic conditions) delivered our desired regioisomer **5.53**.[19]

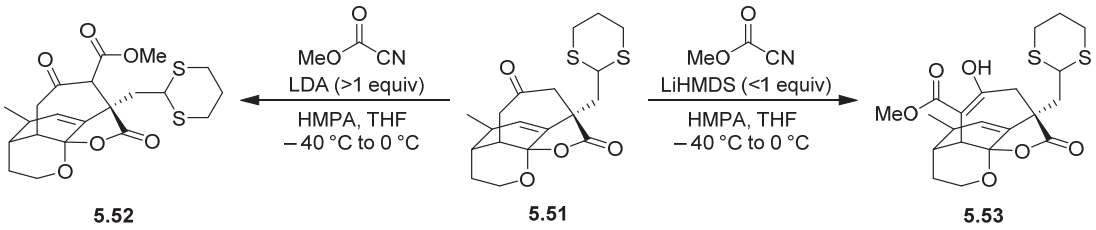

Scheme 5.26 Previous acylation studies

When utilizing our previously developed conditions for the acylation of ketone **5.24**, we found that enol **5.54** could be obtained in low yields (Table 5.11), and we were able to recover unreacted ketone **5.24**. Warming the reaction from 0 °C to room temperature did not improve the yield (Table 5.11, entry 2). We further attempted to completely enolize the ketone by adding additional equivalents of base, followed by the addition of the electrophile, this did produce the desired enol, but only in a low yield (Table 5.11, entry 3).

Table 5.11 Acylation attempts

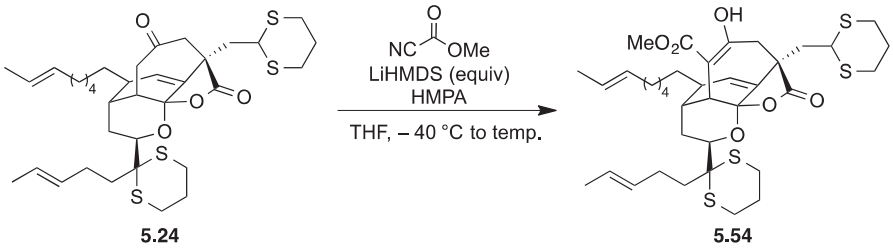

Entry	Equiv	Temp.	Yield
1	0.95	0 °C	17%
2	0.9	rt	6% to 15%
3	0.9 to 1.5	rt	13%
4	1.2	rt	55%

rt = room temperature

All acylation attempts under thermodynamic conditions gave ester **5.54** in low yields. From this observation, we postulated that the thermodynamic enolate was formed

in situ, yet in this system containing the olefinic side chains, thermodynamic enolate could possibly be the undesired regioisomer unlike what we observed in our model substrate. If this was the case, then the undesired enolate regioisomer that was formed was too sterically congested resulting in unreacted thermodynamic enolate being quenched without any addition of the electrophile. This would account for the low yielding reaction and high recovery of starting material. In order to test our rationale for the low reactivity of the reaction, we subjected ketone **5.24** to kinetic enolization conditions (super-stoichiometric base). Under these conditions, we were pleased to obtain enol **5.54** in 55% yield.[3] The regiochemistry of β-keto ester **5.54** was confirmed by HMBC.

5.2.5 Future Directions

Successful acylation of ketone **5.24** with Mander's reagent to form β-keto ester **5.54** led us to consider the final steps needed to complete the total synthesis of phomoidride D (**5.10**). Enol **5.54** is envisioned as furnishing vinyl triflate **5.55**, which upon carbonylative maleic anhydride formation, similar to the route we adopted in the model system (discussed in Chapter 4), will produce **5.56**. Upon the formation of the maleic anhydride **5.56**, the deprotection of both the thioacetal and thioketal are will set the stage for subsequent oxidation of the derived aldehyde to the corresponding acid, thus completing the synthesis.

[3]If the reaction is quenched at – 40 °C, the keto-tautomer is the major tautomer. Like the model system, the enol and keto-tautomers of **5.54** are separable and do not interconvert at room temperature.

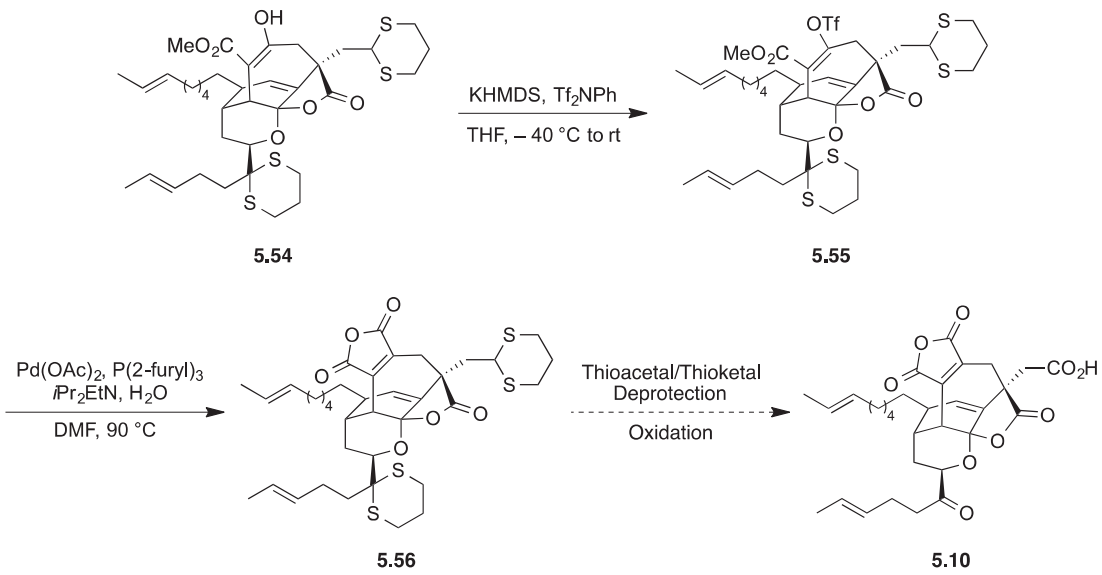

Scheme 5.27 Future direction

5.3 Conclusion

In Chapter Three, we discussed previous synthetic efforts toward phomoidride D (**5.10**) performed in our research group over the period of fifteen years. Creative approaches and brilliant chemistry developed in our first-generation synthetic studies set the foundation for this synthetic odyssey. Unfortunately, attempts to form the maleic anhydride motif at the very end of the first-generation synthesis were unfruitful and required a new strategy for its installation.

The foundations set by the first-generation approach helped guide the model studies employed in our second-generation effort toward an effective late stage installation of the maleic anhydride motif. However, a problematic Wharton fragmentation thwarted these synthetic efforts, leading to a quest for new strategy; a third-generation model study was launched.

As with the second-generation studies, the third-generation approach was initially explored with a model system. In contrast the second-generation approach, the third-

generation approach proved successful in delivering the core structure of phomoidride D (**5.10**). Based on these latter successes, the third-generation approach has been implemented with considerable success on substrates containing the full complement of functionality present in the natural product phomidride D and efforts toward this end continue.

5.4 Experimentals

General.

Unless stated otherwise, all reactions were performed using flame or oven-dried glassware and under an atmosphere of nitrogen. DCM, THF, diethyl ether, benzene, and toluene were dried using a solvent purification system manufactured by SG Water U.S.A., LLC. Acetonitrile, ethyl acetate, pentanes, hexanes, DMF, DMSO, and DCE were supplied by either Fisher Scientific or Sigma-Aldrich and were used as received. Triethylamine, diisopropylamine, and methanol were stirred over calcium hydride and distilled before use. All other commercially available reagents were used as received.

Unless stated otherwise, reactions were monitored by thin-layer chromatography using Silicycle SiliaPlate® TLC glass backed extra hard layer, 60 Å (F-254 indicator, 250 μm thickness). All purifications were performed using Silicyle SiliaFlash® P60 silica (40-63 μm, 230-400 mesh) as a stationary phase. High-resolution mass spectroscopy was performed by the central instrument facility at Colorado State University or on a Thermo Orbitrap ESI mass spectrometer at Baylor University. Single-crystal X-ray crystallography was performed by Brian Newell at Colorado State University or Prof. Caleb Martin at Baylor University. ^{1}H and ^{13}C-NMR spectra were

taken on Varian VNMRS 500, Varian Inova 400, Bruker Ascend 400, and Bruker Ascend 600 cryoprobe spectrometers. Infrared spectra were taken on a Nicolet Avatar 320 FTIR or Bruker Alpha Platinum ATR. Chemical Shifts (δ) are reported in parts per million (ppm) and coupling constants (*J*) are reported in hertz (Hz). The reported chemical shifts are relative to the residual solvent peaks of the indicated deuterated solvents.

Preparation of α-Phenoxy Ketone **5.36**

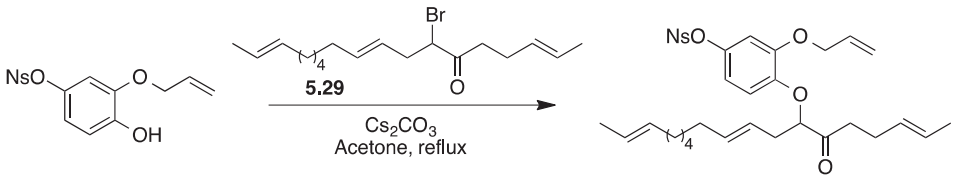

5.30 **5.36**

To a pressure vessel equipped with a magnetic stir bar was added phenol **5.30** (13 g, 37 mmol), α-bromo ketone **5.29** (8.4 g, 25 mmol), cesium carbonate (12 g, 37 mmol), and acetone (62 mL). The reaction vessel was sealed and placed in an oil bath, then heated to 56 °C. The reaction was removed from the heating bath after 2.5 hours. After reaching room temperature, the solution was filtered through a fritted funnel and the solid was washed with EtOAc. Concentration and purification via silica gel flash column chromatography (5% gradient elution from 0% → 50% EtOAc/Hex) afforded ketone **5.36** (9.9 g, 66% yield) as a brown oil.

R_f = 0.24 (25% EtOAc/Hex); ^{1}H-NMR (500 MHz, $CDCl_3$): δ 7.98-7.92 (m, 1H), 7.86-7.79 (m, 2H), 7.67 (ddd, *J* = 7.9, 5.8, 3.0 Hz, 1H), 6.81 (d, *J* = 2.6 Hz, 1H), 6.73-6.62 (m, 2H), 5.96 (ddt, *J* = 17.3, 10.5, 5.3 Hz, 1H), 5.57 (m, 1H), 5.47-5.30 (m, 5H), 5.27 (dq, *J* = 10.5, 1.4 Hz, 1H), 4.49 (dt, *J* = 5.3, 1.5 Hz, 2H), 4.42 (t, *J* = 4.0 Hz, 1H), 2.68-2.45 (m, 4H), 2.22-2.16 (m, 2H), 1.98-1.92 (m, 4H), 1.64-1.56 (m, 6H), 1.35-1.21 (m, 7H); ^{13}C-NMR (125 MHz, $CDCl_3$): δ 210.5, 149.8, 143.6, 135.5, 135.2, 132.4, 132.1,

131.7, 128.5, 126.0, 124.9, 124.8, 123.4, 118.5, 117.1, 114.3, 109.1, 85.5, 70.03, 38.2, 35.8, 32.7, 32.6, 29.6, 29.3, 28.8, 25.9, 18.1, 18.0; FTIR (neat): 29.24, 1716, 1545 cm^{-1}; HRMS (ESI) *m*/*z* Calc'd. for $C_{33}H_{41}NO_8S$ $[M+Na]^+$: 634.2451, found: 634.2461.

Preparation of Ketal **5.37**

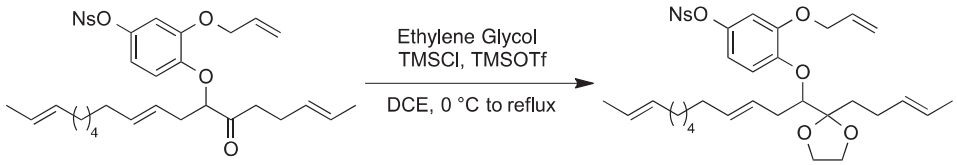

2.36 **2.37**

To a sealed tube under N_2 atmosphere was added ketone **5.36** (9.10 g, 15.0 mmol), ethylene glycol (11.0 mL, 194 mmol) and 1,2-dichloroethane (DCE) (149 mL). The reaction vessel was then cooled in an ice water bath and TMSCl (24.6 mL, 194 mmol) and TMSOTf (0.400 mL, 2.20 mmol) were added. After 10 minutes, the cooling bath was removed and the reaction was allowed to warm to room temperature over 10 minutes, then the N_2 inlet was replaced and the reaction vessel was sealed. The reaction was then placed in an 86 °C oil bath and heated for 6.5 hours, after which the heating bath was removed and the reaction was allowed to cool to room temperature. Upon cooling, the reaction was further cooled in an ice water bath and Et_3N (26.0 mL) was added slowly (vigorous reaction resulting in gas evolution). The solution was transferred to a separatory funnel and washed with H_2O (200 mL). The aqueous was extracted with DCM (3x) and the combined organics were washed with brine before drying over $MgSO_4$. Concentration and purification via silica gel flash column chromatography (5% gradient elution from 0% → 30% EtOAc/Hex) afforded glycol acetal **5.37** (9.00 g, 92% yield) as a brown oil.

R_f = 0.66 (50% EtOAc/Hex); ^{1}H-NMR (600 MHz, $CDCl_3$): δ 7.96-7.89 (m, 1H), 7.83-7.79 (m, 2H), 7.70-7.62 (m, 1H), 6.86-6.79 (m, 1H), 6.74-6.63 (m, 2H), 5.95 (ddt, *J* = 17.4, 10.5, 5.2 Hz, 1H), 5.55-5.31 (m, 7H), 5.28-5.20 (m, 1H), 4.51-4.40 (m, 2H), 4.14-4.09 (m, 1H), 4.04-3.86 (m, 3H), 2.67-2.47 (m, 1H), 2.45-2.37 (m, 1H), 2.22-2.13 (m, 1H), 2.07-2.00 (m, 2H), 1.99-1.86 (m, 4H), 1.78-1.67 (m, 1H), 1.67-1.55 (m, 6H), 1.35-1.17 (m, 7H); ^{13}C-NMR (150 MHz, $CDCl_3$): δ 149.5, 148.9, 142.5, 135.3, 133.4, 132.8, 132.4, 132.0, 131.7, 131.0, 126.2, 125.0, 124.8, 124.7, 118.0, 116.1, 114.1, 111.4, 108.6, 83.8, 69.9, 66.2, 65.9, 34.2, 34.0, 32.7, 29.6, 29.3, 28.8, 26.0, 18.1, 18.0; FTIR (neat): 2923, 1595, 1501 cm^{-1}; HRMS (ESI) *m/z* Calc'd. for $C_{35}H_{45}NO_9S$ $[M+Na]^+$: 678.2707, found: 678.2704.

Preparation of Phenol **5.21**

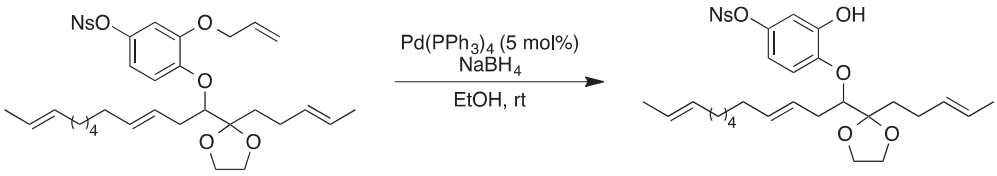

5.37 **5.21**

To a flask equipped with a magnetic stir bar was added ketal **5.37** (9.02 g, 13.8 mmol), $Pd(PPh_3)_4$ (0.794 g, 0.687 mmol), $NaBH_4$ (0.260 g, 6.87 mmol), and the flask was evacuated and backfilled with N_2 three times. EtOH (92.0 mL, degassed by freeze-pump-thaw) was added and the reaction was allowed to stir at room temperature. TLC was used to monitor the reaction progress. The TLC plates were developed using a 50% EtOAc/Hex solution and visualized by $KMnO_4$. After 2 hours, the reaction looked complete, so the reaction was quenched with a saturated aqueous solution of NH_4Cl (20.0 mL). The reaction was diluted with EtOAc (100 mL) and transferred to a separatory funnel, where the organic was washed with H_2O (90.0 mL) and brine. Drying over

Na_2SO_4, concentration, and purification via silica gel flash column chromatography (10% gradient elution from 0% → 60% EtOAc/Hex) afforded phenol **5.21** (7.38 g, 87% yield) as an orange oil.

R_f = 0.19 (25% EtOAc/Hex); ^{1}H-NMR (500 MHz, $CDCl_3$): δ 7.98-7.94 (m, 1H), 7.84-7.78 (m, 2H), 7.67 (ddd, *J* = 7.8, 6.7, 2.2 Hz, 1H), 7.60 (s, 1H), 6.96 (d, *J* = 8.9 Hz, 1H), 6.73 (d, *J* = 2.8 Hz, 1H), 6.61 (dd, *J* = 8.9, 2.9 Hz, 1H), 5.57-5.49 (m, 1H), 5.49-5.30 (m, 5H), 4.08-3.95 (m, 4H), 3.80 (dd, *J* = 7.5, 4.7 Hz, 1H), 2.52-2.41 (m, 2H), 2.15-2.20 (m, 2H), 1.99-1.85 (m, 5H), 1.74 (ddd, *J* = 14.2, 11.0, 5.3 Hz, 1H), 1.64-1.58 (m, 6H), 1.36-1.21 (m, 6H); ^{13}C-NMR (125 MHz, $CDCl_3$): δ 149.3, 145.9, 144.8, 135.4, 134.3, 132.3, 132.0, 131.7, 130.5, 128.7, 125.6, 125.5, 124.9, 124.8, 120.9, 113.2, 111.7, 110.4, 86.2, 66.2, 66.1, 34.8, 34.0, 32.7, 29.6, 29.2, 28.9, 25.9, 18.1, 18.0; FTIR (neat): 3226, 2924, 1602, 1546 cm^{-1}; HRMS (ESI) *m*/*z* Calc'd. for $C_{32}H_{41}NO_9S$ $[M+Cl]^-$: 650.2191, found: 650.2183.

Preparation of α-Acetoxy Ketone **5.27**

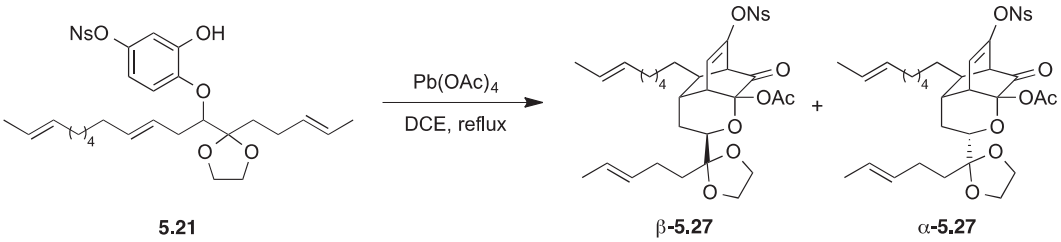

5.21 β-**5.27** α-**5.27**

To a pressure vessel equipped with a magnetic stir bar was added phenol **5.21** (0.87 g, 1.4 mmol), lead tetraacetate ($Pb(OAc)_4$) (0.75 g, 1.7 mmol), and DCE (14 mL). The reaction vessel was stirred at room temperature for 20 minutes after which it was placed into a 90 °C oil bath. After 18 hours, the solution was transferred to a round bottom flask and concentrated. Purification via silica gel flash column chromatography

(10% gradient elution from 0% → 80% EtOAc/Hex) afforded α-acetoxy ketone **5.27** (0.54 g, 72% yield, 1:3 dr α:β) as an orange foam. (Note: diastereomeric ratio was determined using the crude ^{1}H NMR)

R_f = 0.29 (50% EtOAc/Hex); ^{1}H-NMR (400 MHz, $CDCl_3$): δ 8.04-7.98 (m, 1H), 7.86-7.82 (m, 2H), 7.77-7.68 (m, 1H), 6.06 (dd, *J* = 7.7, 2.4 Hz, 0.3H), 6.00 (dd, 12.0, 4.0 Hz, 0.7H), 5.49-5.30 (m, 4H), 4.58 (dd, *J* = 10.6, 6.4 Hz, 0.3H), 4.02-3.84 (m, 4.7H), 3.76 (dd, *J* = 7.7, 2.9 Hz, 0.3H), 3.68 (dd, *J* = 7.6, 3.5 Hz, 0.7H), 3.49 (dd, *J* = 12.2, 2.8 Hz, 0.6H), 3.21 (dt, *J* = 15.7, 2.3 Hz, 1.2H), 2.14-1.86 (m, 8H), 1.84-1.73 (m, 2H), 1.70-1.52 (m, 8H), 1.40-1.18 (m, 8H): ^{13}C-NMR (100 MHz, $CDCl_3$): δ 200.3, 200.2, 194.7, 169.7, 168.2, 148.7, 145.9, 145.4, 135.9, 135.8, 132.6, 132.4, 132.3, 132.2, 131.4, 131.4, 131.0, 130.9, 128.7, 128.1, 125.2, 125.1, 125.0, 125.0, 117.6, 115.9, 110.3, 110.2, 94.2, 93.7, 75.9, 75.8, 75.2, 66.6, 66.5, 66.0, 65.8, 55.5, 55.4, 44.2, 41.3, 41.0, 36.3, 36.0, 35.6, 35.4, 34.9, 34.8, 34.0, 33.9, 32.6, 32.5, 30.6, 29.5, 29.2, 29.1, 29.1, 29.0, 27.0, 26.8, 25.9, 25.8, 22.1, 21.9, 18.1, 18.0, 18.0 cm^{-1}; FTIR (neat); 2927, 1749, 1546 cm^{-1}; HRMS (ESI) *m*/*z* Calc'd. for $C_{34}H_{43}NO_{11}S$ $[M+H]^+$: 674.2635, found: 674.2640.

Preparation of α-Hydroxy Ketone **5.43**

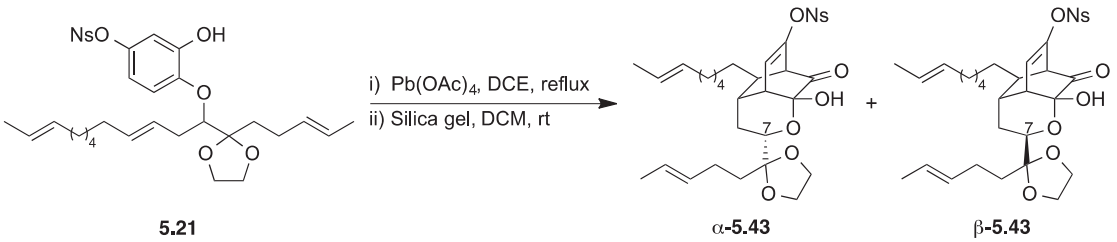

5.21 **α-5.43** **β-5.43**

To a pressure vessel equipped with a magnetic stir bar was added the phenol **5.21** (0.13 g, 0.20 mmol), $Pb(OAc)_4$ (0.11 g, 0.25 mmol), and 1,2-dichloroethane (DCE) (2.0 mL). The reaction vessel was stirred at room temperature for 25 minutes after which it

was placed into a 90 °C oil bath. After 22 hours, the reaction was removed from the heating bath and after an additional hour, it was filtered through a fritted funnel using DCM to rinse the flask. After concentration, the crude oil was dissolved in DCM (3.2 mL) and silica gel (1.1 g) was added. This was allowed to stir at room temperature and the reaction progress was followed by TLC. The TLC plates were developed using a 50% EtOAc/Hexanes solution and visualized by $KMnO_4$. After 23 hours, the silica gel was removed by vacuum filtration and solid was washed with DCM (30 mL) and EtOAc (40 mL). Concentration and purification via silica gel flash column chromatography (10% gradient elution from 0% → 70% EtOAc/Hex) afforded ketone **5.43** (0.080 g, 60% yield, 1:3 dr α:β) as a brown sticky foam. (Note: diastereomeric ratio was determined using the crude ^{1}H NMR)

R_f = 0.28 (50% EtOAc/Hex); ^{1}H-NMR (500 MHz, $CDCl_3$): δ 8.00-7.97 (m, 1H), 7.86-7.81 (m, 2H), 7.73-7.65 (m, 1H), 6.13 (dd, *J* = 7.6, 2.3 Hz, 0.28H), 6.05 (dd, *J* 7.6, 2.5 Hz, 0.82H), 5.47-5.32 (m, 4H), 4.03-3.87 (m, 5H), 3.54-3.41 (m, 1H), 3.30-3.16 (m, 2H), 2.89 (dd, *J* = 7.6, 2.6 Hz, 0.27H), 2.65 (dd, *J* = 7.5, 3.4 Hz, 0.83H), 2.06-1.88 (m, 6H), 1.83-1.69 (m, 2H), 1.66-1.57 (m, 6H), 1.48-1.44 (m, 1H), 1.37-1.23 (m, 8H); ^{13}C-NMR (125 MHz, $CDCl_3$): δ 206.32, 198.24, 148.69, 148.61, 144.82, 144.40, 135.87, 135.84, 133.34, 133.02, 132.23, 132.19, 131.47, 130.85, 130.77, 130.61, 129.99, 127.79, 127.75, 125.27, 125.17, 125.10, 125.05, 125.02, 124.96, 124.27, 124.06, 119.60, 119.48, 110.36, 110.22, 110.19, 110.13, 90.82, 90.40, 73.94, 72.93, 66.66, 66.34, 66.09, 65.57, 65.55, 55.69, 55.67, 55.23, 43.67, 42.67, 40.76, 38.50, 36.21, 35.87, 35.44, 34.77, 34.16, 32.61, 32.56, 30.56, 29.50, 29.48, 29.22, 29.20, 29.10, 28.95, 27.04, 26.92, 26.86, 26.82,

26.10, 25.91, 20.62, 18.08, 18.05, 12.93, 12.85; FTIR (neat): 3410, 29.26, 1746, 1545 cm^{-1}; HRMS (ESI) *m/z* Calc'd. for $C_{32}H_{41}NO_{10}S$ $[M+Na]^+$: 654.2349, found: 654.2355.

Preparation of Silyl Ether **5.44**

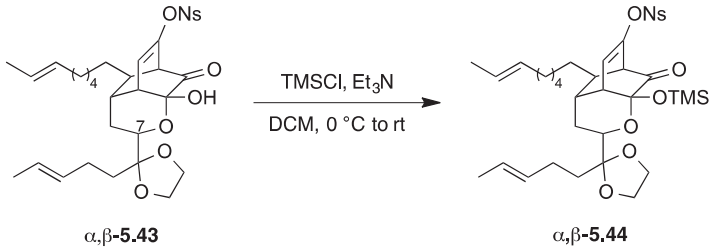

α,β-**5.43** α,β-**5.44**

To a round bottom flask equipped with a magnetic stir bar was added alcohol **5.43** (1.80 g, 2.85 mmol, 1:3 α:β mixture), and DCM (28.5 mL). The solution was cooled in an ice water bath, at which point chlorotrimethylsilane (TMSCl) (0.550 mL, 4.27 mmol) and triethylamine (Et_3N) (0.600 mL, 4.27 mmol) were added. TLC was used to follow the reaction progress and the TLC plates were developed using a 50% EtOAc/Hexanes solution and visualized with CAM. After stirring at 0 °C for 4 hours, TMSCl (0.550 mL, 4.27 mmol) and Et_3N (0.600 mL, 4.27 mmol) were added and the reaction was allowed to slowly warm to room temperature, with the bath, overnight. In the morning, the reaction was cooled to 0 °C, TMSCl (0.550 mL, 4.27 mmol) and Et_3N (0.600 mL, 4.27 mmol) were again added. After four additional hours of slowly warming to room temperature with the bath, the reaction was quenched with the addition of $NaHCO_3$ (14.0 mL). The solution was transferred to a separatory funnel where the layers were separated and the aqueous extracted with DCM (2x). The combined organics were dried over Na_2SO_4. Concentration and purification via silica gel flash column chromatography (teledyne MPLC, 0% → 30% EtOAc/Hex) afforded silyl ether **5.44** (1.73 g, 86% yield, 1:3 α:β mixture) as a yellow oil.

R_f = 0.42 (20% EtOAc/Hex); ^{1}H-NMR (500 MHz, $CDCl_3$): δ 8.01-7.99 (m, 0.25H), 7.98-7.96 (m, 0.75H), 7.86-7.80 (m, 2H), 7.74-7.71 (m, 0.25H), 7.69-7.64 (m, 0.75H), 6.07 (dd, *J* =10.0, 5.0 Hz, 0.25H), 6.04 (dd, *J* = 10.0, 5.0 Hz, 0.75H), 5.48-5.31 (m, 4H), 4.06-3.82 (m, 5H), 3.49-3.45 (m, 1H), 3.15-3.14 (m, 0.25H), 3.08-3.05 (m, 0.75H), 2.73 (dd, *J* = 7.6, 2.7 Hz, 0.25H), 2.55 (dd, *J* = 7.6, 2.7 Hz, 0.75H), 2.09-1.98 (m, 1H), 1.98-1.79 (m, 5H), 1.76-1.51 (m, 8H), 1.44-1.40 (m, 1H), 1.35-1.21 (m, 8H), 0.17 (s, 6.8H), 0.15 (s, 2.2H); ^{13}C-NMR (125 MHz, $CDCl_3$): δ 204.36, 197.75, 148.67, 148.61, 144.90, 144.43, 135.66, 135.62, 132.80, 132.56, 132.42, 132.38, 131.53, 131.47, 130.80, 130.78, 130.74, 130.69, 129.99, 128.48, 128.38, 125.22, 125.15, 125.01, 124.96, 124.94, 124.91, 124.18, 124.01, 119.48, 119.37, 110.64, 110.43, 92.82, 92.39, 73.26, 73.21, 72.70, 66.43, 66.19, 66.18, 66.05, 65.09, 56.19, 56.06, 56.04, 45.71, 43.67, 42.02, 41.35, 35.97, 35.88, 35.49, 34.91, 34.62, 34.55, 34.50, 32.63, 32.56, 30.97, 29.53, 29.50, 29.23, 29.13, 28.37, 27.13, 26.95, 26.90, 26.83, 26.32, 25.90, 20.87, 18.08, 12.92, 1.99, 1.7; FTIR (neat): 2926, 1752, 1651, 1546 cm^{-1}; HRMS (ESI) *m*/*z* Calc'd. for $C_{35}H_{49}NO_{10}SSi$ $[M+Na]^+$: 726.2739, found: 726.2734.

Preparation of Amine **5.46**

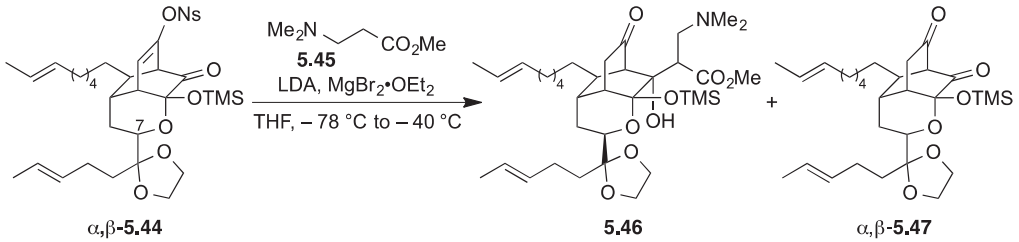

α,β-**5.44** **5.46** α,β-**5.47**

Preparation of a Magnesium Bromide solution in Ether.[20] Magnesium turnings were washed with 1M HCl (15.0 mL), H_2O (30.0 mL), and acetone (60.0 mL). The washed magnesium turnings (1.46 g, 60.0 mmol) were transferred to a schlenk tube

equipped with a magnetic stir bar and placed under vacuum for 30 minutes. Diethyl ether (Et_2O) (50.0 mL) was then added and the reaction vessel was fitted with a water-cooled condenser and 1,2-dibromoethane (0.400 mL, 4.65 mmol) was added. More 1,2-Dibromoethane (3.90 mL, 45.4 mmol) was added slowly via syringe pump over 4 hours. After the addition was complete, the reaction was allowed to stir for 1 hour before being sealed and stirred overnight (slow stirring). The two layers that had formed consisted of Et_2O (top) and a 2.8M solution of $MgBr_2 \bullet OEt_2$ in Et_2O (bottom).

Preparation of Lithium Enolate solution 0.5M in THF. To a round bottom flask equipped with a magnetic stir bar was added diisopropylamine (*i*Pr_2NH) (0.600 mL, 4.26 mmol) and THF (7.74 mL). The solution was cooled in a dry ice/acetone bath and *n*-butyllithium (*n*BuLi) (1.67 mL, 2.43M in hexanes, 4.07 mmol) was added. The reaction was stirred at – 78 °C for 1 hour before the addition of methyl 3-(dimethylamino)propionate (0.550 mL, 3.88 mmol). The resultant mixture was stirred for 30 minutes at – 78 °C before being placed into and ice/salt water bath for 15 minutes and then warmed to room temperature for additional 20 minutes. The enolate solution was cooled again to – 78 °C before use.

Aldol Reaction. To a round bottom flask equipped with a magnetic stir bar was added ketone α,β-**5.44** (0.47 g, 0.67 mmol), $MgBr_2 \bullet OEt_2$ (0.48 mL, 2.8M in Et_2O, 1.3 mmol) and THF (13 mL). The solution was cooled in a dry ice/acetone bath and the enolate solution was slowly added via cannula over 20 minutes. The reaction was stirred at this temperature for an additional 30 minutes before being placed into a dry ice/acetonitrile bath. TLC was used to follow the reaction progress and the TLC plates

were developed using a 25% EtOAc/Hexanes solution (10% MeOH/DCM for product) and visualized with CAM. After 1 hour, the solution was cooled again to – 78 °C and after 20 minutes, the reaction was quenched with the addition of sat. aq. NH_4Cl (6.0 mL). After warming to room temperature, the solution was transferred to a separatory funnel and diluted to EtOAc. The organic layer was dried over Na_2SO_4. Concentration and purification via silica gel flash column chromatography (10% gradient, 0% → 100% EtOAc/Hex) afforded alcohol **5.46** (0.33 g) as a mixture of several compounds along with diketone α,β-**5.47** (0.13 g, 39% yield, 1:2 dr, α:β).

Amine **5.46**. R_f = 0.5 (10% MeOH:DCM); ^{1}H-NMR (500 MHz, $CDCl_3$): δ 8.19-8.17 (m, 1H), 7.83-7.79 (m, 2H), 7.76-7.73 (m, 1H), 5.67 (dd, *J* = 7.4, 2.8 Hz, 1H), 5.47-5.33 (m, 4H), 4.80 (dd, *J* = 10.3, 5.6 Hz, 1H), 4.01-3.86 (m, 5H), 3.67 (s, 3H), 3.19 (dd, *J* = 12.8, 8.9 Hz, 1H), 2.92 (dd, *J* = 8.9, 3.1 Hz, 1H), 2.74 (dd, *J* = 12.8, 3.3 Hz), 2.47-2.42 (m, 1H), 2.30-2.19 (m, 8H), 2.16-1.86 (m, 7H), 1.68-1.58 (m, 7H), 1.43-1.37 (m, 1H), 1.27-1.23 (m, 2H), 1.19-1.05 (m, 6H), 0.17 (s, 9H); ^{13}C-NMR (125 MHz, $CDCl_3$): δ 176.5, 148.9, 148.7, 135.1, 132.1, 131.7, 131.5, 131.4, 130.2, 125.0, 124.8, 124.5, 111.5, 111.4, 100.4, 81.3, 73.7, 66.0, 64.9, 59.8, 52.3, 51.6, 49.1, 47.7, 46.4, 37.5, 36.1, 34.9, 34.7, 32.7, 29.6, 29.5, 28.9, 27.2, 26.6, 18.1, 18.1, 18.0, 2.32; FTIR (neat): 3419, 2927, 1704, 1547 cm^{-1}; HRMS (ESI) *m/z* Calc'd. for $C_{41}H_{63}N_2O_{12}SSi$ $[M+H]^+$:835.3865, found: 835.3866.

Diketone **5.47** *α-Epimer*. R_f = 0.54 (25% EtOAc/Hexanes); ^{1}H-NMR (500 MHz, $CDCl_3$): δ 5.50-5.34 (m, 4H), 4.11-4.02 (m, 2H), 4.00-3.87 (m, 3H), 3.15 (d, *J* = 2.0 Hz, 1H), 2.55-2.48 (m, 1H), 2.38-2.30 (m, 2H), 2.19-2.14 (m, 1H), 2.12-1.92 (m, 6H), 1.89-

1.84 (m, 1H), 1.77-1.66 (m, 2H), 1.66-1.55 (m, 6H), 1.37-1.17 (m, 8H); ^{13}C-NMR (125 MHz, $CDCl_3$): δ 204.8, 199.0, 131.4, 130.7, 125.3, 125.0, 110.7, 96.5, 72.5, 69.3, 66.5, 66.1, 44.1, 40.2, 38.8, 35.4, 35.3, 34.6, 32.7, 32.6, 29.5, 29.1, 26.9, 26.0, 18.1, 1.6; FTIR (neat): 2927, 1757, 1729 cm^{-1}; HRMS (ESI) *m/z* Calc'd. for $C_{41}H_{46}O_6Si$ $[M+Na]^+$:541.2956, found: 541.2958.

Diketone **5.47** *β-Epimer*. R_f = 0.57 (10% EtOAc/Hexanes); ^{1}H-NMR (500 MHz, $CDCl_3$): δ 5.50-5.32 (m, 4H), 4.03-3.89 (m, 5H), 3.62 (dd, *J* 12.2, 2.6 Hz, 1H), 3.22 (d, *J* = 3.1 Hz, 1H), 2.80 (dd, *J* = 19.7, 2.9 Hz, 1H), 2.25 (dd, *J* 19.7, 3.2 Hz, 1H), 2.14-2.06 (m, 2H), 2.02-1.80 (m, 6H), 1.68-1.48 (m, 8H), 1.35-1.19 (m, 8H), 0.15 (s, 9H); ^{13}C-NMR (125 MHz, $CDCl_3$): δ 204.9, 204.6, 131.3, 130.8, 125.03, 125.01, 110.5, 96.1, 73.6, 70.1, 66.2, 65.1, 42.0, 39.9, 39.5, 36.3, 35.9, 34.7, 32.5, 30.3, 29.4, 26.7, 26.4, 18.05, 18.03, 1.7; FTIR (neat): 2927, 1752, 1724 cm^{-1}; HRMS (ESI) *m/z* Calc'd. for $C_{29}H_{46}O_6Si$ $[M+Na]^+$:541.2956, found: 541.2959.

Preparation of Methyl Ester **5.48**

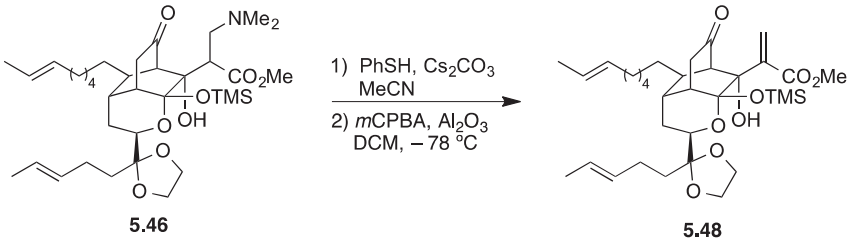

5.46 **5.48**

Nosyl Deprotection. To a round bottom flask equipped with a magnetic stir bar was added the nosyl enol ether **5.46** (0.33 g, 0.40 mmol) and acetonitrile (MeCN) (4.0 mL). Thiophenol (0.061 mL, 0.59 mmol) and cesium carbnonate (Cs_2CO_3) (0.19 g, 0.59 mmol) were then added and the reaction was allowed to stir at room temperature. TLC

was used to follow the reaction progress and the TLC plates were developed using a 20% EtOAc/Hexanes solution and visualized with CAM. After stirring 3.5 hours, the reaction was quenched with the addition of sat. aq. NH_4Cl (2.0 mL) and diluted with EtOAc. The organic layer was separated and dried over Na_2SO_4. Concentration and purification via silica gel flash column chromatography (5% gradient, 5% → 20%; then 100% EtOAc/Hex) afforded the ketone.

Cope Elimination. To a round bottom flask equipped with a magnetic stir bar was added the ketone and DCM (3.1 mL). The solution was cooled in a dry ice/acetone bath and stirred at this temperature for 10 minutes before the addition of 3-chloroperbenzoic acid (*m*CPBA) (0.21 g, 0.32 mmol) as a solution in DCM, which was added slowly dropwise (~ 1 drop/second) to keep the solution temperature consistent. Upon completion of the addition, basic alumina (Al_2O_3) (0.21 g) was added to the solution which was allowed to stir 20 seconds at this temperature before the solution was quickly passed through a plug of basic alumina (12 g) (presaturated with DCM) and vacuum filtered using a 10% MeOH/DCM solution (25 mL) to wash. Concentration and purification of the filtrate via silica gel flash column chromatography (0% → 5% EtOAc/Hex) afforded methyl ester **5.48** (0.11 g, 25% yield from TMS ether α,β-**5.44**) as a clear oil and as a single diastereomer.

R_f = 0.82 (50% EtOAc/Hex); ^{1}H-NMR (500 MHz, $CDCl_3$): δ 5.84 (s, 1H), 5.75 (s, 1H), 5.70 (s, 1H), 5.54-5.35 (m, 4H), 4.89 (dd, *J* = 11.3, 4.2 Hz, 1H), 4.02-3.91 (m, 4H), 3.78 (s, 3H), 2.68 (d, *J* = 2.4 Hz, 1H), 2.45 (dd, *J* = 19.3, 2.3 Hz, 1H), 2.39-2.31 (m, 1H), 2.24-2.04 (m, 2H), 2.04-1.91 (m, 4H), 1.84-1.75 (m, 2H), 1.70-1.57 (m, 9H), 1.36-1.23 (m, 8H), 0.13 (s, 9H); ^{13}C-NMR (125 MHz, $CDCl_3$): δ 213.7, 170.1, 143.7, 131.6, 131.3,

124.9, 124.8, 121.6, 111.4, 100.3, 80.4, 74.6, 66.2, 65.3, 59.3, 52.0, 43.8, 39.5, 36.8, 36.0, 35.0, 33.3, 32.6, 30.0, 29.6, 29.3, 27.0, 26.8, 18.1, 18.0, 1.71; FTIR (neat): 3437, 2926, 1724, 1705 cm^{-1}; HRMS (ESI) *m*/*z* Calc'd. for $C_{33}H_{52}O_8Si$ $[M+Na]^+$: 627.3324, found: 627.3329.

Preparation of tButyl Ester **5.40**

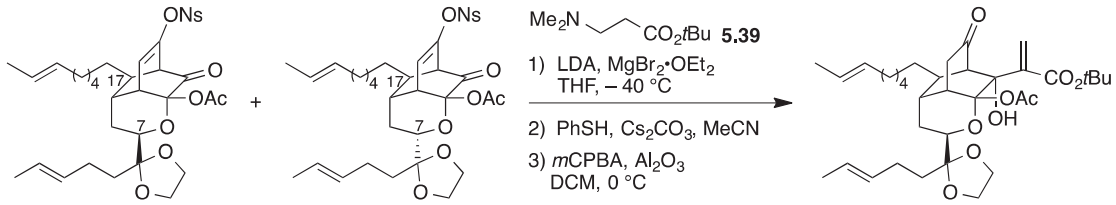

Preparation of the Lithium Enolate. To a round bottom flask equipped with a magnetic stir bar was added *i*Pr_2NH (0.070 mL, 0.48 mmol) and THF (0.50 mL). The solution was cooled in a dry ice/acetone bath and *n*BuLi (0.34 mL, 1.4 M in hexanes, 0.48 mmol) was added. The reaction was then stirred at this temperature for 30 minutes and then placed into a ice/salt water bath for 20 minutes before being cooled again to – 78 °C. After cooling a solution of *t*butyl 3-(dimethylamino)propionate (0.082 mL, 0.48 mmol) in THF (0.30 mL) was added and the reaction was allowed to stir at – 78 °C for an additional hour before use.

Aldol Reaction. To a round bottom flask equipped with a stir bar was added ketone α,β-**5.27** (0.10 g, 0.15 mmol), $MgBr_2$•OEt_2 (0.077 g, 0.30 mmol) and THF (1.0 mL). The solution was then cooled in a dry ice/acetone bath and the lithium enolate solution was added via cannula. TLC was used to follow the reaction progress and the TLC plates were developed using a 50% EtOAc/Hexanes solution and visualized with

$KMnO_4$. After 30 minutes, the reaction was quenched with the addition of sat. aq. NH_4Cl (0.50 mL) and was allowed to warm to room temperature before diluting with EtOAc. The organic was washed with H_2O and brine before being dried over Na_2SO_4. After concentration, the crude mixture was moved on to the next reaction.

Nosyl Deprotection. To a vial equipped with a magnetic stir bar was added the crude nosyl enol ether, Cs_2CO_3 (0.073 g, 0.22 mmol), and MeCN (0.75 mL). Thiophenol (0.023 mL, 0.22 mmol) was added dropwise and the vial was capped and the reaction was stirred at room temperature. TLC was used to follow the reaction progress and the TLC plates were developed using a 50% EtOAc/Hexanes solution and visualized with $KMnO_4$. After 3.5 hours, the reaction was quenched with the addition of sat. aq. NH_4Cl and diluted with EtOAc. The organic layer was washed with brine and dried over Na_2SO_4. Concentration afforded the crude ketone that was moved onto the next reaction.

Cope Elimination. To a vial equipped with a magnetic stir bar was added the crude ketone and DCM (1.2 mL). The solution was cooled in an ice/water bath and *m*CPBA was added. After 5 minutes, the reaction was removed from the cooling bath and after a total of 30 minutes, basic alumina (0.17 g) was added. TLC was used to follow the reaction progress and the TLC plates were developed using a 50% EtOAc/Hexanes solution and visualized with $KMnO_4$. After 4 hours, the reaction was worked up by vacuum filtration and washing the filtrate with sat. aq. $NaHCO_3$ and brine, followed by drying over Na_2SO_4. Concentration and purification via silica gel flash column chromatography (5% gradient, 0% → 35% EtOAc/Hex) afforded *t*butyl ester **5.40** (0.031 g, 34% yield from ketone α,β-**5.27**) as primarily one diastereomer (>20:1 dr).

R_f = 0.45 (15% EtOAc/Hex); ^{1}H-NMR (400 MHz, $CDCl_3$): δ 5.94 (s, 1H), 5.70 (s, 1H), 5.61 (s, 1H), 5.47-5.35 (m, 4H), 4.84 (dd, *J* = 12.5, 4.3 Hz, 1H), 4.07-3.91 (m, 4H), 3.17 (dd, *J* = 3.8, 2.4 Hz, 1H), 2.71-2.67 (m, 1H), 2.39-2.34 (m, 1H), 2.32-1.45 (m, 29H), 1.35-1.21 (m, 8H); ^{13}C-NMR (100 MHz, $CDCl_3$): δ 212.4, 167.7, 167.6, 144.3, 131.5, 131.3, 124.9, 124.8, 123.0, 111.2, 104.0, 82.7, 79.4, 77.0, 66.6, 65.9, 59.0, 38.3, 37.0, 36.7, 35.8, 34.1, 33.3, 32.6, 30.9, 29.5, 29.2, 28.2, 26.9, 26.0, 22.4, 18.1, 18.04; FTIR (neat): 3512, 2926, 1752,1726, 1698 cm^{-1}; HRMS (ESI) *m/z* Calc'd.for $C_{35}H_{52}O_9$ $[M+Na]^+$: 639.3504, found: 639.3508.

Preparation of Lactone **5.38**

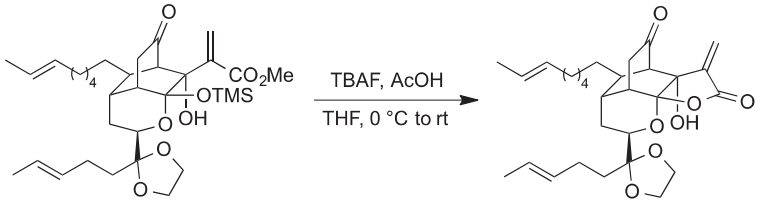

5.48 **5.38**

To a round bottom flask equipped with a magnetic stir bar was added methyl ester **5.48** (0.852 g, 1.41 mmol) and THF (14.0 mL). The solution was then cooled in an ice/water bath and acetic acid (AcOH) (0.400 mL, 7.05 mmol) was added, followed by the addition of tetrabutylammonium fluoride (TBAF) (2.82 mL, 1.0M in THF, 2.82 mmol). TLC was used to follow the reaction progress and the TLC plates were developed using a 50% EtOAc/Hexanes solution and visualized with CAM. After 3.5 hours, TBAF (1.41 mL, 1.0M in THF, 1.41 mmol) was again added followed by another TBAF (1.41 mL, 1.0M in THF, 1.41 mmol) addition after an additional 45 minutes. After a total of 4.25 hours, the reaction was worked up by pouring into H_2O (50.0 mL), the organic layer was washed with brine, and dried over Na_2SO_4. Concentration and

purification via silica gel flash column chromatography (5% gradient, 0% → 40% EtOAc/Hex) afforded lactone **5.38** (0.620 g, 89% yield) as a white foam.

R_f = 0.21 (25% EtOAc/Hex); ^{1}H-NMR (500 MHz, $CDCl_3$): δ 6.49 (s, 1H), 5.99 (s, 1H), 5.51-5.35 (m, 4H), 4.56 (dd, *J* = 12.2, 4.0 Hz, 1H), 4.35 (s, 1H), 4.21-3.89 (m, 4H), 2.73 (d, *J* = 2.5 Hz, 1H), 2.21-1.58 (m, 19H), 1.39-1.17 (m, 8H); ^{13}C-NMR (125 MHz, $CDCl_3$): δ 208.6, 166.0, 139.9, 131.4, 130.8, 130.2, 125.4, 125.0, 110.9, 105.5, 76.7, 75.3, 66.5, 66.2, 59.7, 40.0, 38.6, 37.2, 36.2, 34.2, 33.9, 32.6, 31.1, 29.5, 29.2, 27.0, 25.9, 18.1; FTIR (neat): 3373, 2927, 1777, 1734 cm^{-1}; HRMS (ESI) *m*/*z* Calc'd.for $C_{29}H_{40}O_7$ $[M+Na]^+$: 523.2666, found: 523.2669.

Preparation of Isotwistane **5.22**

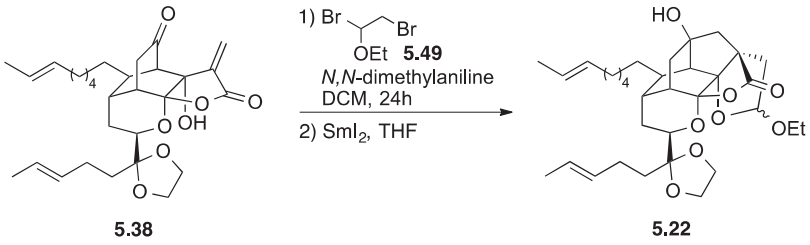

Bromoacetal Functionalization. To a round bottom flask equipped with a magnetic stir bar was added lactone **5.38** (2 x azeotrope with toluene) (0.69 g, 1.4 mmol) and DCM (14 mL). *N,N*-Dimethylaniline (freshly distilled, 150 torr, 155 °C) (0.88 mL, 6.9 mmol) and bromoacetal **5.49** (freshly distilled, ~ 0.2 mmHg, 52 °C) (1.6 g, 6.9 mmol) were then added. TLC was used to follow the reaction progress and the TLC plates were developed using a 50% EtOAc/Hexanes solution and visualized with $KMnO_4$. After 24.5 hours, the reaction was quenched with the addition of sat. aq. $NaHCO_3$ (8.4 mL) and diluted with DCM. The organic layer was washed with brine and dried over $MgSO_4$.

Concentration and purification via silica gel flash column chromatography (5% gradient, 0% → 40% EtOAc/Hex) afforded the ethyl acetal as a green sticky foam.

SmI_2 Formation. To a schlenk tube equipped with a magnetic stir bar and fitted with a water cooled condenser was added samarium powder (0.41 g, 2.7 mmol) and THF (44 mL). A separate solution of 1,2-diiodoethane[4] (1.7 g, 6.0 mmol) in THF (16 mL) was added and the reaction stirred at room temperature until it had turned dark blue in color (45 minutes). The reaction was then placed into a 55 °C bath and heated for 4 hours. The SmI_2 solution (0.10M in THF) was cooled to room temperature before use.

Cascade Cyclization. To a round bottom flask equipped with a magnetic stir bar was added SmI_2 (50 mL, 0.10M in THF, 5.0 mmol). A solution of the ethyl acetal in THF (10 mL) was then added. TLC was used to follow the reaction progress and the TLC plates were developed using a 50% EtOAc/Hexanes solution and visualized with *p*-anisaldehyde stain. The reaction was quenched after 15 minutes with the addition of sat. aq. NH_4Cl (8.0 mL), and 1.0M HCl (3.2 mL). The solution was then diluted with EtOAc and washed with brine before drying over $MgSO_4$. Concentration and purification via silica gel flash column chromatography (5% gradient, 0% → 60% EtOAc/Hex) afforded isotwistane **5.22** (0.48 g, 60% yield from lactone **5.38**, 1:1 dr) as a green sticky foam.

Diastereomer A. R_f = 0.19 (25% EtOAc/Hex); ^{1}H-NMR (500 MHz, $CDCl_3$): δ 5.45 (m, 5H), 4.19 (dd, *J* = 12.3, 2.8, 1H), 4.01-3.95 (m, 4H), 3.74 (dq, *J* = 9.7, 7.1 Hz, 1H), 3.48 (dq, *J* = 9.7, 7.1 Hz, 1H), 2.75 (dd, *J* = 14.2, 5.7 Hz, 1H), 2.37 (d, *J* = 2.7 Hz, 1H), 2.31-1.47 (m, 25H), 1.41-1.24 (m, 6H), 1.20 (t, *J* = 7.1 Hz, 3H); ^{13}C-NMR (125

[4]1,2-diiodoethane was taken up in ether, washed with a 1:1 mixture of sat. aq. $Na_2S_2O_3$, brine, dried over Na_2SO_4, concentrated, and dried under vacuum. Care was taken to exclude light.

MHz, $CDCl_3$): δ 177.7, 131.5, 131.2, 124.9, 124.8, 110.6, 109.5, 107.4, 95.7, 77.9, 74.5, 66.3, 65.5, 64.0, 56.9, 52.0, 51.7, 44.1, 39.3, 37.6, 37.5, 35.8, 33.9, 33.8, 32.7, 31.08, 29.7, 29.4, 28.1, 26.1, 18.1, 18.06, 15.3; FTIR (neat): 3476, 2925, 1780 cm^{-1}; HRMS (ESI) *m*/*z* Calc'd. for $C_{33}H_{48}O_8$ $[M+Na]^+$: 595.3241, found: 595.3240.

Diastereomer B. R_f = 0.46 (50% EtOAc/Hex); ^{1}H-NMR (500 MHz, $CDCl_3$): δ 5.46-5.37 (m, 4H), 5.30 (d, *J* = 4.1 Hz, 1H), 4.19-4.09 (m, 2H), 4.08-4.02 (m, 2H), 3.95-3.91 (m, 1H), 3.87-3.85 (m, 1H), 3.35 (dq, *J* = 9.0, 6.9 Hz, 1H), 2.65 (d, *J* = 12.8 Hz, 1H), 2.17 (d, *J* = 13.0 Hz, 1H), 2.13-1.45 (m, 25H), 1.39-1.23 (m, 6H), 1.13 (t, *J* = 7.0 Hz, 3H); ^{13}C-NMR (125 MHz, $CDCl_3$): δ 177.2, 131.6, 131.0, 125.1, 124.9, 110.7, 108.1, 107.5, 95.3, 79.2, 75.7, 66.5, 66.2, 62.6, 56.6, 52.7, 51.0, 44.0, 39.4, 38.5, 37.6, 36.0, 34.6, 33.8, 32.7, 32.5, 29.6, 29.4, 28.1, 25.9, 18.1, 18.0, 15.0; FTIR (neat): 3460, 2923, 1763 cm^{-1}; HRMS (ESI) *m*/*z* Calc'd. for $C_{33}H_{48}O_8$ $[M+Na]^+$: 595.3241, found: 595.3240.

Preparation of Acetate **5.25**

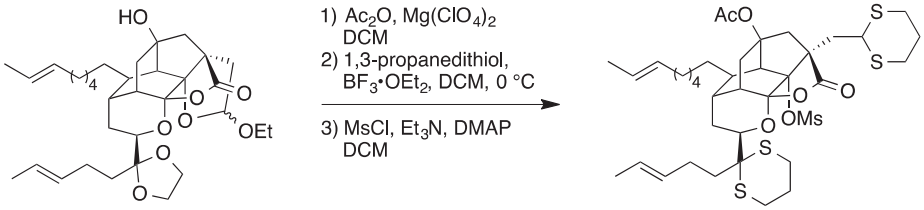

5.22 **5.25**

Acetate Protection. To a round bottom flask equipped with a magnetic stir bar was added alcohol **5.25** (0.10 g, 0.18 mmol) (2 x azeotrope with toluene), $Mg(ClO_4)_2$ (0.041 g, 0.018 mmol), DCM (0.95 mL), and acetic anhydride (0.051 mL, 0.53 mmol). The reaction was stirred at room temperature for 25 hours. TLC was used to follow the reaction progress and the TLC plates were developed using a 25% EtOAc/Hexanes

solution and visualized with CAM. Concentration and purification via silica gel flash column chromatography (10% gradient, 0% → 50% EtOAc/Hex) afforded the acetate (0.11 g) as a colorless oil.

Thioacetal Formation. To a round bottom flask equipped with a magnetic stir bar was added the ethyl acetal (0.11 g, 0.18 mmol) and DCM (1.8 mL). The solution was cooled in and ice/salt water bath and 1,3-propanedithiol (0.097 mL, 0.90 mmol) was added. After 5 minutes, $BF_3 \bullet OEt_2$ (0.11 mL, 0.90 mmol) was added dropwise. TLC was used to follow the reaction progress and the TLC plates were developed using a 25% EtOAc/Hexanes solution and visualized with CAM. After 40 minutes at 0 °C, acetone (0.90 mL) was added and the reaction was allowed to stir an additional 10 minutes before it was quenched with the addition of sat. aq. $NaHCO_3$ (0.90 mL). The organic was washed with sat. aq. NH_4Cl, H_2O, and brine before drying over $MgSO_4$. Concentration and purification via silica gel flash column chromatography (5% gradient, 0% → 30% EtOAc/Hex) afforded the thioacetal (0.087 g).

Mesylate Functionalization. To a round bottom flask equipped with a magnetic stir bar was added the thioacetal (0.087 g, 0.12 mmol), 4-(dimethylamino)pyridine (DMAP) (0.044 g, 0.36 mmol), Et_3N (0.050 mL, 0.36 mmol), and DCM (1.2 mL). The solution was cooled in an ice/salt water bath and methanesulfonyl chloride (0.029 mL, 0.36 mmol) was added dropwise. The reaction was then allowed to slowly warm to room temperature with the bath. TLC was used to follow the reaction progress and the TLC plates were developed using a 25% EtOAc/Hexanes solution and visualized with CAM. After 5.5 hours, the reaction was again cooled to 0 °C and quenched with 1M HCl (0.60

mL). After warming to room temperature, the solution was diluted to DCM and the organic layer was washed with brine before drying over $MgSO_4$. Concentration and purification via silica gel flash column chromatography (5% gradient, 0% → 35% EtOAc/Hex) afforded acetate **5.25** (0.086 g, 60% yield from **5.22**) as a white solid.

R_f = 0.35 (25% EtOAc/Hex); m.p. 78-80 °C; ^{1}H-NMR (500 MHz, $CDCl_3$): δ 5.49-5.31 (m, 4H), 4.81 (dd, *J* = 12.0, 3.2 Hz, 1H), 4.82-4.74 (m, 1H), 3.49-3.44 (m, 1H), 3.63 (s, 3H), 3.30 (d, *J* = 2.4 Hz, 1H), 3.04-2.89 (m, 3H), 2.83-2.78 (m, 2H), 2.63-2.54 (m, 2H), 2.53-2.28 (m, 7H), 2.14-1.92 (m, 9H), 1.89-1.73 (m, 6H), 1.66-1.44 (m, 10H), 1.43-1.28 (m, 6H); ^{13}C-NMR (125 MHz, $CDCl_3$): δ 175.0, 169.5, 131.6, 130.3, 125.9, 124.8, 106.1, 96.0, 84.1, 79.8, 53.4, 52.6, 47.9, 47.8, 42.7, 40.8, 39.7, 38.6, 38.4, 37.0, 35.97, 35.96, 32.6, 32.7, 32.3, 31.2, 30.7, 29.6, 29.2, 28.3, 27.9, 27.3, 27.0, 25.5, 25.0, 21.7, 18.07, 18.05; FTIR (neat): 2923, 1777, 1783 cm^{-1}; HRMS (ESI) *m*/*z* Calc'd. for $C_{38}H_{56}O_8S_5$ $[M+Na]^+$: 823.2471, found: 823.2465.

Preparation of Diol **5.50**

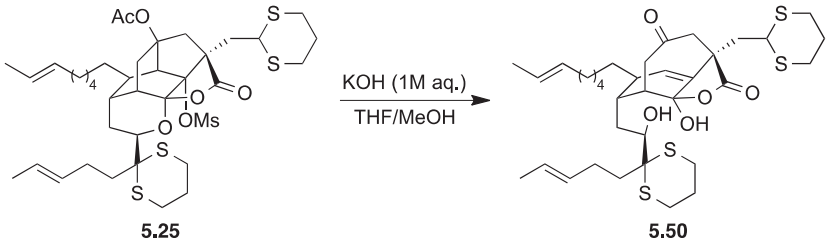

5.25 **5.50**

To a round bottom flask equipped with a magnetic stir bar was added acetate **5.25** (0.32 g, 0.40 mmol), THF (2.0 mL), and MeOH (2.0 mL). To the stirred solution was added an aqueous solution of KOH (2.0 mL, 1.0M, 2.0 mmol) over 30 seconds and the flask was sealed with a glass stopper. After 10 minutes, the reaction was placed into a 40 °C oil bath. TLC was used to follow the reaction progress and the TLC plates were

developed using a 50% EtOAc/Hexanes solution and visualized with CAM. After 5 hours, the reaction was removed from the hot bath and was allowed to cool to room temperature. The reaction was then quenched with the addition of 1M HCl (2.2 mL) until the solution reached a pH ~ 2 and then was diluted with EtOAc. The organic layer was washed with 1M HCl, H_2O, and brine before being dried over Na_2SO_4. Concentration and purification via silica gel flash column chromatography (10% gradient, 0% → 60% EtOAc/Hex) afforded diol **5.50** (0.22 g, 81% yield) as a white foam.

R_f = 0.52 (50% EtOAc/Hex); m.p. 62-64 °C; ^{1}H-NMR (500 MHz, $CDCl_3$): δ 5.66 (d, *J* = 3.5 Hz, 1H), 5.50-5.32 (m, 4H), 5.08 (s, 1H), 4.20-4.07 (m, 2H), 3.18 (s, 1H), 2.96-2.52 (m, 15H), 2.41-2.36 (m, 1H), 2.31-2.14 (m, 5H), 2.10-1.78 (m, 7H), 1.74-1.55 (m, 8H), 1.48-1.42 (m, 1H), 1.38-1.10 (m, 6H); ^{13}C-NMR (125 MHz, $CDCl_3$): δ 205.9, 177.5, 142.3, 132.4, 131.5, 130.4, 125.8, 124.9, 107.5, 68.8, 58.8, 58.7, 48.34, 48.27, 47.2, 42.8, 40.8, 38.9, 38.4, 34.5, 33.7, 32.9, 32.6, 29.6, 29.4, 28.6, 28.3, 27.9, 26.2, 25.4, 25.1, 24.3, 18.07, 18.06; FTIR (neat): 3478, 2923, 1769, 1693 cm^{-1}; HRMS (ESI) *m*/*z* Calc'd. for $C_{35}H_{52}O_5S_4$ $[M+H]^+$: 703.2590, found: 703.2585.

Preparation of Ketone **5.24**

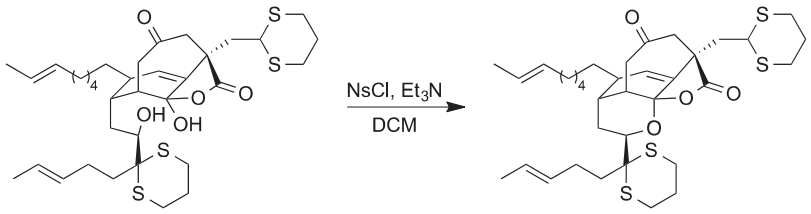

5.50 **5.24**

To a vial equipped with a magnetic stir bar was added diol **5.50** (0.024 g, 0.035 mmol), 4-nitrobenzenesulfonyl chloride (NsCl) (0.016 g, 0.070 mmol), Et_3N (0.015 mL, 0.11 mmol), and DCM (0.40 mL). The vial was capped and the reaction was stirred at

room temperature. TLC was used to follow the reaction progress and the TLC plates were developed using a 50% EtOAc/Hexanes solution and visualized with CAM. After 6 hours, the reaction was quenched with the addition of 1M HCl (0.13 mL) and diluted with DCM. The organic layer was washed with 1M HCl, H_2O, and brine before being dried over $MgSO_4$. Concentration and purification via silica gel flash column chromatography (5% gradient, 0% → 30% EtOAc/Hex) afforded ketone **5.24** (0.016 g, 67% yield) as a white foam.

R_f = 0.43 (25% EtOAc/Hex); m.p. 67-68 °C; ^{1}H-NMR (500 MHz, $CDCl_3$): δ 5.81 (d, *J* = 1.9 Hz, 1H), 5.47-5.29 (m, 4H), 4.20-4.10 (m, 2H), 3.48-3.37 (m, 2H), 2.87-2.81 (m, 2H), 2.76-264 (m, 5H), 2.55 (d, *J* = 14.5 Hz, 1H), 2.50-2.45 (m, 3H), 2.32-1.29 (m, 30H); ^{13}C-NMR (125 MHz, $CDCl_3$): δ 204.9, 175.9, 138.5, 132.2, 131.3, 130.3, 125.9, 125.1, 105.9, 83.8, 60.9, 52.8, 49.5, 45.3, 43.1, 42.7, 41.8, 38.5, 38.3, 37.0, 36.7, 35.5, 32.6, 29.6, 29.1, 29.0, 28.7, 28.4, 28.3, 28.0, 27.3, 25.6, 25.0, 18.08, 18.06; FTIR (neat): 2924, 1790, 1697 cm^{-1}; HRMS (ESI) *m/z* Calc'd. for $C_{35}H_{50}O_4S_4$ $[M+Na]^+$: 685.2484, found: 685.2480.

Preparation of β-Keto Ester **5.54**

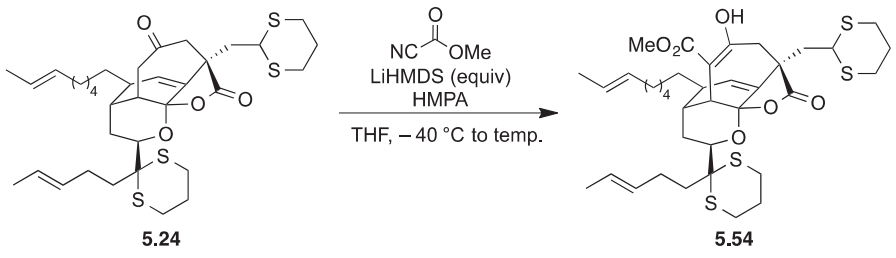

5.24 **5.54**

Thermodynamic Enolate Conditions. To a vial equipped with a magnetic stir bar was added ketone **5.24** (0.025 g, 0.038 mmol) and THF (0.35 mL). The solution was cooled in a dry ice/MeCN bath and lithium bis(trimethylsilyl)amide (LiHMDS) (0.034

mL, 1.0M in THF, 0.034 mmol) was added dropwise. After 30 minutes, the reaction was placed into an ice/salt water for 1.5 hours before being cooled again to – 40 °C. After 10 minutes, hexamethylphophramide (HMPA) (0.072 mL, 0.42 mmol) was added and the reaction was stirred at – 40 °C for additional 20 minutes. A solution of methyl cyanoformate (0.0030 mL, 0.038 mmol) in THF (0.050 mL) was then added dropwise. TLC was used to follow the reaction progress and the TLC plates were developed using a 25% EtOAc/Hexanes solution and visualized with $KMnO_4$. After 50 minutes, the reaction was quenched with the addition of sat. aq. NH_4Cl (0.20 mL) and was allowed to warm to room temperature. The solution was then diluted with EtOAc and the organic layer was washed with H_2O and brine. After drying over Na_2SO_4 and concentration, purification via silica gel flash column chromatography (10% gradient, 0% → 60% EtOAc/Hex) afforded enol **5.54** (0.0047 g, 17% yield) as a colorless residue.

Kinetic Enolate Conditions. To a vial equipped with a magnetic stir bar was added ketone **5.24** (3 x azeotrope with toluene) (0.0085 g, 0.013 mmol) and THF (0.13 mL). The solution was cooled in a dry ice/MeCN and LiHMDS (0.015 mL, 1.0M in THF, 0.015 mmol) was added dropwise. After 30 minutes at – 40 °C, the reaction was placed into an ice/salt water bath. After 1 hour, the reaction was cooled again to – 40 °C and HMPA (0.0022 mL, 0.013 mmol) was added, followed by a solution of methyl cyanoformate (0.0013 mL, 0.015 mmol) in THF (0.05 mL). TLC was used to follow the reaction progress and the TLC plates were developed using a 25% EtOAc/Hexanes solution and visualized with CAM. After stirring at – 40 °C for 1 hour, the cooling bath was removed and the reaction was stirred an additional hour before being quenched with the addition of sat. aq. NH_4Cl (0.10 mL). The solution was diluted with EtOAc and the

organic layer washed with H_2O and brine, before being dried over Na_2SO_4. Concentration and purification via silica gel flash column chromatography (5% gradient, 0% → 25% EtOAc/Hex) afforded enol **5.54** (0.0051 g, 55% yield) as a colorless residue.[5]

Enol Tautomer. R_f = 0.53 (25% EtOAc/Hex); ^{1}H-NMR (500 MHz, $CDCl_3$): δ 13.83 (s, 1H), 5.75 (s, 1H), 5.48-5.31 (m, 4H), 4.20-4.13 (m, 2H), 3.82 (s, 3H), 3.53-3.39 (m, 2H), 3.25-3.18 (m, 1H), 2.90-1.59 (m, 32H), 1.32-1.25 (m, 6H); ^{13}C-NMR (150 MHz, $CDCl_3$): δ 175.8, 174.6, 171.7, 136.5, 131.3, 130.42, 130.36, 125.9, 125.1, 104.4, 100.1, 83.4, 55.1, 52.8, 52.7, 49.2, 44.7, 42.1, 38.6, 36.8, 36.6, 35.9, 35.4, 32.6, 32.1, 29.9, 29.5, 29.0, 28.7, 28.5, 28.1, 28.0, 27.3, 25.6, 25.1, 22.84, 18.1; FTIR (neat): 2923, 1786, 1639, 1573 cm^{-1}; HRMS (ESI) *m*/*z* Calc'd. for $C_{37}H_{52}O_6S_4$ $[M+Na]^+$: 743.2539, found: 743.2534.

Keto Tautomer. R_f = 0.32 (25% EtOAc/Hex); ^{1}H-NMR (600 MHz, $CDCl_3$): δ 5.91 (s, 1H), 5.46-5.30 (m, 4H), 4.19-4.09 (m, 2H), 3.74 (s, 3H), 3.48-3.37 (m, 2H), 3.21 (d, *J* = 4.6 Hz, 1H), 3.09-3.08 (m, 1H), 2.92 (d, *J* = 13.2 Hz, 1H), 2.87-2.82 (m, 2H), 2.79-2.67 (m, 3H), 2.59 (d, *J* = 13.2 Hz, 1H), 2.49-2.42 (m, 2H), 2.34-1.50 (m, 23H), 1.38-1.27 (m, 6H); ^{13}C-NMR (150 MHz, $CDCl_3$): δ 200.8, 174.7, 169.2, 138.8, 131.9, 131.3, 130.2, 126.0, 125.2, 104.5, 84.1, 61.5, 61.4, 53.1, 52.5, 50.0, 45.8, 42.4, 41.9, 38.8, 38.6, 37.6, 35.7, 35.2, 32.6, 29.8, 29.5, 29.0, 28.8, 28.6, 28.3, 28.1, 27.3, 25.6, 24.9, 18.11, 18.09; FTIR (neat): 2919, 1792, 1747, 1706 cm^{-1}; HRMS (ESI) *m*/*z* Calc'd. for $C_{37}H_{52}O_6S_4$ $[M+Na]^+$: 743.2539, found: 743.2534.

[5]Note: If the reaction is quenched at this point the major product is the keto-tautomer. Which does not interconvert to the enol-tautomer, nor does the enol convert to the keto-tautomer.

[1] (a) Njardarson, J. T.; Wood, J. L. *Org. Lett.* **2001**, *3*, 2431. (b) Njardarson, J. T; McDonald, I. M.; Spiegel, D. A.; Inoue, M.; Wood, J. L. *Org. Lett*. **2001**, *3*, 2435. (c) Drutu, I.; Njardarson, J. T.; Wood, J. L. *Org. Lett.* **2002**, *4*, 493.

[2] Murphy, G. K.; Hama, N.; Bedermann, A.; Dong, P.; Schneider, C. M.; McMahon, T. C.; Tao, R. N.; Twenter, B. M.; Spiegel, D. A.; Wood, J. L. *Org. Lett.* **2012**, *14*, 4544.

[3] Lespieau, J. C. *R. Hebd, Seaces Acad. Sci.* **1929**, *30*, 287.

[4] Vo-Quang, Y. C. *R. Hebd. Seaces Acad. Sci*. **1964**, *258*, 4586.

[5] Dobson, N. A.; Raphael, R. A. *J. Chem. Soc.* **1955**, 3558.

[6] (a) Waizumi, N.; Itoh, T.; Fukuyama, T. *Tetrahedron Lett.* **1998**, *39*, 6015. (b) Waizumi, N.; Itoh, T.; Fukuyama, T. *J. Am. Chem. Soc.* **2000**, *122*, 7825. (c) Hayashi, Y.; Itoh, T.; Fukuyama, T. *Org. Lett.* **2003**, *5*, 2235.

[7] (a) Cabrera, A.; Alper, H. *Tetrahedron Lett.* **1992**, *33*, 5007. (b) Corey, E. J.; Boaz, N. W. *Tetrahedron Lett.* **1985**, *26*, 6015. (c) Corey, E. J.; Boaz, N. W. *Tetrahedron Lett.* **1985**, *26*, 6019.

[8] Murphy, G. K.; Shirahata, T.; Hama, N.; Bedermann, A.; Dong, P.; McMahon, T. C.; Twenter, B. M.; Spiegel, D. A.; McDonald, I. M.; Taniguchi, N.; Inoue, M.; Wood, J. L. *J. Org. Chem.* **2013**, *78*, 477.

[9] Tsunoda, T.; Suzuki, M.; Noyori, R. *Tetrahedron Lett.* **1980**, *21*, 1357.

[10] Guibe, F. *Tetrahedron* **1998**, *54*, 2967.

[11] (a) Varala, R.; Sreelatha, N.; Srinivas, R. A. *Synlett* **2006**, 1549. (b) Yu, L. C.; Helquist, P. *Tetrahedron Lett.* **1978**, *37*, 3423. (c) Yu, L. C.; Helquist, P. *J. Org. Chem.* **1981**, *46*, 4536. (d) Yu, L. C.; Helquist, P. *Synthetic Commun.* **1981**, *11*, 591.

[12] Aihara, Y.; Yoshida, A.; Furuta, T.; Wakimoto, T.; Akizawa, T.; Konishi, M.; Kan, T. *Bioorg. Med. Chem. Lett.* **2009**, *19*, 4171.

[13] (a) DePuy, C. H.; King, R. W. *Chem. Rev.* **1960**, *60*, 431. (b) Garcia Martinez, A.; Teso Vilar, E.; Garcia Fraile, A.; de la Moya Cerero, S.; Lora Maroto, B. *Tetrahedron: Asymmetry* **2002**, *13*, 17.

[14] Neilson, T.; Werstiuk, E. S. *Can. J. Chem.* **1971**, *49*, 493.

[15] Di Stefano, S.; Leonelli, F.; Garofalo, B.; Mandolini, L.; Bettolo, R. M.; Migneco, L. M. *Org. Lett.* **2002**, *4*, 2783.

[16] (a) Yoshimoto, K.; Kawabata, H.; Nakamichi, N.; Hayashi, M. *Chem. Lett.* **2001**, 934. (b) Mori, K.; Tominaga, M.; Takigawa, T.; Matsui, M. *Synthesis* **1973**,790.

[17] (a) Stork, G.; Kahn, M. *J. Am. Chem. Soc.* **1985**, *107*, 500. (b) Stork, G.; Mook, R. *J. Am. Chem. Soc.* **1983**, *105*, 3720. (c) Stork, G.; Mook, R.; Biller, S. A.; Rychnovsky, S. D. *J. Am. Chem. Soc.* **1983**, *105*, 3741. (d) Stork, G.; Sher, P. M. *J. Am. Chem. Soc.* **1986**, *108*, 303.

[18] (a) Molander, G. A.; Harris, C. R. *Chem. Rev.* **1996**, *96*, 307. (b) Ananthanarayan, T. P.; Gallagher, T.; Magnus, P. *J. Chem. Soc. Chem. Commun.* **1982**, 709. (c) Fang, J. M.; Chen, M. Y.; Shiue, J. S.; Lu, L.; Hsu, J. L. *Tetrahedron Lett.* **2000**, *41*, 4633. (d) Cabrera, A.; Alper, H. *Tet. Lett.* **1992**, *33*, 5007. (e) Fukuzawa, S.; Tsuchimoto, T. *Synlett* **1993**, 803. (f) Inanaga, J.; Handa, Y.; Tabuchi, T.; Otsubo, K.; Yamaguchi, M.; Hanamoto, T. A. *Tetrahedron Lett.* **1991**, *32*, 6557. (g) Inanaga, J.; Sakai, S.; Handa, Y.; Yamaguchi, M.; Yokoyama, Y. *Chem. Lett.* **1991**, 2117. (h) Shinohara, I.; Okue, M.; Yamada, Y.; Nagaoka, H. *Tetrahedron Lett.* **2003**, *44*, 4649.

[19] (a) Mander, L. N.; Sethi, S. P. *Tetrahedron Lett.* **1983**, *24*, 5425. (b) Hale, K. J.; Grabski, M.; Flasz, J. T. *Org. Lett.* **2013**, *15*, 370.

[20] (a) Screttas, C. G.; Michascrettas, M. *J. Organomet. Chem*. **1985**, *292*, 325. (b) Maji, M. S.; Pfeifer, T.; Studer, A. *Chem. Eur. J.* **2010**, *16*, 5872.

APPENDICES

APPENDIX A

Spectra Relevant to Chapter Two

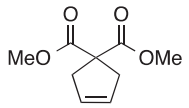

2.32

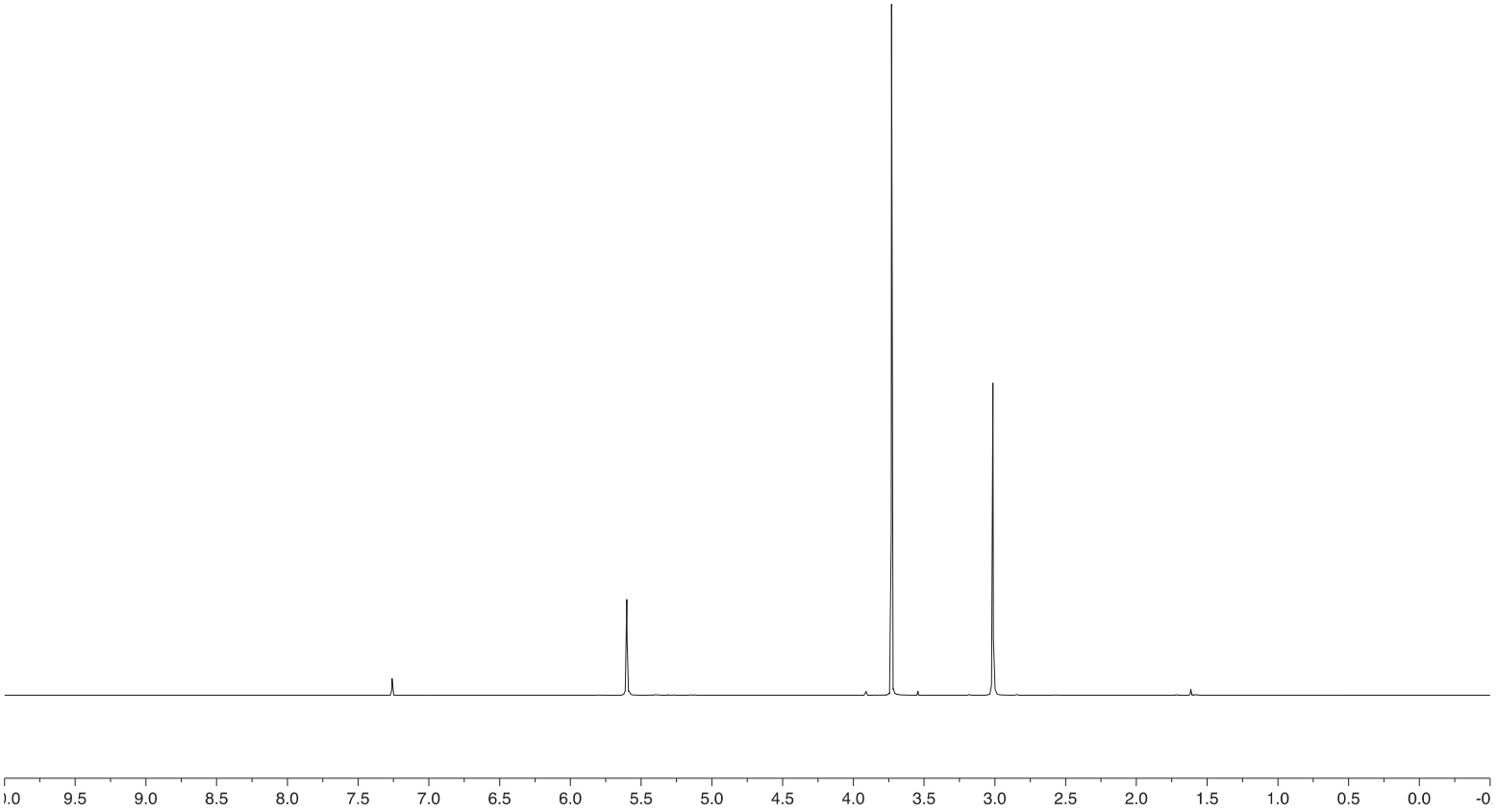

Figure A.10 ^{1}H-NMR (400 MHz; $CDCl_3$) for compound **2.32**

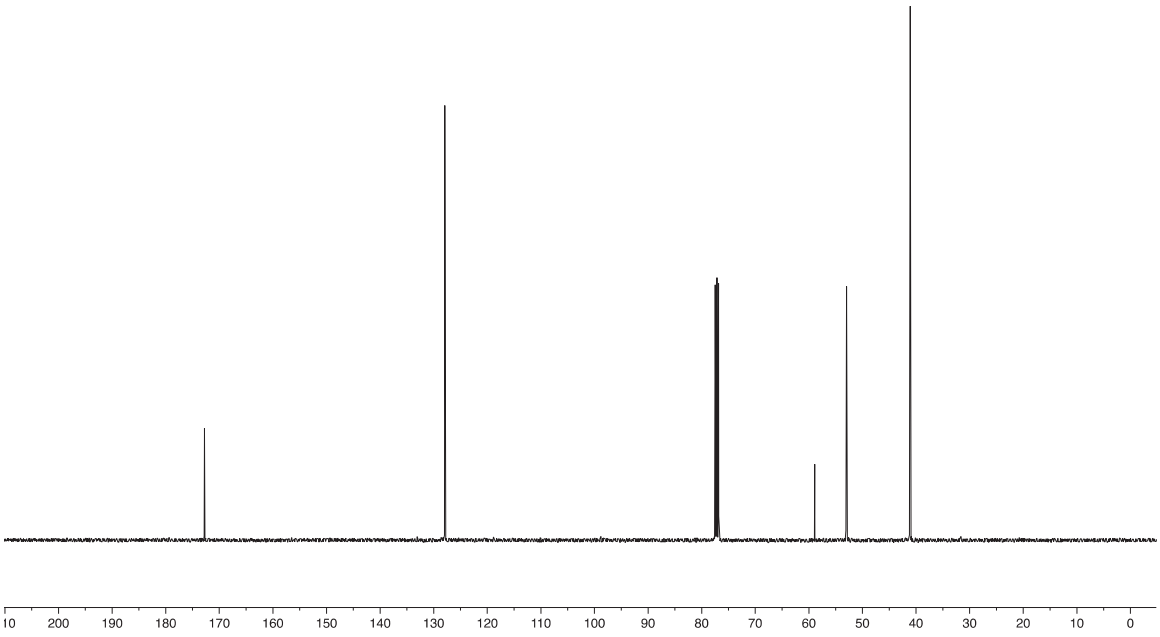

Figure A.11 ^{13}C-NMR spectrum (100 MHz; $CDCl_3$) of compound **2.32**

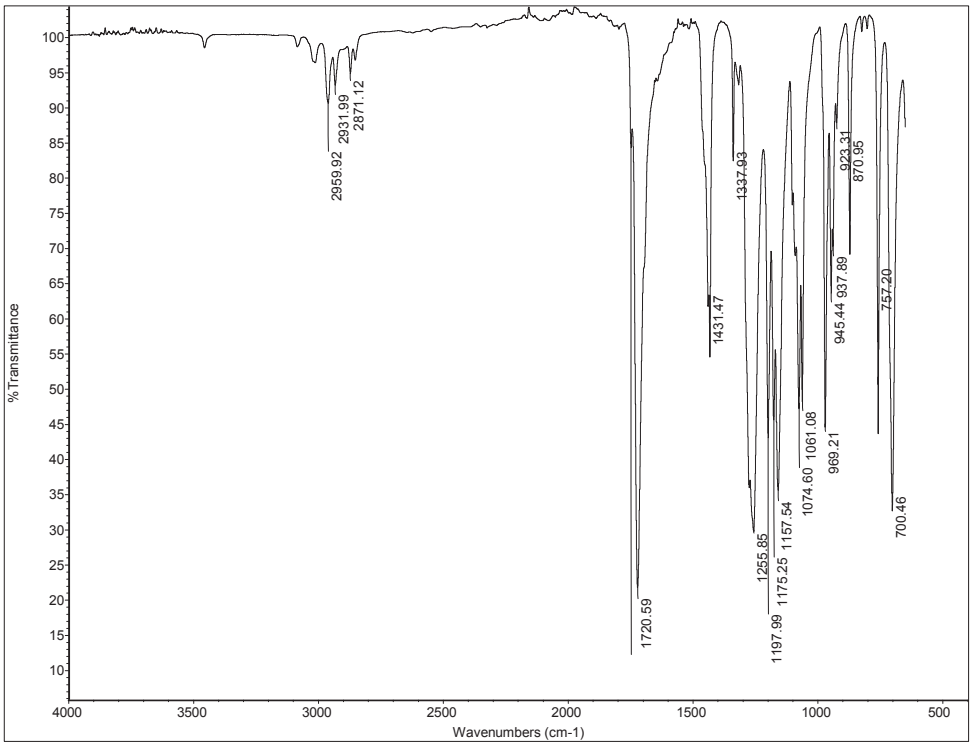

Figure A.12 FTIR spectrum (neat) of compound **2.32**

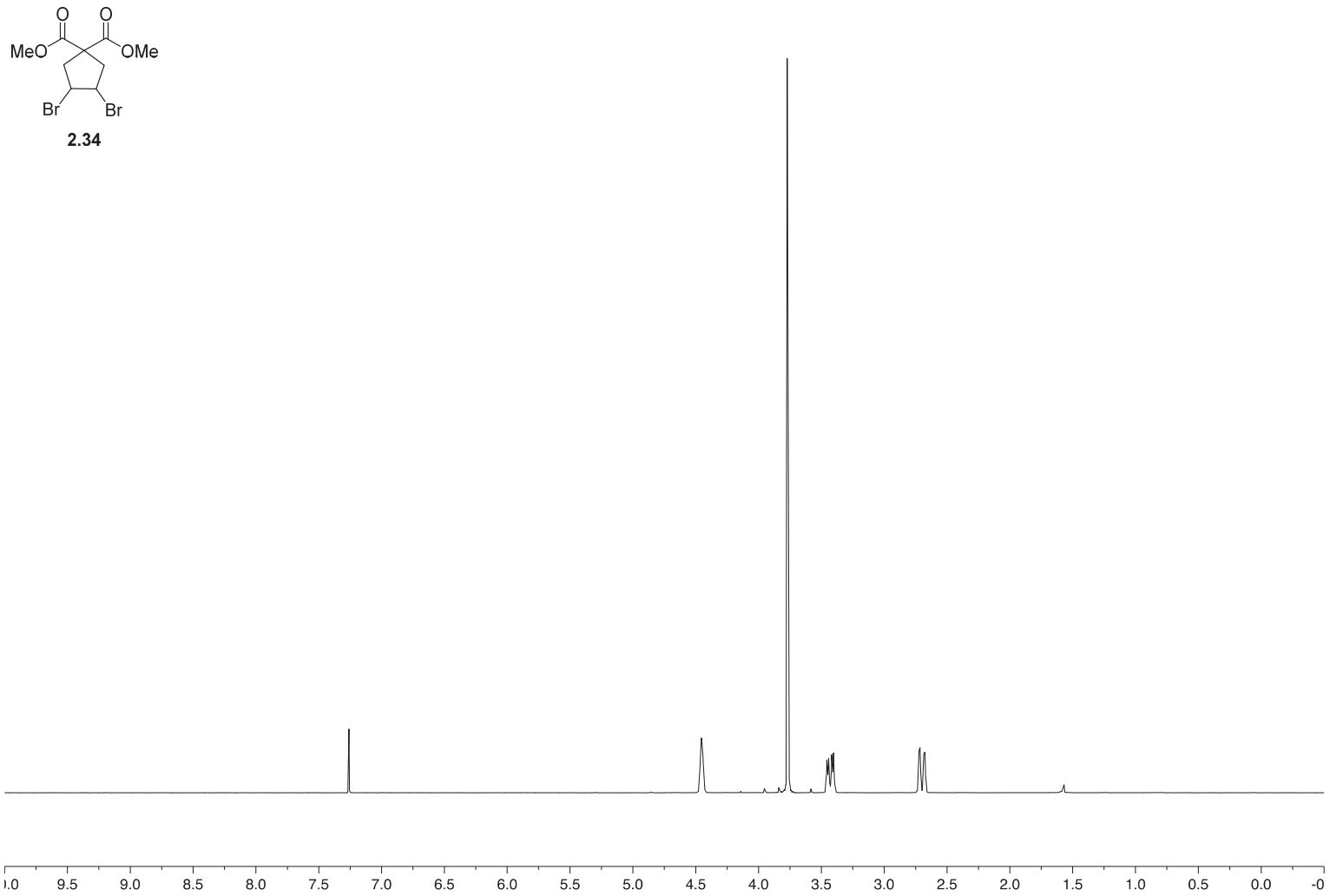

Figure A.13 ^{1}H-NMR (400 MHz; $CDCl_3$) for compound **2.34**

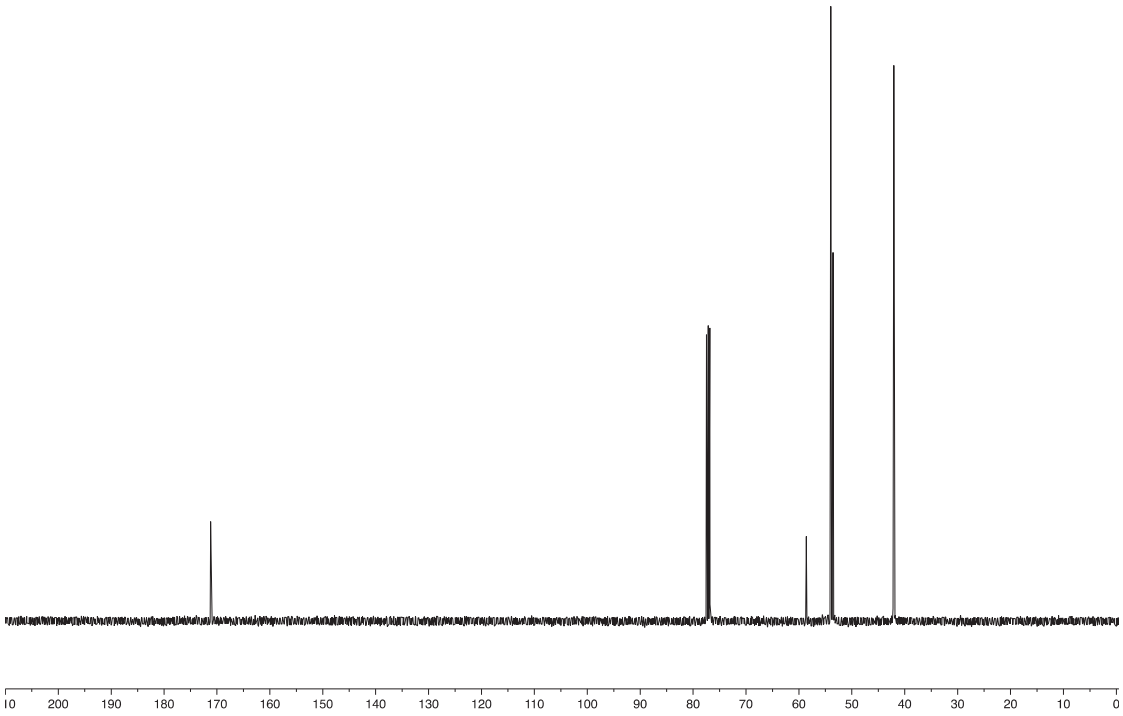

Figure A.14 ^{13}C-NMR spectrum (100 MHz; $CDCl_3$) of compound **2.34**

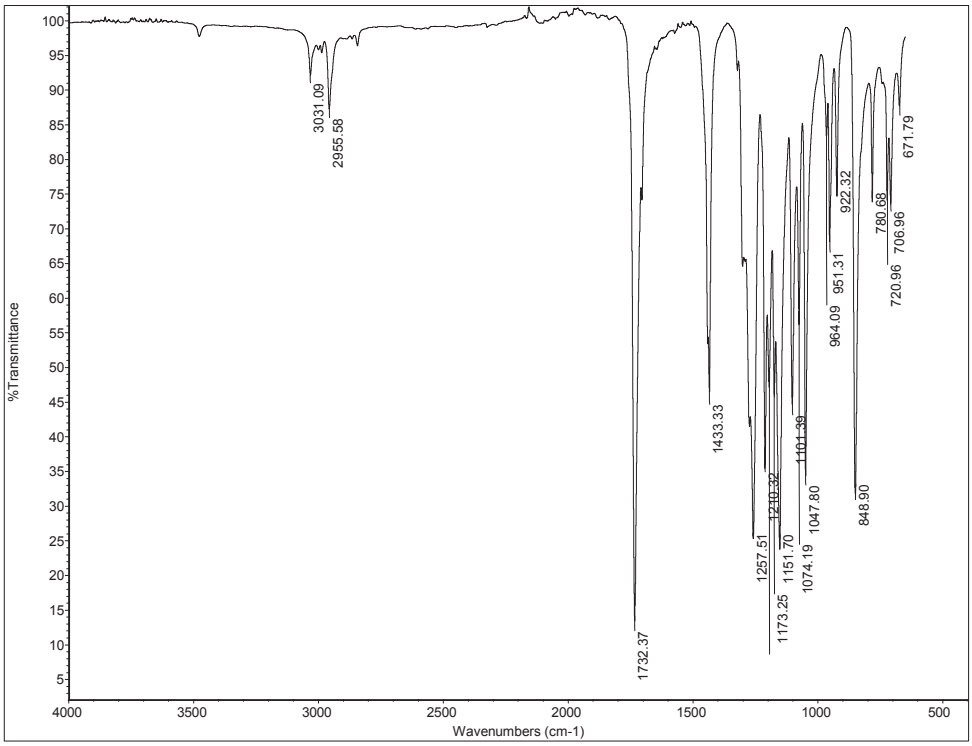

Figure A.15 FTIR spectrum (neat) of compound **2.34**

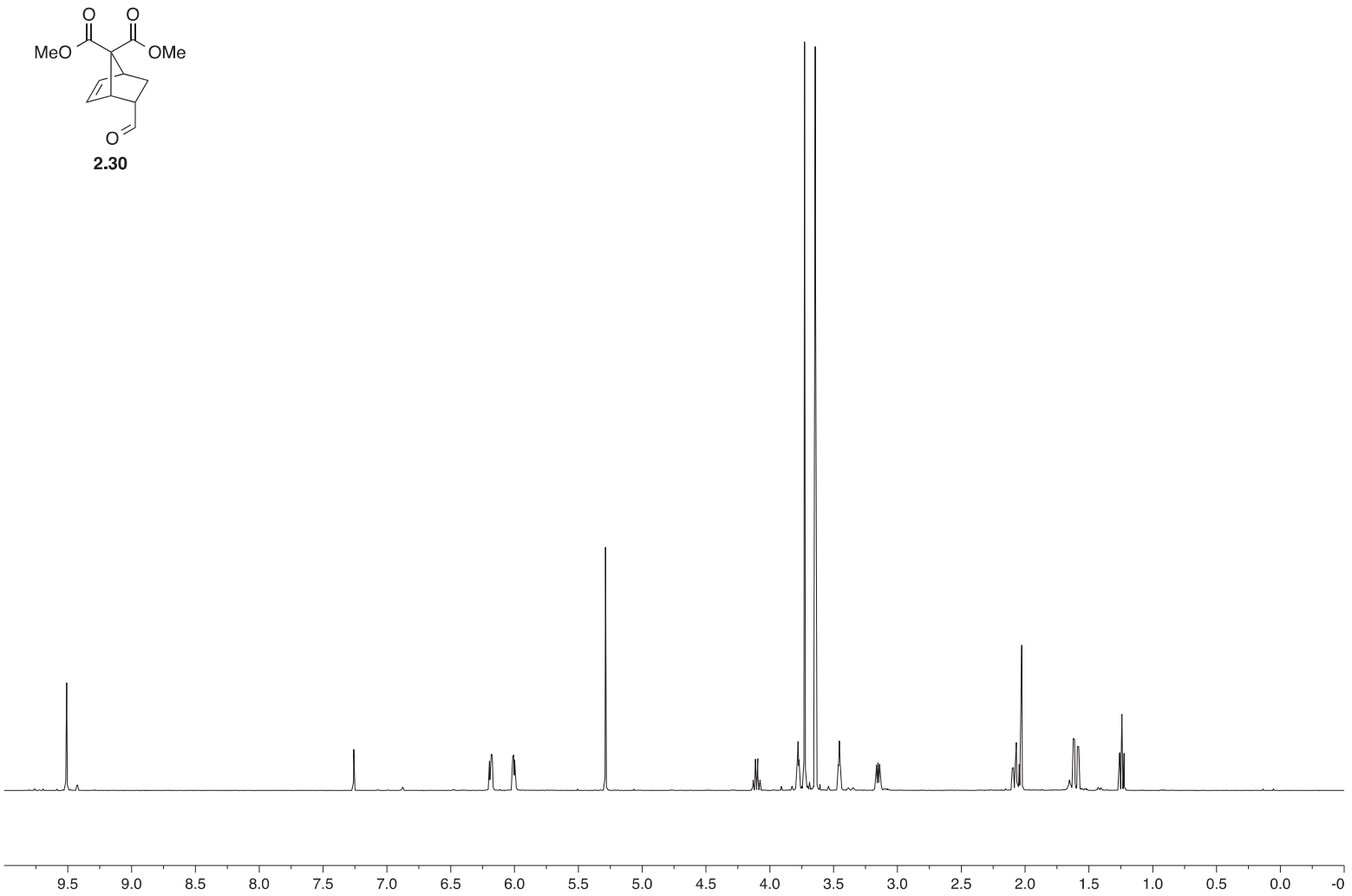

Figure A.16 ^{1}H-NMR (400 MHz; $CDCl_3$) for compound **2.30**

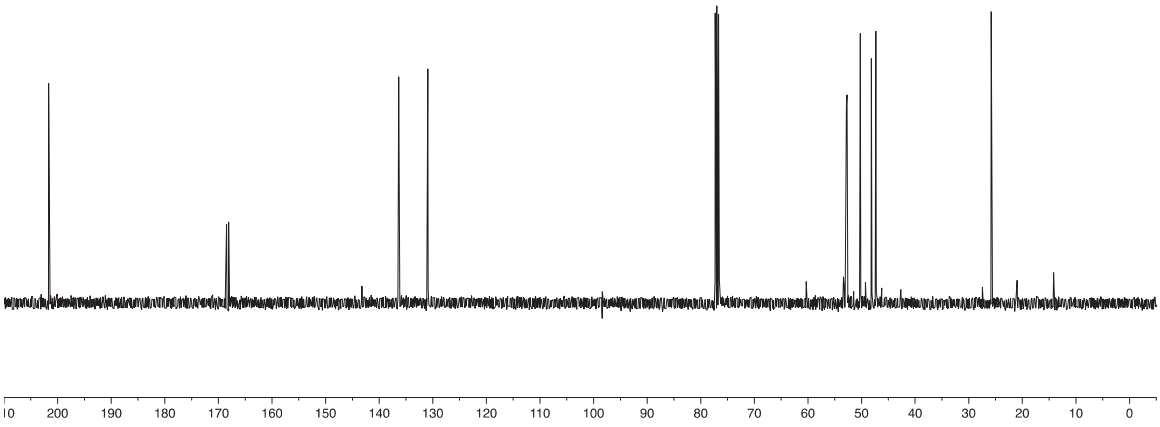

Figure A.17 ^{13}C-NMR spectrum (100 MHz; $CDCl_3$) of compound **2.30**

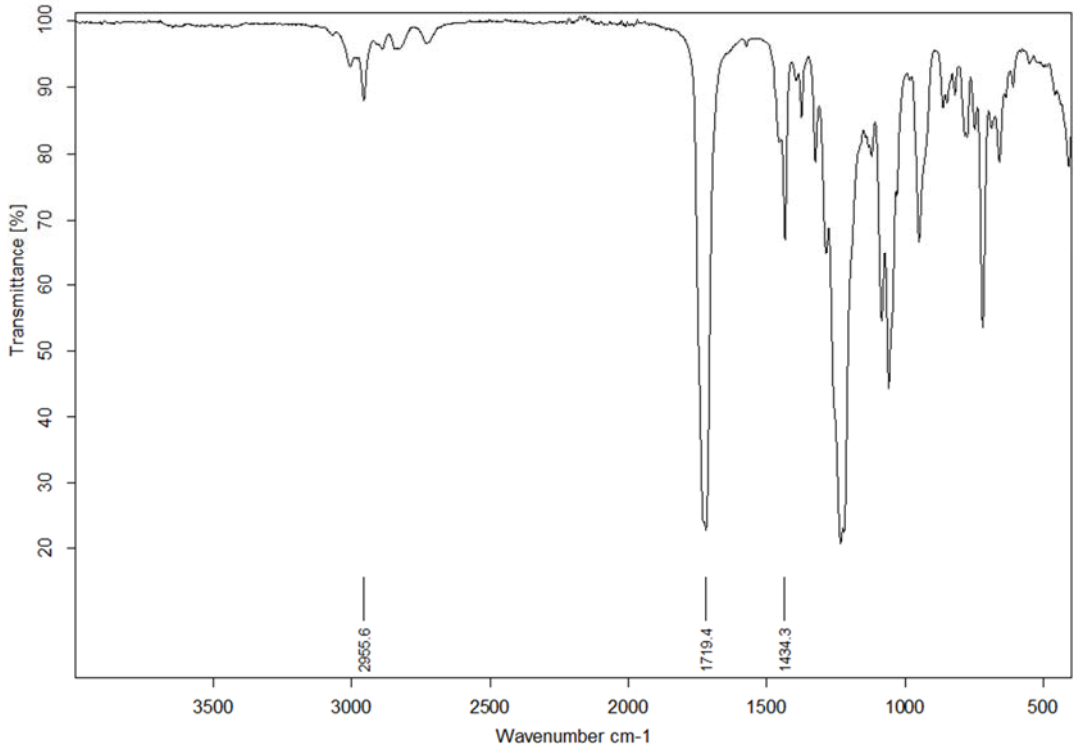

Figure A.18 FTIR spectrum (neat) of compound **2.30**

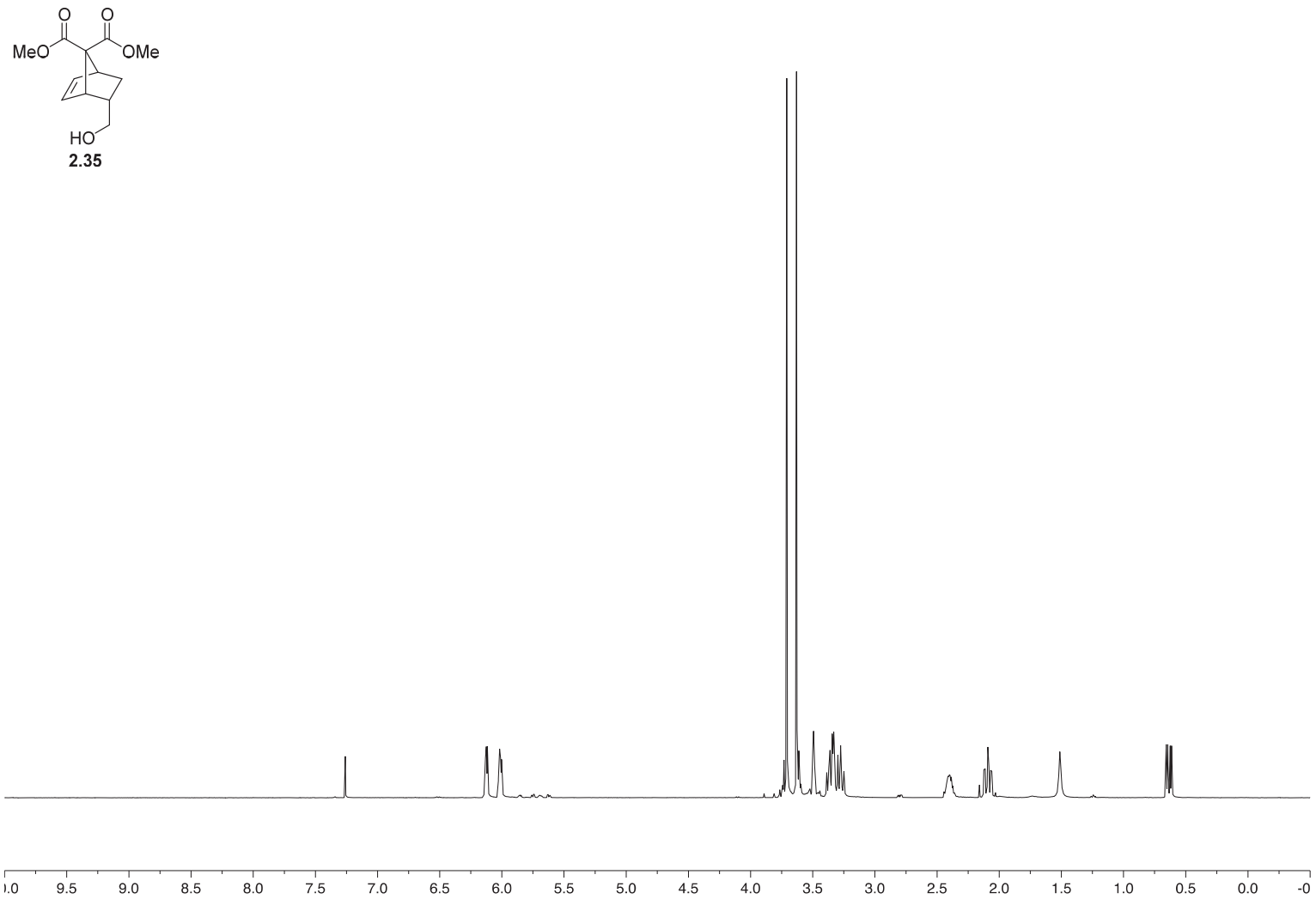

Figure A.19 ^{1}H-NMR (400 MHz; $CDCl_3$) for compound **2.35**

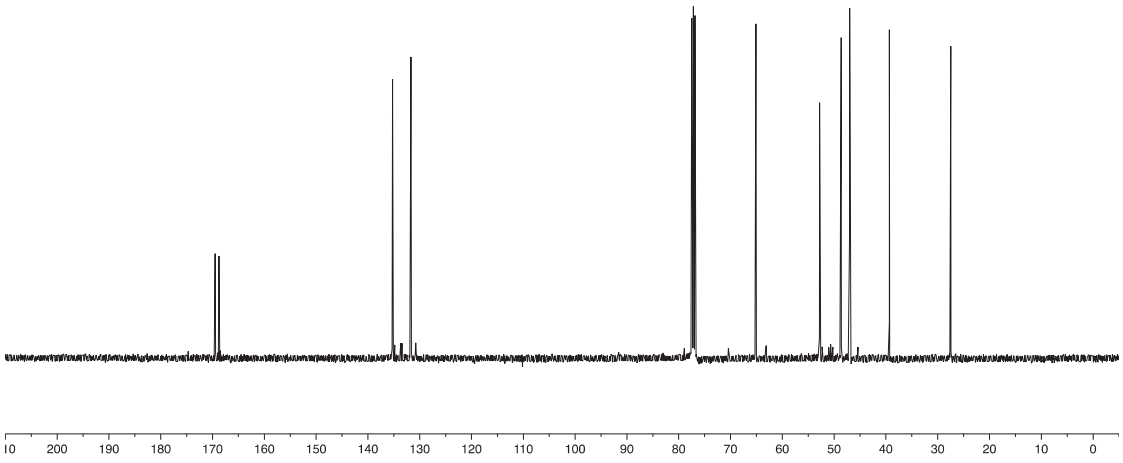

Figure A.20 ^{13}C-NMR spectrum (100 MHz; $CDCl_3$) of compound **2.35**

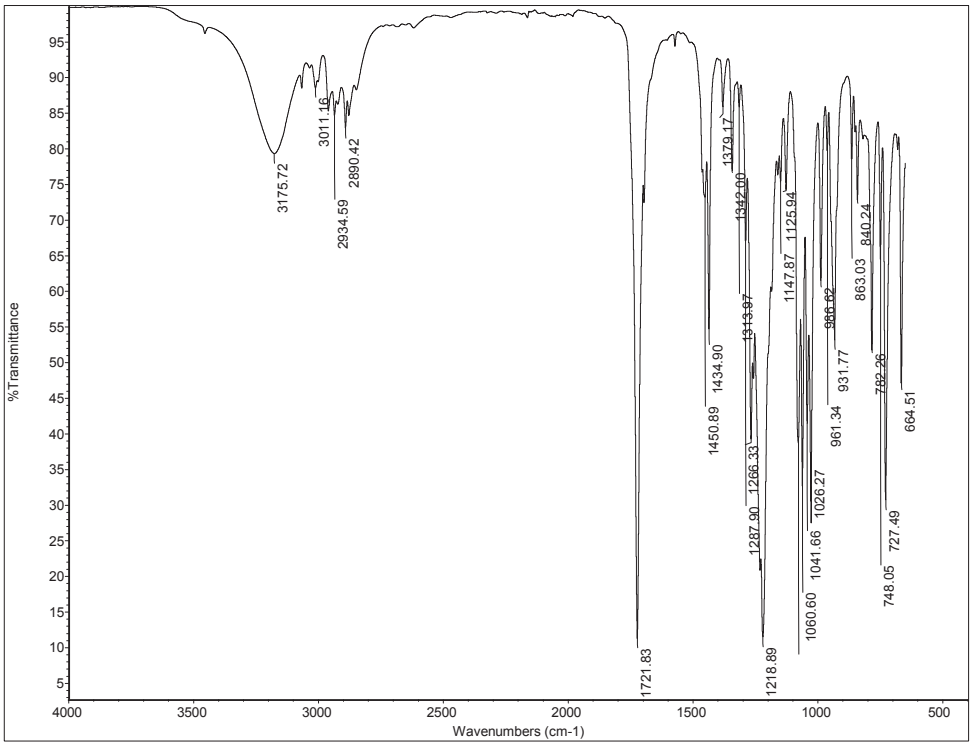

Figure A.21 FTIR spectrum (neat) of compound **2.35**

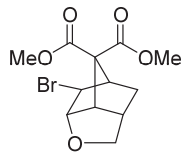

2.36

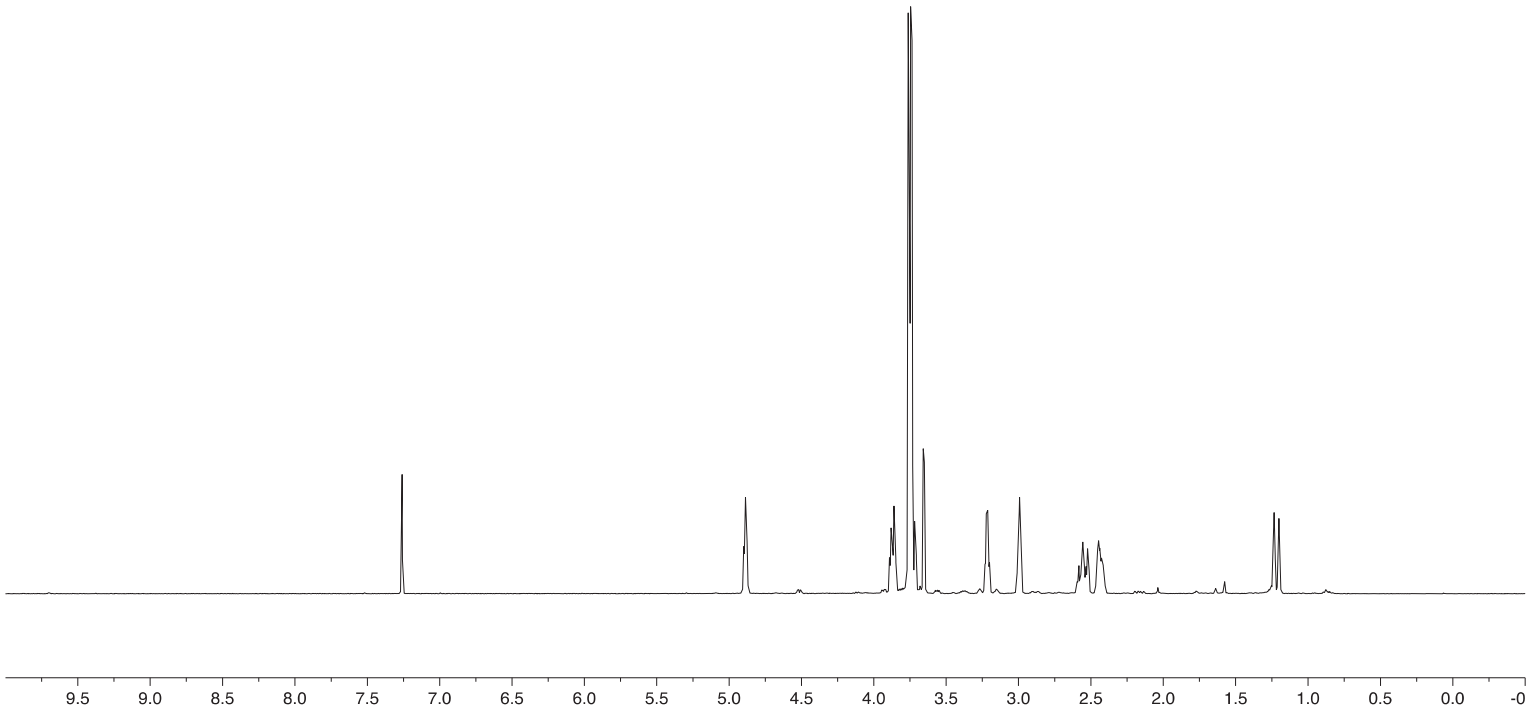

Figure A.22 ^{1}H-NMR (400 MHz; $CDCl_3$) for compound **2.36**

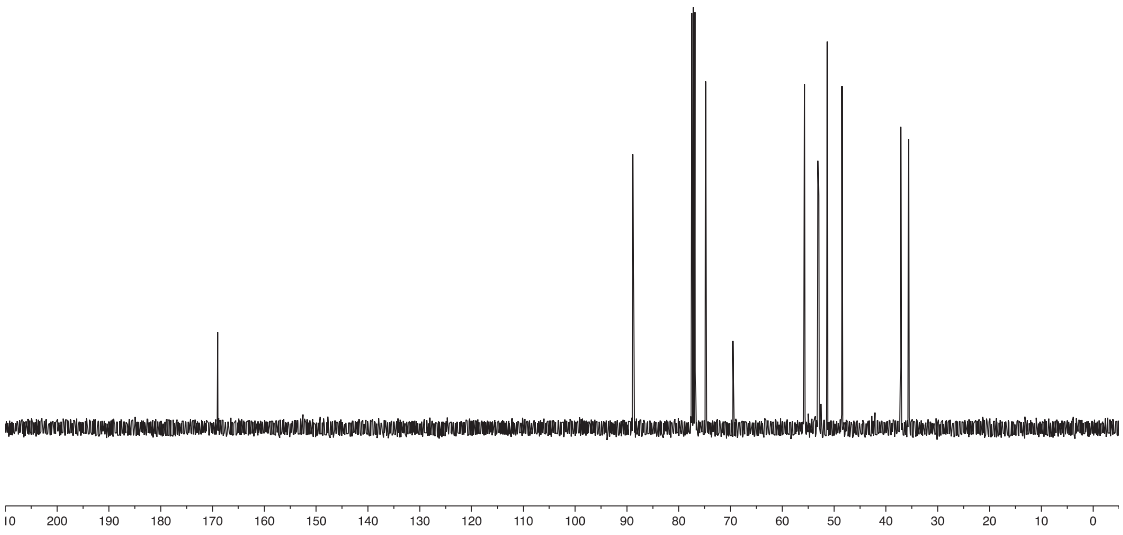

Figure A.23 ^{13}C-NMR spectrum (100 MHz; $CDCl_3$) of compound **2.36**

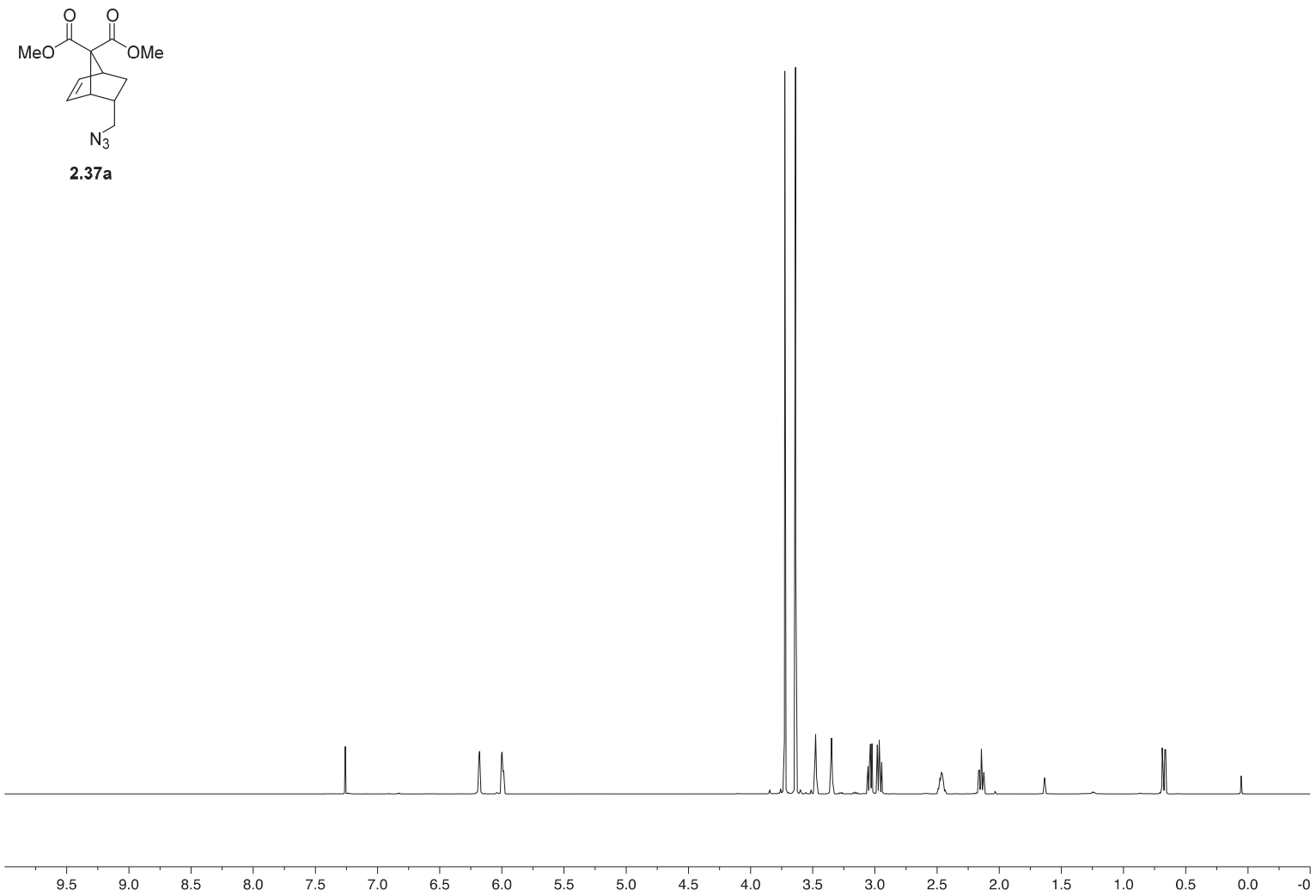

Figure A.24 ^{1}H-NMR (600 MHz; $CDCl_3$) for compound **2.37a**

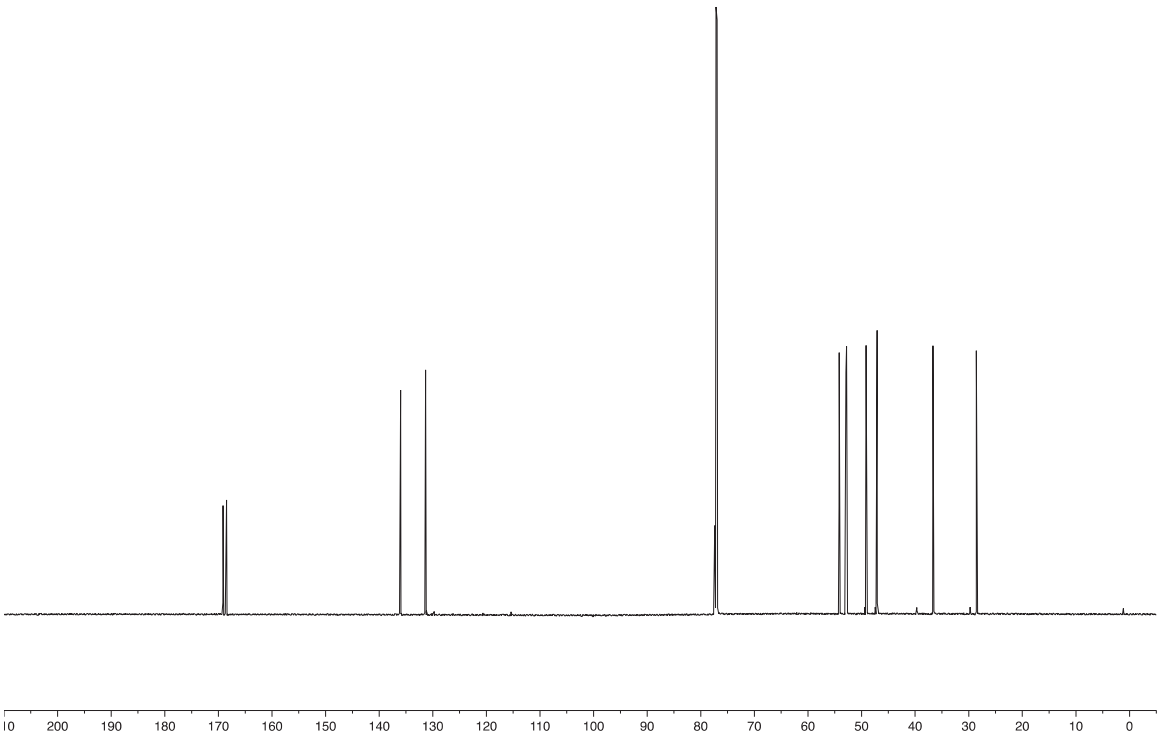

Figure A.25 ^{13}C-NMR spectrum (150 MHz; $CDCl_3$) of compound **2.37a**

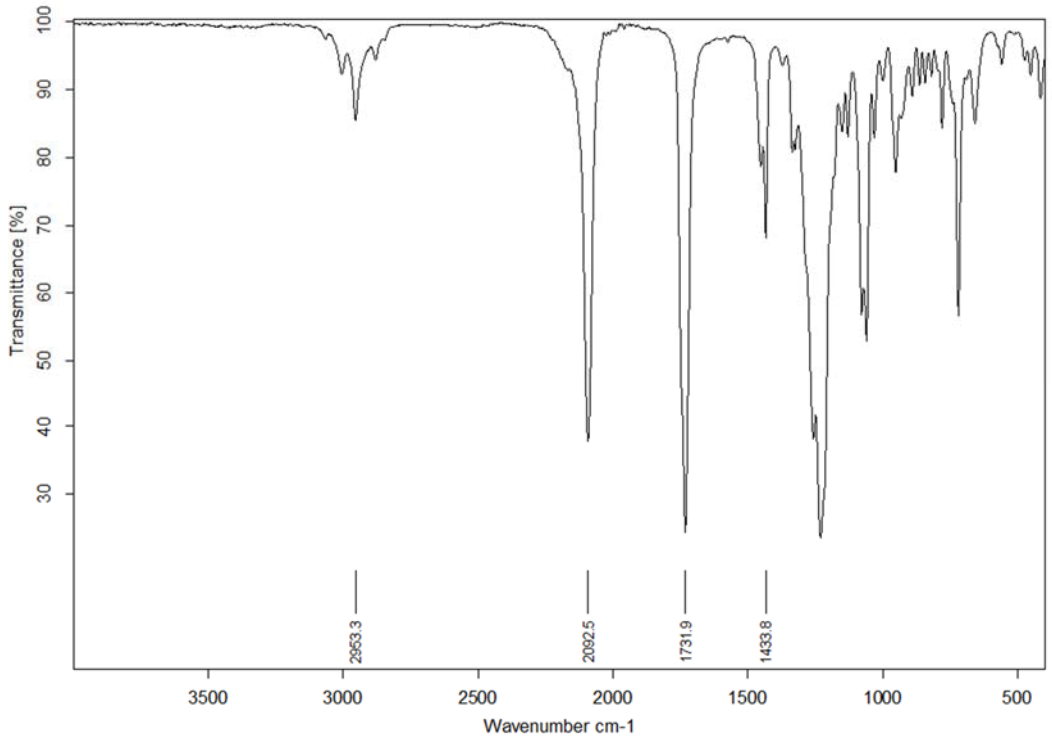

Figure A.26 FTIR spectrum (neat) of compound **2.37a**

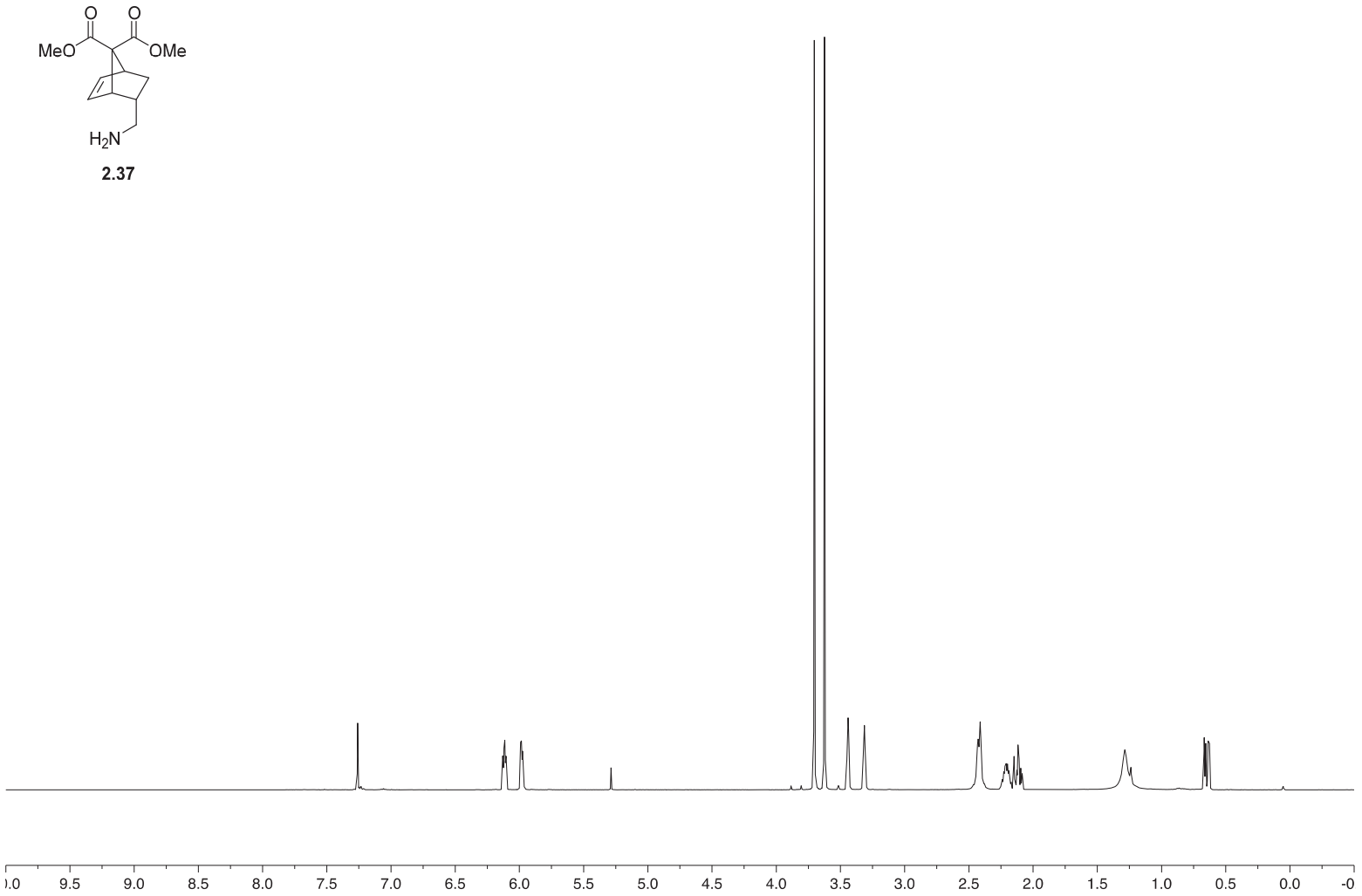

Figure A.27 ^{1}H-NMR (400 MHz; $CDCl_3$) for compound **2.37**

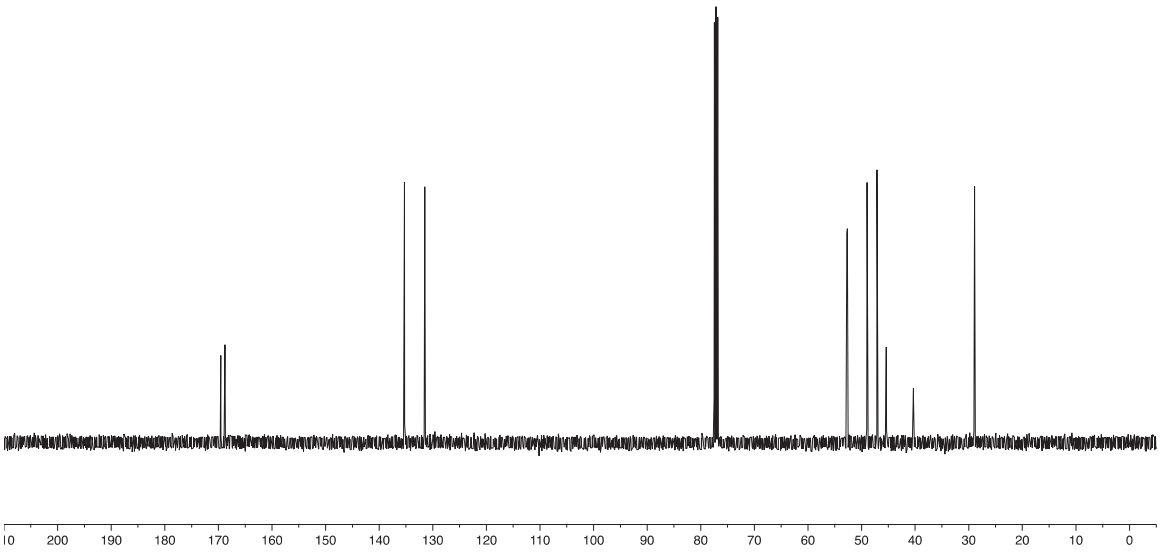

Figure A.28 ^{13}C-NMR spectrum (100 MHz; $CDCl_3$) of compound **2.37**

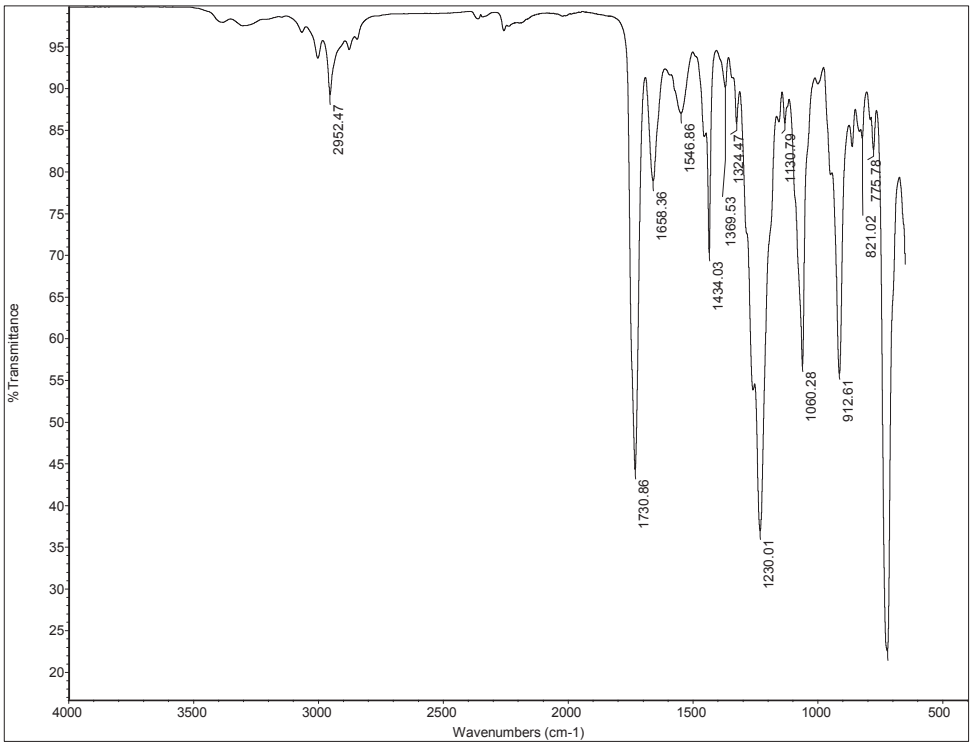

Figure A.29 FTIR spectrum (neat) of compound **2.37**

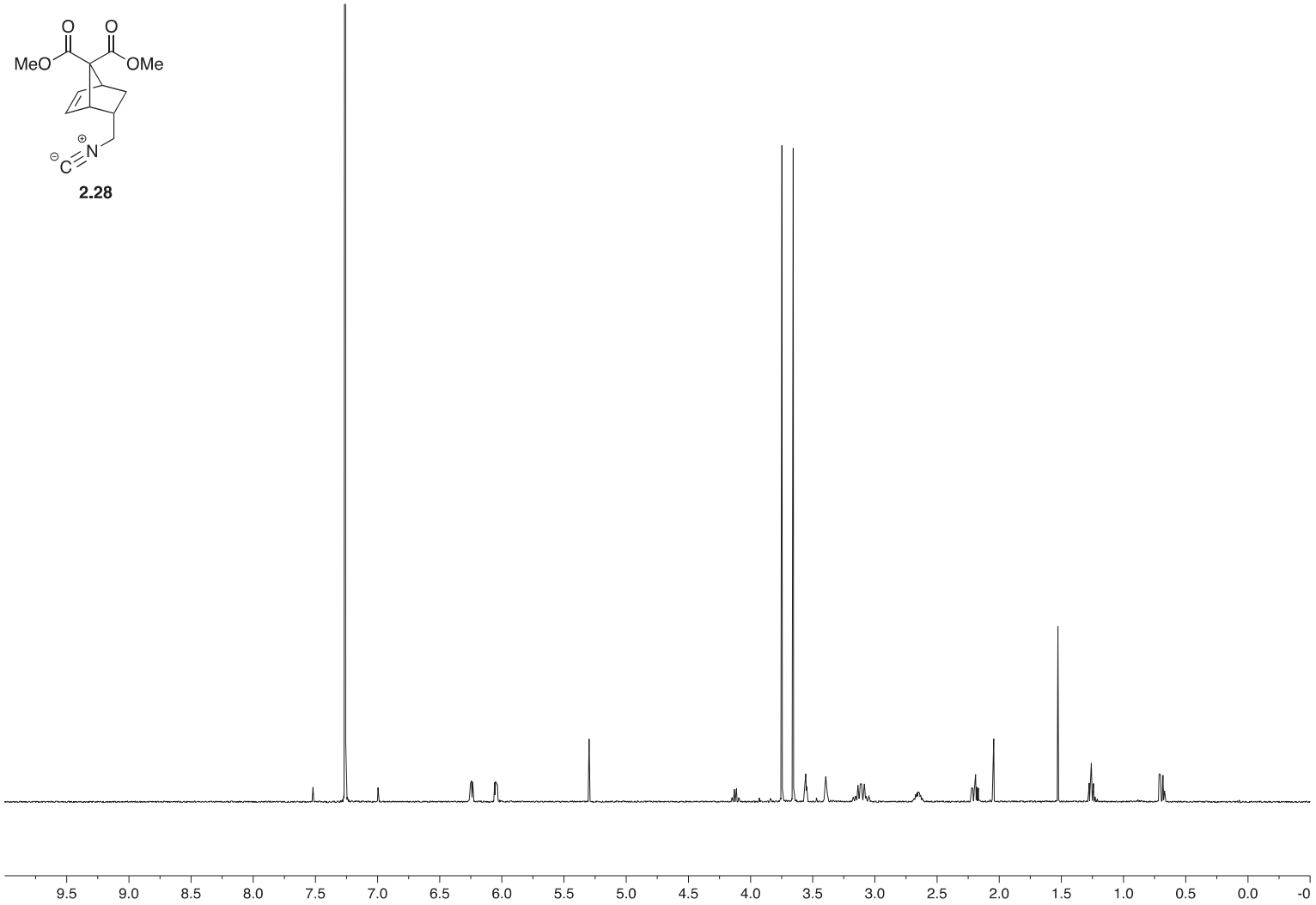

Figure A.30 ^{1}H-NMR (400 MHz; $CDCl_3$) for compound **2.28**

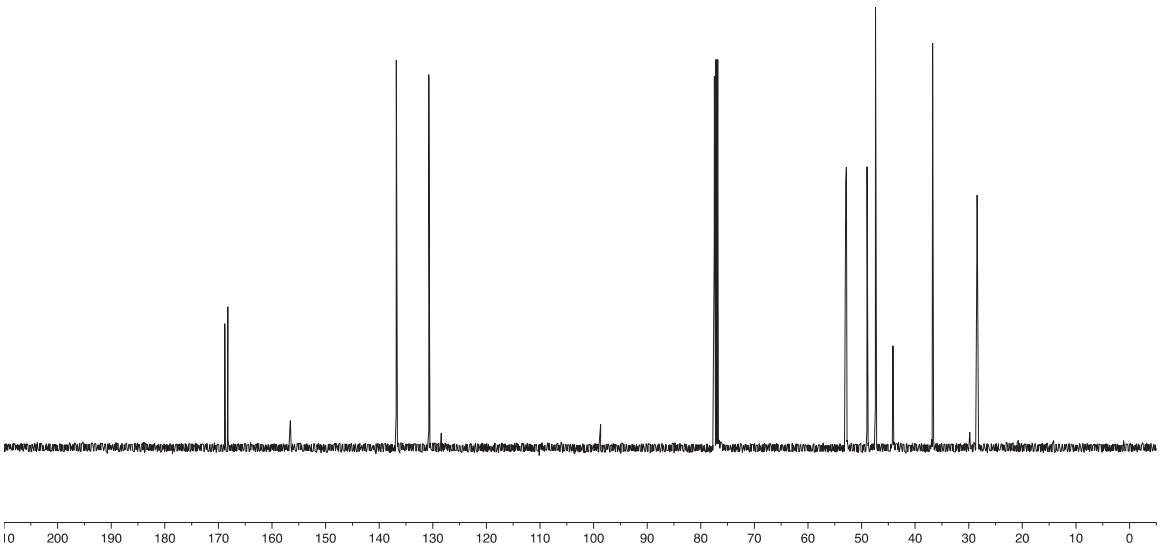

Figure A.31 ^{13}C-NMR spectrum (100 MHz; $CDCl_3$) of compound **2.28**

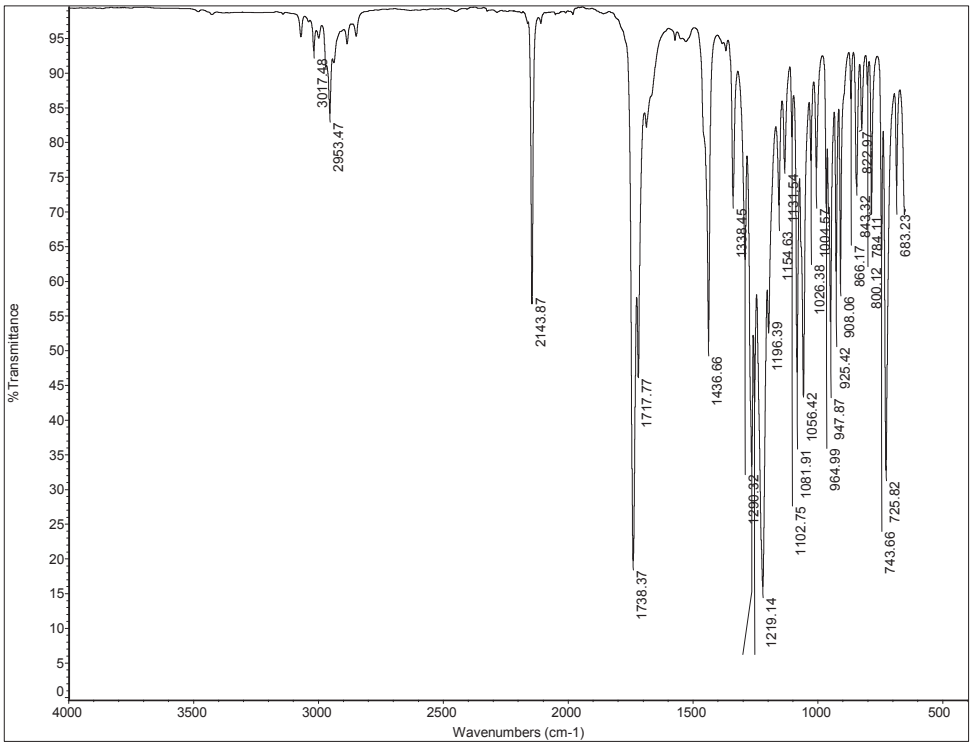

Figure A.32 FTIR spectrum (neat) of compound **2.28**

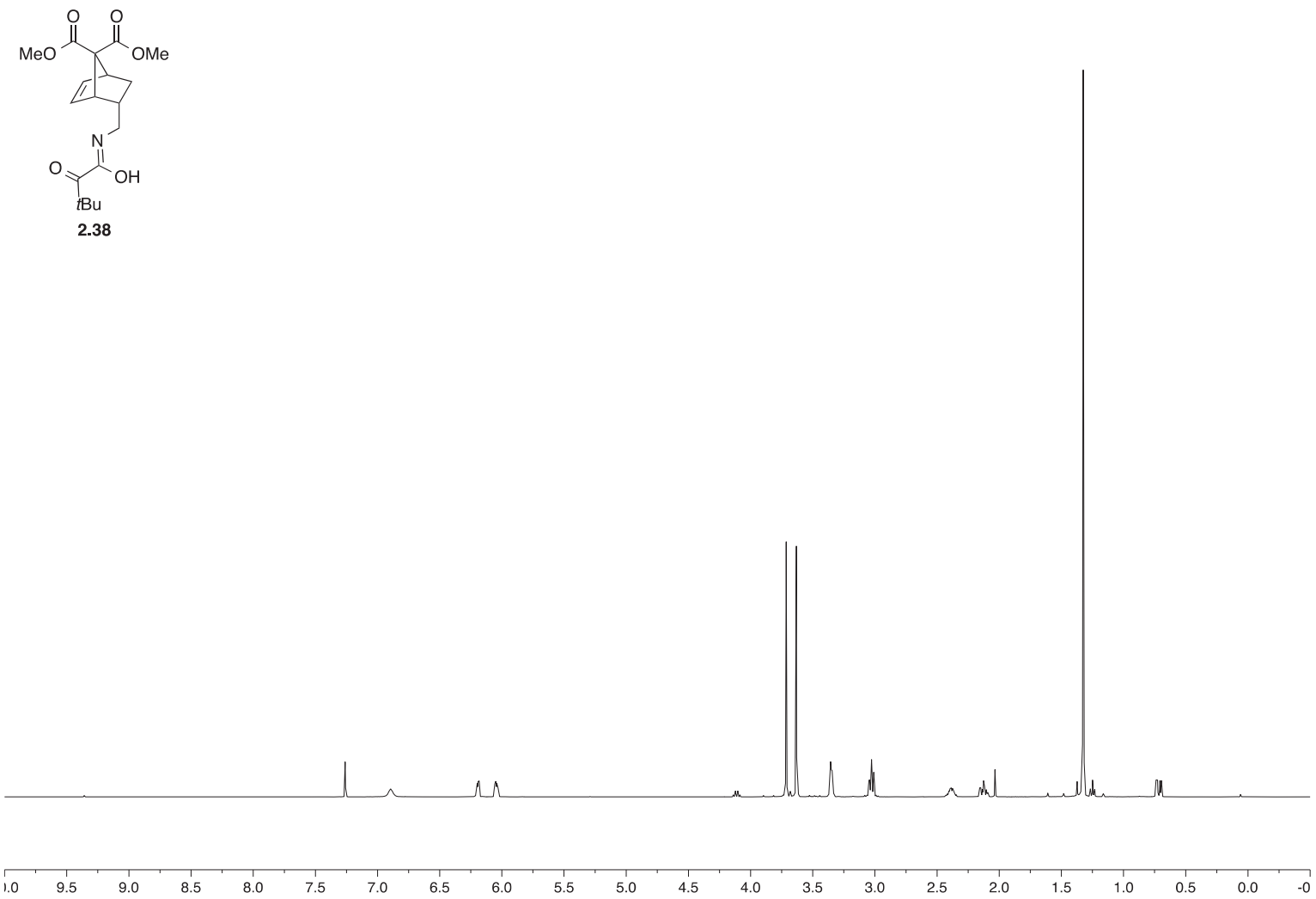

Figure A.33 ^{1}H-NMR (400 MHz; $CDCl_3$) for compound **2.38**

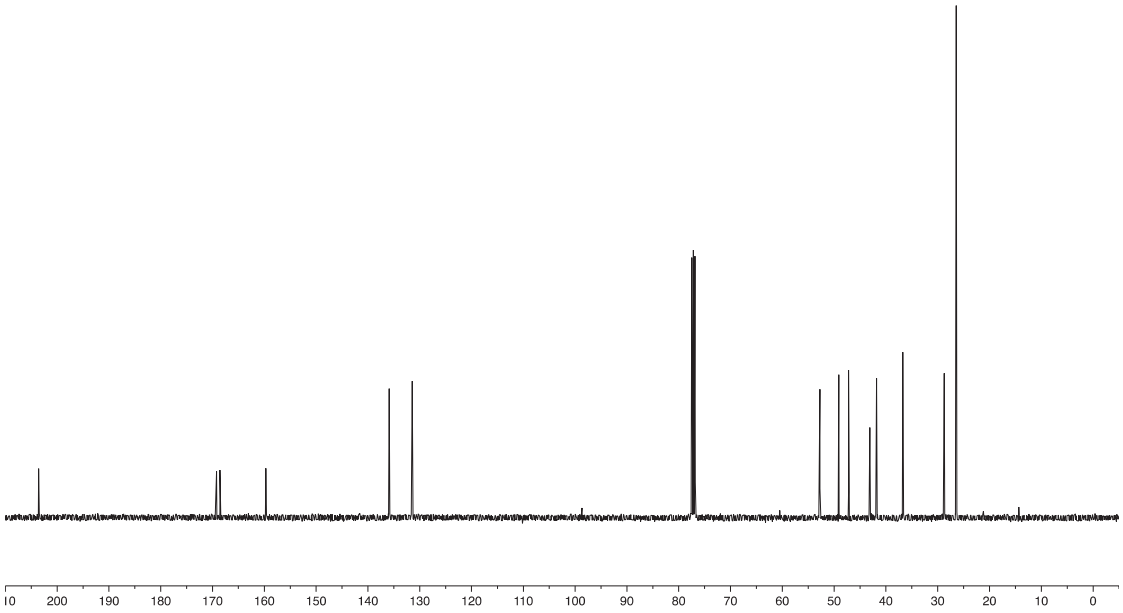

Figure A.34 ^{13}C-NMR spectrum (100 MHz; $CDCl_3$) of compound **2.38**

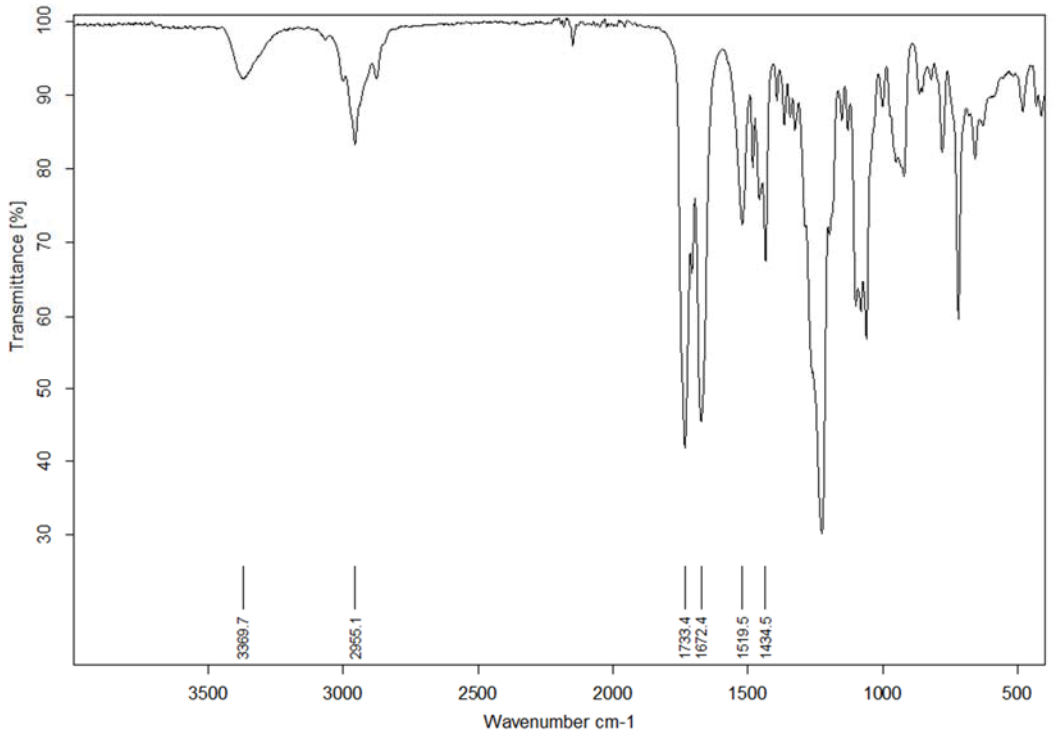

Figure A.35 FTIR spectrum (neat) of compound **2.38**

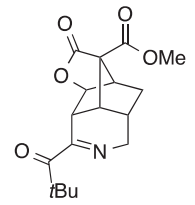

2.39

Figure A.36 ^{1}H-NMR (400 MHz; $CDCl_3$) for compound **2.39**

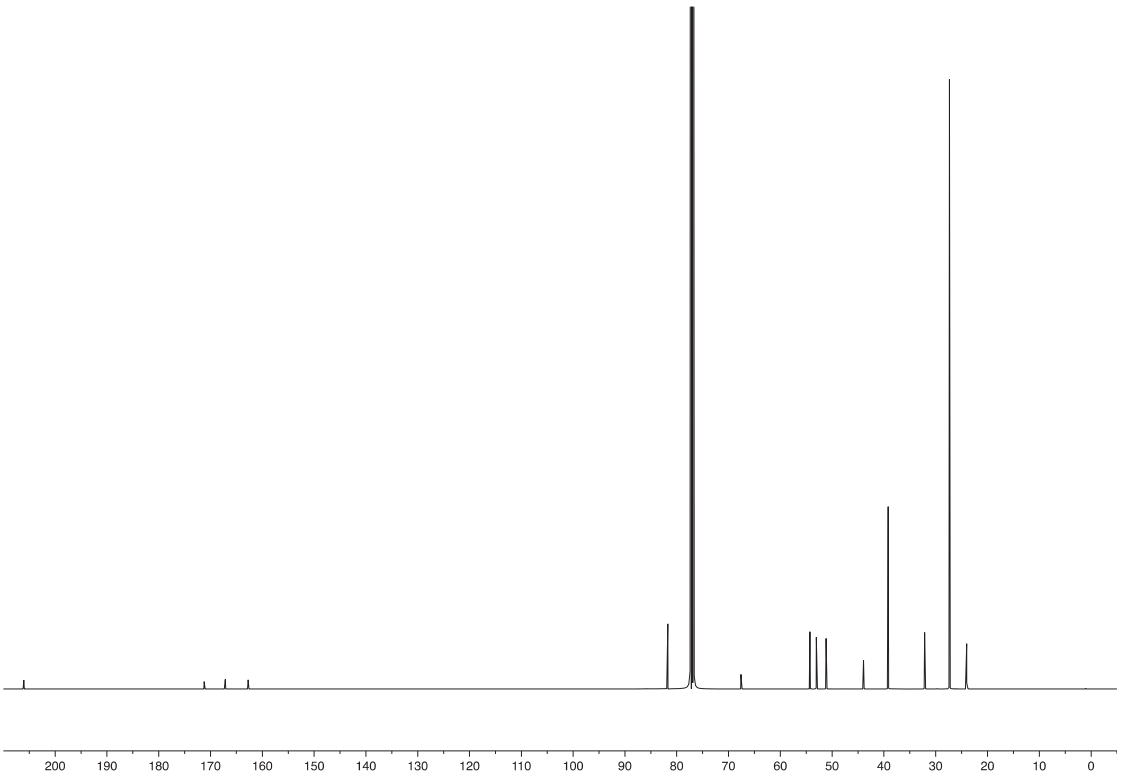

Figure A.37 ^{13}C-NMR spectrum (150 MHz; $CDCl_3$) of compound **2.39**

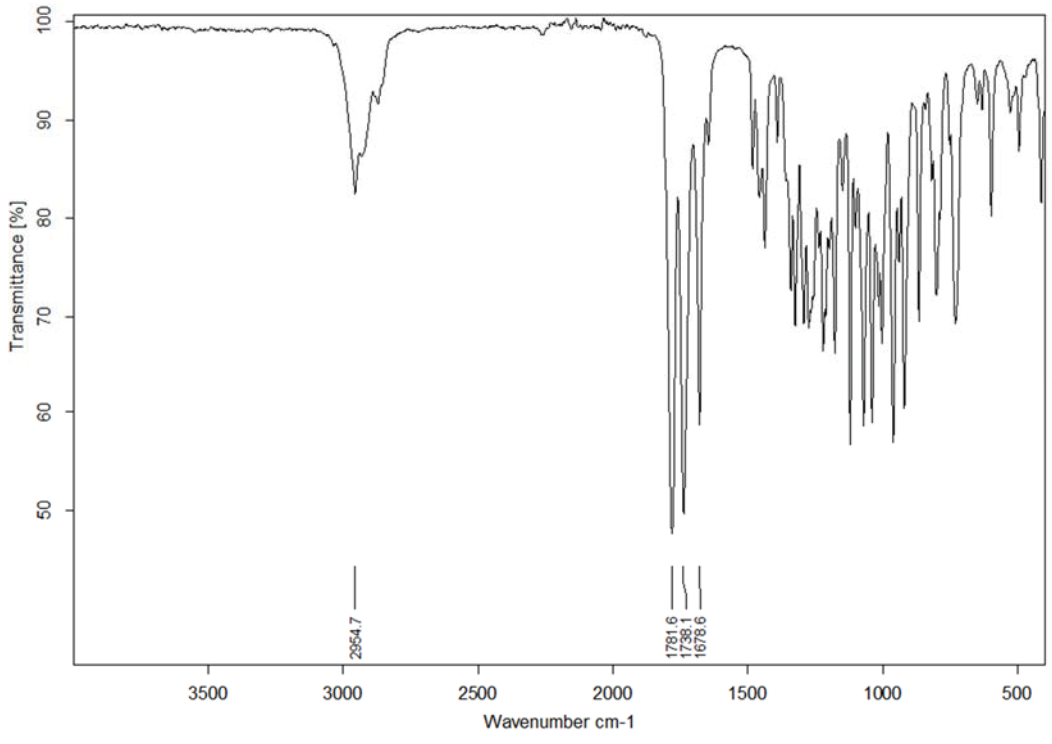

Figure A.38 FTIR spectrum (neat) of compound **2.39**

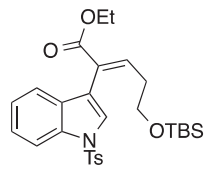

2.27

Figure A.39 ^{1}H-NMR (400 MHz; $CDCl_3$) for compound **2.27**

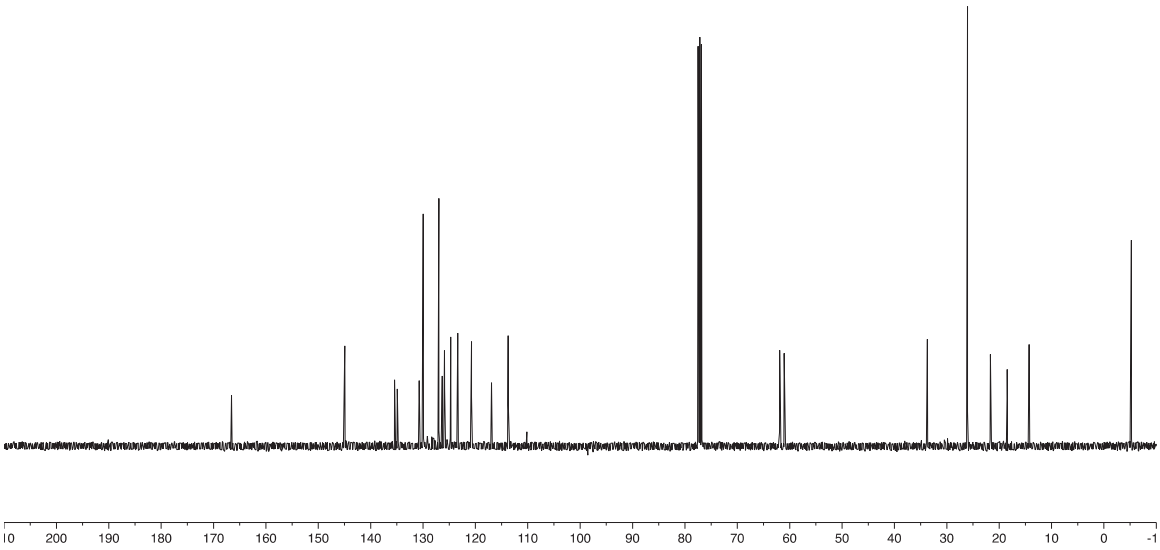

Figure A.40 ^{13}C-NMR spectrum (100 MHz; $CDCl_3$) of compound **2.27**

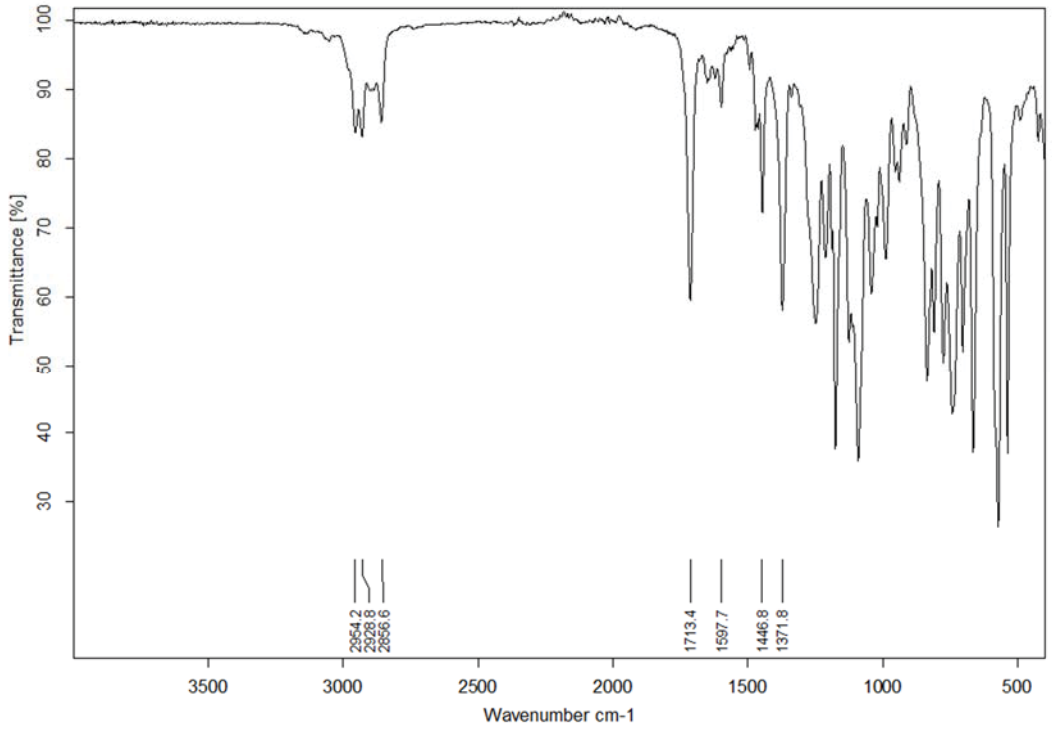

Figure A.41 FTIR spectrum (neat) of compound **2.27**

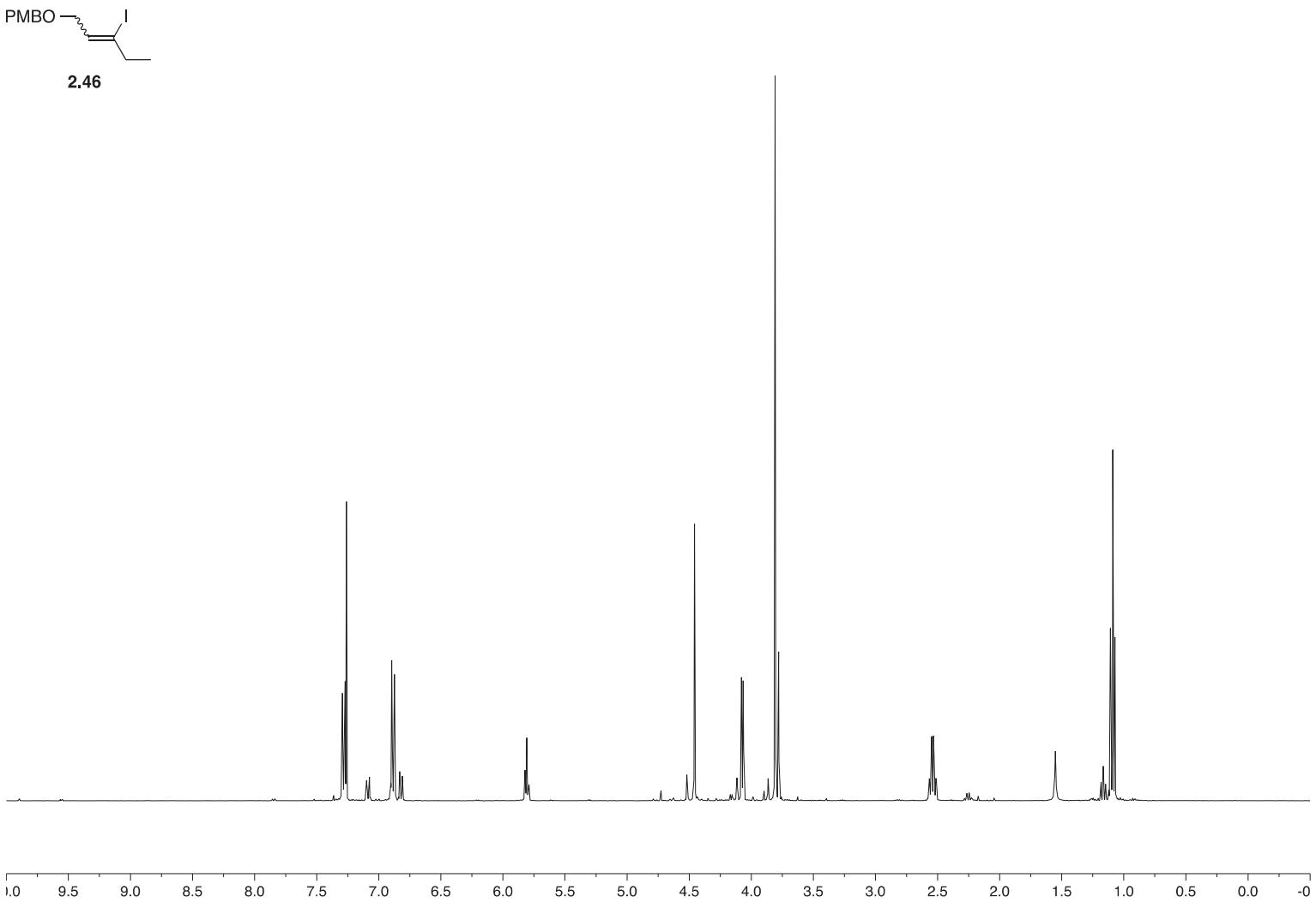

Figure A.42 ^{1}H-NMR (400 MHz; $CDCl_3$) for compound **2.46**

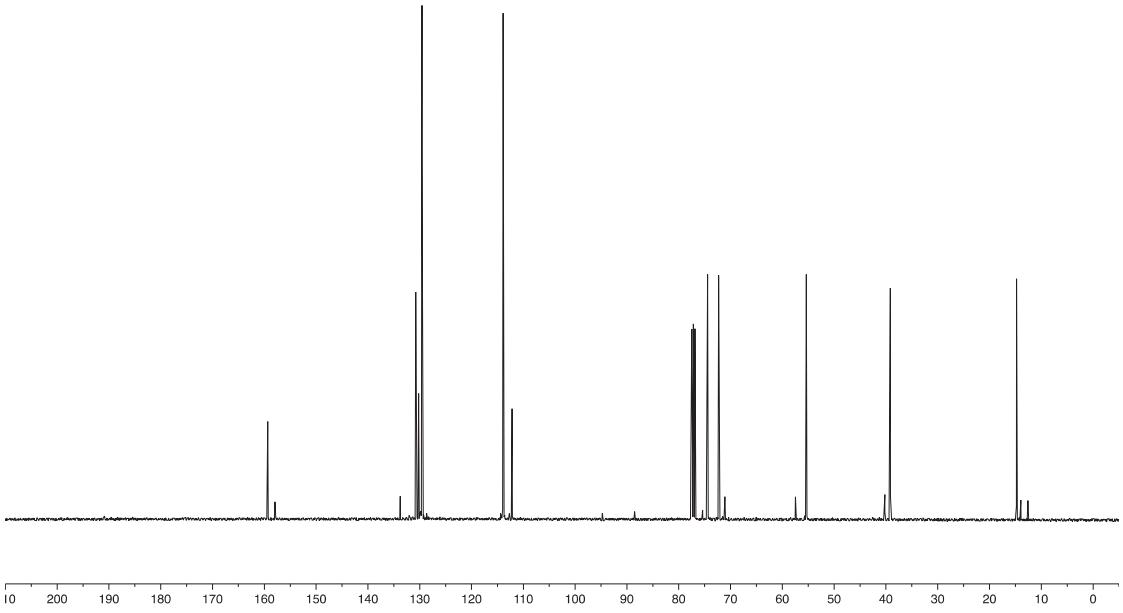

Figure A.43 ^{13}C-NMR spectrum (100 MHz; $CDCl_3$) of compound **2.46**

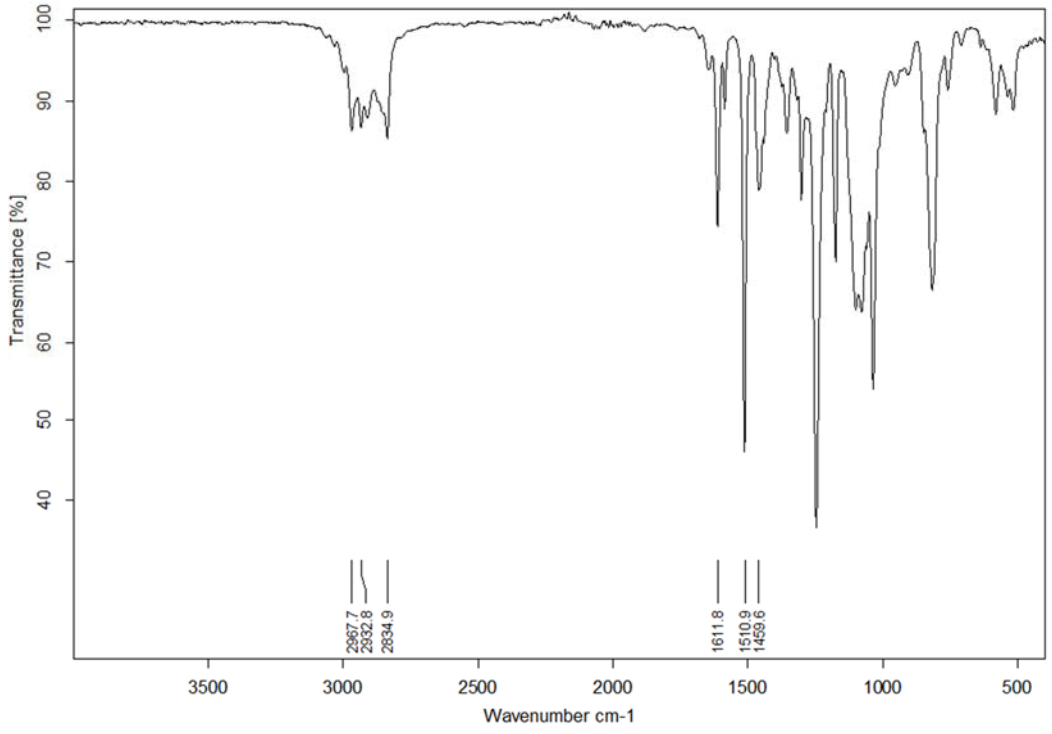

Figure A.44 FTIR spectrum (neat) of compound **2.46**

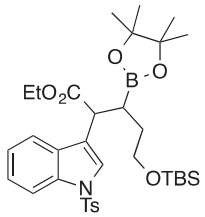

2.55

Figure A.45 ^{1}H-NMR (400 MHz; $CDCl_3$) for compound **2.55**

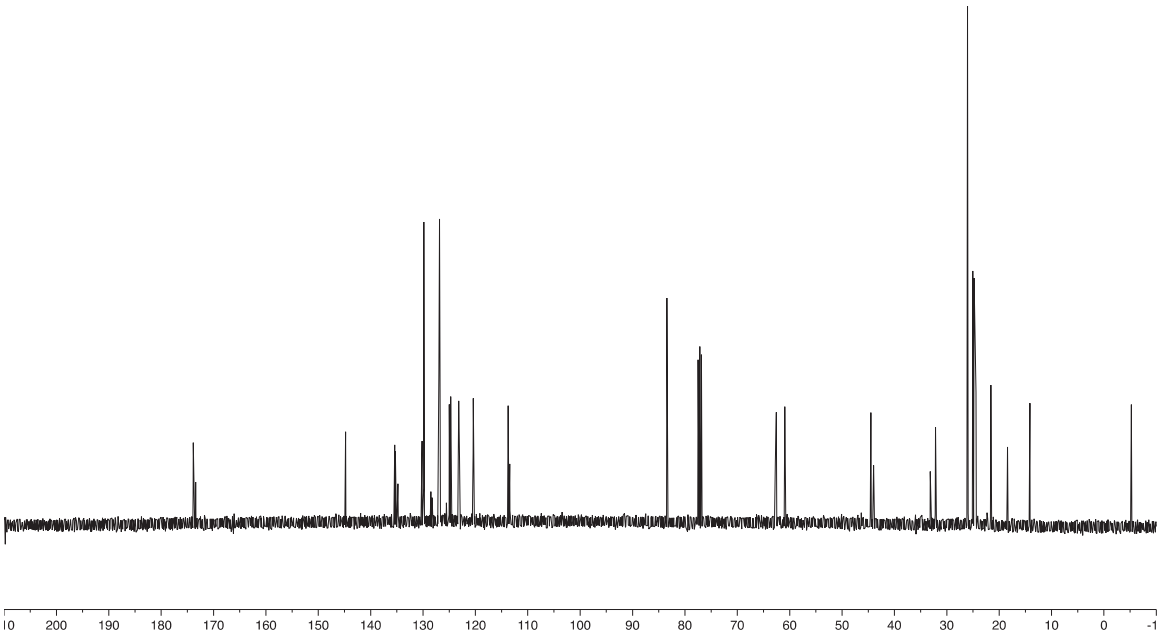

Figure A.46 ^{13}C-NMR spectrum (100 MHz; $CDCl_3$) of compound **2.55**

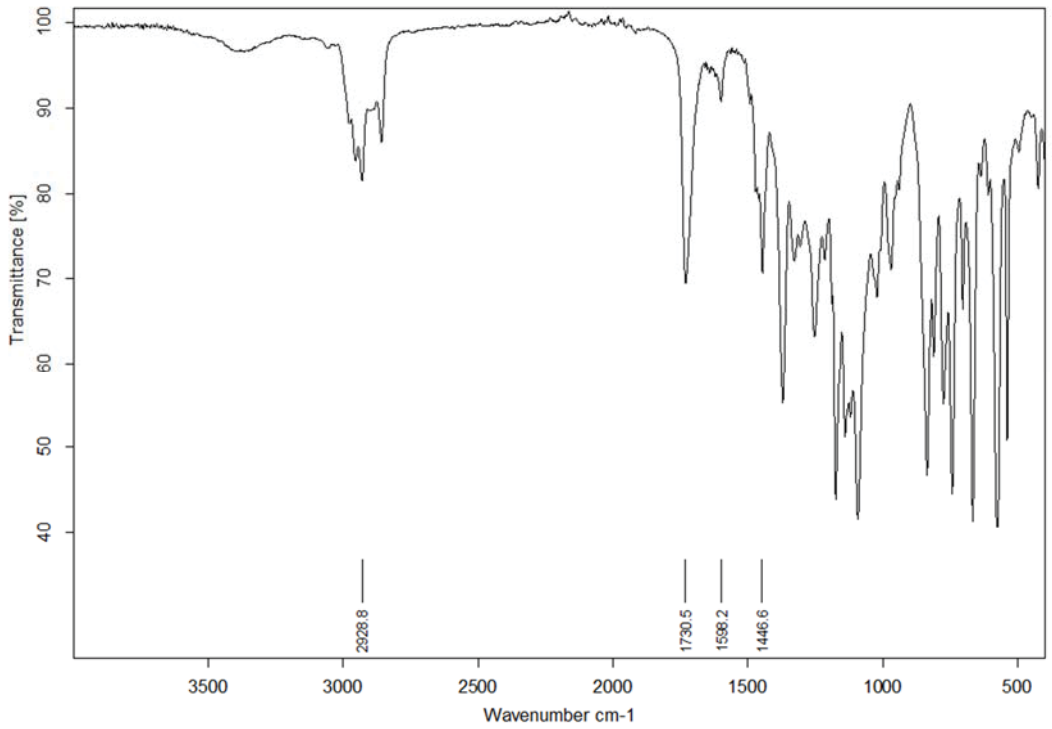

Figure A.47 FTIR spectrum (neat) of compound **2.55**

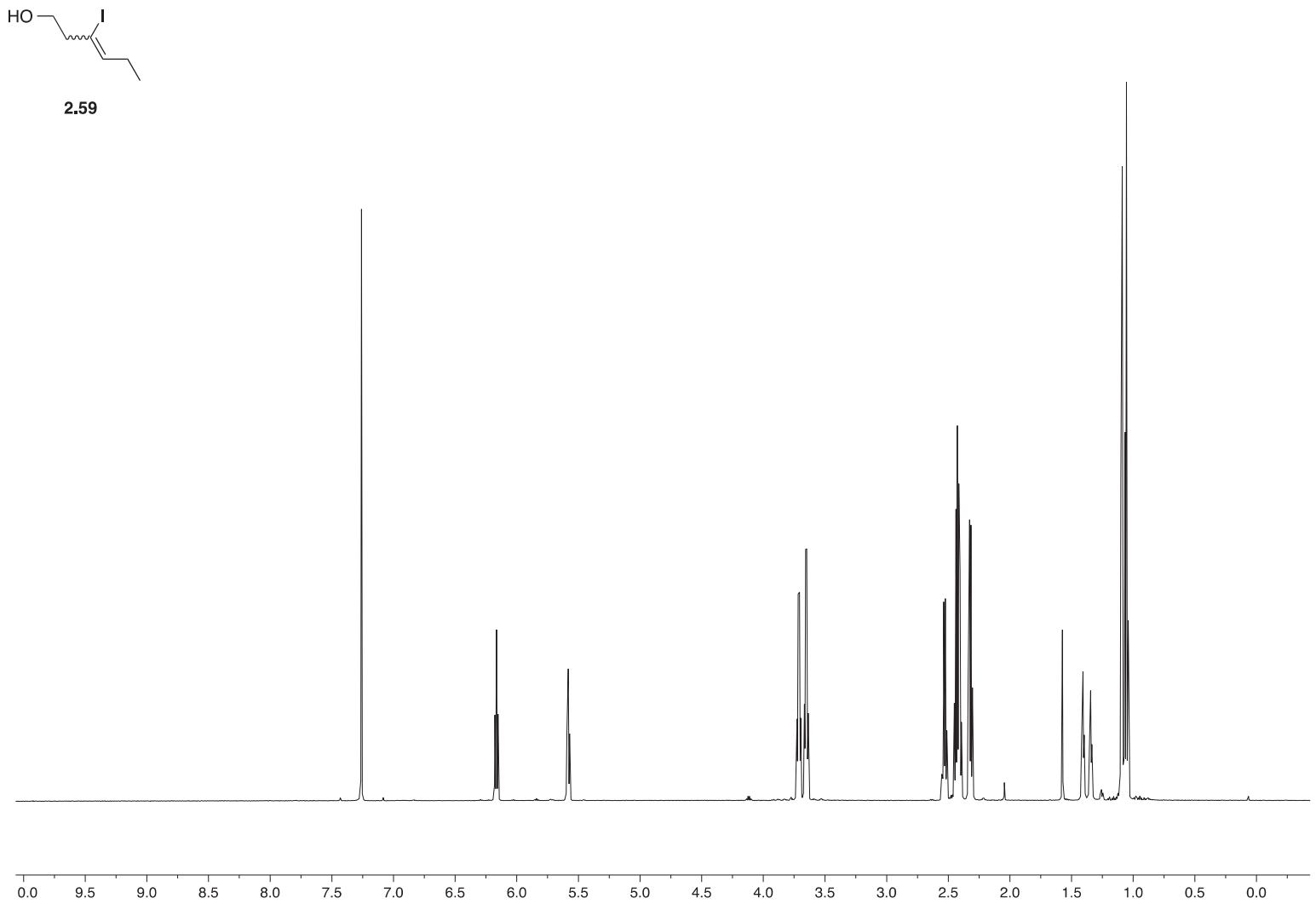

Figure A.48 ^{1}H-NMR (600 MHz; $CDCl_3$) for compound **2.59**

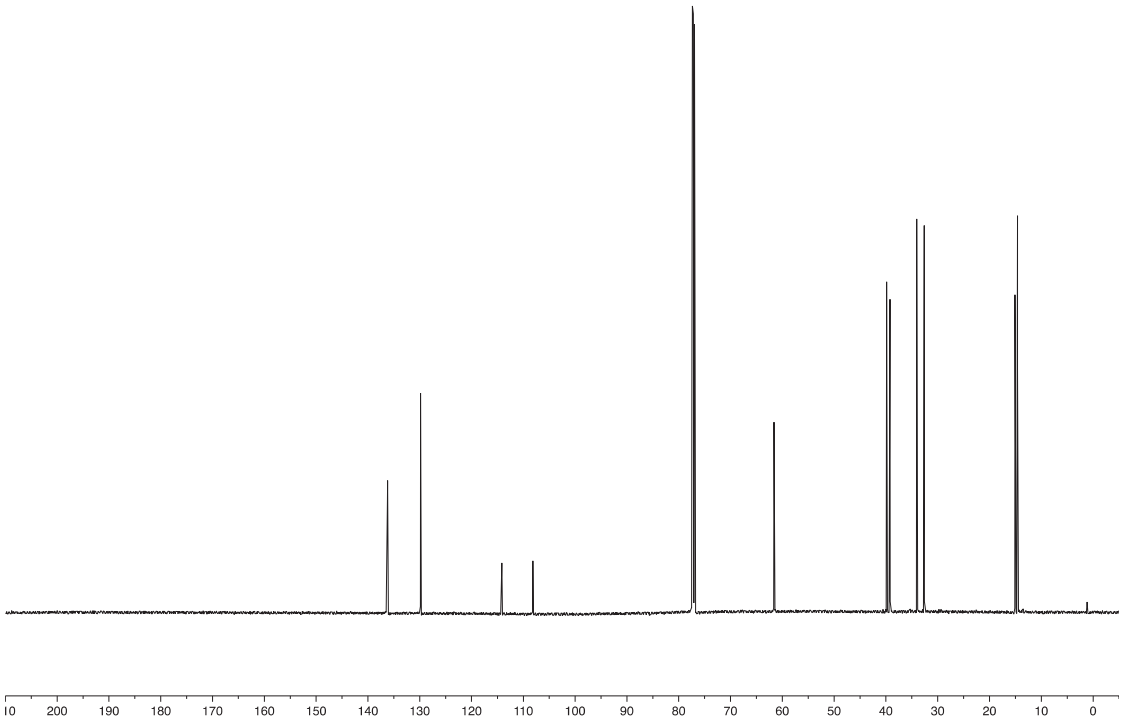

Figure A.49 ^{13}C-NMR spectrum (150 MHz; $CDCl_3$) of compound **2.59**

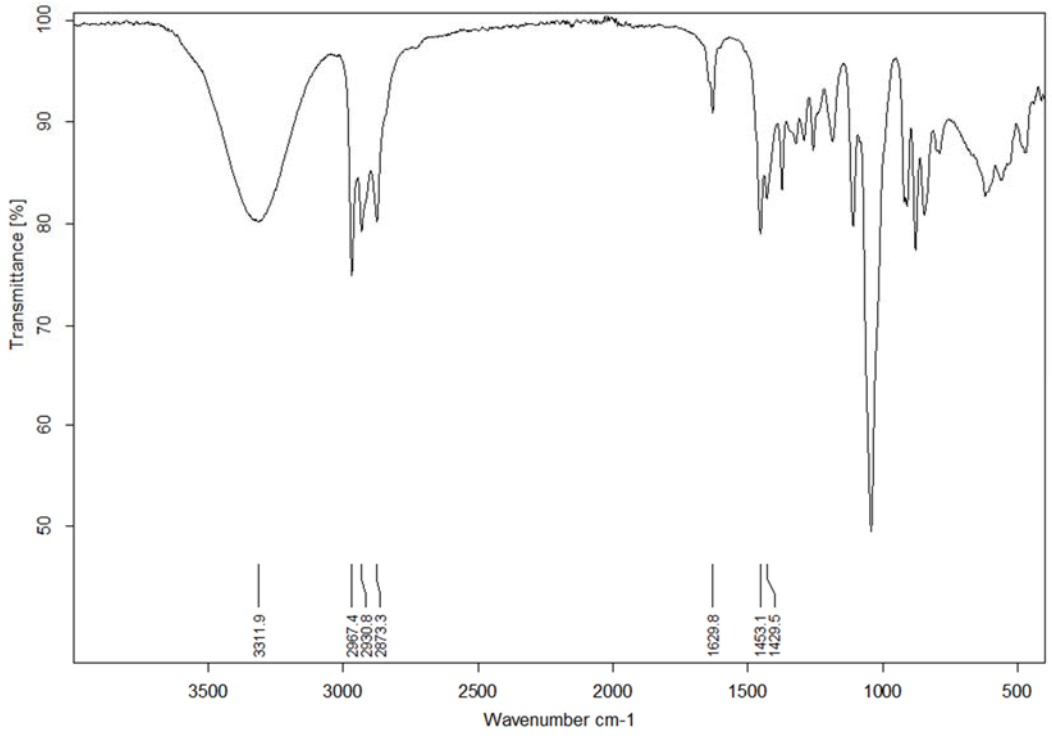

Figure A.50 FTIR spectrum (neat) of compound **2.59**

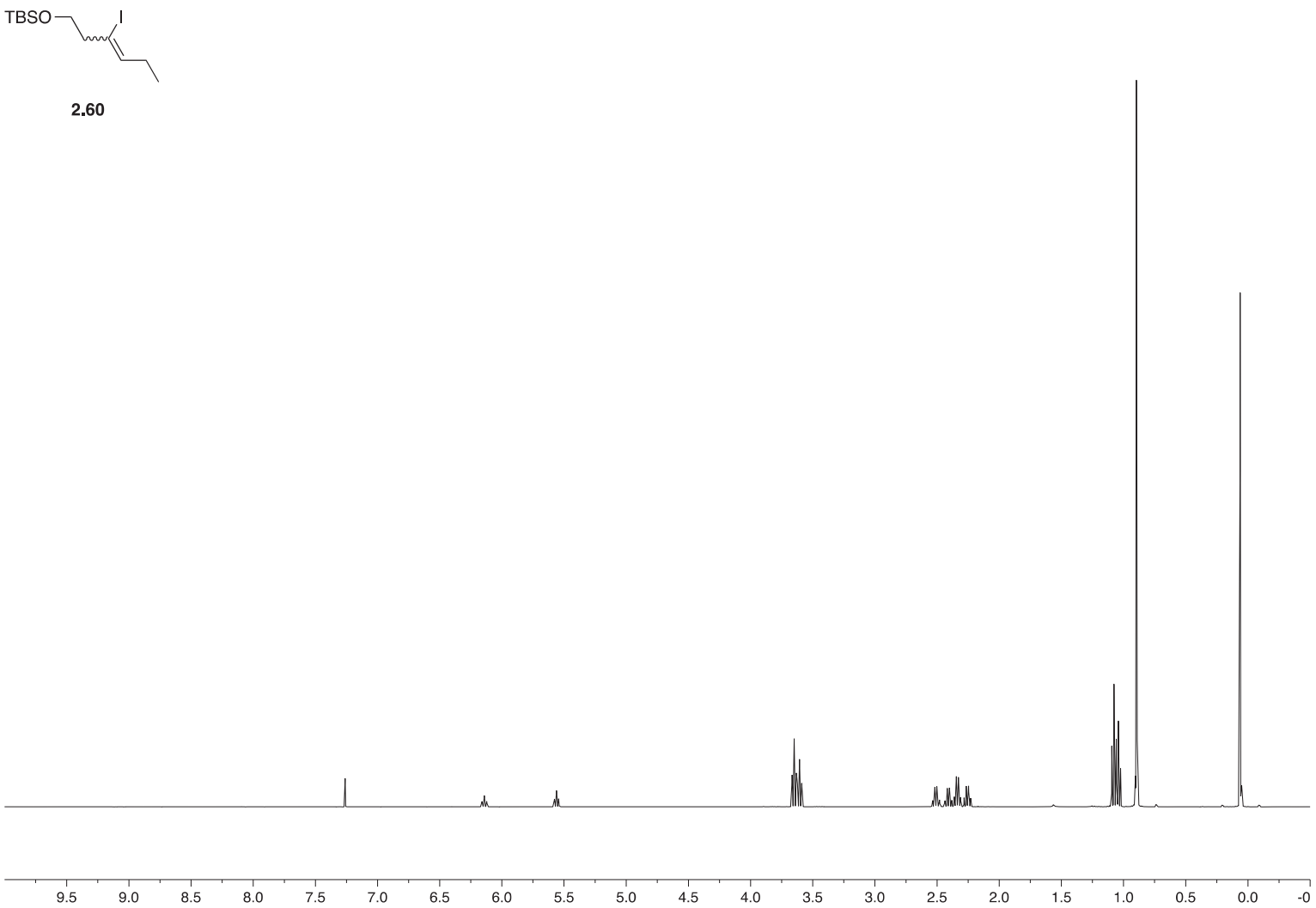

Figure A.51 ^{1}H-NMR (400 MHz; $CDCl_3$) for compound **2.60**

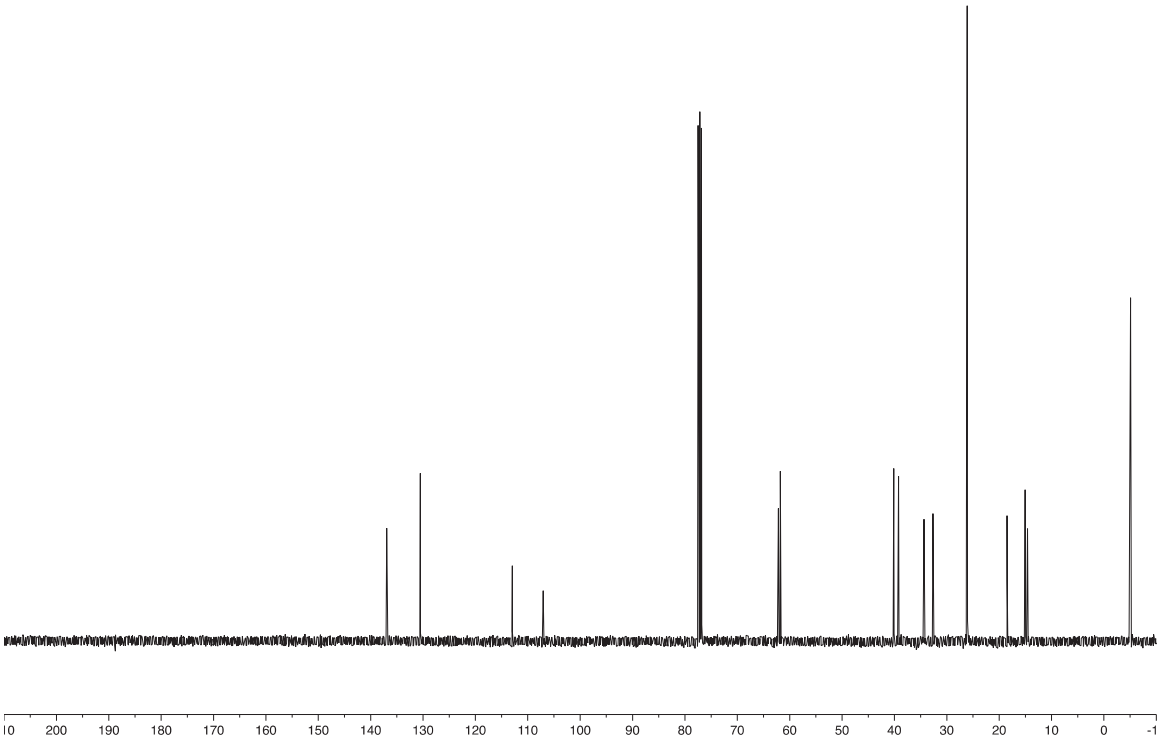

Figure A.52 ^{13}C-NMR spectrum (100 MHz; $CDCl_3$) of compound **2.60**

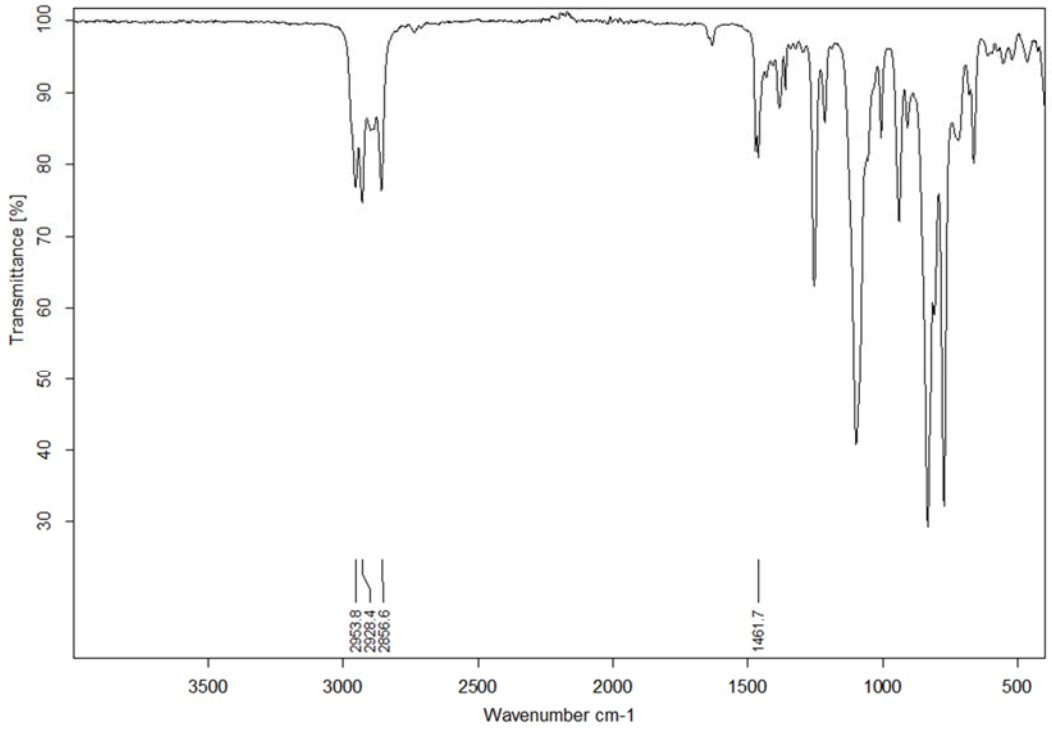

Figure A.53 FTIR spectrum (neat) of compound **2.60**

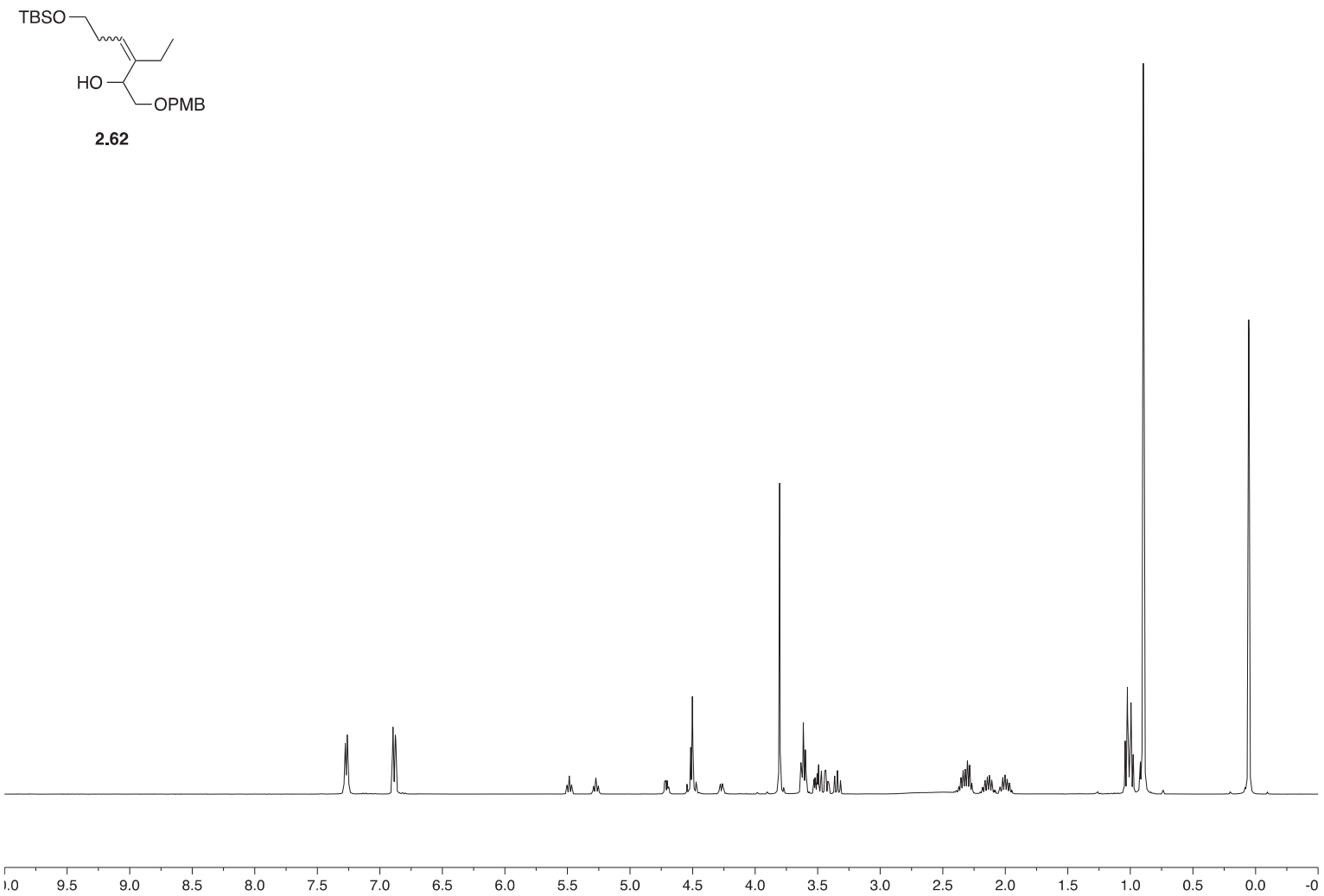

Figure A.54 ^{1}H-NMR (400 MHz; $CDCl_3$) for compound **2.62**

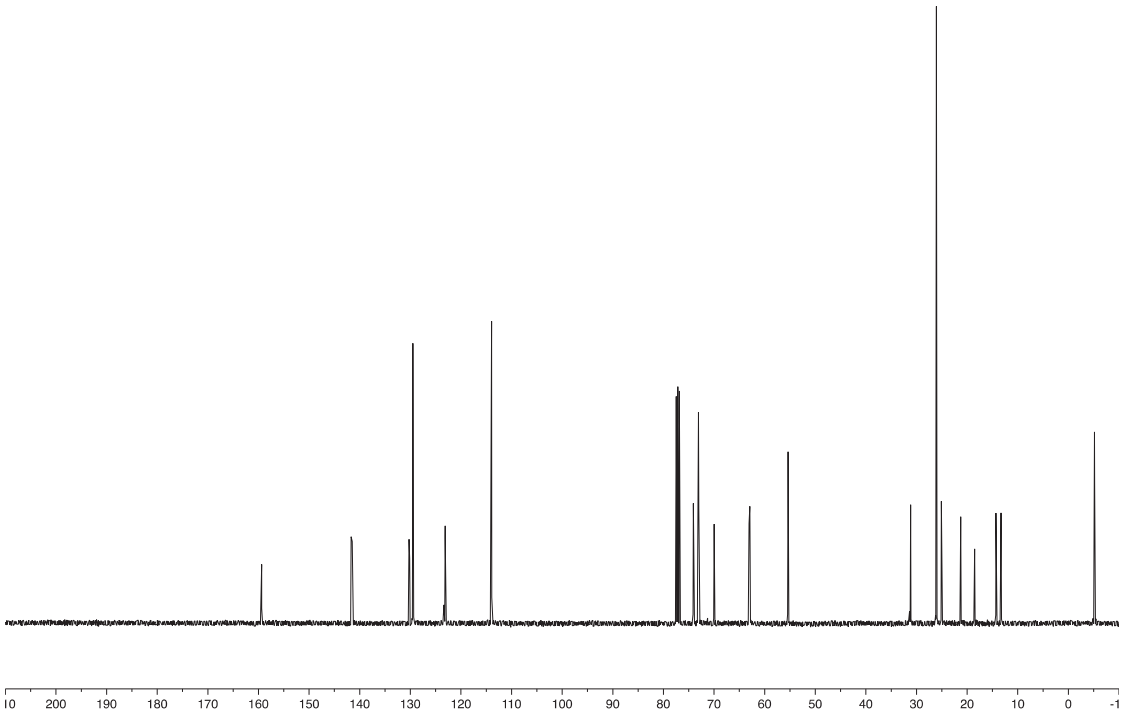

Figure A.55 ^{13}C-NMR spectrum (100 MHz; $CDCl_3$) of compound **2.62**

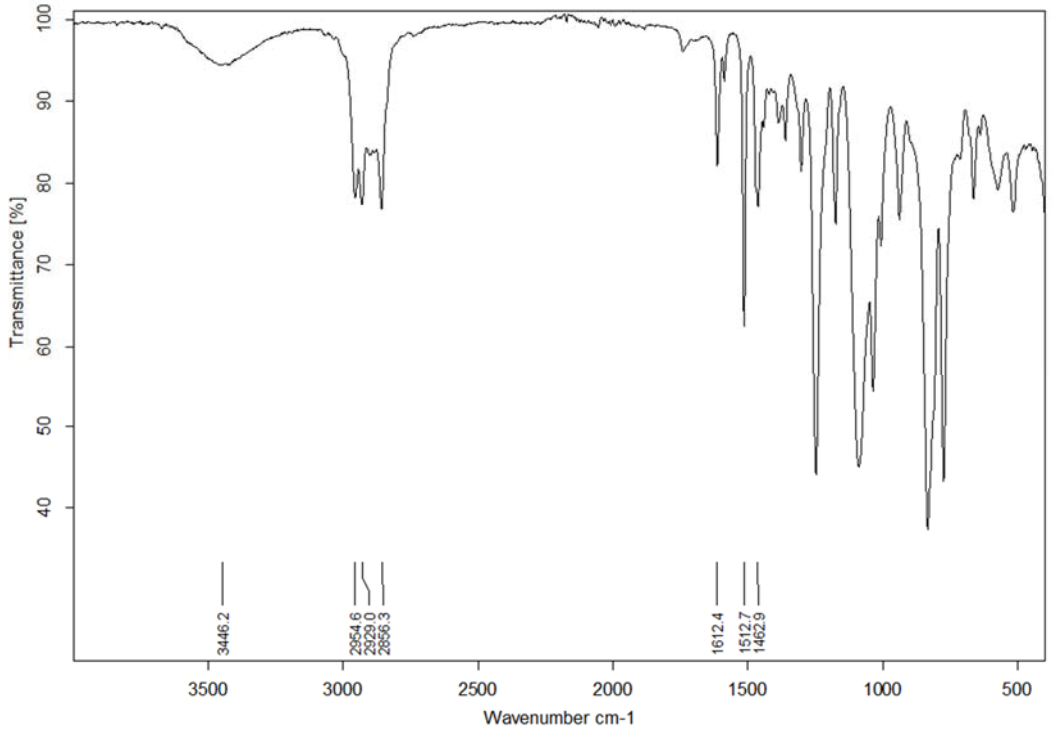

Figure A.56 FTIR spectrum (neat) of compound **2.62**

APPENDIX B

Spectra Relevant to Chapter Four

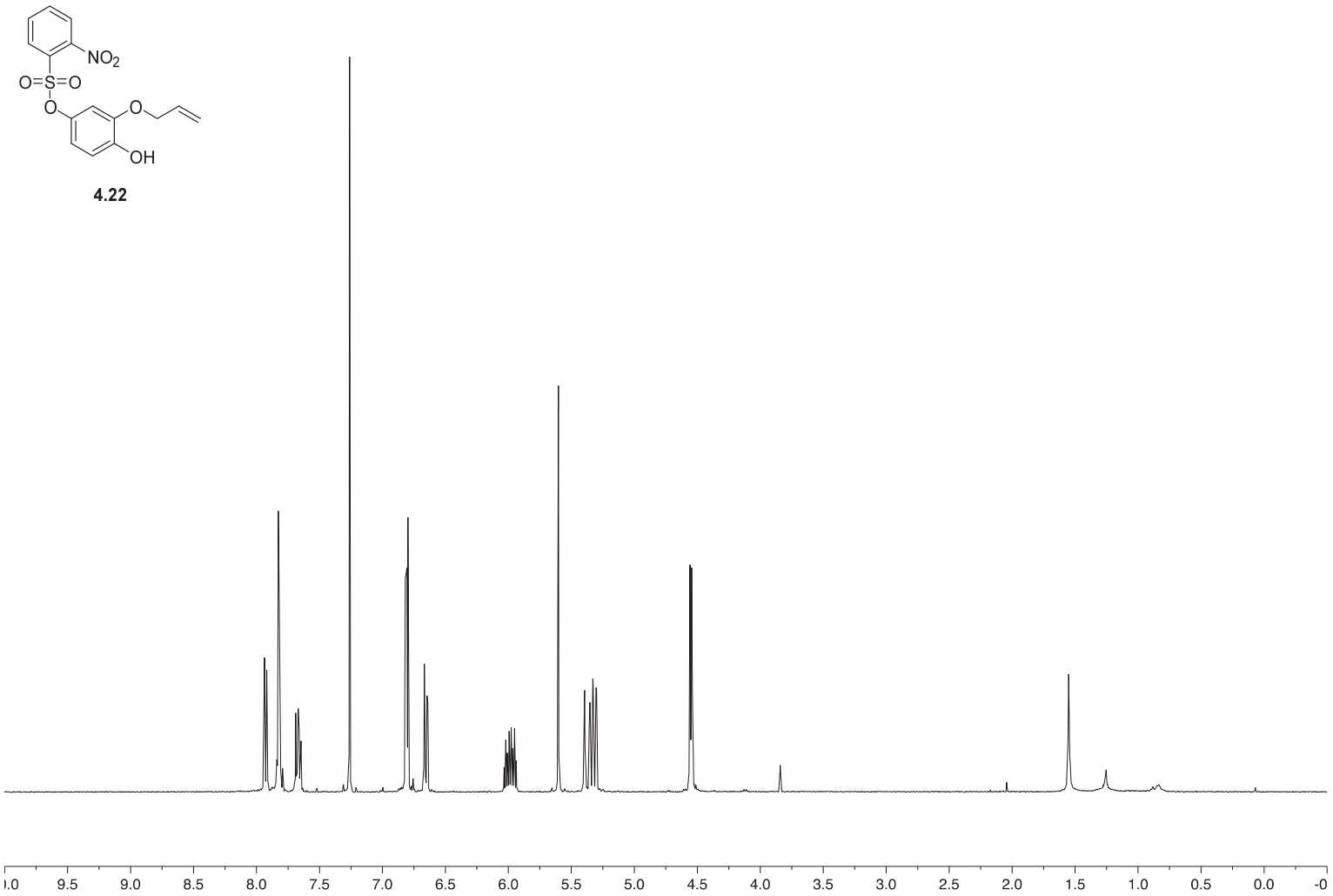

Figure B.10 ^{1}H-NMR (600 MHz; $CDCl_3$) for compound **4.22**

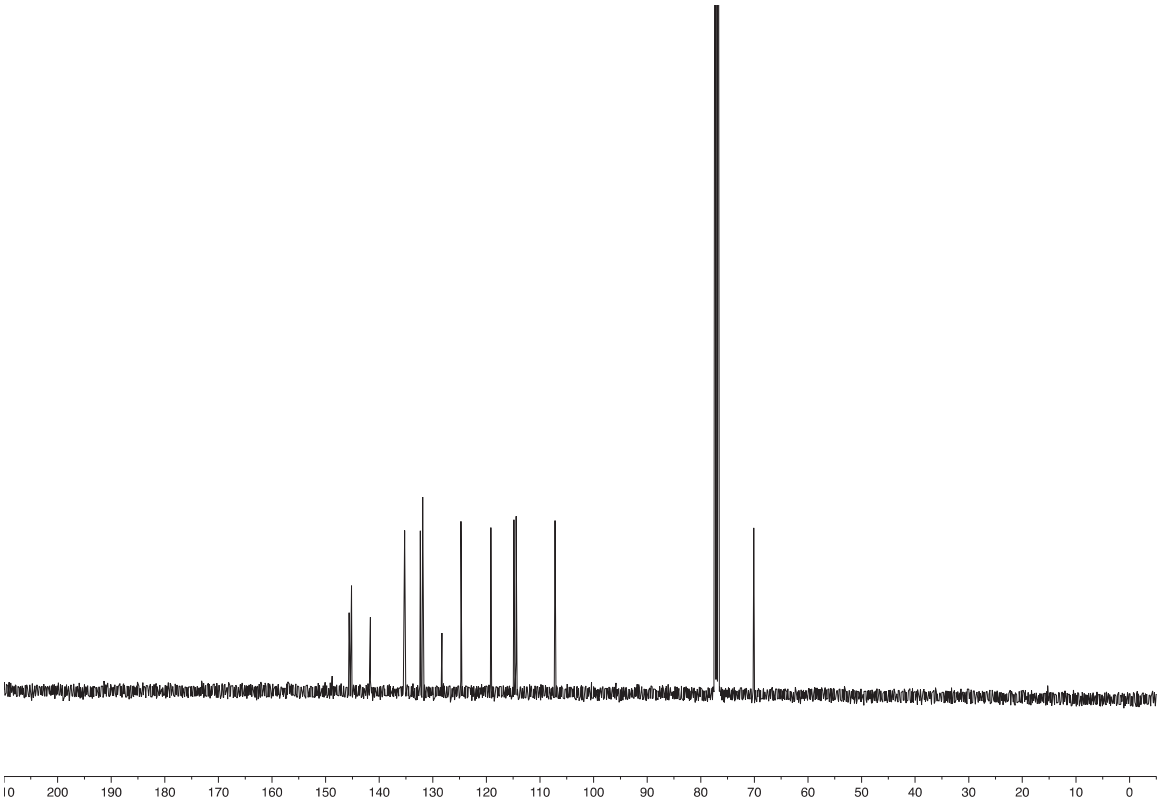

Figure B.11 ^{13}C-NMR spectrum (150 MHz; $CDCl_3$) of compound **4.22**

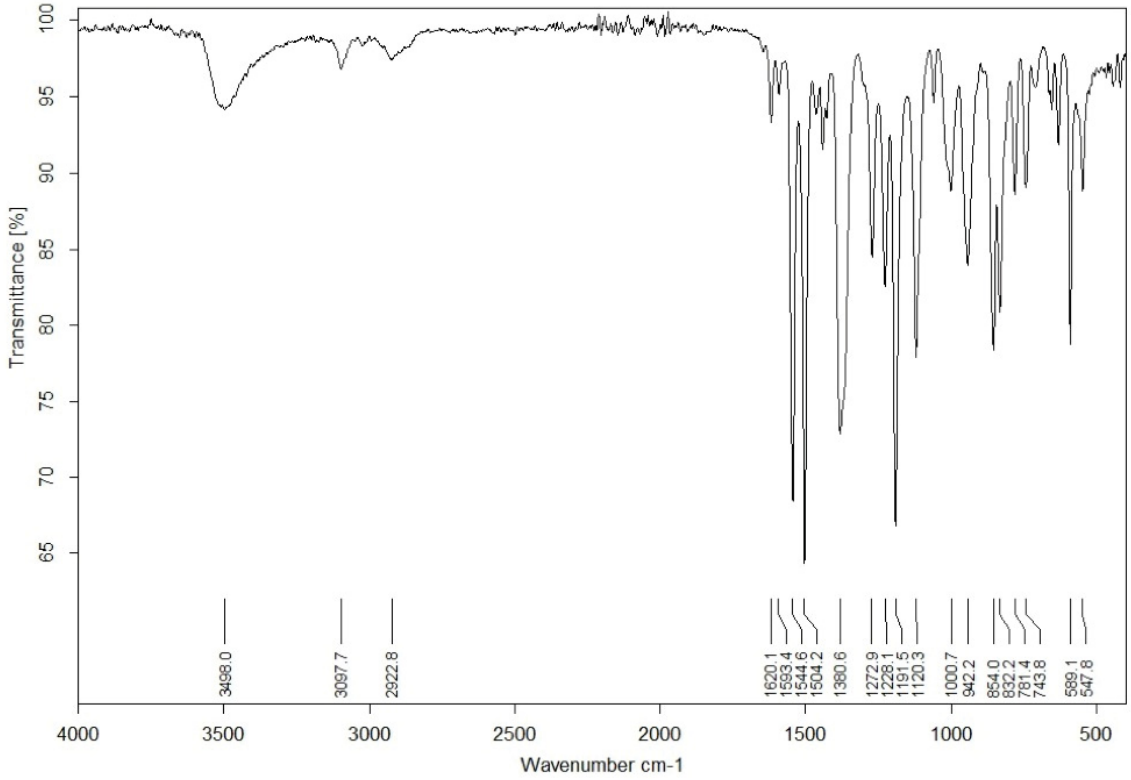

Figure B.12 FTIR spectrum (neat) of compound **4.22**

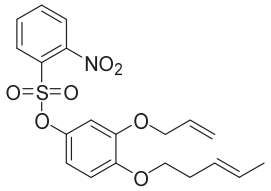

4.24

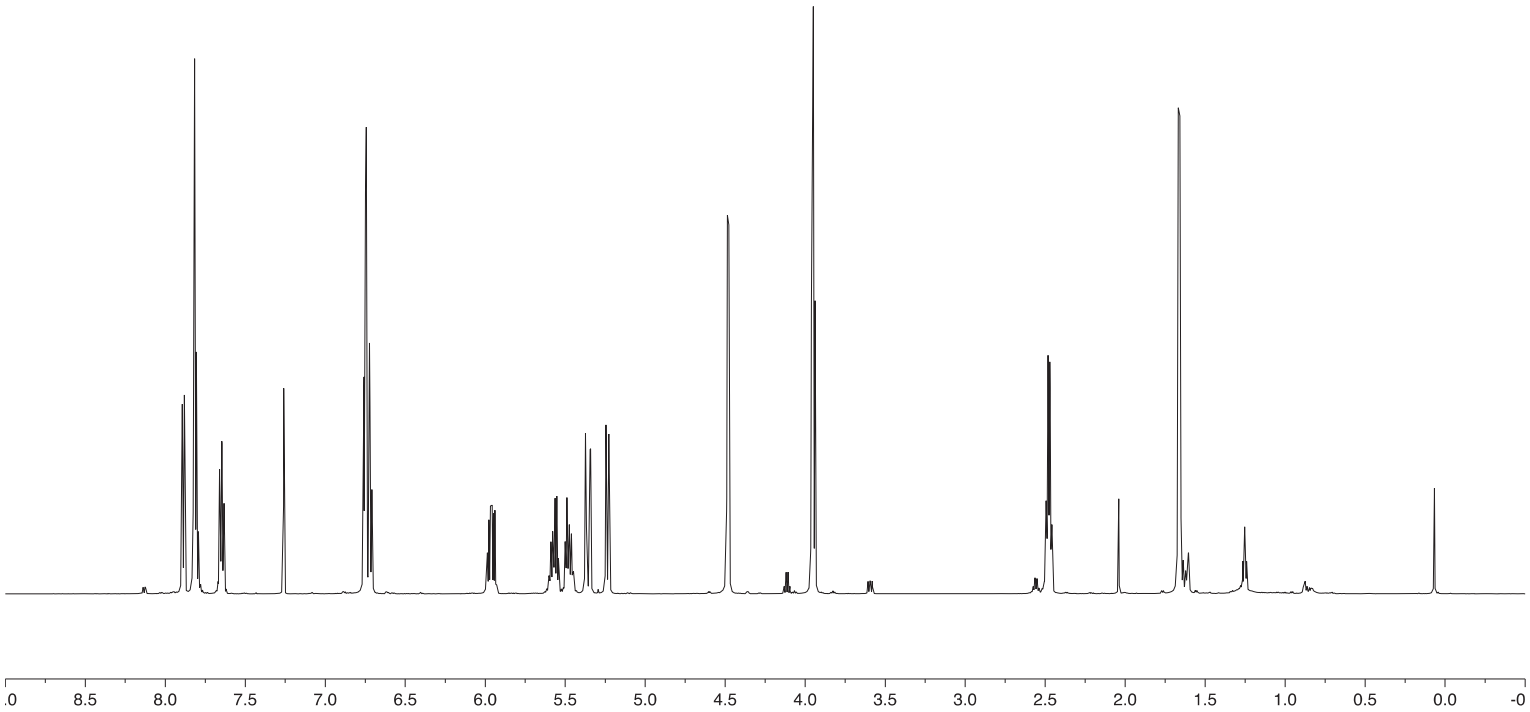

Figure B.13 ^{1}H-NMR (600 MHz; $CDCl_3$) for compound **4.24**

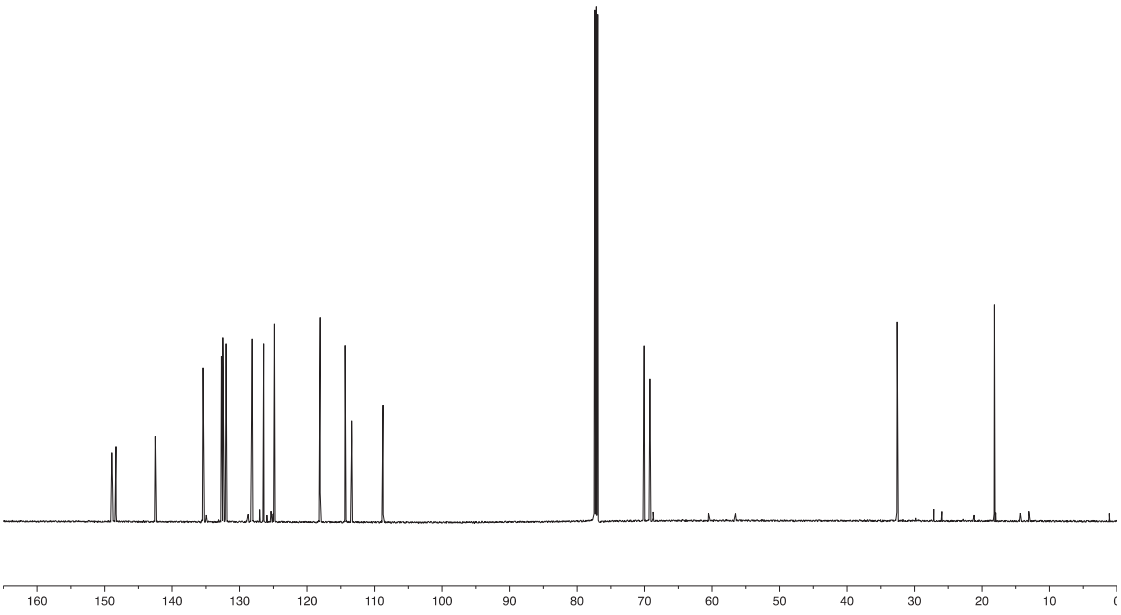

Figure B.14 ^{13}C-NMR spectrum (150 MHz; $CDCl_3$) of compound **4.24**

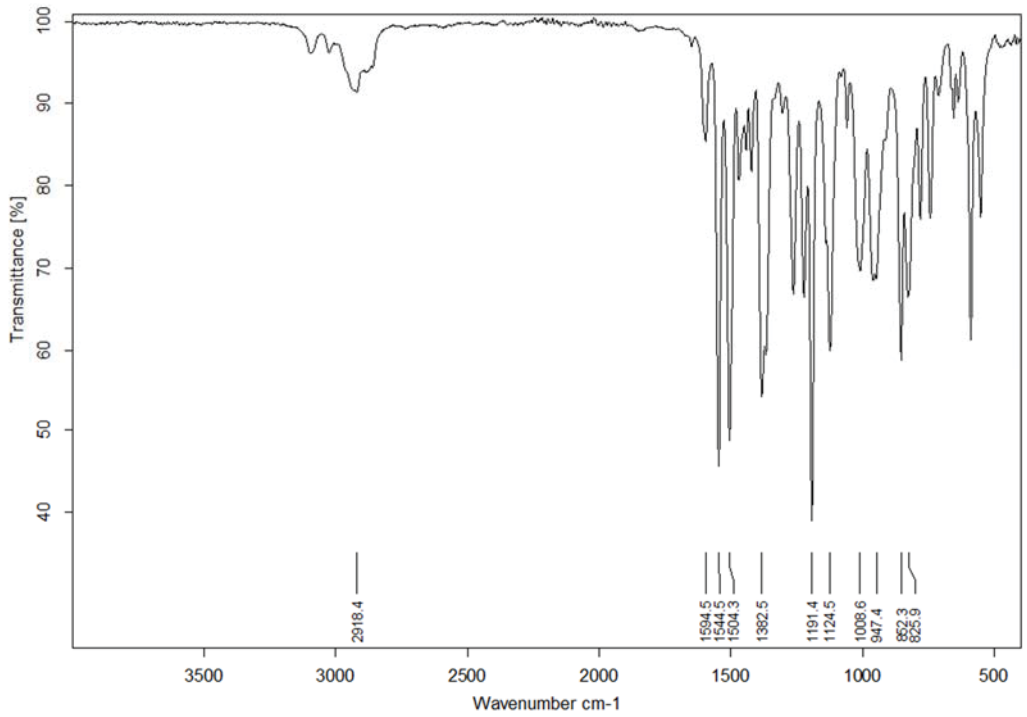

Figure B.15 FTIR spectrum (neat) of compound **4.24**

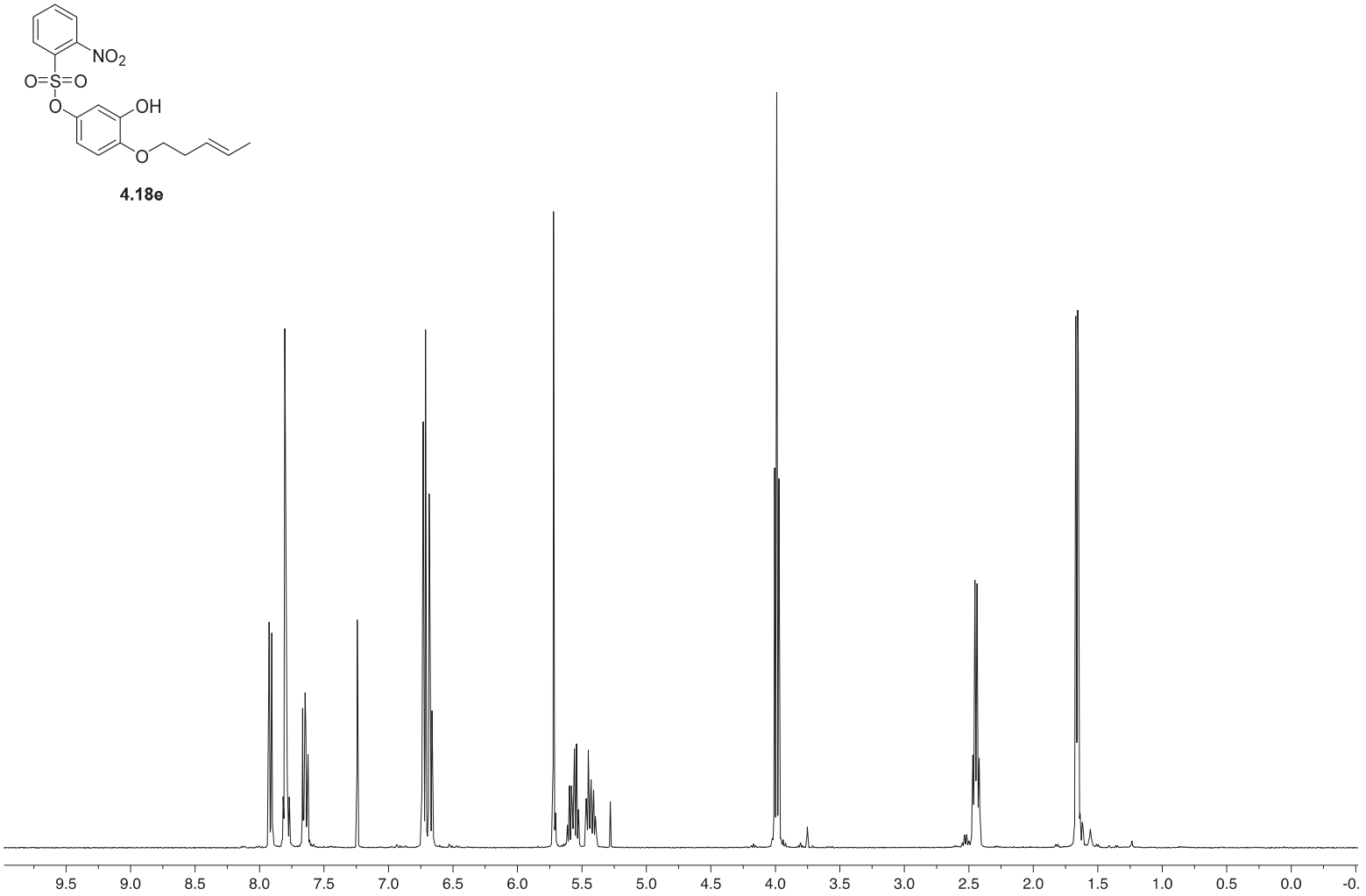

Figure B.16 ^{1}H-NMR (400 MHz; $CDCl_3$) for compound **4.18e**

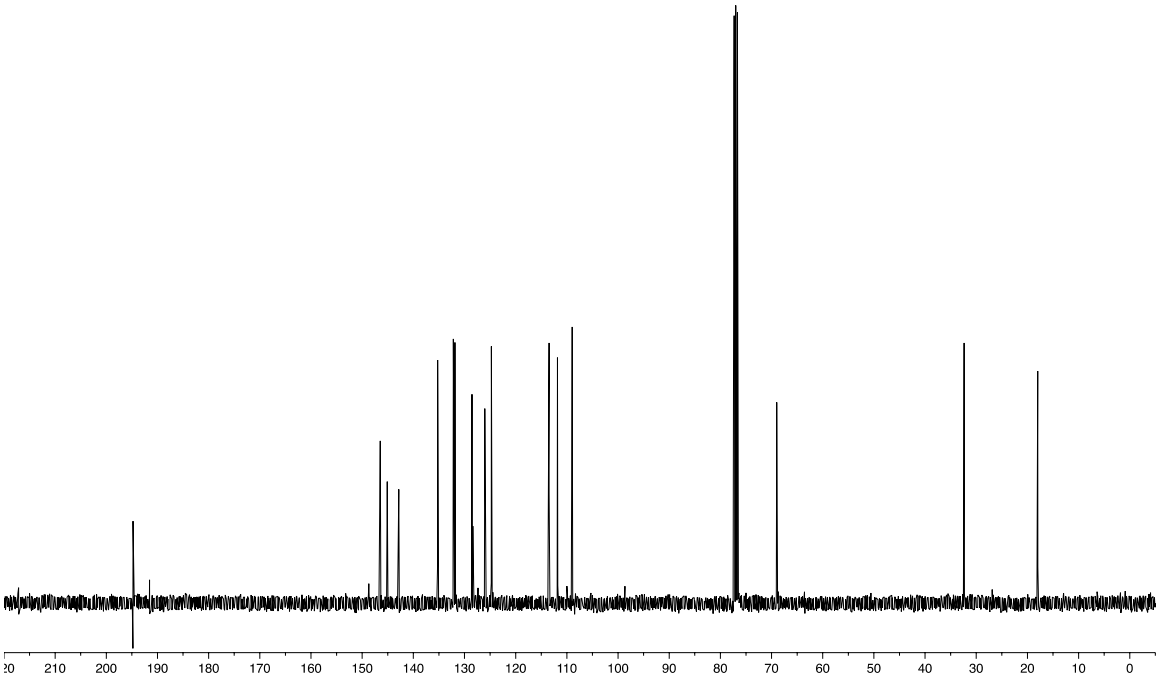

Figure B.17 ^{13}C-NMR spectrum (100 MHz; $CDCl_3$) of compound **4.18e**

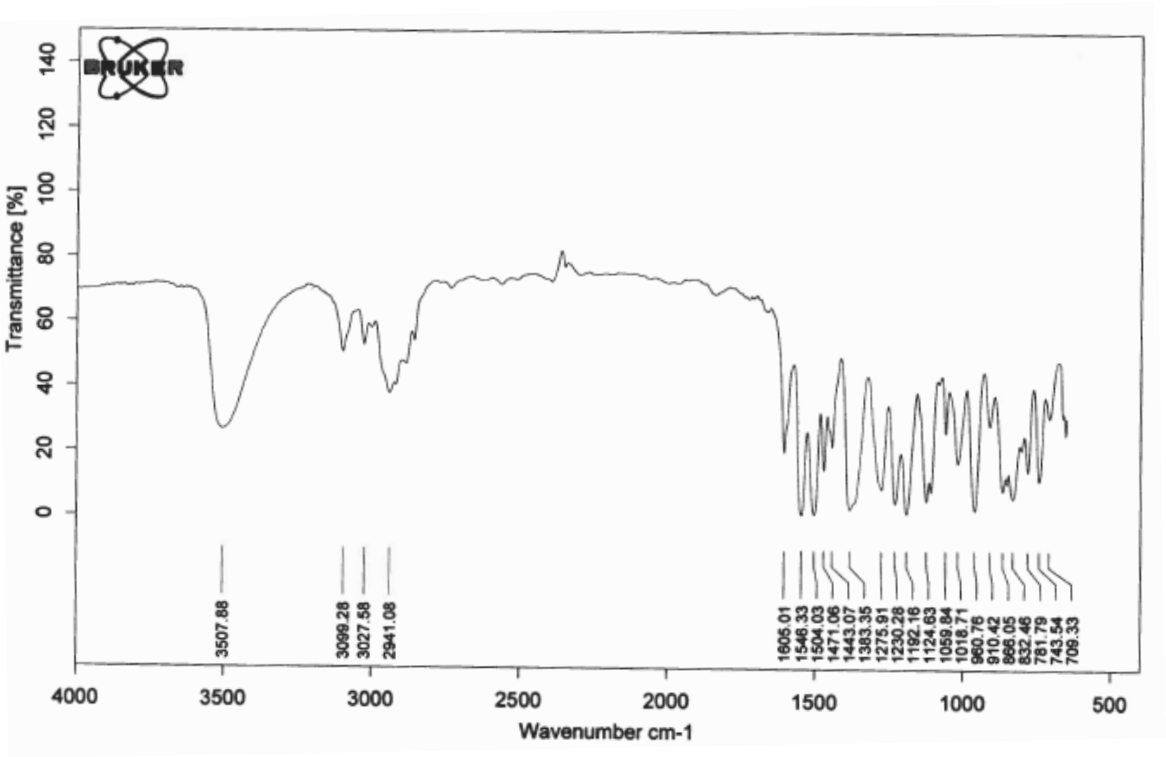

Figure B.18 FTIR spectrum (thin film/NaCl) of compound **4.18e**

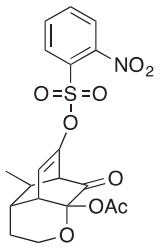

4.16e

Figure B.19 ^{1}H-NMR (400 MHz; Benzene-d_6) for compound **4.16e**

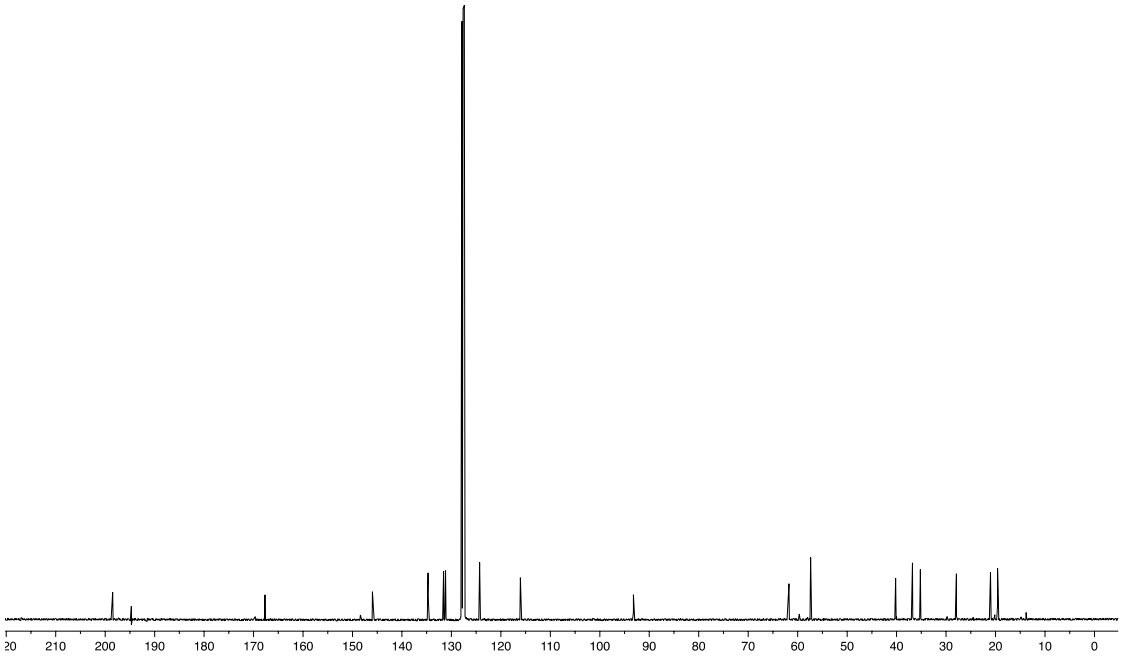

Figure B.20 ^{13}C-NMR spectrum (100 MHz; Benzene-D_6) of compound **4.16e**

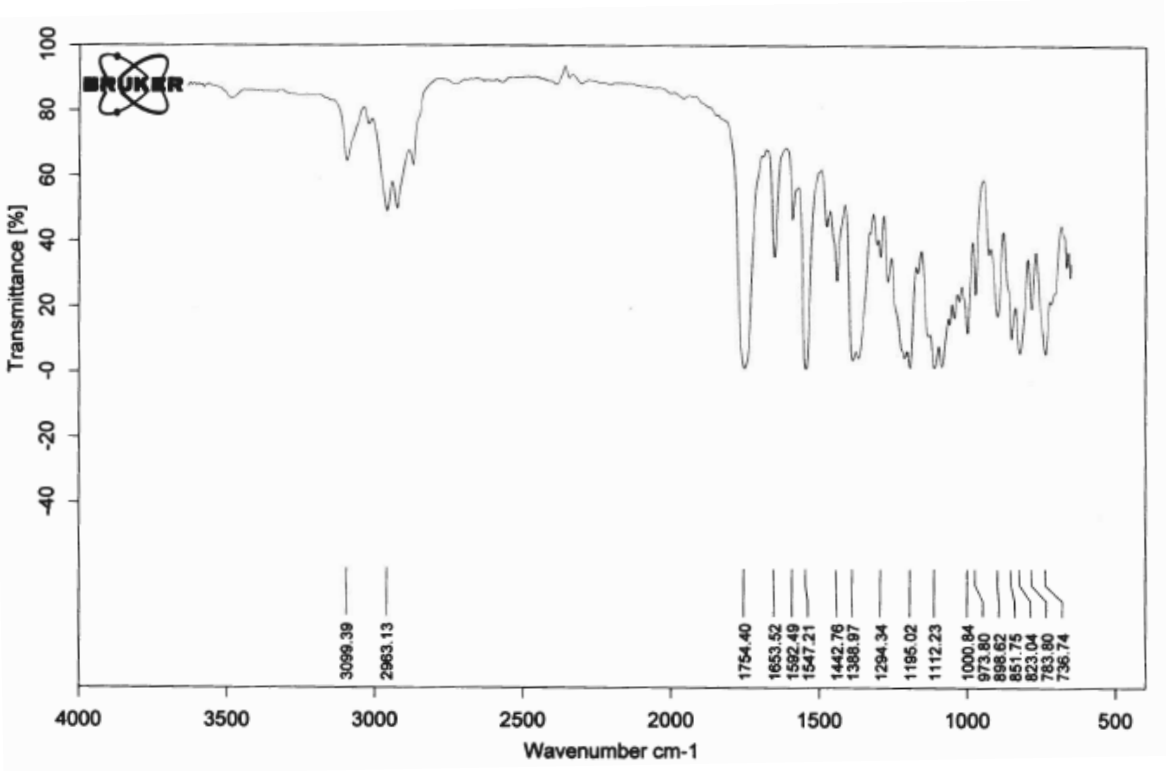

Figure B.21 FTIR spectrum (thin film/NaCl) of compound **4.16e**

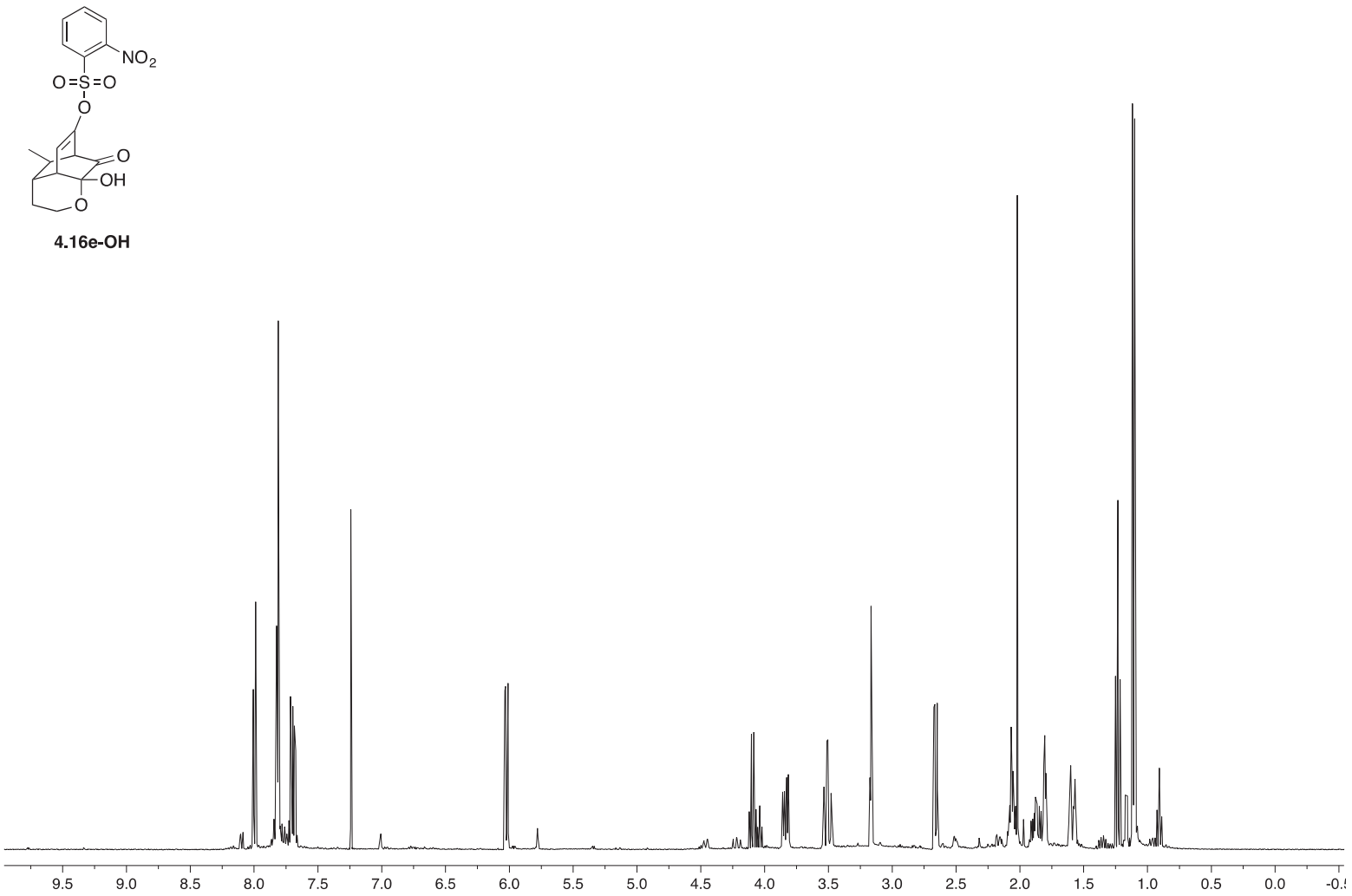

Figure B.22 ^{1}H-NMR (400 MHz; $CDCl_3$) for compound **4.16e-OH**

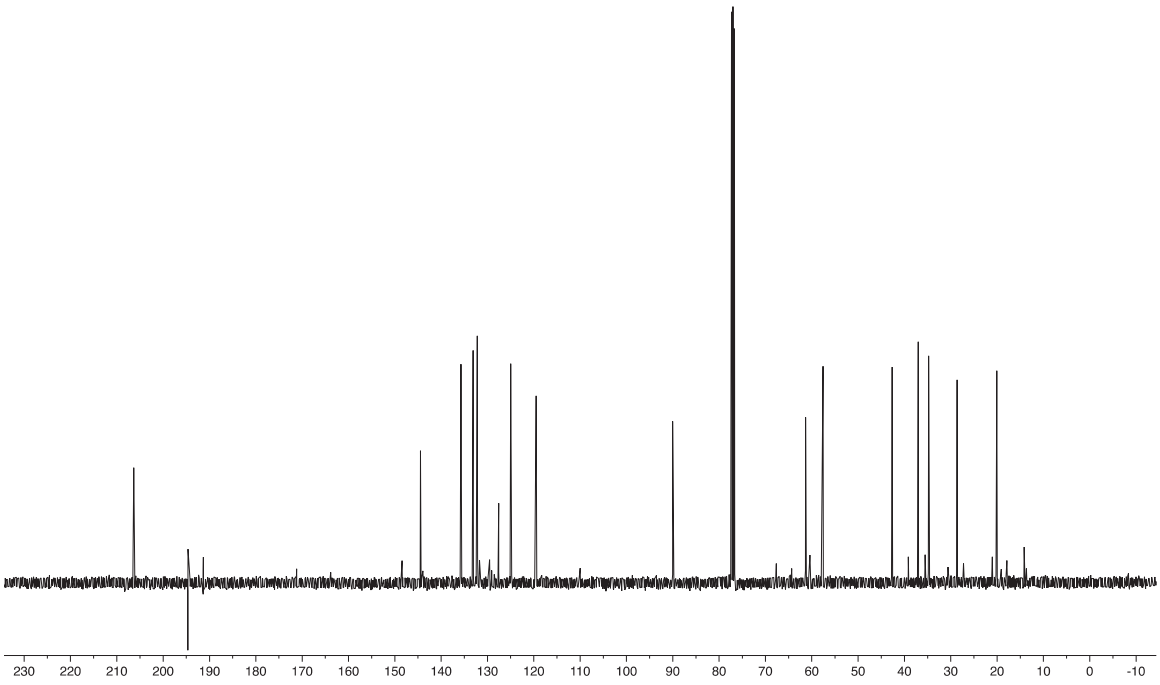

Figure B.23 ^{13}C-NMR spectrum (100 MHz; $CDCl_3$) of compound **4.16e-OH**

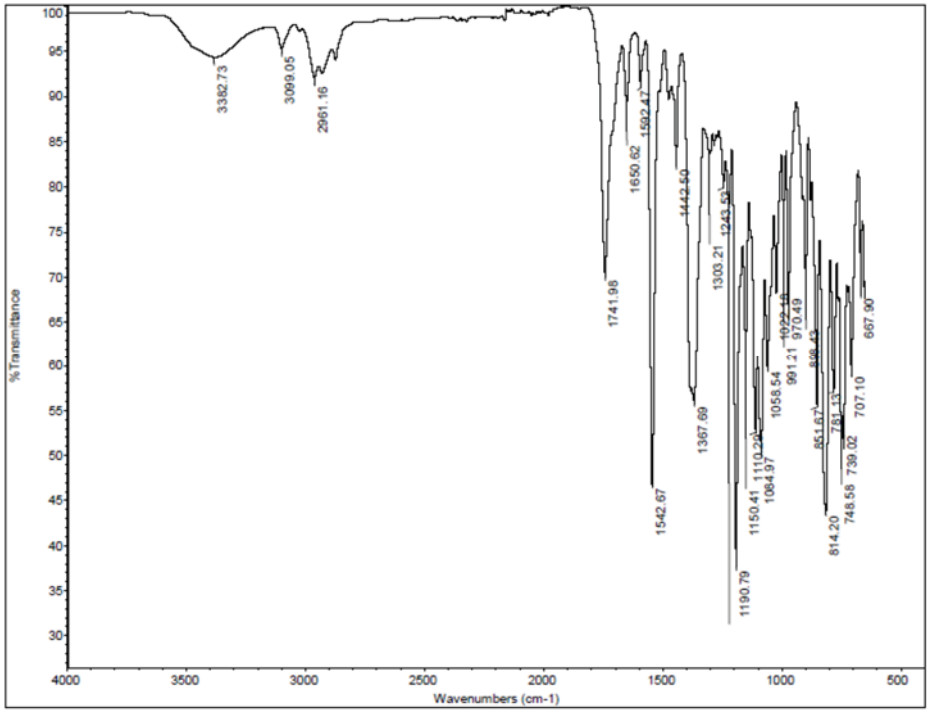

Figure B.24 FTIR spectrum (neat) of compound **4.16e-OH**

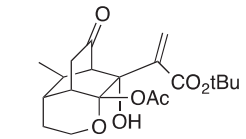

4.27

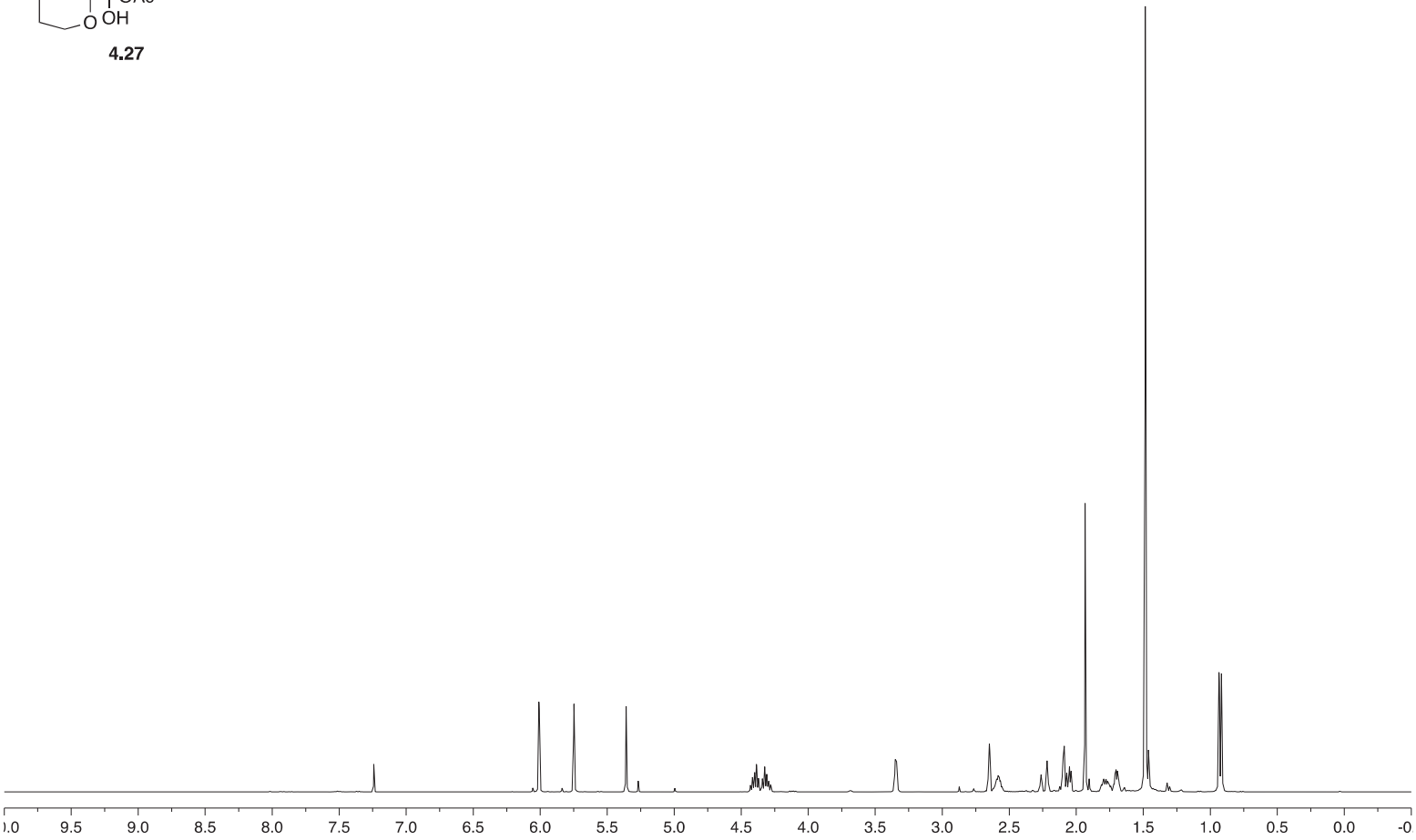

Figure B.25 ^{1}H-NMR (400 MHz; $CDCl_3$) for compound **4.27**

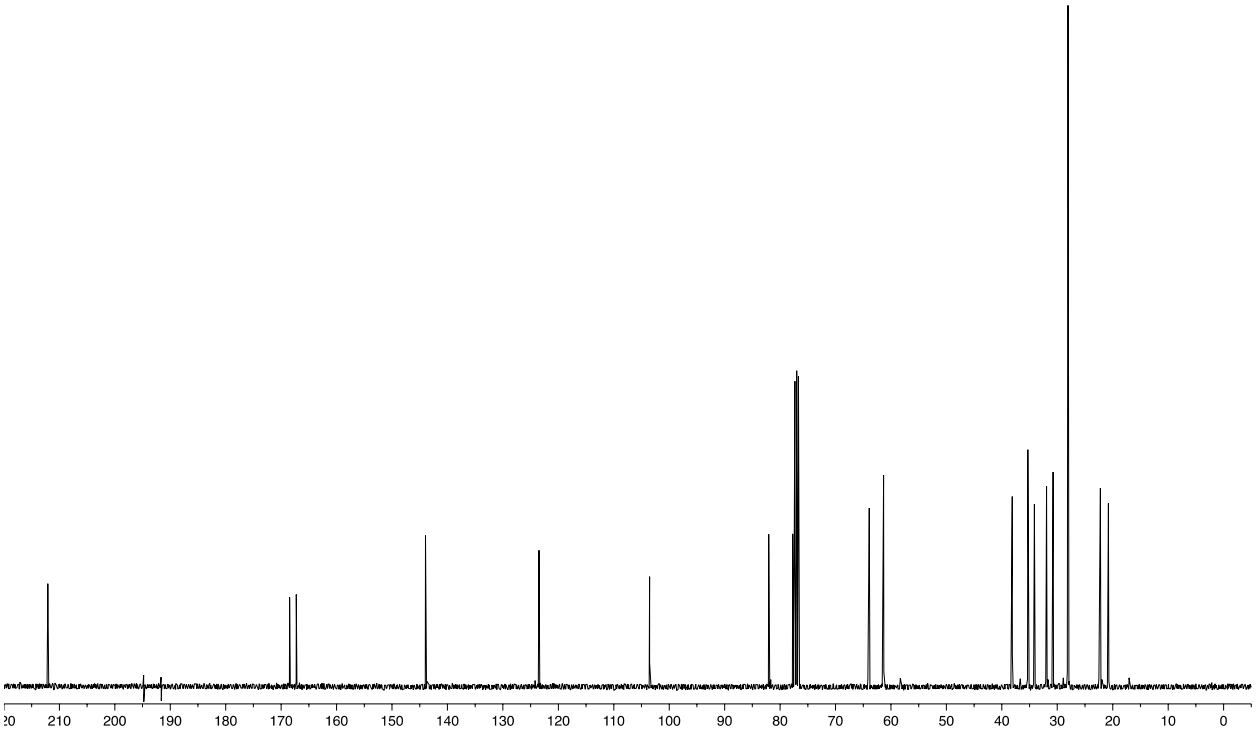

Figure B.26 ^{13}C-NMR spectrum (100 MHz; $CDCl_3$) of compound **4.27**

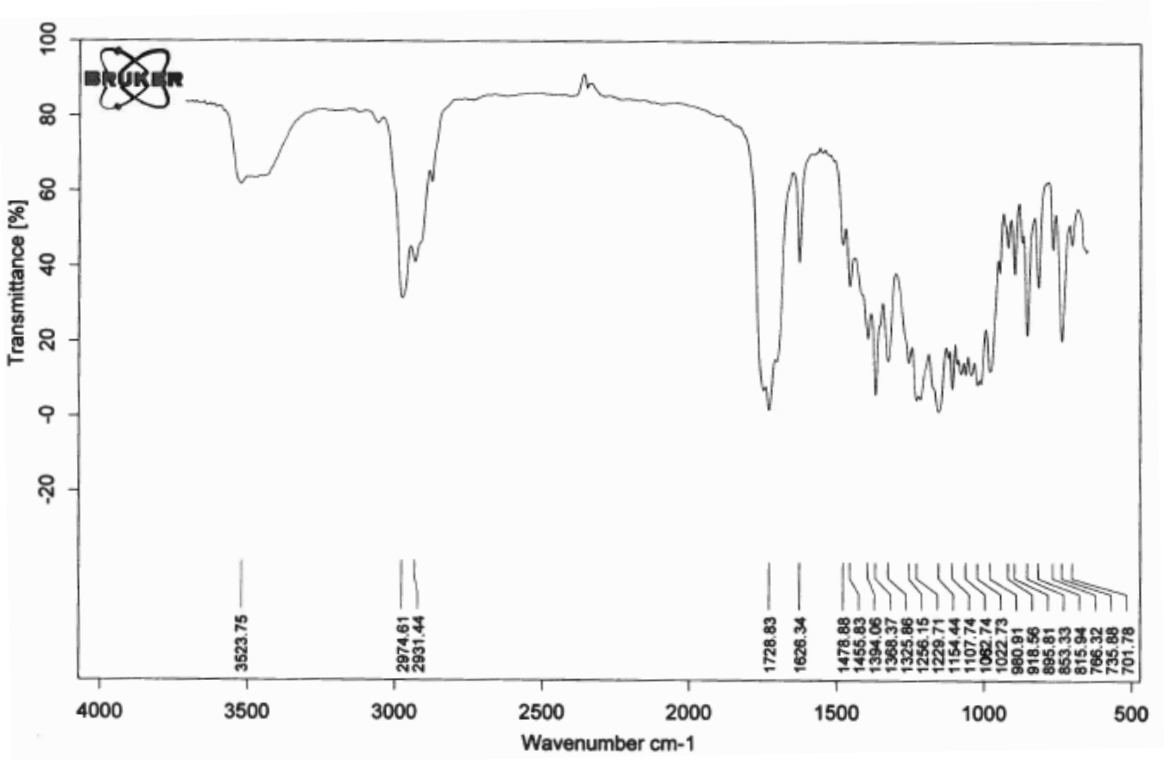

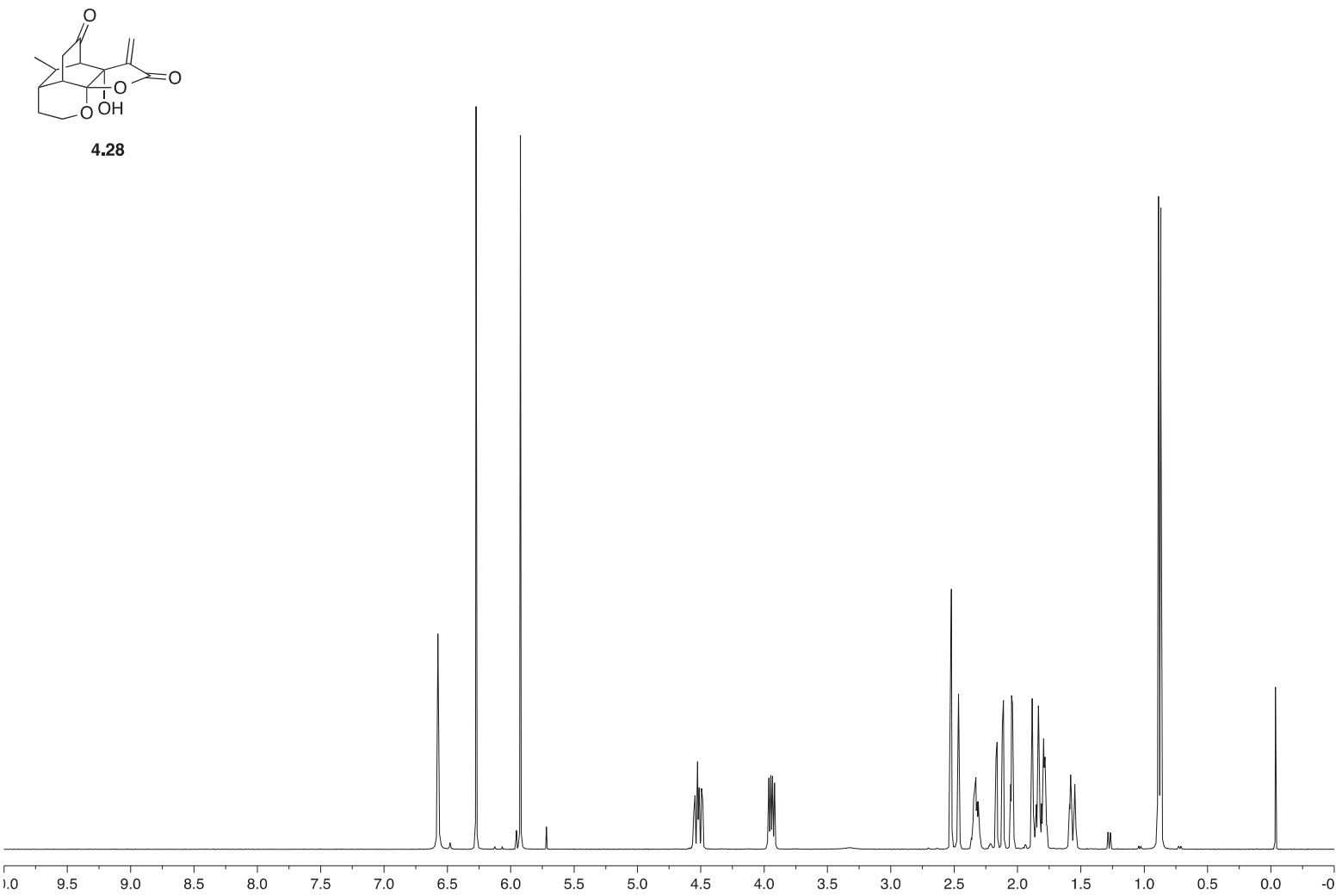

Figure B.28 ^{1}H-NMR (400 MHz; DMSO-d_6) for compound **4.28**

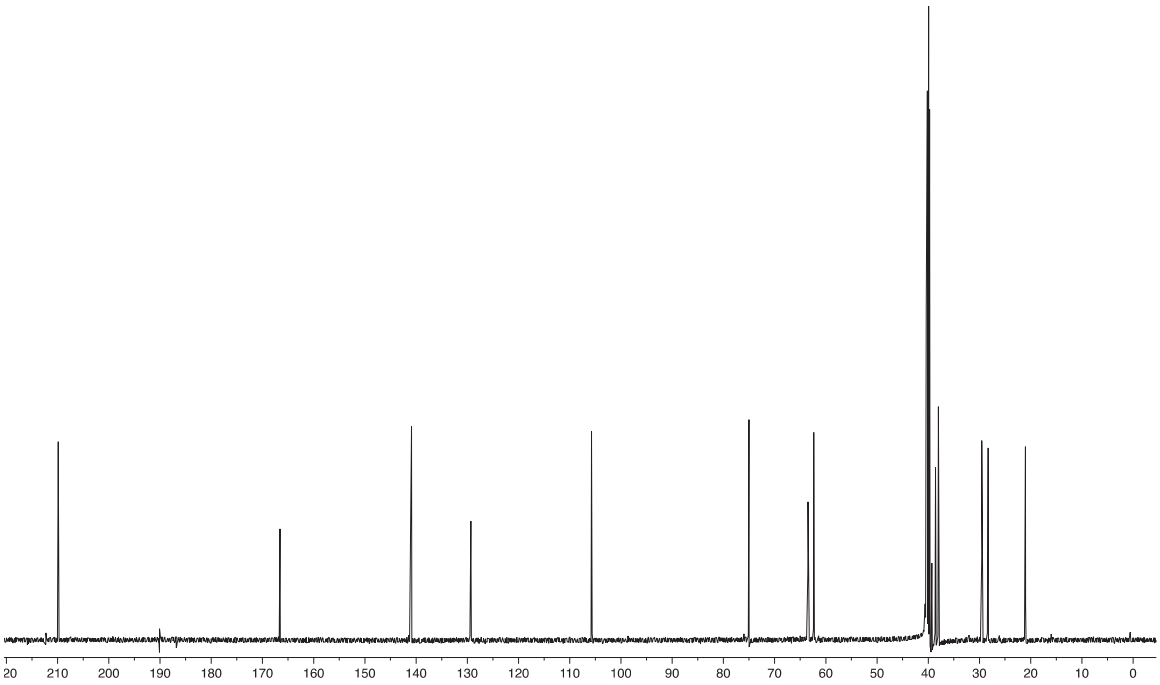

Figure B.29 ^{13}C-NMR spectrum (100 MHz; DMSO-d_6) of compound **4.28**

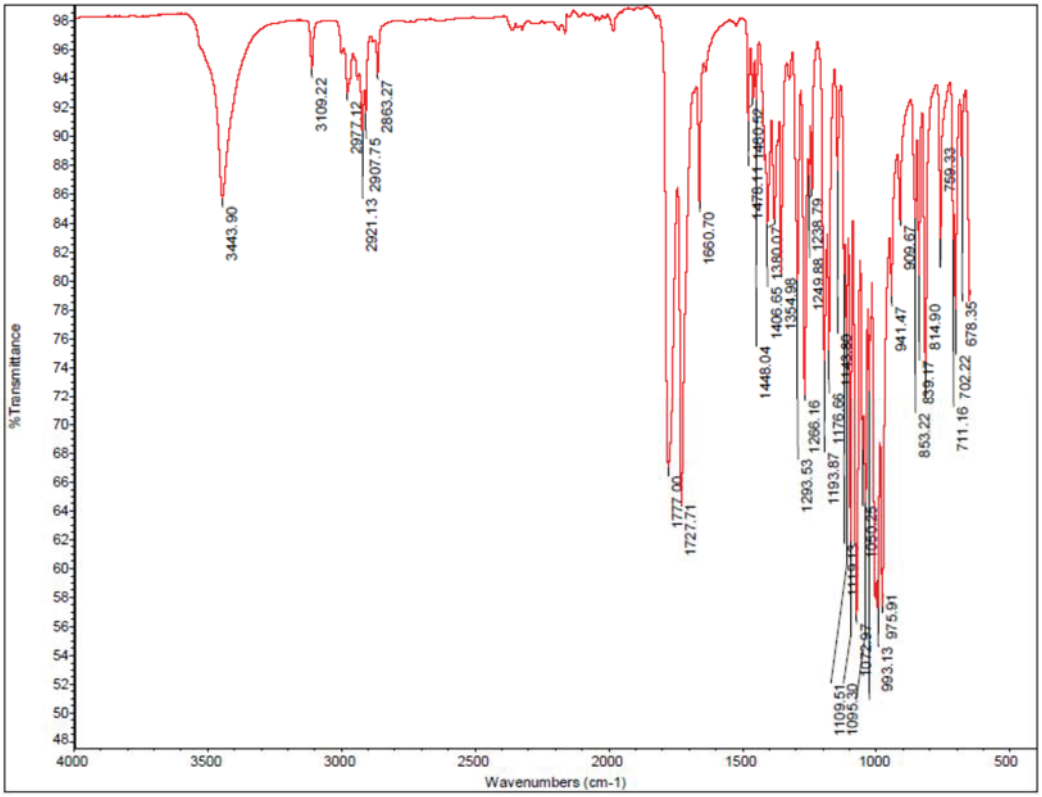

Figure B.30 FTIR spectrum (neat) of compound **4.28**

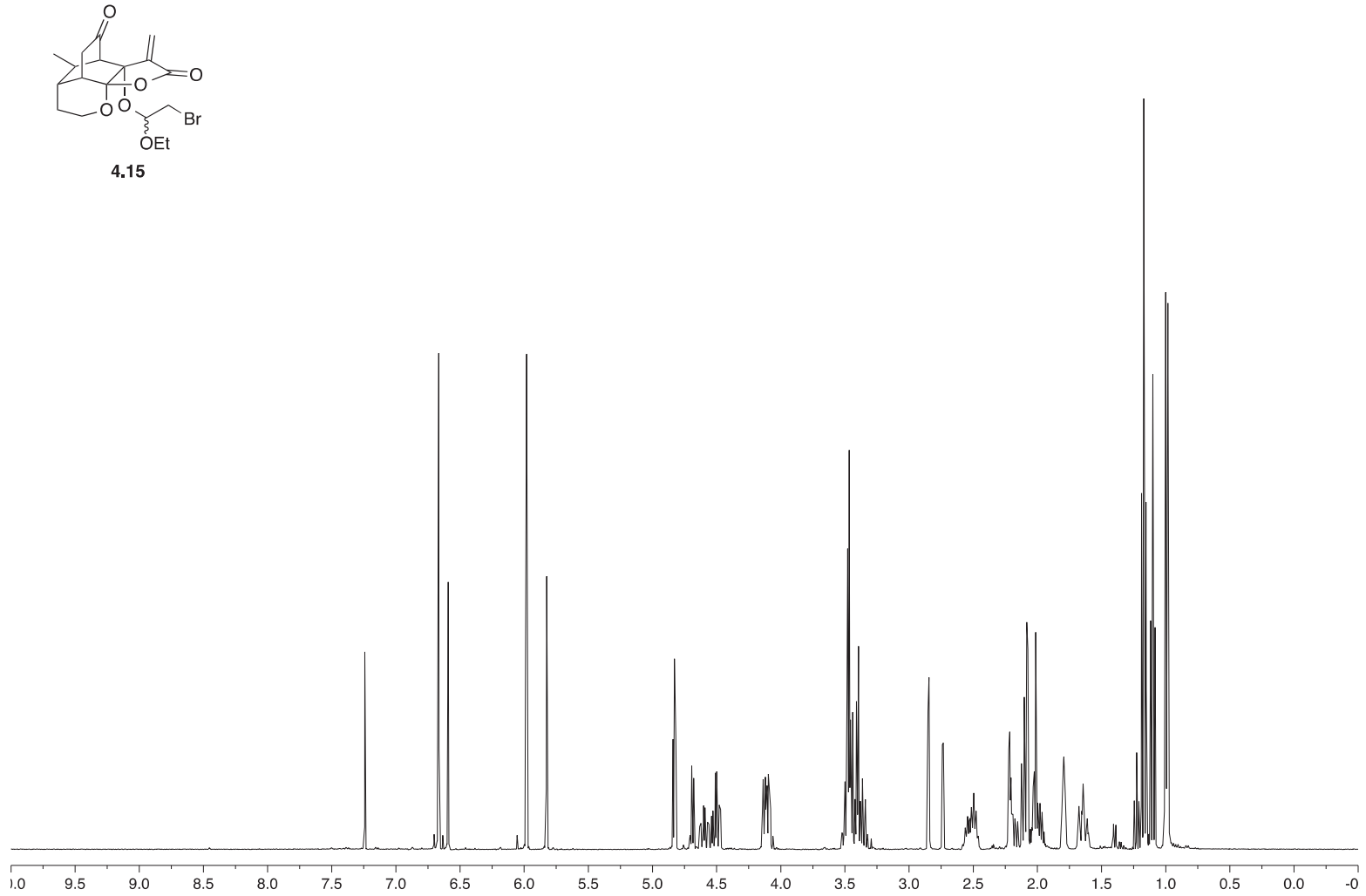

Figure B.31 ^{1}H-NMR (400 MHz; $CDCl_3$) for compound **4.15**

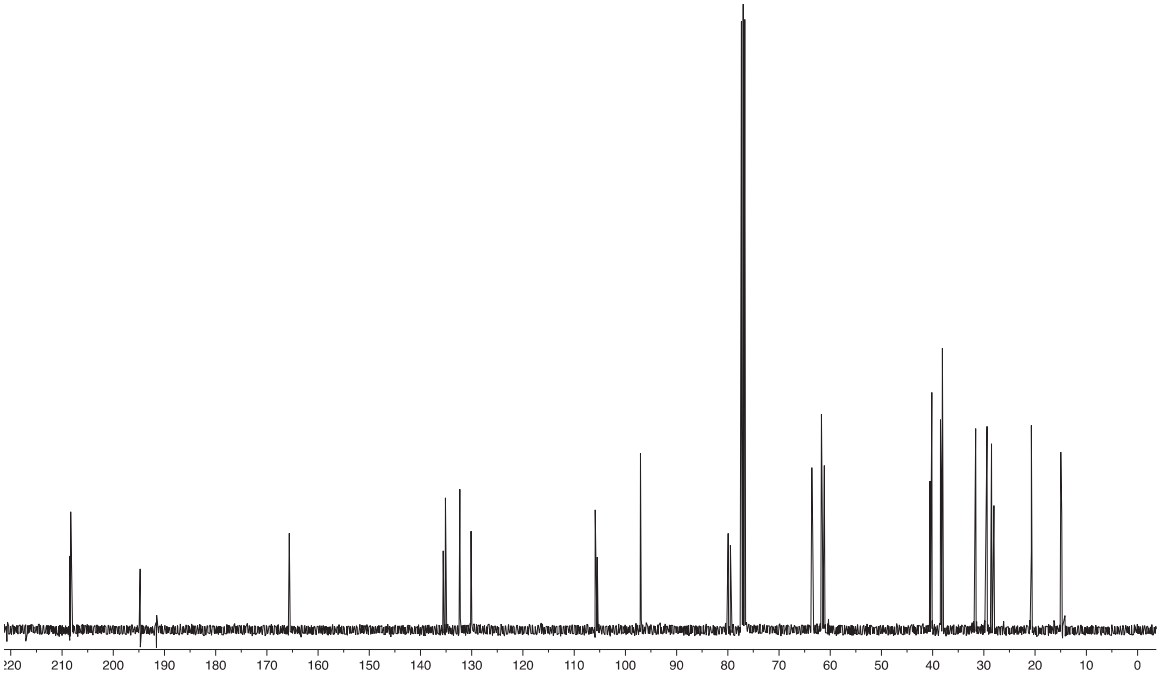

Figure B.32 ^{13}C-NMR spectrum (100 MHz; $CDCl_3$) of compound **4.15**

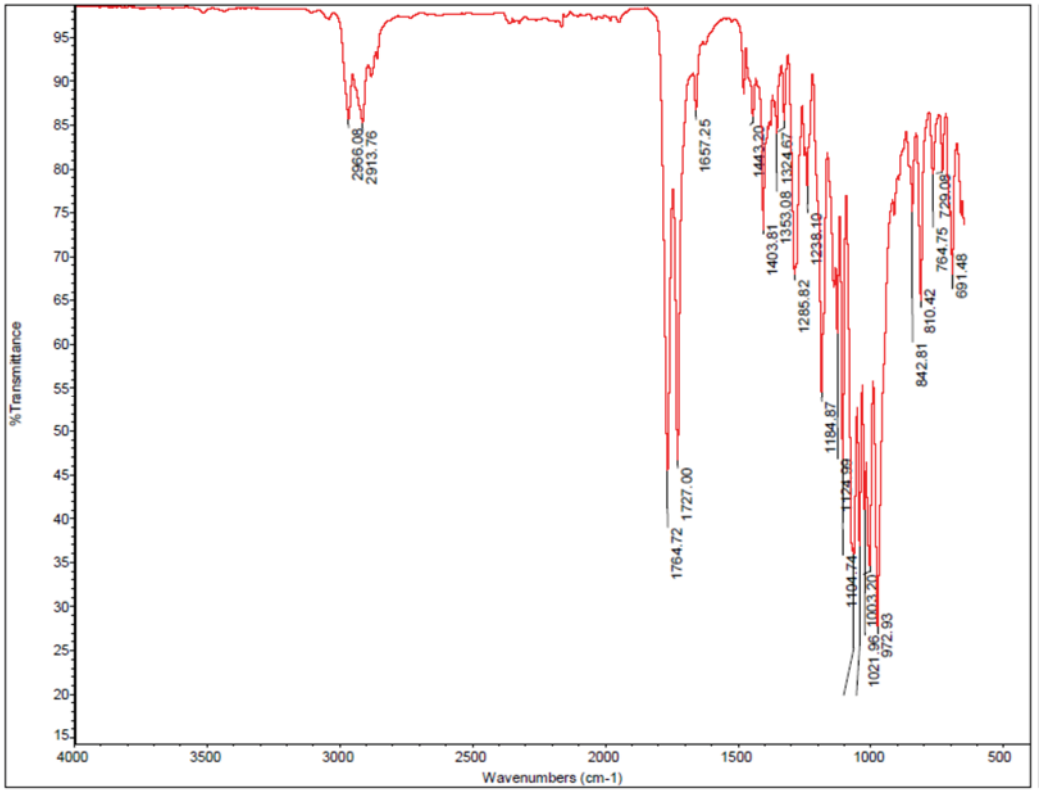

Figure B.33 FTIR spectrum (neat) of compound **4.15**

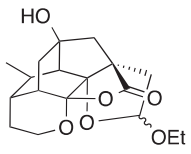

4.14
Diastereomer A

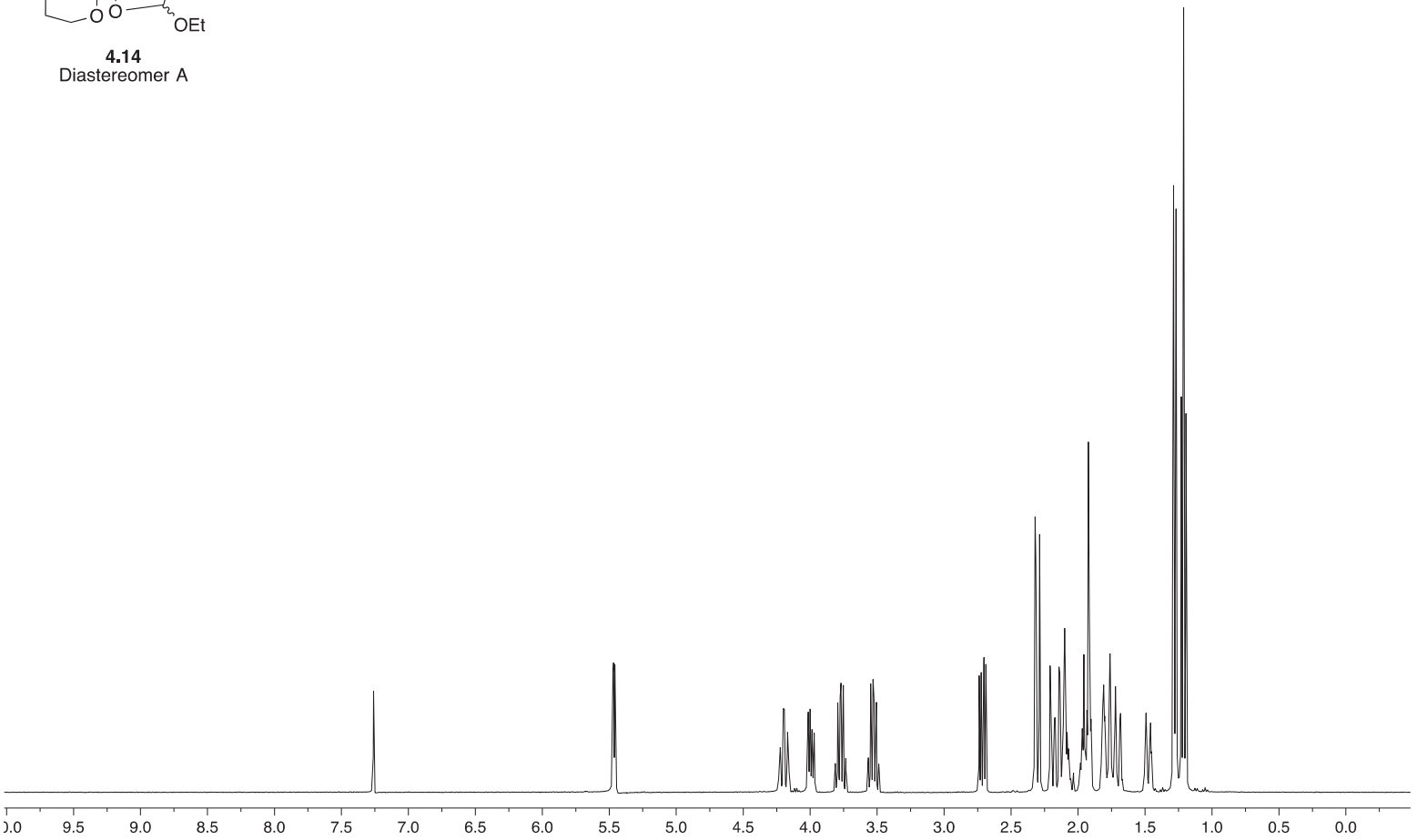

Figure B.34 ^{1}H-NMR (400 MHz; $CDCl_3$) for compound **4.14** Diastereomer A

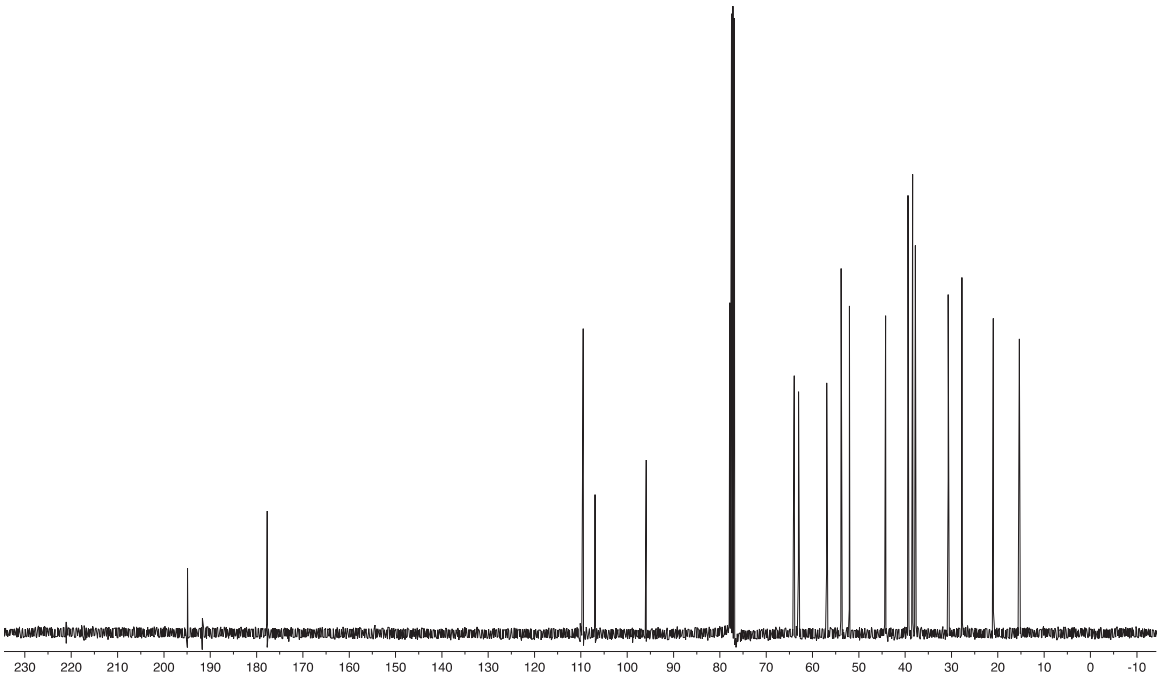

Figure B.35 ^{13}C-NMR spectrum (100 MHz; $CDCl_3$) of compound **4.14** Diastereomer A

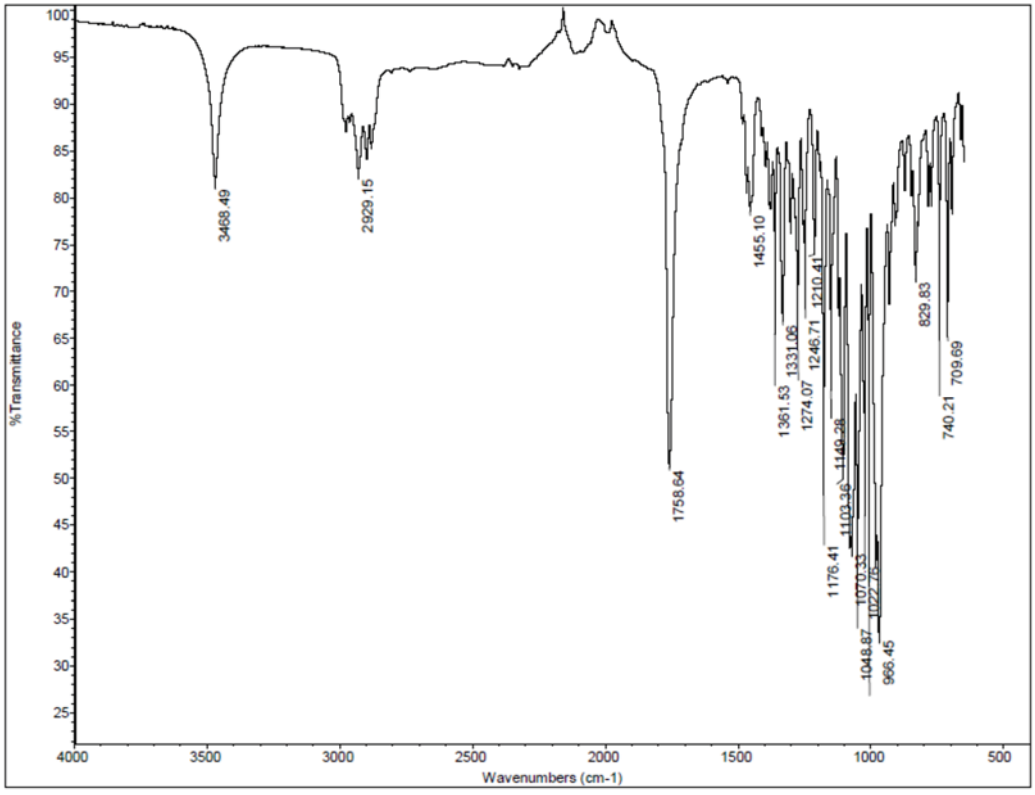

Figure B.36 FTIR spectrum (neat) of compound **4.14** Diastereomer A

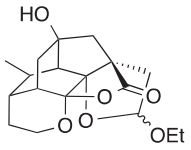

4.14
Diastereomer B

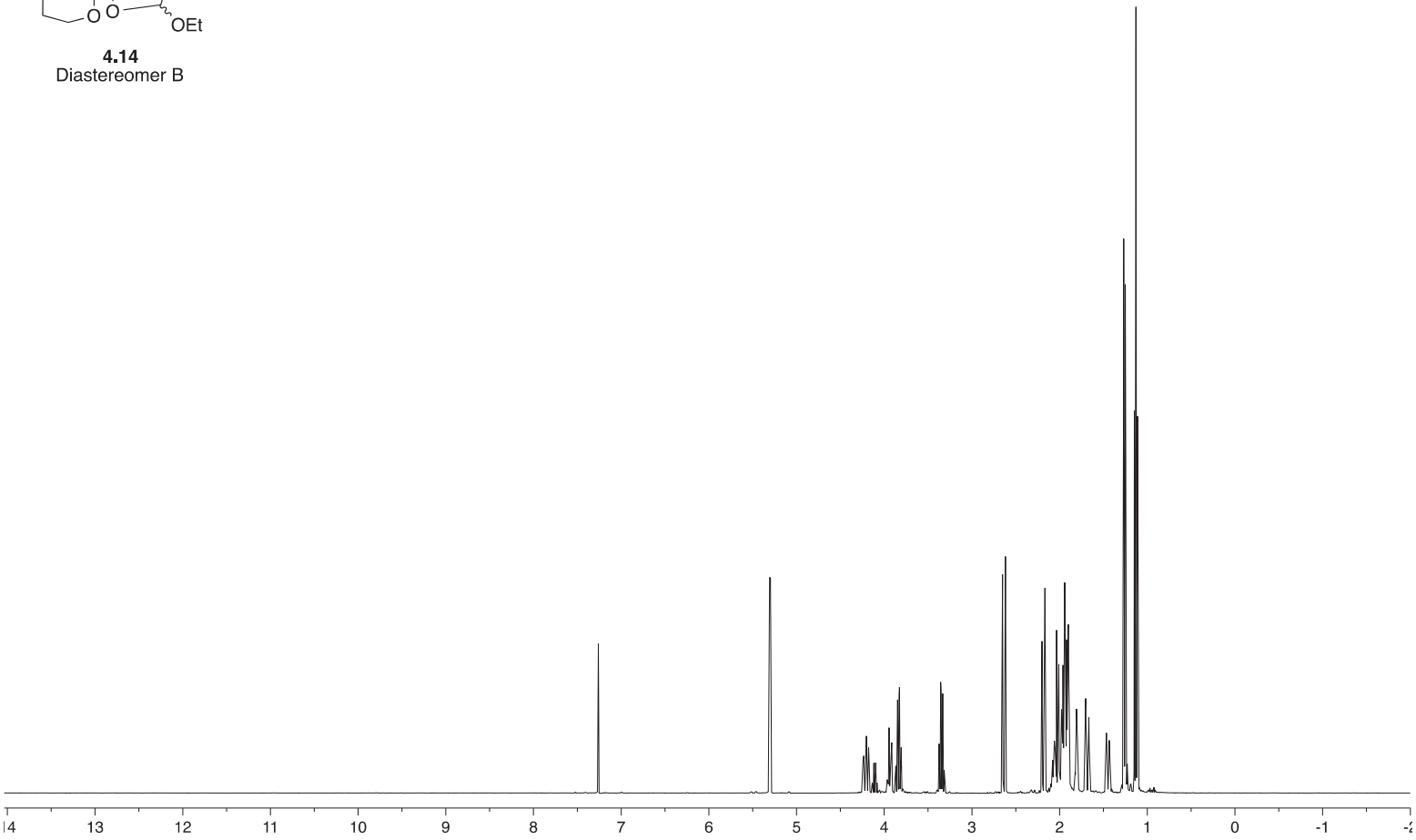

Figure B.37 ^{1}H-NMR (400 MHz; $CDCl_3$) for compound **4.14** Diastereomer B

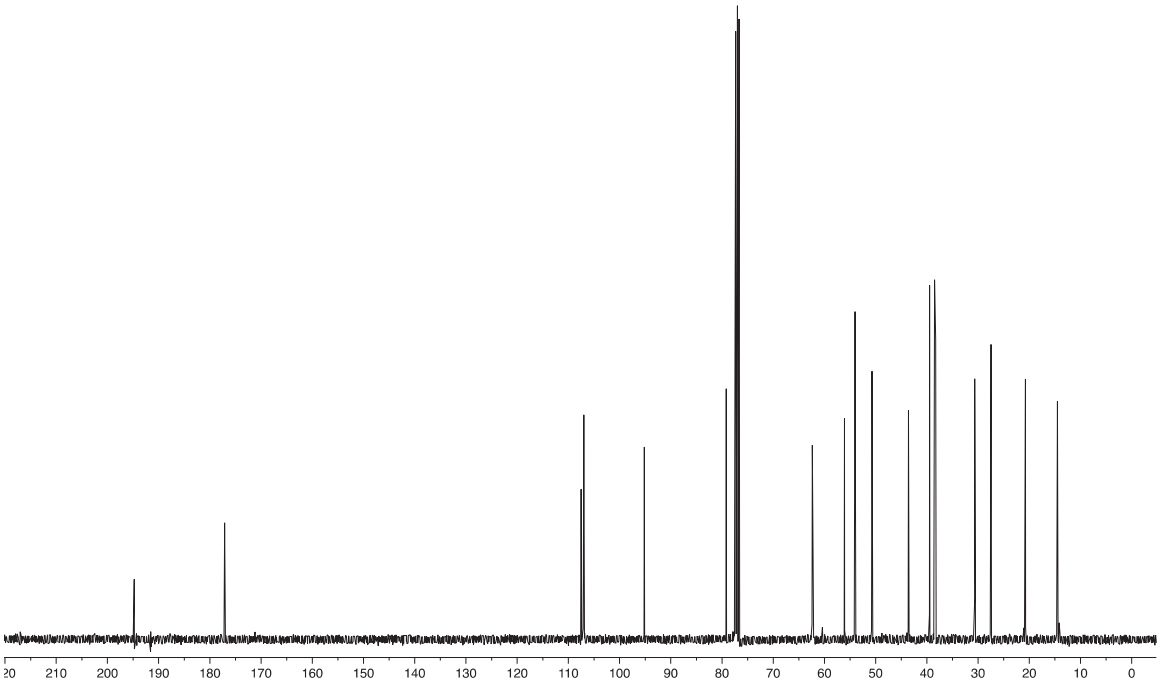

Figure B.38 ^{13}C-NMR spectrum (100 MHz; $CDCl_3$) of compound **4.14** Diastereomer B

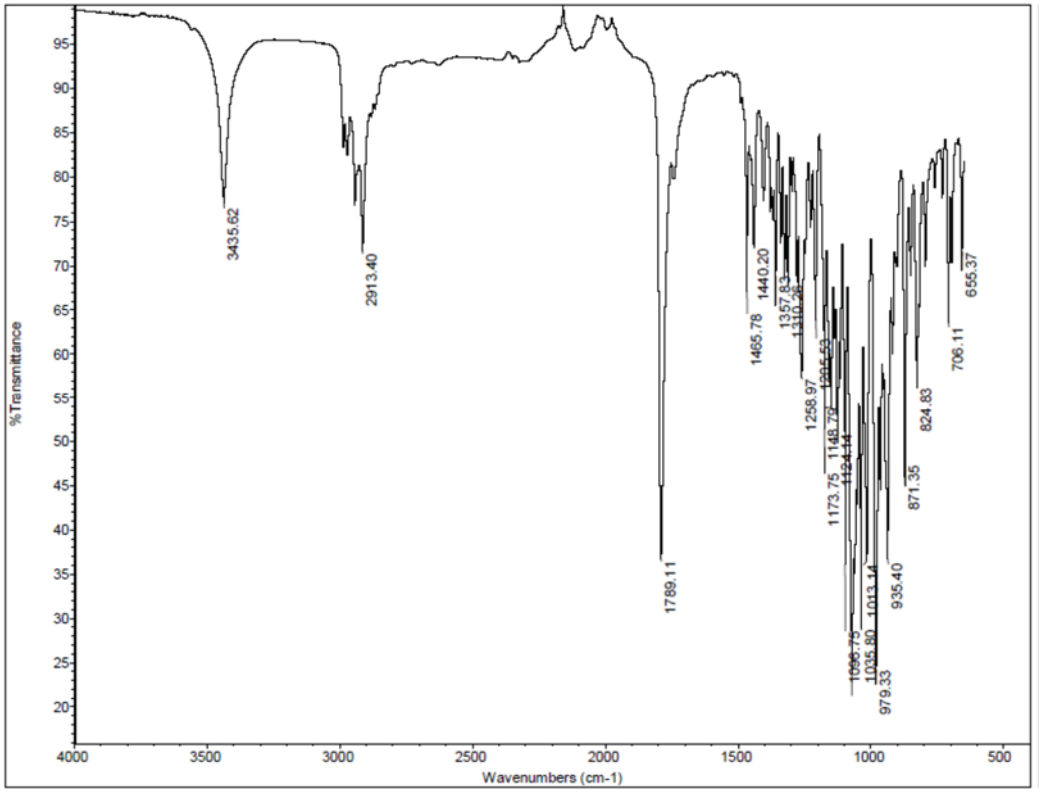

Figure B.39 FTIR spectrum (neat) of compound **4.14** Diastereomer B

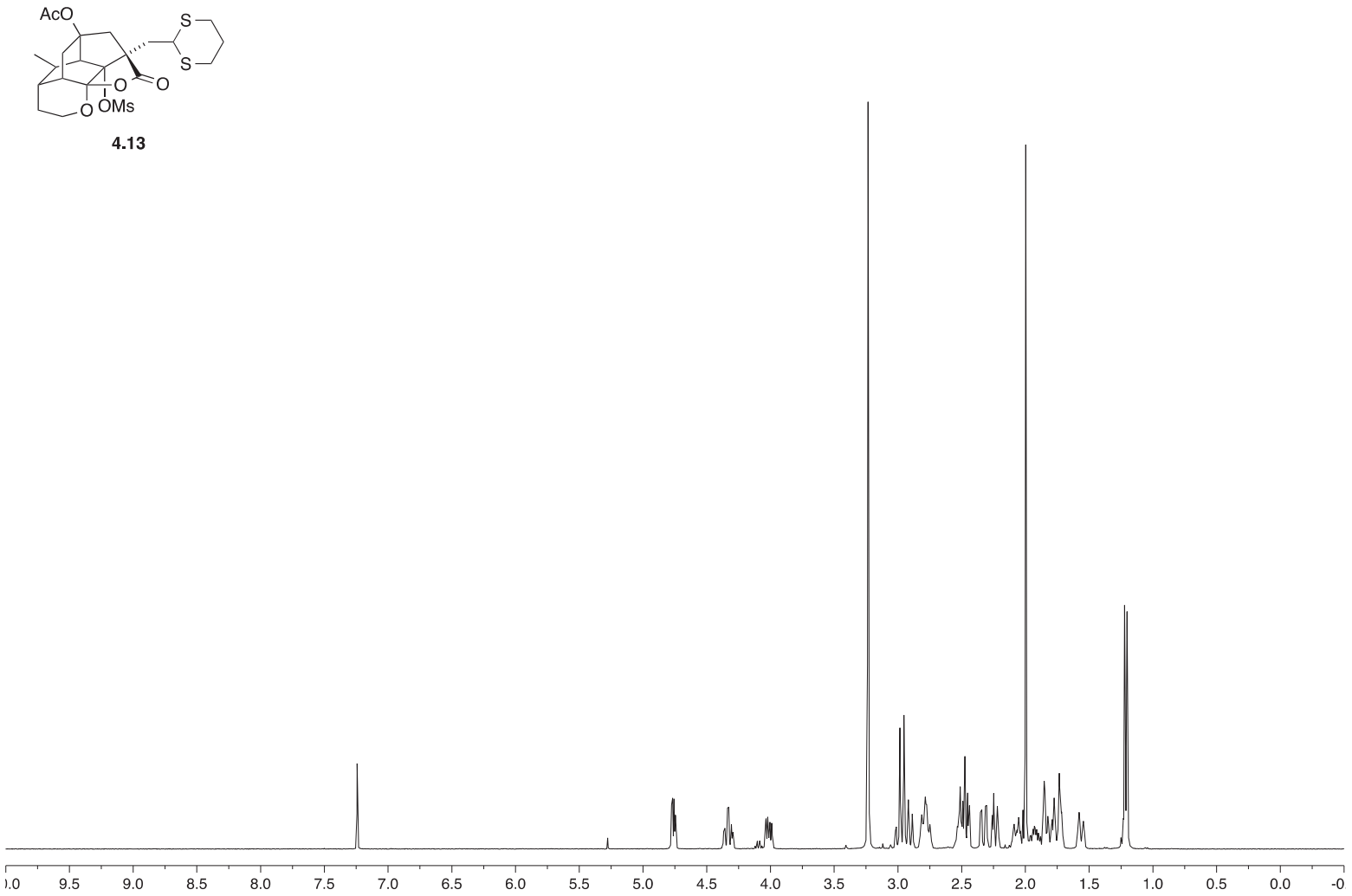

Figure B.40 ^{1}H-NMR (400 MHz; $CDCl_3$) for compound **4.13**

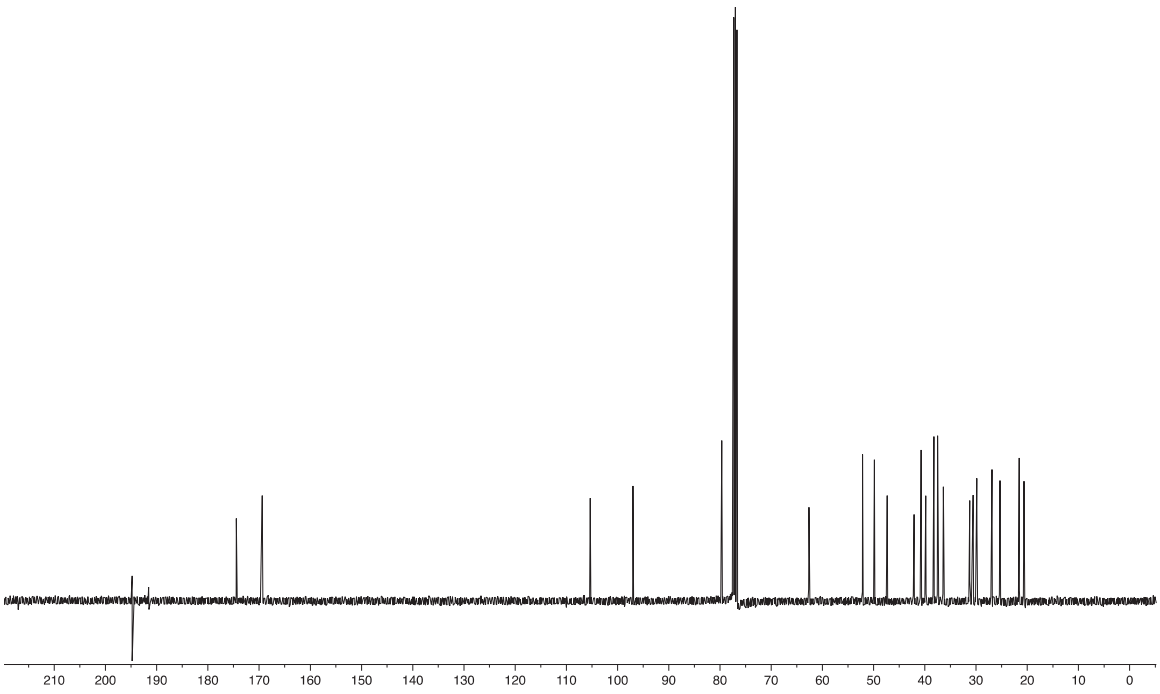

Figure B.41 ^{13}C-NMR specrum (100 MHz; $CDCl_3$) of compound **4.13**

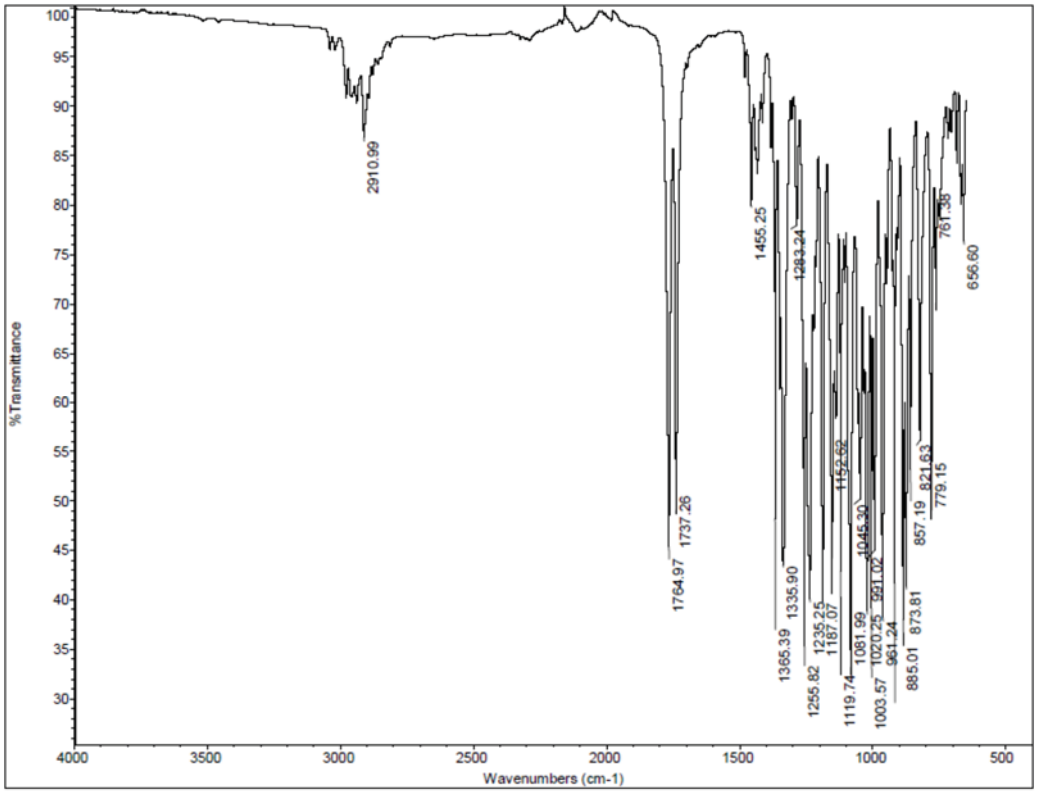

Figure B.42 FTIR spectrum (neat) of compound **4.13**

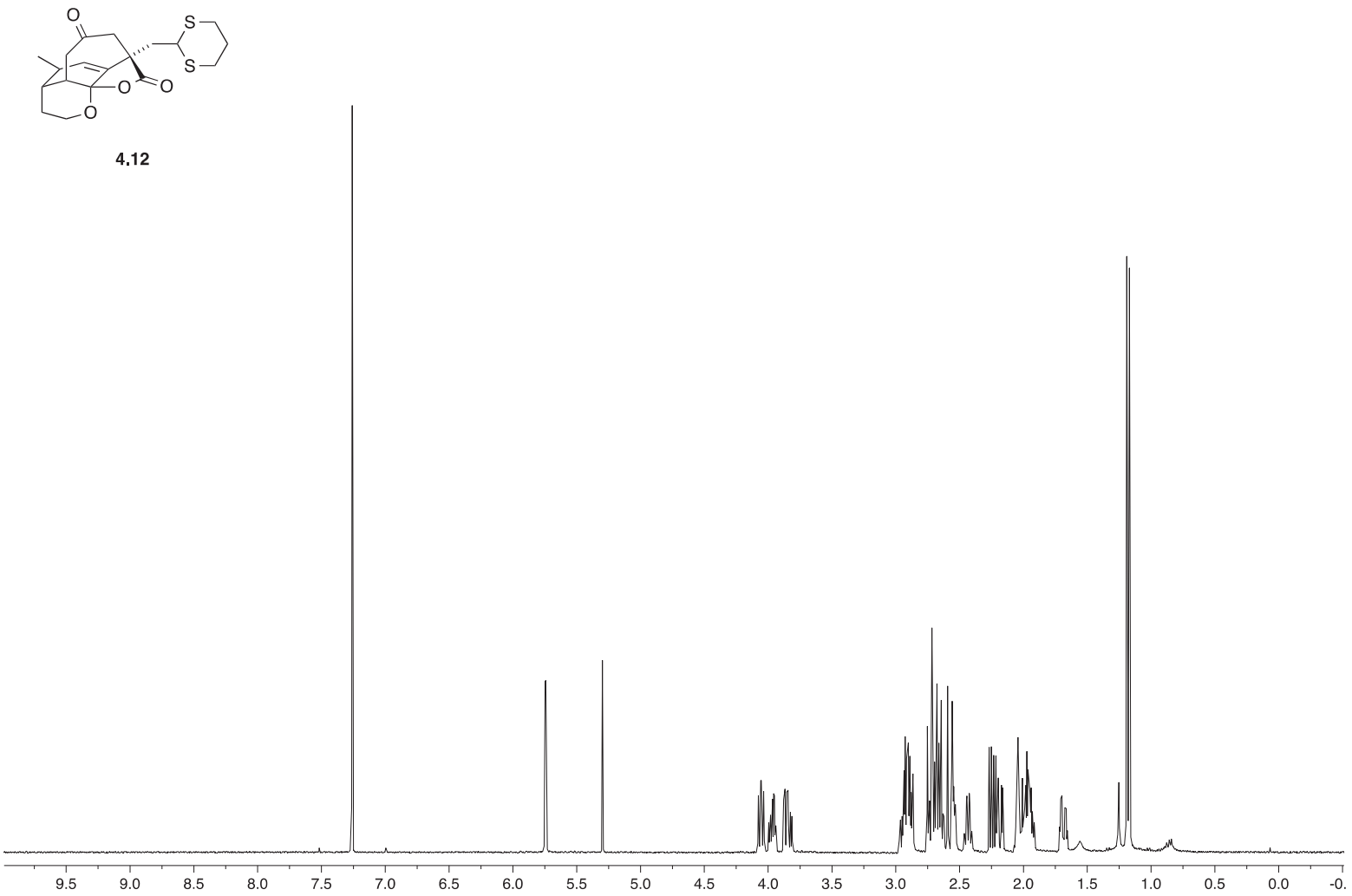

Figure B.43 ^{1}H-NMR (400 MHz; $CDCl_3$) for compound **4.12**

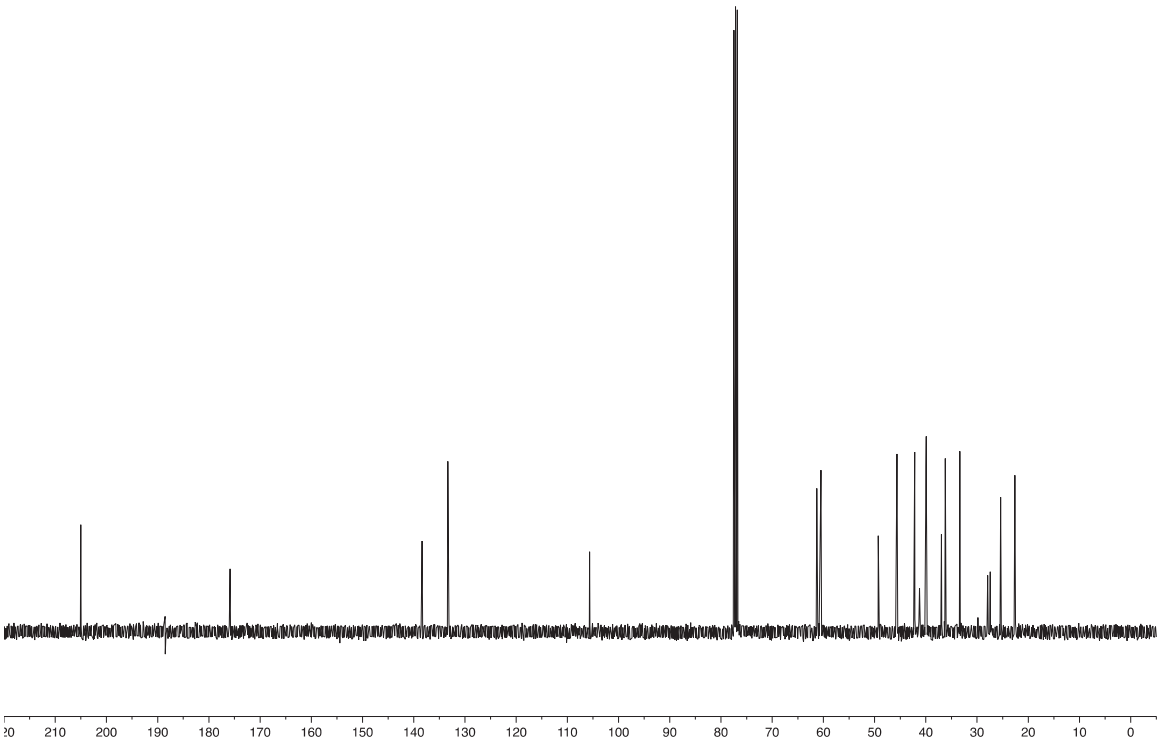

Figure B.44 ^{13}C-NMR spectrum (100 MHz; $CDCl_3$) of compound **4.12**

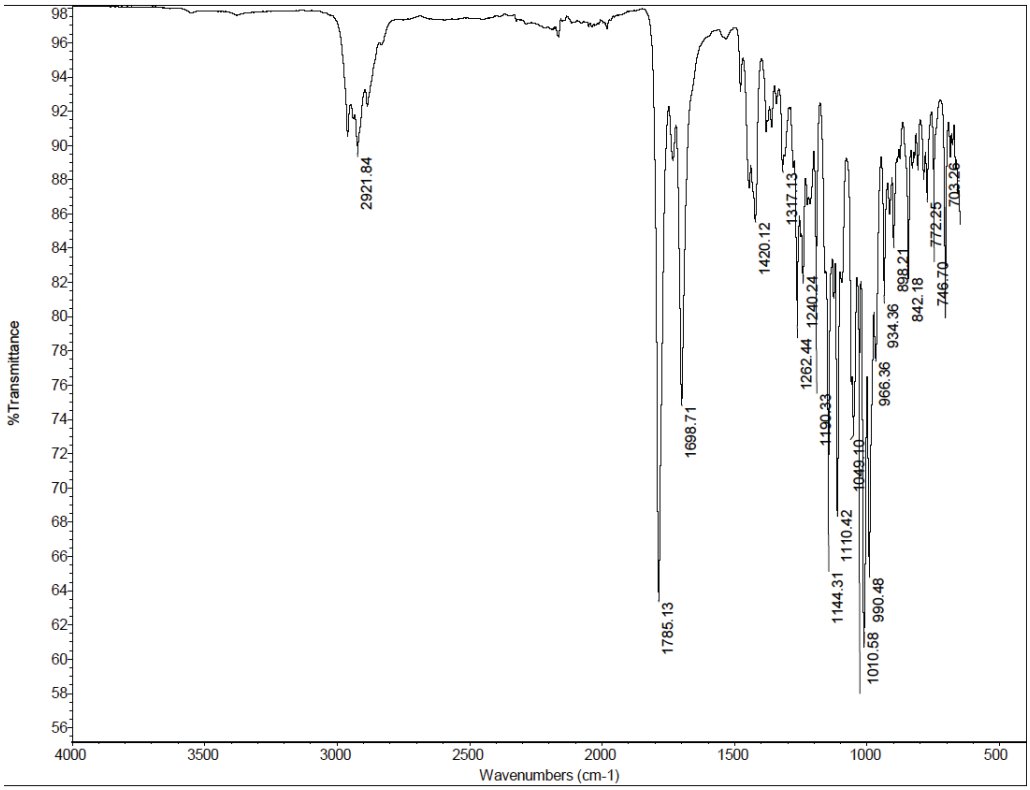

Figure B.45 FTIR spectrum (neat) of compound **4.12**

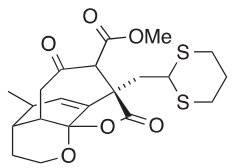

4.32

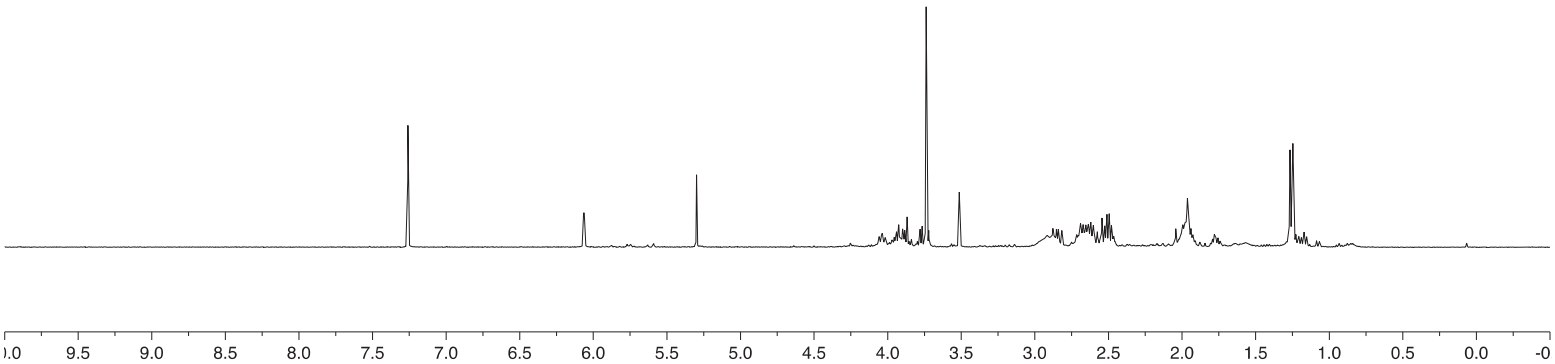

Figure B.46 ^{1}H-NMR (400 MHz; $CDCl_3$) for compound **4.32**

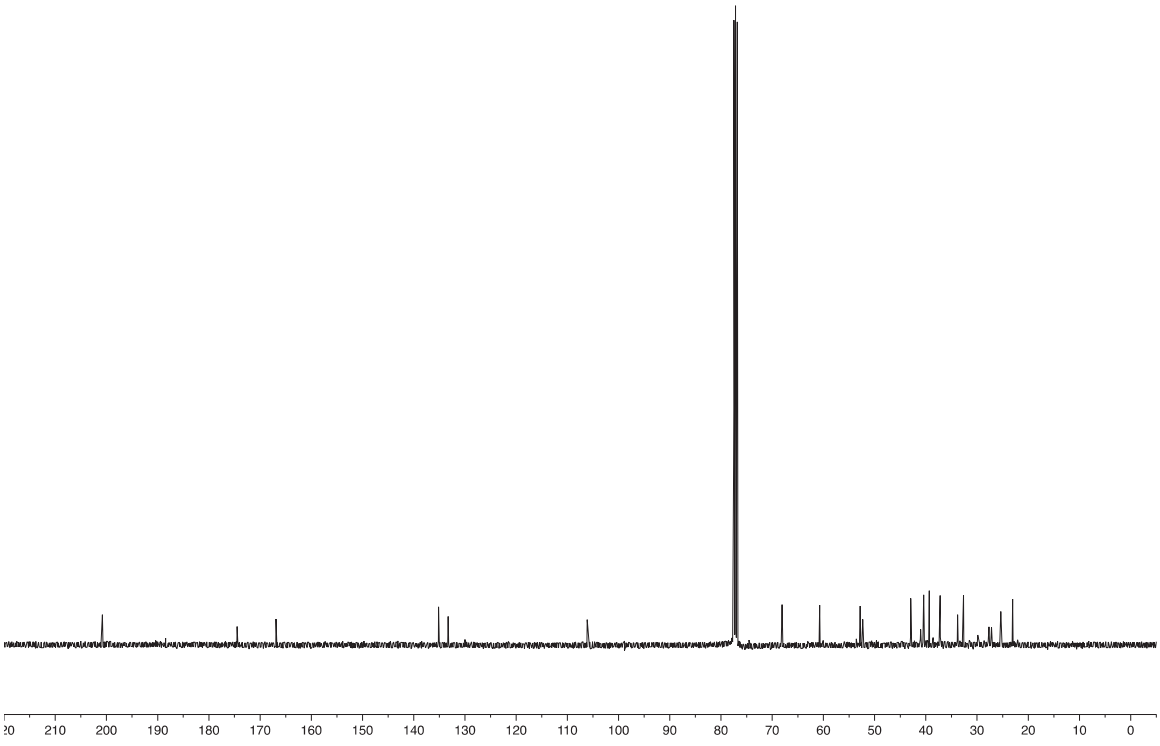

Figure B.47 ^{13}C-NMR spectrum (100 MHz; $CDCl_3$) of compound **4.32**

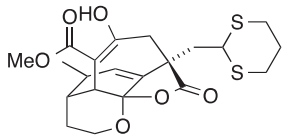

4.31

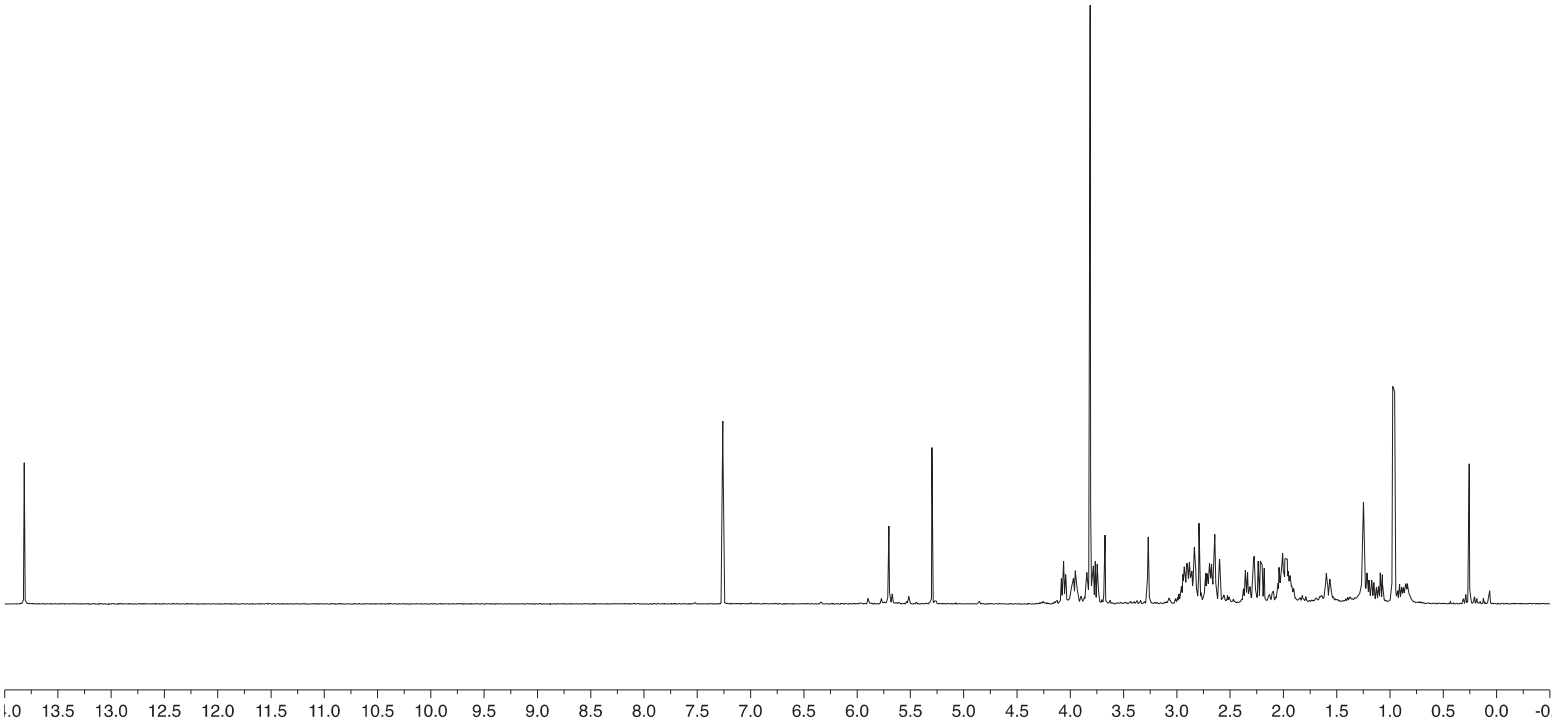

Figure B.48 ^{1}H-NMR (400 MHz; $CDCl_3$) for compound **4.31**

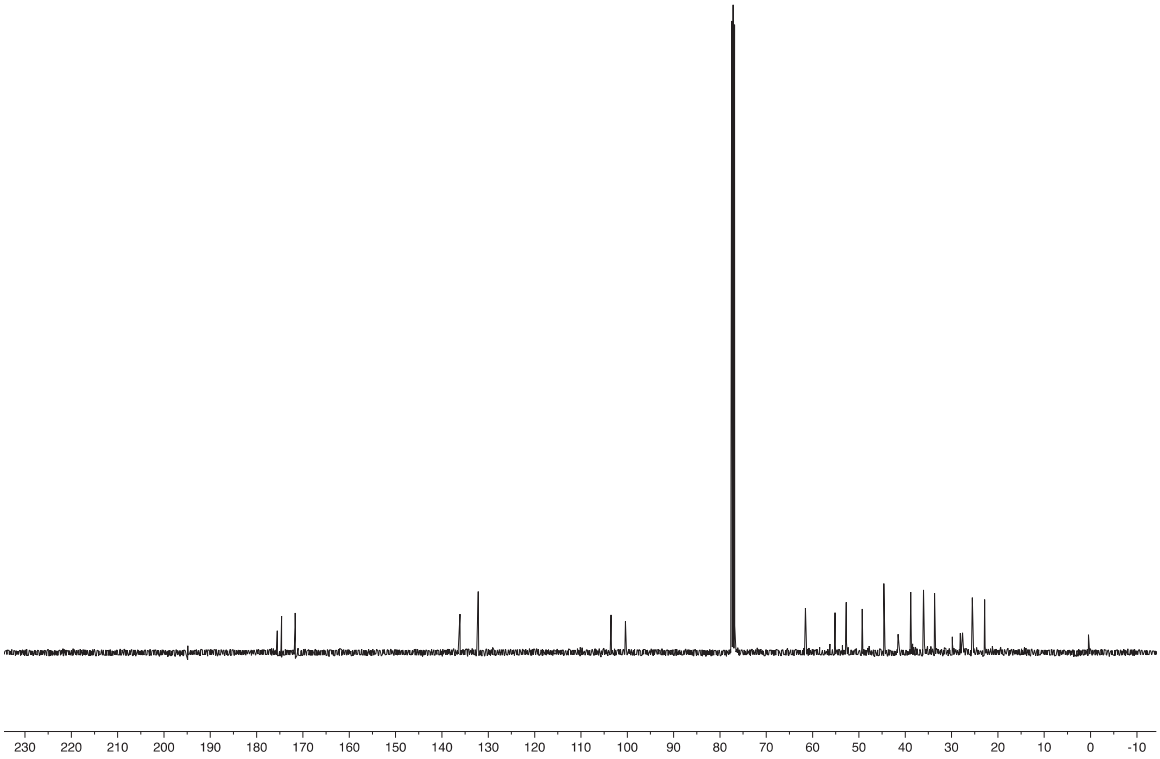

Figure B.49 ^{13}C-NMR (100 MHz; $CDCl_3$) for Compound **4.31**

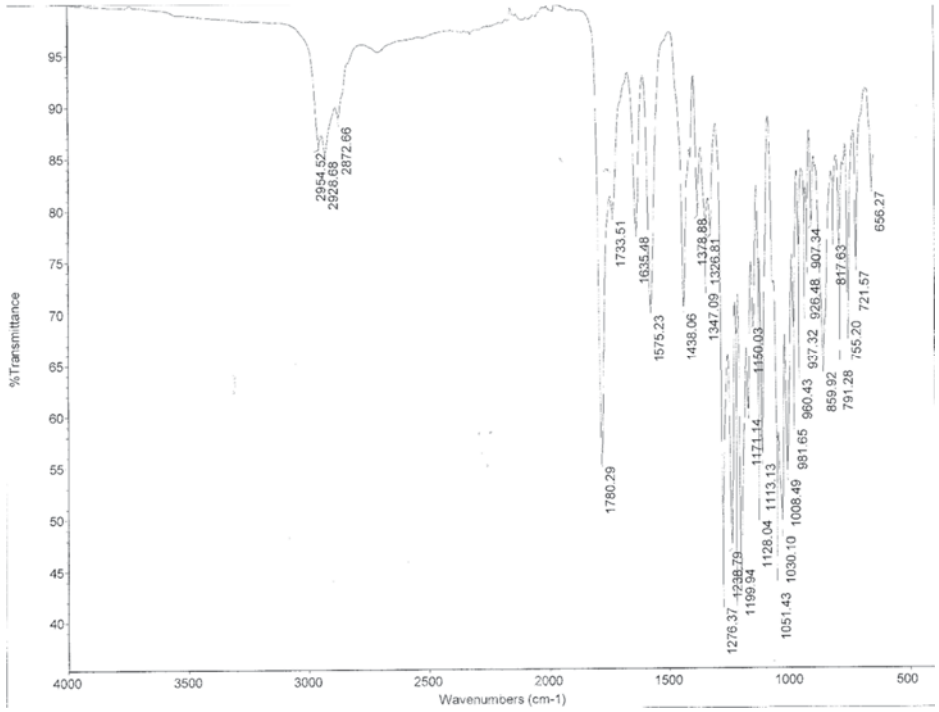

Figure B.50 FTIR spectrum (neat) of compound **4.31**

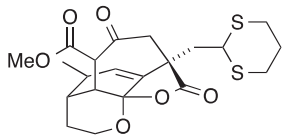

4.11

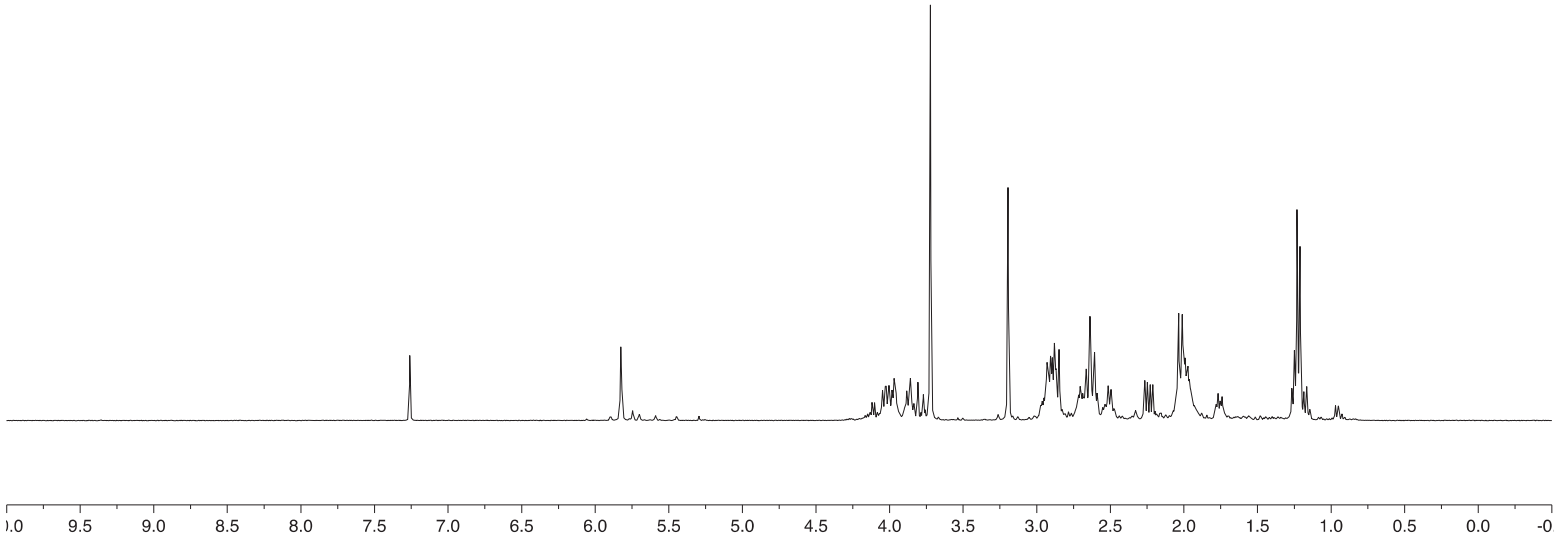

Figure B.51 ^{1}H-NMR (400 MHz; $CDCl_3$) for compound **4.11**

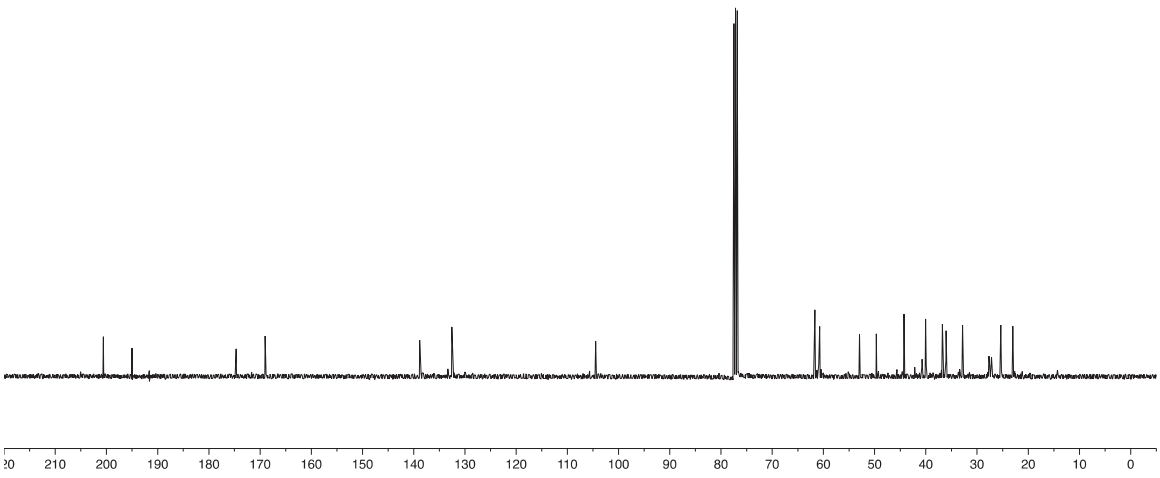

Figure B.52 ^{13}C-NMR spectrum (100 MHz; $CDCl_3$) of compound **4.11**

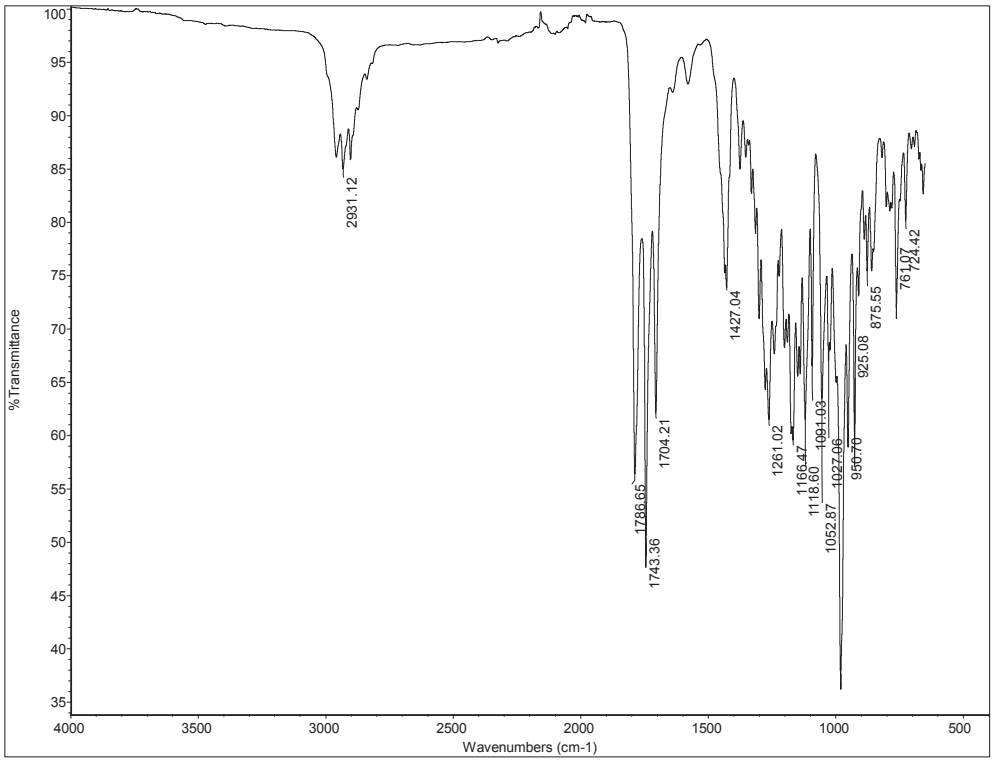

Figure B.53 FTIR spectrum (neat) of compound **4.11**

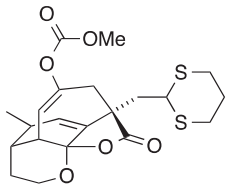

4.31a

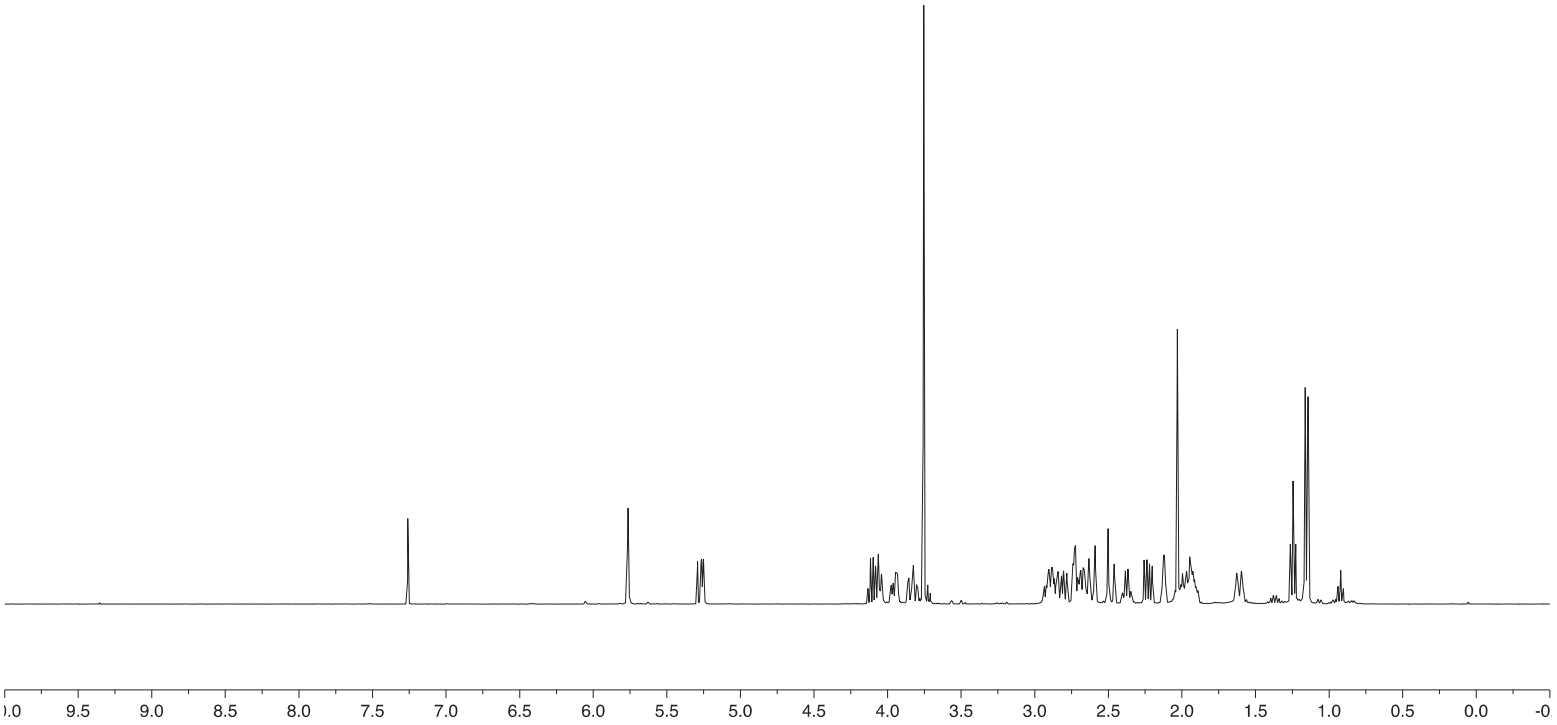

Figure B.54 ^{1}H-NMR (400 MHz; $CDCl_3$) for compound **4.31a**

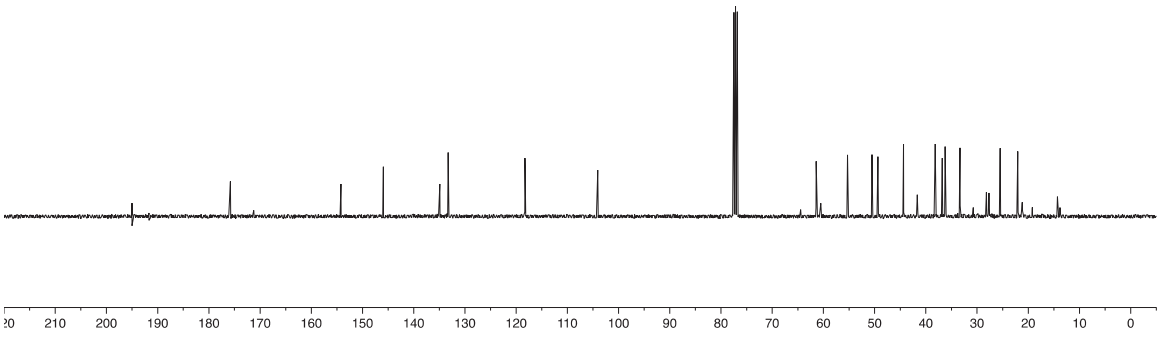

Figure B.55 ^{13}C-NMR spectrum (100 MHz; $CDCl_3$) of compound **4.31a**

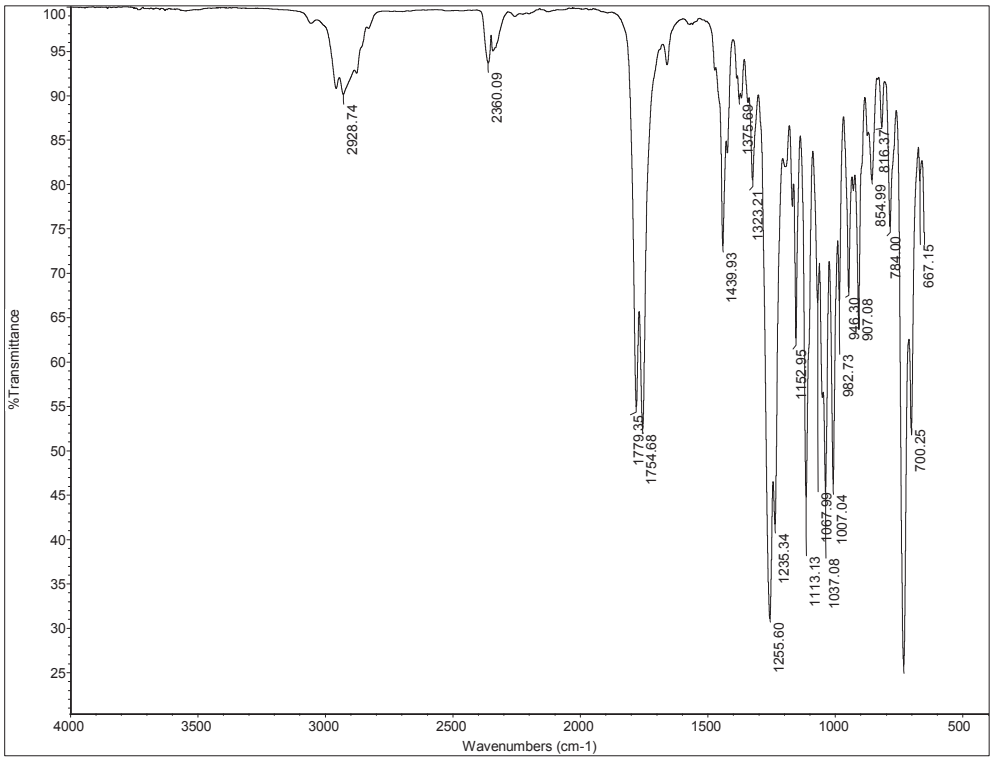

Figure B.56 FTIR spectrum (neat) of compound **4.31a**

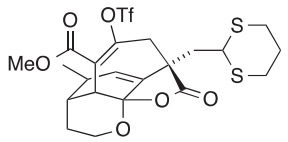

4.33

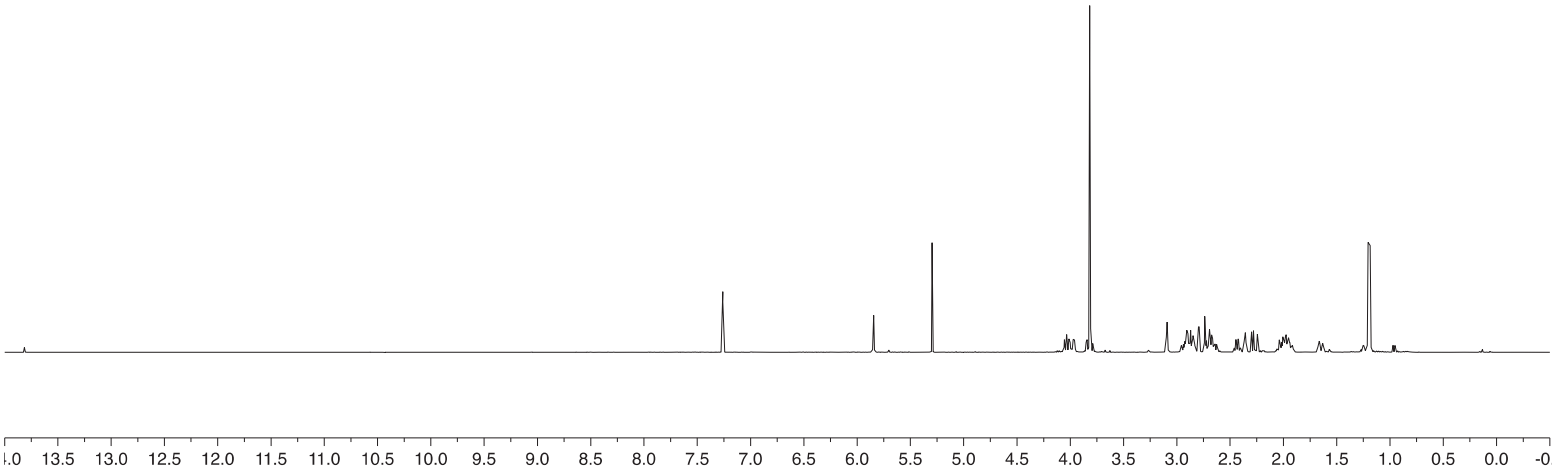

Figure B.57 ^{1}H-NMR (400 MHz; $CDCl_3$) for compound **4.33**

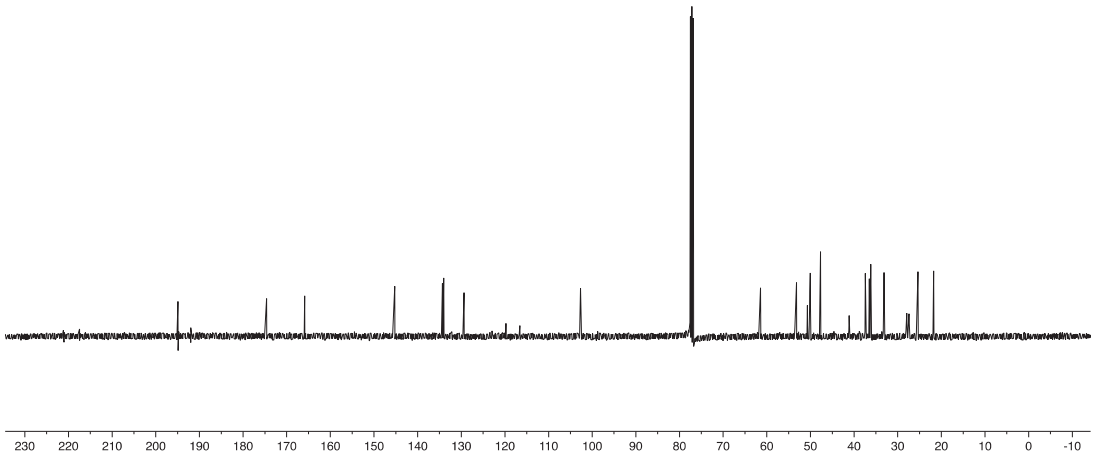

Figure B.58 ^{13}C-NMR spectrum (100 MHz; $CDCl_3$) of compound **4.33**

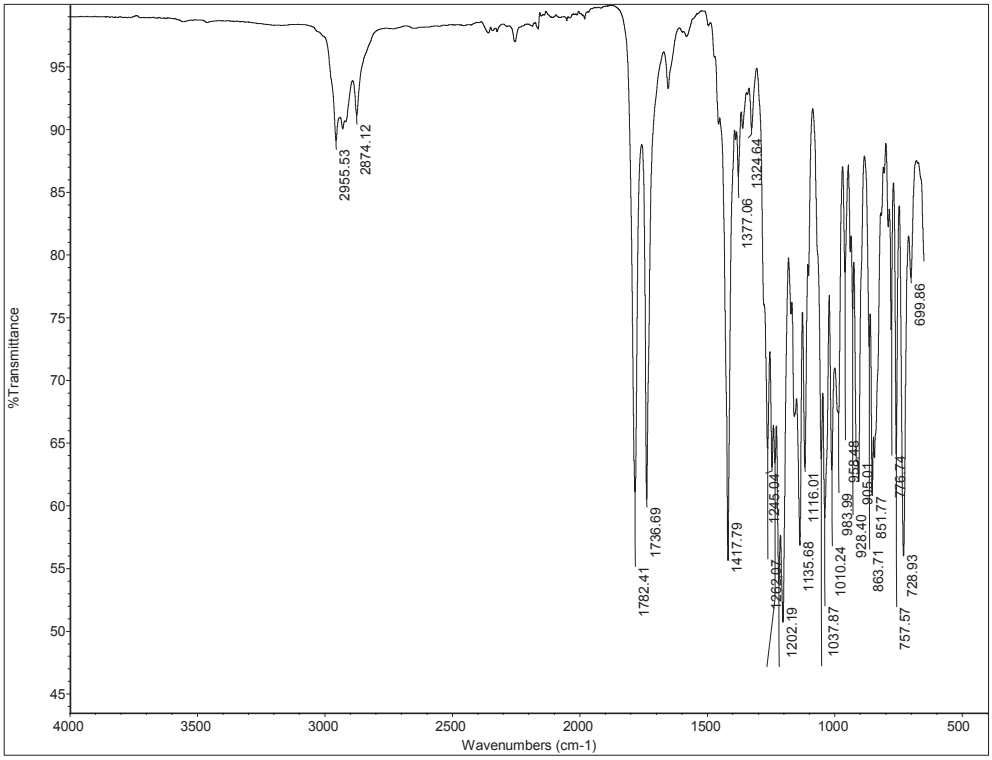

Figure B.59 FTIR spectrum (neat) of compound **4.33**

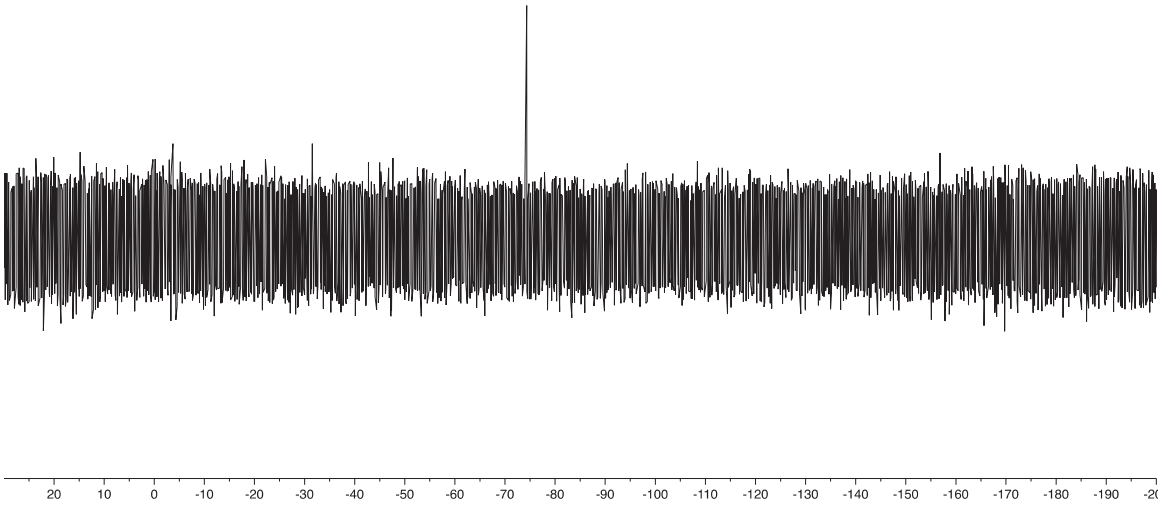

Figure B.60 ^{19}F-NMR spectrum (376 MHz; $CDCl_3$) of compound **4.33**

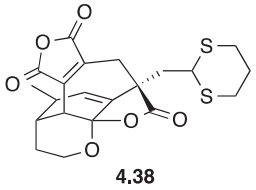

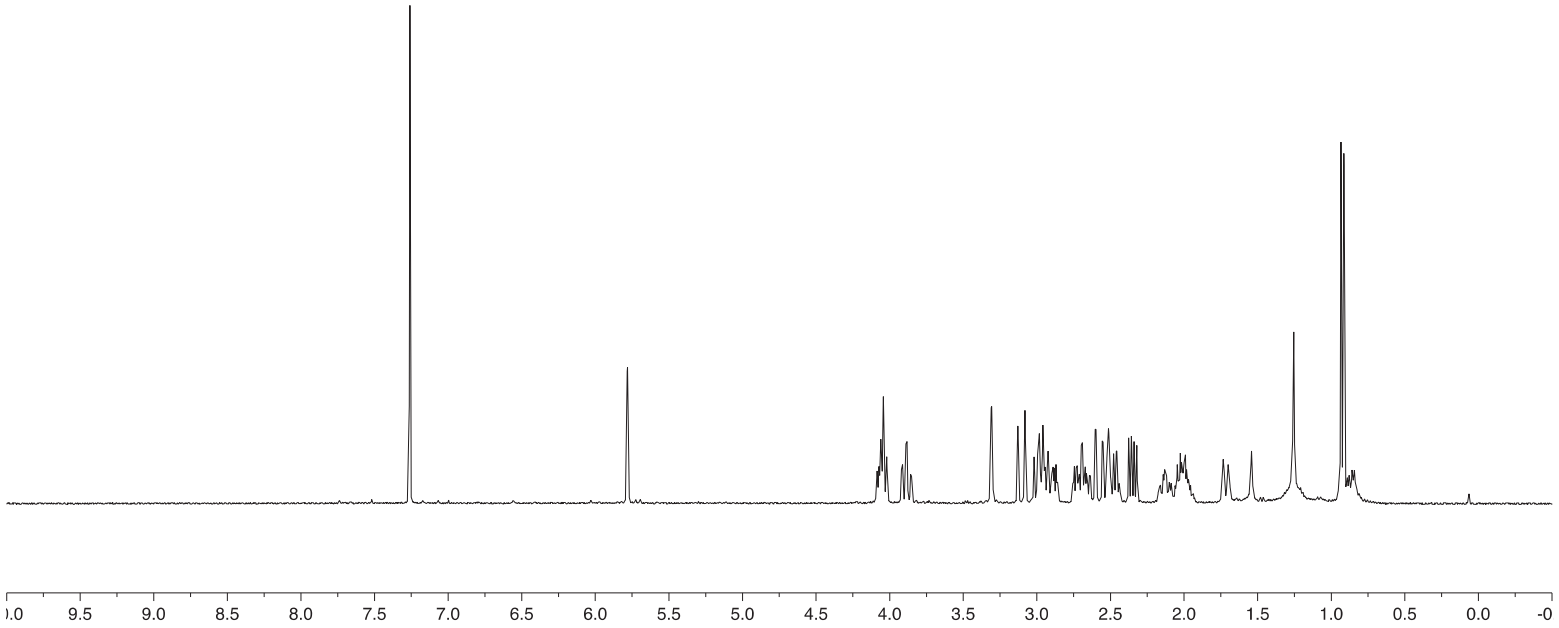

Figure B.61 ^{1}H-NMR (400 MHz; $CDCl_3$) for compound **4.38**

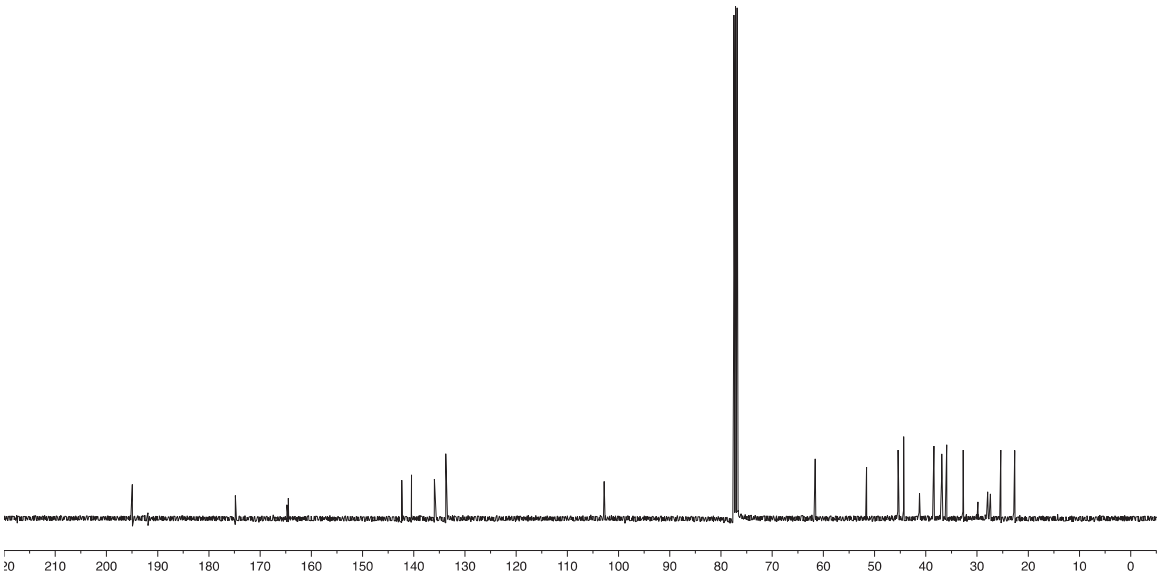

Figure B.62 ^{13}C-NMR spectrum (100 MHz; $CDCl_3$) of compound **4.38**

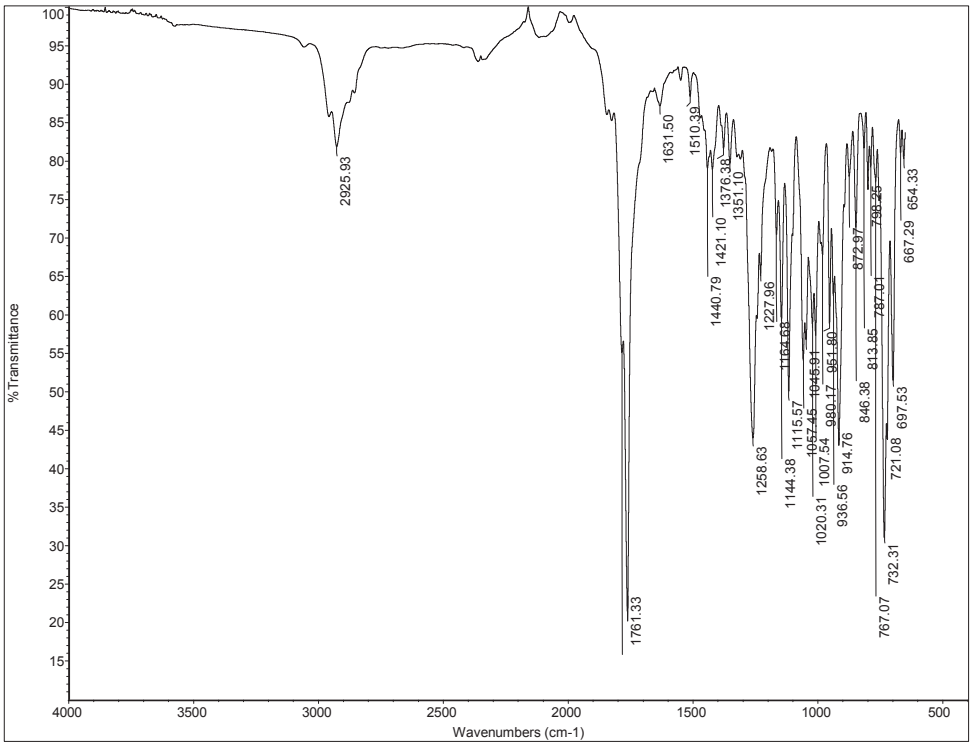

Figure B.63 FTIR spectrum (neat) of compound **4.38**

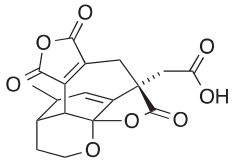

4.10

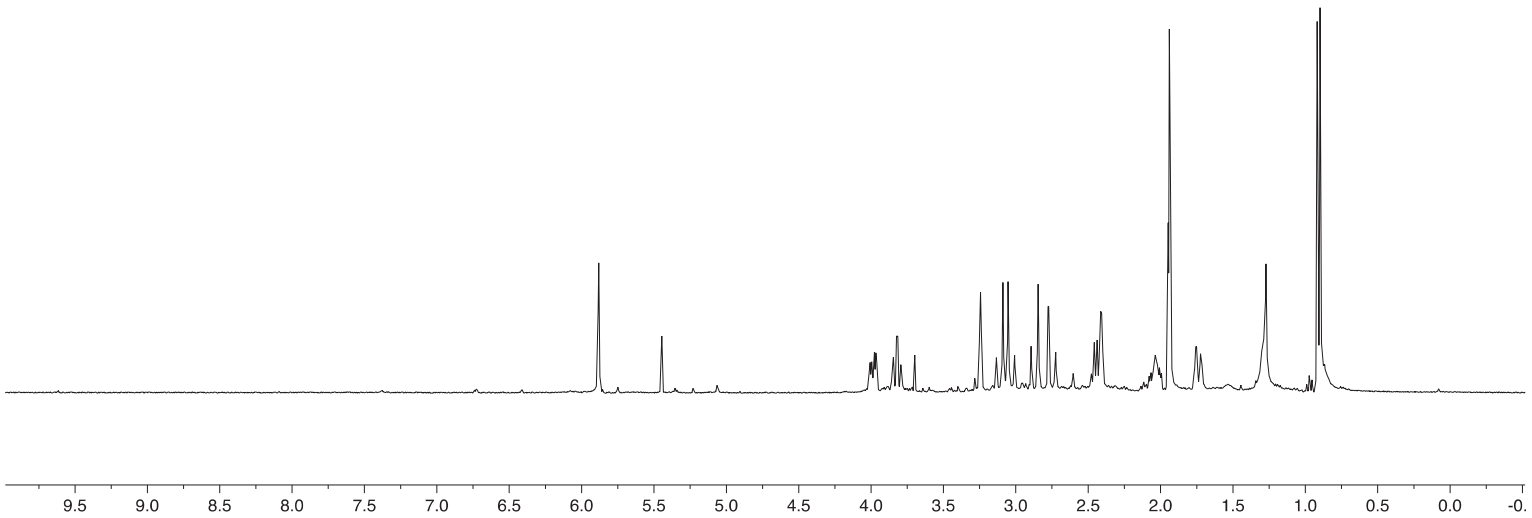

Figure B.64 ^{1}H-NMR (400 MHz; CD_3CN) for compound **4.10**

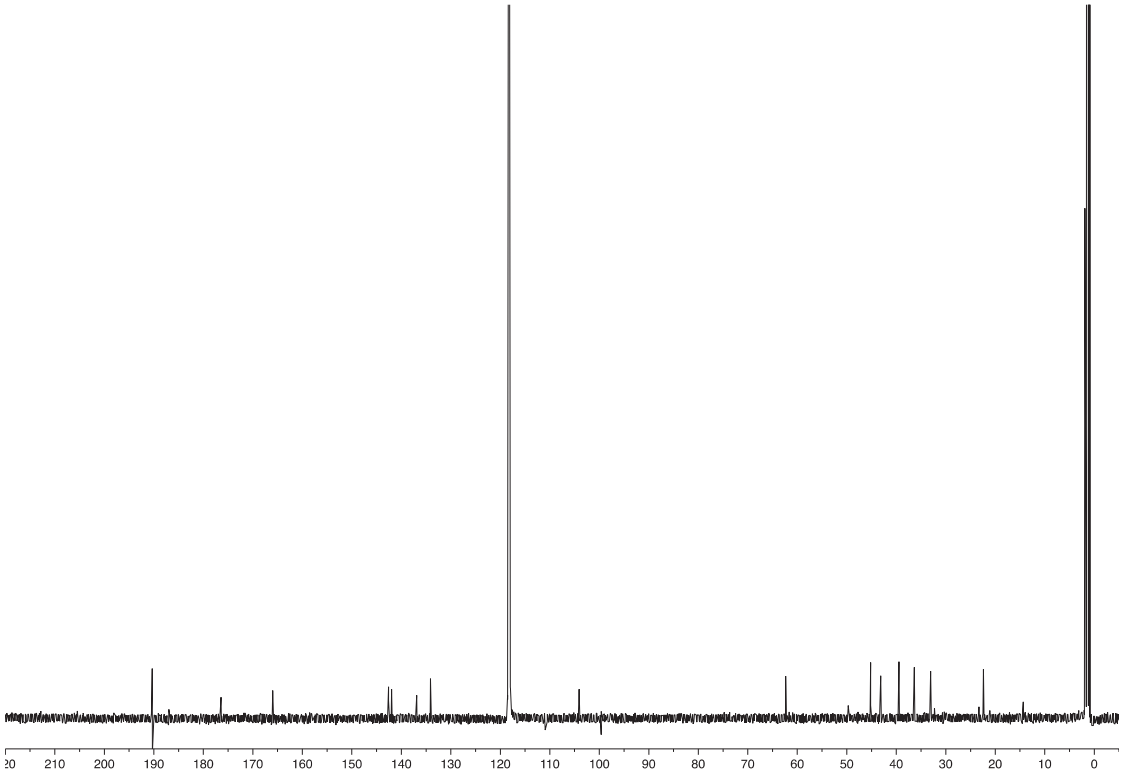

Figure B.65 ^{13}C-NMR spectrum (100 MHz; CD_3CN) of compound **4.10**

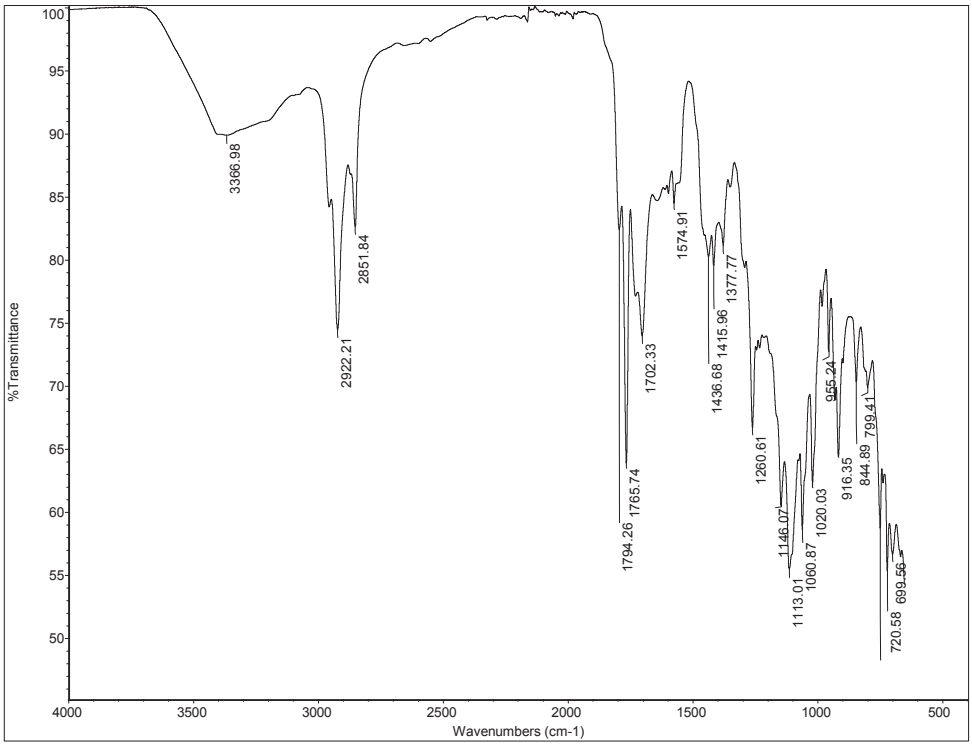

Figure B.66 FTIR spectrum (neat) of compound **4.10**

APPENDIX C

Spectra Relevant to Chapter Five

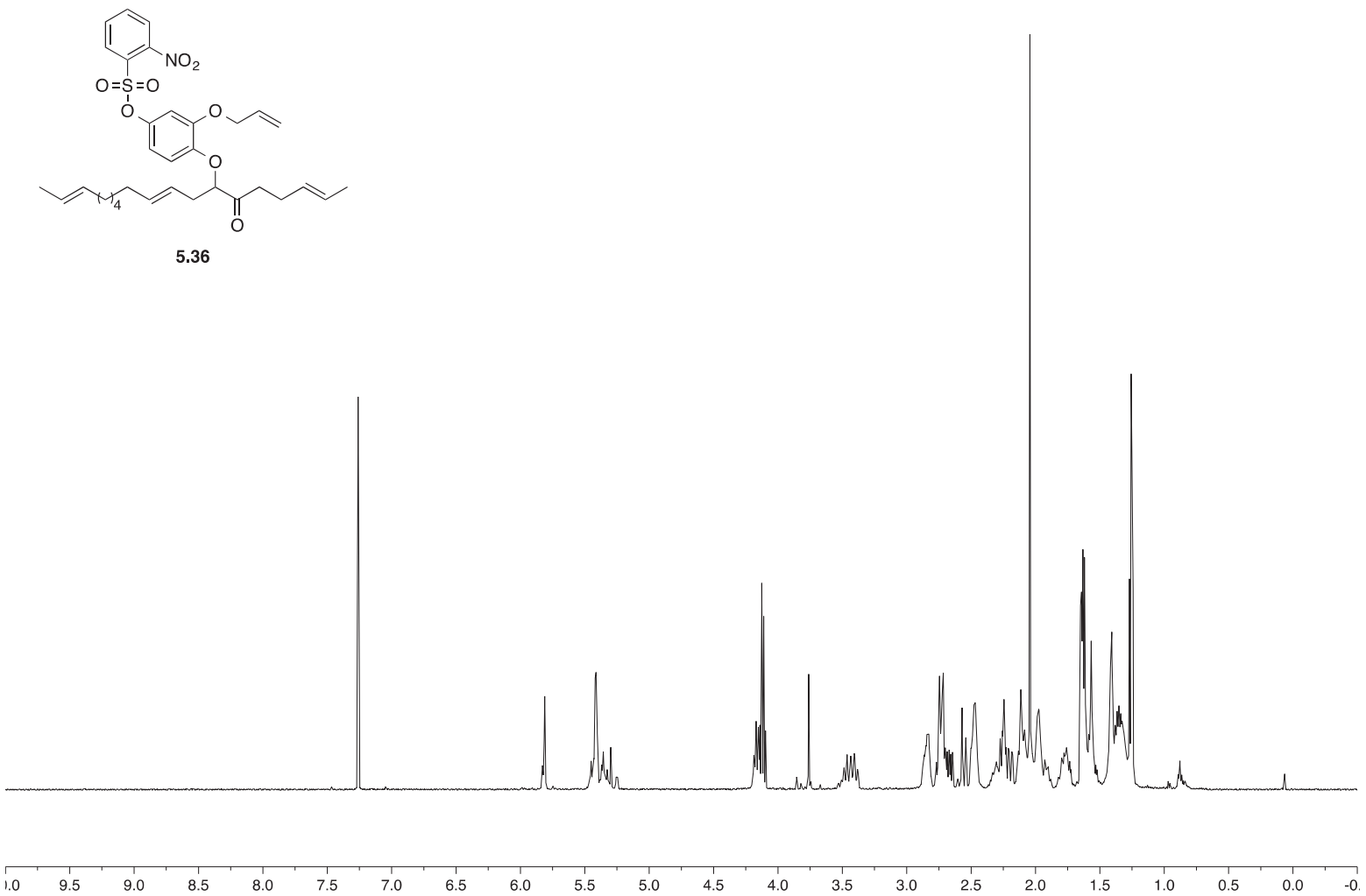

Figure C.10 ^{1}H-NMR (500 MHz; $CDCl_3$) for compound **5.36**

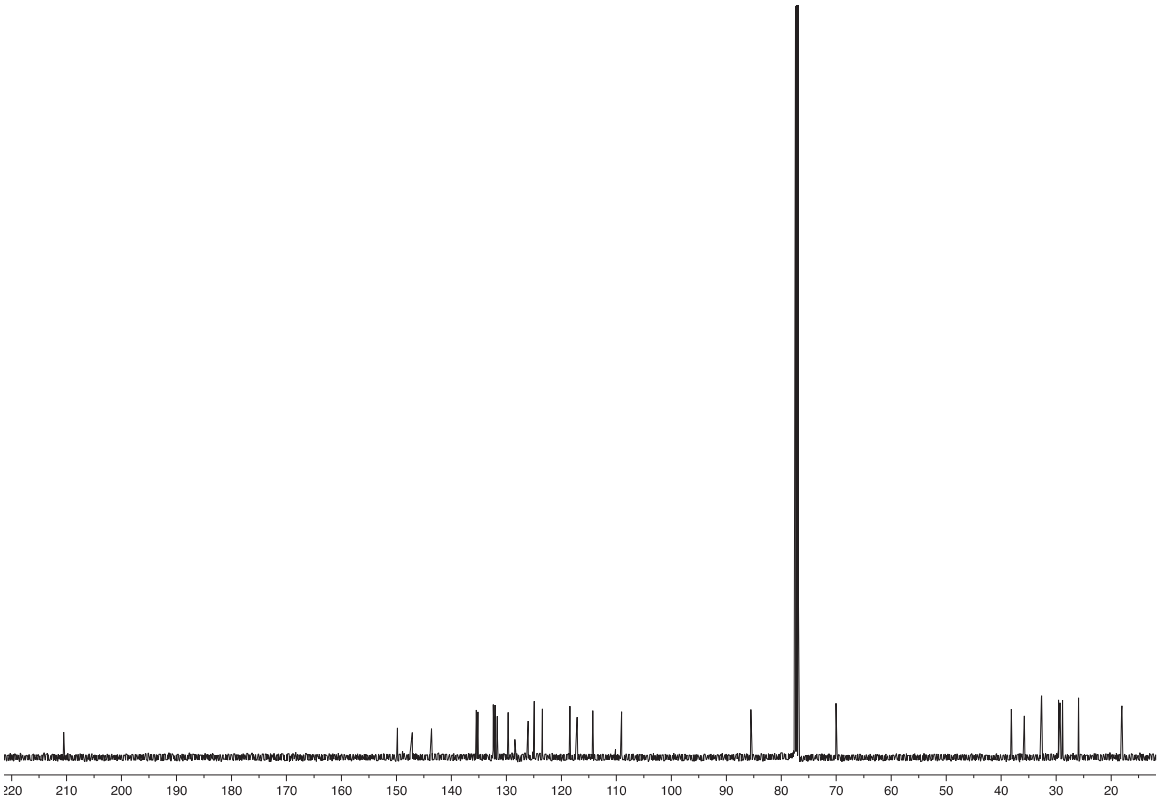

Figure C.11 ^{13}C-NMR spectrum (125 MHz; $CDCl_3$) of compound **5.36**

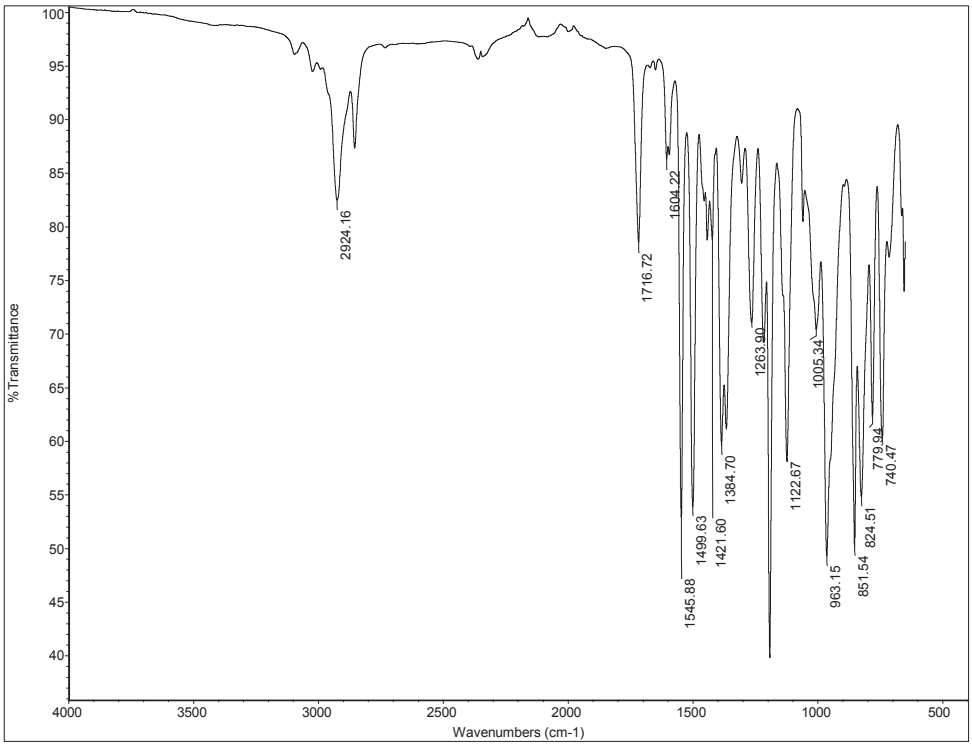

Figure C.12 FTIR spectrum (neat) of compound **5.36**

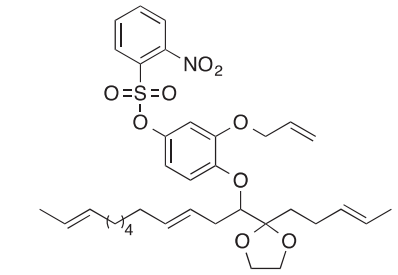

5.37

Figure C.13 ^{1}H-NMR (600 MHz; $CDCl_3$) for compound **5.37**

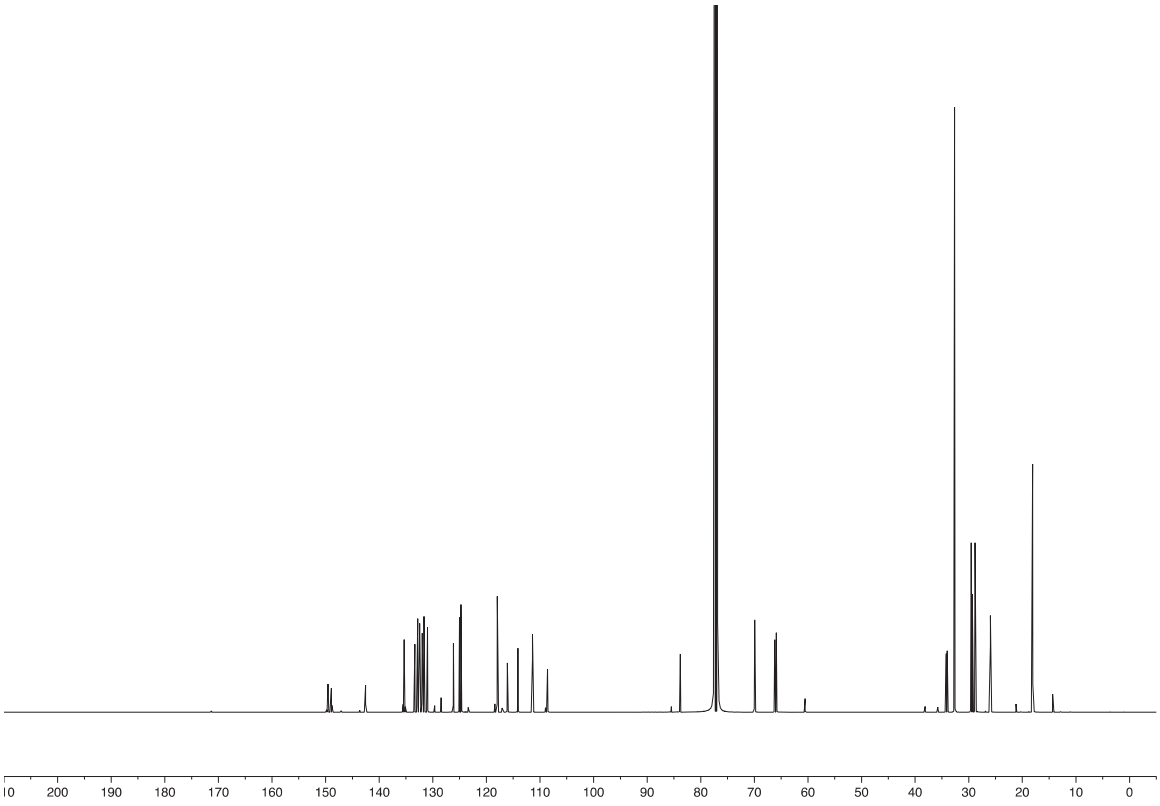

Figure C.14 ^{13}C-NMR spectrum (150 MHz; $CDCl_3$) of compound **5.37**

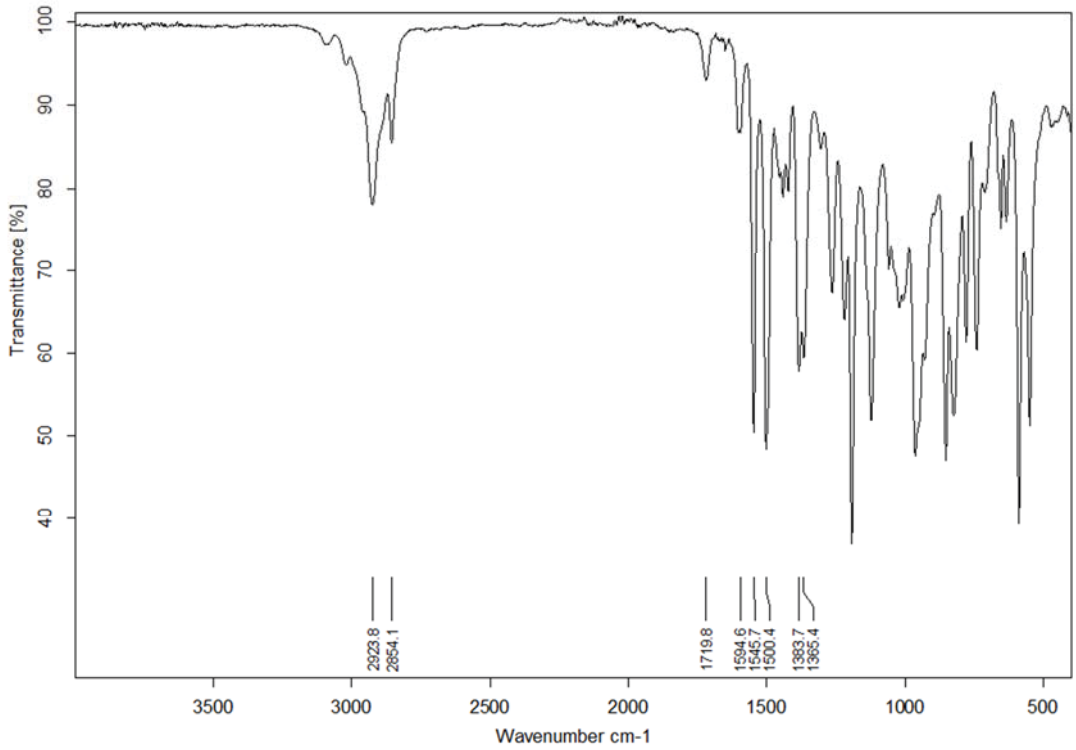

Figure C.15 FTIR spectrum (neat) of compound **5.37**

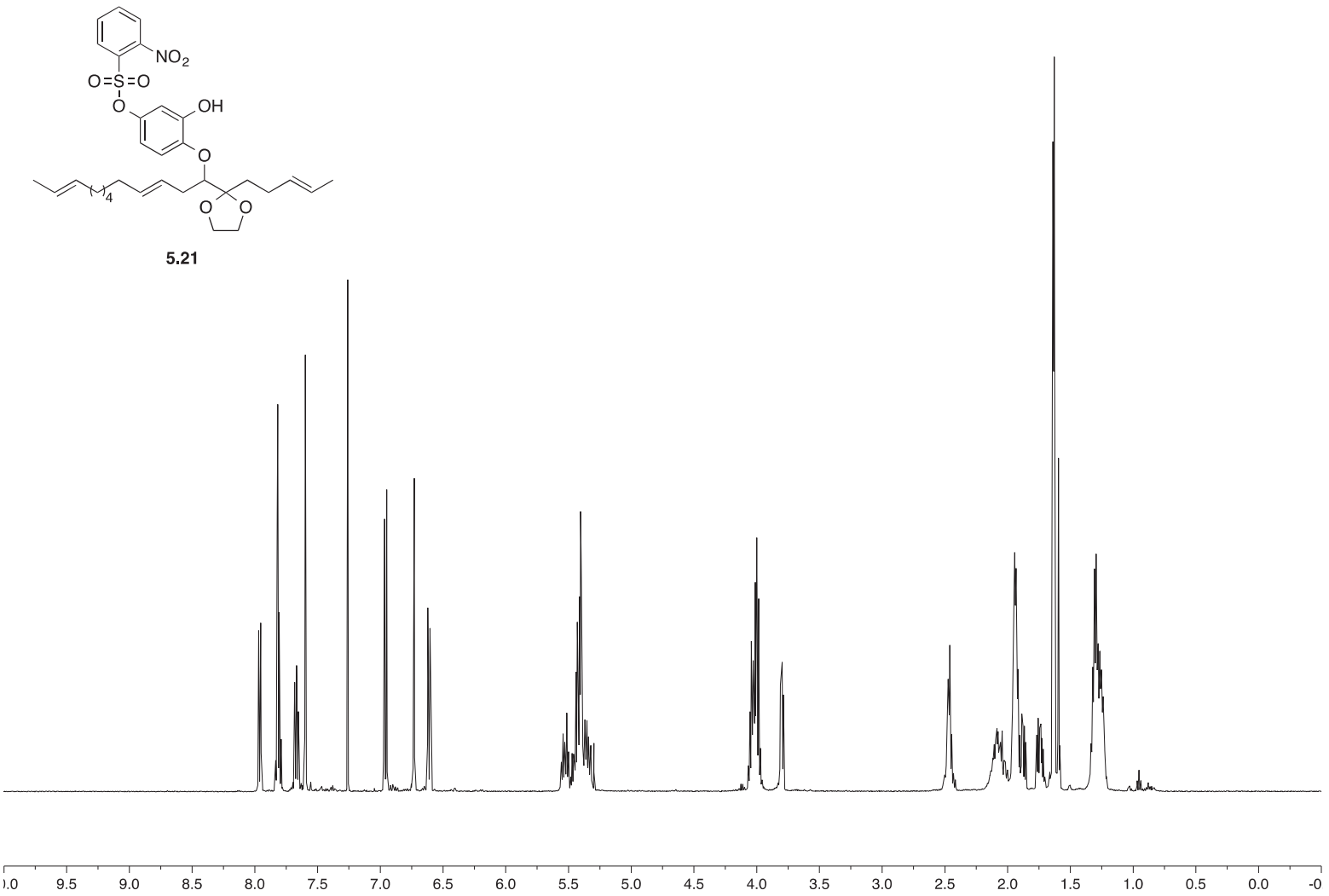

Figure C.16 ^{1}H-NMR (500 MHz; $CDCl_3$) for compound **5.21**

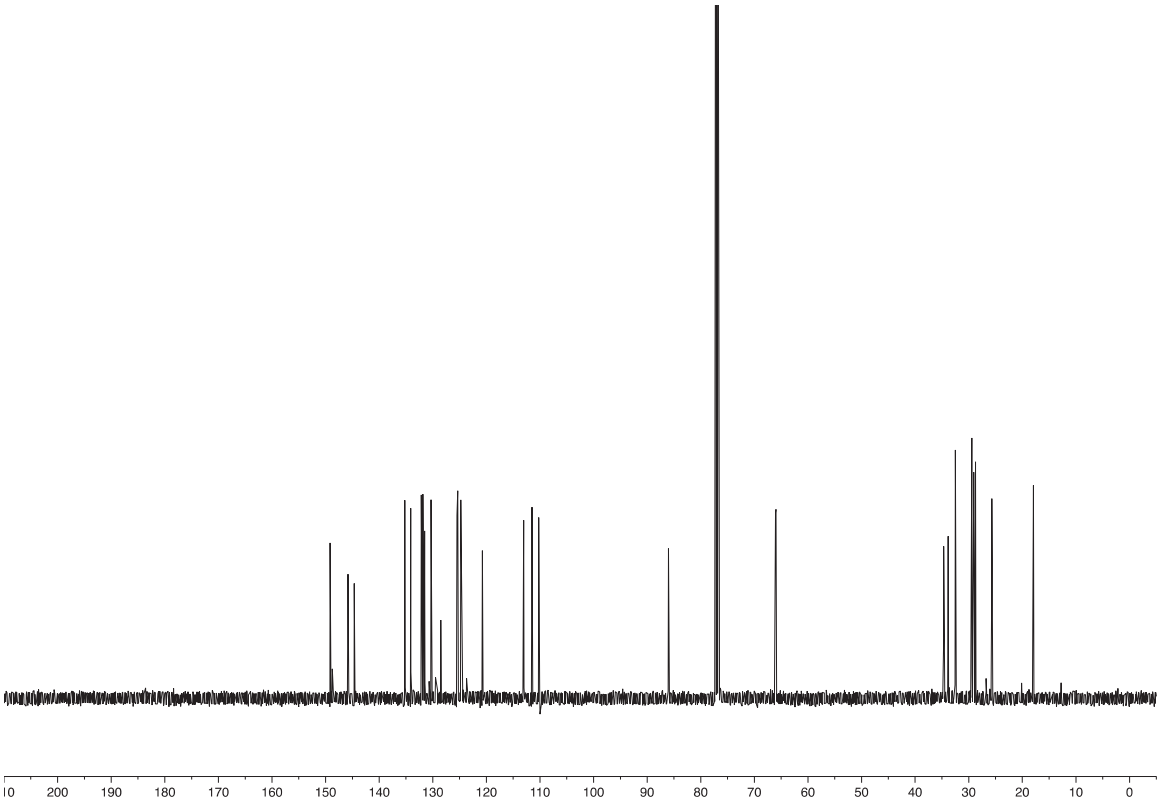

Figure C.17 ^{13}C-NMR spectrum (125 MHz; $CDCl_3$) of compound **5.21**

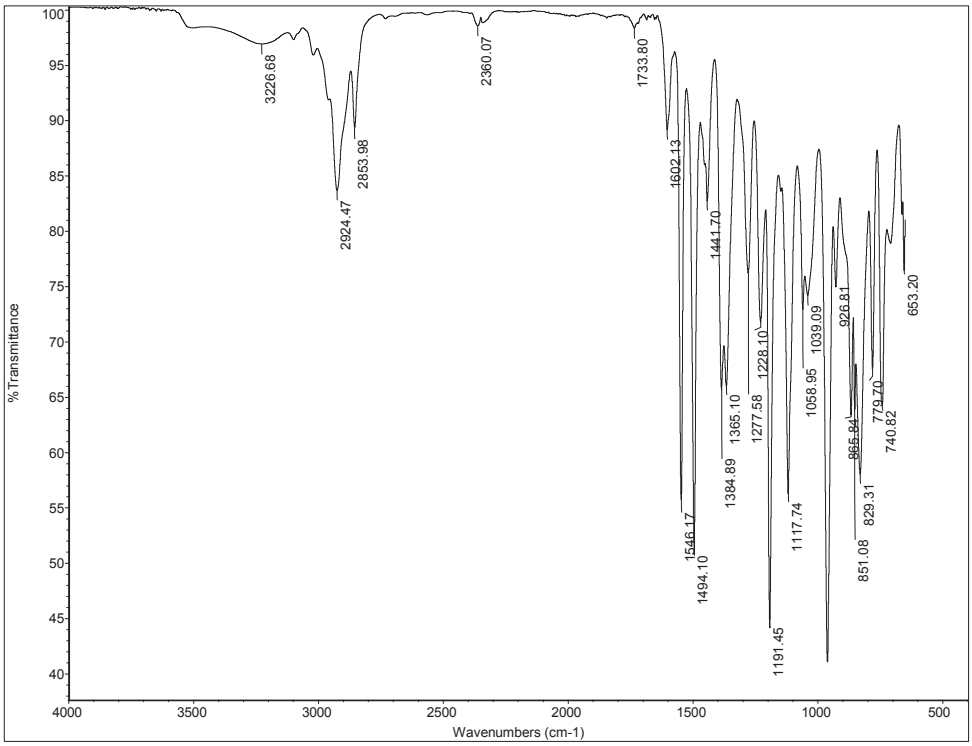

Figure C.18 FTIR spectrum (neat) of compound **5.21**

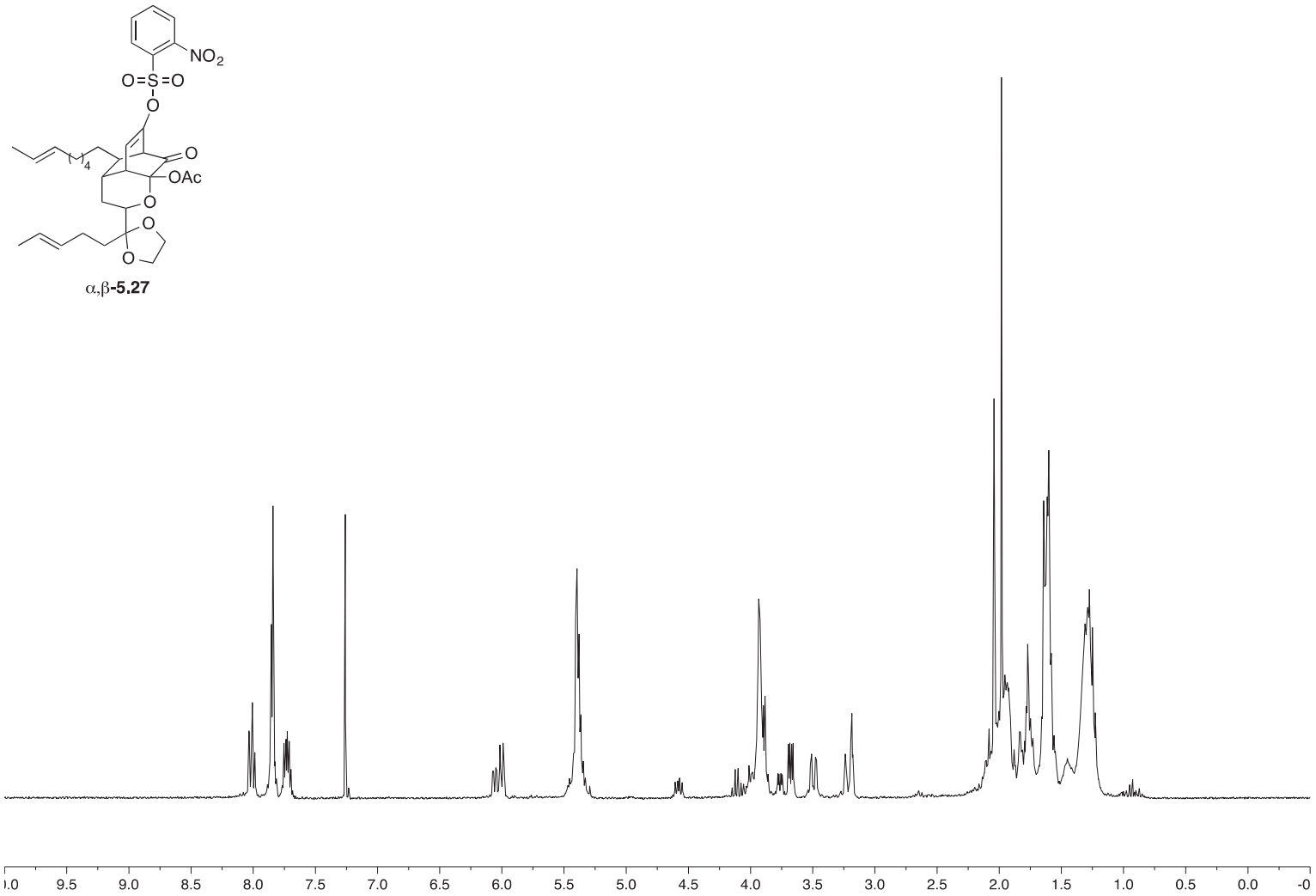

Figure C.19 ^{1}H-NMR (400 MHz; $CDCl_3$) for compound α,β-**5.27**

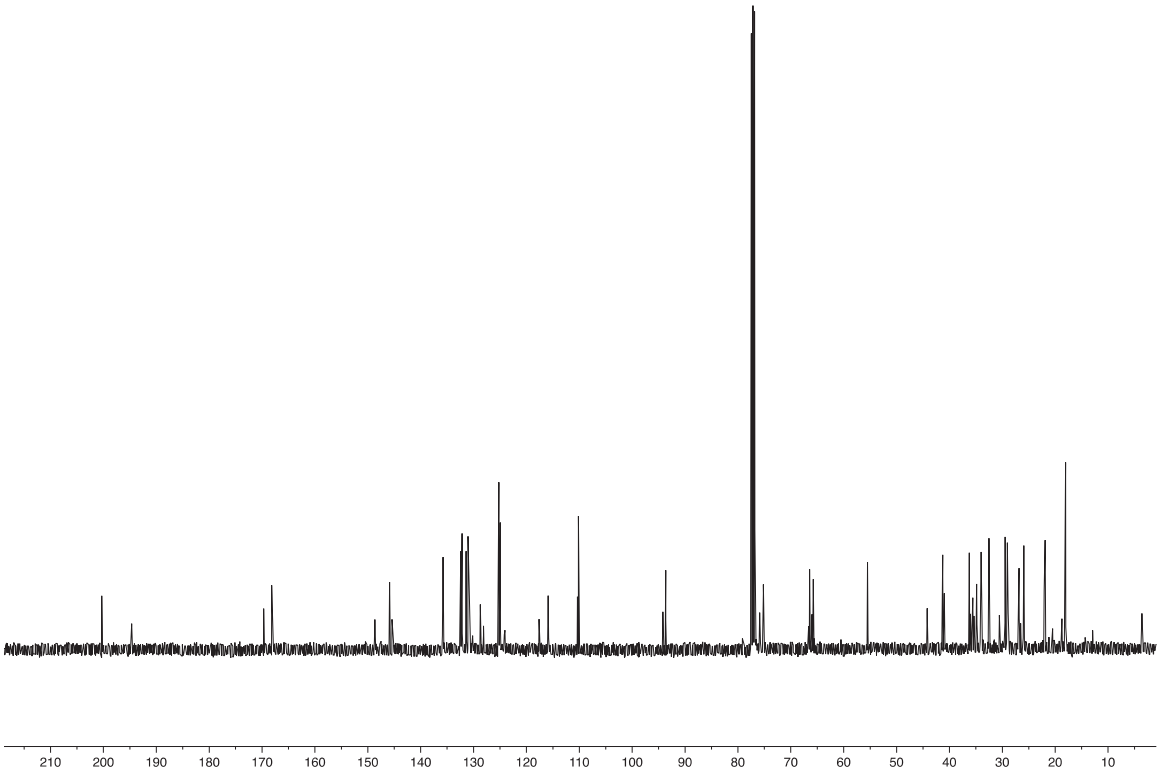

Figure C.20 ^{13}C-NMR spectrum (100 MHz; $CDCl_3$) of compound α,β-**5.27**

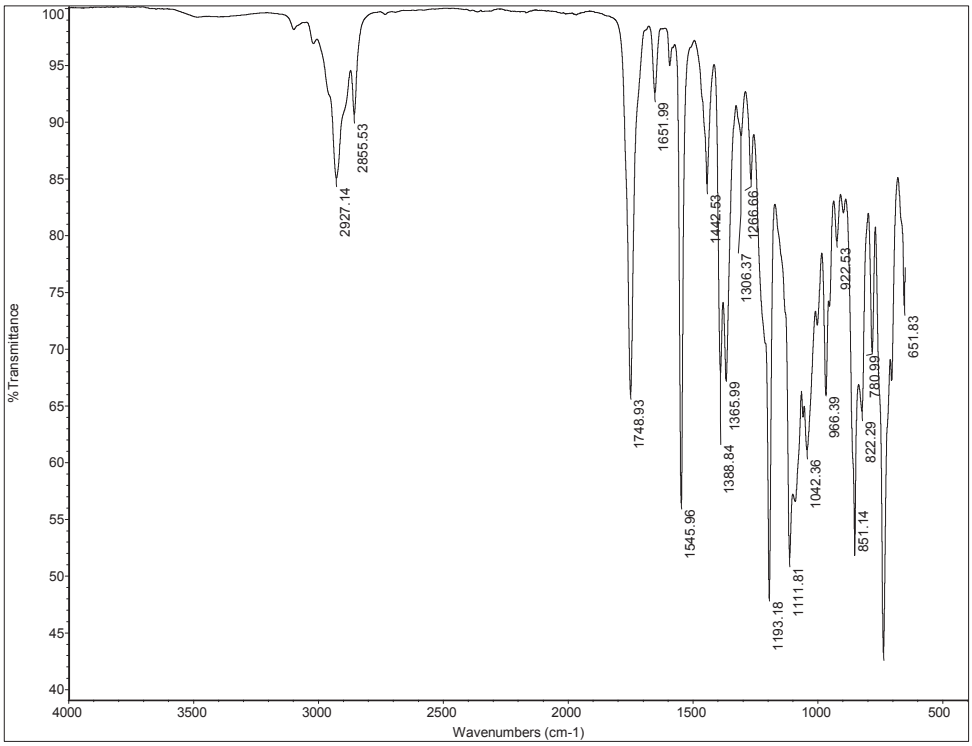

Figure C.21 FTIR spectrum (neat) of compound α,β-**5.27**

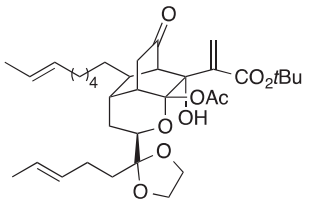

5.40

Figure C.22 ^{1}H-NMR (400 MHz; $CDCl_3$) for compound **5.40**

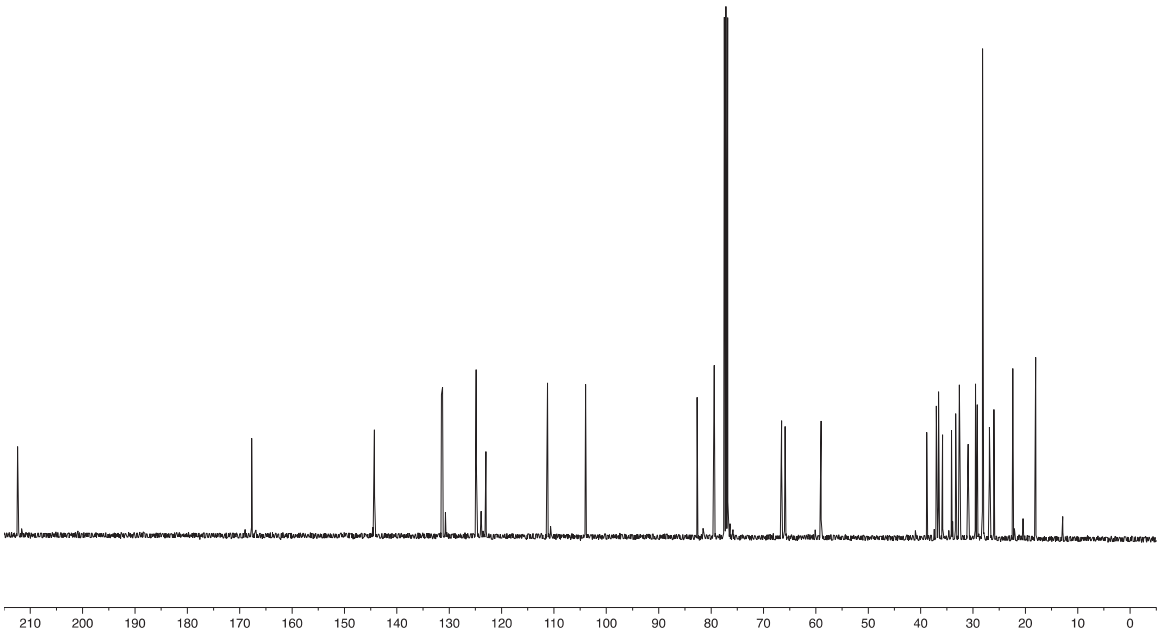

Figure C.23 ^{13}C-NMR spectrum (100 MHz; $CDCl_3$) of compound **5.40**

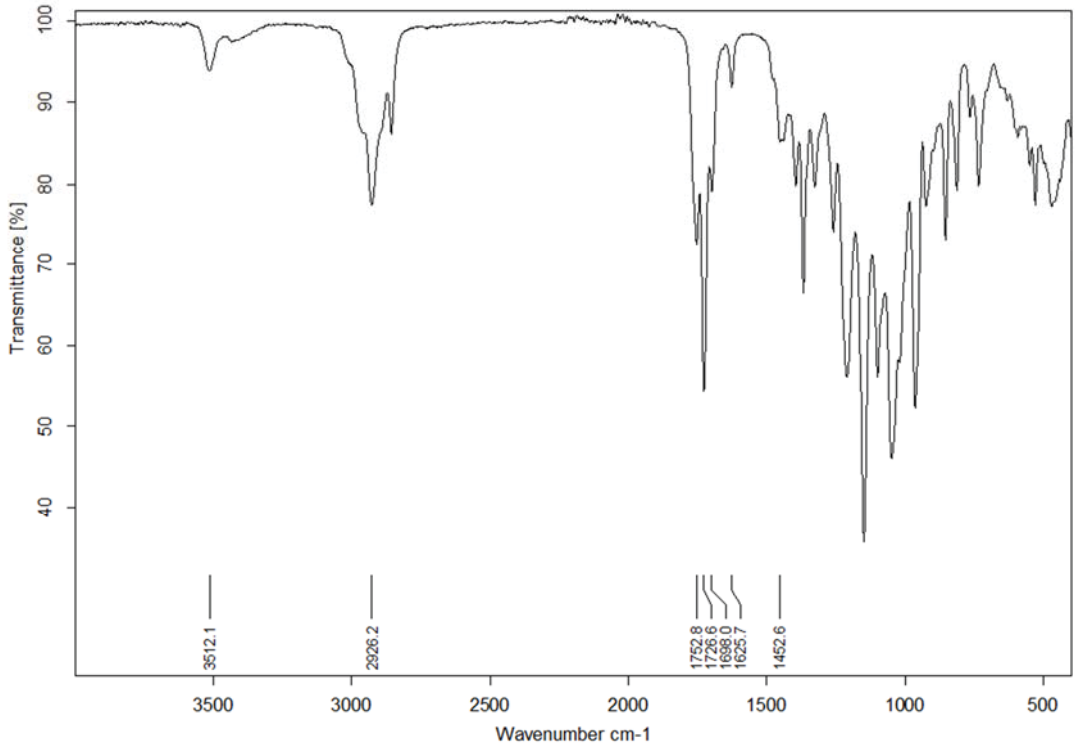

Figure C.24 FTIR spectrum (neat) of compound **5.40**

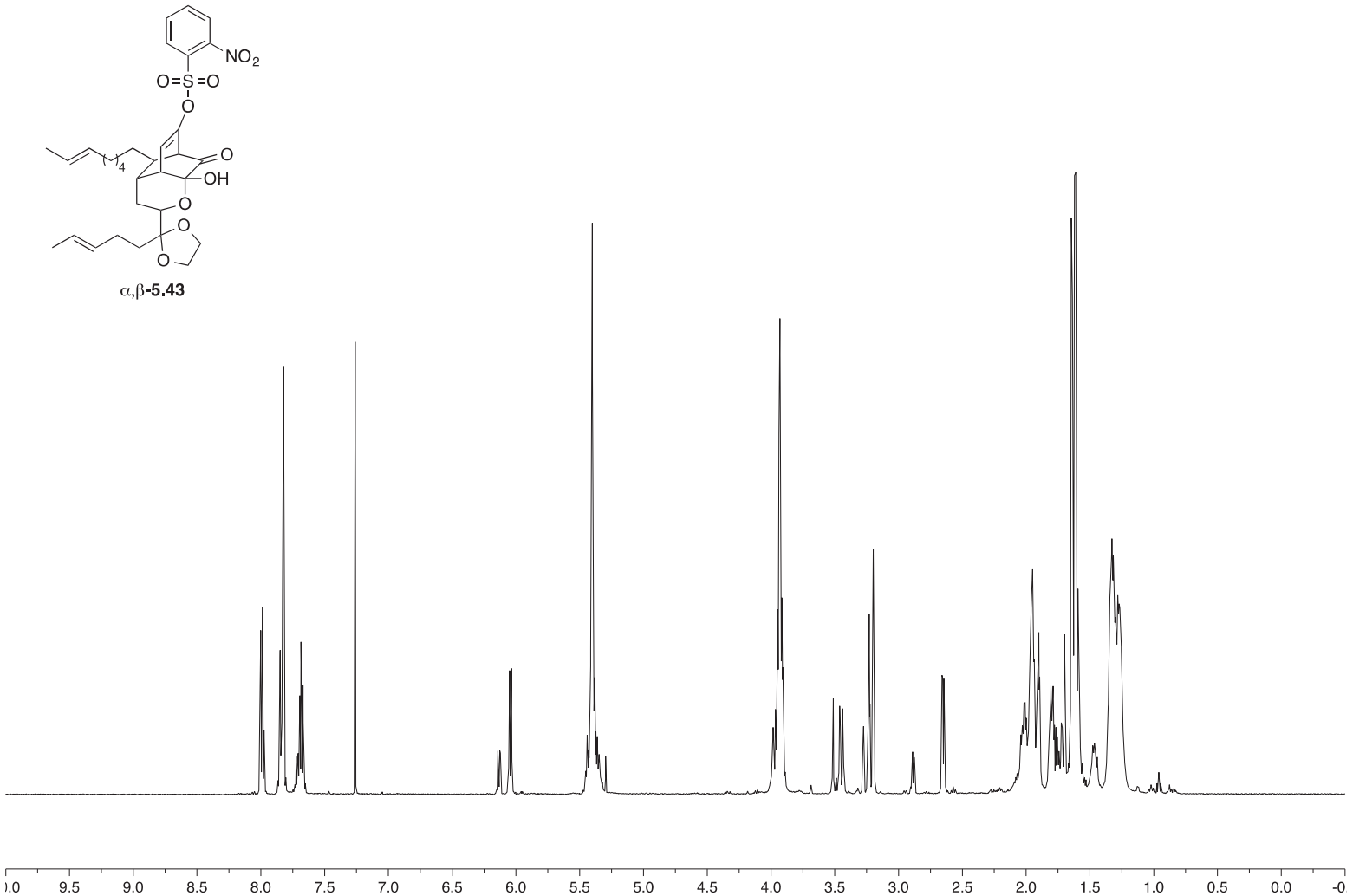

Figure C.25 ^{1}H-NMR (500 MHz; $CDCl_3$) for compound α,β-**5.43**

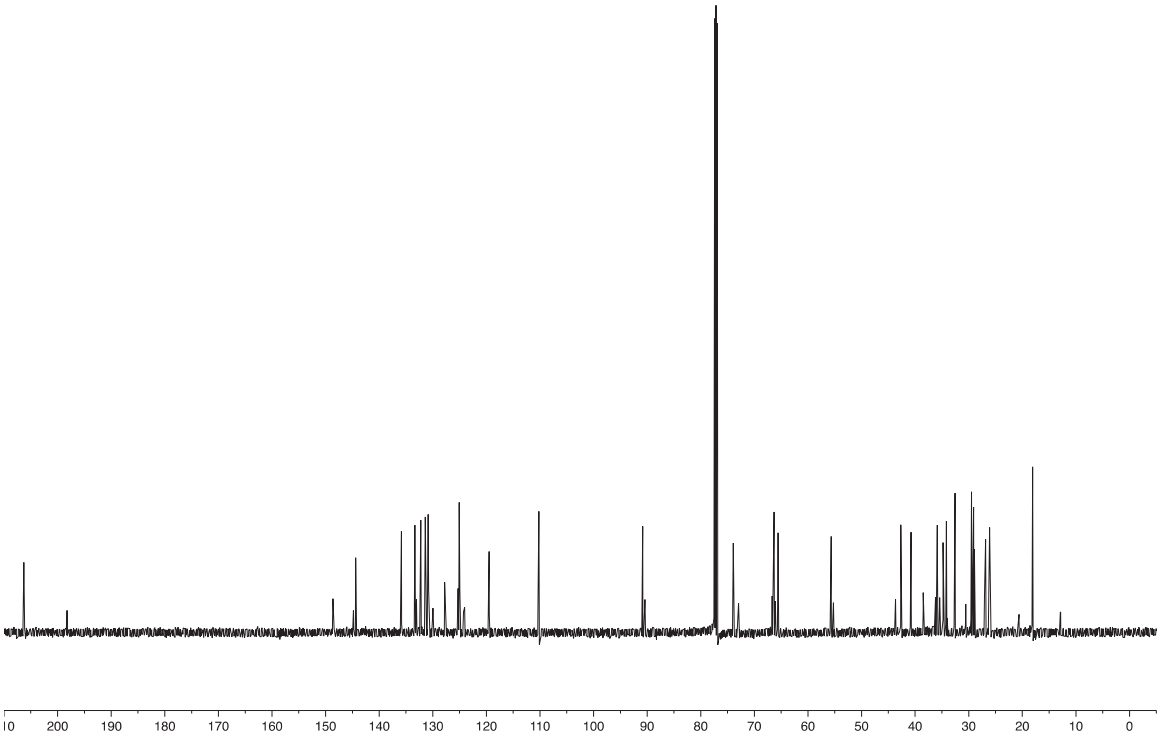

Figure C.26 ^{13}C-NMR spectrum (125 MHz; $CDCl_3$) of compound α,β-**5.43**

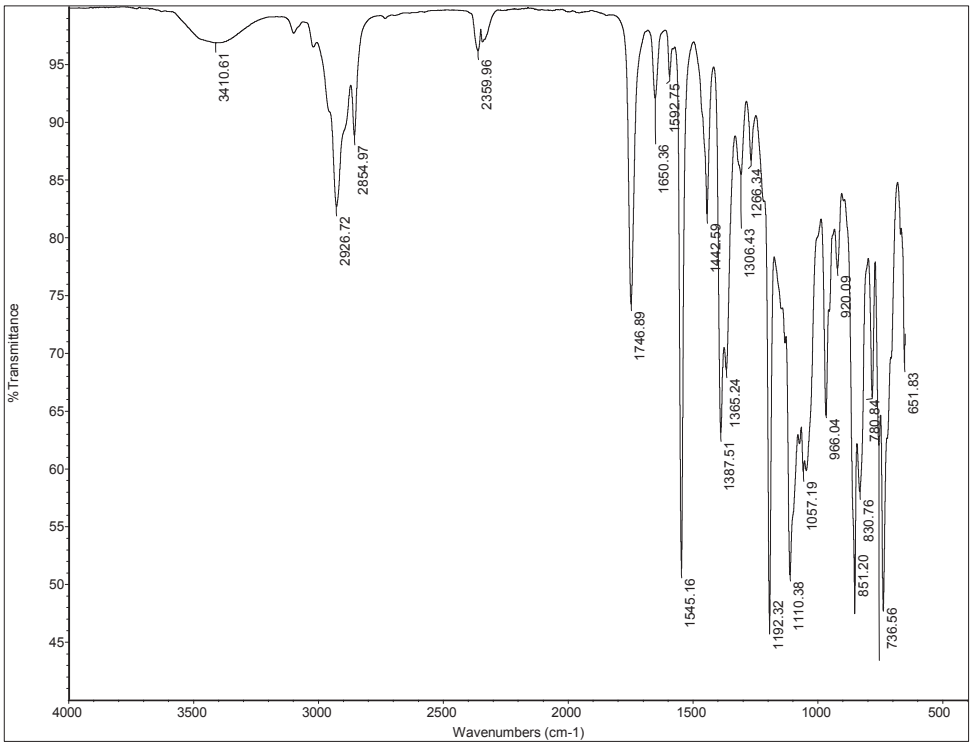

Figure C.27 FTIR spectrum (neat) of compound α,β-**5.43**

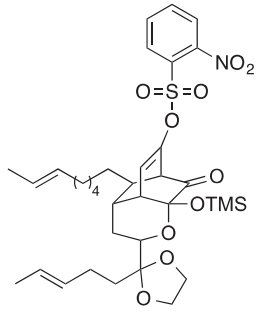

α,β-**5.44**

Figure C.28 ^{1}H-NMR (500 MHz; $CDCl_3$) for compound α,β-**5.44**

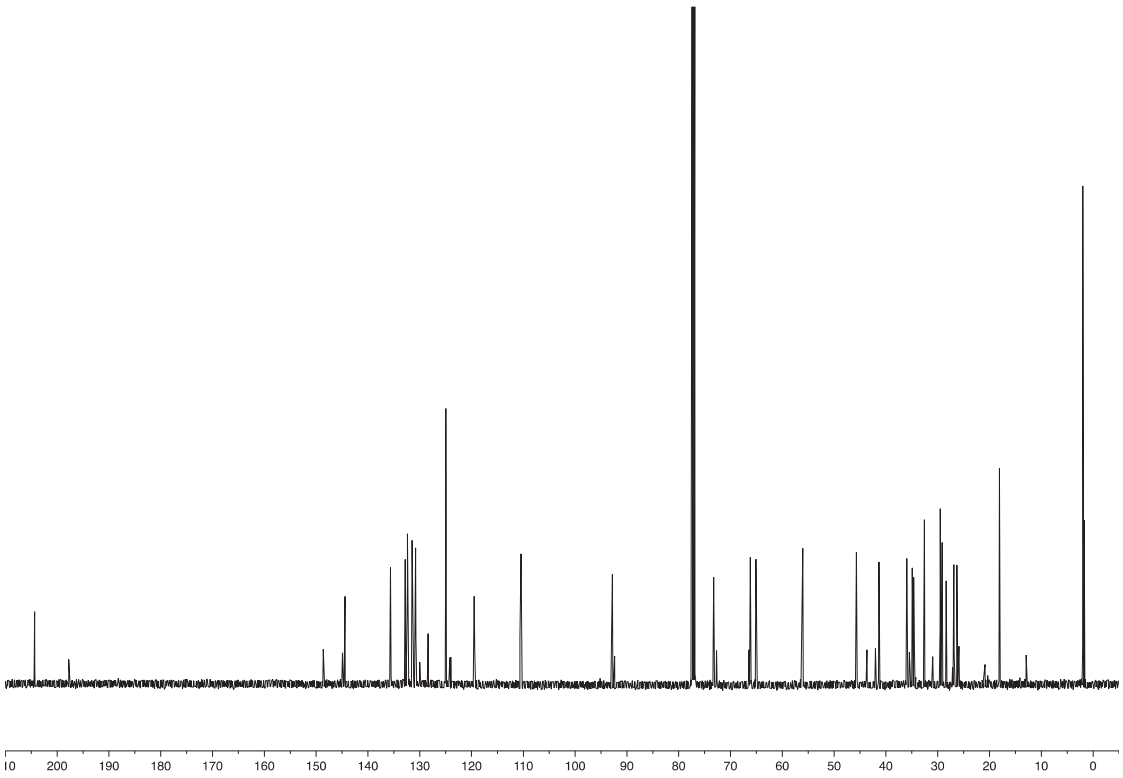

Figure C.29 ^{13}C-NMR spectrum (125 MHz; $CDCl_3$) of compound α,β-**5.44**

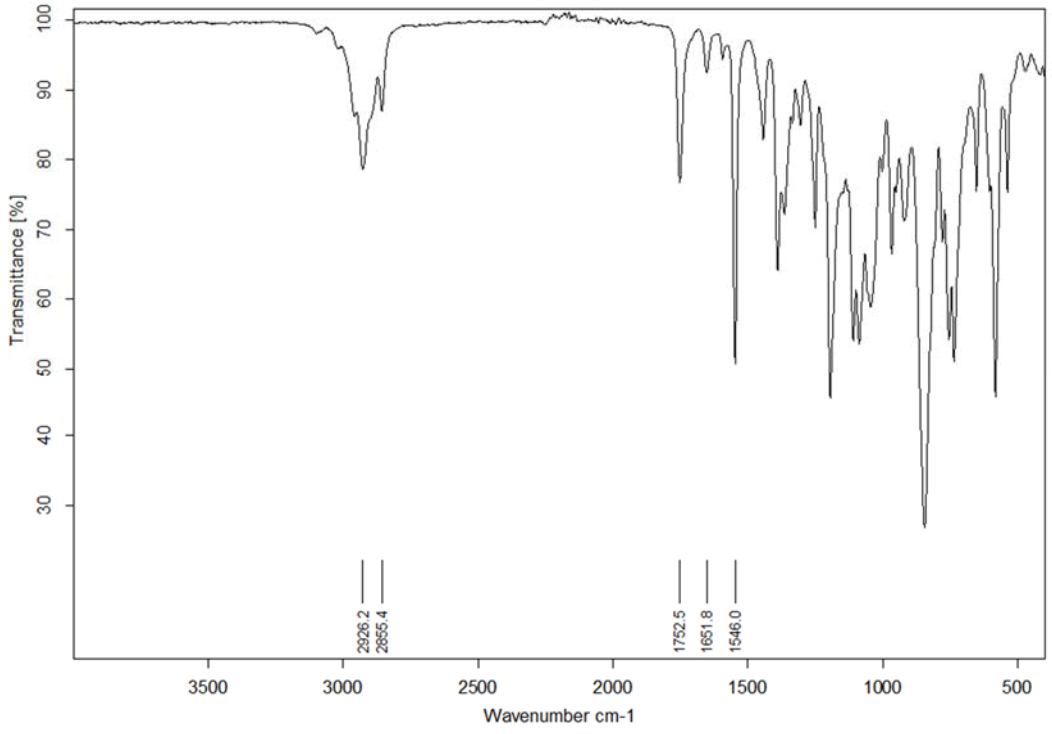

Figure C.30 FTIR spectrum (neat) of compound α,β-**5.44**

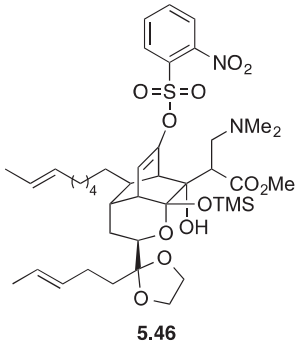

5.46

Figure C.31 ^{1}H-NMR (500 MHz; $CDCl_3$) for compound **5.46**

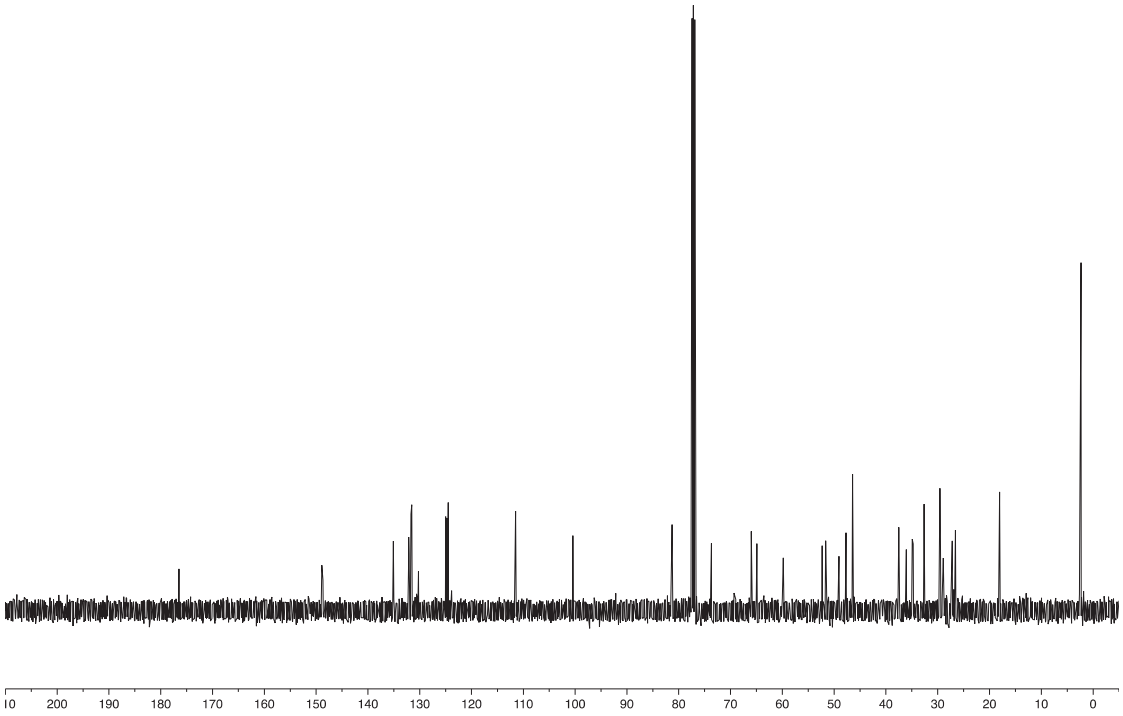

Figure C.32 ^{13}C-NMR spectrum (125 MHz; $CDCl_3$) of compound **5.46**

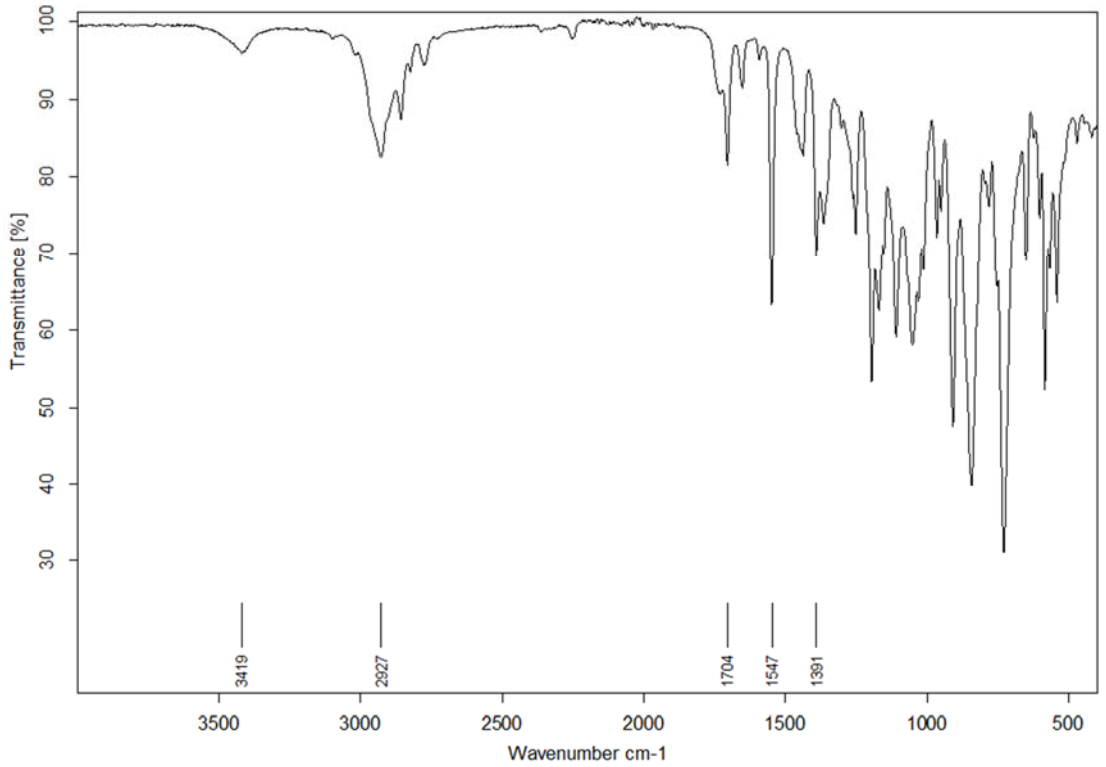

Figure C.33 FTIR spectrum (neat) of compound **5.46**

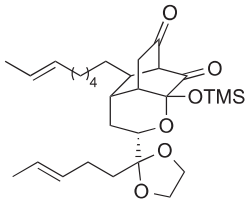

α-**5.47**

Figure C.34 ^{1}H-NMR (500 MHz; $CDCl_3$) for compound α-**5.47**

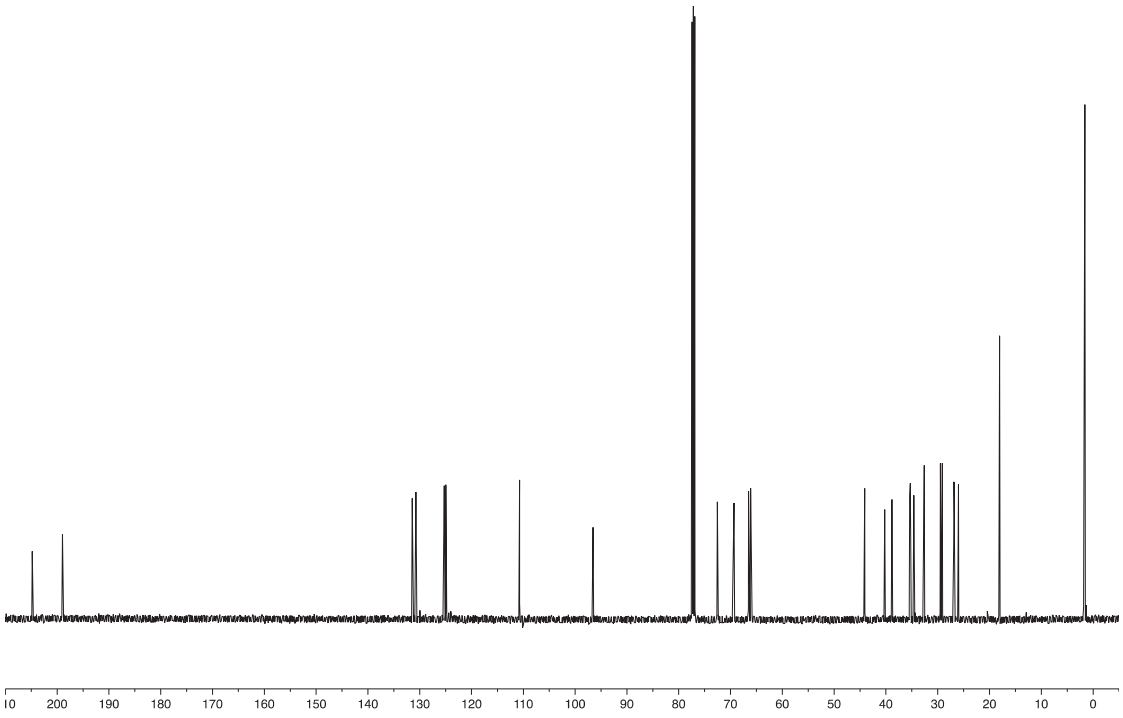

Figure C.35 ^{13}C-NMR spectrum (125 MHz; $CDCl_3$) of compound α-**5.47**

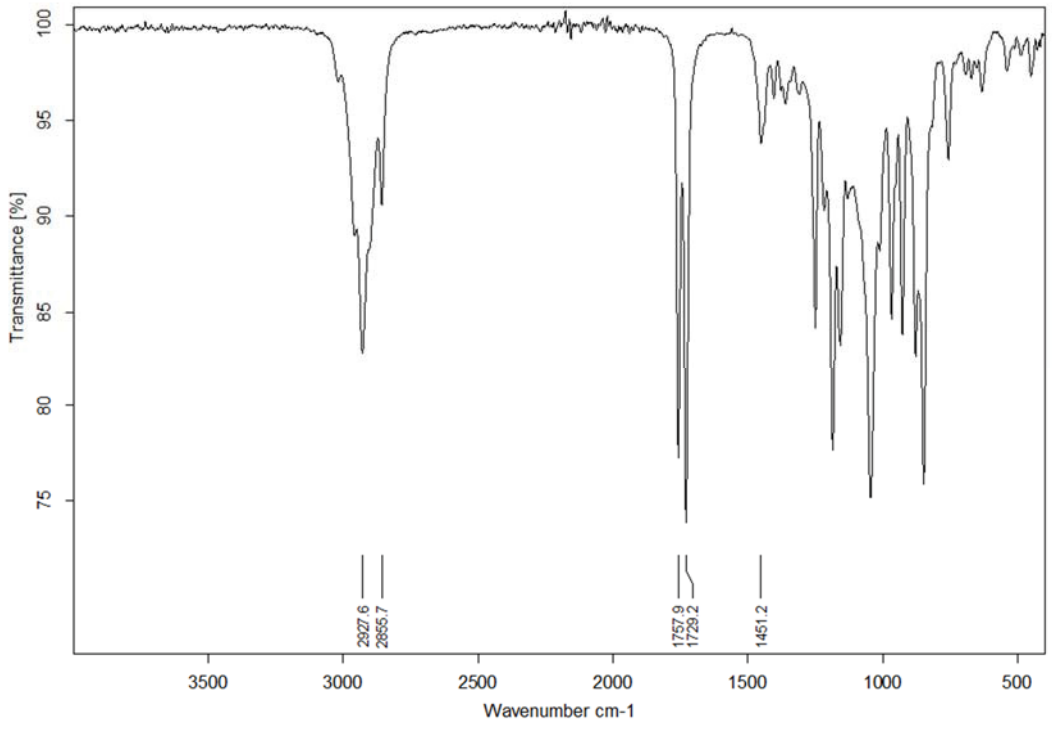

Figure C.36 FTIR spectrum (neat) of compound α-**5.47**

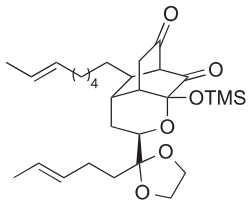

β-**5.47**

Figure C.37 ^{1}H-NMR (500 MHz; $CDCl_3$) for compound β-**5.47**

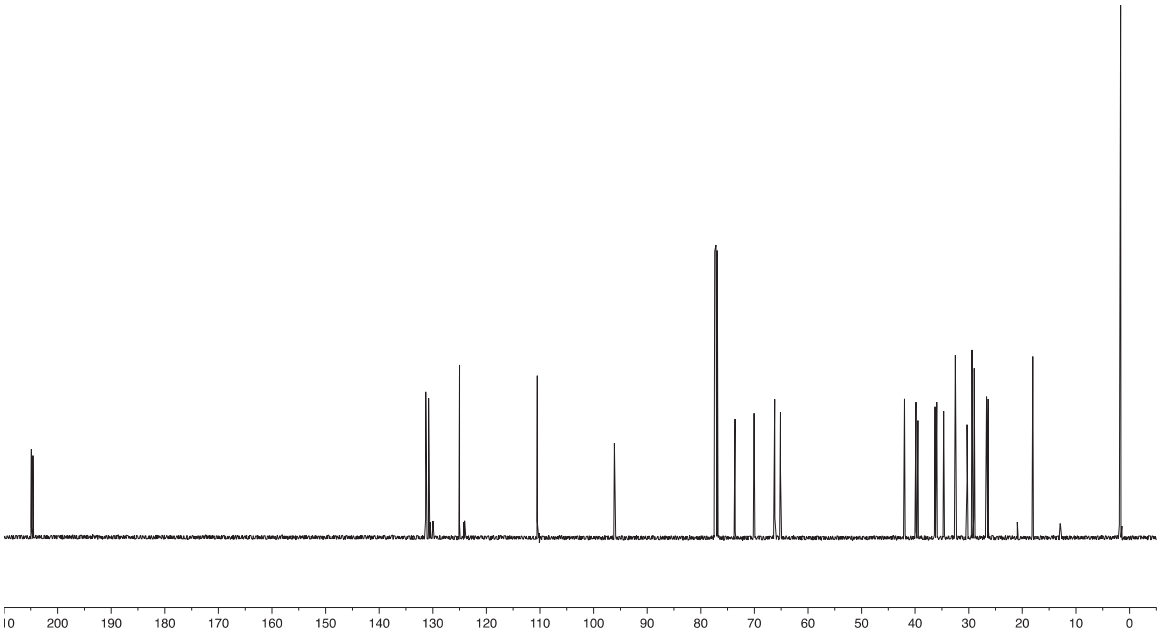

Figure C.38 ^{13}C-NMR spectrum (125 MHz; $CDCl_3$) of compound β-**5.47**

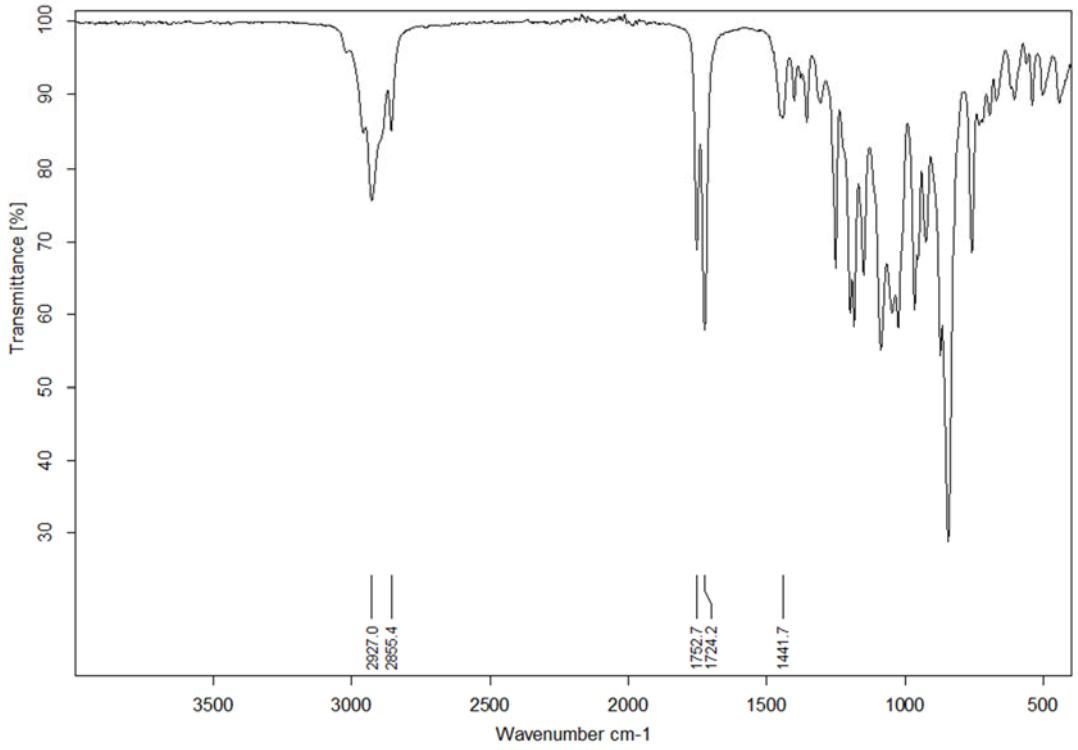

Figure C.39 FTIR spectrum (neat) of compound β-**5.47**

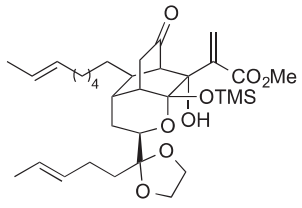

5.48

Figure C.40 ^{1}H-NMR (500 MHz; $CDCl_3$) for compound **5.48**

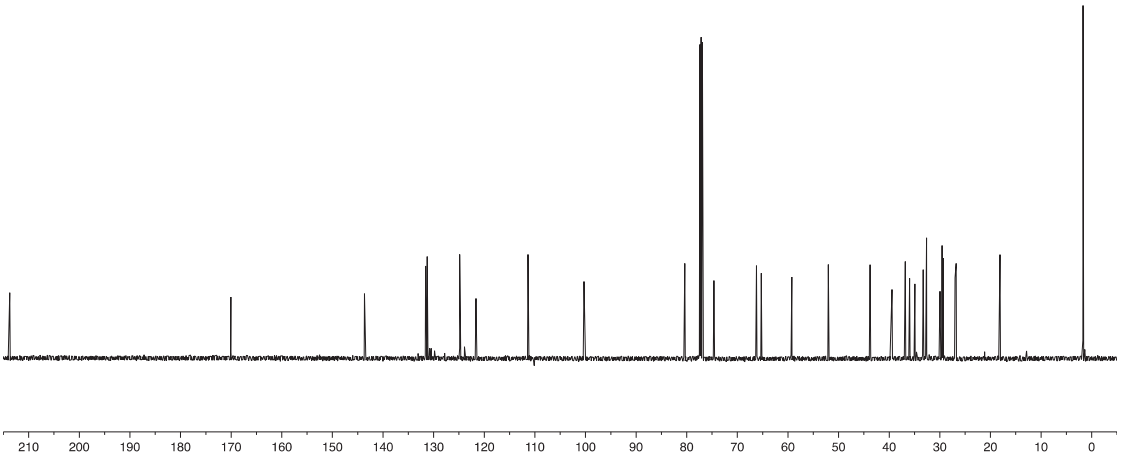

Figure C.41 ^{13}C-NMR spectrum (125 MHz; $CDCl_3$) of compound **5.48**

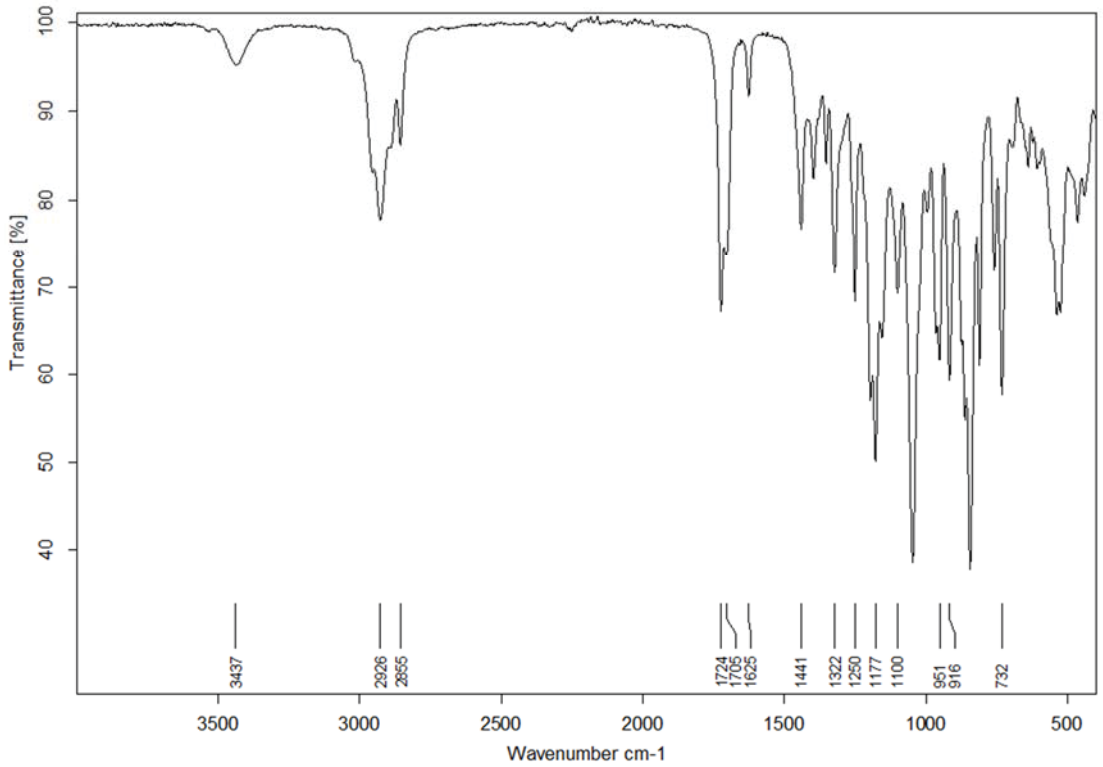

Figure C.42 FTIR spectrum (neat) of compound **5.48**

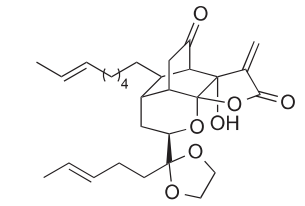

5.38

Figure C.43 ^{1}H-NMR (500 MHz; $CDCl_3$) for compound **5.38**

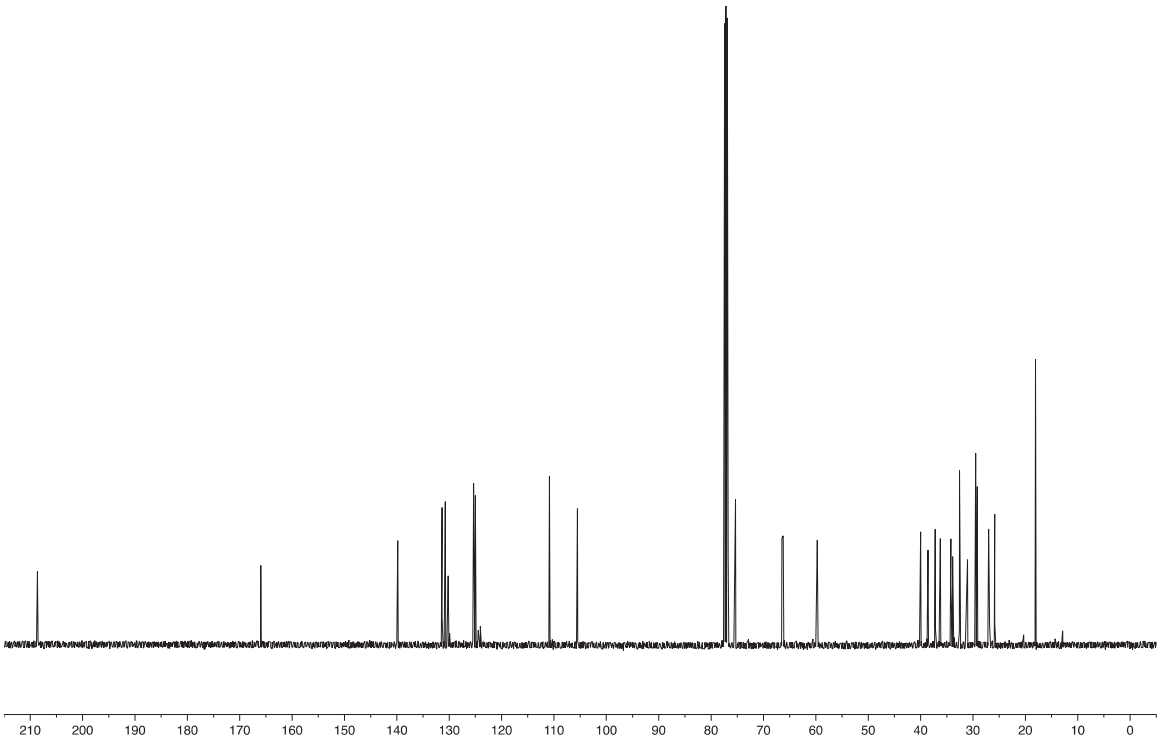

Figure C.44 ^{13}C-NMR spectrum (125 MHz; $CDCl_3$) of compound **5.38**

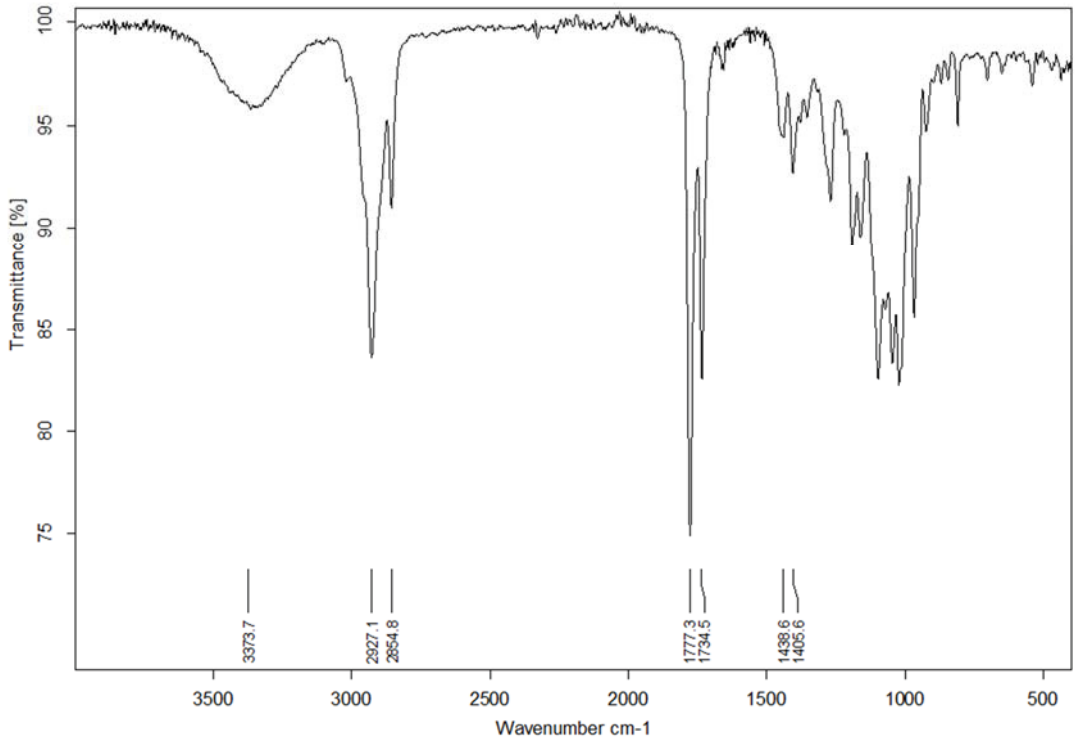

Figure C.45 FTIR spectrum (neat) of compound **5.38**

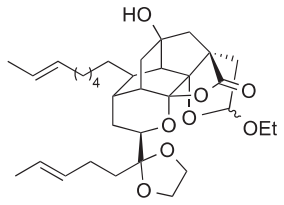

5.22
Diastereomer A

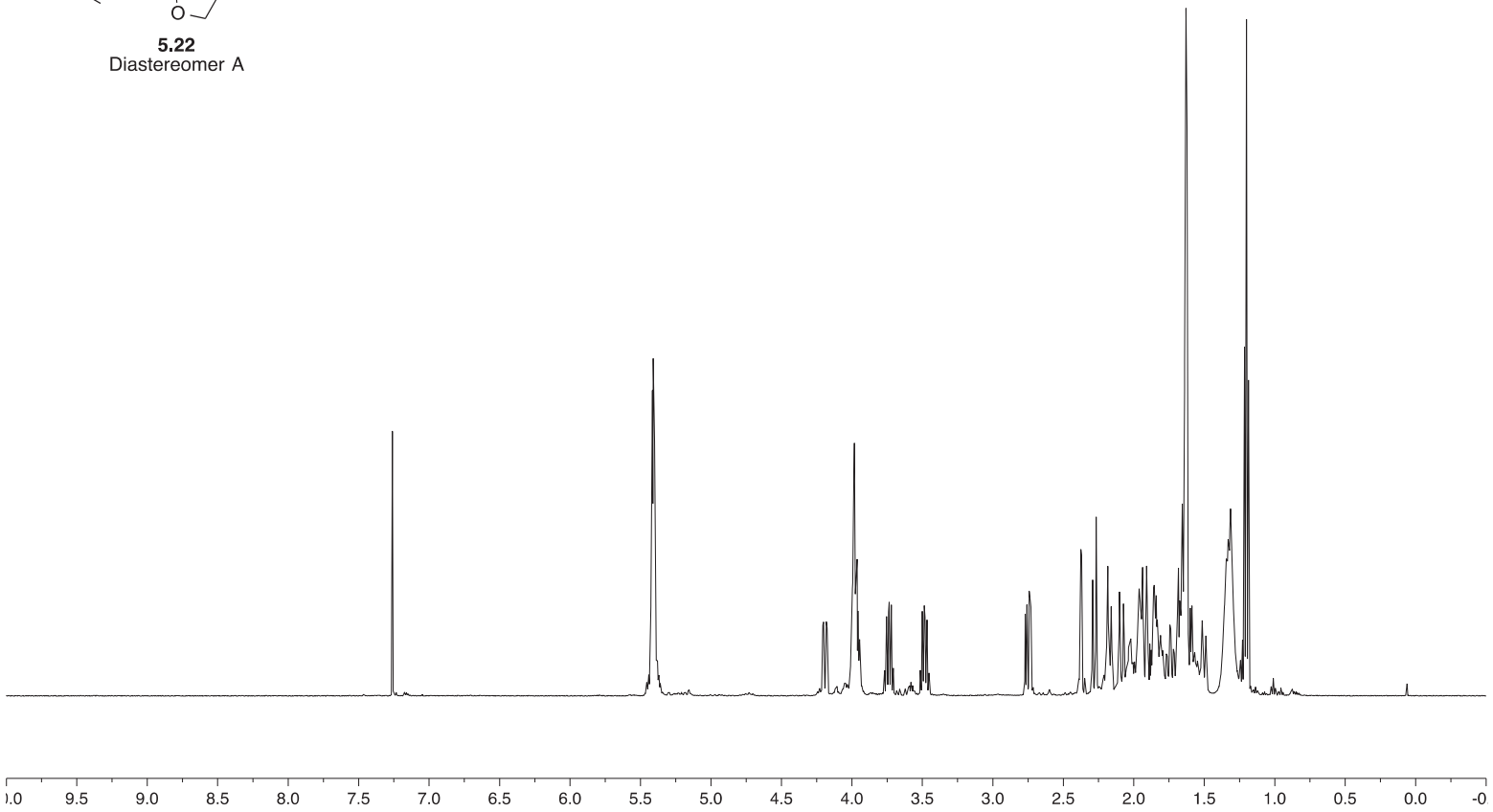

Figure C.46 ^{1}H-NMR (500 MHz; $CDCl_3$) for compound **5.22** Diastereomer A

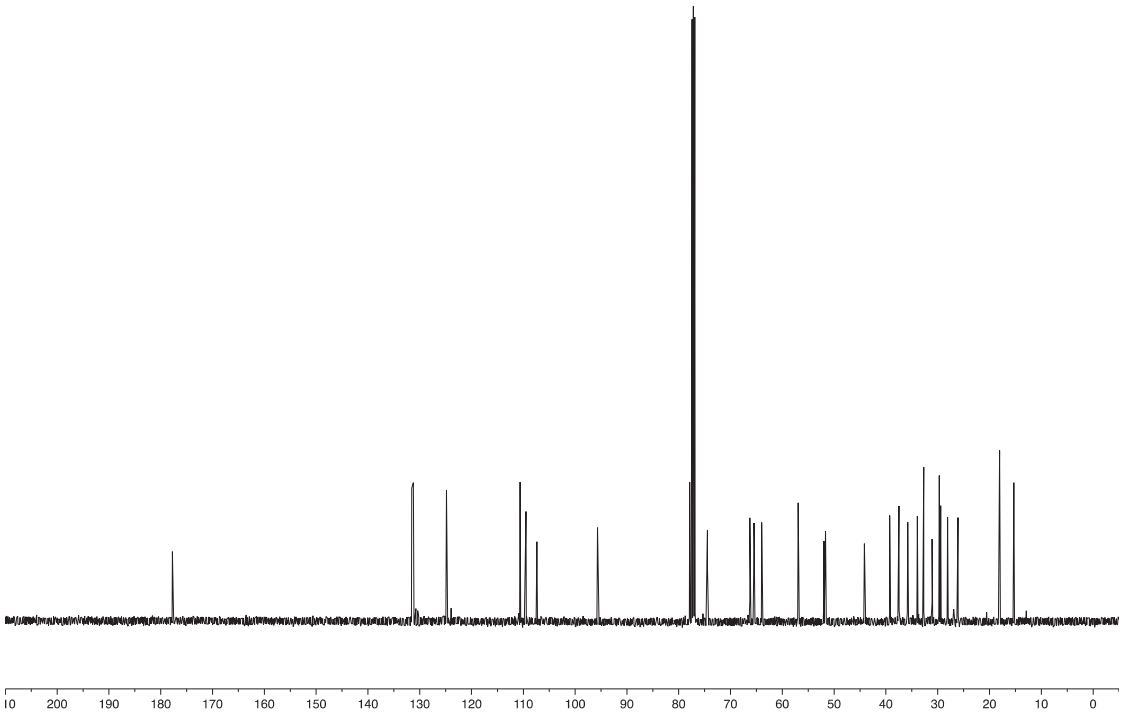

Figure C.47 ^{13}C-NMR spectrum (125 MHz; $CDCl_3$) of compound **5.22** Diastereomer A

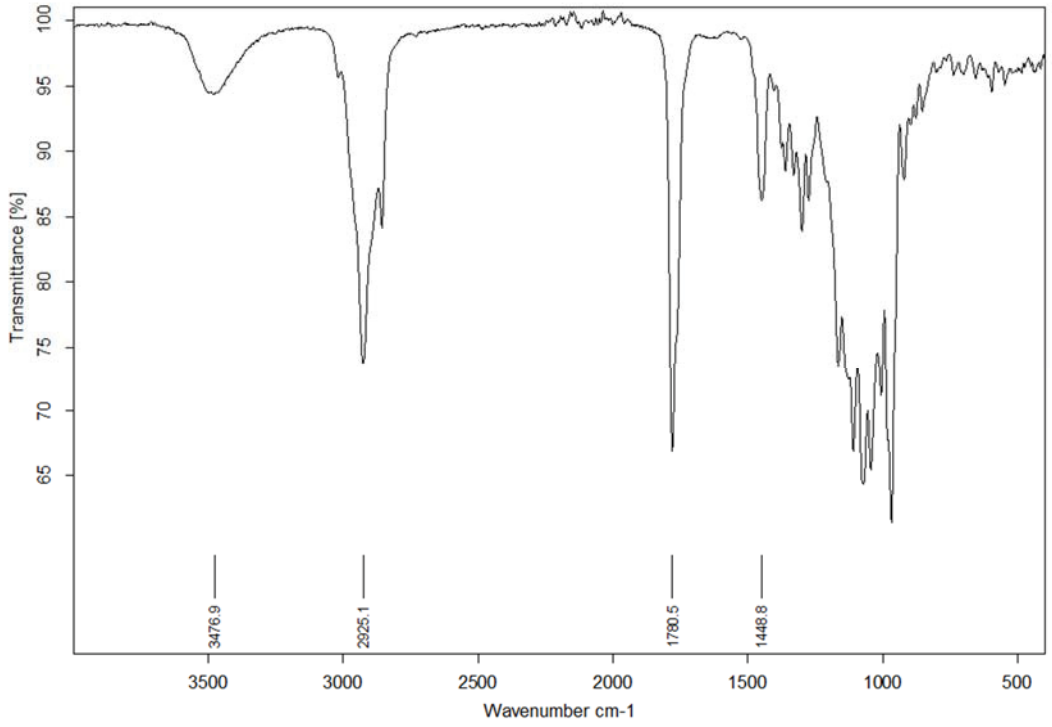

Figure C.48 FTIR spectrum (neat) of compound **5.22** Diastereomer A

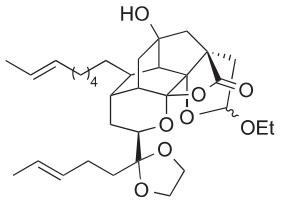

5.22
Diastereomer B

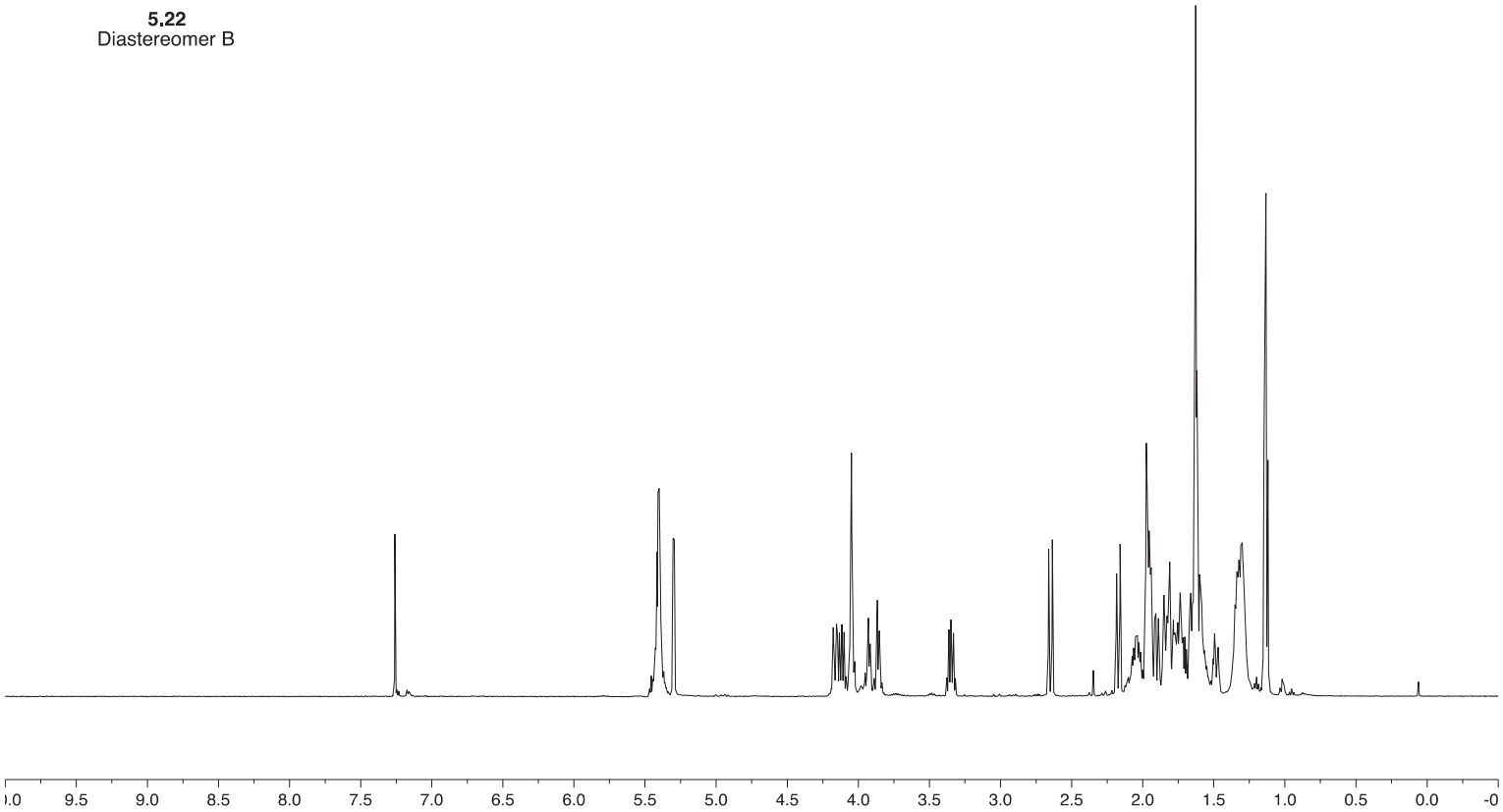

Figure C.49 ^{1}H-NMR (500 MHz; $CDCl_3$) for compound **5.22** Diastereomer B

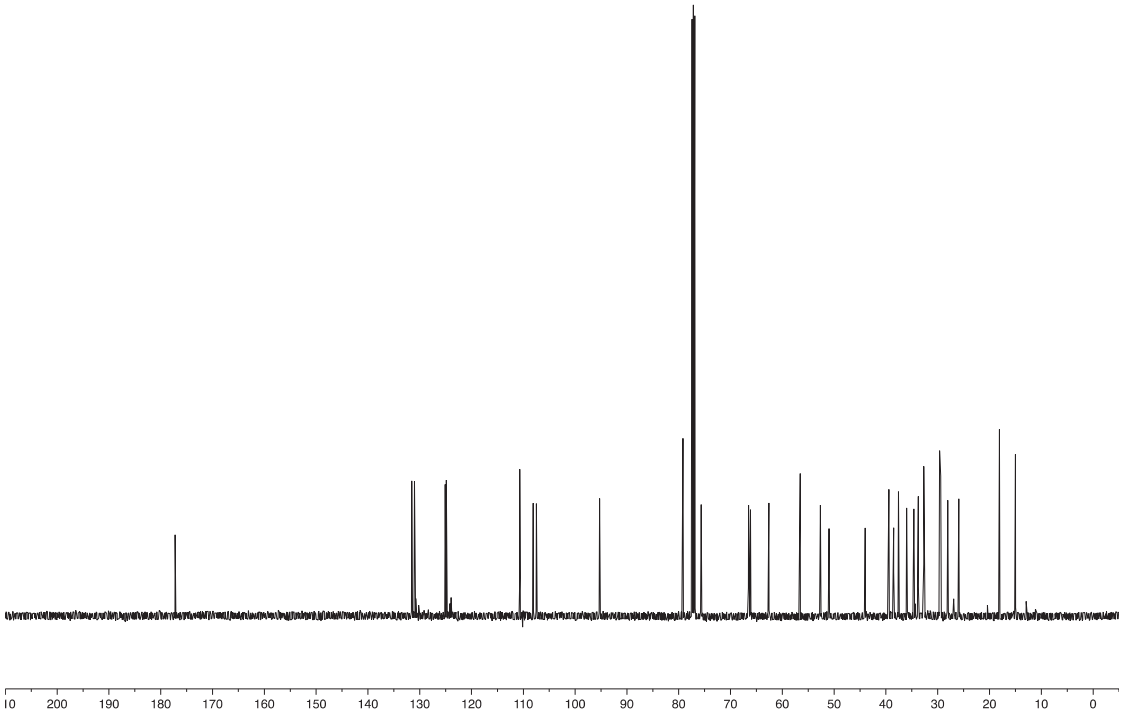

Figure C.50 ^{13}C-NMR spectrum (125 MHz; $CDCl_3$) of compound **5.22** Diastereomer B

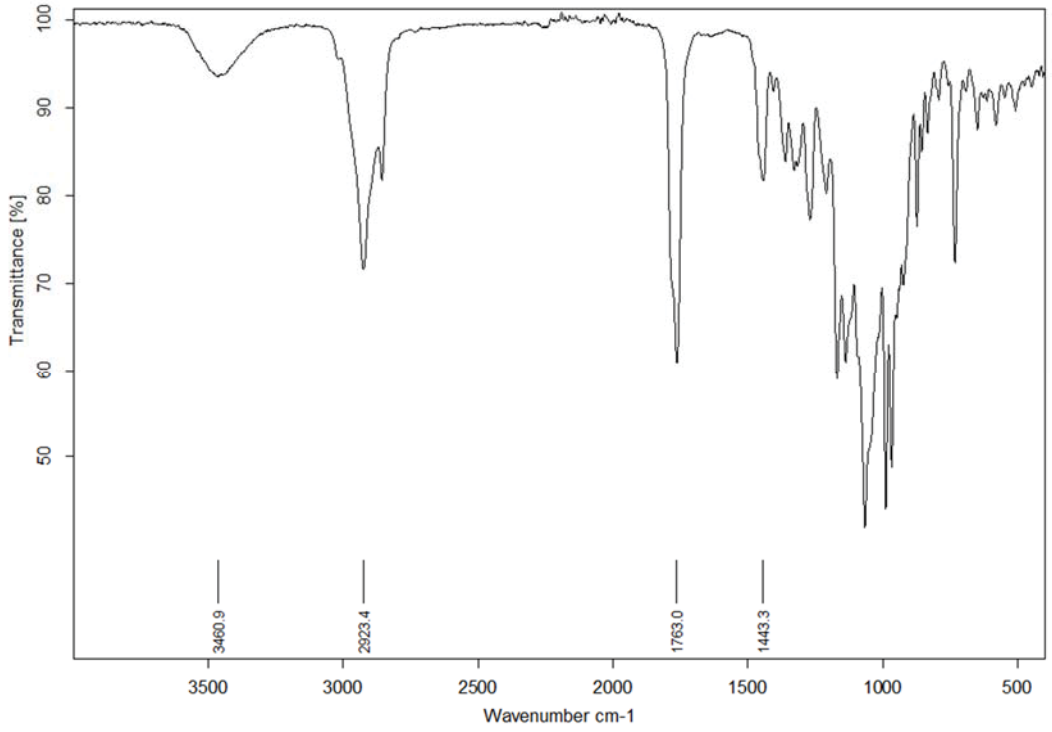

Figure C.51 FTIR spectrum (neat) of compound **5.22** Diastereomer B

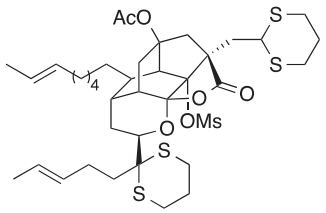

5.25

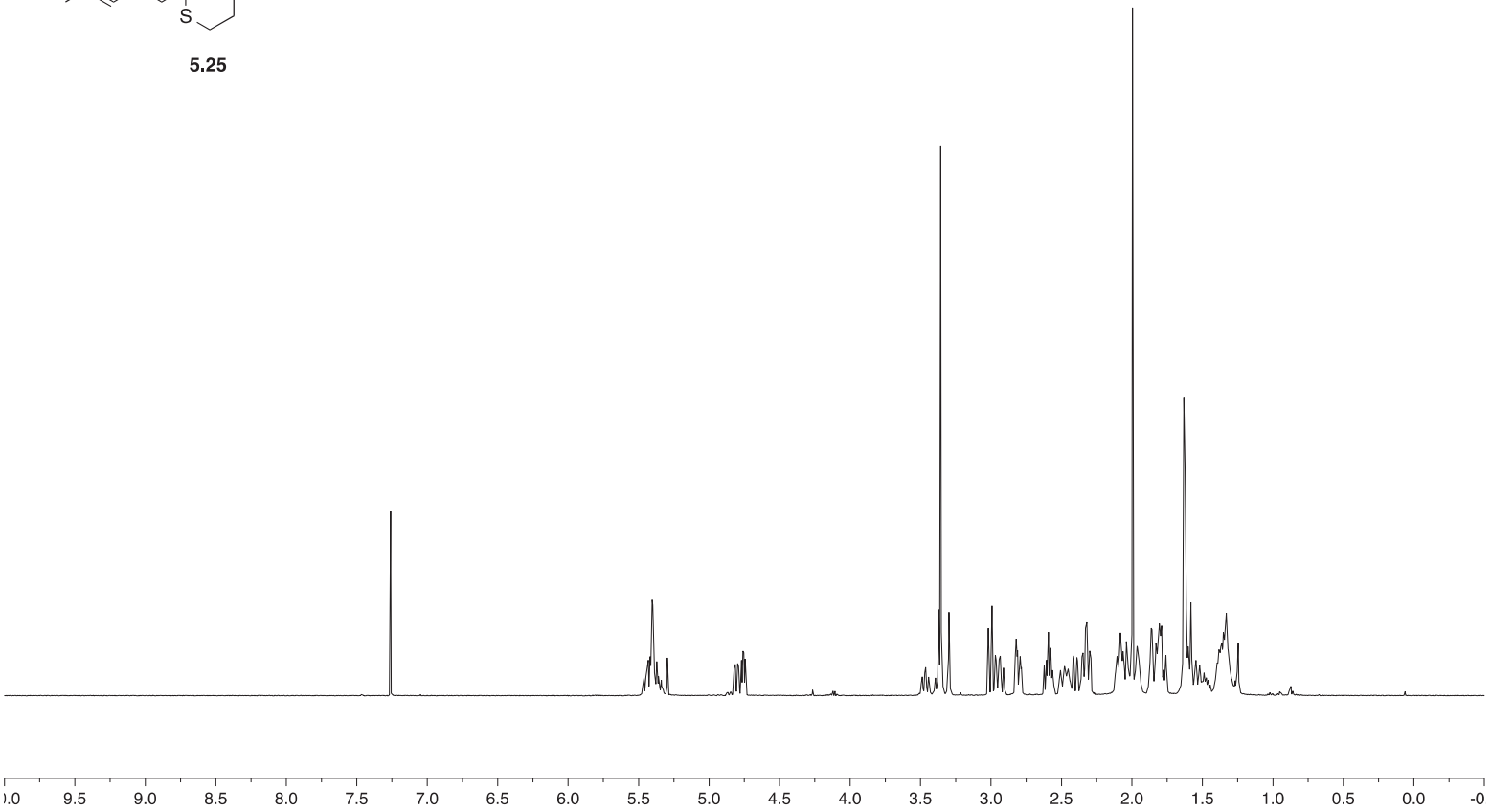

Figure C.52 ^{1}H-NMR (500 MHz; $CDCl_3$) for compound **5.25**

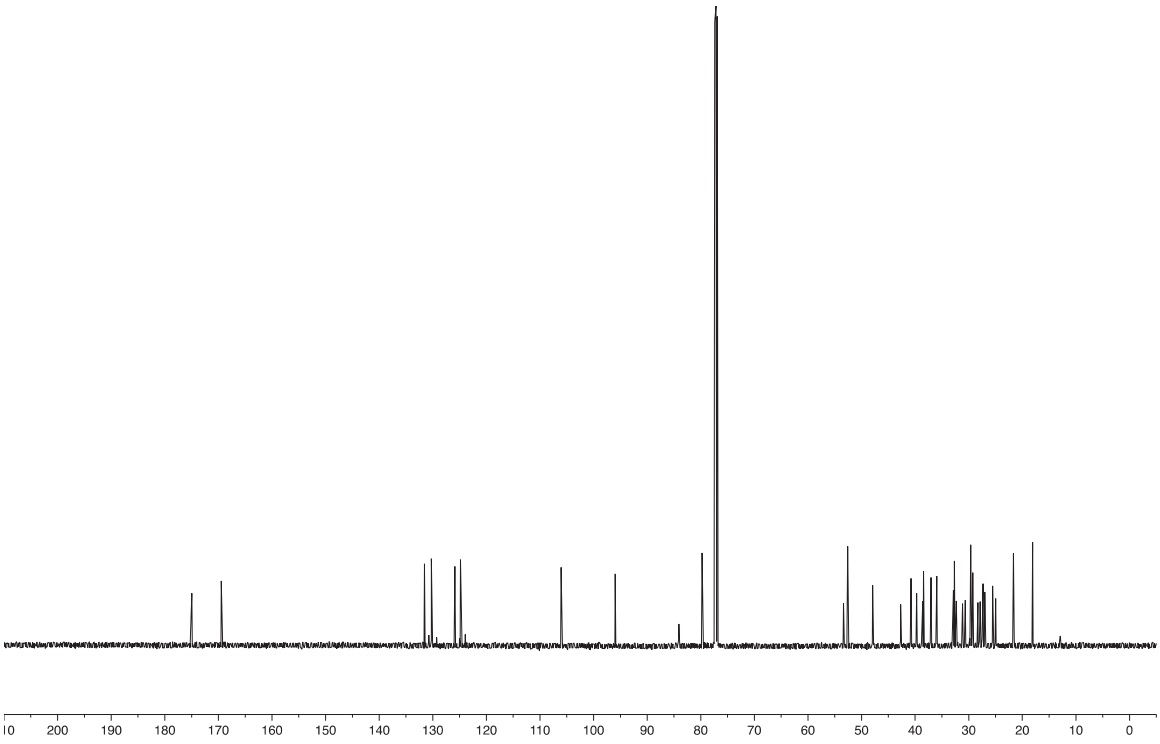

Figure C.53 ^{13}C-NMR spectrum (125 MHz; $CDCl_3$) of compound **5.25**

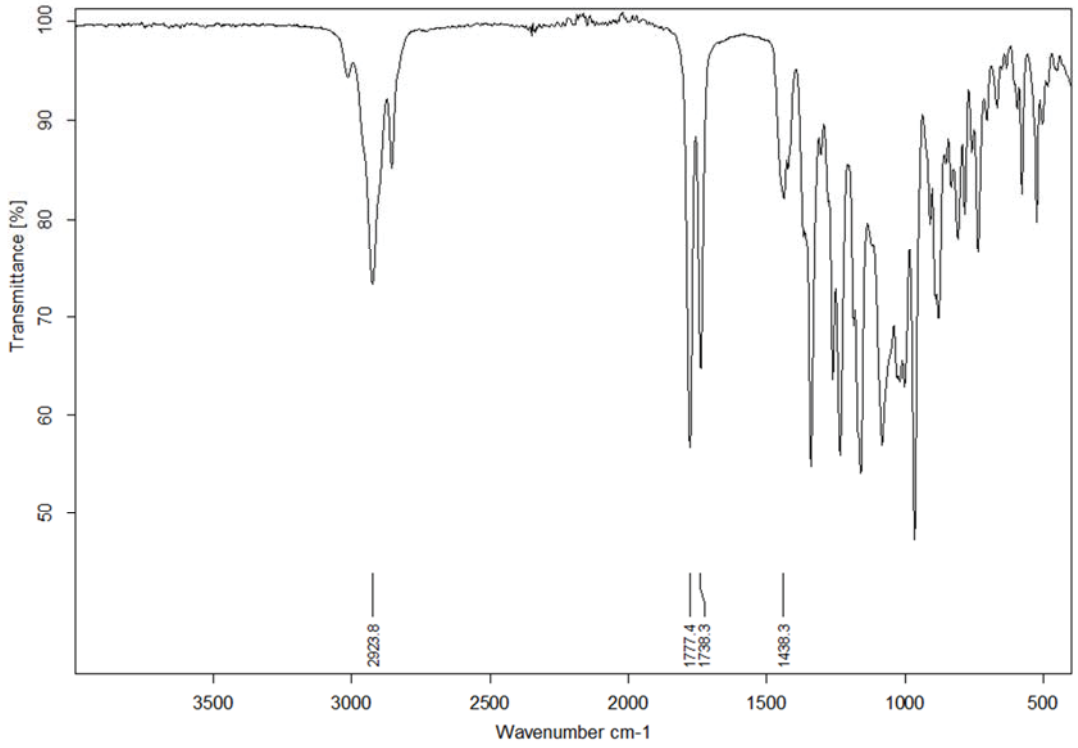

Figure C.54 FTIR spectrum (neat) of compound **5.25**

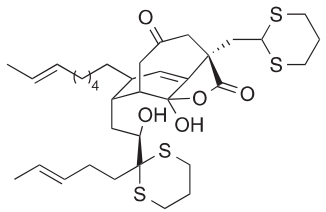

5.50

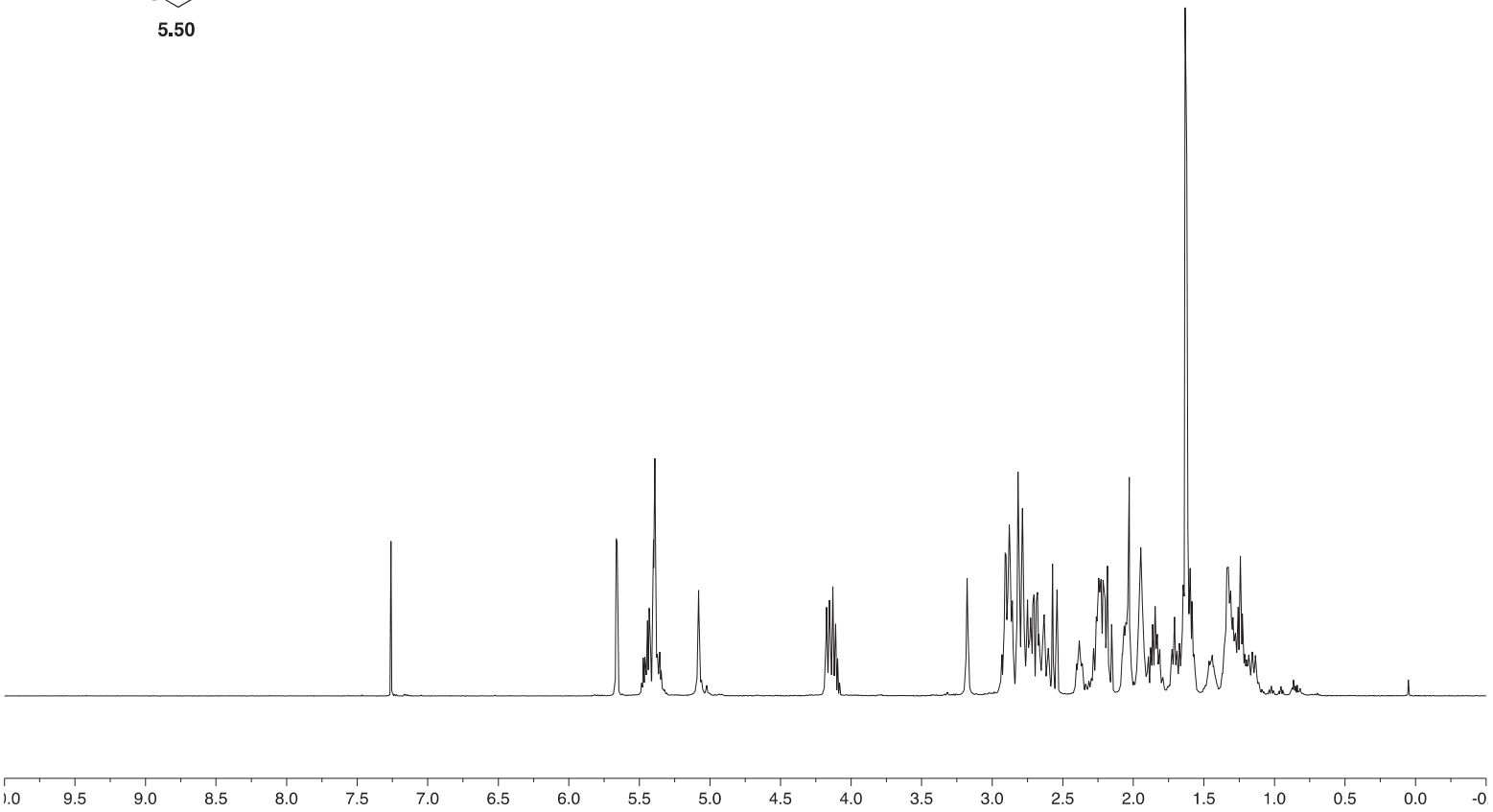

Figure C.55 ^{1}H-NMR (500 MHz; $CDCl_3$) for compound **5.50**

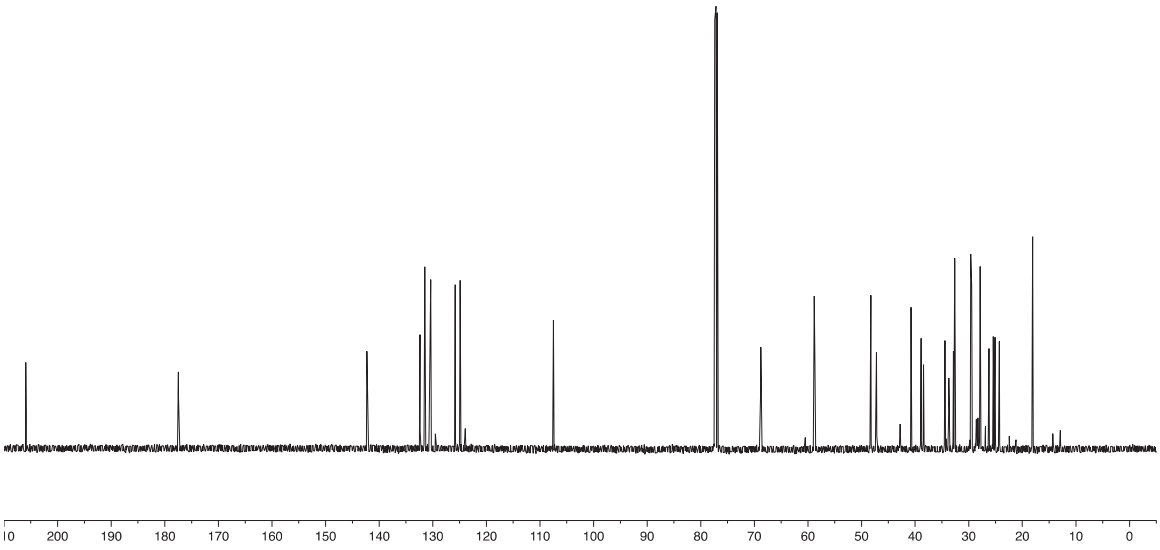

Figure C.56 ^{13}C-NMR spectrum (125 MHz; $CDCl_3$) of compound **5.50**

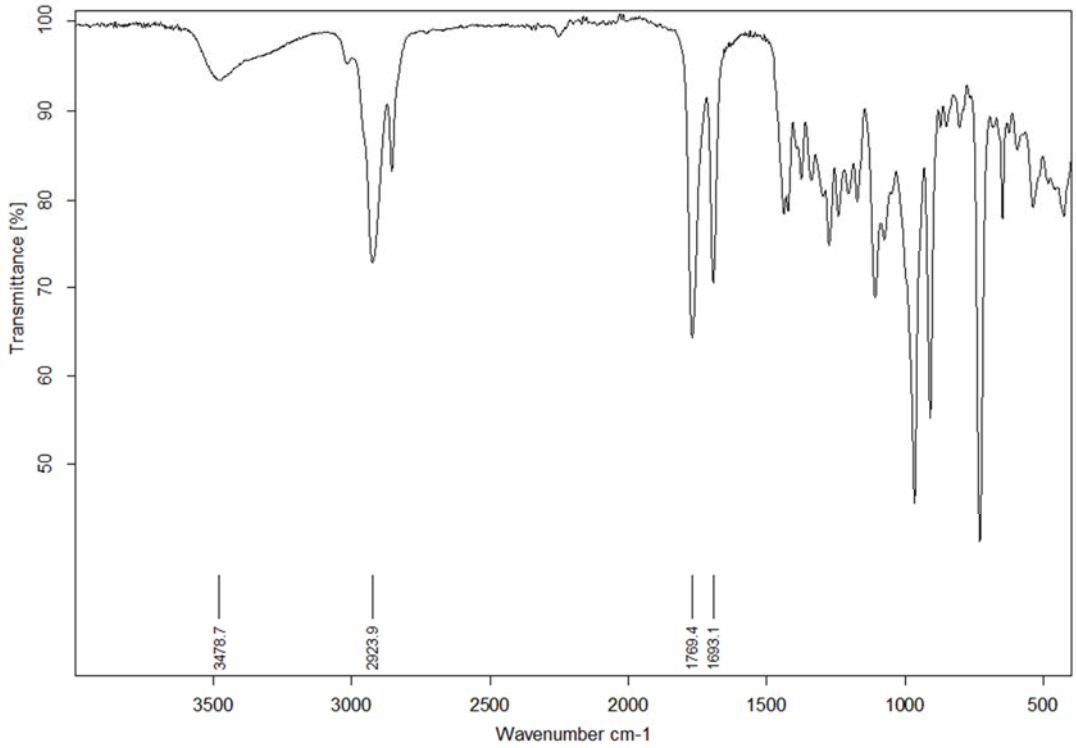

Figure C.57 FTIR spectrum (neat) of compound **5.50**

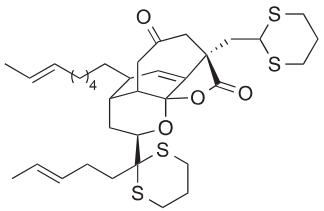

5.24

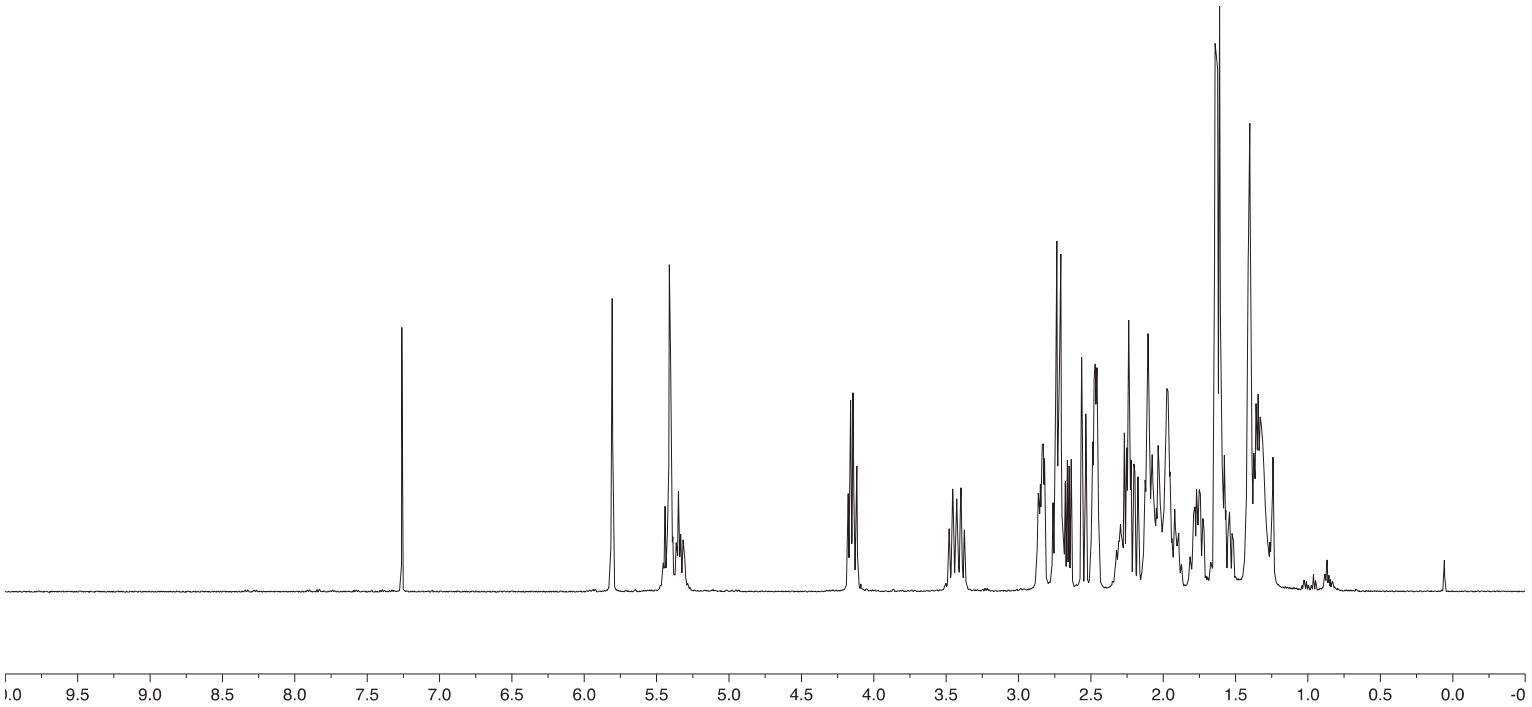

Figure C.58 ^{1}H-NMR (500 MHz; $CDCl_3$) for compound **5.24**

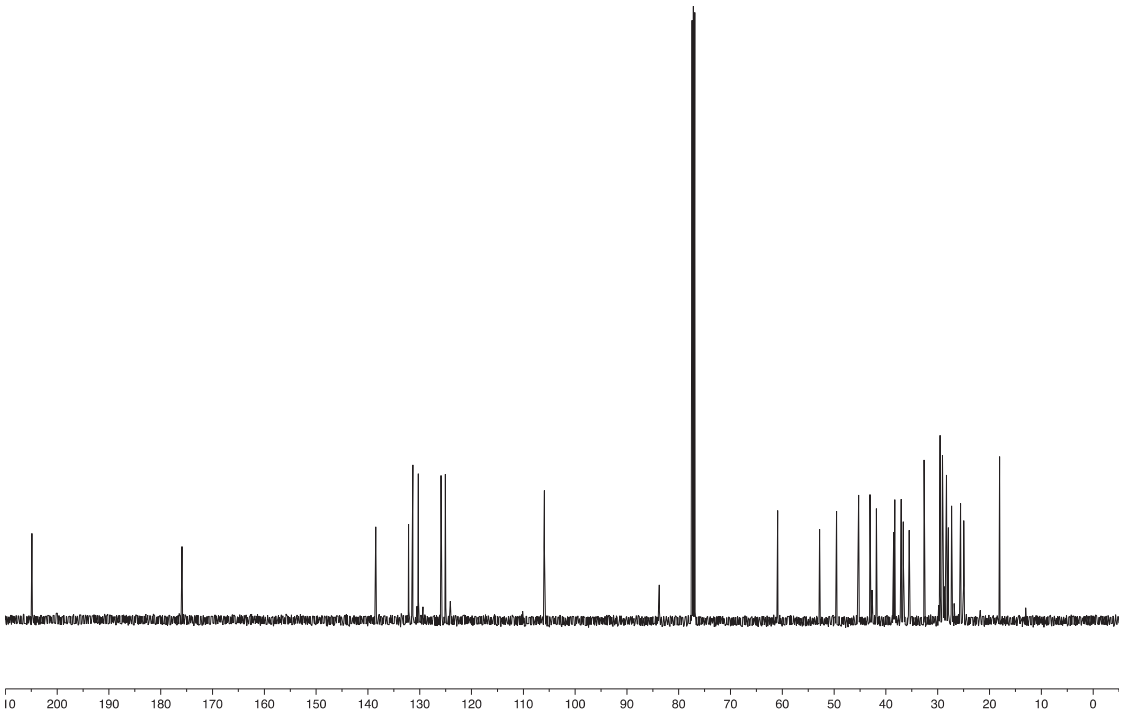

Figure C.59 ^{13}C-NMR spectrum (125 MHz; $CDCl_3$) of compound **5.24**

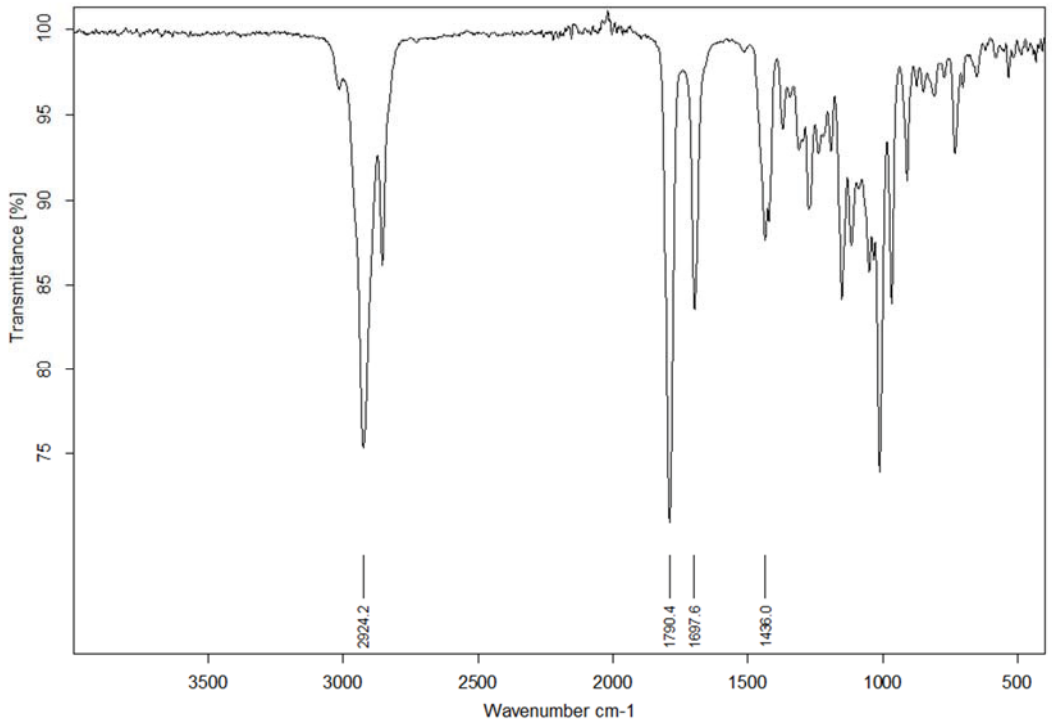

Figure C.60 FTIR spectrum (neat) of compound **5.24**

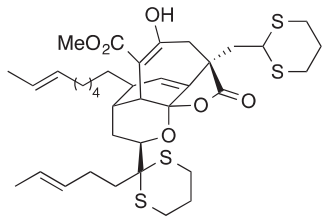

5.54

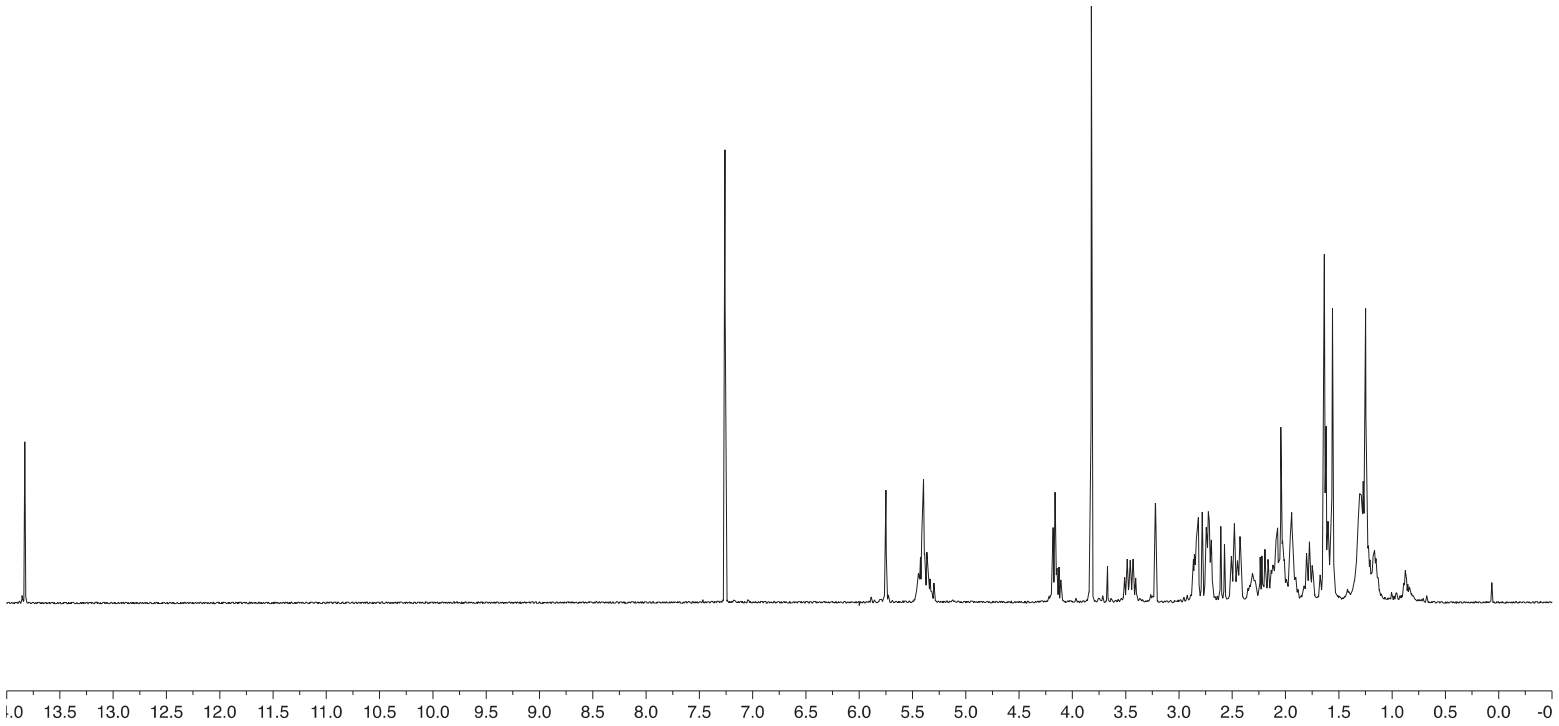

Figure C.61 ^{1}H-NMR (500 MHz; $CDCl_3$) for compound **5.54**

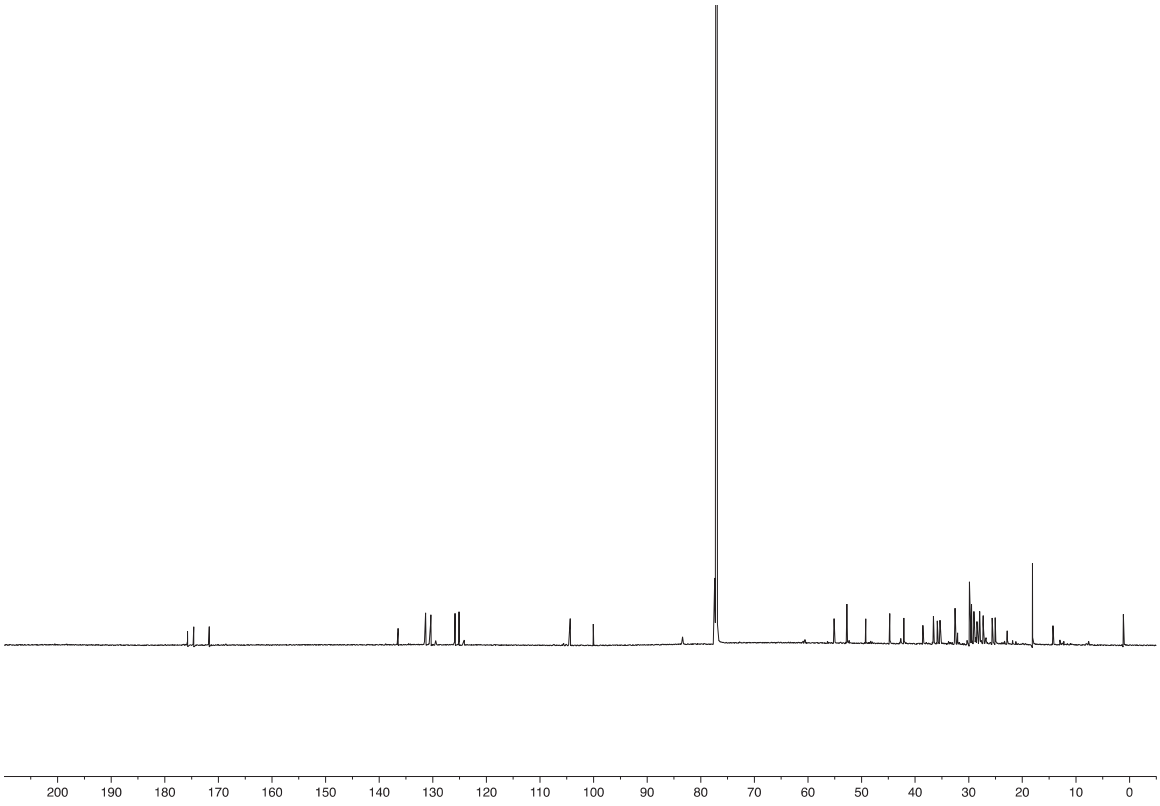

Figure C.62 ^{13}C-NMR spectrum (150 MHz; $CDCl_3$) of compound **5.54**

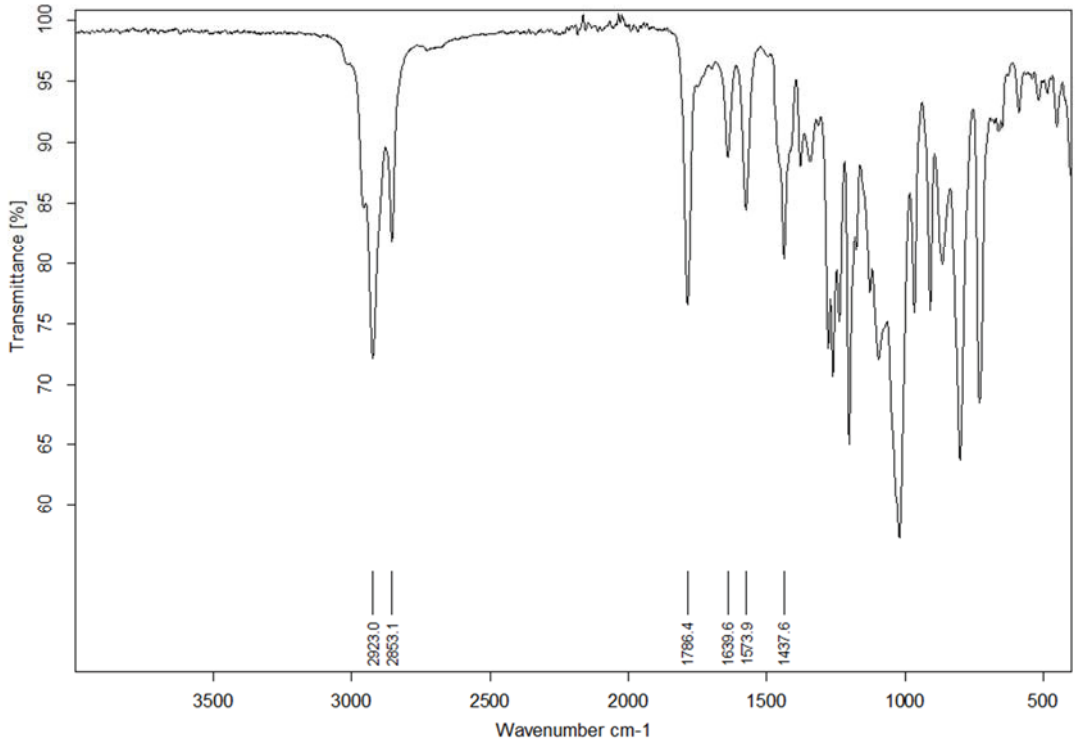

Figure C.63 FTIR spectrum (neat) of compound **5.54**

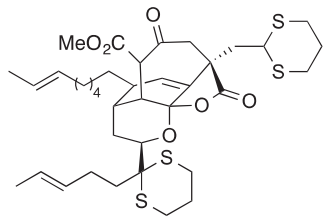

5.54a

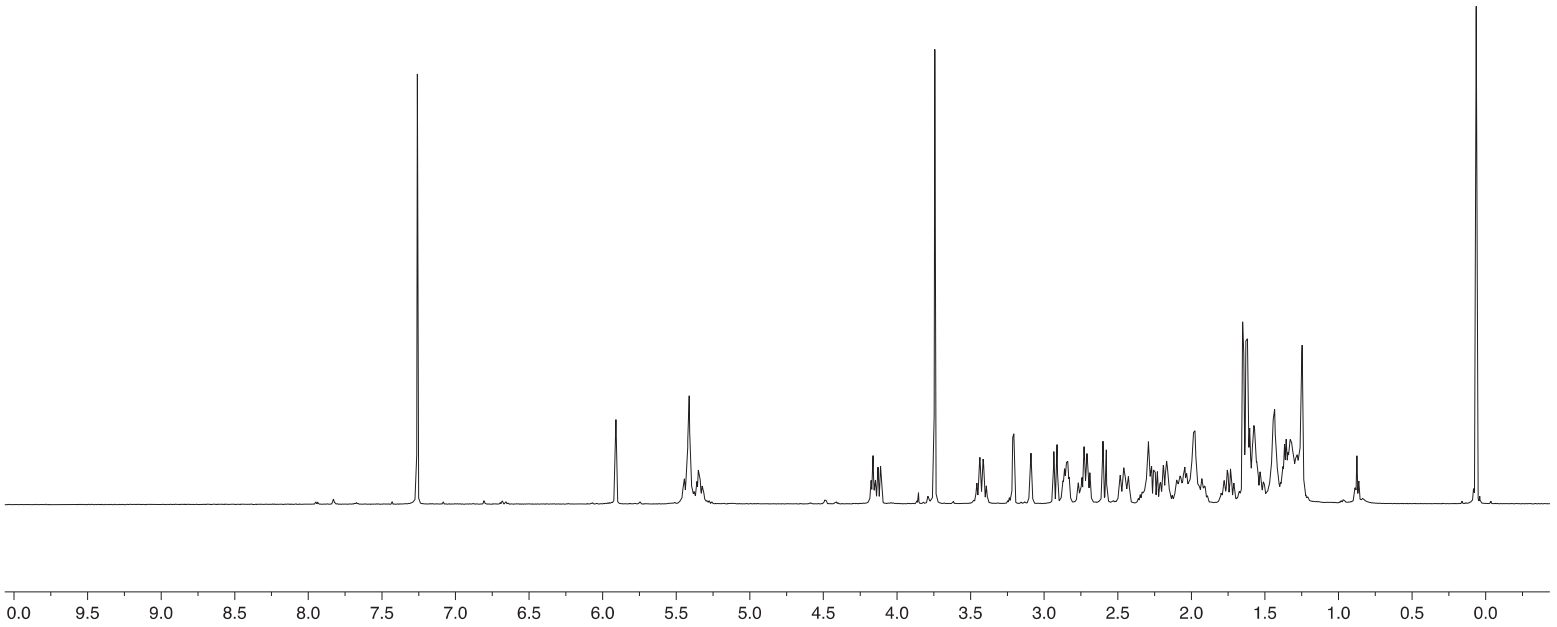

Figure C.64 ^{1}H-NMR (600 MHz; $CDCl_3$) for compound **5.54a**

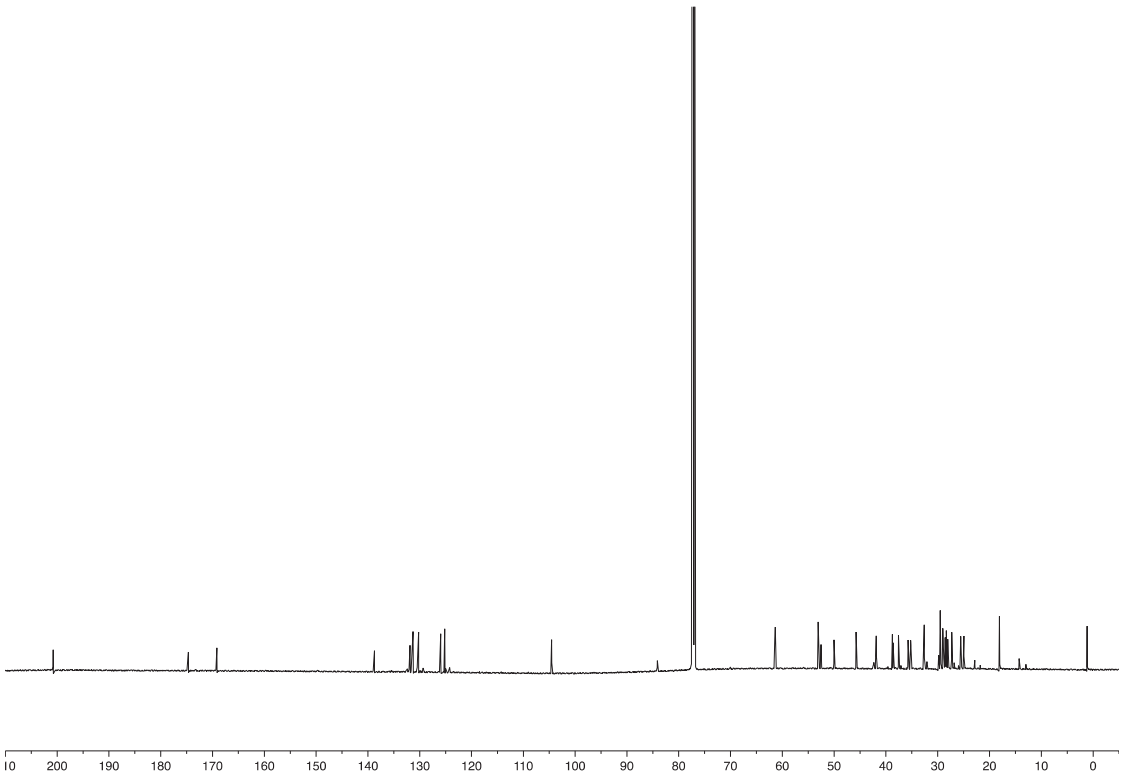

Figure C.65 ^{13}C-NMR spectrum (150 MHz; $CDCl_3$) of compound **5.54a**

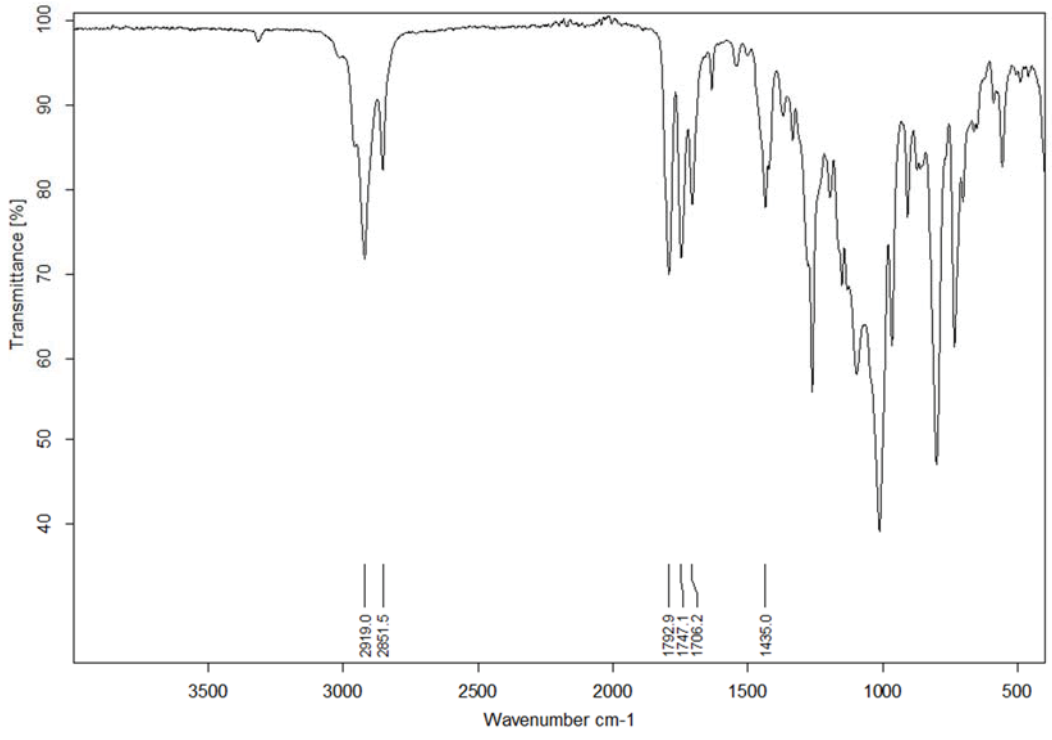

Figure C.66 FTIR spectrum (neat) of compound **5.54a**

APPENDIX D

X-ray Crystallography Reports

D.1 X-ray Crystallography Reports Relevant to Chapter Two

*D.1.1 Crystal Structure Analysis of Norbornane **2.39***

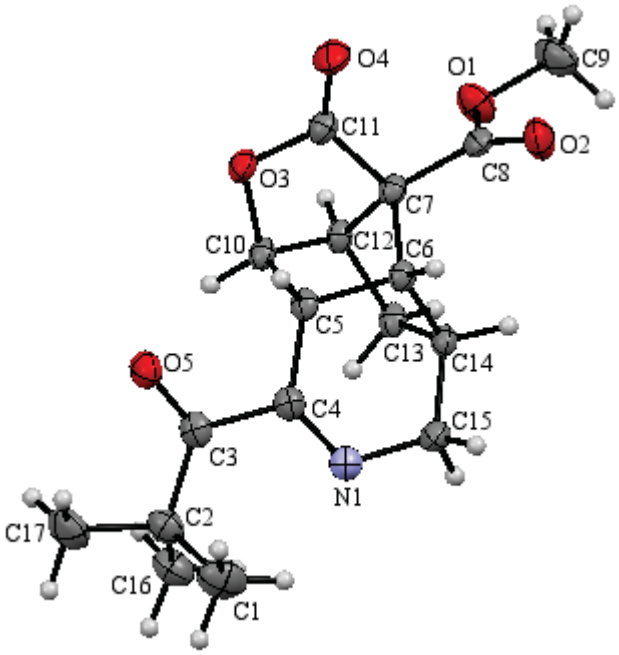

Figure D.10 ORTEP drawing of norbornane **2.39**

Table D.10 Crystal data and structural refinement for norbornane **2.39**

Identification code	JLW7d
Empirical formula	$C_{17}H_{21}NO_5$
Formula weight	319.35
Temperature	150(2) K
Wavelength	0.71073 Å
Crystal system	Monoclinic
Space group	P2(1)/n
Unit cell dimensions	a = 12.0625(9) Å α = 90°
	b = 6.9800(6) Å β = 102.874(3)°.
	c = 19.6097(14) Å γ = 90°.
Volume	1609.6(2) $Å^3$
Z, Calculated density	4, 1.318 Mg/m^3
Absorption coefficient	0.097 mm^{-1}
F(000)	680
Crystal size	0.149 x 0.093 x 0.042 mm
Theta range for data collection	2.226 to 27.102°.
Limiting indices	$-15 \le h \le 15, -8 \le k \le 8, -25 \le l \le 25$
Reflections collected / unique	36214 / 3535 [R_{int} = 0.0860]
Completeness to theta = 25.242	99.9%
Refinement method	Full-matrix least-squares on F^2
Data / restraints / parameters	3535 / 0 / 212
Goodness-of-fit on F^2	1.043
Final R indices [I>2sigma(I)]	R1 = 0.0417, wR2 = 0.0984
R indices (all data)	R1 = 0.0554, wR2 = 0.1068
Largest diff. peak and hole	0.332 and -0.187 $e.Å^{-3}$

Table D.11 Displacement parameters (A^2 x 10^3) for JLW7d. U(eq) is defined as one third of the trace of the orthogonalized U^{ij} tensor.

Atom	x	y	z	U(eq)
O(1)	3893(1)	289(2)	1170(1)	37(1)
O(2)	3844(1)	889(2)	2283(1)	38(1)
O(3)	1714(1)	4817(2)	700(1)	26(1)
O(4)	3465(1)	5132(2)	1384(1)	36(1)
O(5)	-1208(1)	5798(2)	877(1)	32(1)
N(1)	-1001(1)	1225(2)	1600(1)	28(1)
C(1)	-3102(2)	3652(3)	1707(1)	45(1)
C(2)	-2836(1)	3957(2)	983(1)	31(1)
C(3)	-1562(1)	4297(2)	1060(1)	26(1)
C(4)	-683(1)	2777(2)	1365(1)	23(1)
C(5)	522(1)	3377(2)	1374(1)	21(1)
C(6)	1448(1)	2075(2)	1808(1)	21(1)
C(7)	2378(1)	2139(2)	1366(1)	21(1)
C(8)	3442(1)	1036(2)	1668(1)	24(1)
C(9)	4920(2)	-820(3)	1412(1)	45(1)
C(10)	856(1)	3310(2)	654(1)	22(1)
C(11)	2632(1)	4182(2)	1179(1)	25(1)
C(12)	1551(1)	1471(2)	685(1)	22(1)
C(13)	945(1)	-282(2)	895(1)	24(1)
C(14)	999(1)	21(2)	1688(1)	23(1)
C(15)	-139(1)	-211(2)	1891(1)	28(1)
C(16)	-3218(1)	2223(3)	509(1)	38(1)
C(17)	-3469(2)	5737(3)	646(1)	46(1)

Table D.12 Bond Lengths [Å] and angles [°] for norbornane **2.39**

O(1)-C(8)	1.3258(18)	C(13)-H(16)	0.9900
O(1)-C(9)	1.448(2)	C(14)-C(15)	1.521(2)
O(2)-C(8)	1.1992(17)	C(14)-H(15)	1.0000
O(3)-C(11)	1.3566(17)	C(15)-H(13)	0.9900
O(3)-C(10)	1.4647(17)	C(15)-H(14)	0.9900
O(4)-C(11)	1.1963(18)	C(16)-H(7)	0.9800
O(5)-C(3)	1.2156(19)	C(16)-H(5)	0.9800
N(1)-C(4)	1.270(2)	C(16)-H(6)	0.9800
N(1)-C(15)	1.465(2)	C(17)-H(10)	0.9800
C(1)-C(2)	1.538(2)	C(17)-H(11)	0.9800
C(1)-H(1)	0.9800	C(17)-H(12)	0.9800
C(1)-H(9)	0.9800		
C(1)-H(8)	0.9800	C(8)-O(1)-C(9)	115.50(13)
C(2)-C(3)	1.528(2)	C(11)-O(3)-C(10)	105.34(10)
C(2)-C(17)	1.530(2)	C(4)-N(1)-C(15)	118.64(13)
C(2)-C(16)	1.533(2)	C(2)-C(1)-H(1)	109.5
C(3)-C(4)	1.525(2)	C(2)-C(1)-H(9)	109.5
C(4)-C(5)	1.510(2)	H(1)-C(1)-H(9)	109.5
C(5)-C(6)	1.5398(19)	C(2)-C(1)-H(8)	109.5
C(5)-C(10)	1.5513(19)	H(1)-C(1)-H(8)	109.5
C(5)-H(19)	1.0000	H(9)-C(1)-H(8)	109.5
C(6)-C(14)	1.533(2)	C(3)-C(2)-C(17)	108.12(14)
C(6)-C(7)	1.5627(19)	C(3)-C(2)-C(16)	110.02(13)
C(6)-H(20)	1.0000	C(17)-C(2)-C(16)	108.98(14)
C(7)-C(8)	1.501(2)	C(3)-C(2)-C(1)	110.04(13)
C(7)-C(11)	1.521(2)	C(17)-C(2)-C(1)	108.93(14)
C(7)-C(12)	1.5493(18)	C(16)-C(2)-C(1)	110.70(15)
C(9)-H(2)	0.9800	O(5)-C(3)-C(4)	117.12(13)
C(9)-H(3)	0.9800	O(5)-C(3)-C(2)	121.11(14)
C(9)-H(21)	0.9800	C(4)-C(3)-C(2)	121.77(13)
C(10)-C(12)	1.527(2)	N(1)-C(4)-C(5)	126.90(13)
C(10)-H(18)	1.0000	N(1)-C(4)-C(3)	119.75(13)
C(12)-C(13)	1.527(2)	C(5)-C(4)-C(3)	113.30(12)
C(12)-H(4)	1.0000	C(4)-C(5)-C(6)	114.89(12)
C(13)-C(14)	1.5565(19)	C(4)-C(5)-C(10)	115.16(11)
C(13)-H(17)	0.9900	C(6)-C(5)-C(10)	100.47(11)

Table D.12 continued

C(4)-C(5)-H(19)	108.6	C(10)-C(5)-H(19)	108.6
C(6)-C(5)-H(19)	108.6	C(14)-C(6)-C(5)	106.24(11)
C(14)-C(6)-C(7)	102.38(11)	C(13)-C(12)-H(4)	114.8
C(5)-C(6)-C(7)	101.46(10)	C(7)-C(12)-H(4)	114.8
C(14)-C(6)-H(20)	115.0	C(12)-C(13)-C(14)	104.13(11)
C(5)-C(6)-H(20)	115.0	C(12)-C(13)-H(17)	110.9
C(7)-C(6)-H(20)	115.0	C(14)-C(13)-H(17)	110.9
C(8)-C(7)-C(11)	112.06(12)	C(12)-C(13)-H(16)	110.9
C(8)-C(7)-C(12)	121.04(12)	C(14)-C(13)-H(16)	110.9
C(11)-C(7)-C(12)	101.55(11)	H(17)-C(13)-H(16)	108.9
C(8)-C(7)-C(6)	115.02(11)	C(15)-C(14)-C(6)	111.60(12)
C(11)-C(7)-C(6)	111.60(12)	C(15)-C(14)-C(13)	114.06(12)
C(12)-C(7)-C(6)	93.73(10)	C(6)-C(14)-C(13)	102.38(11)
O(2)-C(8)-O(1)	124.50(14)	C(15)-C(14)-H(15)	109.5
O(2)-C(8)-C(7)	124.02(14)	C(6)-C(14)-H(15)	109.5
O(1)-C(8)-C(7)	111.47(12)	C(13)-C(14)-H(15)	109.5
O(1)-C(9)-H(2)	109.5	N(1)-C(15)-C(14)	115.42(12)
O(1)-C(9)-H(3)	109.5	N(1)-C(15)-H(13)	108.4
H(2)-C(9)-H(3)	109.5	C(14)-C(15)-H(13)	108.4
O(1)-C(9)-H(21)	109.5	N(1)-C(15)-H(14)	108.4
H(2)-C(9)-H(21)	109.5	C(14)-C(15)-H(14)	108.4
H(3)-C(9)-H(21)	109.5	H(13)-C(15)-H(14)	107.5
O(3)-C(10)-C(12)	103.11(11)	C(2)-C(16)-H(7)	109.5
O(3)-C(10)-C(5)	104.21(10)	C(2)-C(16)-H(5)	109.5
C(12)-C(10)-C(5)	103.91(11)	H(7)-C(16)-H(5)	109.5
O(3)-C(10)-H(18)	114.7	C(2)-C(16)-H(6)	109.5
C(12)-C(10)-H(18)	114.7	H(7)-C(16)-H(6)	109.5
C(5)-C(10)-H(18)	114.7	H(5)-C(16)-H(6)	109.5
O(4)-C(11)-O(3)	123.15(14)	C(2)-C(17)-H(10)	109.5
O(4)-C(11)-C(7)	129.63(14)	C(2)-C(17)-H(11)	109.5
O(3)-C(11)-C(7)	107.21(12)	H(10)-C(17)-H(11)	109.5
C(10)-C(12)-C(13)	113.11(12)	C(2)-C(17)-H(12)	109.5
C(10)-C(12)-C(7)	105.31(11)	H(10)-C(17)-H(12)	109.5
C(10)-C(12)-H(4)	114.8	H(11)-C(17)-H(12)	109.5

Symmetry transformations used to generate equivalent atoms

Table D.13 The anisotropic displacement factor exponent takes the form: $-2\pi^2 [h^2 a^{*2} U^{11} + ... + 2 h k a^* b^* U^{12}]$

	U11	U22	U33	U23	U13	U12
O(1)	30(1)	40(1)	40(1)	-4(1)	9(1)	11(1)
O(2)	35(1)	43(1)	31(1)	9(1)	0(1)	9(1)
O(3)	30(1)	19(1)	28(1)	5(1)	4(1)	-1(1)
O(4)	35(1)	28(1)	42(1)	4(1)	1(1)	-10(1)
O(5)	31(1)	25(1)	40(1)	3(1)	3(1)	3(1)
N(1)	27(1)	28(1)	28(1)	2(1)	5(1)	0(1)
C(1)	40(1)	58(1)	43(1)	-8(1)	20(1)	1(1)
C(2)	26(1)	33(1)	35(1)	-3(1)	8(1)	4(1)
C(3)	28(1)	24(1)	24(1)	-4(1)	5(1)	3(1)
C(4)	25(1)	23(1)	22(1)	-2(1)	4(1)	1(1)
C(5)	25(1)	16(1)	21(1)	-2(1)	2(1)	0(1)
C(6)	24(1)	20(1)	18(1)	0(1)	3(1)	0(1)
C(7)	24(1)	17(1)	20(1)	0(1)	4(1)	-1(1)
C(8)	24(1)	17(1)	30(1)	3(1)	5(1)	-3(1)
C(9)	27(1)	38(1)	71(1)	-2(1)	12(1)	8(1)
C(10)	27(1)	16(1)	22(1)	1(1)	2(1)	-1(1)
C(11)	29(1)	20(1)	25(1)	1(1)	6(1)	-1(1)
C(12)	26(1)	19(1)	18(1)	0(1)	3(1)	2(1)
C(13)	29(1)	17(1)	24(1)	-1(1)	2(1)	1(1)
C(14)	25(1)	18(1)	24(1)	4(1)	3(1)	2(1)
C(15)	28(1)	25(1)	30(1)	6(1)	5(1)	-3(1)
C(16)	28(1)	42(1)	40(1)	-6(1)	3(1)	0(1)
C(17)	30(1)	45(1)	63(1)	2(1)	10(1)	13(1)

Table D.14 Displacement parameters (A^2 x 10^3) for JLW7d.

Atom	x	y	z	U(eq)
H(1)	-2731	2477	1917	68
H(9)	-3926	3540	1657	68
H(8)	-2818	4746	2009	68
H(19)	640	4710	1562	25
H(20)	1716	2454	2309	25
H(2)	5476	-51	1740	67
H(3)	5238	-1177	1011	67
H(21)	4740	-1980	1647	67
H(18)	202	3411	241	26
H(4)	1910	1268	278	26
H(17)	1339	-1477	815	29
H(16)	147	-341	626	29
H(15)	1564	-886	1968	27
H(13)	-447	-1495	1738	33
H(14)	-8	-169	2408	33
H(7)	-3004	2413	61	56
H(5)	-4046	2084	430	56
H(6)	-2850	1064	735	56
H(10)	-3195	6866	931	69
H(11)	-4286	5578	615	69
H(12)	-3332	5909	176	69

Table D.15

C(17)-C(2)-C(3)-O(5)	1.2(2)
C(16)-C(2)-C(3)-O(5)	120.08(16)
C(1)-C(2)-C(3)-O(5)	-117.69(17)
C(17)-C(2)-C(3)-C(4)	-178.67(13)
C(16)-C(2)-C(3)-C(4)	-59.76(18)
C(1)-C(2)-C(3)-C(4)	62.48(18)
C(15)-N(1)-C(4)-C(5)	-2.6(2)
C(15)-N(1)-C(4)-C(3)	-179.98(12)
O(5)-C(3)-C(4)-N(1)	176.08(13)
C(2)-C(3)-C(4)-N(1)	-4.1(2)
O(5)-C(3)-C(4)-C(5)	-1.61(18)
C(2)-C(3)-C(4)-C(5)	178.23(12)
N(1)-C(4)-C(5)-C(6)	-9.2(2)
C(3)-C(4)-C(5)-C(6)	168.29(11)
N(1)-C(4)-C(5)-C(10)	106.86(16)
C(3)-C(4)-C(5)-C(10)	-75.64(15)
C(4)-C(5)-C(6)-C(14)	38.10(15)
C(10)-C(5)-C(6)-C(14)	-86.13(12)
C(4)-C(5)-C(6)-C(7)	144.77(11)
C(10)-C(5)-C(6)-C(7)	20.55(12)
C(14)-C(6)-C(7)-C(8)	-72.35(14)
C(5)-C(6)-C(7)-C(8)	177.98(11)
C(14)-C(6)-C(7)-C(11)	158.56(11)
C(5)-C(6)-C(7)-C(11)	48.89(13)
C(14)-C(6)-C(7)-C(12)	54.57(12)
C(5)-C(6)-C(7)-C(12)	-55.10(12)
C(9)-O(1)-C(8)-O(2)	2.1(2)
C(9)-O(1)-C(8)-C(7)	-179.44(13)
C(11)-C(7)-C(8)-O(2)	94.06(17)
C(12)-C(7)-C(8)-O(2)	-146.20(15)
C(6)-C(7)-C(8)-O(2)	-34.8(2)
C(11)-C(7)-C(8)-O(1)	-84.43(15)
C(12)-C(7)-C(8)-O(1)	35.31(18)
C(6)-C(7)-C(8)-O(1)	146.70(12)
C(11)-O(3)-C(10)-C(12)	-40.12(13)
C(11)-O(3)-C(10)-C(5)	68.16(13)

Table D.15 continued

C(4)-C(5)-C(10)-O(3)	150.20(12)
C(6)-C(5)-C(10)-O(3)	-85.76(12)
C(4)-C(5)-C(10)-C(12)	-102.12(13)
C(6)-C(5)-C(10)-C(12)	21.92(13)
C(10)-O(3)-C(11)-O(4)	-174.18(14)
C(10)-O(3)-C(11)-C(7)	6.74(14)
C(8)-C(7)-C(11)-O(4)	-20.5(2)
C(12)-C(7)-C(11)-O(4)	-151.05(16)
C(6)-C(7)-C(11)-O(4)	110.18(17)
C(8)-C(7)-C(11)-O(3)	158.54(11)
C(12)-C(7)-C(11)-O(3)	27.95(14)
C(6)-C(7)-C(11)-O(3)	-70.82(14)
O(3)-C(10)-C(12)-C(13)	160.37(11)
C(5)-C(10)-C(12)-C(13)	51.87(14)
O(3)-C(10)-C(12)-C(7)	53.08(11)
C(5)-C(10)-C(12)-C(7)	-55.42(12)
C(8)-C(7)-C(12)-C(10)	-172.07(12)
C(11)-C(7)-C(12)-C(10)	-47.30(12)
C(6)-C(7)-C(12)-C(10)	65.65(11)
C(8)-C(7)-C(12)-C(13)	73.50(15)
C(11)-C(7)-C(12)-C(13)	-161.72(11)
C(6)-C(7)-C(12)-C(13)	-48.77(12)
C(10)-C(12)-C(13)-C(14)	-72.40(14)
C(7)-C(12)-C(13)-C(14)	25.85(14)
C(5)-C(6)-C(14)-C(15)	-57.36(14)
C(7)-C(6)-C(14)-C(15)	-163.38(11)
C(5)-C(6)-C(14)-C(13)	65.04(13)
C(7)-C(6)-C(14)-C(13)	-40.97(13)
C(12)-C(13)-C(14)-C(15)	130.06(13)
C(12)-C(13)-C(14)-C(6)	9.34(14)
C(4)-N(1)-C(15)-C(14)	-17.75(19)
C(6)-C(14)-C(15)-N(1)	49.72(16)
C(13)-C(14)-C(15)-N(1)	-65.71(17)

Symmetry transformations used to generate equivalent atoms:

*D.2.1 Crystal Structure Analysis of maleic anhydride **4.38***

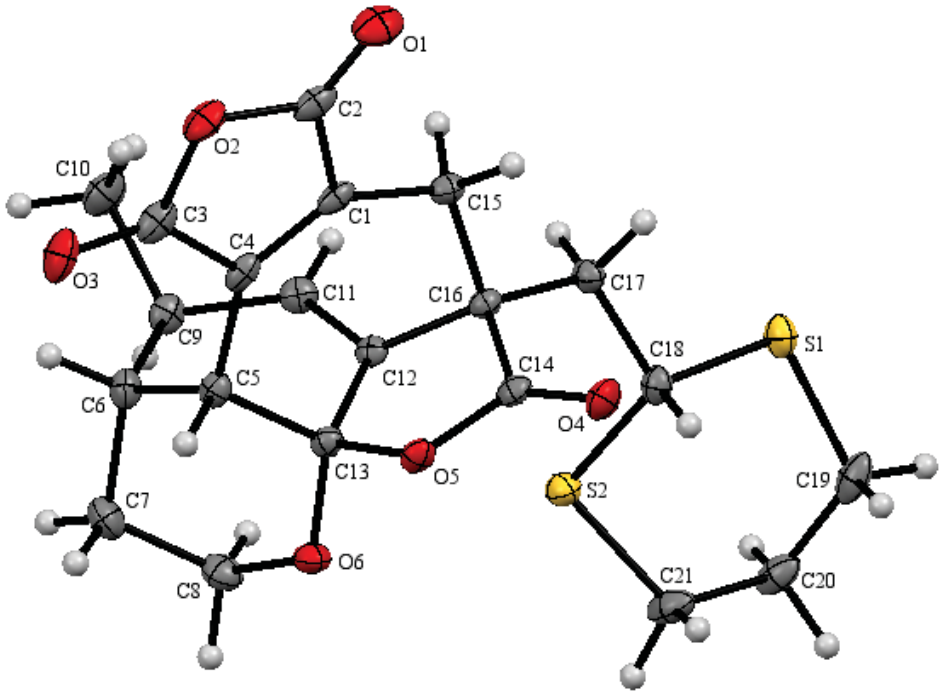

Figure D.11 ORTEP drawing of maleic anhydride **4.38**

Table D.16 Crystal data and structure refinement for maleic anhydride **4.38**.

Identification code	ef12_p212121	
Empirical formula	C21 H22 O6 S2	
Formula weight	434.51	
Temperature	120(2) K	
Wavelength	0.71073 Å	
Crystal system	Orthorhombic	
Space group	P 21 21 21	
Unit cell dimensions	a = 9.0939(12) Å	α = 90°
	b = 12.7592(17) Å	β = 90°
	c = 16.617(2) Å	γ = 90°
Volume	1928.1(4) $Å^3$	
Z	4	
Density (calculated)	1.497 Mg/m^3	
Absorption coefficient	0.314 mm^{-1}	
F(000)	912	
Crystal size	0.21 x 0.16 x 0.12 mm^3	
Theta range for data collection	2.01 to 30.61°.	
Index ranges	$-12 \leq h \leq 13$, $-18 \leq k \leq 18$, $-23 \leq l \leq 23$	
Reflections collected	38440	
Independent reflections	5899 [R_{int} = 0.0399]	
Completeness to theta = 30.61∞	99.6%	
Absorption correction	Semi-empirical from equivalents	
Max. and min. transmission	0.9639 and 0.9367	
Refinement method	Full-matrix least-squares on F^2	
Data / restraints / parameters	5899 / 0 / 263	
Goodness-of-fit on F^2	1.031	
Final R indices [I>2sigma(I)]	R1 = 0.0317, wR2 = 0.0725	
R indices (all data)	R1 = 0.0388, wR2 = 0.0757	
Absolute structure parameter	0.00(4)	
Largest diff. peak and hole	0.335 and -0.200 $e.Å^{-3}$	

Table D.17 Atomic coordinates (x 10^4) and equivalent isotropic displacement parameters ($Å^2$x 10^3) for ef12_p212121. U(eq) is defined as one third of the trace of the orthogonalized U^{ij} tensor.

Atom	x	y	z	U(eq)
C(1)	-1002(2)	755(1)	2308(1)	15(1)
C(2)	-1998(2)	1021(1)	2992(1)	20(1)
C(3)	-3246(2)	1308(1)	1847(1)	20(1)
C(4)	-1774(2)	882(1)	1620(1)	15(1)
C(5)	-1494(2)	635(1)	748(1)	15(1)
C(6)	-1120(2)	1585(1)	192(1)	17(1)
C(7)	-976(2)	1147(1)	-668(1)	22(1)
C(8)	261(2)	351(1)	-702(1)	22(1)
C(9)	299(2)	2176(1)	445(1)	18(1)
C(10)	-87(2)	3190(1)	899(1)	26(1)
C(11)	1296(2)	1513(1)	963(1)	16(1)
C(12)	1085(1)	491(1)	1084(1)	13(1)
C(13)	-167(2)	-85(1)	679(1)	14(1)
C(14)	632(2)	-1152(1)	1713(1)	15(1)
C(15)	548(2)	443(1)	2521(1)	16(1)
C(16)	1440(2)	-120(1)	1840(1)	14(1)
C(17)	3044(2)	-245(1)	2097(1)	16(1)
C(18)	3902(2)	-1063(1)	1611(1)	16(1)
C(19)	6390(2)	-2280(1)	1447(1)	24(1)
C(20)	6328(2)	-2128(1)	535(1)	23(1)
C(21)	4784(2)	-1973(1)	214(1)	25(1)
O(1)	-1796(1)	947(1)	3693(1)	27(1)
O(2)	-3335(1)	1367(1)	2680(1)	22(1)
O(3)	-4226(1)	1587(1)	1424(1)	26(1)
O(4)	730(1)	-1945(1)	2098(1)	20(1)
O(5)	-379(1)	-1044(1)	1123(1)	16(1)
O(6)	60(1)	-454(1)	-109(1)	18(1)
S(1)	5740(1)	-1164(1)	2032(1)	20(1)
S(2)	3915(1)	-766(1)	545(1)	19(1)

Table D.18 Bond lengths [Å] and angles [°] for ef12_p212121.

C(1)-C(4)	1.350(2)	C(19)-C(20)	1.528(2)
C(1)-C(2)	1.4933(19)	C(19)-S(1)	1.8225(16)
C(1)-C(15)	1.507(2)	C(20)-C(21)	1.515(2)
C(2)-O(1)	1.1824(19)	C(21)-S(2)	1.8153(16)
C(2)-O(2)	1.3935(19)		
C(3)-O(3)	1.1893(19)	C(4)-C(1)-C(2)	107.54(12)
C(3)-O(2)	1.3887(19)	C(4)-C(1)-C(15)	135.79(12)
C(3)-C(4)	1.493(2)	C(2)-C(1)-C(15)	116.66(12)
C(4)-C(5)	1.5052(19)	O(1)-C(2)-O(2)	121.85(13)
C(5)-C(13)	1.5215(19)	O(1)-C(2)-C(1)	129.57(14)
C(5)-C(6)	1.561(2)	O(2)-C(2)-C(1)	108.54(12)
C(6)-C(7)	1.540(2)	O(3)-C(3)-O(2)	121.90(14)
C(6)-C(9)	1.552(2)	O(3)-C(3)-C(4)	129.18(14)
C(7)-C(8)	1.517(2)	O(2)-C(3)-C(4)	108.90(13)
C(8)-O(6)	1.4354(18)	C(1)-C(4)-C(3)	107.24(12)
C(9)-C(11)	1.509(2)	C(1)-C(4)-C(5)	134.57(12)
C(9)-C(10)	1.538(2)	C(3)-C(4)-C(5)	118.07(12)
C(11)-C(12)	1.3324(19)	C(4)-C(5)-C(13)	109.44(11)
C(12)-C(13)	1.5129(19)	C(4)-C(5)-C(6)	116.35(12)
C(12)-C(16)	1.5147(19)	C(13)-C(5)-C(6)	104.56(11)
C(13)-O(6)	1.4067(16)	C(7)-C(6)-C(9)	110.88(12)
C(13)-O(5)	1.4418(17)	C(7)-C(6)-C(5)	106.57(12)
C(14)-O(4)	1.2005(17)	C(9)-C(6)-C(5)	113.45(11)
C(14)-O(5)	1.3512(16)	C(8)-C(7)-C(6)	109.94(12)
C(14)-C(16)	1.5219(19)	O(6)-C(8)-C(7)	111.05(12)
C(15)-C(16)	1.5659(19)	C(11)-C(9)-C(10)	109.22(12)
C(16)-C(17)	1.5274(19)	C(11)-C(9)-C(6)	112.47(12)
C(17)-C(18)	1.5342(19)	C(10)-C(9)-C(6)	110.53(12)
C(18)-S(2)	1.8117(14)	C(12)-C(11)-C(9)	123.14(13)
C(18)-S(1)	1.8166(14)	C(11)-C(12)-C(13)	121.16(13)
C(11)-C(12)-C(16)	126.71(12)	O(6)-C(13)-O(5)	102.20(10)
C(13)-C(12)-C(16)	106.22(11)	O(6)-C(13)-C(12)	117.80(11)
O(5)-C(13)-C(12)	106.59(11)	C(12)-C(13)-C(5)	105.66(11)
O(6)-C(13)-C(5)	112.88(11)	O(4)-C(14)-O(5)	121.49(13)
O(5)-C(13)-C(5)	111.59(11)		
O(5)-C(14)-C(16)	109.99(11)		

Table D.18 continued

C(1)-C(15)-C(16)	115.87(11)	S(2)-C(18)-S(1)	112.69(7)
C(12)-C(16)-C(14)	103.11(11)	C(20)-C(19)-S(1)	114.70(11)
C(12)-C(16)-C(17)	119.28(12)	C(21)-C(20)-C(19)	113.61(13)
C(14)-C(16)-C(17)	114.20(11)	C(20)-C(21)-S(2)	114.01(11)
C(12)-C(16)-C(15)	104.60(11)	C(3)-O(2)-C(2)	107.61(11)
C(14)-C(16)-C(15)	104.30(11)	C(14)-O(5)-C(13)	111.49(10)
C(17)-C(16)-C(15)	109.92(11)	C(13)-O(6)-C(8)	114.69(11)
C(16)-C(17)-C(18)	114.17(11)	C(18)-S(1)-C(19)	98.52(7)
C(17)-C(18)-S(2)	112.09(10)	C(18)-S(2)-C(21)	97.00(8
C(17)-C(18)-S(1)	108.28(9)		

Symmetry transformations used to generate equivalent atoms:

Table D.19 Anisotropic displacement parameters ($Å^2 x\ 10^3$) for ef12_p212121. The anisotropic displacement factor exponent takes the form: $-2\pi^2[\ h^2\ a^{*2}U^{11} + ... + 2\ h\ k\ a^*\ b^*\ U^{12}\ ]$

Atom	U^{11}	U^{22}	U^{33}	U^{23}	U^{13}	U^{12}
C(1)	16(1)	9(1)	20(1)	-1(1)	7(1)	-1(1)
C(2)	22(1)	12(1)	25(1)	-2(1)	9(1)	-1(1)
C(3)	18(1)	13(1)	28(1)	2(1)	8(1)	-1(1)
C(4)	12(1)	10(1)	23(1)	1(1)	6(1)	-1(1)
C(5)	12(1)	14(1)	19(1)	0(1)	1(1)	0(1)
C(6)	16(1)	18(1)	18(1)	4(1)	0(1)	2(1)
C(7)	23(1)	26(1)	17(1)	4(1)	-3(1)	0(1)
C(8)	23(1)	27(1)	15(1)	-1(1)	1(1)	0(1)
C(9)	18(1)	15(1)	20(1)	4(1)	4(1)	-2(1)
C(10)	28(1)	15(1)	34(1)	0(1)	2(1)	-1(1)
C(11)	13(1)	17(1)	17(1)	0(1)	3(1)	-3(1)
C(12)	10(1)	15(1)	13(1)	-1(1)	2(1)	0(1)
C(13)	13(1)	13(1)	15(1)	-2(1)	0(1)	-1(1)
C(14)	13(1)	14(1)	18(1)	-3(1)	3(1)	2(1)
C(15)	18(1)	15(1)	15(1)	-2(1)	2(1)	0(1)
C(16)	14(1)	13(1)	14(1)	-1(1)	2(1)	0(1)
C(17)	13(1)	19(1)	16(1)	-2(1)	-1(1)	1(1)
C(18)	12(1)	17(1)	20(1)	2(1)	-1(1)	0(1)
C(19)	12(1)	17(1)	42(1)	3(1)	4(1)	2(1)
C(20)	13(1)	20(1)	37(1)	-8(1)	3(1)	0(1)
C(21)	17(1)	25(1)	33(1)	-14(1)	0(1)	2(1)
O(1)	32(1)	27(1)	22(1)	-2(1)	11(1)	-1(1)
O(2)	19(1)	20(1)	28(1)	-1(1)	11(1)	4(1)
O(3)	18(1)	23(1)	38(1)	8(1)	5(1)	6(1)
O(4)	22(1)	13(1)	25(1)	3(1)	2(1)	1(1)
O(5)	15(1)	12(1)	20(1)	-1(1)	-1(1)	-2(1)
O(6)	21(1)	20(1)	14(1)	-4(1)	0(1)	1(1)
S(1)	14(1)	23(1)	23(1)	2(1)	-3(1)	2(1)
S(2)	18(1)	21(1)	18(1)	-4(1)	-1(1)	3(1)

Table D.20 Hydrogen coordinates (x 10^4) and isotropic displacement parameters ($Å^2$x 10^3) for ef12_p212121.

Atom	x	y	z	U(eq)
H(5)	-2374	265	524	18
H(6)	-1962	2089	206	21
H(7A)	-1911	811	-830	26
H(7B)	-771	1727	-1048	26
H(8A)	293	30	-1244	26
H(8B)	1212	709	-607	26
H(9)	849	2370	-54	21
H(10A)	-681	3019	1373	38
H(10B)	-646	3656	544	38
H(10C)	820	3541	1069	38
H(11)	2114	1839	1216	19
H(15A)	510	-27	2994	19
H(15B)	1092	1081	2683	19
H(17A)	3071	-444	2673	19
H(17B)	3543	441	2043	19
H(18)	3405	-1755	1684	19
H(19A)	7420	-2430	1602	29
H(19B)	5792	-2900	1590	29
H(20A)	6931	-1510	389	28
H(20B)	6768	-2748	271	28
H(21A)	4168	-2572	386	30
H(21B)	4819	-1977	-382	30

*D.3.1 Crystal Structure Analysis of ketone **5.24***

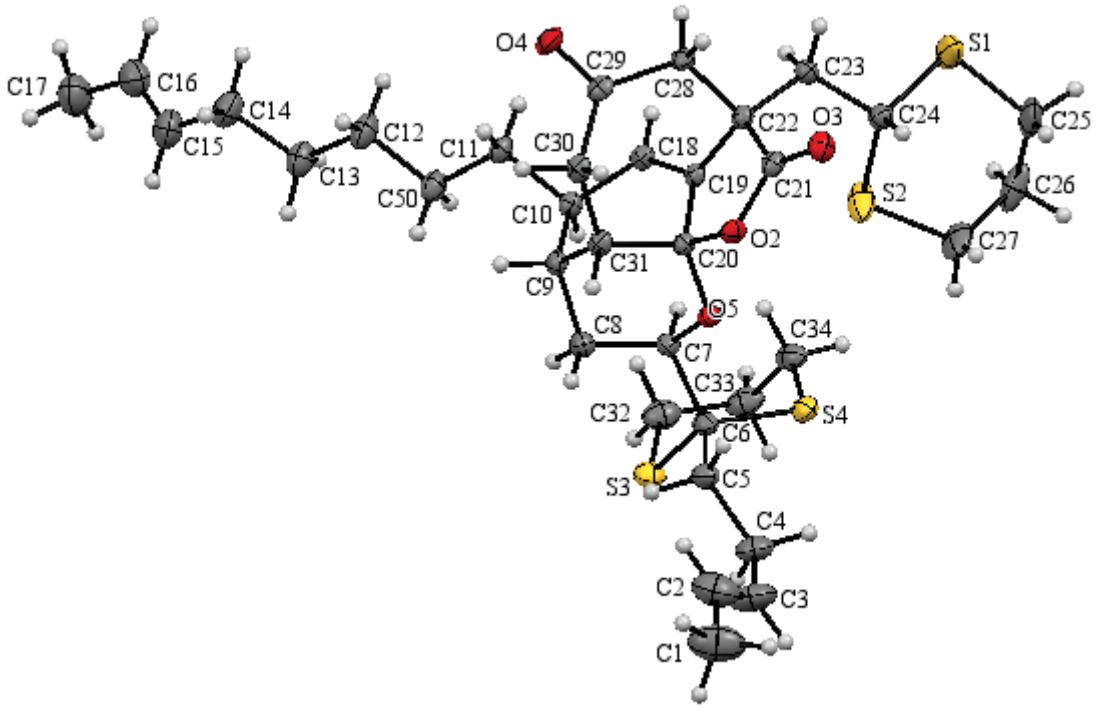

Figure D.12 ORTEP drawing of ketone **5.24**

Table D.21 Crystal data and structure refinement for maleic anhydride **5.24**

Identification code	JLW4
Empirical formula	$C_{35}H_{50}O_4S_4$
Formula weight	662.99
Temperature	150(2) K
Wavelength	0.71073 Å
Crystal system,	Triclinic
Space group	P-1
Unit cell dimensions	a = 10.0340(10) Å, α = 92.308(3)°
	b = 10.6467(11) Å, β = 101.718(3)°
	c = 16.4332(16) Å, γ = 96.139(3)°
Volume	1705.6(3) $Å^3$
Z, Calculated density	2, 1.291 Mg/m^3
Absorption coefficient	0.316 mm^{-1}
F(000)	712
Crystal size	0.142 x 0.085 x 0.062 mm
Theta range for data collection	1.928 to 28.365°
Limiting indices	$-13 \leq h \leq 13$, $-14 \leq k \leq 14$, $-21 \leq l \leq 21$
Reflections collected / unique	65960 / 8503 [R_{int} = 0.0741]
Completeness to theta = 25.242	100.0%
Absorption correction	Semi-empirical from equivalents
Max. and min. transmission	0.9810 and 0.9560
Refinement method	Full-matrix least-squares on F^2
Data / restraints / parameters	8503 / 0 / 388
Goodness-of-fit on F^2	1.074
Final R indices [I>2sigma(I)]	R1 = 0.0666, wR2 = 0.1652
R indices (all data)	R1 = 0.1187, wR2 = 0.2047
Largest diff. peak and hole	1.657 and -1.064 $e.A^{-3}$

Table D.22 Displacement parameters (A^2 x 10^3) for JLW4. U(eq) is defined as one third of the trace of the orthogonalized U^{ij} tensor.

Atom	x	y	z	U(eq)
S(1)	3327(1)	4638(1)	11743(1)	53(1)
S(2)	2464(1)	4712(1)	9873(1)	52(1)
S(3)	1822(1)	4808(1)	6106(1)	31(1)
S(4)	1072(1)	5633(1)	7716(1)	27(1)
C(50)	5555(3)	556(3)	7171(2)	28(1)
O(2)	272(2)	1513(2)	8912(1)	19(1)
O(3)	95(2)	1523(2)	10240(1)	25(1)
O(4)	3625(2)	-1213(2)	9309(2)	28(1)
O(5)	864(2)	2778(2)	7969(1)	19(1)
C(1)	-4904(5)	2884(5)	5335(3)	65(1)
C(2)	-3428(5)	3281(5)	5740(3)	53(1)
C(3)	-2839(4)	4403(4)	5875(3)	50(1)
C(4)	-1397(4)	4878(4)	6258(2)	37(1)
C(5)	-497(3)	3850(3)	6557(2)	26(1)
C(6)	1008(3)	4305(3)	6958(2)	23(1)
C(7)	1713(3)	3218(3)	7406(2)	20(1)
C(8)	1922(3)	2106(3)	6854(2)	22(1)
C(9)	2526(3)	1077(3)	7403(2)	20(1)
C(10)	3946(3)	1587(3)	7952(2)	18(1)
C(11)	4991(3)	625(3)	7954(2)	21(1)
C(12)	6547(4)	-454(3)	7185(2)	35(1)
C(13)	7320(4)	-414(3)	6490(2)	34(1)
C(14)	8110(4)	-1565(3)	6442(3)	38(1)
C(15)	9034(4)	-1466(4)	5846(3)	44(1)
C(16)	10358(4)	-1629(4)	6030(3)	43(1)
C(17)	11311(5)	-1536(5)	5454(3)	56(1)
C(18)	3847(3)	1941(3)	8833(2)	18(1)
C(19)	2655(3)	2026(2)	9062(2)	16(1)
C(20)	1316(3)	1768(3)	8437(2)	16(1)
C(21)	811(3)	1601(3)	9741(2)	20(1)
C(22)	2360(3)	1714(3)	9900(2)	18(1)
C(23)	3048(3)	2574(3)	10681(2)	21(1)

Table D.22 continued

C(24)	2442(3)	3818(3)	10770(2)	21(1)
C(25)	2362(4)	5990(4)	11714(3)	46(1)
C(26)	2434(4)	6764(3)	10978(3)	41(1)
C(27)	1691(5)	6075(3)	10163(3)	47(1)
C(28)	2774(3)	358(3)	10025(2)	20(1)
C(29)	2777(3)	-474(3)	9246(2)	20(1)
C(30)	1689(3)	-541(3)	8434(2)	21(1)
C(31)	1439(3)	613(3)	7906(2)	19(1)
C(32)	3520(4)	5485(4)	6644(2)	37(1)
C(33)	3533(4)	6555(3)	7285(2)	36(1)
C(34)	2892(4)	6133(3)	8009(2)	31(1)

Table D.23 Bond lengths [Å] and angles [°] for ketone **5.24**

S(1)-C(24)	1.802(3)	C(8)-H(8A)	0.9900
S(1)-C(25)	1.815(4)	C(8)-H(8B)	0.9900
S(2)-C(24)	1.790(3)	C(9)-C(31)	1.550(4)
S(2)-C(27)	1.807(4)	C(9)-C(10)	1.553(4)
S(3)-C(32)	1.810(4)	C(9)-H(9A)	1.0000
S(3)-C(6)	1.830(3)	C(10)-C(18)	1.507(4)
S(4)-C(34)	1.807(4)	C(10)-C(11)	1.541(4)
S(4)-C(6)	1.833(3)	C(10)-H(10A)	1.0000
C(50)-C(11)	1.510(4)	C(11)-H(11A)	0.9900
C(50)-C(12)	1.539(5)	C(11)-H(11B)	0.9900
C(50)-H(50A)	0.9900	C(12)-C(13)	1.505(5)
C(50)-H(50B)	0.9900	C(12)-H(12A)	0.9900
O(2)-C(21)	1.356(4)	C(12)-H(12B)	0.9900
O(2)-C(20)	1.437(3)	C(13)-C(14)	1.537(5)
O(3)-C(21)	1.195(4)	C(13)-H(13A)	0.9900
O(4)-C(29)	1.212(4)	C(13)-H(13B)	0.9900
O(5)-C(20)	1.408(3)	C(14)-C(15)	1.479(6)
O(5)-C(7)	1.439(4)	C(14)-H(14A)	0.9900
C(1)-C(2)	1.503(6)	C(14)-H(14B)	0.9900
C(1)-H(1A)	0.9800	C(15)-C(16)	1.333(6)
C(1)-H(1B)	0.9800	C(15)-H(15A)	0.9500
C(1)-H(1C)	0.9800	C(16)-C(17)	1.475(6)
C(2)-C(3)	1.265(6)	C(16)-H(16A)	0.9500
C(2)-H(2A)	0.9500	C(17)-H(17A)	0.9800
C(3)-C(4)	1.481(6)	C(17)-H(17B)	0.9800
C(3)-H(3A)	0.9500	C(17)-H(17C)	0.9800
C(4)-C(5)	1.526(5)	C(18)-C(19)	1.336(4)
C(4)-H(4A)	0.9900	C(18)-H(18A)	0.9500
C(4)-H(4B)	0.9900	C(19)-C(20)	1.508(4)
C(5)-C(6)	1.537(4)	C(19)-C(22)	1.508(4)
C(5)-H(5A)	0.9900	C(20)-C(31)	1.510(4)
C(5)-H(5B)	0.9900	C(21)-C(22)	1.513(4)
C(6)-C(7)	1.553(4)	C(22)-C(23)	1.540(4)
C(7)-C(8)	1.521(4)	C(22)-C(28)	1.554(4)
C(7)-H(7A)	1.0000	C(23)-C(24)	1.530(4)
C(8)-C(9)	1.543(4)	C(23)-H(23A)	0.9900

Table D.23 continued

C(23)-H(23B)	0.9900	H(50A)-C(50)-H(50B)	107.8
C(24)-H(24A)	1.0000	C(21)-O(2)-C(20)	111.5(2)
C(25)-C(26)	1.500(6)	C(20)-O(5)-C(7)	115.0(2)
C(25)-H(25A)	0.9900	C(2)-C(1)-H(1A)	109.5
C(25)-H(25B)	0.9900	C(2)-C(1)-H(1B)	109.5
C(26)-C(27)	1.512(6)	H(1A)-C(1)-H(1B)	109.5
C(26)-H(26A)	0.9900	C(2)-C(1)-H(1C)	109.5
C(26)-H(26B)	0.9900	H(1A)-C(1)-H(1C)	109.5
C(27)-H(27A)	0.9900	H(1B)-C(1)-H(1C)	109.5
C(27)-H(27B)	0.9900	C(3)-C(2)-C(1)	126.5(5)
C(28)-C(29)	1.527(4)	C(3)-C(2)-H(2A)	116.8
C(28)-H(28A)	0.9900	C(1)-C(2)-H(2A)	116.8
C(28)-H(28B)	0.9900	C(2)-C(3)-C(4)	130.0(4)
C(29)-C(30)	1.537(4)	C(2)-C(3)-H(3A)	115.0
C(30)-C(31)	1.546(4)	C(4)-C(3)-H(3A)	115.0
C(30)-H(30A)	0.9900	C(3)-C(4)-C(5)	114.6(3)
C(30)-H(30B)	0.9900	C(3)-C(4)-H(4A)	108.6
C(31)-H(31A)	1.0000	C(5)-C(4)-H(4A)	108.6
C(32)-C(33)	1.517(5)	C(3)-C(4)-H(4B)	108.6
C(32)-H(32A)	0.9900	C(5)-C(4)-H(4B)	108.6
C(32)-H(32B)	0.9900	H(4A)-C(4)-H(4B)	107.6
C(33)-C(34)	1.525(5)	C(4)-C(5)-C(6)	116.2(3)
C(33)-H(33B)	0.9900	C(4)-C(5)-H(5A)	108.2
C(33)-H(33C)	0.9900	C(6)-C(5)-H(5A)	108.2
C(34)-H(34B)	0.9900	C(4)-C(5)-H(5B)	108.2
C(34)-H(34C)	0.9900	C(6)-C(5)-H(5B)	108.2
		H(5A)-C(5)-H(5B)	107.4
C(24)-S(1)-C(25)	98.89(17)	C(5)-C(6)-C(7)	110.6(2)
C(24)-S(2)-C(27)	100.14(17)	C(5)-C(6)-S(3)	106.0(2)
C(32)-S(3)-C(6)	102.89(16)	C(7)-C(6)-S(3)	110.9(2)
C(34)-S(4)-C(6)	101.65(15)	C(5)-C(6)-S(4)	109.0(2)
C(11)-C(50)-C(12)	112.5(3)	C(7)-C(6)-S(4)	109.4(2)
C(11)-C(50)-H(50A)	109.1	S(3)-C(6)-S(4)	110.87(16)
C(12)-C(50)-H(50A)	109.1	O(5)-C(7)-C(8)	109.5(2)
C(11)-C(50)-H(50B)	109.1	O(5)-C(7)-C(6)	105.6(2)
C(12)-C(50)-H(50B)	109.1	C(8)-C(7)-C(6)	116.6(2)

Table D.23 continued

O(5)-C(7)-H(7A)	108.3	C(6)-C(7)-H(7A)	108.3
C(8)-C(7)-H(7A)	108.3		
C(7)-C(8)-C(9)	109.5(2)	C(14)-C(13)-H(13B)	109.1
C(7)-C(8)-H(8A)	109.8	H(13A)-C(13)-H(13B)	107.8
C(9)-C(8)-H(8A)	109.8	C(15)-C(14)-C(13)	113.9(3)
C(7)-C(8)-H(8B)	109.8	C(15)-C(14)-H(14A)	108.8
C(9)-C(8)-H(8B)	109.8	C(13)-C(14)-H(14A)	108.8
H(8A)-C(8)-H(8B)	108.2	C(15)-C(14)-H(14B)	108.8
C(8)-C(9)-C(31)	106.6(2)	C(13)-C(14)-H(14B)	108.8
C(8)-C(9)-C(10)	111.1(2)	H(14A)-C(14)-H(14B)	107.7
C(31)-C(9)-C(10)	113.9(2)	C(16)-C(15)-C(14)	124.6(4)
C(8)-C(9)-H(9A)	108.4	C(16)-C(15)-H(15A)	117.7
C(31)-C(9)-H(9A)	108.4	C(14)-C(15)-H(15A)	117.7
C(10)-C(9)-H(9A)	108.4	C(15)-C(16)-C(17)	126.1(4)
C(18)-C(10)-C(11)	109.8(2)	C(15)-C(16)-H(16A)	116.9
C(18)-C(10)-C(9)	111.9(2)	C(17)-C(16)-H(16A)	116.9
C(11)-C(10)-C(9)	111.5(2)	C(16)-C(17)-H(17A)	109.5
C(18)-C(10)-H(10A)	107.8	C(16)-C(17)-H(17B)	109.5
C(11)-C(10)-H(10A)	107.8	H(17A)-C(17)-H(17B)	109.5
C(9)-C(10)-H(10A)	107.8	C(16)-C(17)-H(17C)	109.5
C(50)-C(11)-C(10)	114.3(3)	H(17A)-C(17)-H(17C)	109.5
C(50)-C(11)-H(11A)	108.7	H(17B)-C(17)-H(17C)	109.5
C(10)-C(11)-H(11A)	108.7	C(19)-C(18)-C(10)	123.0(3)
C(50)-C(11)-H(11B)	108.7	C(19)-C(18)-H(18A)	118.5
C(10)-C(11)-H(11B)	108.7	C(10)-C(18)-H(18A)	118.5
H(11A)-C(11)-H(11B)	107.6	C(18)-C(19)-C(20)	120.9(3)
C(13)-C(12)-C(50)	114.5(3)	C(18)-C(19)-C(22)	125.1(3)
C(13)-C(12)-H(12A)	108.6	C(20)-C(19)-C(22)	107.0(2)
C(50)-C(12)-H(12A)	108.6	O(5)-C(20)-O(2)	102.7(2)
C(13)-C(12)-H(12B)	108.6	O(5)-C(20)-C(19)	117.4(2)
C(50)-C(12)-H(12B)	108.6	O(2)-C(20)-C(19)	106.1(2)
H(12A)-C(12)-H(12B)	107.6	O(5)-C(20)-C(31)	113.4(2)
C(12)-C(13)-C(14)	112.6(3)	O(2)-C(20)-C(31)	111.2(2)
C(12)-C(13)-H(13A)	109.1	C(19)-C(20)-C(31)	105.8(2)
C(14)-C(13)-H(13A)	109.1	O(3)-C(21)-O(2)	121.4(3)
C(12)-C(13)-H(13B)	109.1	O(3)-C(21)-C(22)	128.0(3)

Table D.23 continued

O(2)-C(21)-C(22)	110.5(2)	H(27A)-C(27)-H(27B)	107.6
C(19)-C(22)-C(21)	102.8(2)	C(29)-C(28)-C(22)	117.5(2)
C(19)-C(22)-C(23)	120.0(2)	C(29)-C(28)-H(28A)	107.9
C(21)-C(22)-C(23)	112.7(2)	C(22)-C(28)-H(28A)	107.9
C(19)-C(22)-C(28)	104.5(2)	C(29)-C(28)-H(28B)	107.9
C(21)-C(22)-C(28)	107.0(2)	C(22)-C(28)-H(28B)	107.9
C(23)-C(22)-C(28)	108.9(2)	H(28A)-C(28)-H(28B)	107.2
C(24)-C(23)-C(22)	115.3(2)	O(4)-C(29)-C(28)	116.7(3)
C(24)-C(23)-H(23A)	108.4	O(4)-C(29)-C(30)	118.3(3)
C(22)-C(23)-H(23A)	108.4	C(28)-C(29)-C(30)	124.5(3)
C(24)-C(23)-H(23B)	108.4	C(29)-C(30)-C(31)	122.9(2)
C(22)-C(23)-H(23B)	108.4	C(29)-C(30)-H(30A)	106.6
H(23A)-C(23)-H(23B)	107.5	C(31)-C(30)-H(30A)	106.6
C(23)-C(24)-S(2)	110.9(2)	C(29)-C(30)-H(30B)	106.6
C(23)-C(24)-S(1)	108.2(2)	C(31)-C(30)-H(30B)	106.6
S(2)-C(24)-S(1)	114.70(17)	H(30A)-C(30)-H(30B)	106.6
C(23)-C(24)-H(24A)	107.6	C(20)-C(31)-C(30)	111.5(2)
S(2)-C(24)-H(24A)	107.6	C(20)-C(31)-C(9)	104.3(2)
S(1)-C(24)-H(24A)	107.6	C(30)-C(31)-C(9)	118.1(2)
C(26)-C(25)-S(1)	113.4(3)	C(20)-C(31)-H(31A)	107.5
C(26)-C(25)-H(25A)	108.9	C(30)-C(31)-H(31A)	107.5
S(1)-C(25)-H(25A)	108.9	C(9)-C(31)-H(31A)	107.5
C(26)-C(25)-H(25B)	108.9	C(33)-C(32)-S(3)	114.3(3)
S(1)-C(25)-H(25B)	108.9	C(33)-C(32)-H(32A)	108.7
H(25A)-C(25)-H(25B)	107.7	S(3)-C(32)-H(32A)	108.7
C(25)-C(26)-C(27)	112.8(3)	C(33)-C(32)-H(32B)	108.7
C(25)-C(26)-H(26A)	109.0	S(3)-C(32)-H(32B)	108.7
C(27)-C(26)-H(26A)	109.0	H(32A)-C(32)-H(32B)	107.6
C(25)-C(26)-H(26B)	109.0	C(32)-C(33)-C(34)	113.2(3)
C(27)-C(26)-H(26B)	109.0	C(32)-C(33)-H(33B)	108.9
H(26A)-C(26)-H(26B)	107.8	C(34)-C(33)-H(33B)	108.9
C(26)-C(27)-S(2)	114.1(3)	C(32)-C(33)-H(33C)	108.9
C(26)-C(27)-H(27A)	108.7	C(34)-C(33)-H(33C)	108.9
S(2)-C(27)-H(27A)	108.7	H(33B)-C(33)-H(33C)	107.8
C(26)-C(27)-H(27B)	108.7	C(33)-C(34)-S(4)	113.8(2)
S(2)-C(27)-H(27B)	108.7	C(33)-C(34)-H(34B)	108.8

Table D.23 continued

S(4)-C(34)-H(34B)	108.8	S(4)-C(34)-H(34C)	108.8
C(33)-C(34)-H(34C)	108.8	H(34B)-C(34)-H(34C)	107.7

Symmetry transformations used to generate equivalent atoms:

Table D.24 The anisotropic displacement factor exponent takes the form: $-2\pi^2 [h^2 a^{*2} U^{11} + ... + 2 h k a^* b^* U^{12}]$

	U11	U22	U33	U23	U13	U12
S(1)	60(1)	50(1)	41(1)	-25(1)	-17(1)	30(1)
S(2)	104(1)	26(1)	41(1)	11(1)	37(1)	25(1)
S(3)	37(1)	32(1)	24(1)	9(1)	6(1)	6(1)
S(4)	34(1)	19(1)	26(1)	2(1)	2(1)	8(1)
C(50)	28(2)	26(2)	33(2)	4(1)	14(1)	7(1)
O(2)	14(1)	22(1)	22(1)	2(1)	4(1)	2(1)
O(3)	25(1)	25(1)	28(1)	3(1)	12(1)	1(1)
O(4)	28(1)	19(1)	36(1)	0(1)	1(1)	10(1)
O(5)	20(1)	18(1)	20(1)	4(1)	4(1)	6(1)
C(1)	46(3)	76(3)	63(3)	24(3)	-6(2)	-11(2)
C(2)	54(3)	60(3)	40(2)	14(2)	0(2)	-1(2)
C(3)	41(2)	51(3)	53(3)	20(2)	-7(2)	12(2)
C(4)	36(2)	37(2)	36(2)	14(2)	0(2)	11(2)
C(5)	29(2)	25(2)	23(2)	3(1)	0(1)	6(1)
C(6)	30(2)	18(1)	20(2)	3(1)	1(1)	4(1)
C(7)	23(2)	19(1)	17(1)	2(1)	5(1)	5(1)
C(8)	25(2)	22(2)	20(2)	0(1)	4(1)	5(1)
C(9)	22(2)	18(1)	19(2)	-2(1)	5(1)	3(1)
C(10)	17(1)	17(1)	22(2)	2(1)	6(1)	1(1)
C(11)	18(1)	21(2)	26(2)	2(1)	7(1)	4(1)
C(12)	37(2)	28(2)	46(2)	4(2)	21(2)	11(2)
C(13)	33(2)	32(2)	41(2)	0(2)	15(2)	7(2)
C(14)	34(2)	29(2)	50(2)	-2(2)	10(2)	9(2)
C(15)	50(2)	40(2)	45(2)	-4(2)	14(2)	16(2)
C(16)	51(2)	39(2)	38(2)	-4(2)	6(2)	7(2)
C(17)	54(3)	70(3)	48(3)	-6(2)	15(2)	18(2)
C(18)	15(1)	15(1)	22(2)	0(1)	2(1)	-1(1)
C(19)	17(1)	11(1)	18(1)	-1(1)	3(1)	0(1)
C(20)	16(1)	15(1)	18(1)	2(1)	4(1)	2(1)
C(21)	20(2)	15(1)	24(2)	2(1)	7(1)	2(1)
C(22)	19(1)	15(1)	19(1)	0(1)	3(1)	2(1)
C(23)	22(2)	21(2)	19(2)	0(1)	2(1)	3(1)

Table D.24 continued

C(24)	21(2)	19(1)	23(2)	-1(1)	2(1)	2(1)
C(25)	49(2)	40(2)	48(2)	-21(2)	5(2)	18(2)
C(26)	23(2)	18(2)	83(3)	-12(2)	21(2)	-4(1)
C(27)	76(3)	21(2)	51(2)	8(2)	20(2)	20(2)
C(28)	23(2)	15(1)	20(2)	3(1)	2(1)	4(1)
C(29)	20(2)	13(1)	26(2)	4(1)	6(1)	-1(1)
C(30)	20(2)	15(1)	25(2)	-2(1)	3(1)	-2(1)
C(31)	17(1)	16(1)	23(2)	0(1)	3(1)	0(1)
C(32)	34(2)	36(2)	41(2)	14(2)	8(2)	3(2)
C(33)	33(2)	25(2)	47(2)	9(2)	0(2)	1(2)
C(34)	38(2)	18(2)	31(2)	0(1)	-6(2)	4(1)

Table D.25 Displacement parameters ($Å^2$ x 10^3) for JLW4.

Atom	x	y	z	U(eq)
H(50A)	6041	1392	7103	33
H(50B)	4785	359	6685	33
H(1A)	-5089	1958	5308	97
H(1B)	-5496	3254	5663	97
H(1C)	-5091	3179	4770	97
H(2A)	-2882	2625	5911	64
H(3A)	-3411	5041	5704	60
H(4A)	-1387	5474	6738	44
H(4B)	-991	5358	5847	44
H(5A)	-516	3254	6075	32
H(5B)	-910	3370	6966	32
H(7A)	2627	3584	7743	23
H(8A)	2554	2395	6491	27
H(8B)	1035	1753	6495	27
H(9A)	2650	353	7029	23
H(10A)	4297	2370	7708	22
H(11A)	5763	852	8435	25
H(11B)	4545	-224	8032	25
H(12A)	7217	-345	7723	42
H(12B)	6020	-1300	7157	42
H(13A)	7974	368	6572	41
H(13B)	6665	-380	5955	41
H(14A)	8658	-1671	7003	45
H(14B)	7443	-2333	6280	45
H(15A)	8658	-1272	5294	52
H(16A)	10723	-1825	6584	52
H(17A)	12222	-1698	5747	84
H(17B)	10977	-2163	4983	84
H(17C)	11365	-685	5248	84
H(18A)	4669	2110	9245	21
H(23A)	2988	2096	11179	25
H(23B)	4032	2774	10673	25

Table D.25 continued

H(24A)	1462	3602	10807	25
H(25A)	1391	5685	11703	56
H(25B)	2717	6537	12231	56
H(26A)	3408	6993	10955	49
H(26B)	2029	7558	11052	49
H(27A)	1661	6674	9716	57
H(27B)	735	5796	10203	57
H(28A)	3705	437	10382	23
H(28B)	2143	-91	10337	23
H(30A)	802	-847	8574	25
H(30B)	1901	-1212	8062	25
H(31A)	545	398	7502	23
H(32A)	4003	4807	6926	44
H(32B)	4037	5805	6227	44
H(33B)	3029	7224	7008	43
H(33C)	4492	6927	7505	43
H(34B)	3055	6842	8439	37
H(34C)	3356	5424	8260	37

Table D.26

C(1)-C(2)-C(3)-C(4)	-179.3(5)
C(2)-C(3)-C(4)-C(5)	-1.9(7)
C(3)-C(4)-C(5)-C(6)	179.9(3)
C(4)-C(5)-C(6)-C(7)	167.3(3)
C(4)-C(5)-C(6)-S(3)	-72.4(3)
C(4)-C(5)-C(6)-S(4)	47.0(3)
C(32)-S(3)-C(6)-C(5)	173.9(2)
C(32)-S(3)-C(6)-C(7)	-66.0(2)
C(32)-S(3)-C(6)-S(4)	55.7(2)
C(34)-S(4)-C(6)-C(5)	-173.3(2)
C(34)-S(4)-C(6)-C(7)	65.6(2)
C(34)-S(4)-C(6)-S(3)	-57.01(19)
C(20)-O(5)-C(7)-C(8)	52.9(3)
C(20)-O(5)-C(7)-C(6)	179.2(2)
C(5)-C(6)-C(7)-O(5)	-54.2(3)
S(3)-C(6)-C(7)-O(5)	-171.43(18)
S(4)-C(6)-C(7)-O(5)	66.0(3)
C(5)-C(6)-C(7)-C(8)	67.7(3)
S(3)-C(6)-C(7)-C(8)	-49.6(3)
S(4)-C(6)-C(7)-C(8)	-172.2(2)
O(5)-C(7)-C(8)-C(9)	-55.8(3)
C(6)-C(7)-C(8)-C(9)	-175.6(2)
C(7)-C(8)-C(9)-C(31)	63.1(3)
C(7)-C(8)-C(9)-C(10)	-61.5(3)
C(8)-C(9)-C(10)-C(18)	100.7(3)
C(31)-C(9)-C(10)-C(18)	-19.6(3)
C(8)-C(9)-C(10)-C(11)	-135.8(2)
C(31)-C(9)-C(10)-C(11)	103.8(3)
C(12)-C(50)-C(11)-C(10)	-177.7(3)
C(18)-C(10)-C(11)-C(50)	-159.1(3)
C(9)-C(10)-C(11)-C(50)	76.3(3)
C(11)-C(50)-C(12)-C(13)	-170.2(3)
C(50)-C(12)-C(13)-C(14)	-170.4(3)
C(12)-C(13)-C(14)-C(15)	-171.7(3)
C(13)-C(14)-C(15)-C(16)	127.9(4)
C(14)-C(15)-C(16)-C(17)	-179.9(4)

Table D.26 continued

C(11)-C(10)-C(18)-C(19)	-136.1(3)
C(9)-C(10)-C(18)-C(19)	-11.7(4)
C(10)-C(18)-C(19)-C(20)	0.0(4)
C(10)-C(18)-C(19)-C(22)	147.0(3)
C(7)-O(5)-C(20)-O(2)	-178.3(2)
C(7)-O(5)-C(20)-C(19)	65.7(3)
C(7)-O(5)-C(20)-C(31)	-58.2(3)
C(21)-O(2)-C(20)-O(5)	-122.9(2)
C(21)-O(2)-C(20)-C(19)	0.8(3)
C(21)-O(2)-C(20)-C(31)	115.5(3)
C(18)-C(19)-C(20)-O(5)	-85.3(3)
C(22)-C(19)-C(20)-O(5)	122.5(2)
C(18)-C(19)-C(20)-O(2)	160.7(2)
C(22)-C(19)-C(20)-O(2)	8.4(3)
C(18)-C(19)-C(20)-C(31)	42.4(3)
C(22)-C(19)-C(20)-C(31)	-109.9(2)
C(20)-O(2)-C(21)-O(3)	173.8(3)
C(20)-O(2)-C(21)-C(22)	-9.9(3)
C(18)-C(19)-C(22)-C(21)	-164.2(3)
C(20)-C(19)-C(22)-C(21)	-13.4(3)
C(18)-C(19)-C(22)-C(23)	69.9(4)
C(20)-C(19)-C(22)-C(23)	-139.4(3)
C(18)-C(19)-C(22)-C(28)	-52.5(4)
C(20)-C(19)-C(22)-C(28)	98.3(3)
O(3)-C(21)-C(22)-C(19)	-169.6(3)
O(2)-C(21)-C(22)-C(19)	14.5(3)
O(3)-C(21)-C(22)-C(23)	-39.0(4)
O(2)-C(21)-C(22)-C(23)	145.1(2)
O(3)-C(21)-C(22)-C(28)	80.7(4)
O(2)-C(21)-C(22)-C(28)	-95.3(3)
C(19)-C(22)-C(23)-C(24)	76.5(3)
C(21)-C(22)-C(23)-C(24)	-44.7(3)
C(28)-C(22)-C(23)-C(24)	-163.3(2)
C(22)-C(23)-C(24)-S(2)	-56.3(3)
C(22)-C(23)-C(24)-S(1)	177.1(2)
C(27)-S(2)-C(24)-C(23)	179.6(2)

Table D.26 continued

C(27)-S(2)-C(24)-S(1)	-57.5(2)
C(25)-S(1)-C(24)-C(23)	-177.0(2)
C(25)-S(1)-C(24)-S(2)	58.6(2)
C(24)-S(1)-C(25)-C(26)	-60.3(3)
S(1)-C(25)-C(26)-C(27)	68.6(4)
C(25)-C(26)-C(27)-S(2)	-66.6(4)
C(24)-S(2)-C(27)-C(26)	57.0(3)
C(19)-C(22)-C(28)-C(29)	-23.8(3)
C(21)-C(22)-C(28)-C(29)	84.7(3)
C(23)-C(22)-C(28)-C(29)	-153.2(3)
C(22)-C(28)-C(29)-O(4)	147.2(3)
C(22)-C(28)-C(29)-C(30)	-40.1(4)
O(4)-C(29)-C(30)-C(31)	-125.2(3)
C(28)-C(29)-C(30)-C(31)	62.2(4)
O(5)-C(20)-C(31)-C(30)	-170.1(2)
O(2)-C(20)-C(31)-C(30)	-54.9(3)
C(19)-C(20)-C(31)-C(30)	59.9(3)
O(5)-C(20)-C(31)-C(9)	61.4(3)
O(2)-C(20)-C(31)-C(9)	176.5(2)
C(19)-C(20)-C(31)-C(9)	-68.7(3)
C(29)-C(30)-C(31)-C(20)	-48.2(4)
C(29)-C(30)-C(31)-C(9)	72.6(4)
C(8)-C(9)-C(31)-C(20)	-62.9(3)
C(10)-C(9)-C(31)-C(20)	59.9(3)
C(8)-C(9)-C(31)-C(30)	172.6(2)
C(10)-C(9)-C(31)-C(30)	-64.5(3)
C(6)-S(3)-C(32)-C(33)	-57.1(3)
S(3)-C(32)-C(33)-C(34)	64.5(4)
C(32)-C(33)-C(34)-S(4)	-66.7(4)
C(6)-S(4)-C(34)-C(33)	60.5(3)

Symmetry transformations used to generate equivalent atoms:

BIBLIOGRAPHY

Adams, G. L.; Carroll, P. J.; Smith, A. B. III. *J. Am. Chem. Soc.* **2012**, *134*, 4037.

Adams, G. L.; Carroll, P. J.; Smith, A. B., III. *J. Am Chem. Soc.* **2013**, *135*, 519.

Ahmad, Y.; Fatima, K.; Le Quesne, P. W.; Atta-Ur-Rahman *Phytochemistry* **1983**, *22*, 1017.

Ahmad, Y.; Fatima, K.; Rahman, A.-U.; Occolowitz, J. L.; Solheim, B. A.; Clardy, J.; Garnick, R. L.; Le Quesne, P. W. *J. Am. Chem. Soc.* **1977**, *99*, 1943.

Aihara, Y.; Yoshida, A.; Furuta, T.; Wakimoto, T.; Akizawa, T.; Konishi, M.; Kan, T. *Bioorg. Med. Chem. Lett.* **2009**, *19*, 4171.

Alexakis, A.; Bäckvall, J. E.; Krause, N. Pàmies, O.; Diéguez, M. *Chem. Rev.* **2008**, *108*, 2796.

Almasi, D.; Alonso, D. A.; Nájera, C. *Tetrahedron: Asymmetry* **2007**, *18*, 299.

Ananthanarayan, T. P.; Gallagher, T.; Magnus, P. *J. Chem. Soc. Chem. Commun.* **1982**, 709.

Arcadi, A. *Chem. Rev.* **2008**, *108*, 3266.

Armstrong, A.; Davies, N. G. M.; Martin, N. G.; Rutherford, A. P. *Tetrahedron* **2003**, *44*, 3915.

Ashenhurst, J. A.; Isakovic, L.; Gleason, J. L. *Tetrahedron* **2010**, *66*, 368.

Baldwin, J. E.; Barton, D. H. B.; Bloomer, J. L.; Jackman, L. M.; Rodriguez-Hahn, L.; Sutherland, J. K. *Experientia* **1962**, *18*, 345.

Baldwin, J. E.; Barton, D. H. R.; Sutherland, J. K. *J. Chem. Soc.* **1965**, 1787.

Baloglu, E.; Kingston, D. G. I. *J. Nat. Prod.* **1999**, *62*, 1448.

Banwell, M. G.; Coster, M. J.; Edwards, A. J.; Vögtle, M. *Aust. J. Chem.* **2003**, *56*, 577.

Baran, P. S.; Maimone, T. J.; Richer, J. M. *Nature* **2007**, *446*, 404.

Barton, D. H. R.; Godinho, L. D. S.; Sutherland, J. K. *J. Chem. Soc.* **1965**, 1772.

Barton, D. H. R.; Jackman, L. M.; Rodriguez-Hahn, L.; Sutherland, J. K. *J. Chem. Soc.* **1965**, 1779.

Barton, D. H. R.; Sutherland, J. K. *J. Chem. Soc.* **1965**, 1769.

Bishop, R. *Comp. Org. Synth.* **1991**, *6*, 261.

Bloomer, J. L.; Moppett, C. E.; Sutherland, J. K. *J. Chem. Soc. C* **1968**, 588.

Bredt, J.; Thouet, H.; Schnitz, J. *J. Liebigs Ann. Chem.* **1924**, *437*, 1.

Britten, A. Z.; Smith, G. F. *J. Chem. Soc.* **1963**, 3850.

Buchanan, G. L. *Chem. Soc. Rev.* **1974**, *3*, 41.

Cabrera, A.; Alper, H. *Tet. Lett.* **1992**, *33*, 5007.

Cabrera, A.; Alper, H. *Tetrahedron Lett.* **1992**, *33*, 5007.

Cai, X.-H., Du, Z.-Z.; Luo, X.-D. *Org. Lett.* **2007**, *9*, 1817.

Cai, X.-H.; Tan, Q.-G.; Liu, Y.-P., Feng, T.; Du, Z.-Z.; Li, W.-Q.; Luo, X.-D. *Org. Lett.* **2008**, *10*, 577.

Cardoso, C. L.; Silva, D. H. S.; Tomazela, D. M.; Verli, H.; young, M. C. M.; Furlan, M.; Eberlin, M. N.; da Silva Bolani, V. *J. Nat. Prod.* **2003**, *66*, 1017.

Chatterjee, A.; Mukherjee, B.; Ray, A. B.; Das, B. *Tet. Lett.* **1965**, *6*, 3633.

Chemler, S. R.; Trauner, D.; Danishefsky, S. J. *Angew. Chem. Int. Ed.* **2001**, *40*, 4544.

Chen, C.; Layton, M. E.; Shair, M. D. *J. Am. Chem. Soc.* **1998**, *120*, 10784.

Chen, C.; Layton, M. E.; Sheehan, S. M.; Shair, M. D. *J. Am. Chem. Soc.* **2000**, *122*, 7424.

Chen, X.; Zheng, Y.; Shen, Y. *Chem. Rev.* **2007**, *107*, 1777.

Christoffers, J.; Koripelly, G.; Rosiak, A.; Rössle, M. *Synthesis* **2007**, *9*, 1279.

Chu, C. S.; Lee, T. H.; Liao, C. C. *Synlett* **1994**, 635.

Chu, C. S.; Lee, T. H.; Rao, P. D.; Song L. D.; Liao, C. C. *J. Org. Chem.* **1999**, *64*, 4111.

Ciattini, P. G.; Morera, E.; Ortar, G. *Tet. Lett.* **35**, *35*, 2405.

Clive, D. L. J.; Cheng, H.; Gangopadhyay, P.; Huang, X.; Prabhudas, B. *Tetrahedron* **2004** *60*, 4205.

Clive, D. L. J.; Ou, L. *Tetrahedron Lett.* **2002**, *43*, 4559.

Clive, D. L. J.; Sgarbi, P. W. M.; He, X.; Sun, S.; Zhang, J.; Ou, L. *Can. J. Chem.* **2003**, *81*, 811.

Corey, E. J.; Boaz, N. W. *Tetrahedron Lett.* **1985**, *26*, 6015.

Corey, E. J.; Boaz, N. W. *Tetrahedron Lett.* **1985**, *26*, 6019.

Corey, E. J.; Venkateswarlu, A. *J. Am. Chem. Soc.* **1972**, *94*, 6190.

Courdavault, V.; Burlat, V.; St-Pierre, B.; Giglioli-Guivarc'h, N. *Plant Cell Rep.* **2009**, *28*, 83.

Dabrah, T. T.; Kaneko, T.; Massefski, Jr. W.; Whipple, E. B. *J. Am. Chem. Soc.* **1997**, *119*, 1594.

Davies, P.; Fürstner, A. *Angew. Chem. Int. Ed.* **2007**, *46*, 3410.

Deprés, J.-P.; Greene, A. E. *Organic Syntheses* **2004**, 228.

DePuy, C. H.; King, R. W. *Chem. Rev.* **1960**, *60*, 431.

Di Stefano, S.; Leonelli, F.; Garofalo, B.; Mandolini, L.; Bettolo, R. M.; Migneco, L. M. *Org. Lett.* **2002**, *4*, 2783.

Dmitrienko, G. I.; Savard, M. E.; Friesen, R. W.; Thandi, M. S. *Tet. Lett.* **1985**, *26*, 1691.

Dobson, N. A.; Raphael, R. A. *J. Chem. Soc.* **1955**, 3558.

Dong, P. *Synthetic Approaches Towards Cephalezomine A and Phomoidride D*, PhD Thesis, Colorado State University, Ft. Collins, CO, 2010.

Drutu, I.; Njardarson, J. T.; Wood, J. L. *Org. Lett.* **2002**, *4*, 493.

Endo K.; Ohkubo, T.; Hirokami, M.; Shibata, T. *J. Am. Chem. Soc.* **2010**, *132*, 11033.

Fang, J. M.; Chen, M. Y.; Shiue, J. S.; Lu, L.; Hsu, J. L. *Tetrahedron Lett.* **2000**, *41*, 4633.

Feng, T.; Cai, X.-H.; Zhao, P.-H.; Du, Z.-Z.; Li, W.-Q.; Luo, X.-D. *Planta Med.* **2009**, *75*, 1537.

Fukuzawa, S.; Tsuchimoto, T. *Synlett* **1993**, 803.

Garcia Martinez, A.; Teso Vilar, E.; Garcia Fraile, A.; de la Moya Cerero, S.; Lora Maroto, B. *Tetrahedron: Asymmetry* **2002**, *13*, 17.

Gbur, R. K.; Little. R. D. *J. Org. Chem.* **2012**, *77*, 2134.

Ghosh, R.; Roychowdhury, P.; Chattopadhyay, D. Iitaka, Y. *Acta Crys., Sect. C: Cryst. Struct. Commun.* **1988**, *44*, 2151.

Goldring, W. P. D.; Pattenden, G. *Acc. Chem. Res.* **2006**, *39*, 354.

González, D. F.; Brand, J. P.; Waser, J. *Chem. Eur. J.* **2010**, *16*, 9457.

Guibe, F. *Tetrahedron* **1998**, *54*, 2967.

Guirimand, G.; Guihur, A.; Ginis, O.; Poutrain, P.; Héricourt, F.; Oudin, A.; Lanoue, A.; St-Pierre, B.; Burlat, V.; Courdavault, V. *FEBS Journal* **2011**, *278*, 749.

Hale, K. J.; Grabski, M.; Flasz, J. T. *Org. Lett.* **2013**, *15*, 370.

Harutyunyan, S. R.; den Hartog, T.; Geurts, K.; Minnaard, A. J.; Ferigna, B. L. *Chem. Rev.* **2008**, *108*, 2824.

Havlik, A. J.; Wald, M. M. *J. Am. Chem. Soc.* **1955**, *77*, 5171.

Hayahsi, T.; Yamasaki, K. *Chem. Rev.* **2003**, *103*, 2829.

Hayashi, Y.; Itoh, T.; Fukuyama, T. *Org. Lett.* **2003**, *5*, 2235.

Henry, T. A. *J. Chem. Soc.* **1932**, 2759.

Hrubiec, R. T.; Smith, M. B. *J. Org. Chem.* **1984**, *49*, 431.

Huff, R. K.; Sutherland, J. K.; Moppett, C. E. *J. Chem Soc. Perkin Trans. 1* **1972**, 2584.

Inanaga, J.; Handa, Y.; Tabuchi, T.; Otsubo, K.; Yamaguchi, M.; Hanamoto, T. A. *Tetrahedron Lett.* **1991**, *32*, 6557.

Inanaga, J.; Sakai, S.; Handa, Y.; Yamaguchi, M.; Yokoyama, Y. *Chem. Lett.* **1991**, 2117.

Kercher, T.; Livinghouse, T. *J. Org. Chem.* **1997**, *62*, 805.

Krimen, L. I. *Organic Syntheses* **1988**, *6*, 8.

Kwon, O. Y.; Su, D.-S.; Meng, D. F.; Deng, W.; Danishefsky, S. J. *Angew. Chem. Int. Ed.* **1998**, *37*, 1880.

Kwon, O.; Su, D.-S.; Meng, D.; Deng, W.; D'Amico, C. D.; Danishefsky, S. J. *Angew. Chem. Int. Ed.* **1998**, *37*, 1877.

Lai, C. H.; Shen, Y. L.; Liao, C. C. *Synlett* **1997**, 1351.

Larock, R. C.; Leong, W. W. *Comp. Org. Synth.* **1991**, *4*, 269.

Lautens, M.; Paquin, J.-F. *Org. Lett.* **2003**, *5*, 3391.

Lee, J. C.; McDonald, R.; Hall, D. G. *Nature Chem.* **2011**, *3*, 894.

Lespieau, J. C. *R. Hebd, Seaces Acad. Sci.* **1929**, *30*, 287.

Liao, C. C.; Chu, C. S.; Lee, T. H.; Rao, P. D.; Ko, S.; Song, L. D.; Shiao, H. C. *J. Org. Chem.* **1999**, *64*, 4102.

Livinghouse, T. *Tetrahedron* **1999**, *55*, 9947.

Llopart, C. C.; Joule, J. A. *Arkivoc*, **2004**, (*x*), 20.

Logan, A. W. J.; Parker, J. S.; Hallside, M. S.; Burton, J.W. *Org. Lett.* **2012**, *14*, 2940.

Luedtke, G.; Westling, M.; Livinghouse, T. *Tetrahedron* **1992**, *48*, 2209.

Lygin, A. V.; de Meijere, A. *Angew. Chem. Int. Ed.* **2010**, *49*, 2.

Ma, S.; Liu, F.; Negishi, E. *Tet. Lett.* **1997**, *38*, 3829.

Mahroug, S.; Burlat, V. *Phytochem. Rev.* **2007**, *6*, 363.

Maji, M. S.; Pfeifer, T.; Studer, A. *Chem. Eur. J.* **2010**, *16*, 5872.

Malihi, F.; Clive, D. L. J.; Chang, C.-C.; Minaruzzaman *J. Org. Chem.* **2013**, *78*, 996.

Mander, L. N.; Sethi, S. P. *Tetrahedron Lett.* **1983**, *24*, 5425.

McDonald, I. M. *Progress Toward the Total Synthesis of the Phomoidrides*, Ph. D. Thesis, Yale University, New Haven, CT, 2005.

Meng, D.; Danishefsky, S. J. *Angew. Chem. Int. Ed.* **1999**, *38*, 1485.

Meng, D.; Tan, Q.; Danishefsky, S. J. *Angew. Chem. Int. Ed.* **1999**, *38*, 3197.

Meng, D.; Tan, Q.; Danishefsky, S. J. *Angew. Chem. Int. Ed.* **1999**, *38*, 21.

Mitsudo, K.; Thansandote, P.; Wilhelm, T.; Mariampillai, B.; Lautens, M. *Org. Lett.* **2006**, *8*, 3939.

Molander, G. A.; Harris, C. R. *Chem. Rev.* **1996**, *96*, 307.

Mori, K.; Tominaga, M.; Takigawa, T.; Matsui, M. *Synthesis* **1973**, 790.

Murphy, G. K.; Hama, N.; Bedermann, A.; Dong, P.; Schneider, C. M.; McMahon, T. C.; Tao, R. N.; Twenter, B. M.; Spiegel, d. A.; Wood, J. L. *Org. Lett.* **2012**, *14*, 4544.

Murphy, G. K.; Shirahata, T.; Hama, N.; Bedermann, A.; Dong, P.; McMahon, T. C; Twenter, B. M.; Spiegel, D. A.; McDonald, I. M.; Taniguchi, N.; Inoue, M.; Wood, J. L. *J. Org. Chem.* **2013**, *78*, 477.

Nayak, M.; Batra, S. *Tet. Lett.* **2010**, *51*, 510.

Neilson, T.; Werstiuk, E. S. *Can. J. Chem.* **1971**, *49*, 493.

Nicolaou, K. C.; Ajito, K.; Patron, A. P.; Khatuya, H.; Richter, P. K.; Bertinato, P. *J. Am. Chem. Soc.* **1996**, *118*, 3059.

Nicolaou, K. C.; Baran, P. S. *Angew. Chem. Int. Ed.* **2002**, *41*, 2678.

Nicolaou, K. C.; Baran, P. S.; Jautelat, R.; He, Y.; Fong, K. C.; Choic, H. S.; Yoon, W. H.; Zhong, Y. L. *Angew. Chem. Int. Ed.* **1999**, *38*, 549.

Nicolaou, K. C.; Baran, P. S.; Zhong, Y. L.; Fond, K. C.; He, Y.; Yoon, W. H.; Choi, H. S. *Angew. Chem. Int. Ed.* **1999**, *38*, 1676.

Nicolaou, K. C.; Baran, P. S.; Zhong, Y. L; Fong, K. C.; Choi, H. S. *J. Am. Chem. Soc.* **2002**, *124*, 2190.

Nicolaou, K. C.; Baran, P. S.; Zhong, Y.-L.; Choi, H-S.; Yoon, W. H.; He, Y.; Fong, K. C. *Angew. Chem. Int. Ed.* **1999**, *38*, 1669.

Nicolaou, K. C.; Baran, P. S.; Zhong, Y.-L.; Fong, K. C.; He, Y.; Yoon, W. H.; Choi, H.-S. *Angew. Chem. Int. Ed.* **1999**, *38*, 1676.

Nicolaou, K. C.; He, Y.; Fong, K. C.; Yoon, W. H.; Choi, H. s.; Zhong, Y. L.; Baran, P. S. *Org. Lett.* **1999**, *1*, 63.

Nicolaou, K. C.; Jung, J. K.; Yoon, W. H.; He, Y.; Zhong, Y. L.; Baran. P.S. *Angew. Chem. Int. Ed.* **2000**, *124*, 1829.

Nicolaou, K. C.; Jung, J.; Yoon, W. H.; Fong, K. C.; Choi, H. S.; He, Y.; Zong, Y. L. Baran, P. S. *J. Am. Chem. Soc.* **2002**, *124*, 2183.

Nicolaou, K. C.; Postema, M. H. D.; Miller, N. D.; Yang, G. *Angew. Chem. Int. Ed.* **1997**, *36*, 2821.

Nicolaou, K. C.; Zhong, Y. L.; Baran, P. S.; Zhong, Y. L.; Fong, K. C.; Choi, H. S.; Yoon, W. H. *J. Am. Chem. Soc.* **2002**, *124*, 2202.

Njardarson, J. T.; McDonald, I. M.; Speigel, D. A.; Inoue, M.; Wood, J. L. *Org. Lett.* **2001**, *3*, 2435.

Njardarson, J. T.; Wood, J. L. *Org. Lett.* **2001**, *3*, 2431.

Njardarson, J. T; McDonald, I. M.; Spiegel, D. A.; Inoue, M.; Wood, J. L. *Org. Lett*. **2001**, *3*, 2435.

Ohmura, T.; Agwano, T.; Suginome, M. *J. Am. Chem. Soc.* **2010**, *132*, 13191.

Patil, N. T; Yamamoto, Y. *Chem. Rev.* **2008**, *108*, 3395.

Rao, P. D.; Chen, C. H.; Liao, C. C. *Chem. Comm.* **1998**, 155.

Rapoport, H.; Onak, T. P.; Hughes, N. A.; Reinecke, M. G. *J. Am. Chem. Soc.* **1958**, *80*, 1601.

Rottländer, M.; Baymond, L.; Cahiez, G.; Knochel, P. *J. Org. Chem.* **1999**, *64*, 1080.

Saegusa, T.; Ito, Y.; Kobayashi, S.; Hirota, K. *J. Am. Chem. Soc.* **1967**, *89*, 2240.

Saeugusa, T.; Ito, Y.; Kinoshita, H.; Tomita, S. *J. Org. Chem.* **1971**, *36*, 3316.

Schnoes, H. K.; Biemann, K.; Mokry, H. K.; Kompis, I.; Chatterjee, A.; Ganguli, G. *J. Org. Chem.* **1966**, *31*, 1641.

Screttas, C. G.; Michascrettas, M. *J. Organomet. Chem*. **1985**, *292*, 325.

Shang, J.-H.; Cai, X.-H.; Feng, T.; Zhao, Y.-L.; Wang, J.-K.; Zhang, L.-Y.; Yan, M.; Luo, X.-D. *J. Ethnopharmacol.* **2010**, *129*, 174.

Shang, J.-H.; Cai, X.-H.; Zhao, Y.-L.; Feng, T.; Luo, X.-D. *J. Ethnopharmacol*. **2010**, *129*, 293.

Sheehan, S. M.; Lalic, G.; Chen, J. S.; Shair, M. D. *Angew. Chem. Int. Ed.* **2000**, *39*, 2714.

Shi, J.; Manolikakes, G.; Yeh, C.-H.; Guerrero, C. A.; Shenvi, R. A.; Shigehisa, H.; Baran, P. S. *J. Am. Chem. Soc.* **2011**, *133*, 8014.

Shibahara, S.; Fujino, M.; Tashiro, Y.; Okamoto, N.; Esumi, T; Takahashi, K.; Ishihara, J.; Hatakeyama, S. *Synthesis* **2009**, *17*, 2935.

Shinohara, I.; Okue, M.; Yamada, Y.; Nagaoka, H. *Tetrahedron Lett.* **2003**, *44*, 4649.

Smith, J. M.; Moreno, J.; Boal, B. W.; Garg, N. K. *Angew. Chem. Int. Ed.* **2014**, *53*, 2.

Smith, J. M.; Moreno, J.; Boal, B. W.; Garg, N. K. *J. Am. Chem. Soc.* **2014**, *136*, 4504.

Smith, M. W.; Snyder, S. A. *J. Am. Chem. Soc.* **2013**, *135*, 12964.

Spencer, P.; Agnelli, F.; Sulikowski, G. A. *Org. Lett.* **2001**, *3*, 1443.

Spencer, P.; Agnelli, F.; Williams, H. J.; Keller, N. P.; Sulikowski, G. A. *J. Am. Chem. Soc.* **2000**, *122*, 420.

Spiegel, D. A.; Njardarson, J. T.; McDonald, I. M.; Wood, J. L. *Chem. Rev.* **2003**, *103*, 2691.

Spiegel, D. A.; Njardarson, J. T.; Wood, J. L. *Tetrahedron* **2002**, *58*, 6545.

Stöckigt, J.; Zenk, M. H. *FEBS Lett.* **1977**, *79*, 233.

Stork, G.; Kahn, M. *J. Am. Chem. Soc.* **1985**, *107*, 500.

Stork, G.; Mook, R. *J. Am. Chem. Soc.* **1983**, *105*, 3720.

Stork, G.; Mook, R.; Biller, S. A.; Rychnovsky, S. D. *J. Am. Chem. Soc.* **1983**, *105*, 3741.

Stork, G.; Sher, P. M. *J. Am. Chem. Soc.* **1986**, *108*, 303.

Stork, G.; Zhao, K. *Tetrahedron Lett.* **1989**, *30*, 287.

Subramanium, G.; Hiraku, O.; Hayashi, M.; Koyano, T.; Komiyama, K.; Kam, T.-S. *J. Nat. Prod.* **2007**, *70*, 1783.

Sulikowski, g.; Agnelli, F.; Spencer, P.; Koomen, J. M.; Russell, D. H. *Org. Lett.* **2002**, *4*, 1447.

Tan, Q.; Danishefsky, S. J. *Angew. Chem. Int. Ed.* **2000**, *39*, 4509.

Trost, B. M.; Haffner, C. D.; Jebaratnam, D. J.; Krische, M. J.; Thomas, A. P. *J. Am. Chem. Soc.* **2008**, *130*, 16176.

Tsunoda, T.; Suzuki, M.; Noyori, R. *Tetrahedron Lett.* **1980**, *21*, 1357.

Twenter, B. *Synthetic Approaches Toward the Phomoidrides*, Ph. D. Thesis, Yale University, New Haven, CT, 2008.

Varala, R.; Sreelatha, N.; Srinivas, R. A. *Synlett* **2006**, 1549.

Vo-Quang, Y. C. *R. Hebd. Seaces Acad. Sci*. **1964**, *258*, 4586.

Vutukuri, D. R.; Bharathi, P.; Yu, Z.; Rajasekaran, K.; Trans, M.; Thayumanavan, S. *J. Org. Chem.* **2003**, *68*, 1146.

Waizumi, N.; Itoh, T.; Fukuyama, T. *J. Am. Chem. Soc.* **2000**, *122*, 7825.

Waizumi, N.; Itoh, T.; Fukuyama, T. *Tetrahedron Lett.* **1998**, *39*, 6015.

Warner, P. M. *Chem. Rev.* **1989**, *89*, 1067.

Wenkert, E.; Wickberg, B. *J. Am. Chem. Soc.* **1965**, *87*, 1580.

Wesling, M.; Livinghouse, T. *Tet. Lett.*, **1985**, *26*, 5389.

Westling, M.; Livinghouse, T. *J. Am. Chem. Soc.* **1987**, *109*, 590.

Westling, M.; Smith, R.; Livinghouse, T. *J. Org. Chem.* **1986**, *51*, 1159.

Yamada, H.; Wada, Y.; Tanimoto, S.; Okano, M. *Bull. Chem. Soc. Jpn.* **1982**, *55*, 2480.

Yang, D.; Xu, M. *Org. Lett.* **2001**, *3*, 1785.

Yasui, Y.; Takeda, H.; Takemoto, Y. *Chem. Pharm. Bull.* **2008**, *56*, 1567.

Yates, P.; Auski, H.; *Can. J. Chem.* **1979**, *57*, 2853.

Yates, P.; Macas, T. S. *Can. J. Chem.* **1988**, *66*, 1.

Yoshimitsu, T.; Sasaki, S.; Arano, Y.; Nagaoka, H. *J. Org. Chem.* **2004**, *69*, 9262.

Yoshimoto, K.; Kawabata, H.; Nakamichi, N.; Hayashi, M. *Chem. Lett.* **2001**, 934.

Yoshimura, Y.; Kusanagi, T.; Kibayashi, C.; Yamazaki, N.; Aoyagi, S. *Heterocycles* **2008**, *75*, 1329.

Yu, L. C.; Helquist, P. *J. Org. Chem.* **1981**, *46*, 4536.

Yu, L. C.; Helquist, P. *Synthetic Commun.* **1981**, *11*, 591.

Yu, L. C.; Helquist, P. *Tetrahedron Lett.* **1978**, *37*, 3423.

Yu, M.; Zhang, G.; Zhang, L. *Org. Lett.* **2007**, 2147.

Zu, L.; Boal, B. W.; Garg, N. K. **2011**, *133*, 8877.

About the Author

Aaron was born in October of 1986 in Madison, Wisconsin to Jeff and Donna Bedermann. Growing up in the Midwest with an older sister and younger brother, he enjoyed spending most his time outside camping, fishing, or playing hockey. Although he preferred to be outside, his parents made it a point to support and cultivate a desire for knowledge. While attending LaFollette High School, he ran cross-country, played hockey and lacrosse, and more importantly found an interest in chemistry. During his senior year, Aaron was accepted into the College of Engineering at the University of Wisconsin, Madison.

After his first year at the University of Wisconsin, Aaron was accepted into the Department of Chemical and Biological Engineering, but soon decided his interest was not in the field of engineering. His continued passion for chemistry only grew upon joining the research group of Professor Richard P. Hsung. While working in Professor Hsung's research group, Aaron found that he enjoyed not only organic chemistry but also research. Before graduating in 2009 with a BS in chemistry, he decided to pursue graduate studies at Colorado State University.

Aaron then joined the synthetic organic research group of Professor John L. Wood, where he began his studies toward the total synthesis of scholarisine A. While at CSU, Aaron was awarded a graduate teaching award and was invited to attend the 2013 ACS Organic Division Graduate Research Symposium. In August of 2013, Aaron moved with John L. Wood to Baylor University in order to complete his graduate studies toward

the total synthesis of phomoidride D, where he received his Ph.D. in December of 2014. Aaron has accepted a position as a postdoctoral research associate in the laboratory of Professor Timothy F. Jamison at the Massachusetts Institute of Technology and will start in January of 2015.